

**THE JOURNAL OF  
THE INSTITUTE OF METALS**

TS  
200  
15

THE JOURNAL  
OF THE  
INSTITUTE OF METALS

VOLUME LXXIX

1951

EDITOR

N. B. VAUGHAN, M.Sc.

*The Right of Publication and of Translation is Reserved*



*The Institute of Metals is not responsible either for the statements made or  
for the opinions expressed in the following pages*

LONDON  
PUBLISHED BY THE INSTITUTE OF METALS  
4 GROSVENOR GARDENS, S.W.1  
1951

Copyright]

[Entered at Stationers' Hall

## PAST-PRESIDENTS.

Sir WILLIAM HENRY WHITE, K.C.B., LL.D., D.Eng., Sc.D., F.Inst.Met., F.R.S.,  
1908-1910 (*deceased*).

Sir GERARD ALBERT MUNTZ, Bart., 1910-1912 (*deceased*).

Professor WILLIAM GOWLAND, A.R.S.M., F.R.S., 1912-1913 (*deceased*).

Professor ALFRED KIRBY HUNTINGTON, A.R.S.M., 1913-1914 (*deceased*).

Engineer Vice-Admiral Sir HENRY JOHN ORAM, K.C.B., F.Inst.Met., F.R.S.,  
1914-1916 (*deceased*).

Sir GEORGE THOMAS BEILBY, LL.D., D.Sc., F.R.S., 1916-1918 (*deceased*).

Professor Sir HENRY CORT HAROLD CARPENTER, M.A., Ph.D., D.Sc., D.Met.,  
A.R.S.M., F.Inst.Met., F.R.S., 1918-1920 (*deceased*).

Engineer Vice-Admiral Sir GEORGE GOODWIN GOODWIN, K.C.B., LL.D.,  
F.Inst.Met., 1920-1922 (*deceased*).

LEONARD SUMNER, O.B.E., M.Sc., J.P., F.Inst.Met., 1922-1924 (*deceased*).

Professor-Emeritus THOMAS TURNER, M.Sc., A.R.S.M., F.Inst.Met.,  
1924-1926 (*deceased*).

Sir JOHN DEWRANCE, G.B.E., F.Inst.Met., 1926-1928 (*deceased*).

WALTER ROSENHAIN, D.Sc., B.C.E., F.Inst.Met., F.R.S., 1928-1930 (*deceased*).

RICHARD SELIGMAN, Ph.nat.D., F.Inst.Met., 1930-1932.

Sir HENRY FOWLER, K.B.E., LL.D., D.Sc., 1932-1934 (*deceased*).

HAROLD MOORE, C.B.E., D.Sc., Ph.D., F.Inst.Met., 1934-1936.

WILLIAM ROBB BARCLAY, O.B.E., F.Inst.Met., 1936-1938 (*deceased*).

CECIL HENRY DESCH, D.Sc., LL.D., Ph.D., F.Inst.Met., F.R.S., 1938-1940.

The Hon. RICHARD MARTIN PETER PRESTON, D.S.O., 1940-1942.

Lieut.-Colonel Sir JOHN HENRY MAITLAND GREENLY, K.C.M.G., C.B.E., M.A.,  
F.Inst.Met., 1942-1944 (*deceased*).

Sir WILLIAM THOMAS GRIFFITHS, D.Sc., 1944-1946.

Colonel Sir PAUL GOTTLIEB JULIUS GUETERBOOK, K.C.B., D.S.O., M.C.,  
T.D., D.L., J.P., M.A., A.D.C., F.Inst.Met., 1946-1948.

Sir ARTHUR JOHN GRIFFITHS SMOUT, J.P., 1948-1950.

HUBERT SANDERSON TASKER, B.A., 1950-1951.



# OFFICERS AND COUNCIL

FOR THE YEAR 1951-1952

---

## PRESIDENT :

PROFESSOR A. J. MURPHY, M.Sc.

## PAST-PRESIDENTS :

COLONEL SIR PAUL GUETERBOCK, K.C.B., D.S.O., M.C., T.D., D.L.,  
J.P., M.A., A.D.C., F.Inst.Met.  
SIR ARTHUR SMOUT, J.P.  
H. S. TASKER, B.A.

## VICE-PRESIDENTS :

MAJOR C. J. P. BALL, D.S.O., M.C.  
A. B. GRAHAM.  
P. V. HUNTER, C.B.E.  
PROFESSOR H. O'NEILL, D.Sc., M.Met.

C. J. SMITHELLS, M.C., D.Sc.  
PROFESSOR F. C. THOMPSON, D.Met.,  
M.Sc.

## HONORARY TREASURER :

W. A. C. NEWMAN, O.B.E., B.Sc., A.R.S.M., A.R.C.S., D.I.C.

## ORDINARY MEMBERS OF COUNCIL :

ALFRED BAER, B.A.  
G. L. BAILEY, M.Sc.  
E. A. BOLTON, M.Sc.  
N. I. BOND-WILLIAMS, B.Sc.  
D. F. CAMPBELL, M.A., A.R.S.M.  
K. W. CLARKE.  
C. H. DAVY.  
T. M. HERBERT, M.A.  
H. W. G. HIGNETT, B.Sc.

E. H. JONES.  
L. B. PFEIL, O.B.E., D.Sc., A.R.S.M.,  
F.R.S.  
A. R. POWELL.  
PROFESSOR A. G. QUARRELL, D.Sc.,  
Ph.D., A.R.C.S., D.I.C.  
PROFESSOR G. V. RAYNOR, M.A.,  
D.Sc., D.Phil.  
CHRISTOPHER SMITH.

## EX-OFFICIO MEMBERS OF COUNCIL :

(Chairmen of Local Sections)

BIRMINGHAM : BERNARD THOMAS.  
LONDON : E. A. G. LIDDIARD, M.A.  
OXFORD : H. M. FINNISTON, B.Sc.,  
Ph.D., A.R.T.C.

SCOTTISH : JOHN ARNOTT.  
SHEFFIELD : M. M. HALLETT, M.Sc.  
SOUTH WALES : E. A. HONTOIR, B.Sc.

---

## REPRESENTATIVES OF OTHER BODIES.

The following, in accordance with Article 32, represent Government departments and allied societies at Council meetings for purposes of liaison :

### ADMIRALTY :

CAPTAIN (E) L. A. B. PEILE, D.S.O.,  
M.V.O., R.N.

### IRON AND STEEL INSTITUTE :

RICHARD MATHER, B.Met.

### INSTITUTION OF METALLURGISTS :

E. W. COLBECK, M.A.  
L. ROTHERHAM, M.Sc.

### WAR OFFICE :

MAJOR-GENERAL S. W. JOSLIN,  
C.B.E., M.A.

---

## SECRETARY :

LIEUT.-COLONEL S. C. GUILLAN, T.D.

### ASSISTANT SECRETARY :

MAJOR R. E. MOORE.

### EDITOR OF PUBLICATIONS :

N. B. VAUGHAN, M.Sc.

**CHAIRMEN AND HONORARY SECRETARIES OF THE  
LOCAL SECTIONS.**

at 31 December 1951.

**Birmingham.**

*Chairman* : BERNARD THOMAS, Leigh House, Bradmore Road,  
Wolverhampton.

*Hon. Secretary* : E. H. BUCKNALL, M.Sc., "Ardarroch", 264 Harborne  
Park Road, Harborne, Birmingham 17.

*Hon. Treasurer* : R. CHADWICK, M.A., 5 Fairmead Rise, King's Norton,  
Birmingham 30.

**London.**

*Chairman* : E. A. G. LIDDIARD, M.A., Fulmer Research Institute, Stoke  
Poges, Bucks.

*Hon. Secretary* : E. C. RHODES, Ph.D., B.Sc., The Mond Nickel Company, Ltd.,  
Development and Research Department, Bashley Road, London, N.W.10.

*Hon. Treasurer* : J. D. GROGAN, B.A., Metallurgy Division, National  
Physical Laboratory, Teddington, Middlesex.

**Oxford.**

*Chairman* : H. M. FINNISTON, B.Sc., Ph.D., A.R.T.C., Atomic Energy  
Research Establishment, Harwell.

*Hon. Secretary* : B. R. T. FROST, B.Sc., Ph.D., Atomic Energy Research  
Establishment, Harwell.

*Hon. Treasurer* : J. C. ARROWSMITH, M.Met., Pressed Steel Company of  
Great Britain, Ltd., Oxford.

**Scottish.**

*Chairman* : JOHN ARNOTT, G. and J. Weir, Ltd., Cathcart, Glasgow.

*Hon. Secretary* : MATTHEW HAY, A. Cohen and Co., Ltd., Craigton Industrial  
Estate, Barfillan Drive, Cardonald, Glasgow, S.W.2.

*Hon. Treasurer* : N. J. MACLEOD, Steven and Struthers, Ltd., 86 Eastvale Place,  
Kelvinhaugh, Glasgow, C.3.

**Sheffield.**

*Chairman* : M. M. HALLETT, M.Sc., Sheepbridge Engineering, Ltd.,  
Chesterfield.

*Hon. Secretary and Treasurer* : A. J. MACDOUGALL, M.Met., Department of  
Applied Science, The University, St. George's Square, Sheffield 1.

**South Wales.**

*Chairman* : E. A. HONTOIR, B.Sc., Rio Tinto Co., Ltd., Port Talbot.

*Hon. Secretary* : K. M. SPRING, 36 Beechwood Road, Uplands, Swansea.

*Hon. Treasurer* : W. H. GRENFELL, "The Woods", Bryn Terrace, Mumbles,  
Swansea.

**CORRESPONDING MEMBERS TO THE COUNCIL.**

at 31 December 1951.

**Australia.**

Professor H. K. WORNER, D.Sc.,  
Professor of Metallurgy, University of Melbourne, Carlton, N.3, Melbourne,  
Victoria.

**Belgium.**

H. P. A. FÉRON,  
Administrateur-Directeur, Visseries et Tréfileries Réunies, 2 Avenue  
Général Leman, Haren, Bruxelles.

**Canada.**

Professor BRUCE CHALMERS, Ph.D., D.Sc.,  
Department of Metallurgical Engineering, University of Toronto, Toronto 5,  
Ontario.

Professor G. LETENDRE, B.A., Ph.D., Professor of Metallurgy and  
Director, Department of Mining and Metallurgical Engineering, Faculty of  
Sciences, Laval University, Boulevard de l'Entente, Quebec City, P.Q.

**France.**

Professor P. A. J. CHEVENARD,  
Directeur Scientifique, Société Anonyme de Commentry-Fourchambault et  
Decazeville, 84 rue de Lille, Paris 7e.

JEAN MATTER, Vice-Président et Directeur-Général, Société Centrale des  
Alliages Légers, Issoire, Puy-de-Dôme.

**India.**

N. P. GANDHI, M.A., B.Sc., A.R.S.M., D.I.C.,  
Kennaway House, Proctor Road, Girgaon, Bombay 4.

**Italy.**

LENO MATTEOLI, Dott.chim.,  
Vice-Director, Istituto Scientifico Tecnico Ernesto Breda, Sesto S. Giovanni,  
Milano.

**Netherlands.**

M. HAMBURGER, Director, N.V. Royal Nederlandsche Lood- en Zinkpletterijen  
voorheen A.D. Hamburger, Leidschekade 30, Utrecht.

**South Africa.**

G. H. STANLEY, D.Sc., A.R.S.M.,  
24 Duncombe Road, Forest Town, Johannesburg, Transvaal.  
Professor L. TAVERNER, A.R.S.M., D.I.C., Professor of Metallurgy and  
Assaying, University of the Witwatersrand, Johannesburg, Transvaal.

**Spain.**

Professor J. ORLAND, M.Sc., M.A., Ph.D., D.D., Head of the Department  
of Metallography and Strength of Materials, Instituto Católico  
de Artes e Industrias, Alberto Aguilera 23, Madrid.

**Sweden.**

Professor CARL BENEDICKS, Fil.Dr., Dr.-Ing.e.h., Dr.Techn.h.c.,  
Drottninggatan 95 B., Stockholm.

Professor AXEL HULTGREN, Professor of Metallography, Kungl. Tekniska  
Högskolan, Stockholm.

**Switzerland.**

Professor A. VON ZEERLEDER, Dr.-Ing., Director, Research Laboratories,  
Société Anonyme pour l'Industrie de l'Aluminium Chippis,  
Rosenbergstrasse 25, Neuhausen a./Rheinfall.

**United States of America.**

Professor R. F. MEHL, Ph.D., Eng.D., Sc.D., Director, Metals Research  
Laboratory, Carnegie Institute of Technology, Pittsburgh, Pa.

Professor C. S. SMITH, Sc.D., Professor of Metallurgy and Director of the  
Institute for the Study of Metals, University of Chicago, Chicago 37, Ill.

Dr. R. A. WILKINS, Vice-President, Revere Copper and Brass, Inc., Rome, N.Y.







PROFESSOR A. J. MURPHY, M.Sc. \*  
(President, 1951-52).



# CONTENTS

## MINUTES OF PROCEEDINGS

	PAGE
May Lecture, 23 May 1951 . . . . .	xiii
Election of Members . . . . .	xiii
May Lecture . . . . .	xv
Annual Autumn Meeting, Italy, 16-25 September 1951 . . . . .	xvi
Official Opening . . . . .	xvi
Welcome to Members and Visitors from Overseas . . . . .	xvi
Nomination of Officers for 1952-53 . . . . .	xvi
Senior Vice-President for 1952-53 . . . . .	xvii
Elections of Members . . . . .	xvii
Discussion of Papers (17 September) . . . . .	xxiii
Visits (17 September) . . . . .	xxiii
Autumn Lecture . . . . .	xxiii
Discussion of Papers (18 September) . . . . .	xxiii
Votes of Thanks . . . . .	xxiv
Visits (18 September) . . . . .	xxiv
Banquet . . . . .	xxiv
Visits (19-24 September) . . . . .	xxv
List of Patrons . . . . .	xxvi

## PAPERS AND DISCUSSIONS

	PAGE
<b>1294. The Hardness and Strength of Metals.</b> By D. Tabor, Ph.D.	1
Discussion . . . . .	465
<b>1295. Mechanism of Precipitation in Aluminium-Magnesium Alloys.</b> By E. C. W. Perryman, M.A., A.I.M., and G. B. Brook, B.Met. . . . .	19
<b>1296. Heat Extraction at Corners and Curved Surfaces in Sand Moulds.</b> By R. W. Ruddle, M.A., A.I.M., and R. A. Skinner, B.Sc. . . . .	35
Discussion . . . . .	475
<b>1297. The Effect of Copper, Silicon, and Magnesium on the Mechanical Properties of Aluminium Alloys of the D.T.D. 424 Type.</b> By E. Scheuer, Dr.rer.nat., S. J. Williams, L.I.M., and J. Wood, M.Sc. . . . .	57
<b>1298. The Application of Hydrogen Equilibrium-Pressure Measurements to the Investigation of Titanium Alloy Systems.</b> By A. D. McQuillan, Ph.D., B.Sc. . . . .	73
<b>1299. Some New Observations on the Mechanism of Fatigue in Metals.</b> By W. A. Wood, D.Sc., and A. K. Head, B.A., B.Sc. . . . .	89

	PAGE
	<i>Papers. Discn.</i>
1300. The Stability of the $\text{Co}_2\text{Al}_3$ -Type Structure in the Aluminium-Rich Alloys of the Aluminium-Iron-Cobalt-Nickel System. By M. B. Waldron, B.Sc., Ph.D., A.I.M. . . . .	103
1301. Presidential Address. By Professor A. J. Murphy, M.Sc., F.I.M. . . . .	117
1302. Slip and Polygonization in Aluminium. By R. W. Cahn, B.A., Ph.D. . . . .	129
1303. Three Basic States in the Mechanism of Deformation of Metals at Different Temperatures and Strain-Rates. By W. A. Wood, D.Sc., G. R. Wilms, M.Eng.Sc., and W. A. Rachinger, M.Sc. . . . .	159
1304. The Constitution of Titanium-Rich Alloys of Iron and Titanium. By H. W. Worner, M.Sc. . . . .	173
1305. The Effect of Mould Material and Alloying Elements on Metal/Mould Reaction in Copper-Base Alloys. By N. B. Rutherford, B.Sc., A.I.M. . . . .	189
Discussion . . . . .	477
1306. The Intermetallic Compounds in the Alloys of Aluminium and Silicon with Chromium, Manganese, Iron, Cobalt, and Nickel. By J. N. Pratt, B.Sc., Ph.D., and Professor G. V. Raynor, M.A., D.Sc. . . . .	211
1307. The Variation with Strain-Rate of the Mechanism of Deformation of a Lead-Thallium Alloy. By R. C. Gifkins, B.Sc., A.I.M. . . . .	233
1308. Copper-Nickel-Iron Alloys Resistant to Sea-Water Corrosion. By G. L. Bailey, M.Sc., F.I.M. . . . .	243
Discussion . . . . .	478
1309. Observations on Some Wrought Aluminium-Zinc-Magnesium Alloys. By Maurice Cook, D.Sc., Ph.D., F.I.M., R. Chadwick, M.A., F.I.M., and N. B. Muir, B.Sc., A.I.M. . . . .	293
Discussion . . . . .	482
1310. The Ageing Characteristics of Binary Aluminium-Copper Alloys. By H. K. Hardy, Ph.D., M.Sc., A.R.S.M., A.I.M. . . . .	321
1311. The Titanium-Hydrogen System for Magnesium-Reduced Titanium. By A. D. McQuillan, Ph.D., B.Sc. . . . .	371
1312. A Provisional Constitutional Diagram of the Chromium-Titanium System. By (Mrs.) M. K. McQuillan, M.A. . . . .	379
1313. An X-Ray Study of the Phases in the Copper-Titanium System. By Nils Karlsson . . . . .	391
1314. Science in the Service of the Community. Forty-First May Lecture. By The Right Hon. Sir John Anderson, P.C., G.C.B., G.C.S.I., G.C.I.E., F.R.S. . . . .	407
1315. Grain-Boundary Energies in Silver. By A. P. Greenough, B.A., and Ronald King, B.Sc. . . . .	415
1316. The Study of Recrystallization in Zinc by Direct Observation. By G. Brinson and A. J. W. Moore, B.Sc., Ph.D. . . . .	429

	PAGE
	<i>Papers. Discn.</i>
<b>1317. Internal Friction and Grain-Boundary Viscosity of Tin.</b> By L. Rotherham, M.Sc., A. D. N. Smith, B.A., and G. B. Greenough, Ph.D. . . . .	439
Discussion . . . . .	486
<b>1318. Roller Levelling of Magnesium Alloy Sheet.</b> By E. A. Calnan, B.Sc., and A. E. L. Tate, A.I.M. . . . .	455
Joint Discussion on the Papers by Dr. H. K. Hardy: "The Effect of Small Quantities of Cd, In, Sn, Sb, Tl, Pb, or Bi on the Ageing Characteristics of Cast and Heat- Treated Aluminium-4% Copper-0.15% Titanium Alloy", and "The Tensile Properties of Heat-Treated Aluminium- Copper and Aluminium-Copper-Cadmium Alloys of Com- mercial Purity" ( <i>J. Inst. Metals</i> , 1950-51, <b>78</b> , 169, 657)	487
Discussion on the Paper by Mr. R. W. Ruddle and Mr. A. L. Mincher: "The Influence of Alloy Constitution on the Mode of Solidification of Sand Castings" ( <i>J. Inst. Metals</i> , 1950-51, <b>78</b> , 229) . . . . .	493
Joint Discussion on the Papers by Mr. R. F. Tylecote: "The Adherence of Oxide Scales on Copper" and "The Oxi- dation of Copper at 350°-900° C. in Air" ( <i>J. Inst. Metals</i> , 1950-51, <b>78</b> , 301, 327) . . . . .	496
Discussion on the Paper by Mr. H. G. Baron and Professor F. C. Thompson: "Friction in Wire Drawing" ( <i>J. Inst.</i> <i>Metals</i> , 1950-51, <b>78</b> , 415) . . . . .	500
Additional Discussion on the Paper by Professor A. H. Cottrell and Dr. V. Aytakin: "The Flow of Zinc under Constant Stress" ( <i>J. Inst. Metals</i> , 1950, <b>77</b> , 389, 597) .	505
Obituary Notice . . . . .	506
Name Index . . . . .	509

# LIST OF PLATES

	Professor A. J. Murphy, M.Sc., President	<i>frontispiece</i>
I-VI.	Paper by Mr. E. C. W. Perryman and Mr. G. B. Brook . . . . .	<i>between pp. 24 and 25</i>
VII-VIII.	Paper by Dr. E. Scheuer, Mr. S. J. Williams, and Mr. J. Wood . . . . .	<i>between pp. 64 and 65</i>
IX-X.	Paper by Dr. A. D. McQuillan . . . . .	<i>between pp. 80 and 81</i>
XI-XIV.	Paper by Dr. W. A. Wood and Mr. A. K. Head . . . . .	<i>between pp. 96 and 97</i>
XV-XVI.	Paper by Dr. M. B. Waldron . . . . .	<i>between pp. 110 and 111</i>
XVII-XXIV.	Paper by Dr. R. W. Cahn . . . . .	<i>between pp. 148 and 149</i>
XXV-XXVI.	Paper by Dr. W. A. Wood, Mr. G. R. Wilms, and Mr. W. A. Rachinger . . . . .	<i>between pp. 164 and 165</i>
XXVII-XXVIII.	Paper by Mr. H. W. Worner . . . . .	<i>between pp. 180 and 181</i>
XXIX-XXX.	Paper by Mr. N. B. Rutherford . . . . .	<i>between pp. 204 and 205</i>
XXXI-XXXIV.	Paper by Dr. J. N. Pratt and Professor G. V. Raynor . . . . .	<i>between pp. 220 and 221</i>
XXXV-XXXVIII.	Paper by Mr. R. C. Gifkins . . . . .	<i>between pp. 236 and 237</i>
XXXIX-XLII.	Paper by Mr. G. L. Bailey . . . . .	<i>between pp. 258 and 259</i>
XLIII-XLVI.	Paper by Dr. M. Cook, Mr. R. Chadwick, and Mr. N. B. Muir . . . . .	<i>between pp. 306 and 307</i>
XLVII.	Paper by Dr. A. D. McQuillan . . . . .	<i>facing p. 378</i>
XLVIII-LXIX.	Paper by (Mrs.) M. K. McQuillan . . . . .	<i>between pp. 386 and 387</i>
L-LI.	Paper by Mr. A. P. Greenough and Mr. R. King . . . . .	<i>between pp. 422 and 423</i>
LII-LIX.	Paper by Mr. G. Brinson and Dr. A. J. W. Moore . . . . .	<i>between pp. 430 and 431</i>
LX.	Paper by Mr. E. A. Calnan and Mr. A. E. L. Tate . . . . .	<i>facing p. 460</i>
LXI.	Discussion on the papers by Dr. H. K. Hardy . . . . .	<i>facing p. 488</i>

# THE INSTITUTE OF METALS

## MINUTES OF PROCEEDINGS

### ANNUAL MAY LECTURE

A GENERAL MEETING of the Institute of Metals was held at the Royal Institution, Albemarle Street, London, W.1, on Wednesday, 23 May 1951, at 6.30 p.m., the President, Professor A. J. Murphy, M.Sc., occupying the Chair.

The minutes of the Annual General Meeting, held in London on 13, 14, and 15 March 1951, were taken as read.

#### ELECTIONS OF ORDINARY MEMBERS, JUNIOR MEMBERS, AND STUDENT MEMBERS

The SECRETARY (Lieut.-Colonel S. C. Guilan, T.D.) announced that, since the last General Meeting, the following 35 Ordinary Members, 1 Junior Member, and 19 Student Members had been elected :

#### ELECTED ON 16 APRIL 1951

##### *As Ordinary Members*

COLEMAN, Geoffrey, Manager, British United Shoe Machinery Company, Ltd., Hildyard Road, Leicester.

DE MERRE, Marcel, O.B.E., Administrateur-Directeur Général, Société Général Métallurgique de Hoboken, Anvers, Belgium.

DUNLOP, Samuel Hamilton, General Manager, Central Marine Engine Works, West Hartlepool.

GILLESPIE, William George, Deputy Managing Director, West Rand Engineering Works (Pty.), Ltd., Little Birmingham, Krugersdorp, Transvaal, South Africa.

HAMER, Robert Dennis, B.Sc., Dipl.Ing., Vice-President and Director, Aluminium Laboratories, Ltd., Banbury, Oxon.

HAYWARD, Eric, Dane Street House, Chilham, near Canterbury, Kent.

HEATON, Roger Noel, Secretary, British Non-Ferrous Metals Federation, 132 Hagley Road, Birmingham 16.

KLEMENT, John F., B.S., M.E., Chief Metallurgist, Ampeco Metal, Inc., 1745 S. 38th Street, Milwaukee 15, Wis., U.S.A.

LAWLEY, Bernard, Director, Thomas Lawley, Ltd., 109 Unett Street, Birmingham.

LAWLEY, Gerald, Director, Jones and Rooke (1948), Ltd., 86-92 Northwood Street, Birmingham 3.

MCCONNELL, John Lawson, M.C., Chairman, Goodlass Wall and Lead Industries, Ltd., 14 Finsbury Circus, London, E.C.2.

MACWATTERS, Lieut.-Colonel Gerald, O.B.E., T.D., Manager, Capper Pass and Son, Ltd., Bedminster Smelting Works, Bristol.

PRICHARD, Evan Wynne, B.Sc., Technical Assistant, Department of Atomic Energy, Ministry of Supply, Springfield, near Salwick, Preston, Lancs.

- REYNOLDS, Thomas, Works Manager, Hughes-Johnson Stampings, Ltd., Langley Green, Birmingham.
- SCHENKEL, John Robert Harry, Works Metallurgist, Charles Clifford and Son, Ltd., Dogpool Mills, Birmingham.
- THEOBALD, John Richard, B.Sc., Assistant Works Manager, Mersey White Lead Co., Ltd., Sankey Bridges, Warrington, Lancs.
- WATSON, *Lieut.-Colonel* Nigel, O.B.E., Metallurgist, Oesterreichische Alpine Montangesellschaft, Leoben, Austria.

*As Student Members*

- ATKINS, John William, Student Metallurgical Chemist, John Dale, Ltd., London Colney, St. Albans, Herts.
- BEISHON, Ronald John, Student of Metallurgy, Battersea Polytechnic, London, S.W.11.
- BURRILL, William James, B.Sc., Student of Metallurgy, King's College, Newcastle-upon-Tyne.
- EIOHEN, Erwin, B.Met.E., Student of Metallurgy, Ohio State University, Columbus 10, O., U.S.A.
- ISGAR, John Ernest, Assistant Metallurgist, Ransome and Rapier, Ltd., Waterside Works, Ipswich.
- WHITEHEAD, Trevor Joseph, Student of Metallurgy, College of Technology, Manchester 13.
- WINDLE, John Michael, Student-Metallurgist, Rolls Royce, Ltd., Bankfield, Barnoldswick, via Colne, Lancs.

ELECTED ON 25 APRIL 1951

*As Ordinary Members*

- BROENNIMANN, Markus, B.S., Metallurgist, Cerro de Pasco Copper Corporation, La Oroya, Peru.
- COOKSON, Roland Antony, O.B.E., Director, Associated Lead Manufacturers, Ltd., Crescent House, Newcastle-on-Tyne 1.
- DUPONT, Max, Manager, Centre de Documentation Sidérurgique, 6 Rue de Lota, Paris 16e, France.
- HARDY, John, A.Met., A.I.M., Regional Works Metallurgist, Railway Executive, Western Region, Mechanical and Electrical Engineer's Department, Swindon, Wiltshire.
- HENSCHKE, Erhard Rudolf, Chief Engineer, Loewy Engineering Company, Ltd., Branksome Grange, St. Aldhelm's Road, Bournemouth.
- JONAH, David Alonzo, Sc.M., Librarian, Brown University Library, Providence 12, R.I., U.S.A.
- KIRKPATRICK, Leonard Henry, A.M., Librarian, University of Utah Library, Salt Lake City, Utah, U.S.A.
- SULLY, William John, Director and Works Manager, Sterling Metals, Ltd., Gypsy Lane Works, Nuneaton.

*As Junior Member*

- THOMPSON, Ronald Alexander, Technical Assistant, Imperial Chemical Industries, Ltd., Metals Division, Landore, Swansea.

*As Student Members*

- DAVIES, David Howell, Student, Metallurgy Department, University College, Swansea.
- DUNCAN, John Alexander, Student of Metallurgy, Battersea Polytechnic, London, S.W.11.



- FRICKER, Dennis John, Research Laboratories, The British Aluminium Co., Ltd., Chalfont Park, Gerrards Cross, Buckinghamshire.
- HALL, Edward George, Technical Assistant, Research Laboratories, The British Aluminium Co., Ltd., Chalfont Park, Gerrards Cross, Buckinghamshire.
- HYAM, Elmer Donald, B.A., Research Student, Department of Metallurgy, University of Cambridge.
- SHAMI, Wahid-Uz-Zaman, B.Sc., Assistant Section Officer, A/46, Metallurgical Department, Royal Arsenal, Woolwich, London, S.E.18.
- TOOR, Amanullah Khan, M.Sc., A.S.O. Trainee, A/46, Royal Arsenal, Woolwich, London, S.E.18.

ELECTED ON 21 MAY 1951

*As Ordinary Members*

- BUSHELL, Thomas Wyvern, A.Eng., Surveyor for Metals, Lloyd's Register of Shipping, Albert Road, Middlesbrough, Yorks.
- COLE, *Brigadier* Alan Giffard, O.B.E., Personal Assistant to the Chairman and Managing Director, Magnesium Elektron, Ltd., Bath House, 82 Piccadilly, London, W.1.
- COUDEL, Jean, Directeur-Général, Forges de la Providence, Marchienne-au-Pont, Belgium.
- DAWKINS, Alfred Ernest, B.Sc., A.I.C., F.R.I.C., Chief Superintendent, Defence Research Laboratories, Private Bag No. 4, Ascot Vale, Victoria, Australia.
- EGLINTON, Samuel Sydney Edward, Regional Sales Manager, Imperial Chemical Industries, Ltd., Metals Division, Glasgow.
- FITZGERALD, Timothy, Research Metallurgist, National Gas Turbine Establishment, Whetstone, Leicester.
- FREYNIK, Henry Stanley, Chief Metallurgist, The Riverside Metal Company, Riverside, N.J., U.S.A.
- HOWELL, Leonard Philip, Engineer, Northern Aluminium Co., Ltd., Rogerstone, Mon.
- LODDER, *Ir.* Jacob, M.Sc., Senior Chemist, N. V. Mekog, Velsen, Holland.
- MOGHE, Dinker, B.Sc., Assistant Works Manager, Ordnance Factory, Ambar-nath, India.

*As Student Members*

- FIEDLER, Howard C., B.S., S.M., Graduate Student, Metallurgy Department, Massachusetts Institute of Technology, Cambridge, Mass., U.S.A.
- FROST, Michael Andrew, Student of Metallurgy, University of Sheffield.
- HANNAFORD, Robert Heath, Shift Supervisor, Electrolytic Refining and Smelting Co. Pty., Ltd., Port Kembla, N.S.W., Australia.
- MACLEAN, Timothy Lachlan, Student of Metallurgy, Battersea Polytechnic, London, S.W.11.
- WILLIAMS, Thomas Howard, Laboratory Assistant, Bristol Aeroplane Co., Ltd., Filton, Bristol.

MAY LECTURE

The President then introduced The Right Hon. Sir JOHN ANDERSON, P.C., G.C.B., G.C.S.I., G.C.I.E., F.R.S., who delivered the Forty-First May Lecture on "Science in the Service of the Community" (see this volume, pp. 407-414).

Professor F. C. THOMPSON, D.Met., M.Sc. (Vice-President) proposed a hearty vote of thanks to Sir John Anderson for his lecture. The motion was put to the meeting and carried with acclamation.

The lecturer was afterwards entertained to dinner by the Council.

## ANNUAL AUTUMN MEETING

THE FORTY-THIRD ANNUAL AUTUMN MEETING of the Institute of Metals was held in Italy from Sunday to Wednesday, 16 to 25 September 1951, by invitation of the Associazione Italiana di Metallurgia. The meeting opened in Venice, the General Meetings on Monday and Tuesday, 17 and 18 September, being held in the Cà Foscari, on the Grand Canal, when the President, Professor A. J. Murphy, M.Sc., occupied the Chair.

**Sunday, 16 September**

The official opening of the Autumn Meeting of the Institute of Metals and of the annual meeting of the Associazione Italiana di Metallurgia took place in the Palazzo Ducale (Doge's Palace), Venice, at 9.30 a.m., when the Mayor of Venice welcomed the members of both societies to the city. The Presidents of local industrial associations and Professor Antonio Segni, Secretary for Public Education, also welcomed the members. Speeches of reply to the welcome were made by Cav. A. Daccò, President of the Associazione Italiana di Metallurgia, and by Professor A. J. Murphy, President of the Institute of Metals.

Later in the morning a reception for members and their ladies, of both societies, was given by the Mayor and the Municipality of Venice at the Cà Farsetti.

In the afternoon, by invitation of the Industrial Associations of Venice, a visit was paid, by steamer, to the Island of Murano, in the Lagoon.

**Monday, 17 September**

A scientific session was held at 9.30 a.m. in the Cà Foscari, when the President, Professor A. J. Murphy, M.Sc., took the Chair.

The President expressed the Council's pleasure at the large attendance of members and guests, and he welcomed members of the Iron and Steel Institute, who, by special invitation, had joined the meeting at the conclusion of a meeting of the Iron and Steel Institute in Austria. He stated that, in addition to those from Italy and Great Britain, members were present from Austria, Belgium, Egypt, France, Germany, India, the Netherlands, Norway, Spain, Sweden, Switzerland, and the United States of America. Mr. E. A. Langham attended as official delegate of the Indian Institute of Metals, and Honorary Corresponding Members to the Council for Italy (Dott. Leno Matteoli), Switzerland (Professor Dr.-Ing. A. von Zeerleder), and the United States of America (Professor C. S. Smith) were present.

The minutes of the previous General Meeting, held in London on 23 May 1951, were taken as read.

**NOMINATION OF OFFICERS FOR 1952-53**

The SECRETARY (Lieut.-Colonel S. C. Guilan, T.D.) announced that the following members would retire from the Council at the 1952 Annual General Meeting, as required by the Articles of Association :

*President :*

Professor A. J. MURPHY, M.Sc.

*Past-President :*

Colonel Sir PAUL GUETERBOCK, K.C.B., D.S.O., M.C., T.D., D.L., J.P.,  
M.A., A.D.C.

*Vice-Presidents :*

Major C. J. P. BALL, D.S.O., M.C.  
C. J. SMITHELLS, M.C., D.Sc.

*Honorary Treasurer :*

W. A. C. NEWMAN, O.B.E., A.R.S.M., A.R.C.S., D.I.C.

*Ordinary Members of Council :*

D. F. CAMPBELL, M.A., A.R.S.M.  
T. M. HERBERT, M.A.  
H. W. G. HIGNETT, B.Sc.  
A. R. POWELL

He stated that, in accordance with Article 19, Professor A. J. MURPHY, M.Sc., would fill the vacancy as Past-President, and that, in accordance with Article 22, the Council had nominated the following members to fill the other vacancies :

*As President :*

C. J. SMITHELLS, M.C., D.Sc.

*As Vice-Presidents :*

G. L. BAILEY, M.Sc.  
S. F. DOREY, C.B.E., D.Sc., F.R.S.

*As Honorary Treasurer :*

E. H. JONES

*As Ordinary Members of Council :*

N. P. INGLIS, Ph.D., M.Eng.  
IVOR JENKINS, D.Sc.  
A. G. RAMSAY, B.Sc., Ph.D.  
H. SUTTON, D.Sc.  
Major P. LITHERLAND TEED, A.R.S.M.  
W. J. THOMAS

He reminded members of their rights, under Article 22, to make other nominations, if desired, before the conclusion of the meeting.

SENIOR VICE-PRESIDENT FOR 1952-53

The SECRETARY announced that, in accordance with Article 42, the Council had elected Professor F. C. THOMPSON, D.Met., M.Sc., as Senior Vice-President for 1952-53, and that he would be their next nomination for the Presidency.

ELECTIONS OF ORDINARY MEMBERS, JUNIOR MEMBERS, AND  
STUDENT MEMBERS

The SECRETARY announced that since the last General Meeting, the following 104 Ordinary members, 10 Junior Members, and 23 Student Members had been elected :

ELECTED ON 6 JULY 1951

*As Ordinary Members :*

AHMAD, Shafiq, Superintendent, Melting Department, Pakistan Mint, Lahore, Pakistan.  
BOLLIGER, Max, Head of Chemical Research Department, Cendres et Métaux S.A., Bienne, Switzerland.

- BUCKMAN, Peter, Research and Development Engineer, Morris Motors, Ltd., Radiators' Branch, Oxford.
- BURKE, Thomas Joseph, M.S., Metallurgist, Johnson Bronze Company, 440 S. Mill Street, Newcastle, Pa., U.S.A.
- COLLIER, Claude William, Works Chemist, Ericsson Telephones, Ltd., Beeston, Notts.
- DACÒ, *Cav.* Aldo, President, Associazione Italiana di Metallurgia, via S. Paolo 10, Milan, Italy.
- DEFREYN, Joseph Emile Ghislain, Ing. civil des Mines, Directeur, S.A. Laminaires et Tréfileries de Hal, Hal, Belgium.
- EL LIETHY, Kadry Foad, B.Sc., Metallurgical Engineer, Ministry of Defence, Cairo, Egypt.
- ELTON, Miles, M.A., Director, Elton, Levy and Co., Ltd., 1-4 St. Ermin's (West Side), Caxton Street, London, S.W.1.
- FOX, Kenneth William, Surveyor of Forgings and Castings, Lloyd's Register of Shipping, Fenchurch Street, London, E.C.3.
- FREJACQUES, Maurice, Dr.ès.Sci., Chef du Service de Recherches, Compagnie Alais, Froges et Camargue de Pechiney, 23 rue Balzac, Paris 8e, France.
- FRYE, John H., Jr., Ph.D., Metallurgist, Oak Ridge National Laboratory, Oak Ridge, Tenn., U.S.A.
- ISMAIL, Yousef, B.Sc., Metallurgical Engineer, Ministry of Defence, Cairo, Egypt.
- KENDRICK, *Ing.* George André, Senior Draughtsman, Production Drawing Office, Gestetner, Ltd., Fawley Road, London, N.17.
- LLOYD, Eric Gilbert, B.Sc.Eng., Experimental Officer, Metallurgical Department, Royal Small Arms Factory, Enfield Lock, Middlesex.
- MADINE, James Aloysius, Assistant Technical Superintendent, High Duty Alloys, Ltd., Winscales, Distington, Cumberland.
- METZL, *Ing.* John, Director, Strebor Diecasting Company, Ltd., Windley Works, Wolsey Street, Radcliffe, Lancs.
- MORCOUS, Shoukry, B.Sc., Engineer in Charge of Non-Ferrous Metals Works, Ministry of Defence, Cairo, Egypt.
- MYERS, Rupert Horace, Ph.D., M.Sc., Senior Research Officer, C.S.I.R.O., seconded to Atomic Energy Research Establishment, Harwell, Didcot, Berks.
- NICOLAU, *Ingénieur-Général* Jean Pierre, Directeur de l'Institut Supérieur des Matériaux et de la Construction Mécanique, 233 Boulevard Raspail, Paris, France.
- PETERSEN, Edward Jacob, B.Ch.E., Metallurgist, U.S. Naval Ordnance Laboratory, White Oak, Silver Spring 19, Md., U.S.A.
- POOLE, Howard John, Works Manager, Leopold Lazarus, Ltd., St. Stephens Street, Birmingham 6.
- PORRO, Giovanni, Dr.Ing., Technical Manager, Società Metallurgica Italiana, Borgo Pinti 99, Florence, Italy.
- ROBERTS, William James, Editor, "Product Finishing", Sawell Publications, Ltd., 4 Ludgate Circus, London, E.C.4.
- ROWLEY, Edward, Chief Chemist, James Neill and Company (Sheffield), Ltd., Composite Steel Works, Napier Street, Sheffield 11.
- SIEBEL, Gustav, Dr.Phil., Metallurgist, Aluminium-Walzwerke Singen G.m.b.H., Singen-Hohentwiel, Germany.
- WALTON, Ronald Newton, Engineer, United Steel Companies (India), Ltd., Himalaya House, Hornby Road, Bombay, India.
- WARD, Samuel Henry Dewick, M.B.E., Chief Process Engineer, Ericsson Telephones, Ltd., Beeston, Notts.
- WOOD, David Baker, A.B., S.B., Development Engineer, Aluminum Company of America, 2210 Harvard Avenue, Cleveland 5, O., U.S.A.

*As Junior Member*

LAWRIE, John Arthur Noel, Metallographer, Australian Aluminium Company Pty., Ltd., P.O. Box 12, Granville, N.S.W., Australia.

*As Student Members*

BULLEN, Francis Peter, B.Sc., Research Student, Baillieu Laboratory, Melbourne University, Melbourne, Vic., Australia.

CALDICOTT, Peter David, Student of Metallurgy, University College, Cardiff.

DONOVAN, Maurice, Student of Metallurgy, Battersea Polytechnic, London, S.W.11.

HARDWICK, Henry Cecil, Student of Metallurgy, Battersea Polytechnic, London, S.W.11.

HU, Hsun, M.S., Graduate Student, University of Notre Dame, Notre Dame, Ind., U.S.A.

HULL, Derek, Student of Metallurgy, University College, Cardiff.

SUDBURY, Michael Peter, Student of Metallurgy, Sheffield University.

SUTER, John William, B.Sc., Research Student, University of Melbourne, Melbourne, Vic., Australia.

THORLEY, Raymond Thomas, B.Sc., Research Metallurgist, Aluminium Laboratories, Ltd., Banbury, Oxon.

WILLIAMS, Dean Nesbit, M.S., Graduate Student, Missouri School of Mines and Metallurgy, Rolla, Mo., U.S.A.

ELECTED ON 18 JULY 1951

*As Ordinary Members*

ALLARD, Marc, Ing. civil des Mines, Directeur, Institut de Recherches de la Sidérurgie, 185 rue President Roosevelt, Saint Germain-en-Laye (S. et O.), France.

BLYTH, Howard Neville, B.A., Lecturer, Royal School of Mines, Prince Consort Road, London, S.W.7.

BUNTON, John Darrah, Chief Metallurgist, C.A.V. Ltd., Warple Way, Acton, London, W.3.

CHEN, Neng-Kuan, Dr. Eng., Research Associate, Department of Mechanical Engineering, The Johns Hopkins University, Baltimore 18, Md., U.S.A.

CLAXTON, Cyril Charles, Joint Managing Director, Sheffield Twist Drill and Steel Company, Ltd., Sheffield.

ELLIS, Dennis Thomas, Chief Metallurgist, Jaguar Cars, Ltd., Coventry.

ENGLISH, Alan, Blast Furnace Shift Manager, Appleby-Frodingham Steel Co., Ltd., Scunthorpe, Lincs.

FATTAH, Mohamed Ahmed Abdel, B.Sc., Engineer, Ministry of Defence, Cairo, Egypt.

HARRIS, Arthur Clement, Assoc. Met., Research Metallurgist, Simon-Carves, Ltd., Cheadle Heath, Stockport.

HAUT, Frederick Joseph Georg, B.Sc., Constructional Engineer, Boxmoor Engineering Corporation, Ltd., Watford, Herts.

JONES, Sir Lewis, J.P., Secretary, The South Wales Siemens Steel Association, North Hill, 2 St. James' Crescent, Swansea.

LEWIS, George Leonard, Sales Engineer, Vickers (Eastern), Ltd., Killick Building, Home Street, Bombay, India.

LITTLEWOOD, Frederick Richard Edward, Chief Designer, British Sewing Machines, Ltd., Lombard Road, London, S.W.19.

LOMBARDI, Dott. Paolo, Technical Management Official, Società Metallurgica Italiana, Borgo Pinti 99, Florence, Italy.

O'CONNOR, Kenneth James, Manager, Foundry Sheet and Strip Division, Dominion Foils (Canada) Ltd., Cap de la Madeleine, Quebec, Canada.

- ORLANDO, *Dott.* Giuseppe, Vice-Chairman, Società Metallurgica Italiana, Borgo Pinti 99, Florence, Italy.
- PEPLOW, Douglas Boraston, Metallurgist, British Electricity Authority, Southern Division, 111 High Street, Portsmouth.
- PRASAD, Rajendra, B.Sc., Assistant Professor of Metallurgy, College of Mining and Metallurgy, Benares Hindu University, Benares, India.
- PRYOR, Horace, Works Manager, Humber Ltd., Coventry.
- ROBINSON, Eric Arthur, M.C., Managing Director, The Superheater Company, Ltd., 53 Haymarket, London, S.W.1.
- RUSHWORTH, David, Fuel Economist, Albion Chambers, King Street, Nottingham.
- SALAH EL-DIN NESSIM, Ahmed, B.Sc., Engineer, Ministry of Defence, Cairo, Egypt.
- SANDBERG, Alexander Christer Edward, B.Sc., Consulting Engineer, 40 Grosvenor Gardens, London, S.W.1.
- SARGEANT, Colin Wilfred, Works Manager, James Evans and Son, Ltd., Victoria Works, Bromford Lane, West Bromwich.
- SCORTECCI, *Dott.* Massimo, General Secretary, Istituto Italiano della Saldatura, Via XX Settembre 8, Genoa, Italy.
- SNEDDEN, George Thomas, Colvilles, Ltd., Crosshill Street, Motherwell, Lanarkshire.
- SPARKS, Edward John, Chemist, Blackburn Generating Station, British Electricity Authority, Blackburn, Lancs.
- TALINI, *Dott.* Renzo, Chief of Chemical Laboratories, Società Metallurgica Italiana, Fornaci di Barga, Lucca, Italy.
- WOOD, Harold Carrington, General Sales Manager, Wellman Smith Owen Engineering Corporation, Ltd., 25 Wilton Road, London, S.W.1.
- YATES, Harry, Managing Director, Smith and McLean, Ltd., 179 West George Street, Glasgow, C.2.

*As Junior Member*

- MITCHELL, Neville Meruyan, Metallurgist, Royal Aircraft Establishment, Farnborough, Hants.

*As Student Members*

- BRAINE, William Alan, Staveley Iron and Chemical Company, Ltd., Chesterfield.
- MCLENNAN, John Andrew, Trainee Metallurgist, Metal Manufactures, Ltd., Port Kembla, N.S.W., Australia.
- MIRZA, Mohammad Razi, B.A., Technical Apprentice, John I. Thornycroft and Co., Ltd., Woolston, Southampton.
- NAYLOR, Graham Lewis, Metallurgical Apprentice, Stewarts and Lloyds, Ltd., Bilston, Staffs.
- PLACKETT, John Ronald, Student of Metallurgy, University of Birmingham.
- ROLLS, Roger, Research Assistant, Taylor Brothers and Co., Ltd., Trafford Park Steel Works, Manchester, 21.

ELECTED ON 9 AUGUST 1951

*As Ordinary Members*

- AMÉEN, Einar Louis, Managing Director, Surahammars Bruks Aktiebolag, Surahammar, Sweden.
- ANDRESEN, Erling, Stavanger Electro-Staalverk A/S, Jörpeland, Norway.
- BROADBENT, Brian Lynn, Thomas Broadbent and Sons, Ltd., Central Ironworks, Huddersfield, Yorks.
- CHANDLER, Henry, Vice-President, Vanadium Corporation of America, 420 Lexington Avenue, New York 17, N.Y., U.S.A.



- CLAYTON, William Wikeley Ward, M.I.Mech.E., Chairman and Managing Director, Hudswell, Clarke and Company, Ltd., Railway Foundry, Jack Lane, Leeds 10.
- CORFIELD, Reginald Holbeche, B.A., Managing Director, Corfield-Sigg, Ltd., and Corfield and Buckel, Ltd., Trafalgar Works, Station Road, Merton Abbey, London, S.W.19.
- DAVIES, Ivor Bowen, In Charge of Light Alloy Test House, Richard Thomas and Baldwins, Ltd., Byass Works, Port Talbot, Glam.
- DEWHIRST, Eric Victor, A.I.M., Chief Metallurgist, Specialloid, Ltd., Black Bull Street, Leeds 10.
- DURAN RIGOL, Enrique, Ingeniero Industrial, Productos AGMA, S.A., Refineria de Aluminio, Ronda San Pedro, 32, 1, A, Barcelona, Spain.
- GIFKINS, Robert Cecil, B.Sc., A.I.M., Research Officer, Commonwealth Scientific and Industrial Research Organization, Baillieu Laboratory, University of Melbourne, Carlton N.3, Vic., Australia.
- HANCOCK, Peter Francis, B.A., F.I.M., Chief Metallurgist, Birlec, Ltd., Tyburn Road, Erdington, Birmingham 24.
- HOGAN, Leonard McNamara, B.Sc., Student, Metallurgy Department, University of Melbourne, Melbourne, Vic., Australia.
- KIRKUP, William Brookes, T.D., B.A., G.I.Mech.E., Brass Rolling and Extrusion Mill Engineer, Vickers-Armstrongs, Ltd., Elswick, Newcastle-on-Tyne 4.
- LEROY, *Ing.* André Georges Paul, Directeur, Institut de Soudure, 32 Boulevard de la Chapelle, Paris 18e, France.
- MALCOR, Henri, 12 rue de la Rochefoucauld, Paris 9e, France.
- MATUSCHKA, Bernhard, Dr.Mont.Ing., Consulting Engineer, Vereinigte Österreichische Eisen und Stahlwerke, Linz, Austria.
- MUIR, Neil Baird, B.Sc., A.I.M., Technical Officer (Metallurgical), Research Department, Imperial Chemical Industries, Ltd., Metals Division, Kynoch Works, Witton, Birmingham 6.
- PLANTEMA, *Ir.* Frederik J., Acting Chief, Materials Section, Nationaal Luchtvaartlaboratorium, Sloterweg 145, Amsterdam-W., Holland.
- RIDGE, Charles William, O.B.E., Assoc.Met., F.I.M., General Manager, Scaw Metals, Ltd., P.O. Box 6334, Johannesburg, Transvaal, South Africa.
- STAPLES, Ronald Thomas, Production Metallurgist, T.I. Aluminium, Ltd., Redfern Road, Tyseley, Birmingham 11.
- VARGAS, *Professor* Fernando Gonzalez, Professor of Metallurgy, Universidad Nacional Autonoma de México and the Instituto Politecnico Nacional, Mexico City.

*As Junior Members*

- AULD, John Hugh, B.Met.E., Metallurgist, Metallurgy Department, Royal Aircraft Establishment, Farnborough, Hants.
- McKINLAY, Dudley Frederick Alexander, Electrometallurgist, Standard Telephones and Cables, Ltd., New Southgate, London, N.11.
- PITTS, Gordon Roy, B.Sc., G.I.Mech.E., Metallurgist, Bristol Aeroplane Co., Ltd., Aircraft Division, Filton, Bristol.
- VAUGHAN, Thomas Bernard, Metallurgist, Walter Somers and Co., Ltd., Halesowen, Birmingham.

*As Student Members*

- EVANS, Ronald Ernest, Trainee, Research Department, Imperial Chemical Industries, Ltd., Metals Division, Witton, Birmingham 6.
- HINES, John Grahame, B.A., Research Student, Department of Metallurgy, The University, Pembroke Street, Cambridge.
- TAYLOR, Ian, Laboratory Assistant, Fulmer Research Institute, Ltd., Stoke Poges, Bucks.

## ELECTED ON 4 SEPTEMBER 1951

*As Ordinary Members*

- ARDERN, Lawrence L., Librarian, College of Technology, Manchester 1.  
 BINDER, William Oakley, B.Sc., Research Metallurgist, Union Carbide and Carbon Research Laboratory, Inc., P.O. Box 580, Niagara Falls, N.Y., U.S.A.  
 COLMANT, Raymond, Works Director, Sollac, Seremange, (Moselle), France.  
 CROOKS, Laurence Edward, Chief Control Officer, Control Commission for Germany, Metallurgical Industries Department, Land Commissioner's Office, Düsseldorf, B.A.O.R., 4.  
 DAWIHL, Walther, Dr.Ing.habil., Société Franco-Sarroise de Métaux Durs, Ursulinenstrasse 43, Sarrebruch/Sarre.  
 DEVEREUX, Wallace Deane, Deputy Managing Director, Structural and Mechanical Development Engineers, Ltd., Slough, Bucks.  
 ELSTUB, St. John, B.Sc., Production Director (Wrought Metals), Imperial Chemical Industries, Ltd., Metals Division, Witton, Birmingham 6.  
 FERRALL, Lorin L., Director of Metallurgy, Crucible Steel Company of America, P.O. Box 88, Pittsburgh 30, Pa., U.S.A.  
 FLETCHER, Frank, B.Sc., Research Engineer, Hopkinson's, Ltd., Huddersfield.  
 GOICOECHEA, Manuel, Director and General Manager, Hierro Maleable de Mexico, Viena no. 16-Department 12, Mexico City, Mexico.  
 GRAHAM, Robert, Ph.D., B.Sc., A.R.T.C., Metallurgist, Shell Refining and Marketing Co., Ltd., Thornton Research Centre, P.O. Box 1, Chester.  
 HOUGHTON, Frank, Director, Pickford, Holland and Co., Ltd., Sheffield.  
 JOLIVET, Henri, Directeur, Service Général des Recherches, Société d'Electro-Chimie, 10 rue du Général Foy, Paris 8e, France.  
 MARTINEZ, Giorgio, M.A., Director, Barron and Crowther, Ltd., Eastleigh, Hants.  
 NOURSE, Louis M., A.B., M.S., Librarian, St. Louis Public Library, St. Louis 3, Mo., U.S.A.  
 OWE, Aage Willand, Managing Director, A/S Ardal og Sunndal Verk, Nedre Vollgate 4, P.O. Box 180, Oslo, Norway.  
 PRICE, Bartlett Root, M.S., Westinghouse Electric Corporation, East Pittsburgh, Pa., U.S.A.  
 SANDSTRÖM, Karl Eric Viktor, Chairman, S. and M. Engineering Pty., Ltd., 88 Fox Street, Johannesburg, Transvaal, South Africa.  
 SHERWOOD, Charles Noel, B.Comm., Public Relations Officer, Metals Division, Imperial Chemical Industries Ltd., Witton, Birmingham 6.  
 TAGLIAFERRI, Ing. Leone, General Manager, Leone Tagliaferri & C.S.p.A., via Principe Eugenio 11, Milan, Italy.  
 TENLAND, Eng. Waldemar, Hedåsvägen, 47d, Sandviken, Sweden.  
 VANICK, James Sebold, B.S., International Nickel Company, Inc., 67 Wall Street, New York 5, N.Y., U.S.A.  
 WHITE, Charles M., President, Republic Steel Corporation, Room 1707, Republic Building, Cleveland 1, O., U.S.A.  
 WILLNERS, Sven Harry, A.B. Ferrolegeringar, P.O. Box 16150, Stockholm 16, Sweden.

*As Junior Members*

- BROWN, Derek James, B.Sc., Metallurgist, Magnesium Elektron, Ltd., Clifton Junction, near Manchester.  
 DEVEREUX, Robert Wayne, Assistant to Works Superintendent, Southern Forge, Ltd., Langley, Bucks.  
 HAGEL, William P., B.Met.Eng., Junior Metallurgist, Oak Ridge National Laboratory, Oak Ridge, Tenn., U.S.A.  
 HARRIS, Ian Robert, Research Metallurgist, The British Aluminium Company, Ltd., Chalfont Park, Gerrards Cross, Bucks.

*As Student Members*

CINA, Bernard, B.Sc., Student of Metallurgy, Sheffield University.

HOLDER, Sydney George, Jr., M.Sc., Student of Metallurgy, University of Tennessee, Knoxville, Tenn., U.S.A.

LIV, Tien Shih, M.S., Graduate Student, University of Notre Dame, Ind. U.S.A.

THOMAS, Wilbert Roy, M.A.Sc., Graduate Student, University of Toronto, Canada.

DISCUSSION OF PAPERS

The following papers were presented and discussed. In each case a vote of thanks to the authors was proposed by the Chairman and carried with acclamation.

"Copper-Nickel-Iron Alloys Resistant to Sea-Water Corrosion", by G. L. Bailey, M.Sc., F.I.M.

"The Influence of Alloy Constitution on the Mode of Solidification of Sand Castings", by R. W. Ruddell, M.A., A.I.M., and A. L. Mincher, B.Sc.

"The Adherence of Oxide Scales on Copper", by R. F. Tylecote, M.A., M.Sc., A.I.M. With an Appendix on "The Temperature of the Oxide Scale on Copper During Hot Rolling", by R. Eborall, M.A.

"The Oxidation of Copper at 350°-900° C. in Air", by R. F. Tylecote, M.A., M.Sc., A.I.M.

VISITS

During the morning the ladies, accompanied by guides, visited the Basilica of S. Marco and the Palazzo Ducale, and in the afternoon visited the Palazzo Rezzonico.

In the afternoon, members visited the works of Ilva. Alti Forni e Acciaierie d'Italia; Industria Nazionale Alluminio; Società Alluminio Veneto per Azioni; Società Industriale "San Marco"; Società Montevecchio; and the Società Vetrocoke.

AUTUMN LECTURE

In the evening the Twenty-Second Autumn Lecture was delivered, in the Cà Giustianian, by Professor ROBERTO PIONTELLI on "Electrochemistry and the Science of Metals". The Chair was taken by the President.

At the conclusion, a hearty vote of thanks to the lecturer was proposed and carried with acclamation.

The lecture is published in the *Journal*, 1951-52, vol. 80, pp. 99-107.

Tuesday, 18 September

The meeting was resumed at 9.30 a.m. at the Cà Foscari, the President, Professor A. J. MURPHY, M.Sc., occupying the Chair.

DISCUSSION OF PAPERS

The following papers were presented and discussed. In each case a vote of thanks to the authors was proposed by the Chairman and carried with acclamation.

"Friction in Wire Drawing", by H. G. Baron, M.Sc., and Professor F. C. Thompson, D.Met., M.Sc.

"Observations on Some Wrought Aluminium-Zinc-Magnesium Alloys", by Maurice Cook, D.Sc., Ph.D., F.I.M., R. Chadwick, M.A., F.I.M., and N. B. Muir, B.Sc., A.I.M.

"The Effect of Small Quantities of Cd, In, Sn, Sb, Tl, Pb, or Bi on the Ageing Characteristics of Cast and Heat-Treated Aluminium-4% Copper-0.15% Titanium Alloy", by H. K. Hardy, Ph.D., M.Sc., A.R.S.M., A.I.M.

"The Tensile Properties of Heat-Treated Aluminium-Copper and Aluminium-Copper-Cadmium Alloys of Commercial Purity", by H. K. Hardy, Ph.D., M.Sc., A.R.S.M., A.I.M.

#### VOTES OF THANKS

The CHAIRMAN moved :

"That the best thanks of the Institute of Metals be, and are hereby, extended to :

(a) The President and Council of the Associazione Italiana di Metallurgia for their kind invitation to hold this meeting in Italy;

(b) The Mayor of Venice, the Secretary for Public Education, and the President of the Associazione Industriali della Provincia di Venezia for their welcome to Venice;

(c) Professor Carlo Panzeri, the members of the Executive Committee, Dr. Leno Matteoli (Honorary Corresponding Member to the Council for Italy), and the Honorary Secretaries for Venice (Ing. L. Piana and Dr. Tirelli), Milan (Dr. Lo Pinto), and Florence (Dr. Paolo Lombardi), and the members of the Ladies' Committee, for the detailed arrangements for this meeting, which have been so carefully planned for the comfort and enjoyment of those attending;

(d) Dr. Lo Pinto and the staff of the Associazione Italiana di Metallurgia for helping with the administrative work in connection with the meeting;

(e) The Municipality of Venice and the Industrial Associations of Venice, Porto Marghera, and Florence for their generous hospitality;

(f) The Directors of the Istituto Sperimentale dei Metalli Leggeri and of the Società Adriatica di Elettricità; the Società Alluminio Veneto per Azioni; the Società Ernesto Breda; the Società Dalmine; the Società F.I.A.T.; the Società Ilva; the Società Industria Nazionale Alluminio; the Società Metallurgia Italiana; the Società Montevercchio; the Società Industriale "San Marco"; the Società Vetrocokes, and their staffs, for their kind invitations to visit their works and laboratories, and for their generous hospitality;

(g) All others who have contributed to the success of this meeting."

The motion was seconded, put to the meeting and carried with acclamation.

Cav. A. DACCÒ, President of the Associazione Italiana di Metallurgia, and Dott. LENO MATTEOLI, Honorary Corresponding Member to the Council for Italy, briefly replied.

#### VISITS

The ladies paid visits, accompanied by guides, in the morning to the School of S. Rocco and the Chiesa di S. Maria Gloriosa dei Frari, and in the afternoon to the Chiesa della Salute and the Galleria dell' Accademia di Belle Arti.

In the afternoon members visited the works of : Ilva. Alti Forni e Acciaierie d'Italia; Industria Nazionale Alluminio; Società Alluminio Veneto per Azioni; Società Industriale "San Marco"; Società Montevercchio; and the Società Vetrocokes.

#### BANQUET

In the evening a joint Banquet of the Associazione Italiana di Metallurgia and of the Institute of Metals was held at the Grand Hotel des Bains, Lido Venezia. The Chair was taken by Cav. ALDO DACCÒ, President of the Associazione Italiana di Metallurgia.

**Wednesday, 19 September**

## VISITS

In the morning, visits were paid by members and their ladies to the Chiesa di SS. Giovanni e Paolo, the Chiesa di S. Maria dei Miracoli, the Basilica di S. Marco and the Palazzo Ducale.

A party of members and ladies left Venice in the morning by road for Florence; another party left by road in the afternoon for Milan, taking tea at Gardone on Lake Garda.

**Thursday, 20 September**

## BOLZANO

A party of members and ladies left Venice by road for Bolzano, visiting, en route, the power station of the Società Adriatica di Elettricità at Piave (Soverzene). They took lunch at Cortina d'Ampezzo, by invitation of the Società.

## MILAN

Visits were paid to the steel and tube works of the Società Dalmine at Bergamo; the works of Ilva. Alti Forni e Acciaierie d'Italia at Lovere; the Istituto Scientifico Tecnico Ernesto Breda, Milan; or the Società Italiana Ernesto Breda, Milan. Those visiting Bergamo and Lovere were entertained to lunch by the companies. Other members and ladies took part in a sight-seeing tour in Milan, and in the afternoon visited the triennial Exhibition of Decorative Art in that city.

**Friday, 21 September**

## BOLZANO

Members visited the work of I.N.A. Industria Nazionale Alluminio, while ladies paid a visit to the Bolzano International Fair or took part in an excursion in the Bolzano area.

Later in the day they left by road for Milan.

## MILAN

Members visited the Istituto Sperimentale dei Metalli Leggeri at Novara. They were joined by their ladies for lunch at Stresa and, after a steamer trip on Lake Maggiore, the party returned in the evening to Milan.

## TURIN

A party of members left Milan by train for Turin, where in the morning they visited the steel works and rolling mills of F.I.A.T., and in the afternoon the motor-car works of the company.

**Saturday, 22 September**

In the morning members and ladies in Milan visited the Istituto Scientifico Tecnico Ernesto Breda; the works of the Società Italiana Ernesto Breda; the Pinacoteca di Brera; or took part in a sight-seeing tour of Milan.

In the afternoon the parties of members and ladies in Milan and Turin left by train for Florence.

**Sunday, 23 September**

FLORENCE

In the morning, members and their ladies took part in a sight-seeing tour of Florence, and attended a reception by the Industrial Associations of Florence.

In the afternoon, they were the guests of the Società Metallurgica Italiana at a garden party in the grounds of the palace of the company in the Borgo Pinti.

**Monday, 24 September**

FLORENCE

All-day visits were paid, by road, to the works of the Società Metallurgica Italiana at Fornaci di Barga (Lucca) or of Ilva. Alti Forni e Acciaierie d'Italia at Piombino. Members were entertained to lunch by the companies. Ladies visited Pisa.

Members joined the ladies in Pisa in the evening. The party was entertained to dinner in Pisa by the Società Metallurgica Italiana, and returned to Milan by road.

**Tuesday, 25 September**

The meeting concluded, and members left Florence by special train.

## ITALIAN MEETING

### PATRONS

The following were members of the Comitato d'onore :

SEGNÍ, Ecc. Professore Antonio, Ministro della Pubblica Istruzione, Roma (*Presidente*).

COLONNETTI, Professore Gustavo, Presidente Consiglio Nazionale Ricerche, Roma.

GARGIULO, Ecc. dr. Attilio, Prefetto, Venezia.

GAGGIA, Sen. ing. Achille, Presidente Società S.A.D.E., Venezia.

SPANIO, Professore Angelo, Sindaco di Venezia.

FERRO, Professore Guido, Magnifico Rettore Università, Padova.

LUZZATO, Professore Gino, Rettore dell' Istituto Universitario di Economia e Commercio di Venezia.

FISCA, Ing. G. Favaretto, Presidente Deputazione Provinc., Venezia.

DALL' ARMI, Ing. G. Battista, Presidente Associazione Industriale, Venezia.

BARBINI, Cav. Uff. Giovanni, Presidente Camera Commercio Agricoltura e Industria, Venezia.

FOSCARI, Conte dr. Adriano, Presidente, Rotary Club, Venezia.

BERNABÓ, Cav. del Lavoro Marco, Vice-Presidente, Società S.A.V.A., Venezia.

BERIA, Ing. Biagio, Amministratore Delegato Società Vetrocoke, Venezia.

BRASS, Avv. Alessandro, Presidente Società Industriale "San Marco", Venezia.

CARDELLI, Dr. Dante, Amministratore Delegato Società I.N.A., Milano.

GIAMMARCO, Ing. Giuseppe, Presidente Associazione Industriale Marghera, Porto Marghera (Venezia).

MORANDI, Dr. Luigi, Presidente Istituto Sperimentale Metalli Leggeri, Novara.



ORLANDO, Dr. Salvatore, Presidente Società Metallurgica Italiana, Firenze.  
 PASQUATO, Dr. Michelangelo, Presidente Ufficio Regionale Associazione Industriale, Veneto, Venezia.  
 RATTI di Desio, Conte Ing. Franco, Presidente Società Dalmine, Milano.  
 ROLANDI, Ing. Giovanni, Amministratore Delegato Società Montevecchio, Milano.  
 ROSSI, Ing. Ernesto, Presidente Società Ilva, Genova.  
 TACCONI, Ing. Domenico, Direttore Sezione Siderurgica Fiat, Torino.

*Official Representatives of the Consiglio Nazionale delle Ricerche :*

GIORDANI, Professore Francesco.	PIONTELLI, Professore Roberto.
CAMBI, Professore Livio	MAZZOLENI, Professore Francesco.
DE CARLI, Professore Felice.	

MEMBERS OF THE ORGANIZING COMMITTEE

PANSERI, Professore Carlo ( <i>Chairman</i> ).	MATTEOLI, Dr. Leno.
ANDREAUS, Dr. Vittorio.	SIGNORA, Dr. Mario.
BALDI, Dr. Francesco.	VALMARANA, Conte Andrea di.

*Honorary Secretaries :*

GALLI, Dr. Mario.	PIANA, Ing. Luciano (Venezia).
GARLATTI, Ing. Renato.	TIRELLI, Dr. Bruno (Venezia).
LECIS, Dr. Piero.	LOMBARDI, Dr. Paolo (Firenze).
LIGGERI, Dr. Concetto.	LO PINTO, Dr. Giovanni (Milano).
MASOCH, Dr. Giuseppe.	

MEMBERS OF THE LADIES' COMMITTEE

BARONI, Luisetta.	OLIVO, Maria Luisa.
BRUZZONE, Leopoldina.	PANSERI, Giovanna Maria.
CUTTICA, Maria.	PETRELLI, Maria.
DE CARLI, Franca.	PORRO, Elena.
DUPUIS, Silvia.	REGGIORI, Piermaria.
FALCK da Zara, Maly.	ZAMPI, Lina.
LAMPUGNANI, Noemi.	ZAZZARONI, Adele.
MATTEOLI, Marietta.	ZOJA, Lucrezia.



# THE HARDNESS AND STRENGTH OF METALS.\*

1294

By D. TABOR,† Ph.D.

## SYNOPSIS.

If a spherical indenter of fixed diameter is used to make hardness indentations, as in the Brinell test, it is found that the load  $W$  necessary to produce an indentation of chordal diameter  $d$  is given by the relation  $W = kd^n$ , where  $k$  is a constant and  $n$  another constant (the Meyer index), which depends on the degree of work-hardening of the metal. If indenters of different diameters  $D$  are used, a more general relation, first derived by Meyer, also holds,  $W = Ad^n/D^{n-2}$ . A theoretical explanation of these equations is given, and it is shown that the stress/strain curve of the metal may be derived from the hardness measurements. If the stress/strain curve obeys a simple power relation of the type  $Y = b\epsilon^x$ , where  $Y$  is the yield stress under uniaxial tension (or frictionless compression),  $b$  a constant,  $\epsilon$  the strain, and  $x$  the work-hardening index, it may be shown that  $x$  is very nearly equal to  $n - 2$ . It is thus possible to deduce the true stress/strain curve, the nominal stress/strain curve, and the ultimate tensile strength of a metal from its Brinell hardness number and its Meyer index. The analysis shows that, to a first approximation, the ratio of the ultimate tensile strength  $T_u$  to the Brinell hardness  $H_B$  is independent of the nature of the metal. It depends primarily on the degree of work-hardening of the metal, i.e. on the work-hardening index  $x$ , or the Meyer index  $n$ . A series of curves is drawn showing the variation of the ratio  $T_u/H_B$  with the Meyer index  $n$ , and it is shown that materials as diverse as tool steel, work-hardened nickel, and annealed copper all lie near the theoretical curves.

A similar analysis is given for pyramidal indenters such as are used in making Vickers hardness measurements.

## I.—INTRODUCTION.

It is usual to define the hardness of a metal in terms of its resistance to local indentation. A hard indenter is pressed into the surface of the metal under a specified load and, when equilibrium is reached, a suitable measurement is made of the size of the indentation. In some cases the depth of the indentation is measured, but the most satisfactory methods are those involving a measurement of the area of the indentation. In the Brinell test a hard steel ball is used as the indenter, and the diameter of the resulting indentation is measured. The hardness is then expressed as the ratio of the load to the curved area of the indentation (Brinell hardness), or as the ratio of the load to the projected area of the indentation (Meyer hardness). The hardness in both cases has the dimensions of pressure.

With spherical indenters experiments show that, for a ball of fixed

\* Manuscript received 27 June 1950.

† Research Group on the Physics and Chemistry of Rubbing Solids, Department of Physical Chemistry, Cambridge University.

## 2 Tabor: The Hardness and Strength of Metals

diameter, the chordal diameter  $d$  of the permanent impression is related to the applied load  $W$  by a relation of the type :

$$W = kd^n \quad . \quad . \quad . \quad . \quad . \quad . \quad (1)$$

where  $k$  and  $n$  are suitable constants for the material.<sup>1</sup> The value of  $n$  usually lies between 2 and 2.5, and is a measure of the degree of work-hardening of the metal. For fully annealed metals  $n$  is nearly 2.5, whilst for highly worked metals it approaches a value of 2.

If balls of different diameters are used, equations similar to (1) are obtained. The Meyer index  $n$  for a given metal specimen remains almost unchanged, but the constant  $k$  depends on the diameter  $D$  of the ball. Meyer showed that over a wider range of experimental conditions the following general relation is obeyed :

$$W = A \frac{d^n}{D^{n-2}} \quad . \quad . \quad . \quad . \quad . \quad . \quad (2)$$

If conical or pyramidal indenters are used, as in the Ludwik and Vickers hardness tests respectively, a simpler relation of the type :

$$W = kd^{2.0} \quad . \quad . \quad . \quad . \quad . \quad . \quad (3)$$

is found. The power of  $d$  remains constant at the value 2 over a wide range of loads and indenter angles, but  $k$  depends on the angle of the cone or pyramid.

Experimental observations show that there is a direct relation between the hardness of a metal and its ultimate tensile strength  $T_u$ . If the Brinell hardness  $H_B$  is expressed in kg./mm.<sup>2</sup>, the tensile strength may be written :

$$T_u = cH_B \quad . \quad . \quad . \quad . \quad . \quad . \quad (4)$$

where  $c$  has a value depending on the nature of the metal under examination. Typical values of  $c$  given by O'Neill<sup>2</sup> are reproduced in Table I.

In general, it would seem that with metals for which the Meyer

TABLE I.—Values of  $c$  for Various Metals.

Metal	Meyer Index, $n$	$c$	
		$T_u$ , kg./mm. <sup>2</sup>	$T_u$ , tons/in. <sup>2</sup>
Heat-Treated Alloy Steels . . . . .	2.1	0.33	0.21
Heat-Treated Carbon Steels . . . . .	—	0.34	0.215
Mild Steel . . . . .	2.2	0.36	0.23
Nickel : annealed . . . . .	2.50	0.49	0.31
„ work-hardened . . . . .	2.27	0.41	0.26
Copper : annealed . . . . .	2.45	0.52	0.33
Brass : „ . . . . .	2.53	0.55	0.35
„ drawn . . . . .	2.2	0.41	0.26

index  $n = 2.2$  or less the value of  $c$  is of the order of  $0.35$  ( $T_u$  in  $\text{kg./mm.}^2$ ) or  $0.22$  ( $T_u$  in  $\text{tons/in.}^2$ ). If the value of the Meyer index is higher than  $2.2$ , the value of  $c$  is usually greater.

In what follows it will be briefly shown that relations (1), (2), (3), and (4) may be deduced from simple physical considerations.

## II.—THE STRESS/STRAIN CHARACTERISTICS OF “IDEAL” AND OF REAL METALS.

Before discussing the indentation process in detail it is convenient to describe briefly the stress/strain characteristics of metals. An “ideal” plastic metal is one which does not strain-harden. The stress/strain curve of such a metal is shown in Fig. 1. The full line is the true stress, and it is seen that over the region  $OA$  the strain increases linearly with the stress. This is the elastic region of deformation, and the slope of  $OA$  is a measure of Young’s modulus of the metal. At the point  $L$  plastic deformation begins, and the stress at which this occurs (the elastic limit or yield stress  $Y$ ) remains constant however much the metal is deformed. This means in effect that deformation does not produce work-hardening of the metal. The dotted curve shows the nominal stress/strain curve for the same metal under tension, the “nominal stress” being defined as the tensile force at any stage divided by the original cross-section of the specimen. It is seen that the ultimate tensile strength  $T_u$  is reached immediately after plastic flow has begun and has essentially the same value as the yield stress  $Y$  of the metal. No real metals are known which possess “ideal” plastic properties, but it is possible to obtain a close approximation to them (see below).

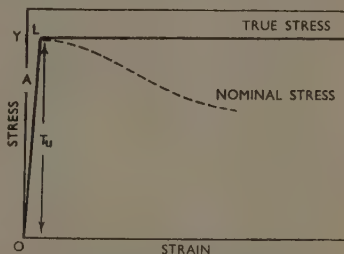


FIG. 1.—Stress/Strain Curves for an “Ideal” Plastic Material.

In practice all metals work-harden as a result of plastic deformation and the stress/strain curve is of the type shown in Fig. 2, in which the yield stress  $Y$  increases with the deformation  $\epsilon$  to which it has been subjected.\* With many metals the relation between  $Y$  and  $\epsilon$  may be expressed by an equation of the form :

$$Y = b\epsilon^x \quad . \quad . \quad . \quad . \quad . \quad . \quad (5)$$

\* This does not take into account the special behaviour of annealed mild steel and some aluminium alloys that show an initial yield value (the upper yield point) which is followed by a drop in the yield stress for subsequent small strains. Even with these materials, however, the yield stress for larger strains increases with strain in a manner similar to that shown in Fig. 2.

for strains that are not too large.<sup>3</sup> The dotted curve in Fig. 2 is the nominal stress/strain curve for the same metal under tension. It is seen that the ultimate tensile strength  $T_u$  is reached only after appreciable plastic flow has occurred.

Fig. 2 shows how such a metal may be used to provide a close approximation to an ideal plastic metal. If the metal is deformed to the point  $D$  and the stress then removed, the specimen recovers elastically along the line  $DO'$ . Consequently if a specimen is used that has already been plastically deformed by an amount of strain corresponding to  $OO'$ , any further deformation starts from the point  $O'$  as the new origin. The stress/strain curve then follows the course  $O'DE$  in which the stress involving plastic deformation increases only slightly with further

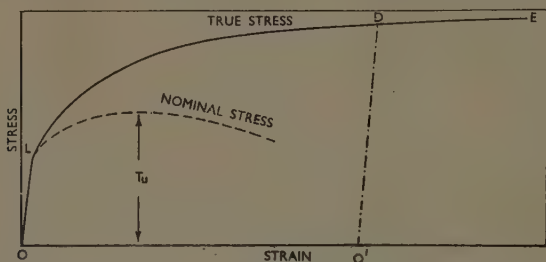


FIG. 2.—Stress/Strain Curves for a Typical Metal which Undergoes Strain-Hardening.

deformation. This is a simple and effective way of obtaining metal specimens which approach the “ideal” plastic material described in Fig. 1.

### III.—THE DEFORMATION OF METALS BY A SPHERICAL INDENTER.

The behaviour must first be considered of an “ideal” plastic metal when a hard spherical indenter is pressed on to its surface. To begin with the deformations are elastic and the stress and displacements are given by Hertz’s celebrated equations.<sup>4</sup> The region of contact is a circle, and the mean pressure  $P$  over the area of contact is proportional to  $W^{\frac{1}{3}}$ , where  $W$  is the load. As  $W$  is increased, the stresses in the metal increase until a stage is reached at which the elastic limit (or yield stress)  $Y$  of the metal is exceeded. An analysis by Timoshenko<sup>5</sup> and more recently by Davies<sup>6</sup> shows that this occurs when :

$$P \approx 1.1Y \quad . \quad . \quad . \quad . \quad . \quad . \quad (6)$$

At this stage the amount of plastic deformation is limited to a small



region below the surface of the area of contact. As the load is increased the region over which plastic flow occurs grows in size and there is a gradual increase in the value of  $P$ . An upper limit is reached (at a load 150–200 times that at which the first onset of plastic deformation occurs) where the mean pressure  $P$  remains almost constant and does not increase appreciably with further increases in  $W$ . At this stage, according to the theoretical work of Hencky <sup>7</sup> and Ishlinsky,<sup>8</sup> the mean pressure  $P$  has a value of the order of :

$$P \approx 3Y \quad . \quad . \quad . \quad . \quad . \quad . \quad (7)$$

Hence the variation of  $P$  with load  $W$  should follow the curve shown in Fig. 3.  $OL$  represents the purely elastic region where  $P$  varies as  $W^{\frac{1}{2}}$ ; the point  $L$  represents the onset of plasticity ( $P \approx 1.1Y$ ), while  $MN$  marks the range over which the whole of the material around the indenter is flowing plastically and  $P$  is almost independent of  $W$ .

Most practical hardness measurements are carried out in the range  $MN$ , so that for "ideal" plastic metals the Meyer hardness (or  $P$ ) is simply three times the elastic limit or yield stress  $Y$  of the metal. This is shown very simply by making large indentations in metals which have been very heavily work-hardened so that they approach ideal conditions. Some typical results are given in Table II, where the yield stress was found

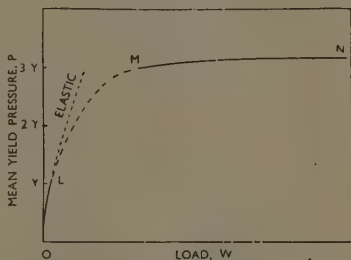


FIG. 3.—Schematic Curve Showing Variation of Yield Pressure  $P$  with Load  $W$ , as a Spherical Indenter is Pressed into the Surface of an "Ideal" Plastic Metal.

TABLE II.—Yield-Stress Values from Compression Experiments on Heavily Work-Hardened Metals.

Metal	$Y$ , kg./mm. <sup>2</sup>	$P$ , kg./mm. <sup>2</sup>	$P/Y$
Tellurium Lead . . . . .	2.1	6.1	2.9
Aluminium . . . . .	12.3	34.5	2.8
Copper . . . . .	31	88	2.8
Mild Steel . . . . .	65	190	2.8

from careful compression experiments using well-lubricated anvils. The value of  $P$  increased slightly with the size of the indentation owing to the increased confinement of the displaced material (see also)



where  $c$  again has a value of about 2.8. The next step is to consider how  $Y_r$  varies with the size of the indentation formed.

Suppose the indentation has a chordal diameter  $d$  and a radius of curvature  $r$ . Its shape is determined solely by the ratio  $d/r$ . To a first approximation  $r$  is equal to the radius of curvature of the indenter, so that  $r = D/2$ .\* Consequently the shape is determined by the ratio  $d/D$ . Now the strain produced in a metal is a dimensionless parameter referring to a fractional change in shape. Consequently the representative strain  $\epsilon_r$  corresponding to the representative yield stress  $Y_r$  will be simply a function of  $d/D$ . We may therefore write :

$$\epsilon_r = f(d/D) \quad . \quad . \quad . \quad . \quad . \quad . \quad (9)$$

This means essentially that geometrically similar indentations (determined by the ratio  $d/D$ ) produce the same effective strain. This is, of course, only valid when the region of plastic flow around the indentation does not extend to the boundaries of the specimen. The yield stress is again a direct function of the strain  $\epsilon$ , so that :

$$Y_r = \phi(\epsilon_r) = \phi\left[f\left(\frac{d}{D}\right)\right] \quad . \quad . \quad . \quad . \quad . \quad (10)$$

Combining equation (10) with equation (8a) we have :

$$P = c\phi\left[f\left(\frac{d}{D}\right)\right] \quad . \quad . \quad . \quad . \quad . \quad (11)$$

This relation implies that geometrically similar indentations have the same Meyer hardness or yield pressure  $P$ .

By a semi-empirical method described in a previous paper<sup>10</sup> it may be shown that the function in equation (9) is approximately a linear one. If the strain is expressed as a percentage strain, equation (9) becomes approximately :

$$\epsilon_r = 20(d/D) \quad . \quad . \quad . \quad . \quad . \quad (9a)$$

A simple example will make this clearer. Suppose a 10-mm. ball is pressed into a metal surface and forms an indentation of chordal diameter 5 mm. The ratio  $d/D$  is equal to  $\frac{1}{2}$ . This means, according to equation (9a), that the representative strain is equivalent to a strain of 10%. From the stress/strain curve of the metal we may determine the representative yield stress  $Y_r$  corresponding to a strain of 10%.

\* Owing to the release of elastic stresses when the load is removed the permanent indentation has a radius of curvature greater than that of the indenter itself. The true radius of curvature of the permanent indentation,  $r_1$ , may be readily calculated in terms of the plastic and elastic constants of the metal (Tabor<sup>10</sup>). The effect, in so far as it affects the following treatment, is appreciable only for shallow indentations, unless the metal is extremely hard. For simplicity the difference between  $r$  and  $r_1$  has therefore been ignored.

## 8 Tabor: The Hardness and Strength of Metals

Then the mean pressure  $P$  involved in producing the indentation will have a value of about  $2.8Y_r$ .

These conclusions can be used to compare the stress/strain characteristics of a metal with its hardness values. Fig. 4 shows the results obtained for partially annealed aluminium, highly annealed copper, and

mild steel. For the hardness results,  $P$  has been plotted against  $d/D$ . To obtain the stress/strain curves, cylindrical specimens were compressed between well-lubricated anvils. The applied force divided by the cross-section of the specimen at any stage gives the true yield stress, whilst the strain is expressed as the fractional change in cross-sectional area of the specimen. In Fig. 4, the yield stress has been multiplied by 2.8, and the strain axis adjusted so that the strain, in per cent., is equal to  $20d/D$ . It is seen that there is close agreement between the stress/strain curves and the hardness results. This analysis has also been extended to materials which have been plastically deformed by various amounts before the hardness

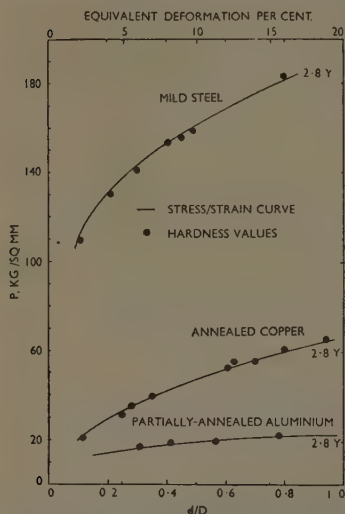


FIG. 4.—Correlation of Stress/Strain Curves with Hardness Values of Steel, Copper, and Aluminium.

measurements were made. A series of  $P/(d/D)$  curves are obtained which are displaced along the strain axis by amounts equal to the initial deformation of the specimen. The hardness curves so obtained lie close to the extended stress/strain curve.<sup>10</sup>

### IV.—THE DERIVATION OF MEYER'S LAWS.

It is not difficult to derive Meyer's equations from these results. To a first approximation the representative strain  $\epsilon_r$  is equivalent to  $20d/D$ . The stress/strain curve may be represented by a power relation of the type  $Y = b\epsilon^x$ , so that the representative yield stress is given by:

$$Y_r = b\epsilon_r^x = b'\left(\frac{d}{D}\right)^x$$

where  $b'$  is a new constant.

Hence 
$$P = \frac{4W}{\pi d^2} = cb' \left( \frac{d}{D} \right)^x$$

or 
$$W = A \frac{d^{x+2}}{D^x} \quad \dots \quad (12)$$

where  $A$  is a new constant. Replacing  $x + 2$  by  $n$  we have :

$$W = A \frac{d^n}{D^{n-2}}$$

which contains the two main laws of Meyer. (See equation (2).)

According to this result the work-hardening index  $x$  of a metal is roughly equal to  $n - 2$ , where  $n$  is the Meyer index. Some results taken from O'Neill<sup>2</sup> show that this is approximately true (see Table III).

TABLE III.—Relation of Work-Hardening Index to Meyer Index.

Metal	Typical Values of Meyer Index, $n$	$n - 2$	Work-Hardening Index, $x$
Mild Steel A . . . .	2.25	0.25	0.259
Yellow Brass . . . .	2.44	0.44	0.404
"    " : cold drawn .	2.10	0.10	0.194
Copper L . . . . .	2.45	0.45	0.414
Steel 1A . . . . .	2.25	0.25	0.24
Steel 6A . . . . .	2.28	0.28	0.18
Nickel : annealed . . .	2.50	0.50	0.43
"    rolled . . . .	2.14	0.14	0.07
Aluminium : annealed . .	2.20	0.20	0.15

V.—BRINELL HARDNESS AND ULTIMATE TENSILE STRENGTH.

It has already been shown that for a fully work-hardened metal the ratio  $T_u/H_B$  should have a value of about 0.37 if  $T_u$  is expressed in kg./mm.<sup>2</sup>.

A more general relation may now be derived between  $T_u$  and  $H_B$  for metals of any degree of work-hardening. Consider a typical stress/strain curve of a tensile specimen where this time stress  $Y$  is plotted against the fractional increase in length  $\epsilon$ . It may again be assumed that :

$$Y = b\epsilon^x \quad \dots \quad (5a)$$

where  $x = n - 2$  and  $n$  is the Meyer index. This curve is shown by the full line in Fig. 5. If at any point the fractional increase in length is  $\epsilon$ ,

## 10 Tabor: The Hardness and Strength of Metals

the length of the specimen is  $1 + \epsilon$ . Since there is a negligible volume change during plastic deformation, the cross-section of the specimen will have been reduced by  $\frac{1}{1 + \epsilon}$ , so that the nominal stress  $T$  will be given by  $T = \frac{Y}{1 + \epsilon}$ . It follows from equation (5a) that the variation of  $T$  with  $\epsilon$  will be :

$$T = \left( \frac{b}{1 + \epsilon} \right) \epsilon^x \quad . \quad . \quad . \quad (13)$$

The value of  $\epsilon$  at which this becomes a maximum is found by differenti-

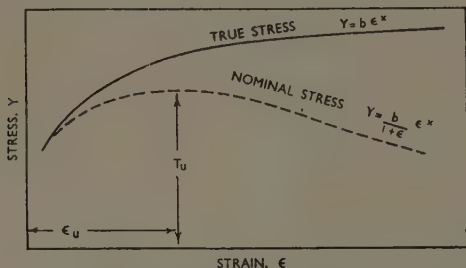


FIG. 5.—The True and Nominal Stress/Strain Curves for a Metal which Undergoes Strain-Hardening.

ating  $T$  in equation (13) with respect to  $\epsilon$  and putting it equal to zero. This gives a value :

$$\epsilon = \frac{x}{1 - x} \quad . \quad . \quad . \quad (14)$$

Inserting this value of  $\epsilon$  in equation (13), we obtain the maximum value of the nominal tensile stress  $T_u$  :

$$T_u = b(1 - x) \left( \frac{x}{1 - x} \right)^x \quad . \quad . \quad . \quad (15)$$

The hardness value is now determined in terms of the stress/strain curve. Suppose the indentation formed in the hardness measurement has a size of  $d/D = \frac{1}{2}$ , the representative strain corresponds to  $\epsilon_r = 10\%$  or  $\epsilon_r = 0.1$ . Consequently, using equation (5a), the representative yield stress  $Y_r$  becomes :

$$Y_r = b(0.1)^x.$$

Thus the yield pressure  $P$  may be written :

$$P = 2.8b(0.1)^x \quad . \quad . \quad . \quad (16)$$

Since for an indentation of this size the ratio of the curved area of the



indentation to the projected area is 1.07, the Brinell hardness number  $H_B$  will be about 7% less than  $P$ , i.e. :

$$H_B = 2.6b(0.1)^x \quad . \quad . \quad . \quad (17)$$

Combining equations (15) and (17) we obtain :

$$\frac{T_u}{H_B} = \frac{1-x}{2.6} \left( \frac{10x}{1-x} \right)^x \quad . \quad . \quad . \quad (18)$$

The value of this ratio for values of  $x$  ranging from 0 to 0.6 (corresponding to values of  $n$  ranging from 2 to 2.6) is given in Table IV and plotted in Fig. 6.

TABLE IV.—Ratio  $T_u/H_B$  for an Indentation  $d/D = \frac{1}{2}$ .

$x$	0	0.1	0.2	0.3	0.4	0.5	0.6
$T_u/H_B$	0.38	0.35	0.37	0.42	0.49	0.60	0.81

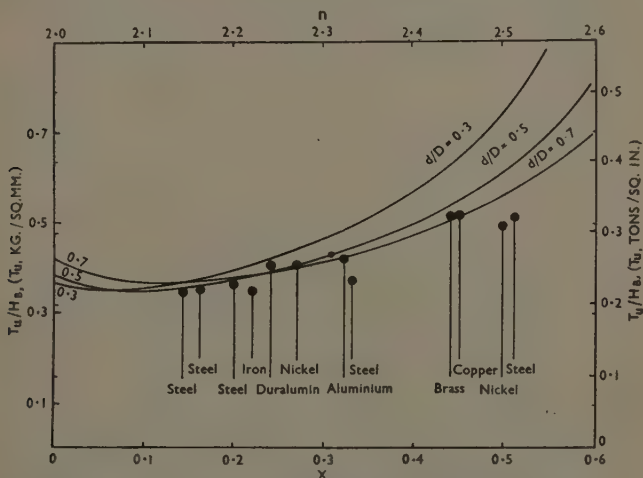


FIG. 6.—Ratio of Ultimate Tensile Strength to Brinell Hardness as a Function of the Work-Hardening Index  $x$ .

Since most Brinell hardness measurements are made with indentations ranging from  $d/D = 0.3$  to  $d/D = 0.7$ , similar calculations have been made for these values of  $d/D$ . The results are also plotted in Fig. 6. It is seen that all the curves have the same characteristics. For values of the Meyer index ranging between 2 and 2.2 the ratio is roughly constant at a value of about 0.36 when  $T_u$  is in kg./mm.<sup>2</sup> or 0.23 when

## 12 Tabor: The Hardness and Strength of Metals

$T_u$  is in tons/in.<sup>2</sup>. For higher values of the Meyer index the ratio increases and reaches an upper value which is about 50% greater.

The results obtained from practical experiments, based on values given by O'Neill,<sup>2</sup> are shown in circles for metals including work-hardened nickel, annealed copper, and tool steel. It is seen that the general trend is similar to the theoretical curves, and the points lie very close to the curve for  $d/D = 0.7$ . If the constant  $c$  in the relation  $P = cY$  had been taken as being equal to 3 instead of 2.8, the observed results would lie around the theoretical curve for  $d/D = 0.5$ . Better agreement than this cannot be expected, since the assumptions involved in the derivation of  $T_u/H_B$  are of an approximate nature. First, it has been assumed that  $x = n - 2$ ; secondly, that the representative strain in the hardness measurements is equal to  $20d/D$ . These assumptions are only approximately true. The third and probably the most serious assumption is that the stress/strain curve can be represented by a relation  $Y = b\epsilon^x$ . This only holds over a limited range of strains, so that for larger strains the results are no longer reliable.

This is shown by some experiments with annealed copper. The Brinell hardness for  $d/D = 0.5$  was  $H_B = 45$  kg./mm.<sup>2</sup>. The Meyer index was  $n = 2.50$  so that  $x = 0.5$ . According to Table IV the ratio  $T_u/H_B$  should be 0.6, so that the ultimate tensile strength should be  $T_u = 27$  kg./mm.<sup>2</sup> (or 17 tons/in.<sup>2</sup>). Similarly, from equation (14), the strain corresponding to  $T_u$  should be  $\frac{x}{1-x} = 1$ , i.e. an extension of 100%. The observed values were  $T_u = 23$  kg./mm.<sup>2</sup> (or 15 tons/in.<sup>2</sup>) and the corresponding extension  $\epsilon = 56\%$ .

The reason for this divergence is seen if the true stress/strain curve of the specimen is compared with the hardness values. The results are shown in Fig. 7, the observed stress/strain curve being drawn as the full line. The true stress is the applied tension at any stage divided by the cross-section at that stage. If slight necking has occurred the cross-section of the neck is used. The strain is the linear strain obtained from the extension of the specimen when the extension is uniform. If there has been slight necking, the equivalent linear strain is calculated from the reduction in area at the neck. On the same curve the hardness values of the original specimen are plotted. The values of  $P$  have been divided by 2.8, and the size of the indentation placed along the strain axis such that  $d/D = 1$  is equivalent to 20% strain. It is seen that the hardness values lie extremely close to the stress/strain curve. However, the stress/strain curve corresponding to these hardness values has a power of  $\epsilon$  equal to 0.5. If the corresponding curve of the form  $Y = b\epsilon^{0.5}$  is drawn, the broken line is obtained. This

coincides with the observed stress/strain curve over the first 25% strain, but diverges from it increasingly at higher strains. A much better fit over the portion of the stress/strain curve lying between strains of 20 and 60% is obtained using a relation  $Y = be^{0.35}$  (dotted line). This does not agree at all well with the hardness observations, but conforms well to that part of the stress/strain curve in which the maximum tensile stress occurs. Using a value of  $x = 0.35$  in equation (14) the strain corresponding to  $T_u$  is  $\frac{0.35}{0.65} = 54\%$ , which is close to the observed value of 56%.

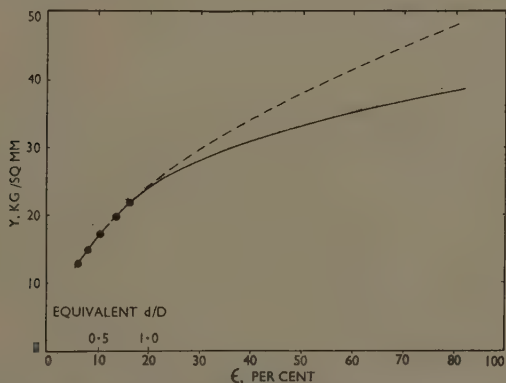


FIG. 7.—Comparison of True Stress/Strain Curve with Hardness Values.

KEY.

- Observed stress/strain curve.
- hardness values.
- - - Theoretical curve  $Y = be^{0.5}$  (from hardness).
- ..... Curve  $Y = be^{0.35}$ .

It is clear from these results that the hardness values provide a reliable measure of the shape of that part of the stress/strain curve which lies within the first 25% of strain. If the maximum tensile stress occurs within this limit the values of  $T_u/H_B$  derived in the above treatment will be reliable. For this to occur the value of  $x$  must be 0.2 or less. This corresponds to values of the Meyer index  $n$  of 2.2 or less. For higher values of  $n$ , the strain corresponding to  $T_u$  is greater than 25%. If the significant portion of the stress/strain curve still follows the stress/strain equation derived from the hardness values, the values of  $T_u/H_B$  will still be reliable. In general, however, the stress/strain curve flattens off with increasing strain, so that the observed value of

$T_u$  and the observed value of the corresponding strain will be less than that given by the above analysis.

These considerations show that the ratio of the ultimate tensile strength to the Brinell hardness depends essentially on the degree of work-hardening of the metal. It does not depend primarily on the nature of the metal itself except in so far as the stress/strain curve of the metal departs from the simple power curve derived from the hardness measurements. Apart from this fundamental limitation the hardness values provide a direct means of determining the ultimate tensile strength of a metal and, as is shown in Fig. 6, the general trend of the experimental results and the actual values of  $T_u/H_B$  are reasonably close to the theoretical values.

#### VI.—THE DEFORMATION OF METALS BY CONICAL OR PYRAMIDAL INDENTERS.

When a metal is deformed by a conical or pyramidal indenter the shape of the indentation remains constant whatever the size of the indentation. Consequently, the stress and strain patterns in the deformed material remain geometrically similar whatever the size of the indentation. For this reason the yield pressure is essentially constant and is independent of the load  $W$ . Consequently, if  $d$  is the diameter or diagonal of the indentation the yield pressure is proportional to  $W/d^2$ , and since this is constant  $W = kd^2$ . The value of the constant depends on the hardness of the metal and on the shape of the indenter. For a sharply pointed indenter it will be greater than for one of large semi-angle. This is because the friction between the face of the indenter and the indentation becomes more important the smaller the angle of the cone or pyramid. In addition the displaced material is more strongly confined the sharper the indenter. However, for an indenter of fixed angle the constant  $k$  depends only on the hardness of the metal.

If conical or pyramidal indentations are made in a material of fixed elastic limit or yield stress  $Y$  (i.e. one that is not work-hardened by indentation) it is found that there is a direct relation between  $Y$  and the mean yield pressure  $P$ . As mentioned above, the factor of proportionality varies with the angle of the indenter, but for a cone or pyramid of semi-angle lying between  $60^\circ$  and  $90^\circ$  it is roughly constant and for the usual conditions of lubrication it has a value of about 3. This is shown in Table V, where the indentations have been made with a standard Vickers diamond pyramid.

Since the Vickers pyramid hardness number  $H_D$  is defined as the load divided by the *surface* area of the indentation, it is smaller than  $P$ . From the geometrical shape of the pyramid it may be shown that

$H_D = 0.93P$ , so that, for work-hardened metals,  $H_D = 0.93P = 0.93 \times 3.2Y \approx 3Y$ .

For materials that work-harden and so experience an increase in  $Y$ , the amount of work-hardening produced by the indentation process again varies with the shape of the indenter. By an empirical

TABLE V.—*Relation Between Y and P for Work-Hardened Metals.*

Metal	$Y$ , kg./mm. <sup>2</sup>	$P$ , kg./mm. <sup>2</sup>	$P/Y$
Tellurium Lead . . .	2.1	6.7	3.2
Aluminium . . .	12.3	39.5	3.2
Copper . . .	27	88	3.3
Mild Steel . . .	70	227	3.2

method it may be shown that, with the pyramid used in the Vickers test, the indentation increases the effective yield stress of the metal by an amount equivalent to a strain of about 8% (Tabor<sup>10</sup>). Thus if we take a metal specimen and deform it by an amount  $\epsilon_0$ , the Vickers hardness value at this stage of deformation will be approximately three times the yield stress of the metal at a deformation of  $\epsilon = \epsilon_0 + 8\%$ .

TABLE VI.—*Relation Between Elastic Limit and Vickers Hardness Number.*

Metal	Initial-Deformation, $\epsilon_0$ , %	$(\epsilon_0 + 8)$ , %	$Y$ , kg./mm. <sup>2</sup>	$cY$	Observed Vickers Hardness Number
Mild Steel . . .	0	8	55	$c = 2.9$ 159	156
	6	14	62	176	177
	10	18	66	190	187
	13	21	67	194	193
	25	33	73	211	209
Annealed Copper .	0	8	15	$c = 3.0$ 45	39
	6	14	20	60	58
	12.5	20.5	23.3	70	69
	17.5	25.5	25	75	76
	25	33	26.6	80	81

This is shown in Table VI, where it is seen that there is reasonably good agreement between the observed values of the Vickers hardness number and those calculated from the stress/strain characteristics of the metal. In addition it is clear from the value of the indentational strain (8%) and from the value of  $c$  (2.9–3) that the Vickers hardness

number will be close to the Brinell hardness number over an appreciable range of hardness values.

### VII.—VICKERS HARDNESS NUMBER AND ULTIMATE TENSILE STRENGTH.

A relation may be derived between the Vickers hardness number  $H_D$  and the ultimate tensile strength  $T_u$  in a manner similar to that

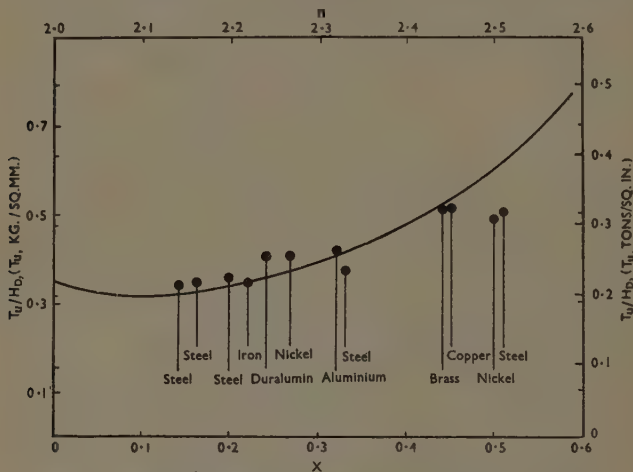


FIG. 8.—Ratio of Ultimate Tensile Strength to Vickers Hardness as a Function of the Work-Hardening Index  $x$ .

described above. If the true stress/strain curve of the metal may be expressed by a relation  $Y = b\epsilon^x$ ,  $T_u$  is given by equation (15), viz :

$$T_u = b(1 - x) \left( \frac{x}{1 - x} \right)^x$$

where  $x$  is again assumed to be equal to  $n - 2$ , and  $n$  is the Meyer index. If the Vickers pyramid produces an indentational strain of 8% the representative yield stress is given by  $Y_r = b(0.08)^x$ , so that the Vickers hardness number is given by :

$$H_D = 2.9Y_r = 2.9b(0.08)^x.$$

Consequently the ratio of  $T_u$  to  $H_D$  is given by :

$$\frac{T_u}{H_D} = \frac{1 - x}{2.9} \left( \frac{12.5x}{1 - x} \right)^x \quad (19)$$

The result is plotted in Fig. 8. It should be noted that here again the



value of the ratio still involves the Meyer index  $n$ . The practical values obtained from Brinell hardness data <sup>2</sup> are plotted on the same figure and it is seen that the agreement with the theoretical curve is reasonably good. The same sort of divergence, particularly for higher values of  $n$ , is observed as in Fig. 6.

### VIII.—CONCLUSIONS.

These results show that indentation hardness measurements are essentially a measure of the elastic limit (or yield stress) of the metal under examination. For metals which do not work-harden appreciably, the hardness value for both the Brinell and the Vickers indenter is approximately three times the yield stress. For metals which work-harden appreciably, the indentation process itself produces an increase in the yield stress of the metal. With conical or pyramidal indenters the indentation is geometrically similar whatever its size, so that the work-hardening produced by the indentation is always, geometrically, the same. Consequently the hardness value does not depend on the size of the indentation and is, therefore, independent of the load. For this reason the Vickers pyramid indenter gives a single value for the hardness of a metal.

With spherical indenters, however, the shape of the indentation depends on the ratio  $d/D$ . The larger this value, the greater the amount of work-hardening produced by the indentation and the greater the resulting hardness value. For this reason the Brinell hardness values depend on the ball diameter  $D$ , on the chordal diameter  $d$  of the indentation, and on the load  $W$ , and the behaviour follows Meyer's general relation  $W = Ad^n/D^{n-2}$ , where  $n$  is the Meyer index. If the true stress/strain curve may be represented by a relation of the type  $Y = b\epsilon^x$  where  $Y$  is the yield stress,  $\epsilon$  is the strain, and  $x$  the work-hardening index, it is found that, to a close approximation  $x = n - 2$ . It is thus possible to derive the true stress/strain curve of a metal from hardness values obtained with a spherical indenter. By this means the nominal stress/strain curve and consequently the ultimate tensile strength may be calculated. The analysis provides a theoretical basis for the empirical observation that the tensile strength in tons/in.<sup>2</sup> is approximately 0.22 times the Brinell hardness for certain steels. The analysis shows further that this type of relation is of much wider application. To a first approximation the ratio of the tensile strength to the Brinell hardness is independent of the metal under consideration: it depends primarily on the degree of work-hardening of the metal, i.e. on the work-hardening index  $x$  or the Meyer index  $n$ . Thus for work-hardened metals ( $n = 2.2$ ) the ratio has a value of about 0.22; for highly

## 18 Tabor : The Hardness and Strength of Metals

annealed metals ( $n = 2.5$ ) the ratio has a value of about 0.36. If a curve is drawn showing the variation of this ratio with the Meyer index  $n$  it is found that materials as diverse as tool steel, work-hardened nickel, and annealed copper, all lie near the theoretical curve. This analysis, of course, becomes less reliable if the stress/strain curve departs markedly from a simple power relation of the type  $Y = be^x$ . It will also cease to be valid if important structural changes occur in the tensile test which do not occur in the hardness measurements. This presumably applies to certain austenitic steels and also to materials containing serious flaws. For other metals, however, there is a reasonably sound theoretical basis for deriving the ultimate tensile strength from the hardness number and the Meyer index of the metal.

### ACKNOWLEDGEMENTS.

The author wishes to thank Dr. F. P. Bowden for his constant encouragement, Mrs. C. Tipper for helpful discussions, the Ministry of Supply (Air) for a grant to the Laboratory, and the Anglo-Iranian Oil Co., Ltd., for a grant for equipment.

### REFERENCES.

1. E. Meyer, *Z.V.d.I.*, 1908, **52**, 645, 740, 835.
2. H. O'Neill, "The Hardness of Metals and Its Measurement". London : 1934 (Chapman and Hall, Ltd.).  
H. O'Neill, *Proc. Inst. Mech. Eng.*, 1944, **151**, 115.
3. A. Nádaí, "Plasticity". New York : 1931 (McGraw-Hill Book Co., Inc.).
4. H. Hertz, *J. reine angew. Math.*, 1886, **92**, 156.
5. S. Timoshenko, "Theory of Elasticity", p. 344. New York : 1934 (McGraw-Hill Book Co., Inc.).
6. R. M. Davies, *Proc. Roy. Soc.*, 1949, [A], **197**, 416.
7. H. Hencky, *Z. angew. Math. Mech.*, 1923, **3**, 241.
8. A. J. Ishlinsky, *Zhur. Priklad. Mat. Mekh.*, 1944, **8**, 233.
9. R. F. Bishop, R. Hill, and N. F. Mott, *Proc. Phys. Soc.*, 1945, **57**, 147.
10. D. Tabor, *Proc. Roy. Soc.*, 1948, [A], **192**, 247.

# MECHANISM OF PRECIPITATION IN ALUMINIUM-MAGNESIUM ALLOYS.\*

By E. C. W. PERRYMAN,<sup>†</sup> M.A., A.I.M., MEMBER, and G. B. BROOK,<sup>‡</sup>  
B.Met., STUDENT MEMBER.

(Communication from The British Non-Ferrous Metals Research Association.)

## SYNOPSIS.

The precipitation mechanism in commercial-purity aluminium-7% magnesium and high-purity aluminium-10% magnesium alloy has been investigated by metallographic methods, and by hardness and X-ray measurements. The effect of 0.5 and 1% zinc on the rate of precipitation and hardening of the former alloy was also studied.

Precipitation took place first in the grain boundaries and then within the grains and not until the latter process occurred did hardening begin. The magnitude of the hardening was small, though it was increased both in rate and extent by the zinc additions. High degrees of supersaturation favoured the formation of a Widmanstätten structure.

X-ray examination showed that precipitation in the aluminium-7% magnesium alloy was of the continuous type at 200° and 250° C. At 125° C. continuous and discontinuous precipitation took place together; continuous precipitation within the precipitated new solid solution then followed. The latter mode of precipitation was also found in the aluminium-10% magnesium alloy at temperatures up to and including 300° C. Continuous precipitation in the precipitated new solid solution has not previously been observed, and a possible reason for its occurrence is suggested. The new solid solution was not detected by metallographic examination, possibly because, as X-ray examination showed, the orientations of the new and old solid solutions were the same.

X-ray analysis confirmed the findings of other workers in that the beta precipitate first formed was unstable and as ageing proceeded transformed into the equilibrium form.

## I.—INTRODUCTION.

IN the course of an investigation<sup>1</sup> of the mechanism of the stress-corrosion of aluminium-7% magnesium alloy, it was found that the stress-corrosion susceptibility was closely related to the metallographic structure. No systematic examination had previously been made of the decomposition of aluminium-magnesium alloys, and it was therefore decided to study further the nature of the precipitate formed during ageing and to determine what ageing treatments produced maximum internal strains, as it was thought possible that these strains might play an important part in the stress-corrosion process. The effect of small additions of zinc on the process of decomposition was

\* Manuscript received 19 May 1950. The work described in this paper was made available to members of the B.N.F.M.R.A. in a confidential research report issued in June 1949.

<sup>†</sup> Investigator, British Non-Ferrous Metals Research Association, London.

<sup>‡</sup> Fulmer Research Institute, Ltd., Stoke Poges, Bucks.; formerly Bursar, British Non-Ferrous Metals Research Association, London.

also investigated, as these had been found to exercise a marked effect on the stress-corrosion susceptibility of the alloys.

As regards previous work, Fink and (D. W.) Smith<sup>2</sup> found that during the decomposition at 100°, 200°, and 300° C. of an alloy containing 10.3% magnesium, precipitation of  $Mg_2Al_3$  occurred before any change in lattice parameter could be detected and before the yield strength or elongation had substantially changed. The first particles of precipitate, which appeared at the grain boundaries, had no measurable effect on the yield strength or elongation, but these properties altered as soon as precipitation took place within the grains. The first change of lattice parameter was shown by the diffraction rings becoming more diffuse in the direction of decreasing lattice spacing, indicating that continuous\* precipitation was occurring. As the ageing continued the diffraction rings became more diffuse and the yield strength increased. These authors also found that after ageing at 300° C. for 80 hr. the equilibrium beta phase was precipitated, while after ageing at 200° C. for 136 hr. the precipitate had a different structure.

Brick, Phillips, and (A. J.) Smith<sup>3</sup> investigated the decomposition of aluminium-10% magnesium alloy at 175°, 250°, and 300° C. by X-ray measurements. In the early stages of ageing there was a slight fall in the lattice parameter which they attributed to the relief of quenching stresses. At all temperatures the precipitation reaction was indicated on the X-ray photographs by the appearance of new lines having approximately the lattice parameter of the solid solution in equilibrium at the temperature of ageing. The lines of the supersaturated solid solution decreased in intensity while the new solid-solution lines became more intense as ageing proceeded, indicating discontinuous\* precipitation, contrary to the findings of Fink and Smith.<sup>2</sup> The rate of decomposition was also found to increase with decreasing grain-size. Lacombe,<sup>4</sup> investigating the decomposition of alloys containing 9, 11, 12, and 13.5% magnesium, found no change in lattice parameter of the 9% magnesium alloy on ageing for up to 4 hr. at 200° C. The other three alloys showed first a small increase in lattice parameter and then a decrease. X-ray measurements indicated the existence

\* Discontinuous precipitation is said to take place when the supersaturated-solid-solution lines in the X-ray spectra decrease in intensity and, at the same time, new lines appear, corresponding to the solid solution in equilibrium at the temperature of ageing. These new lines increase in intensity until the lines of the original solid solution disappear. In general, discontinuous precipitation starts at the grain boundaries and spreads into the grains. Continuous precipitation is said to take place when the X-ray lines from the supersaturated solid solution gradually move from their original position to the position corresponding to the equilibrium composition at the temperature of ageing. Normally, when continuous precipitation occurs the precipitate takes the form of the Widmanstätten structure.

of two forms of the beta phase, a non-equilibrium form  $\beta'$  and the equilibrium form  $\beta$ . Calvet and his co-workers<sup>5</sup> investigated the decomposition of alloys containing 7.4 and 11.8% magnesium. Their results appear to agree with those of Fink and Smith<sup>2</sup> in so far as a general decrease in lattice parameter occurred as the ageing time at 200° C. increased, indicating continuous precipitation. There was no change in lattice parameter until precipitate was visible within the grains. Magnesium-rich zones, similar to the Guinier-Preston zones found in aluminium-copper alloys could not be detected. However, since aluminium and magnesium have approximately the same X-ray scattering power it would be almost impossible to differentiate between the matrix, on the one hand, and areas rich in magnesium but of the same crystal structure, on the other.

Geisler, Barrett, and Mehl<sup>6</sup> claim to have shown that platelets of a coherent transition phase are formed on {100} matrix planes during the ageing of aluminium-10% magnesium alloy. This conclusion is based on the presence of streaks in Laue photographs of single crystals, which are interpreted as due to thin platelets acting as two-dimensional diffraction gratings. Growth of the platelets then occurs until a Widmanstätten structure is obtained, with the precipitate appearing as plates on {100} planes. Subsequent platelet formation takes place on {120} planes. There is an important difference between these results for aluminium-magnesium and those for aluminium-copper alloys, namely, in the former streaks in the Laue diagram were found only when there was a large amount of visible precipitate, while in the latter no visible precipitate is present when the streaks in the Laue diagram first appear. These authors also studied the decomposition of aluminium-10% magnesium alloy by electrical-resistivity measurements and found an increase in resistivity just before the rapid decrease resulting from matrix depletion, and suggested that the increase was due to strains set up by the formation of coherent platelets. On the other hand, Mott<sup>7</sup> has shown that an increase in resistivity on ageing can be accounted for by change in particle size, the increase taking place when the particle size is in the range 5-10 Å. More recently Matyáš<sup>8</sup> has shown theoretically that the change in electrical resistance of aluminium-copper and aluminium-silver alloys can be explained by variation in particle size.

## II.—EXPERIMENTAL WORK.

### 1. *Alloys Investigated.*

Materials examined included: (a) commercial-purity aluminium-7% magnesium alloy (18 S.W.G.), and (b) super-purity aluminium-

10% magnesium alloy. The 10% magnesium alloy was made from 99.99% aluminium and 99.99% distilled magnesium, chill-cast ingots  $9 \times 4\frac{1}{2} \times 1$  in. being cut into slabs  $4\frac{1}{2} \times 2 \times 1$  in. and soaked at  $450^{\circ}\text{C}$ . before hot pressing to a thickness of  $\frac{1}{2}$  in. All sections examined were cross-sections of the original ingot.

In addition to these two alloys three commercial-purity alloys containing 0, 0.5, and 1% zinc were examined. Chill-cast ingots  $9 \times 4 \times 1$  in. made from commercial-purity materials were soaked at  $420^{\circ}\text{C}$ . overnight, and hot pressed to a thickness of  $\frac{1}{2}$  in. After a further heat-treatment of 2 hr. at  $420^{\circ}\text{C}$ . they were hot rolled to 18 S.W.G. sheet according to the following schedule: (i) cross rolled to  $\frac{1}{4}$  in. in 0.06 in. passes, (ii) soaked for 1 hr. at  $420^{\circ}\text{C}$ ., (iii) rolled down to 0.063 in. in 0.03 and 0.015 in. passes, (iv) soaked for 1 hr. at  $420^{\circ}\text{C}$ ., and (v) rolled to 0.048 in. in three passes of 0.005 in.

The compositions of the alloys are given in Table I.

TABLE I.—*Composition of Alloys.*

Alloy Mark	Mg, %	Mn, %	Fe, %	Si, %	Zn, %
MNY	7.4	0.20	0.34	0.16	...
NCM	9.44	<0.001 *	0.05 *	0.005 *	n.d. *
NEE	7.80	0.21	0.25	0.11	...
NEF	7.44	0.15	0.20	0.11	0.51
NEG	7.74	0.21	0.20	0.11	1.06

\* Determined spectrographically.  
n.d. = not detected.

## 2. Hardness Measurements and Microscopic Examination.

The same specimen,  $2 \times 1$  cm., was used for all the Vickers hardness measurements at each ageing temperature, with the exception that separate specimens of the aluminium-7% magnesium alloy were used for each ageing time at  $200^{\circ}\text{C}$ . Each hardness measurement given is the mean of four impressions. Microscopic examination was carried out on the cross-section of the sheet, specimens being mechanically polished and etched with Wassermann's reagent. This reagent consists of equal parts of 0.5% hydrofluoric acid and of a mixture containing 2 c.c. hydrochloric acid, 20 c.c. nitric acid, and 50 c.c. 10% potassium dichromate. The etching time necessary decreased as the ageing time or temperature increased.

All ageing treatments were carried out in an air oven, except the ageing at  $125^{\circ}\text{C}$ . which was done in an oil bath. Ageing treatments were given after an initial solution-treatment of 3 hr. at  $420^{\circ}\text{C}$ . for the 7%, and 6 hr. at  $450^{\circ}\text{C}$ . for the 10% magnesium alloy.



### 3. *X-Ray Measurements.*

Lattice parameters were determined by taking back-reflection scanning photographs using Cu radiation with a nickel filter and an exposure of 40 m.amp. hr. The specimens were etched to remove any worked layer due to polishing, and were oscillated 6 times/min. through  $\pm 5^\circ$  about a vertical axis through the specimen at right angles to the X-ray beam, whilst 1 cm.<sup>2</sup> of its surface was scanned in 20 min. This gave reasonably uniform rings with the largest-grained material. A single specimen was used throughout the ageing at any one temperature, except for the 7% magnesium alloy at 200° C., where separate specimens were used for each ageing time. Parameter values given are accurate to  $\pm 0.0004$  kX., except for specimens giving very diffuse rings. All measurements were made at room temperature, i.e. 20° C., which never varied by more than 3° C. The errors in parameter measurements due to temperature changes were thus less than the experimental error.

To record the diffractions from the beta precipitate, small wires, 3 mm. square, were cut from suitably aged sheet specimens and etched in 10% sodium hydroxide solution to a thickness of 0.3 mm. X-ray diffraction photographs were taken in a 19-cm. powder camera using Co radiation monochromatized by reflection from the (200) planes of a cleaved calcite crystal. The cleaved surface was slightly ground to improve the efficiency of reflection. By this means  $K\alpha$  radiation with a small white component was obtained and an exposure of 1600 m.amp. hr. was sufficient.

## III.—RESULTS.

### 1. *Microscopic Examination.*

#### (a) *Commercial-Purity Aluminium-7% Magnesium Alloy.*

Microscopic examination was carried out after ageing for various times at 125°, 200°, and 250° C. after solution-treatment. At all temperatures the precipitate appeared first at the grain boundaries and later within the grains. The rate of precipitation at the boundaries varied from one grain boundary to another, depending upon the relative orientations of the neighbouring grains, large orientation differences giving high rates of precipitation and vice versa. As the ageing temperature rose the rate of precipitation both at the grain boundaries and within the grains increased, and the precipitated particles became larger (see Figs. 1, 2, and 3, Plate I). On ageing for long times at 125° C. a Widmanstätten structure was formed (see Fig. 4, Plate I). The first sign of this appeared after 19 days, and on further ageing the rods increased in number and size. The precipitate seems to come out as rods in three main directions; it is unlikely that

it comes out as plates for the flat section of a plate has never been found, whereas in Fig. 4 the small round particles could well be the cross-sections of rods. Fig. 5 (Plate II) shows a specimen which was overstrained 10% and then aged at 125° C. for 141 days (cf. Fig. 4). Overstraining has prevented the formation of the Widmanstätten structure. On ageing at the higher temperatures the tendency to form a Widmanstätten structure was markedly reduced; for example, at 125° C. the structure was completely made up of rods, at 200° C. a few rods were formed, while at 250° C. there were practically none. Ageing for long times at the higher temperatures caused the precipitate to coagulate and grow in size, (see Fig. 6, Plate II). Overstraining the material before ageing increased the rate of precipitation, especially at the grain boundaries.

(b) *Commercial-Purity Aluminium-7% Magnesium Alloy with Small Additions of Zinc.*

Alloys were examined containing 0.5 and 1% zinc aged at 75°, 100°, 125°, and 200° C. for various times: (i) after solution-treatment, and (ii) after solution-treatment and 10% overstrain. The mode of precipitation was the same as for the commercial-purity aluminium-7% magnesium alloy, increasing temperatures giving more rapid precipitation. With increasing zinc content, however, the rate of precipitation at the grain boundaries was markedly retarded, though there was more precipitate within the grains in the zinc-bearing alloys (see Figs. 7 and 8, Plate II). This presumably is due to the fact that the solid solubility of magnesium in aluminium is restricted by the presence of zinc. For example, at 200° C. the solubility is reduced from about 3 to 1% by the addition of 0.5% zinc.<sup>9</sup>

Overstraining the material before ageing caused the precipitate to come out more rapidly than was the case in material not overstrained, especially at the grain boundaries.

(c) *Super-Purity Aluminium-10% Magnesium Alloy.*

After ageing for various times at 200°, 230°, 250°, and 300° C., microstructures similar to those of the 7% magnesium alloy were observed, the main difference being that the precipitate was coarser. Again the tendency to form a Widmanstätten structure decreased as the ageing temperature rose and was entirely absent on ageing at 300° C. The formation of a Widmanstätten structure thus appears to depend on the degree of super-saturation, which varies with the temperature of ageing. Figs. 9 and 10 (Plate III) show the structures after ageing at 230° C. for 2 hr. and 300° C. for 6 hr.; the grain-boundary zone denuded of precipitate, referred to earlier, is apparent, especially

ALUMINIUM-7% MAGNESIUM ALLOY.



FIG. 1.—Solution-treated and aged at 125° C. for 2 days.  $\times 1500$ .



FIG. 2.—Solution-treated and aged at 200° C. for 2 days.  $\times 1000$ .

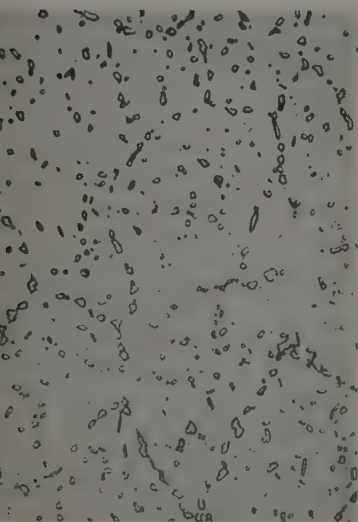


FIG. 3.—Solution-treated and aged at 250° C. for 2 days.  $\times 1000$ .

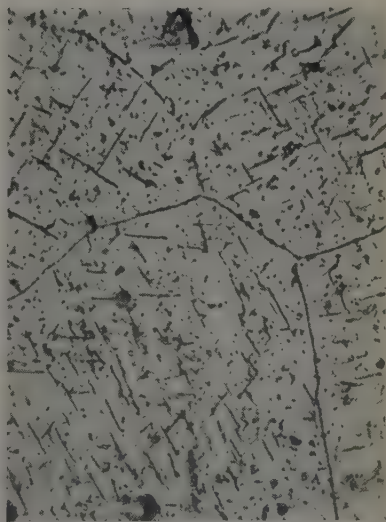


FIG. 4.—Solution-treated and aged at 125° C. for 141 days.  $\times 1500$ .

## ALUMINIUM-7% MAGNESIUM ALLOY.

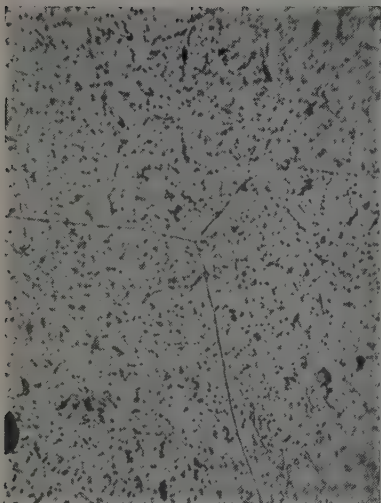


FIG. 5.—Solution-treated, overstrained 10%, and aged at 125° C. for 141 days.  $\times 1500$ .

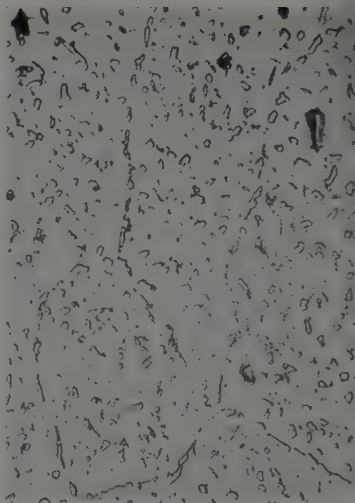


FIG. 6.—Solution-treated and aged at 200° C. for 63 days.  $\times 1000$ .



FIG. 7.—Solution-treated and aged at 100° C. for 2 days.  $\times 500$ .



FIG. 8.—Alloy containing 1% Zinc, solution-treated and aged at 100° C. for 2 days.  $\times 500$ .

ALUMINIUM-10% MAGNESIUM ALLOY.



FIG. 9.—Solution-treated and aged at 230° C. for 2 hr.  $\times 500$ .



FIG. 10. Solution-treated and aged at 300° C. for 6 hr.  $\times 500$ .

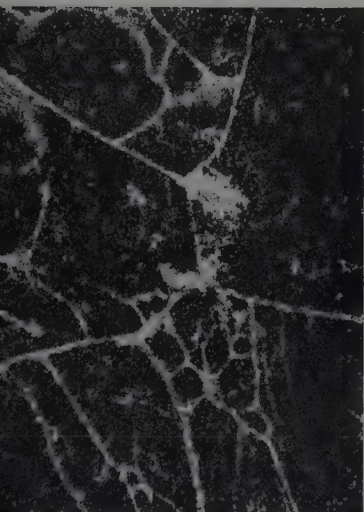


FIG. 11.—Solution-treated and aged at 200° C. for 7 days. Heavily etched.  $\times 100$ .

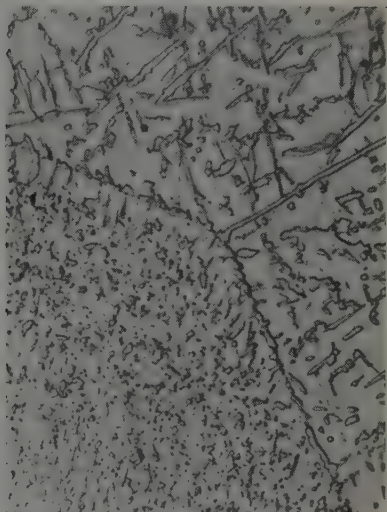


FIG. 12.—Same as Fig. 11, lightly etched. Showing coarse precipitation in white areas revealed in Fig. 11.  $\times 1500$ .

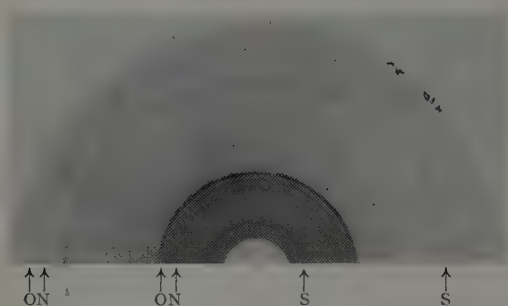


FIG. 13.—Back-Reflection Photograph of Solution-treated Aluminium-10% Magnesium Alloy, aged at 200° C. for 1 day.

*O* = Old solid-solution doublet.      *N* = New solid-solution doublet.  
*S* = Calibration lines.



FIG. 14.—X-Ray Photograph of Aluminium-10% Magnesium Alloy, solution-treated and aged at 230° C. for 12 hr.



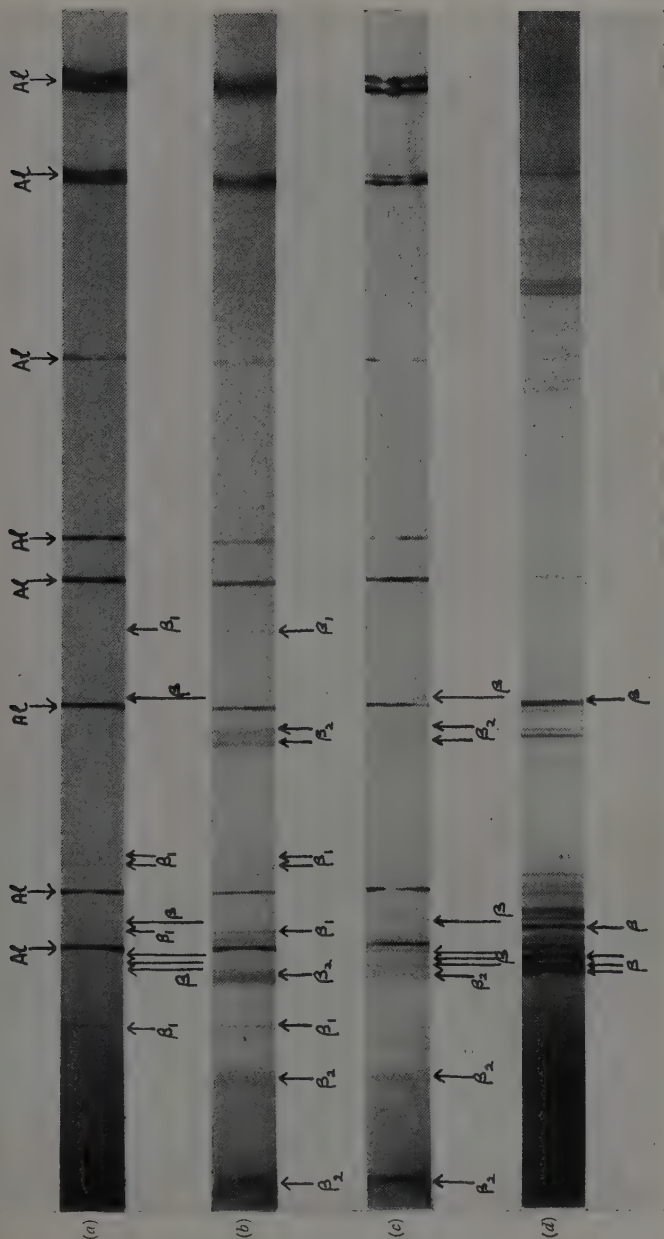


FIG. 15.—X-Ray Diffraction Photographs of Aluminium-Magnesium Alloys.

- (a) Aluminium-7% Magnesium Alloy, solution-treated and aged at 200° C. for 53 days.  
 (b) Aluminium-7% Magnesium Alloy, solution-treated and aged at 125° C. for 357 days.  
 (c) Aluminium-10% Magnesium Alloy, solution-treated and aged at 230° C. for 12 days.  
 (d)  $Mg_2Al_3$  annealed at 250° C.

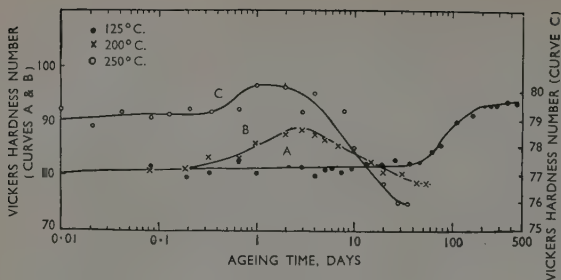


Fig. 16.—Age-Hardening Curves for Commercial-Purity Aluminium-7% Magnesium Alloy.

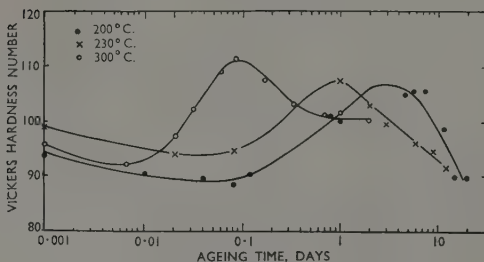


Fig. 17.—Age-Hardening Curves for Super-Purity Aluminium-10% Magnesium Alloy.

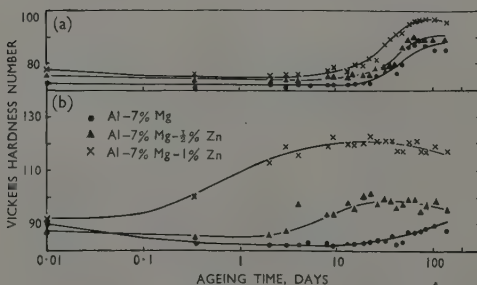


Fig. 18.—Age-Hardening Curves for Commercial-Purity Aluminium-7% Magnesium Alloy with and without Small Additions of Zinc.

(a) Homogenized, aged at 125° C.

(b) Homogenized, overstrained 10%, and aged at 125° C.

in Fig. 9. On ageing for longer times precipitation ultimately took place in these denuded zones, but was coarser than elsewhere. The denuded zones appeared not only at the grain boundaries but also within the grains, forming a subgranular network. Fig. 11 (Plate III) shows such a structure on a specimen heavily etched with 0.5% hydrofluoric acid, the dark areas being those in which heavy precipitation has occurred. Fig. 12 (Plate III) shows the same structure at a higher magnification with the coarser precipitate within the denuded zone.

## 2. Hardness Measurements.

Figs. 16 and 17 (Plate VI) show the ageing curves for the aluminium-7% and aluminium-10% magnesium alloys, respectively. As the ageing temperature increases, the time to attain maximum hardness decreases.

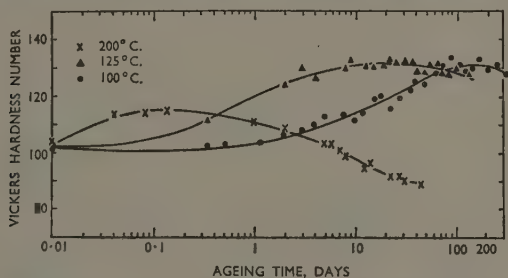


FIG. 19.—Age-Hardening Curves for Aluminium-7% Magnesium-1% Zinc Alloy, Overstrained 10% before Ageing.

The initial fall in hardness of the 10% magnesium alloy is probably due to the relief of internal strains set up during quenching.

Fig. 18 (Plate VI) shows the ageing curves at 125° C. for commercial-purity aluminium-7% magnesium alloy with and without small additions of zinc. As the zinc content increased the maximum hardness increased in magnitude and was reached in a shorter time; this also occurred after ageing at 100° and 200° C. Overstraining before ageing caused the maximum hardness to be reached sooner and produced a larger variation in hardness with zinc content. As with the binary aluminium-magnesium alloys, raising the ageing temperature shortened the time to attain maximum hardness (Fig. 19). These results suggest that hardening is associated with precipitation within the grains because (i) no hardening occurred in the binary aluminium-magnesium alloys until such precipitation had taken place and (ii) the rate and amount of intragranular precipitate increased with the zinc content. That grain-boundary precipitation produces no hardening is shown by the fact

that (a) grain-boundary precipitation was complete before hardening began in the aluminium-magnesium alloys, and (b) as the zinc content increased the rate of precipitation at the grain boundaries lessened, while hardening started earlier.

As precipitation is a diffusion process, the rate of precipitation can be expressed as a function of temperature by means of the equation :

$$r = ae^{-Q/RT}$$

where  $a$  = a constant,  $Q$  = the activation energy,  $R$  = the gas constant, and  $T$  = the absolute temperature. If the reciprocal of the ageing time needed for maximum hardness is taken as a measure of the rate of reaction and plotted against the reciprocal of the absolute tem-

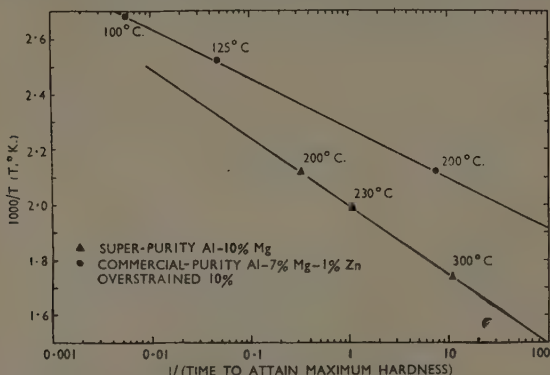


FIG. 20.—Effect of Temperature on Time to Attain Maximum Hardness.

perature, the activation energy  $Q$  can be obtained from the slope of the resulting straight line. Fig. 20 shows such curves for super-purity aluminium-10% magnesium alloys and commercial-purity 7% magnesium-1% zinc alloy overstrained 10% after solution-treatment, the results being taken from Figs. 17 and 19 respectively. Gayler<sup>10</sup> has shown for aluminium-copper alloys that cold work before ageing does

TABLE II.—Effect of Zinc on Activation Energy.

Alloy	Activation Energy from Fig. 20, cal.
Super-purity Aluminium-10% Magnesium	31,900 *
Commercial-purity Aluminium-7% Magnesium-1% Zinc	48,700

\* Seitz<sup>12</sup> gives a value of 38,500 cal.

not alter the slope of the line but merely displaces it to shorter ageing times, and it therefore appears that the zinc increases the activation energy of the precipitation process. Table II gives the activation energies for these alloys.

In agreement with Jetter and Mehl,<sup>11</sup> the activation energy determined from the age-hardening curves is lower than that obtained by Seitz from diffusion data.

### 3. X-Ray Examination.

#### (a) Lattice-Parameter Measurements.

(i) *Aluminium-7% Magnesium Alloy.*—Fig. 21 shows how the lattice parameter of the aluminium-7% magnesium alloy varied with

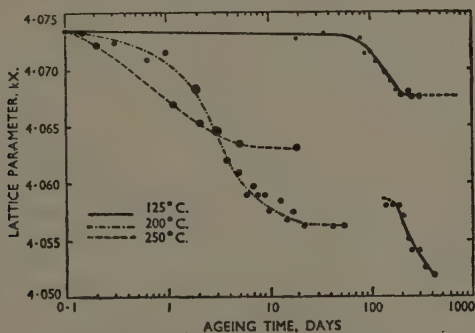


FIG. 21.—Variation of Lattice Parameter with Ageing Time for Commercial-Purity Aluminium-7% Magnesium Alloy.

time of ageing at 125, 200°, and 250° C. The size of the spot represents the diffuseness of the diffraction rings, a small spot indicating a sharp ring, and a large spot a diffuse ring. At 250° C. the rings were always sharp, while at 200° C. the rings became diffuse, being most diffuse after about 2 days and then becoming sharp again. As there was no appreciable hardening at 250° C. and the maximum diffuseness at 200° C. occurred at the same time as maximum hardness, the diffuseness is probably due to internal strains set up during precipitation. At both ageing temperatures the change in lattice parameter is continuous, reaching a constant value corresponding to the composition of the equilibrium solid solution at the temperature of ageing. This occurred earlier at 250° C. than at 200° C. (Fig. 21).

Ageing at 125° C., as distinct from 200° and 250° C., was not accompanied by a continuous decrease in parameter throughout the

ageing process. After approximately 46 days, the time at which hardening began, the diffraction rings started to become diffuse though no change in lattice parameter had taken place. Precipitate was then visible at the grain boundaries and within the grains. With longer ageing times the diffuseness increased (see Fig. 21) and at the same time there was a decrease in parameter. After 163 days the diffraction appearing in the position of the  $\alpha_2$  ring of each doublet was much broader and at least as intense as that in the corresponding  $\alpha_1$  position. On further ageing this effect strengthened and up to 236 days the lattice parameter decreased, showing that continuous precipitation was occurring. After 236 days the  $\alpha_2$  ring appeared to be duplex, a further faint ring appearing inside the  $\alpha_2$  ring. This faint ring was due to the  $\alpha_2$  diffraction of a new solid solution of lower parameter and the reason why, at an earlier stage in the precipitation, the  $\alpha_2$  ring of the supersaturated solid solution had become more intense relative to the  $\alpha_1$  ring was that the two rings were superimposed. On further ageing the new solid-solution lines decreased in parameter and increased in intensity, whilst the parameter of the old solid-solution lines remained constant and decreased in intensity. Fig. 21 shows the change in lattice parameter of the old and new solid solutions, the size of spot again representing the diffuseness of the diffraction rings. It should be remembered that discontinuous precipitation may have been occurring from the beginning of the ageing process, but because of the lack of sensitivity of the X-ray method the new solid solution may not have been detected in the early stages. At 125° C., therefore, the ageing process appears to be first continuous, though some discontinuous precipitation may have been taking place, then discontinuous, followed by continuous precipitation in the new solid solution.

(ii) *Aluminium-10% Magnesium Alloy*.—Table III gives the results of lattice-parameter measurements on the super-purity 10% magnesium alloy aged at 200°, 230°, and 300° C.

In the initial stages of ageing there is a decrease in parameter of the supersaturated solid solution, and new solid-solution lines appear which increase in intensity and decrease in parameter as ageing proceeds. As mentioned above, it is possible that discontinuous precipitation was taking place during the initial stages of ageing, though the results show that continuous precipitation occurs at the same time as discontinuous. Thus, in this alloy also, precipitation appears to be first continuous, then discontinuous, followed by continuous precipitation in the new solid solution. The diffraction rings for the old solid solution increased in diffuseness while the hardness was increasing, and the new solid-solution lines which first appeared just before or



at maximum hardness were also diffuse. This diffuseness remained until the old solid-solution rings had disappeared and then the new solid-solution rings began to sharpen. Fig. 13 (Plate IV) shows a typical photograph of a 10% magnesium specimen aged at 200° C. for 1 day. The old and new solid-solution doublet can be seen, approximately 20% of new solid solution being present.

TABLE III.—*Lattice-Parameter Measurements (kX.) on Super-Purity Aluminium-10% Magnesium Alloy.*

Ageing Time	Ageing Temperature					
	200° C.		230° C.		300° C.	
	Old solid solution	New solid solution	Old solid solution	New solid solution	Old solid solution	New solid solution
	kX.	kX.	kX.	kX.	kX.	kX.
As quenched	4.091 <sub>7</sub>	...	4.091 <sub>7</sub>	...	4.091 <sub>7</sub>	...
1 hr. "	...	...	...	...	4.090 <sub>8</sub> (99)	...
2 " "	...	...	4.091 <sub>0</sub> (100)	...	...	...
3 " "	...	...	...	...	4.086 <sub>8</sub> (40)	4.072 <sub>9</sub> (60)
6 " "	...	...	...	...	4.084 <sub>8</sub> (20)	4.073 <sub>8</sub> (80)
12 " "	...	...	4.088 <sub>8</sub> (60)	4.065 <sub>7</sub> (40)	...	4.072 <sub>8</sub> (100)
1 day "	4.083 <sub>1</sub> (80)	4.059 <sub>8</sub> (20)	N.M. (5)	4.063 <sub>8</sub> (95)	...	4.070 <sub>8</sub> (100)
3 days "	4.082 <sub>4</sub> (30)	4.057 <sub>7</sub> (70)	...	4.060 <sub>7</sub> (100)	...	...
7 " "	N.M. (5)	4.057 <sub>4</sub> (95)	...	...	...	...
12 " "	N.M. (1)	4.057 <sub>0</sub> (99)	...	4.059 <sub>1</sub> (100)	...	...

N.M. = Not measurable. Figures in brackets give estimated percentage of solid solution.

The X-ray photographs indicated that the new solid solution had the same orientation as the old. Fig. 14 (Plate IV) shows a photograph of the 10% magnesium alloy, solution-treated and aged at 230° C. for 12 hr., in which the specimen was oscillated but not scanned, hence giving individual spots instead of continuous rings. The diffractions from the corresponding grain of new and old solid solution can be seen to be on the same layer line, showing that the new solid solution has the same orientation as the old. This is probably the reason why it has not been possible to reveal the new solid solution by etching.

Another feature of the X-ray photographs is that the background between the two solid-solution doublets became more and more intense as the discontinuous precipitation proceeded, so that although most of the alloy consisted of the two main solid solutions there were small regions of intermediate composition, i.e. some continuous precipitation was occurring.

#### (b) Structure of Beta Precipitate.

For comparison with the aged wires a photograph (Fig. 15d, Plate V) was taken of annealed filings from an alloy cast to the composition

of the beta phase (36% magnesium), which gave interplanar spacings in agreement with Lacombe's<sup>4</sup> equilibrium beta. Photograms of the 7% magnesium alloy aged at 125° C. for 357 days and at 200° C. for 53 days, and of the 10% magnesium alloy aged at 230° C. for 12 days, are also given in Fig. 15 (Plate V).

Three types of pattern were obtained from the precipitate in addition to the solid-solution lines :

(1) Sharp diffractions which did not correspond to the equilibrium beta pattern and will be called  $\beta_1$ .

(2) Diffuse diffractions which also did not correspond to equilibrium beta and will be called  $\beta_2$ . The spacing of these lines corresponded to those of some of the sharp  $\beta_1$  lines.

(3) Sharp diffractions which corresponded to the equilibrium beta (called  $\beta$ ). It is possible that  $\beta_1$  and  $\beta_2$  have the same structure, but for the sake of clarity they have been differentiated. Some of the weak  $\beta_1$  lines correspond with weak lines in the equilibrium  $\beta$  structure.

On ageing the 7% magnesium alloy at 200° C. sharp  $\beta_1$  lines appeared after about 3 days, and after 7 days equilibrium  $\beta$  lines were observed. After 53 days (Fig. 15a) the equilibrium  $\beta$  lines were predominant, and only the strongest  $\beta_1$  lines remained. At this temperature continuous precipitation occurred throughout.

On ageing the 7% magnesium alloy at 125° C.  $\beta_1$  lines were first observed after 80 days and became stronger up to 156 days. On further ageing some of the  $\beta_1$  lines became diffuse and more intense, giving the  $\beta_2$  pattern (Fig. 15b). At the same time discontinuous precipitation started. The equilibrium  $\beta$  pattern was not observed on ageing at 125° C. for up to 411 days, the pattern remaining as shown in Fig. 15b.

The diffraction pattern from the 10% magnesium alloy aged for 12 days at 230° C. showed only the  $\beta_2$  lines and the strongest equilibrium  $\beta$  lines (Fig. 15c). In this specimen precipitation was discontinuous.

In general, these results confirm those of previous workers<sup>2,4</sup> that the precipitate first formed during the ageing of aluminium-magnesium alloys is not stable and later transforms into the equilibrium beta precipitate. Up to 411 days, however, the 7% magnesium alloy aged at 125° C. showed no lines due to equilibrium beta. When continuous precipitation takes place the unstable precipitate  $\beta_1$  transforms directly to the equilibrium beta, whereas when precipitation is discontinuous there is an intermediate stage which gives rise to the diffuse lines which have been called  $\beta_2$ .

The structure of the equilibrium beta phase is incompletely known, and it has not been possible to determine structures which would

account for the  $\beta_1$  and  $\beta_2$  patterns. Consequently, it is not possible to say whether  $\beta_1$  and  $\beta_2$  have two distinct structures (i.e. whether three forms of beta can exist), or whether the  $\beta_1$  and  $\beta_2$  patterns are derived from the same structure. No suggestions can therefore be put forward as to the mechanism of formation of beta.

#### IV.—DISCUSSION OF THE RESULTS.

X-ray analysis shows that precipitation from the supersaturated solid solution of 7% magnesium in aluminium is entirely continuous at ageing temperatures of 200° and 250° C. At 125° C., however, precipitation was at first apparently continuous, then discontinuous together with continuous, followed by continuous precipitation in the new solid solution. The latter precipitation mechanism was also found for super-pure aluminium-10% magnesium alloy at temperatures up to 300° C. The continuous precipitation in the new solid solution may be caused either (i) by precipitation in the new solid solution areas, or (ii) by diffusion of solute away from these areas to the already precipitated  $\text{Mg}_2\text{Al}_3$ , or possibly a combination of the two. From the results obtained it is not possible to say which of these processes is taking place. Gayler<sup>14</sup> asserts that, in general, discontinuous precipitation is followed by continuous, though Cohen<sup>15</sup> by X-ray measurements has shown that on ageing a silver-copper alloy at low temperatures continuous precipitation precedes the discontinuous variety. For a similar alloy aged at high temperatures, Gayler<sup>13</sup> by microscopic examination found the reverse to be true. Geisler, Barrett, and Mehl<sup>16</sup> by microscopic examination also found continuous precipitation preceding discontinuous during the ageing of an aluminium-silver alloy.

Gayler<sup>13</sup> suggests that the type of precipitation is controlled by the degree of supersaturation, high degrees of supersaturation favouring discontinuous precipitation. The occurrence of continuous precipitation is then accounted for by assuming that it takes place when the solid solution has become sufficiently depleted by the discontinuous precipitation. Hardy<sup>17</sup> points out that the objection to Gayler's theory is that the whole of the crystal would have to provide solute for discontinuous precipitation, thus necessitating diffusion over improbably long distances, and the proposed mechanism would, moreover, be expected to alter the lattice parameter of the old solid solution. Instead, Hardy<sup>17</sup> suggests that if the lattice strain set up by precipitation provides sufficient energy for fragmentation and recrystallization, precipitation is of the discontinuous type.

The present results do not favour Gayler's proposal, because for

the same degree of supersaturation (2.9% magnesium) (see Table IV), discontinuous precipitation occurred in the 10% magnesium alloy but not in the 7% alloy. It must be pointed out, however, that the former alloy was of high purity, while the latter was of commercial purity. Nevertheless, the results do lend support to Hardy's view, in that when discontinuous precipitation occurred, the magnitude of hardening (i.e. degree of lattice strain) was always greater than when continuous precipitation occurred. Similar results have been found for aluminium-zinc alloys.<sup>18</sup>

TABLE IV.—*Effect of Temperature and Degree of Supersaturation on Precipitation.*

Ageing Temperature, °C.	Aluminium-7% Magnesium Alloy		Aluminium-10% Magnesium Alloy	
	Degree of Supersaturation, % Mg.	Type of Precipitation	Degree of Supersaturation, % Mg.	Type of Precipitation
125	5.40	Discontinuous	7.44	n.d.
200	4.30	Continuous	6.34	Discontinuous
230	3.70	n.d.	5.74	Discontinuous
250	2.90	Continuous	4.94	Discontinuous
300	0.80	n.d.	2.84	Discontinuous

n.d. = not determined.

Gayler<sup>14</sup> considers that the new solid solution which is formed during discontinuous precipitation has a composition corresponding to that which is in equilibrium at the temperature of ageing, i.e. no change in lattice parameter of the new solid solution should occur on further ageing at the same temperature. The results for the aluminium-magnesium alloys clearly disprove this, for on further ageing at the same temperature the lattice parameter of the new solid solution decreases. Fink and Smith<sup>19</sup> obtained similar results for an aluminium-5% copper alloy. Cohen,<sup>15</sup> however, for a silver-copper alloy found no change in lattice parameter of the new solid solution on further ageing. The main difference between the three systems, aluminium-magnesium, aluminium-copper, and silver-copper, is that, on ageing, the precipitate first appearing in the aluminium-magnesium and aluminium-copper alloys is not the equilibrium form, while the precipitate in the silver-copper alloys is the equilibrium copper-rich solid solution. It can be shown<sup>21</sup> that if the first-formed precipitate is a non-equilibrium type then the new solid solution which is precipitated during discontinuous precipitation will have a solute concentration greater than that of the solid solution in equilibrium at the temperature of ageing. If the non-equilibrium precipitate then changes to the

equilibrium form, as it does in the aluminium-magnesium and aluminium-copper systems, the new solid solution must also change to the equilibrium solid solution (see Fig. 22). Thus, when discontinuous precipitation takes place in the aluminium-magnesium and aluminium-copper alloys a change in the lattice parameter of the new solid solution is to be expected during subsequent ageing at the same temperature.

When discontinuous precipitation occurs, it is usually accompanied by the formation of new solid solution starting at the grain boundaries and spreading into the grains, but this has not been observed with the aluminium-magnesium alloys. This is possibly because the orientation of the new solid solution is the same as the old, tending to prevent differentiation by chemical etching. Continuous precipitation, on the other hand, is generally accompanied by the formation of a Widmanstätten structure, but for the aluminium-magnesium alloys continuous and discontinuous precipitation are both accompanied by the Widmanstätten structure, and as the ageing temperature increases the tendency for this structure to form lessens, the temperature at which it occurs being higher for the 10% than the 7% magnesium alloy. These results are in agreement with those obtained by Geisler, Barrett, and Mehl.<sup>6</sup> The Widmanstätten structure observed in the aluminium-magnesium alloys appears to consist of "rods" precipitated along three crystallographic directions.

From the contradictory results obtained by Geisler *et al.*<sup>6</sup> and Calvet *et al.*<sup>5</sup> as to the existence of platelet formation (i.e. Guinier-Preston zones) on ageing aluminium-magnesium alloys, it is not possible to say whether hardening is due to coherency strains or not. Hardening does not occur in the aluminium-magnesium alloys until visible precipitation has taken place within the grains, and the magnitude of hardening is very much smaller than in the aluminium-copper, aluminium-silver, and aluminium-zinc alloys, where platelet formation is known to occur. The Widmanstätten type of precipitation was observed before hardening had begun, which together with Gayler's<sup>20</sup> observation that this type of precipitation takes place when the strains

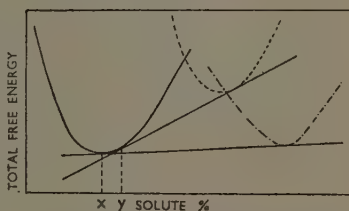


Fig. 22.—Diagram Showing how Concentration of Solid Solution Changes from  $y\%$  to  $x\%$  as the Non-Equilibrium Precipitate Transforms to the Equilibrium Form.

KEY.  
 — Free-energy curve for a solid solution.  
 - - - Free-energy curve for non-equilibrium precipitate.  
 - · - · - Free-energy curve for equilibrium precipitate.

resulting from platelet formation have, in the main, been relieved, suggests that hardening in the aluminium-magnesium alloys is not due to strains set up by the formation of coherent platelets but is possibly attributable to the growth of precipitated particles, maximum hardness being obtained at a critical particle size.

X-ray analysis confirms the results of other workers in that the beta precipitate which is first formed is unstable, and as ageing proceeds transforms into the equilibrium form.

#### ACKNOWLEDGEMENTS.

The work recorded in this paper was undertaken as part of a research on the stress-corrosion of light alloys carried out for the Principal Director of Scientific Research (Aircraft), Ministry of Supply.

The authors wish to thank the Chief Scientist, Ministry of Supply, and the Director and Council of the British Non-Ferrous Metals Research Association for permission to publish this paper. They are also indebted to Dr. M. L. V. Gayler, Dr. A. G. Quarrell, and Mr. R. J. Eborall for many helpful discussions.

#### REFERENCES.

1. E. C. W. Perryman and S. E. Hadden, *J. Inst. Metals*, 1950, **77**, 207.
2. W. L. Fink and D. W. Smith, *Trans. Amer. Inst. Min. Met. Eng.*, 1937, **124**, 162.
3. R. M. Brick, A. Phillips, and A. J. Smith, *Trans. Amer. Inst. Min. Met. Eng.*, 1935, **117**, 102.
4. P. Lacombe, *Rev. Mét.*, 1944, **41**, 180, 217, 259.
5. J. Calvet, A. Guinier, P. Jacquet, and A. Silberstein, *Compt. rend.*, 1939, **208**, 1903, and *Métaux et Corrosion*, 1939, **14**, 139.
6. A. H. Geisler, C. S. Barrett, and R. F. Mehl, *Trans. Amer. Inst. Min. Met. Eng.*, 1943, **152**, 201.
7. N. F. Mott, *J. Inst. Metals*, 1937, **60**, 267 (discussion).
8. Z. Matyáš, *Phil. Mag.*, 1949, [vii], **40**, 324.
9. W. L. Fink and L. A. Willey, *Trans. Amer. Inst. Min. Met. Eng.*, 1937, **124**, 78.
10. M. L. V. Gayler, *J. Inst. Metals*, 1946, **72**, 543.
11. J. K. Jetter and R. F. Mehl, *Trans. Amer. Inst. Min. Met. Eng.*, 1943, **152**, 166.
12. F. Seitz, "The Physics of Metals," p. 180. 1943: New York (McGraw-Hill Book Co., Inc.).
13. M. L. V. Gayler and W. E. Carrington, *J. Inst. Metals*, 1947, **73**, 625.
14. M. L. V. Gayler, *J. Inst. Metals*, 1947, **73**, 681.
15. M. Cohen, *Trans. Amer. Inst. Met. Eng.*, 1937, **124**, 138.
16. A. H. Geisler, C. S. Barrett, and R. F. Mehl, *Trans. Amer. Inst. Min. Met. Eng.*, 1943, **152**, 182.
17. H. K. Hardy, *J. Inst. Metals*, 1948-49, **75**, 707.
18. E. C. W. Perryman and J. C. Blade, *J. Inst. Metals*, 1950, **77**, 263.
19. W. L. Fink and D. W. Smith, *Trans. Amer. Inst. Min. Met. Eng.*, 1936, **122**, 284.
20. M. L. V. Gayler, *Inst. Metals: Symposium on Internal Stresses*, 1948, p. 255. (Monograph and Report Series, No. 5.)
21. H. Lipson and A. J. C. Wilson, *J. Iron Steel Inst.*, 1940, **142**, 107p.



# HEAT EXTRACTION AT CORNERS AND CURVED SURFACES IN SAND MOULDS.\*

1296

By R. W. RUDDLE,† M.A., A.I.M., MEMBER, and R. A. SKINNER,‡ B.Sc., STUDENT MEMBER.

(Communication from The British Non-Ferrous Metals Research Association.)

## SYNOPSIS.

The rate at which a sand mould removes heat from corners (both external and re-entrant) and curved surfaces of castings has been determined by means of temperature measurements made in the mould. Heat is extracted considerably more rapidly from a convex surface or an external corner of a casting than from a plane surface; the difference is decreased by increasing the radius of the surface or by radiusing the corner. The rate of heat extraction at a re-entrant corner is slightly less than that from a plane surface. The solidification times of castings can be roughly calculated using a mathematical analysis of the heat flow through a plane surface, and more accurate estimates are possible by using the correction factors given in this paper for corner and curvature effects.

## I.—INTRODUCTION.

IN previous work<sup>1</sup> on the chilling power of mould materials, the rate at which a plane wall of a sand mould removes heat from a casting was determined experimentally and shown to be represented by a mathematical equation with good accuracy.

The solidification times of sand-cast pure aluminium cylinders calculated on this basis exceeded those observed,<sup>2</sup> and it was concluded that heat extraction from the corners and curved surfaces of the cylinder is considerably greater than that from the plane faces. The present work was therefore undertaken with the object of determining how much more rapidly heat is removed from these locations in comparison with the plane mould wall. It was hoped that the results of these determinations would enable calculations of the freezing times of castings to be made with greater accuracy than hitherto possible.

## II.—THEORY.

The mathematics of the rate of heat extraction by a plane mould wall have been discussed in an earlier paper.<sup>1</sup> For the plane mould face, the total quantity of heat extracted at any given time may be

\* Manuscript received 14 June 1950. The work described in this paper was made available to members of the B.N.F.M.R.A. in a confidential research report issued in August 1949.

† Head of Melting and Casting Section, British Non-Ferrous Metals Research Association, London.

‡ Formerly Research Bursar, now Investigator, British Non-Ferrous Metals Research Association, London.

determined mathematically if the physical constants of the mould material are known, or may be estimated by measuring the area under the experimentally determined graph of the temperature distribution in the mould. Mathematical analysis of the heat extraction by corners and cylindrical mould surfaces is complicated, and in some important cases no solutions are available. Recourse was therefore made to empirical determination, the results obtained being compared, where possible, with those computed mathematically.

The method employed was briefly as follows. The temperature distribution around the mould corner or cylindrical mould wall was determined experimentally and the results obtained were plotted as two-

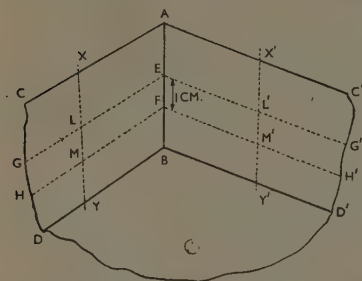


FIG. 1.—Diagram of Corner in Mould.

dimensional isothermal diagrams (in the case of the corners) or one-dimensional temperature/distance curves (in the case of the cylindrical mould walls). The heat content of the mould was calculated in the manner described in Appendix I (p. 53), after measuring each diagram with a planimeter. In each experiment the heat content of the mould was thus calculated for several different times

after the mould was filled; the figures so obtained enabled the total heat extracted by the mould to be plotted against the time.

To make the following sections of the paper readily understandable, it is necessary to define some of the terms used in connection with corners. This may best be done with the aid of Fig. 1, which is a three-dimensional illustration of a right-angled corner (edge) of a mould viewed from inside the mould cavity. In this figure the corner is formed by the two planes  $ABDC$  and  $ABD'C'$  which intersect in the line  $AB$ . The length of the line  $AB$  is termed the length of the corner. For obvious reasons, in considering the heat extraction by corners, it is desirable to refer the results obtained to corners of unit length, i.e. to the corner of a 1-cm.-thick slice of the mould at right angles to  $AB$ ; this is indicated in Fig. 1 by the dotted lines  $EG$ ,  $FH$ , &c. In the description below of the experimental results a corner of 1 cm. length should therefore be understood unless otherwise stated.

It is convenient to express the results obtained with corners as the difference between the heat extracted by the areas adjacent to the

corner and that extracted by a plane mould wall of equal area. The results described later show that beyond a certain distance from the corner the isotherms in the mould are substantially unaffected by the corner; this distance is indicated in Fig. 1 by the lines  $XY$  and  $X'Y'$ . The influence of the corner is therefore confined to the areas  $EFML$  and  $EFM'L'$  and the difference in heat referred to above is the heat extracted through these areas less the heat extracted by an equal area of a plane mould wall.

It should be pointed out that the positions of the lines  $XY$  and  $X'Y'$  are in a sense arbitrary, there being no sharp line of demarcation between the region of the mould affected by the corner and the region in which the isotherms are parallel to the mould wall.\* However, the exact position of  $XY$  and  $X'Y'$  is unimportant, for, provided that these lines are far enough from the apex of the corner, the difference between the heat extracted by the corner and that extracted by an equal area of a plane mould wall is not sensibly affected by the magnitude of the areas  $EFML$  and  $EFM'L'$ .

### III.—MATERIALS AND TECHNIQUE.

The following mould shapes were investigated :

- (1) External corners (edges) : \* (a) Left sharp (about  $\frac{1}{32}$  in. rad.)
- (b) Rounded to  $\frac{1}{2}$  in. rad. (c) Rounded to 1 in. rad.
- (2) A sharp re-entrant corner (edge) of about  $\frac{1}{32}$  in. rad.†
- (3) Cylindrical surfaces of the following dimensions : (a) 2 in. ;
- (b) 3 in. ; (c) 5 in. dia.

All the corners investigated were right-angled. The general technique was similar to that described in the earlier paper.<sup>1</sup>

The casting used for the experiments with external corners was a 6-in. cube with two vertical edges left sharp, one rounded to  $\frac{1}{2}$  in. and one rounded to 1 in. rad. ; only one of these corners was studied in a single experiment. The casting was run through a  $1\frac{1}{4}$ -in.-dia. downgate into the centre of the top face of the casting.

For the re-entrant corner a cylindrical casting was used, 12 in. dia.  $\times$  6 in. high, with a right-angled "cheese" of 7 in. arm-length missing and providing the re-entrant corner. The  $1\frac{1}{4}$ -in.-dia. downgate was attached to the top surface of the casting at a point near the circumference opposite to the apex of the missing part.

The dimensions of the castings employed for the experiments with cylindrical surfaces were as follows : 2 in. dia.  $\times$  4 in. long, 3 in. dia.  $\times$  6 in. long, 5 in. dia.  $\times$  10 in. long. All these castings were moulded with

\* Rigorously, the corner should be regarded as extending to infinity.

† The external and re-entrant corners referred to are respectively external and re-entrant corners of the casting, not of the mould cavity.

their longitudinal axes horizontal and were run at one end through  $1\frac{1}{4}$ -in.-dia. downgates attached to the upper surfaces of the cylinders.

The moulds were made from silica sand of the grading given below, bonded with 5% bentonite :

B.S. Sieve Nos.	Percentage
— 30 + 44	2.2
— 44 + 60	23.8
— 60 + 100	64.3
— 100 + 150	6.1
— 150 + 200	2.4

The moulds were dried at 120° C. for 15 hr. and were allowed to cool to room temperature before casting. After drying, the moulds had a bulk density of about 1.50 g./c.c.

Sand temperatures were measured by moulding a grid of up to 28 Chromel/Alumel thermocouples (28 B. and S. gauge) into the drag in the positions shown in the figures giving the observed isotherms. The parting plane was built up well above the plane of the thermocouples. The couple wires were arranged to approach the weld beads approximately along the isotherms, to minimize any conduction of heat along the wires; after casting, the couple positions were measured with a pair of dividers after carefully scraping the sand away.

Most of the work was carried out using the aluminium-30% copper alloy employed in earlier work;<sup>1</sup> with this alloy the interface temperature remains substantially constant for a long period. An alloy of copper with 0.5% lead was used to investigate the effect of higher interface temperature on the heat extraction at corners. Normal melting and degassing techniques for each alloy were employed, and the melts were poured with approximately 100° C. superheat. The moulds were filled as rapidly as possible. The time zero was taken at half-way through pouring.

The sand temperatures were recorded by the Tinsley D.C. amplifier and a high-speed pen recorder used previously.<sup>1</sup> The amplifier was arranged to give full-scale deflection of the recorder for a 12 mV. input; any excess potential from the couples was backed-off by a calibrated potentiometer suppression unit. A motor-driven selector switch connected each couple in turn to the amplifier; the speed of the switch was adjusted so that each couple was connected for about 2 sec. The accuracy of measurement was  $\pm 4^\circ$  C.

#### IV.—RESULTS AND DISCUSSION.

##### 1. *External Corners.*

Figs. 2-4 show the isotherms round the sharp, the  $\frac{1}{2}$ -in.-radius, and 1-in.-radius corners 15 min. after pouring, respectively; these

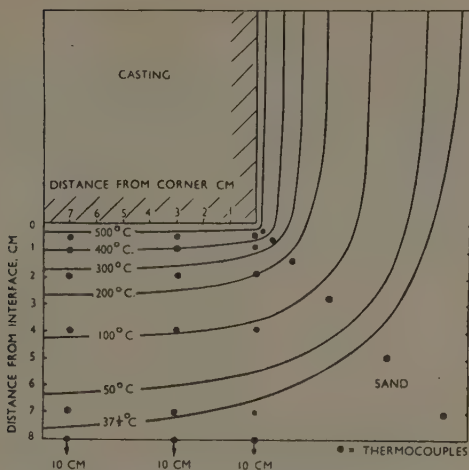


FIG. 2.—Isotherms at a Sharp Corner of a Sand Mould 15 min. after Pouring. Interface temperature 548° C.

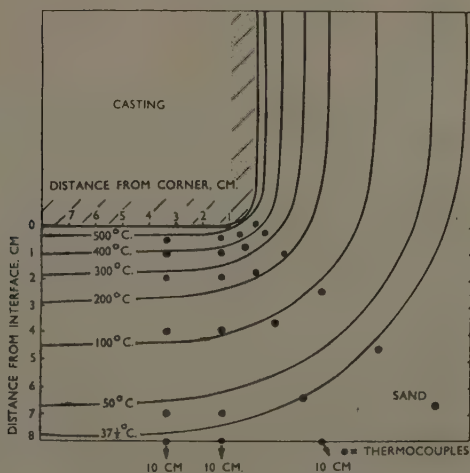


FIG. 3.—Isotherms at a Corner Rounded to  $\frac{1}{2}$  in. rad., of a Sand Mould 15 min. after Pouring. Interface temperature 548° C.

figures were all obtained using an aluminium-30% copper alloy casting (interface temperature  $548^{\circ}\text{C.}$ ). It can be seen that the effect of the corner extends for about 5-8 cm. on either side of the corner; at greater distances the isotherms are practically straight and parallel to the mould walls. Furthermore, the effect of the corner is small at distances beyond about 3-5 cm. from the apex, so that for most practical purposes the corner effect may be regarded as being concentrated in the 3 cm. of mould on either side.

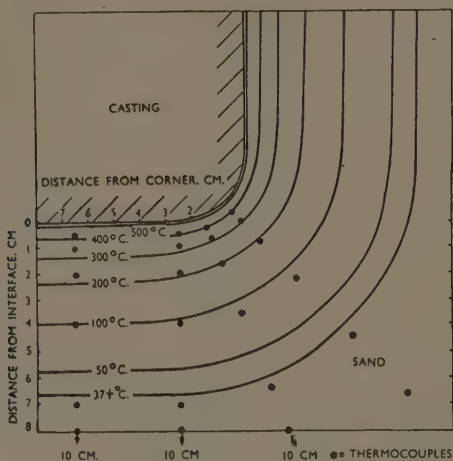


FIG. 4.—Isotherms at a Corner Rounded to 1 in. rad., of a Sand Mould 15 min. after Pouring. Interface temperature  $548^{\circ}\text{C.}$

Fig. 5 illustrates the difference between the amounts of heat extracted from unit length of these corners and the amounts of heat that would have been extracted by an equal area of a plane wall face; these differences were calculated from the heat contents of the mould measured as described in Section II and Appendix I and are plotted for times up to 30 min.

The curves in Fig. 5 show that corners extract a considerable amount of heat in excess of that removed in the same time by the equivalent plane wall, the difference being greatest for the sharp corner and least for the 1-in.-radius corner. The difference curves are all approximately straight lines passing through the origin, suggesting that the equation giving the rate of heat extraction ( $dQ/dt$ ) by a corner is of the form;



$$\frac{dQ}{dt} = \frac{nqt^{\frac{1}{2}}}{2} + C \quad . \quad . \quad . \quad . \quad . \quad (1)$$

where  $q$  is the mould constant for the plane wall,<sup>1</sup> \*  $n$  is the number of square centimetres of mould surface involved, and  $C$  is a constant. Integration of this equation between the limits 0 and  $t$  yields :

$$Q = nqt^{\frac{3}{2}} + Ct \quad . \quad . \quad . \quad . \quad . \quad (2)$$

In this equation the term  $nqt^{\frac{3}{2}}$  represents the amount of heat that would be removed by a plane mould wall of the same area (proportional to the square root of the time), and the term  $Ct$  represents the difference

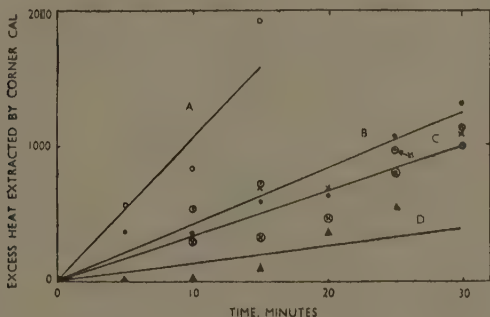


FIG. 5.—Excess Heat Extracted by Corners.

KEY.

- A ○ Sharp corner; interface temperature 1083° C.  
 B ● " " " " 548° C.  
 C × " " " " (repeat experiment).  
 D ▲ " " 1 in. " " " " (repeat experiment).

between the heat removed by the corner and that extracted in the same time by an equal area of plane mould wall—this latter term is directly proportional to the time and is the quantity plotted in Fig. 5. These curves yield the following approximate values for the constant  $C$  for an interface temperature of 548° C. :

	$C$
Sharp corner . . . . .	41 cal./cm. min.
$\frac{1}{2}$ -in.-rad. corner . . . . .	33 cal./cm. min.
1-in.-rad. corner . . . . .	13 cal./cm. min.

\* The mould constants calculated from the temperature measurements were 107 cal./cm.<sup>2</sup> min.<sup>1</sup> at 548° C. and 260 cal./cm.<sup>2</sup> min.<sup>1</sup> at 1083° C. These figures differ slightly from those given for synthetic sand in the earlier paper,<sup>1</sup> probably largely on account of small differences in the grading, &c., of the mould materials used.

The isotherms in the sand round a sharp corner of a copper casting (interface temperature  $1083^{\circ}\text{C.}$ ) are shown in Fig. 6, and the quantity of extra heat extracted by this corner is plotted against time in Fig. 5. The value of  $C$  obtained from this curve is  $104\text{ cal./cm. min.}$  Comparison of the difference curves for the sharp corners in the aluminium- and copper-base castings shows that the differences are approximately in the ratio of the chilling powers of the mould material at the two interface temperatures concerned, as would be expected on theoretical grounds. Thus the values of the constant  $C$  for the copper- and aluminium-base alloy castings are respectively  $104$  and  $41\text{ cal./cm. min.}$ ; the ratio of

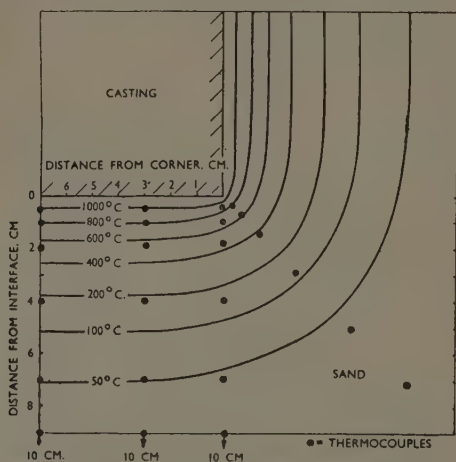


FIG. 6.—Isotherms at a Sharp Corner of a Sand Mould 15 min. after Pouring. Interface temperature  $1083^{\circ}\text{C.}$

these figures is approximately 2.5; the respective chilling powers are  $260$  and  $107\text{ cal./cm.}^2\text{ min.}^{\frac{1}{2}}$ , the ratio between these quantities being about 2.4.

The values of  $C$  given above are the corrections to be applied for every centimetre length of the corner. They can be employed to calculate the solidification times of castings, but their use renders the calculation somewhat cumbersome, necessitating the solution of a quadratic equation.

A simpler method is to employ a factor equal to :

$$\frac{\text{Heat removed by corner}}{\text{Heat removed by plane mould wall of equal area}}$$

The factor is, of course, equal to :

$$\frac{nqt^{\frac{1}{2}} + Ct}{nqt^{\frac{1}{2}}} = 1 + \frac{Ct^{\frac{1}{2}}}{nq} \quad . \quad . \quad . \quad . \quad . \quad (3)$$

and is therefore a function of surface area. Consequently, to make use of the factor it is necessary to define the area over which the effect of the corner is spread; in the present work the corner is regarded as extending for 3 cm. on either side for the sharp corner and the corner of  $\frac{1}{2}$  in. rad., and for 4 cm. in the case of the 1-in.-rad. corner. When the value of the factor is known, the "effective area" (i.e. the equivalent area of plane mould wall) of the corner may be obtained by multiplying the area of the corner by the factor.

Equation (3) also shows that the factor is a function of time, and Table I gives average values calculated for solidification times of up to 2 hr.

TABLE I.—Values of the Corner Factor  $\left(1 + \frac{Ct^{\frac{1}{2}}}{nq}\right)$ .

Solidification Time, min.	Factor Value		
	Sharp Corner (3 cm.)*	$\frac{1}{2}$ -in.-rad. Corner (3 cm.)*	1-in.-rad. Corner (4 cm.)*
5	1.1	1.1	1.0
10	1.2	1.2	1.0
15	1.2	1.2	1.1
20	1.3	1.2	1.1
25	1.3	1.3	1.1
30	1.4	1.3	1.1
40	1.4	1.3	1.1
50	1.5	1.4	1.1
60	1.5	1.4	1.1
75	1.6	1.5	1.1
90	1.6	1.5	1.1
105	1.7	1.5	1.2
120	1.7	1.6	1.2

\* Corners assumed to extend for these distances on either side of the apex.

Since the factor varies with time, the appropriate value must be obtained by a preliminary calculation of the solidification time, in which corner effects are ignored. The factor can then be used to compute a more accurate value of the solidification time. The method is illustrated in the calculation in Section V (p. 50).

## 2. Re-Entrant Corners.

The isotherms for a re-entrant corner cast in aluminium-30% copper are shown in Fig. 7, and it will be seen that the effect of the corner extends over a much longer distance than in the case of an

external corner, viz. up to 12 cm. or more, 15 min. after pouring. The curve for the heat content of the corner, measured over a 14 cm. square section, is given in Fig. 8, together with the curve for the heat that would have been extracted by the same area of a plane mould face; this latter curve was determined at the same time as the curve for the corner. The curve for the re-entrant corner falls slightly below that for the flat face, but the difference is small and possibly inside the limits of experimental error. An almost identical curve was obtained on repeating the experiment.

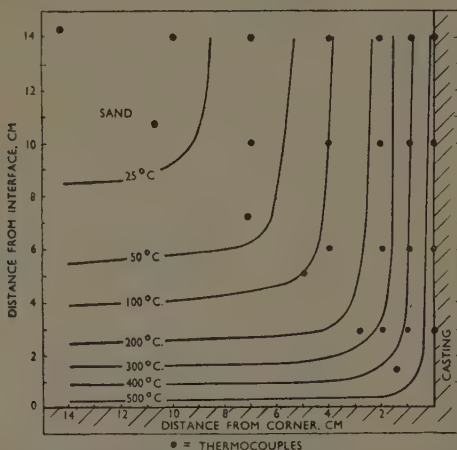


FIG. 7.—Isotherms at a Re-Entrant Corner 15 min. after Casting.  
Interface temperature 548° C.

A mathematical solution of this problem is available,<sup>3</sup> and this shows that the difference between the rate of heat extraction by a re-entrant corner of unit length and a plane mould wall of equal area is  $4K(\theta - \theta_0)/\pi$  cal./sec., where  $K$  is the thermal conductivity of the mould,  $\theta$  is the temperature of the metal/mould interface, and  $\theta_0$  is the initial temperature of the mould. It follows that the difference in the total heat extracted in a time  $t$  is  $4Kt(\theta - \theta_0)/\pi$  cal.

Since  $K$  is very small for a sand mould (approximately 0.0014 C.G.S. units), the difference to be expected is also small, amounting after 30 min. to about 10% of the heat extracted in that time by a plane mould wall. The experimental results obtained are therefore in substantial agreement with the mathematical analysis, and it seems

safe to conclude that, for sand moulds, the rate of heat extraction at a re-entrant corner is only slightly less than that at a plane mould wall.

At first sight this conclusion is at variance with the well-known fact that solidification is retarded at re-entrant corners in castings. Actually there is no discrepancy, because the conclusion merely states that the chilling power over the area of the re-entrant corner is little different from that of a plane mould face of equal area and ignores the fact that in a re-entrant corner this area of mould face affects the solidification

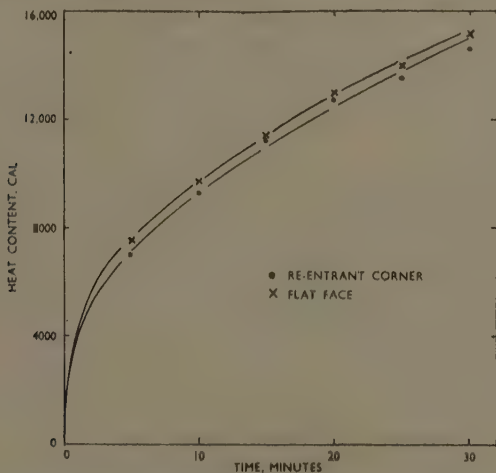


FIG. 8.—Diagram Showing Heat Extracted from a Re-Entrant Corner of a Casting by the Sand up to 14 cm. on either side of the corner. The heat extracted by a flat face of equal area is also shown.

of a greater volume of metal. The effect of a re-entrant corner on the solidification of a casting is readily seen from Fig. 9. In this figure a uniform skin of solid metal (the regions  $ABCD$  and  $AB'C'D'$ ) is assumed to form on the mould walls corresponding with the removal of a certain amount of heat by the mould. If this happens it is obvious that a prism of liquid metal (shown in Fig. 9 as the area  $ABEB'$ ), from which no heat has been extracted, will exist at the apex of the corner. In practice the skin formed is not of uniform thickness owing to conduction within the casting, and some solidification takes place at the apex, the solidification front being of the shape shown by the full line in Fig. 9; it is clear, however, that solidification is considerably retarded at the apex. It is, of course, true that the small difference in the rate

of heat extraction of the corner compared with the plane wall will be concentrated in the immediate region of the apex, and this might be an additional reason for the slow solidification at this point. However, the difference involved is small and can cause only a secondary effect.

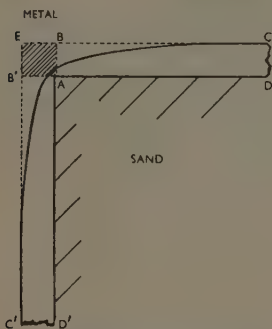


FIG. 9.—Diagram Showing How a Re-Entrant Corner Affects Solidification.

Similar reasoning in reverse applies to the external corner, but in this instance the fact that the mould corner extracts heat considerably more rapidly than the corresponding area of plane wall is an additional reason for the rapid solidification which occurs at such corners.

Although both theory and experiment show that the rate of heat extraction at a right-angled re-entrant corner is very little different from that of an equal area of plane mould wall, it is evident that this will no longer be true if the angle of the corner becomes more acute; a thin tongue of

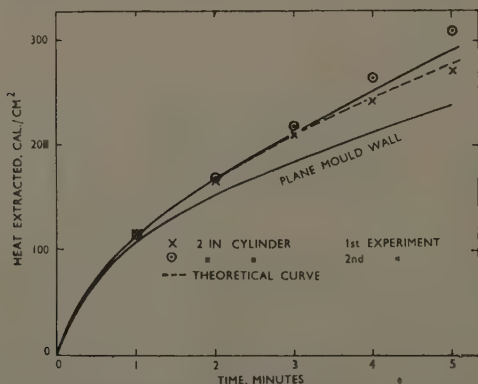


FIG. 10.—Heat Extracted per Unit Area from a 2-in.-dia. Cylinder. Interface temperature 548° C.

sand, for example, would clearly remove heat considerably more slowly than the corresponding area of plane wall. However, the conclusion reached probably covers the majority of cases met with in



practice, and is not likely to be invalidated by the presence of a radius at the corner.

### 3. Cylindrical Surfaces.

The heat-extraction curves for the 2-in.-dia. cylinder are given in Fig. 10, and similar curves for the 3-in.- and 5-in.-dia. cylinders in Fig. 11; the curve of Fig. 10 is replotted in Fig. 11 to render comparison

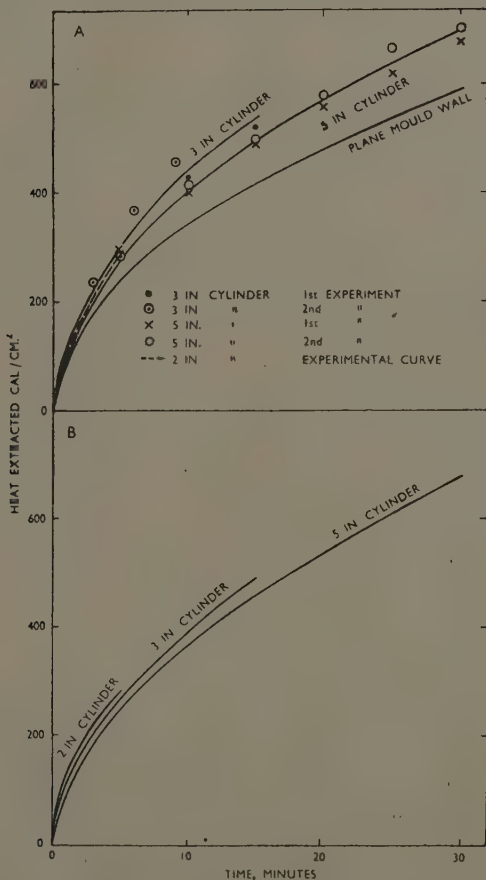


FIG. 11.—Heat Extracted per Unit Area from 3-in.- and 5-in.-dia. Cylinders.

A. Observed results.

B. Theoretical curves.

easy, and the heat-extraction curve for the plane mould wall is reproduced in both figures. Each curve represents the mean of two sets of experimental results.

The two figures show that the heat extracted per unit area of mould face from the 3-in.-dia. cylinder is slightly greater than from the 5-in.-dia. cylinder; the difference between the 2- and 3-in.-dia. cylinders is very small, the two curves almost coinciding. In all cases the total heat extracted in a given time was considerably in excess of that extracted by a plane mould wall.

The flow of heat from a cylindrical surface of a casting may be evaluated mathematically using a treatment based on that given by Jaeger<sup>4</sup> and described in Appendix II (p. 55) of the present paper. Theoretical heat-extraction curves have thus been constructed for each of the three cylinders, and are included in Figs. 10 and 11. The agreement between the theoretical and observed curves is fairly good, especially for the 2-in.- and 5-in.-dia. cylinders, and this confirms the validity of the mathematical approach. In the case of the 3-in.-dia. cylinder the agreement is not quite so good, the observed curve for this cylinder being anomalous in that it indicates a slightly higher rate of heat extraction than with the 2-in.-dia. cylinder. The difference between the curves for the 2-in.- and 3-in.-dia. cylinders is, however, small, and is probably within the limits of experimental error. It may be noted that had the results of the second experiment with the 3-in.-dia. cylinders (circled dots in Fig. 11 (A)) been ignored and only the results of the first experiment (dots in Fig. 11 (A)) been used, the curve would have fallen between those for the 2-in.- and 5-in.-dia. cylinders, as predicted by theory.

The influence of cylindrical surfaces may be allowed for in calculations of the solidification times of castings by employing a factor similar to that already given for mould corners :

$$\frac{\text{Heat removed by cylindrical surface}}{\text{Heat removed by plane mould wall of equal area}}$$

Values of the factor for solidification times up to 2 hr. are given in Table II. Both the observed and calculated factors are included in Table II; the calculated factors are recommended in preference to the observed factors, in view of the scatter shown by the points from which the experimental heat-extraction curves were constructed. It may be noted that where the experimental scatter (viewed as a percentage of the total heat) is least—i.e. at short times in the case of the 2-in.-dia. cylinders and long times in the case of the 5-in.-dia. cylinders—the agreement between the calculated and observed factors is very close.

It will be noted that the cylinder correction factors are in some cases greater than those for the radiused corners, despite the fact that the radii of the corners studied were generally smaller than those of the cylindrical surfaces. The reason for this apparent discrepancy is that, for purposes of calculation, the corner is regarded as extending for some distance on either side of the radiused part. The factors quoted for the radiused corners therefore represent the mean heat extraction through a cylindrical surface and two plane surfaces, and are therefore smaller than is the case if a cylindrical surface alone is considered.

TABLE II.—*Factor Values for Cylindrical Surfaces.*

Solidification Time, min.	Factor Value					
	2-in.-dia.		3-in.-dia.		5-in.-dia.	
	Calculated	Observed	Calculated	Observed	Calculated	Observed
1	1.07	1.06	1.02	...	1.01	...
2	1.10	1.10	1.04	...	1.01	...
3	1.12	1.14	1.05	...	1.02	...
4	1.14	1.18	1.07	...	1.03	...
5	1.16	1.22	1.09	1.25	1.04	1.17
10	1.28	...	1.14	1.28	1.06	1.17
15	1.32	...	1.19	1.27	1.10	1.18
20	1.35	...	1.26	...	1.12	1.18
25	1.37	...	1.30	...	1.14	1.18
30	1.39	...	1.32	...	1.17	1.19
40	1.45	...	1.34	...	1.23	...
50	1.50	...	1.37	...	1.26	...
60	1.54	...	1.40	...	1.28	...
75	...	...	1.44	...	1.30	...
90	...	...	1.47	...	1.32	...
105	...	...	1.50	...	1.34	...
120	...	...	1.53	...	1.35	...

#### 4. *Influence of the Mode of Solidification of the Casting.*

The experiments at the lower interface temperature were carried out using castings made in a eutectiferous alloy which solidifies in a more or less "pasty" manner.<sup>2,5</sup> It seemed possible, however, that castings in materials solidifying by "skin-formation" might be more prone to contract away from the mould wall, thereby reducing the rate at which the mould removes heat; these effects might, furthermore, be localized in certain parts of the casting. It is clear that effects of this nature, besides reducing the overall rate of heat extraction, might also affect the values of the empirical factors given in Section IV.1 and IV.3 above.

To determine whether such contraction effects are, in fact, important in "skin-forming" castings, a few of the experiments described above, in which the heat extraction by the mould from corners and cylindrical surfaces was measured, were repeated using castings made in pure aluminium. In each case the rate of heat extraction was found to be higher than with the corresponding castings in the eutectiferous aluminium-30% copper alloy, in proportion to the higher mould constant for an interface temperature equal to the melting point of aluminium. The values of the empirical factors in Table I were unaffected.

For example, with a pure aluminium casting, the value of the difference constant,  $C$ , for the sharp corner was found to be 47 cal./cm. min., compared with the figure of 41 cal./cm. min. obtained with the aluminium-30% copper alloy; the ratio between these two values is 1.15 : 1. The mould constants for the interface temperatures concerned ( $660^{\circ}$  and  $548^{\circ}$  C.) are 124 and 107 cal./cm.<sup>2</sup> min.<sup>3</sup>, these figures also being in the ratio 1.15 : 1. Similar results were obtained in experiments with cylindrical castings made in pure aluminium.

It was therefore concluded that, if it occurred, contraction away from the mould wall of the solid metal shell in the "skin-forming" castings did not appreciably affect the rate of heat extraction. The empirical factors given in Tables I and II may therefore be confidently used with sand castings solidifying by "skin-formation".

#### V.—CALCULATION OF THE SOLIDIFICATION TIME OF THE CASTINGS.

In previous work,<sup>2</sup> corner and surface-curvature effects were neglected in calculating the solidification times of cylinder castings, and this resulted in the calculated times being considerably in excess of those observed. For example, the time of solidification calculated for a 5-in.-dia. aluminium cylinder was 36 min., but the observed time was only 25.8 min.<sup>(2)</sup> Application of the data obtained in the present work to such calculations in order to make allowance for the increased heat extraction at corners and curved surfaces (but neglecting the runner system) results in greatly improved accuracy. The calculation of the solidification time of the aluminium cylinder cited above, when thus modified, yields a time of 23.4 min.—a figure showing good agreement with experiment. Other examples of similar improved agreement are given in another report.<sup>5</sup>

Since the primary object of the present work is the assembly of data which will enable the solidification times of castings to be calculated accurately, it is appropriate to describe in detail the way in which these calculations may be made.

As an example, suppose that it is required to calculate the solidification time of a 5-in.-dia.  $\times$  10-in. cylinder cast in copper with 100° C. superheat.

The data used in making the calculations are :

Melting point of copper	.	.	.	.	.	1083° C.
Heat of fusion of copper	.	.	.	.	.	49 cal./g. <sup>(6)</sup>
Specific heat of liquid copper	.	.	.	.	.	0.118 cal./g. °C. <sup>(6)</sup>
Casting weight	.	.	.	.	.	26,800 g.

The heat content of the casting above the solidus is therefore :

$$26,800 (49 + 100 \times 0.118) = 1,629,000 \text{ cal.}$$

The surface of the casting may be divided into four areas as shown in Fig. 12: *A*, the cylindrical surface to within 3 cm. of the ends (774 cm.<sup>2</sup>); *B*, the cylindrical surfaces within 3 cm. of the corners (239 cm.<sup>2</sup>); *C*, the annuli on the end faces, 3 cm. from the corner (183 cm.<sup>2</sup>); *D*, the areas inside the annuli (71 cm.<sup>2</sup>). The total heat extracted from the casting in time *t* is found in the following way. Each of the four areas *A*, *B*, *C*, and *D* is multiplied by the appropriate factors \*

(given in Section IV) to take into account the corner and surface-curvature effects, and the sum of these may be regarded as the "effective area" of the casting, i.e. the equivalent area of plane mould wall. The solidification time is then calculated in the usual way,<sup>2</sup> using the effective area instead of the true area.

As explained in Section IV, a preliminary calculation must first be made to ascertain the values of the corner and surface-curvature correction factors to be employed. The complete calculation is given below.

#### *Preliminary Calculation.*

This calculation neglects corner and surface-curvature effects, and is carried out as described in an earlier paper.<sup>2</sup>

The total heat *Q* (in calories), extracted from the casting by the mould, is given by <sup>1,6</sup>

$$Q = Aq\sqrt{t}$$

\* The area *B* must be multiplied by two factors since this area is a part of the corner as well as of the cylindrical surface. The factor for the area *D* is, of course, unity.

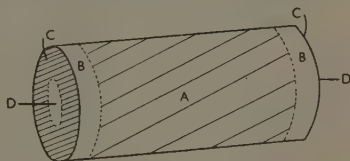


FIG. 12.—Diagram Illustrating the Division of the Surface of a 5-in.-dia.  $\times$  10 in. Cylinder for the Purpose of Calculating the Solidification Time.

where  $q$  is the "mould constant",<sup>1</sup> in this case equal to 260 cal./cm.<sup>2</sup> min. <sup>$\frac{1}{2}$</sup>  (interface temperature 1083° C.),  $A$  is the surface area of the casting (1267 cm.<sup>2</sup>), and  $t$  is the time of total solidification. Inserting the appropriate numerical values there is obtained :

$$\sqrt{t} = \frac{1,629,000}{260 \times 1267}$$

and

$$t = 24.5 \text{ min.}$$

### *Final Calculation.*

Tables I and II, and the above approximate solidification time, indicate that the correction factors to be used in the final calculation are 1.3 for the corners and 1.1 for the cylindrical surfaces.

The "effective area" of the casting is therefore :

$$(774 \times 1.1) + (239 \times 1.3 \times 1.1) + (183 \times 1.3) + 71 = 1502 \text{ cm.}^2$$

Hence

$$\sqrt{t} = \frac{1,629,000}{260 \times 1502}$$

and

$$t = 17.4 \text{ min.}$$

If desired, the calculation may be repeated a second time using new values of the correction factors obtained by entering Tables I and II with the calculated solidification time of 17.4 min.; however, the gain in accuracy is usually too small to justify the extra effort involved.

The calculated solidification time of 17.4 min. is in fair agreement with the figure of 14.0 min. observed experimentally<sup>5</sup> and is considerably more accurate than the time of 24.5 min. computed by the simpler method, which takes no account of corner and curvature effects.

In making the calculation it has been assumed that the factor for the curved corner is the same as that for a straight one, but the error so incurred is unlikely to be large.

## VI.—SUMMARY AND CONCLUSIONS.

The work described in this paper may be briefly summarized as follows :

(1) Experimental investigation of the temperature distribution at the corners (edges) of sand moulds has shown that a right-angled corner of a mould extracts heat from a casting considerably more rapidly than a plane mould wall. The heat extracted in a given time through the area bounded by lines 3 cm. either side of a sharp corner is



greater than that extracted by a plane mould wall by a factor which is independent of the temperature of the metal/mould interface, but is dependent on time and is reduced by radiusing the corner. Average values of the factor are tabulated for solidification times up to 2 hr.

(2) The rate at which a sand mould extracts heat from a right-angled re-entrant corner of a casting is a little less than that at which heat is removed by a plane mould face of equal area. In this case the corner is taken as comprising the area bounded by lines 14 cm. on either side of the apex.

(3) A cylindrical sand-mould surface extracts heat faster than a plane surface; the factors involved are tabulated for times up to 2 hr.

(4) The data obtained can be used to calculate the solidification times of castings of simple shape with fair accuracy. The way in which these calculations are carried out is illustrated in an example.

#### ACKNOWLEDGEMENTS.

The authors are indebted to the Director and Council of the British Non-Ferrous Metals Research Association for permission to publish this paper. They gratefully acknowledge the advice and assistance received from their colleagues, in particular Dr. A. G. Quarrell and Mr. W. A. Baker; their thanks are also due to Dr. E. T. Goodwin of the National Physical Laboratory for help with the mathematical aspects of the problem.

#### APPENDIX I.

##### EXPERIMENTAL DETERMINATION OF THE HEAT CONTENTS OF MOULD CORNERS AND CYLINDRICAL MOULD WALLS.

The heat contents of the moulds studied in this work were calculated in the following way from experimentally determined temperature-distribution graphs of the kind shown in Figs. 2-4 and 6-7. In each case these calculations were made for several different times after the beginning of the experiment.

##### *Mould Corner.*

The total quantity of heat,  $Q$ , extracted by a mould at any given time,  $t$ , after casting, is the product of the density,  $\rho$ , the specific heat,  $c$ , and the temperature,  $\theta$ , above the initial temperature of the mould, integrated over that volume of the mould which has risen appreciably in temperature.

The isotherms in the sand at a mould corner are depicted diagram-

matically in Fig. 13. In the neighbourhood of the corner the isotherms are curved but a little distance from the corner they become practically straight and parallel to the mould wall; in Fig. 13 the boundaries between the straight and curved portions are indicated by the lines  $AB$  and  $A'B'$ —these boundaries are of course arbitrary since there is no sharp line of demarcation.

The heat removed in time  $t$  by the corner of the mould, i.e. by the area\* of sand bounded by the lines  $BA$ ,  $AO$ ,  $OA'$ ,  $A'B'$  may be estimated in the following way if the positions of the isotherms are plotted. The mean temperature† of the sand in the area  $\alpha_1$  ( $AOA'L'L$ ) is approximately  $(\theta_i + \theta_1)/2$ , where  $\theta_1$  is the temperature

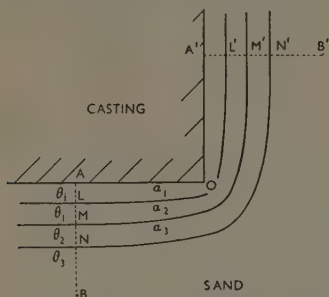


FIG. 13.—Diagram Illustrating the Method of Calculating the Heat Extracted by a Two-Dimensional Corner of a Mould.

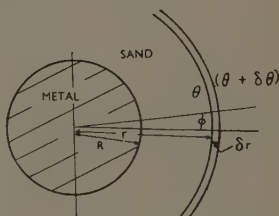


FIG. 14.—Diagram Illustrating the Calculation of Heat Extraction by a Cylindrical Mould Wall.

at the interface (this approximation is justified if the isotherms are taken sufficiently close together); the quantity of heat absorbed by this area is therefore  $\frac{1}{2}(\theta_i + \theta_1)\alpha_1\rho c = Q_1$ . The area  $\alpha_1$  can be obtained by measuring the diagram with a planimeter. The heat absorbed by the area  $\alpha_2$  ( $LL'M'M$ ) is similarly  $\frac{1}{2}(\theta_1 + \theta_2)\alpha_2\rho c = Q_2$  and is found in the same way. The procedure is repeated for the areas  $\alpha_3$ ,  $\alpha_4$ , &c., until the values of  $Q$  obtained become negligible in comparison with the experimental error and the total heat in the corner is then obtained by summing  $Q_1$ ,  $Q_2$ , &c.

### Cylindrical Mould Wall.

The heat absorbed by a cylindrical mould wall is estimated in a somewhat different way. The isotherms round a cylindrical casting

\* A slice perpendicular to the mould wall and of unit thickness is considered; it is therefore permissible to refer to areas of the mould rather than to volumes.

† The initial temperature of the mould is taken as zero.

are, for reasons of symmetry, themselves cylindrical surfaces; on a transverse section perpendicular to the axis of the cylinder they will therefore appear as concentric circles as in Fig. 14.

Taking the unit deep sector defined by the angle  $\phi$  at the centre of the cylinder of radius  $R$  and assuming that the mould temperatures at distances of  $r$  and  $(r + \delta r)$  are  $\theta$  and  $(\theta + \delta\theta)$  above the initial mould temperature, then the mass of the small unit between  $r$  and  $(r + \delta r)$  is :

$$\rho r \phi \delta r,$$

so that the heat gained by this unit is :

$$\rho r \phi c \theta \cdot \delta r.$$

Therefore the heat gained by the whole sector is :

$$\int_R^\infty r \phi \rho c \theta \cdot dr.$$

This heat has been extracted through a mould face of area  $R\phi$ , and hence the heat extracted per unit of mould surface is :

$$\frac{\rho c \phi}{R \phi} \int_R^\infty r \theta \cdot dr$$

But since  $r dr = d\left(\frac{r^2}{2}\right)$

it follows that the heat extracted per unit mould surface is :

$$\frac{\rho c}{R} \int_R^\infty \theta \cdot d\left(\frac{r^2}{2}\right).$$

Hence the heat extracted by unit mould surface in a time  $t$  may be estimated by plotting the temperature in the mould against  $(r^2/2)$ , measuring the area under the curve, and multiplying by the appropriate constants.

## APPENDIX II.

### CALCULATION OF HEAT EXTRACTION BY CYLINDRICAL MOULD WALLS.

The flow of heat from an infinitely long cylindrical surface, maintained at constant temperature, into the surrounding region (in this case the mould), assumed to extend to infinity in all directions, has been treated mathematically by Jaeger,<sup>4</sup> who gives the following expression for the flux of heat,  $\partial Q/\partial t$ , across the cylindrical surface :

$$\frac{\partial Q}{\partial t} = \frac{4K(\theta - \theta_0)}{a\pi^2} \int_0^\infty \frac{e^{-au^2} du}{u[J_0^2(ua) + Y_0^2(ua)]} = \frac{4K(\theta - \theta_0)}{a\pi^2} I(0, 1; x)$$

where  $\theta$  = temperature of the cylindrical surface (constant),

$\theta_0$  = initial temperature of the mould,

$a$  = radius of cylindrical surface,

$K$  = thermal conductivity of the mould material,

$\alpha$  = temperature diffusivity of the mould material =  $K/\rho c$ ,  
where  $\rho$  = density and  $c$  = specific heat,

and 
$$I(0, 1; x) = \int_0^\infty \frac{e^{-au^2} du}{u[J_0^2(ua) + Y_0^2(ua)]} \text{ where } x = at/a^2$$

The integral  $I(0, 1; x)$  may be evaluated by approximation methods and a short table of values is given by Jaeger and Clarke.<sup>7</sup>

It follows from the above equation that the quantity of heat  $Q$  absorbed by the mould in time  $t$ , per unit area of mould surface, is given by

$$\begin{aligned} Q &= \frac{4K(\theta - \theta_0)}{a\pi^2} \int_0^t I(0, 1; x) \cdot dt \\ &= \frac{4Ka(\theta - \theta_0)}{\pi^2\alpha} \int_0^x I(0, 1; x) \cdot dx \end{aligned}$$

The integral in the right-hand side of the above equation may be evaluated by integration of the series for  $I(0, 1; x)$ .<sup>7</sup>

In computing the theoretical heat-extraction curves in Figs. 10 and 11, the values of thermal properties were either those used in earlier work<sup>1</sup> (density and specific heat), or were calculated from mould-temperature measurements made during the course of the present work, in the way described in the earlier paper<sup>1</sup> (thermal conductivity).

#### REFERENCES.

1. R. W. Ruddle and A. L. Mincher, *J. Inst. Metals*, 1949-50, **76**, 43.
2. R. W. Ruddle, *J. Inst. Metals*, 1950, **77**, 1.
3. H. S. Carslaw and J. C. Jaeger, "Conduction of Heat in Solids." London: 1947 (Oxford University Press).
4. J. C. Jaeger, *Proc. Roy. Soc. Edinburgh*, 1941/43, **61**, 223.
5. R. W. Ruddle and A. L. Mincher, *J. Inst. Metals*, 1950-51, **78**, 229.
6. R. W. Ruddle, "The Solidification of Castings: A Review of the Literature," *Inst. Metals Monograph and Rep. Series*, No. 7, 1950.
7. J. C. Jaeger and M. Clarke, *Proc. Roy. Soc. Edinburgh*, 1941/43, **61**, 229.

# THE EFFECT OF COPPER, SILICON, AND MAGNESIUM ON THE MECHANICAL PROPERTIES OF ALUMINIUM ALLOYS OF THE D.T.D. 424 TYPE.\*

By E. SCHEUER,† Dr. rer. nat., MEMBER, S. J. WILLIAMS,‡ L.I.M., MEMBER, and J. WOOD,§ M.Sc., MEMBER.

## SYNOPSIS.

The optimum copper content for alloys of the D.T.D. 424 type is generally believed to be about 3%. After the last war it became necessary to use scrap material of a higher copper content than this in making the alloys, and it was therefore thought desirable to investigate the effect of variations in the copper, magnesium, and silicon contents of the alloy on its mechanical properties.

With this end in view the ultimate tensile stress, proof stress, elongation, and Brinell hardness of 81 alloys were determined and recorded in contour diagrams based on the ternary diagram for aluminium-copper-silicon alloys. The investigation included alloys with four different magnesium contents (0.00, 0.08, 0.15, and 0.25%). Graphs are also given showing the effect of varying either the copper or silicon content while keeping the other constituents constant. From these a contour diagram has been drawn to indicate the limits of composition which must be adhered to if the specified mechanical properties are to be realized.

## I.—INTRODUCTION.

THE aluminium alloy to specification D.T.D. 424 has, in recent years, become one of the most popular alloys for sand casting and gravity die-casting. The composition range laid down by the specification is as follows :

Cu, %	Mg, %	Si, %	Fe, %	Mn, %	Ni, %
2.0-4.0	0.15 max.	3.0-6.0	0.8 max.	0.3-0.7	0.35 max.
Zn, %	Pb, %	Sn, %	Tl, %	Fe + Mn, %	Al, %
0.3 max.	0.05 max.	0.04 max.	0.2 max.	1.3 max.	Remainder

The specified mechanical properties of this alloy, using standard D.T.D. sand-cast test-bars are : ultimate tensile stress, 9 tons/in.<sup>2</sup>, and elongation on 2 in., 2%.

This alloy has a specified composition range which allows of its being made from secondary materials, using a mixture of Duralumin scrap

\* Manuscript received 1 July 1950.

† Chief Metallurgist and Head of Laboratories, International Alloys, Ltd., Aylesbury, Bucks.

‡ Metallurgist, International Alloys, Ltd.

§ Assistant Chief Metallurgist, International Alloys, Ltd.

|| Limits in accordance with A.D.M. 475.

containing about 4% copper and 0.5% silicon, and low-copper aluminium scrap containing less than 1% copper. Scrap materials of high silicon content, if available, are included, and also rock silicon for the adjustment of the silicon content. Within the limits of the D.T.D. 424 specification, the optimum composition is generally considered to lie at about 3% copper and about 5% silicon. No evidence has, however, been published as to the reasons for this preference.

After the war, the normal pre-war types of scrap material were not available for a considerable period, and the major source of raw material for the secondary smelters was redundant and broken-down aircraft. The predominant aluminium alloy used in aircraft structural components is Duralumin, or similar copper-containing aluminium alloys, the copper content of which ranges from 3.5 to 4.8%. When using this raw material it is not possible by addition of 5% silicon alone to reduce the copper content to the supposed optimum figure of 3%. The use of considerable proportions of expensive pure aluminium would be required to do this.

The producers of the D.T.D. 424 type of alloy were confronted with the alternatives of increasing its price or of departing from what was thought to be the optimum composition. As no detailed evidence of the effect of such a departure on the properties of the alloy was available in the literature, it was decided to investigate the influence of the copper content on the mechanical properties.

Among the other constituents, magnesium and silicon are those that may be expected to have a strong influence on the mechanical properties of the alloy, and alterations in the percentages of these elements would be expected to offset, to a certain extent, the changes brought about by the increased copper content. Fortunately, the quantities of magnesium and silicon can be arbitrarily adjusted in the alloying process without the need for making additions of pure aluminium. Silicon can be added, as required, as rock silicon and magnesium can be added or eliminated by metallurgical treatment during alloying.

The investigation was planned to include variations of these three components—copper, magnesium, and silicon—in order to determine what adjustments were possible to meet the raw-material situation. To keep the volume of work within practicable limits (81 alloys had to be tested), the experiments were limited to standard D.T.D. sand-cast test-bars. Furthermore, the tests were restricted to tensile and hardness tests.

It was not possible at the time to extend the programme to include the examination of other important properties of the alloys, such as their age-hardening and casting characteristics, but later some work on



age-hardening was carried out and an investigation of casting properties is in hand.

The experiments described in the present paper were, therefore, undertaken in order to establish the relationship between the copper, silicon, and magnesium contents, and the mechanical properties of D.T.D. sand-cast test-bars.

## II.—PLAN OF INVESTIGATION.

The official specification for the composition of D.T.D. 424 alloy is as given on p. 57, but for engineering purposes, a new specification, B.S. 1490, LM 4, has been introduced. This differs from D.T.D. 424 in respect of the silicon, lead, and tin contents. The new limits are :

Silicon	.	.	.	.	4.0-6.0%, instead of 3.0-6.0%
Lead	.	.	.	.	0.1% max., instead of 0.05% max.
Tin	.	.	.	.	0.05% max., instead of 0.04% max.

The requirements regarding mechanical properties make it necessary to produce the alloy to closer limits than those permitted by the specification. This applies particularly to the elongation, there being relatively little difficulty in securing the specified ultimate tensile stress over a wide range of composition.

In order to obtain reliable graphs in the specification range, it was considered necessary to extend the range of compositions studied beyond the specified limits. Thus, for copper, with specified limits of 2.0-4.0%, the range investigated covered 0-5.0%; for silicon (specified limits, 3.0-6.0%), it was 0-6.0%, and for magnesium (specified limit, 0.15% max.) 0-0.25%.

The copper and silicon contents of the alloys were selected to cover adequately the actual specified composition range of D.T.D. 424. The range of magnesium concentrations was covered by the four values : nil, 0.08, 0.15, and 0.25%. In order to reduce the number of alloys studied, only a selection of the copper and silicon concentrations was tested with all four magnesium contents.

The copper and silicon contents investigated are shown in the ternary composition diagram (Fig. 1). The key indicates which magnesium contents were tested with each copper and silicon content.

Apart from the copper, silicon, and magnesium contents, all alloys were made up to a composition with impurity contents near to the maximum values that would occur in aircraft scrap. The values selected were :

Fe, %	Mn, %	Ni, %	Zn, %	Pb, %	Sn, %	Ti, %
0.60	0.60	0.10	0.25	0.10	0.05	0.05

The following tests were carried out: 0.1% proof stress, ultimate tensile stress, percentage elongation on 2 in., and Brinell hardness (10-mm. ball with 1000 kg. load or 5-mm. ball with 250 kg.).

Alloys containing copper and magnesium will, of course, age-harden after casting, even without special heat-treatment. Although it was not intended to study the effects of age-hardening in this series of tests, it was necessary to eliminate fluctuations of mechanical properties due to variations in cooling speed and ageing time. In order to avoid errors from this source, the machining and testing were all completed within 4 hr. of casting. If, for any reason, bars could not be tested within this period, they were kept in a refrigerator until testing was possible. The cooling of test-bars was also standardized, the bars being allowed

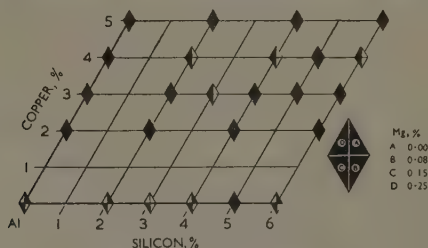


FIG. 1.—Ternary Composition Diagram Showing Alloys Tested.

to remain in the mould for 45 min. after casting, at the end of which time they had cooled to about 180° C. The bars were then taken from the moulds and quenched in cold water.

### III.—METHOD OF MELTING, CASTING, AND TESTING.

In order to secure the greatest possible consistency in the minor constituents and impurities it was decided to use four master alloys, whose nominal compositions are shown in Table I.

TABLE I.—Nominal Composition of Master Alloys.

Master Alloy	Cu, %	Mg, %	Si, %	Fe, %	Mn, %	Ni, %	Zn, %	Pb, %	Sn, %	Ti, %
1	5.0	...	...	0.60	0.60	0.10	0.25	0.10	0.05	0.05
2	5.0	...	6.0	0.60	0.60	0.10	0.25	0.10	0.05	0.05
3	...	...	6.0	0.60	0.60	0.10	0.25	0.10	0.05	0.05
4	...	...	...	0.60	0.60	0.10	0.25	0.10	0.05	0.05

All alloys were prepared by combining these four master alloys in various proportions. Each alloy was given a code number of two

numerals, with a suffix letter, the numerals indicating the copper and silicon contents, respectively, and the suffix letters *A*, *B*, *C*, and *D*, magnesium contents of 0, 0.08, 0.15, and 0.25%, respectively. Thus, an alloy with copper 3, silicon 4, and magnesium 0.15% was identified by the code number 34C.

The first melt of each alloy always contained sufficient material to produce six or seven test-bars and two samples for chemical and spectrographic analysis. Subsequent rechecks were all made using sufficient material to produce two test-bars and one analysis sample. At least two, and in most cases three, melts of each alloy were made, the sequence of melting being arranged in a random order.

Melting was carried out in Salamander crucibles in a producer-gas-fired furnace. The crucible wall was treated with a small quantity of 85:15 salt-fluorspar mixture before use. The metal was melted and heated to 750° C., well mixed, and then degassed by plunging in 1% by weight of Foundry Services Degasser No. 7 powder wrapped in aluminium foil. The melt was subsequently skimmed and allowed to stand in a hot electric-resistance furnace, the temperature of which was regulated so as to allow the metal to cool to the casting temperature in 20–30 min., the surface of the melt being skimmed about three times during this standing period. The magnesium additions, when required, were always made just before casting. Test-bars were cast by hand-ladle at 700° C. in the case of the large melts and from the crucible, also at 700° C., with the smaller recheck melts. The pouring time was 10–15 sec. for the test-bars, excluding the feeder head. The moulds were the standard D.T.D. type made of red Mansfield sand and were oven-dried and cooled to room temperature before using.

TABLE II.—*Typical Analyses of the Master Alloys.*

Alloy No.	Cu, %	Mg, %	Si, %	Fe, %	Mn, %	Ni, %	Zn, %	Pb, %	Sn, %	Tl, %
1	4.91	<0.02	0.16	0.62	0.62	0.13	0.27	0.10	0.10	0.054
2	5.05	<0.02	6.10	0.62	0.62	0.12	0.25	0.12	0.10	0.056
3	0.06	<0.02	6.20	0.62	0.62	0.11	0.27	0.09	0.05	0.050
4	0.06	<0.02	0.20	0.60	0.61	0.11	0.28	0.10	0.05	0.049

All bars were tested to determine the ultimate tensile stress and percentage elongation on 2 in. Proof-stress and Brinell-hardness tests were carried out on the second and last-but-one bar of each melt of 6 or 7 bars, and on the first bar in the case of each recheck melt.

Some typical analyses of the master alloys and test bars are shown in Tables II and III.

As the sample for the analysis of the test-bars was cast at the same time as the bars themselves, the magnesium contents given on the graph shown in Fig. 15, p. 71, represent the actual magnesium contents of the test-bars. The loss of magnesium during the remelting and

TABLE III.—*Typical Analyses of Test-Bars.*

Test-Bar Code No.	Cu, %	Mg, %	Si, %	Fe, %	Mn, %	Ni, %	Zn, %	Pb, %	Sn, %	Ti, %
56D	4.95	0.26	5.91	0.63	0.62	0.14	0.27	0.10	0.07	0.056
42C	4.06	0.152	2.09	0.60	0.60	0.12	0.26	0.10	0.06	0.048
30A	3.05	<0.02	0.14	0.59	0.63	0.11	0.24	0.11	0.07	0.050
24B	2.01	0.081	4.02	0.62	0.58	0.15	0.26	0.11	0.04	0.050

degassing of ingots for test-bars is of the order of 20% of the content. The loss is negligible below 0.04% magnesium. The loss of magnesium when remelting ingots in production foundries for the manufacture of castings is likely to be considerably less, and it is estimated that in this case the difference between ingots and finished castings is in the order of 0.05% magnesium, being slightly less for ingots of low magnesium content and slightly more for ingots of high magnesium content.

#### IV.—RESULTS OF TESTS.

##### 1. *Mechanical Properties.*

The results of the tests are given in the form of graphs (Figs. 2–11). Figs. 2 and 3 show, respectively, the effect of variation of copper content on alloys with no silicon, and the effect of variation of silicon on alloys with no copper content. Figs. 4–7 indicate the effect of silicon on alloys with 2, 3, 4, and 5% copper. Figs. 8–11 represent the same results plotted to show the effect of copper content on alloys with 2, 4, 5, and 6% silicon. Each graph contains two or four curves corresponding to the different magnesium contents used.

Each average value is derived from at least two separate melts and at least four test-bars. In Figs. 10 and 11, the scatter of the individual results is indicated by vertical lines which are connected by horizontal lines to the point representing the average figure. If no vertical line is shown, the agreement of the individual results is within 0.1 ton/in.<sup>2</sup> for the ultimate and proof stress, 0.1% for the elongation, and 1 kg./mm.<sup>2</sup> in the case of the Brinell hardness. The scatter in the other graphs was found to be of similar magnitude and, for reasons of simplicity, it is not indicated.

Proof stress and hardness show a fairly steady rise with increasing copper or silicon content, which is more marked for copper additions

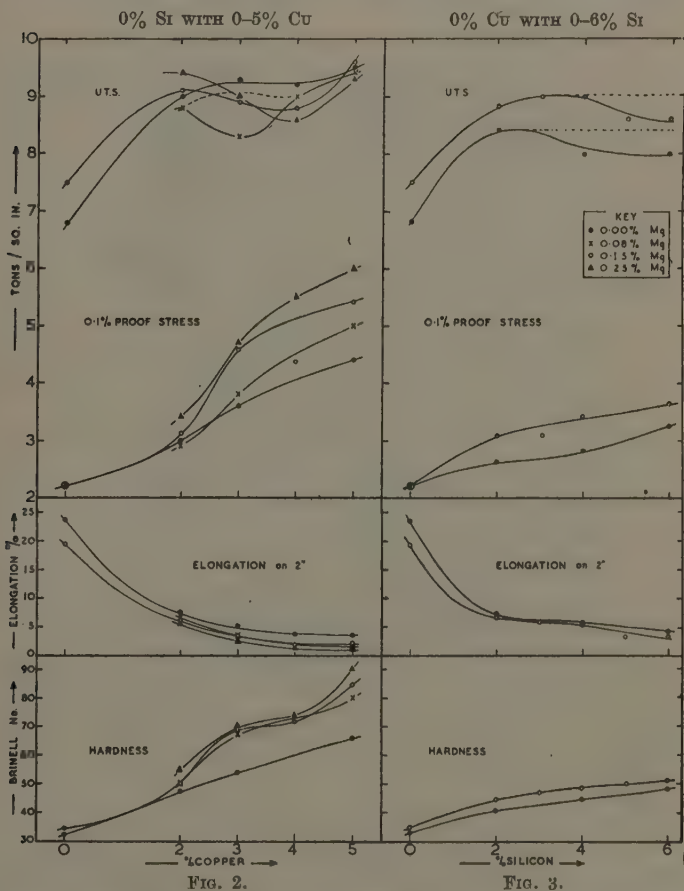
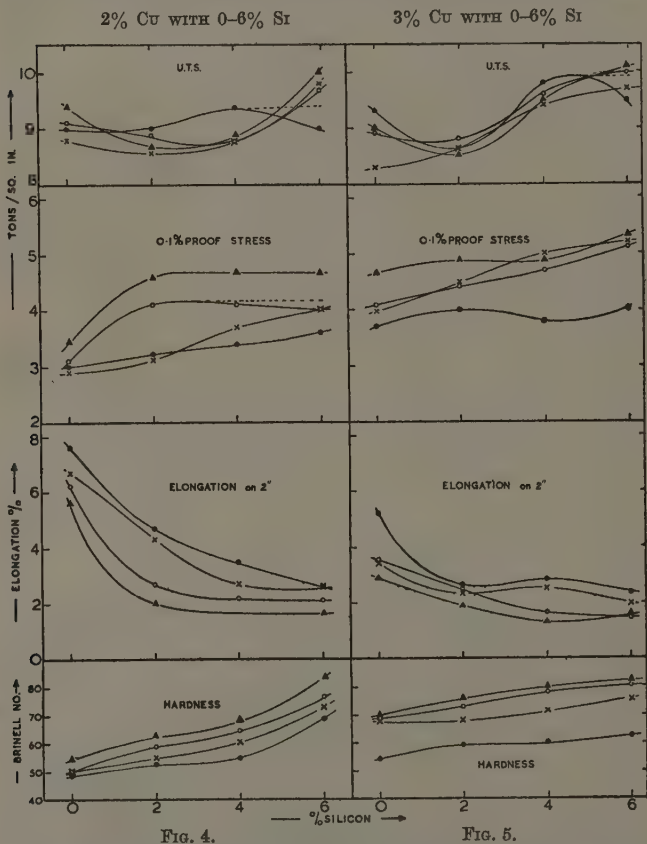


FIG. 2.—Effect of Variation of Copper Content (0-5%) on Mechanical Properties of Alloys with no Silicon Content.

FIG. 3.—Effect of Variation of Silicon Content (0-6%) on Mechanical Properties of Alloys with no Copper Content.

than for silicon additions of the same magnitude. The elongation drops rather steeply in the lower range of additions, and comparatively little

in the higher ranges. The ultimate stress generally increases with the copper and silicon content. The curves are drawn through all deter-



FIGS. 4-5.—Effect of Variation of Silicon Content (0-6%) on Mechanical Properties of Alloys Containing 2% Copper (Fig. 4) and 3% Copper (Fig. 5). Key as in Fig. 3.

mined points without attempting to idealize their shape, and therefore, in view of the small differences between the graphs on one diagram, intersection of the curves occurs in a number of cases.

On the graphs where there is a strong likelihood that one point of



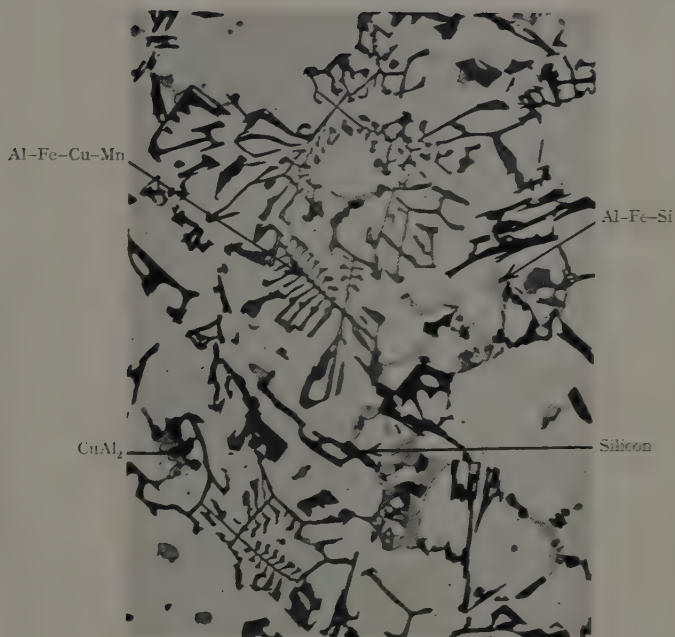


FIG. 16.—Typical Microstructure of D.T.D. 424 Test-Bar.  
Unetched.  $\times 200$ .

Identification of constituents in bar No. 45C  
(Cu 4, Si 5, Mg 0.15%).

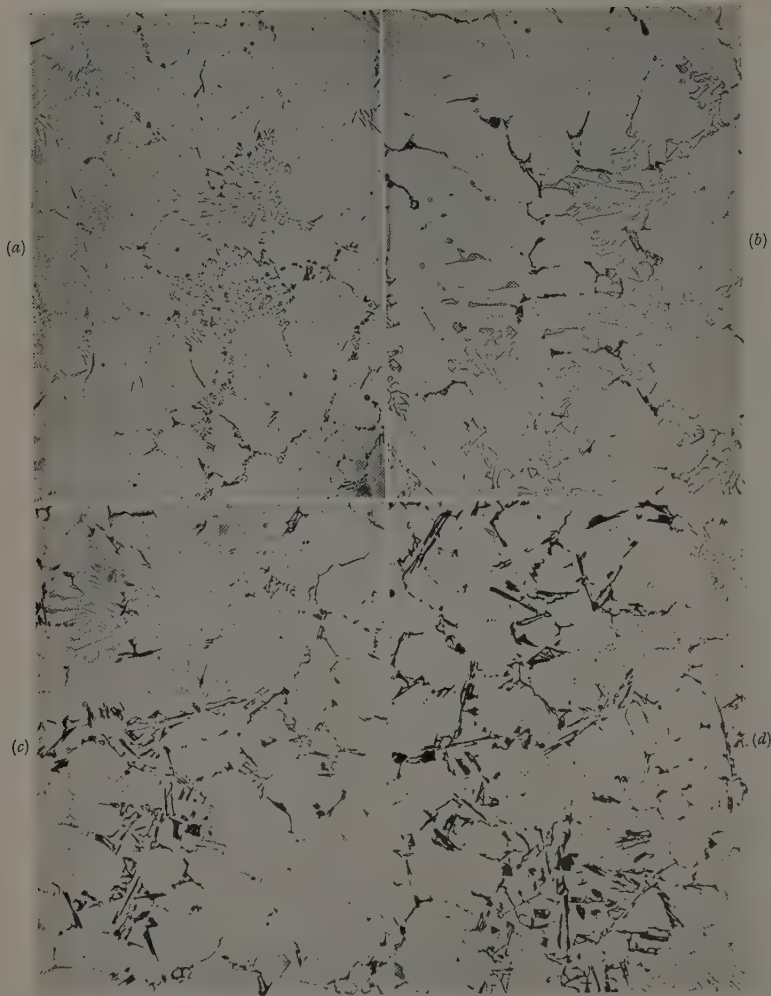


FIG. 17(a)-(d).—Microstructures of Alloys with 0.15% Magnesium and Varying Copper and Silicon Contents. Unetched.  $\times 100$ . Reduced by 1/5 in reproduction.

(a) Cu 0.00, Si 0.15%.

(c) Cu 4.00, Si 5.00%.

(b) Cu 3.00, Si 2.00%.

(d) Cu 5.00, Si 6.00%.

one particular line is anomalous, the probable position of the ideal curve is indicated by a dotted line.

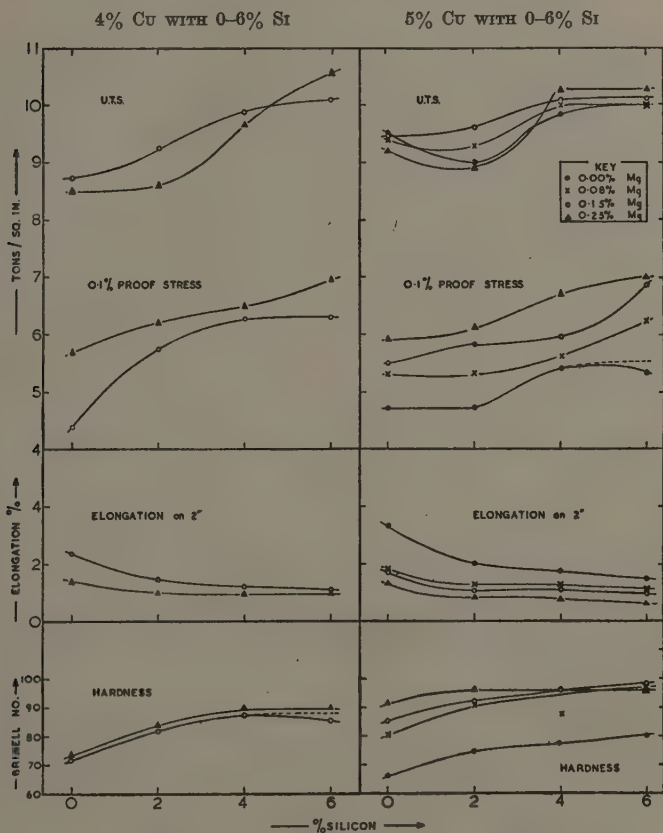


FIG. 6.

FIG. 7.

FIGS. 6-7.—Effect of Variation of Silicon Content (0-6%) on Mechanical Properties of Alloys Containing 4% Copper (Fig. 6) and 5% Copper (Fig. 7).

In order to obtain a comprehensive picture of the results, the graphs in Figs. 12, 13, and 14 have been plotted on the ternary aluminium-silicon-copper diagram for alloys containing 0.15% magnesium, with contour lines interpolated between the results obtained. The tensile

stress (Fig. 12) rises sharply from 7 to 8.75 tons/in.<sup>2</sup> between the aluminium corner and a line connecting roughly the points 0% silicon, 1.5% copper and 0% copper, 2% silicon. In

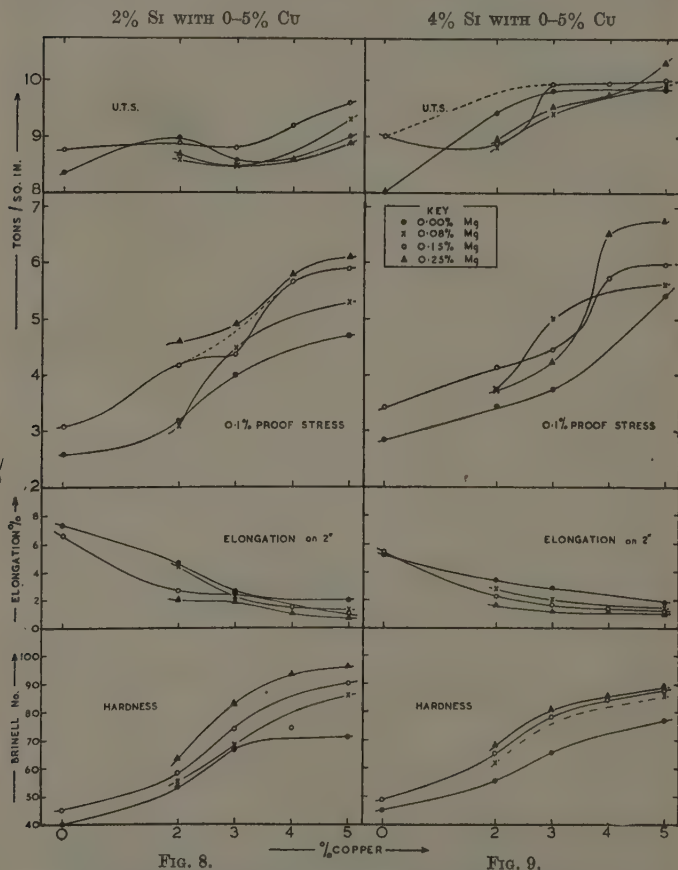


FIG. 8.

FIG. 9.

Figs. 8-9.—Effect of Variation of Copper Content (0-5%) on Mechanical Properties of Alloys Containing 2% Silicon (Fig. 8) and 4% Silicon (Fig. 9).

1.5% copper and 0% copper, 2% silicon and then much more slowly from 8.75 to 9.0 tons/in.<sup>2</sup>, this value being reached along a line connecting the points 0% silicon, 4.5% copper and 0% copper, 7% silicon. In

the region of higher copper and silicon contents, roughly to the right of the contour line representing 9 tons/in.<sup>2</sup>, the tensile stress increases

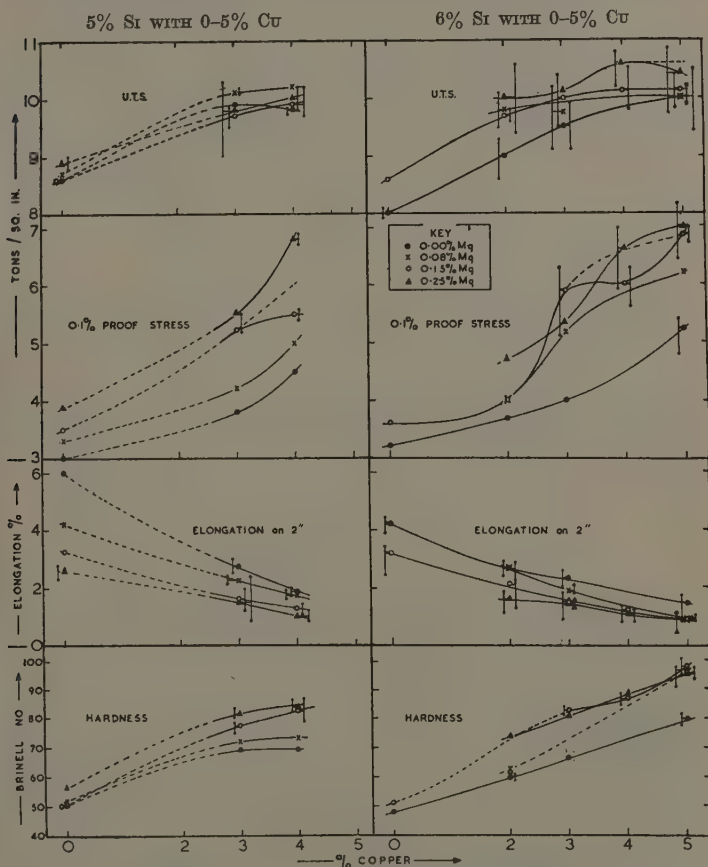


FIG. 10.

FIG. 11.

FIGS. 10-11.—Effect of Variation of Copper Content (0-5%) on Mechanical Properties of Alloys Containing 5% Silicon (Fig. 10) and 6% Silicon (Fig. 11).

again more steeply. Between the lines 8.75 and 9.0 tons/in.<sup>2</sup> there is a region of more or less uniform values of the tensile stress over a considerable range of composition.

The elongation curve (Fig. 13) drops sharply near the aluminium corner and flattens out markedly in a zone roughly between the points

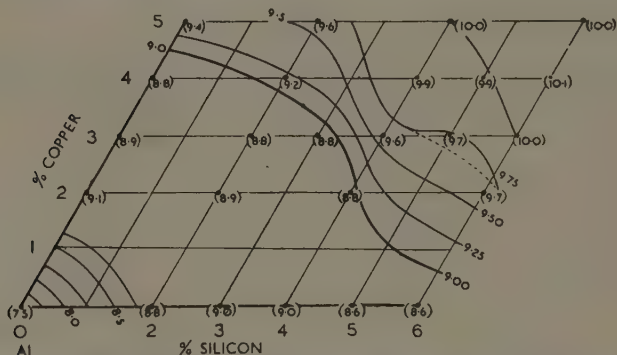


FIG. 12.—Contour Diagram Showing U.T.S. Results Obtained with Alloys of the 0.15% Magnesium Series. Contours at 0.25 ton/in.<sup>2</sup> intervals. Actual U.T.S. results in parentheses.

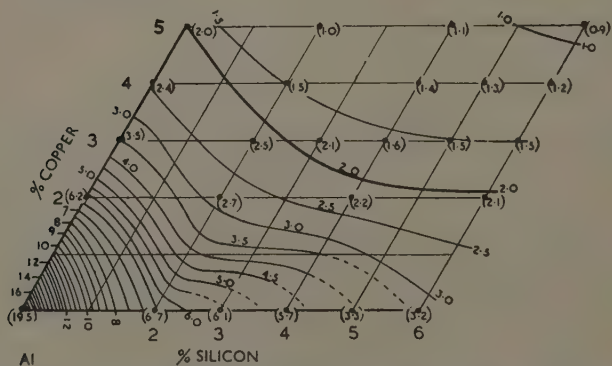


FIG. 13.—Contour Diagram Showing Elongation Results Obtained with Alloys of the 0.15% Magnesium Series. Contours at 0.5% elongation intervals. Actual elongation results in parentheses.

0% silicon, 3.5% copper (3% elongation) and 0% copper, 3% silicon (6% elongation). There seems to be no steep drop corresponding to the increased gradient of the tensile stress at higher copper and silicon contents. If there were, however, it might not be conspicuous, as the

elongation has already fallen to about 1% in the zone where the second steeper gradient of tensile stress was observed.

The graphs representing proof stress and Brinell hardness (Fig. 14) are very similar to one another. The rise in both properties is more pronounced with addition of copper than with the addition of silicon. The two zones which characterize the tensile stress graph, i.e. one of pronounced and one of slight gradient, are scarcely recognizable. The increase is steeper in a zone roughly between the points 0% silicon, 2-4% copper and 6% silicon, 1-3% copper.

The various magnesium contents have not been incorporated in

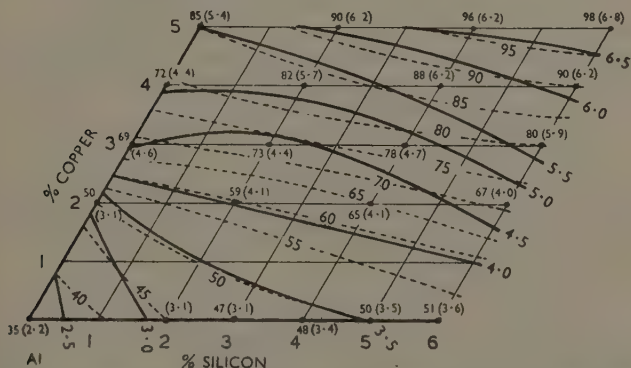


FIG. 14.—Contour Diagram Showing Proof-Stress and Brinell-Hardness Results Obtained with Alloys of the 0.15% Magnesium Series. Actual proof-stress results in parentheses.

Proof stress curves —————

Brinell hardness curves - - - - -

the ternary graphs. From the binary graphs it can be seen that the tensile stress is not very much affected by variation in magnesium content, the values for 0.25% magnesium being less than 1 ton/in.<sup>2</sup> higher than the values for nil magnesium. The elongation is comparatively more markedly affected, the drop produced by adding 0.25% magnesium being of the order of 1% at low copper and silicon contents and about 0.5% at high copper and silicon contents. The values for alloys with 0.08% magnesium and 0.15% magnesium seem to be very close together.

The diagram showing the ultimate tensile stress figures (Fig. 12) differs from that showing proof stress and hardness in that the rise in tensile strength due to increasing copper and silicon contents falls in two separate zones of concentration, the first one lying between 0 and



2% of both constituents, the second starting roughly on a line representing compositions where the sum of the copper and silicon contents is about equal to 6%. Between these zones the results show a comparatively slow rise with increasing additions, but this rise is not very consistent, and in some cases low results occur.

Comparing the contour lines for ultimate tensile stress with those for 0.1% proof stress and hardness, which exhibit a fairly steady rise with increasing additions, one is led to the conclusion that the alloys of a certain zone and composition are weakened by the presence of an unfavourable structure. The most probable cause of this weakening of the structure is, in the opinion of the authors, intercrystalline shrinkage. This form of shrinkage is connected with the presence of comparatively small volume percentages of eutectic. From the constitution of the alloys used in these experiments, the zone in which copper + silicon is of the order of 3-5% is that most likely to contain the maximum amount of intercrystalline shrinkage.

While attempts to prove the existence of significant amounts of intercrystalline shrinkage in the alloys in this zone by density measurements, and microscopic and radiographic examination, have been unsuccessful, it is not possible at the moment to offer a more probable explanation of the particular shape of the graph of ultimate tensile stress.

## 2. Microstructure.

Typical microstructures of test-bars (taken near the fracture) are shown in Fig. 16 (Plate VII) and Fig. 17 (a)-(d) (Plate VIII). Fig. 16 provides the identification of the main constituents, while Fig. 17 (a)-(d) shows larger areas of a selection of alloys with increasing copper and silicon contents. The increase in the proportion of the various copper-, manganese-, and silicon-containing constituents is very marked between Fig. 17 (a) and Fig. 17 (d). In spite of this, however, the size of the branches of primary aluminium dendrites remains the same for all alloys investigated, while these dendrite branches are more and more completely surrounded by the brittle eutectic crystals as the concentration of copper and silicon increases.

## V.—CONCLUSIONS.

Figs. 15 (a) and (b) summarize the practical results of the investigation. Fig. 15 (a) contains contour lines connecting compositions with respect to copper, silicon, and aluminium contents giving an ultimate tensile stress of 9 tons/in.<sup>2</sup> and an elongation of 2% for the various magnesium contents. The composition range of the official D.T.D. 424

specification is indicated by the outlined parallelogram. The shape of the lines has been slightly simplified in order to give the best estimate of their true arrangement based on the experimental results.

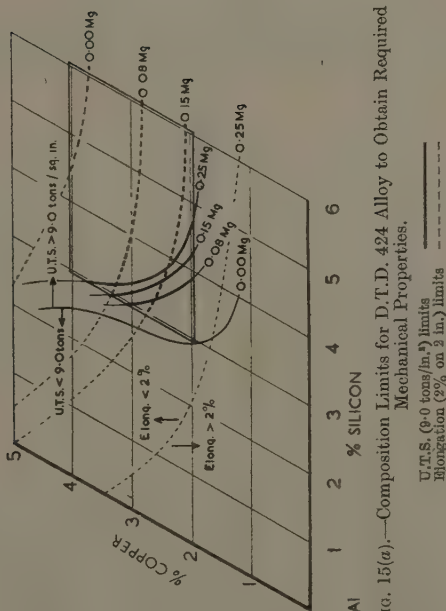


FIG. 15(a).—Composition Limits for D.T.D. 424 Alloy to Obtain Required Mechanical Properties.

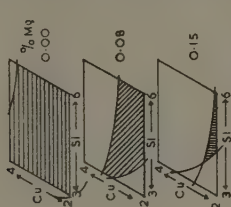


FIG. 15(b).—Composition Ranges for Required Mechanical Properties: Effect of Magnesium Content. (See outlined composition range in Fig. 15(a).)

which satisfies the specification of 2% minimum elongation. In order to make clearer the permissible concentration field for the various magnesium contents three small diagrams for 0.00, 0.08, and 0.15% magnesium have been added as Fig. 15 (b), in which the fields of concentration of copper and silicon which produce mechanical properties meeting the specification are shaded. It can be seen that with no magnesium the required mechanical properties can be obtained throughout the whole range of specified copper and silicon contents, with the exception of one small area with the highest quantity of alloying constituents. With rising magnesium content the range of permissible copper and silicon contents narrows considerably, however, and with a magnesium content of 0.25% no practicable working range of copper and silicon contents remains.

#### ACKNOWLEDGEMENTS.

The authors are indebted to the Directors of International Alloys, Ltd., in whose laboratories the work was carried out, for permission to publish this paper.

# THE APPLICATION OF HYDROGEN EQUILIBRIUM - PRESSURE MEASUREMENTS TO THE INVESTIGATION OF TITANIUM ALLOY SYSTEMS.\*

By A. D. McQUILLAN,† Ph.D., B.Sc.

## SYNOPSIS.

A method is described for the investigation of equilibrium relations in certain alloy systems, which depends on the measurement of hydrogen pressures in equilibrium with a very dilute solution of hydrogen in the alloys. The method is illustrated by a theoretical treatment of a hypothetical, simplified system, and is then applied to a series of alloys in a limited region of the titanium-copper and titanium-iron systems. It is found that both copper and iron depress the  $\alpha \rightleftharpoons \beta$  transformation in titanium. The effect of these addition elements on the solubility of hydrogen in the titanium-rich  $\beta$  solid solution has been examined.

## I.—INTRODUCTION.

In a previous paper<sup>1</sup> the author has described a study of the allotropic transformation temperature of titanium metal by measuring the variation with temperature of the equilibrium pressure of hydrogen in a very dilute solution of hydrogen in the metal. This method has now been applied to the study of phase transformations in limited regions of binary alloy systems of titanium with other metals.

Solutions of atomic hydrogen in homogeneous metallic phases which obey the laws of ideal dilute solutions can be shown to exhibit, in a closed system, a hydrogen equilibrium pressure  $p$ , which is given by the equation :

$$p = kc^2e^{\frac{Q}{RT}} \quad . \quad . \quad . \quad . \quad . \quad (1)$$

where  $c$  is the concentration of the dissolved hydrogen,  $T$  the absolute temperature,  $Q$  the heat of solution of 1 g.-molecule of hydrogen in the metal, and  $k$  a constant. The quantities  $Q$  and  $k$  are independent of hydrogen concentration and temperature, but will depend in general on the crystal structure and composition of the phase in which the hydrogen is dissolved. If the logarithm of the hydrogen equilibrium pressure is plotted as a function of the reciprocal of the absolute temperature for a given concentration of hydrogen dissolved in a homo-

\* Manuscript received 3 August 1950.

† Senior Research Officer, Physical Metallurgy Section, Commonwealth Scientific and Industrial Research Organization, Baillieu Laboratory, University of Melbourne, Australia.

geneous metallic phase of constant composition, a linear relationship will be obtained. In a binary alloy which can exist in a number of single-phase conditions at different temperatures, the  $\log p$  against  $1/T$  curves will be linear in each single-phase region, but each linear portion of the curve will be characterized by the particular values of  $Q$  and  $k$  for the phase.

In a two-phase alloy, the dissolved hydrogen will distribute itself between the two phases in such a way that the two solutions have the same equilibrium pressure. The hydrogen equilibrium pressure for a two-phase alloy will therefore be a function of the relative amounts of the two phases present and of the values of  $Q$  and  $k$  for the co-existing phases. This hydrogen pressure can be readily calculated when the quantities  $Q$  and  $k$  are known.

From equation (1), the hydrogen equilibrium pressure  $p$  for a hydrogen concentration  $c$  at any given temperature in a particular phase is given by :

$$p^{\frac{1}{2}} = Kc,$$

where  $K$  is the equilibrium constant, and has the value :

$$K = (ke^{\frac{Q}{RT}})^{\frac{1}{2}}.$$

If, in an alloy containing two phases,  $\alpha$  and  $\beta$ ,  $n$  represents the number of hydrogen atoms dissolved in  $N$  atoms of the alloy,  $a$  the fraction of alloy atoms in the  $\alpha$  phase, and  $x$  the number of hydrogen atoms dissolved in that phase, the hydrogen equilibrium pressure  $\bar{p}$  of the alloy at a given temperature is expressed by the relationship :

$$\bar{p}^{\frac{1}{2}} = K_a \frac{x}{aN} = K_\beta \frac{(n-x)}{(1-a)N}$$

where  $K_a$  and  $K_\beta$  are the equilibrium constants for hydrogen solutions in the  $\alpha$  and  $\beta$  phases of the alloy, respectively.

Hence

$$x = \frac{aK_\beta n}{K_a(1-a) + aK_\beta}$$

and

$$\bar{p}^{\frac{1}{2}} = \frac{n}{N} \cdot \frac{K_\beta}{\left\{1 - a\left(1 - \frac{K_\beta}{K_a}\right)\right\}}.$$

Since  $\frac{n}{N} = c$ , where  $c$  is the hydrogen concentration in the whole alloy :

$$p^{\frac{1}{2}} = \frac{cK_\beta}{\left\{1 - a\left(1 - \frac{K_\beta}{K_a}\right)\right\}} \quad \dots \quad (2)$$

and by rearranging :

$$a = \frac{1 - \frac{K_\beta}{\bar{p}^{1/2}/c}}{1 - \frac{K_\beta}{K_\alpha}} \quad \dots \quad (3)$$

With a knowledge of  $Q$  and  $k$ , the quantities  $K_\alpha$  and  $K_\beta$  may therefore be evaluated at any temperature, and substitution of the appropriate experimentally determined values of  $\bar{p}$  in equation (3) enables the relative amounts of the two phases in the alloy at any temperature to be determined.

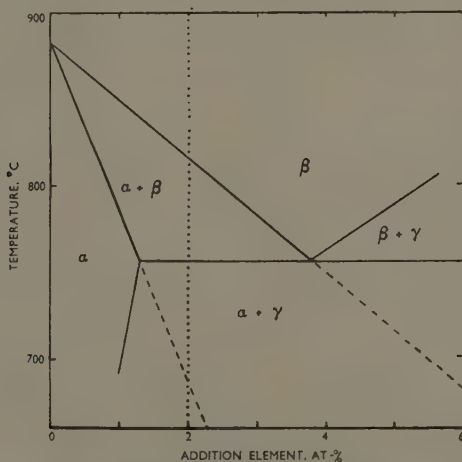


FIG. 1.—Hypothetical Equilibrium Diagram with Eutectoid Transformation.

To illustrate the form of the hydrogen pressure/temperature curve to be expected when an alloy passes through a number of different phase regions, equation (2) may be used to calculate the  $\log p$  against  $1/T$  curve for a simplified hypothetical eutectoid binary system of the type shown in Fig. 1, in which the  $\beta/(\alpha + \beta)$  and  $\alpha/(\alpha + \beta)$  boundaries are linear. For the purpose of this calculation it will be assumed that the values of  $k$  and  $Q$  are independent of the composition of a particular phase, and the values of  $k$  and  $Q$  for the  $\alpha$  and  $\beta$  phases will be taken to be those for  $\alpha$ - and  $\beta$ -titanium. In practice,  $k$  and  $Q$  would be expected to change with the composition of a phase, and the effect on the  $\log p$  against  $1/T$  curves of such changes will be examined when discussing the results obtained for real systems.

The atomic fraction of the  $\alpha$  phase present in an alloy containing 2 at.-% addition element, determined from the hypothetical equilibrium diagram, is shown as a function of temperature in Fig. 2. Once the alloy has entered the  $(\alpha + \beta)$  region, the atomic fraction of the  $\alpha$  phase present increases with decreasing temperature. When the alloy does not cross a eutectoid horizontal and the diagram is of the form shown by the broken lines in Fig. 1, the atomic fraction of  $\alpha$  phase will increase to unity in the manner shown by the broken line in Fig. 2. If a eutectoid line is reached, however, the amount of  $\alpha$  phase in the alloy will increase isothermally at the eutectoid temperature to a new value, depending on the position in the equilibrium diagram of the  $\gamma$  phase.

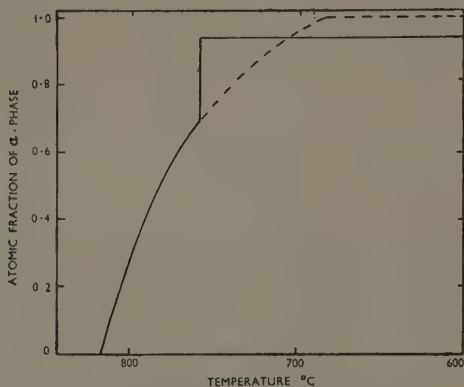


FIG. 2.—Atomic Fraction of  $\alpha$  Phase Present in the 2 at.-% Alloy of Hypothetical System as a Function of Temperature.

In this hypothetical case the amount of  $\alpha$  phase present in the alloy below the eutectoid horizontal has been assigned an arbitrary value. It will be assumed that the solubility of hydrogen in the  $\gamma$  phase, which contains a relatively large amount of addition element, is small and will be taken to be zero. The form of the  $\log p$  against  $1/T$  curve for the particular alloy may be calculated using equation (2).

In Fig. 3,  $ABCD$  represents the  $\log p$  against  $1/T$  curve for pure titanium containing 0.05 at.-% hydrogen. Over the temperature interval covered by the part of the curve  $AB$ , the titanium is in the  $\beta$  condition, but at 882.5° C. the  $\alpha \rightleftharpoons \beta$  transformation occurs and the hydrogen pressure increases isothermally from  $B$  to  $C$ . Below this transformation temperature the titanium is in the  $\alpha$  condition and the hydrogen pressure follows the line  $CD$ .



The pressure/temperature curve for the hypothetical 2 at.-% alloy containing 0.05 at.-% hydrogen is also presented in Fig. 3. In conformity with the initial assumption that the addition element has no effect on the  $\log p$  against  $1/T$  curves for pure phases, the line  $AB$  produced to  $E$  represents the  $\beta$  phase of the alloy. At  $E$  the alloy begins to transform, and a sharp discontinuity occurs in the  $\log p$  against  $1/T$  curve. In the  $(\alpha + \beta)$  region the pressure follows the curve  $EG$ , and if, as indicated by the broken line in Fig. 1, this transformation were completed, the hydrogen pressure would continue to follow the curve

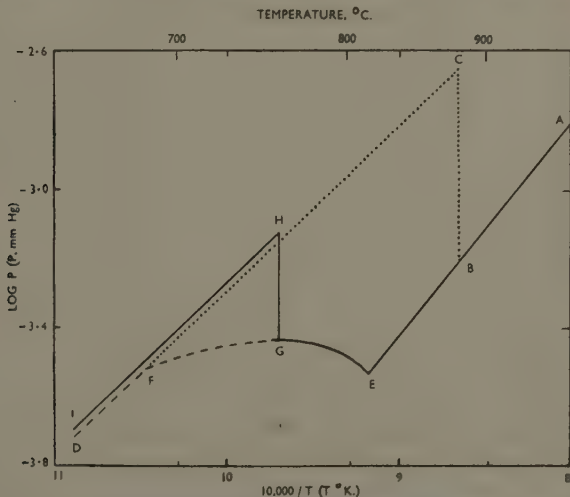


FIG. 3.—Form of  $\log p$  against  $1/T$  Curves for Hypothetical 2 at.-% Alloy Compared with Curve for Pure Titanium.

$EF$  until at  $F$ , when all the alloy is in the  $\alpha$  form, a second pressure discontinuity would occur. At temperatures below that represented by the point  $F$ , the pressure/temperature curve for the alloy would coincide with the line  $CD$  for pure  $\alpha$ -titanium. In the eutectoid system, however, the hydrogen pressure suddenly increases along the vertical line  $GH$  at the temperature at which the alloy passes through the eutectoid horizontal. The pressure represented by  $H$  is greater than the pressure of the hydrogen in pure  $\alpha$ -titanium at the same temperature. Below the eutectoid temperature the alloy contains a certain amount of  $\gamma$  phase, and hence the amount of  $\alpha$  phase in which the constant amount of hydrogen is dissolved is less than that which would be present if the alloy

consisted wholly of  $\alpha$  phase. Therefore, the hydrogen concentration in the  $\alpha$  phase of the  $(\alpha + \gamma)$  alloy will be increased. Equation (1) shows that an increase in hydrogen concentration must bring about an increase in the hydrogen pressure, and hence the pressure/temperature curve *HI* of the  $(\alpha + \gamma)$  alloy will lie above that for pure  $\alpha$ -titanium. In cases where the solubility of hydrogen in the  $\gamma$  phase is negligibly small, the increase in pressure,  $\Delta p$ , due to the presence of the  $\gamma$  phase is given by :

$$\Delta p = \frac{1}{a^2} \quad . \quad . \quad . \quad . \quad . \quad . \quad . \quad . \quad (4)$$

where  $a$  is the atomic fraction of the  $\alpha$  phase present in the two-phase alloy.

## II.—PREPARATION OF SPECIMENS.

The titanium-copper and titanium-iron alloys used in this investigation were prepared from spectroscopically pure copper and iron. The titanium metal was produced by the van Arkel method and was shown to contain about 0.07 at.-% impurities, the principal impurity being 0.02 at.-% iron.

The alloy specimens were prepared by melting in an argon-arc furnace. The argon in the furnace was purified by maintaining a separate piece of titanium in a molten condition in the furnace for 20 min. before melting the alloys. The alloy samples weighed only 3 g., and it was therefore possible to keep the whole sample molten at the same time. The smallness of the sample caused a high rate of cooling of the melts and enabled ingots to be produced which showed no large-scale segregation. An analysis of the alloys after melting indicated that no tungsten had been introduced from the electrode or copper from the water-cooled hearth.

The ingots were hot-swaged into rods at a temperature of 500° C. and annealed at 1000° C. for 70 hr. to remove any micro-inhomogeneities. After hot working in air, the samples had a superficial oxygen-contaminated zone which was removed before the annealing treatment. To prevent contamination of the specimens during the prolonged heating at 1000° C., they were inserted in a hollow titanium block contained in a silica tube which was then evacuated and sealed. Diffusion of gas through the heated walls of the sealed silica tube was prevented by surrounding it by another tube which was continuously evacuated. A piece of pure titanium subjected to this melting and homogenizing treatment showed no significant increase in hardness. Since the hardness of titanium is exceptionally sensitive to oxygen and nitrogen contamination, it was considered that the alloy specimens remained substantially uncontaminated by this treatment.

After the final homogenizing treatment the surface of the specimen was again mechanically cleaned. A marked reduction in the amount of gaseous contamination of the specimen was obtained when, after the final surface cleaning, the specimen was rapidly mounted in the apparatus and the apparatus evacuated.

### III.—APPARATUS AND EXPERIMENTAL PROCEDURE.

The alloy specimen, weighing about 0.5 g. was heated in a narrow-bore silica tube to which was connected a Pirani gauge of small internal volume. It is essential that the internal volume of this part of the apparatus, in which the hydrogen equilibrium pressure is to be established, shall be as small as possible to ensure that the amount of hydrogen necessary to create the equilibrium hydrogen pressure shall be negligible compared with the amount of hydrogen dissolved in the specimen. The pure hydrogen for these experiments was generated by the thermal decomposition of titanium hydride, and the amount necessary to give a hydrogen concentration of 0.05 at.-% when dissolved in the specimen was measured by collecting the hydrogen in a reservoir of known volume at a predetermined pressure. A full and detailed account of the apparatus and experimental procedure has already been given in a previous paper on the hydrogen-pressure method as applied to titanium.<sup>1</sup>

It was found that when the alloy was in a single-phase condition, the hydrogen pressure attained the equilibrium value at any temperature above 400° C. in a few minutes. In a two-phase region, however, the rate of attainment of the hydrogen equilibrium pressure depends on the rate of the phase-transformations occurring in the alloy. For the two groups of alloys studied in this work, periods of up to 1 hr. were required for the attainment of equilibrium. At lower temperatures, the time became inconveniently long.

### IV.—THE TITANIUM-COPPER SYSTEM.

Alloys containing 0.5, 1, 2, 3.5, and 5 at.-% copper were examined by the hydrogen equilibrium-pressure method over the temperature range 950°–725° C. The log  $p$  against  $1/T$  curves for these alloys, all of which contained 0.050 at.-% hydrogen, are shown in Fig. 4.

The form of the curves closely resembles that of the hypothetical curve (Fig. 3). At high temperatures the log  $p$  against  $1/T$  curves are linear, indicating that all the alloys are in a single-phase condition. The discontinuities indicate the beginning of the transformation of the  $\beta$  solutions, and occur at temperatures which decrease progressively with increasing copper content. Copper additions to titanium, therefore, reduce the temperature at which the  $\alpha \rightleftharpoons \beta$  transformation occurs,

Alloys containing 0.5 and 1 at.-% copper have log  $p$  against  $1/T$  curves which, after passing through a curved ( $\alpha + \beta$ ) region, again become linear at lower temperatures. These resemble the hypothetical curve for the binary system in which an alloy transforms completely to the  $\alpha$  phase at low temperatures. The curves for the 2, 3.5, and 5 at.-% copper alloys exhibit a sudden increase in hydrogen pressure at 776° C.; the increase becoming more marked the higher the copper content of the alloy. At temperatures below 776° C., the curves lie substantially

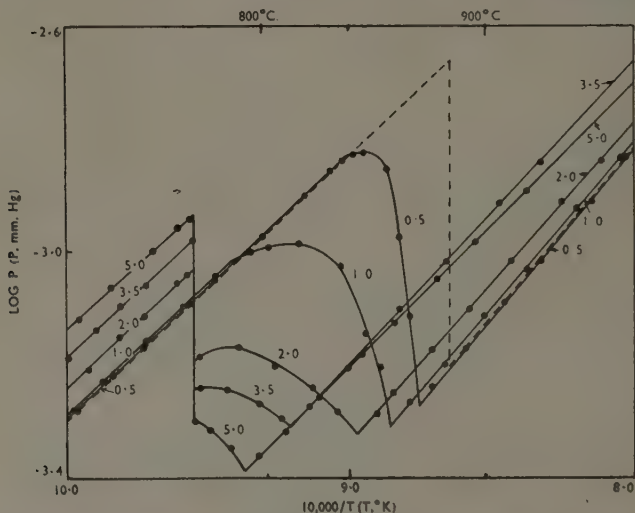


FIG. 4.—Log  $p$  against  $1/T$  Curves for a Series of Titanium-Copper Alloys. The figures on the curves give the copper content in at.-%. The broken line represents the log  $p$  against  $1/T$  curve for pure titanium containing the same amount of hydrogen.

parallel to the equivalent portion of the curve for the 1 at.-% alloy, but are displaced in the direction of higher hydrogen pressures, the displacement increasing with the copper content of the alloy. This behaviour indicates that alloys containing 2 at.-% and greater amounts of copper pass through a eutectoid horizontal at 776° C.

If the temperatures at which discontinuities occur in the log  $p$  against  $1/T$  curves for these alloys are plotted as a function of the copper concentration, the equilibrium diagram shown in Fig. 5 is obtained. The solubility of copper in  $\alpha$ -titanium is restricted to a maximum of about 1.25 at.-%, whereas the  $\beta$  phase extends over a much greater

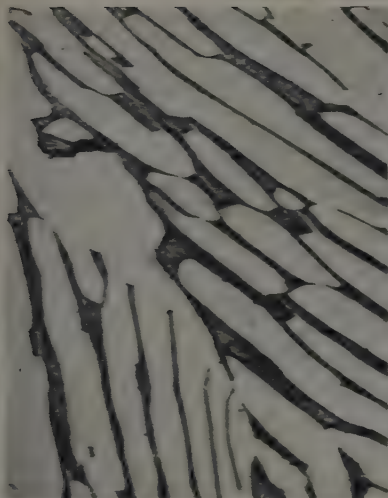


Fig. 6. 50% Cu-50% Sn alloy, slowly cooled from 900° to 800° C., and for 16 hr. at 800° C., and annealed.

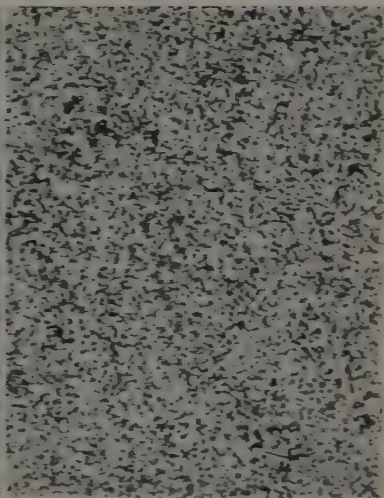


Fig. 7. 50% Cu-50% Sn alloy, slowly cooled from 900° to 800° C., and for 16 hr. at 800° C., and annealed for 168 hr. at 750° C.

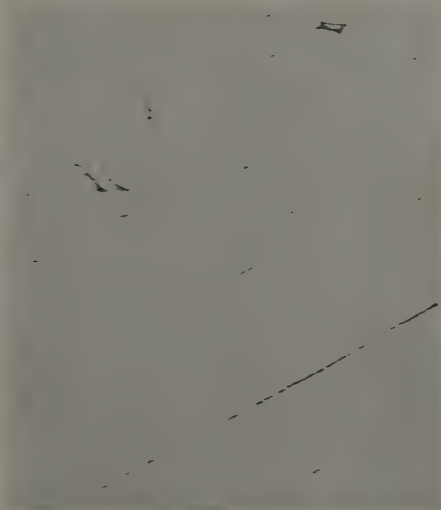


Fig. 8. 50% Cu-50% Sn alloy, slowly cooled from 900° to 800° C., and for 16 hr. at 800° C., and annealed.

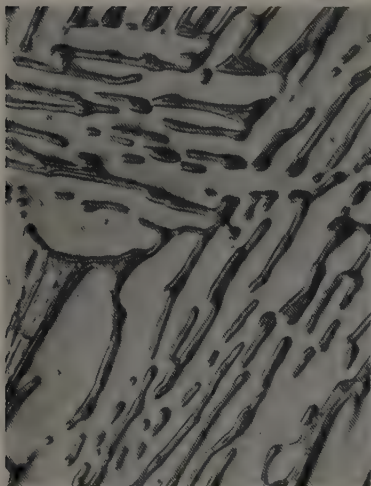


FIG. 9.—0.5 at.-% Iron Alloy, slowly cooled from 900° to 810° C., held for 16 hr. at 810° C., and quenched.



FIG. 10. 1.0 at.-% Iron Alloy, slowly cooled from 900° to 850° C., held for 16 hr. at 850° C., and quenched.

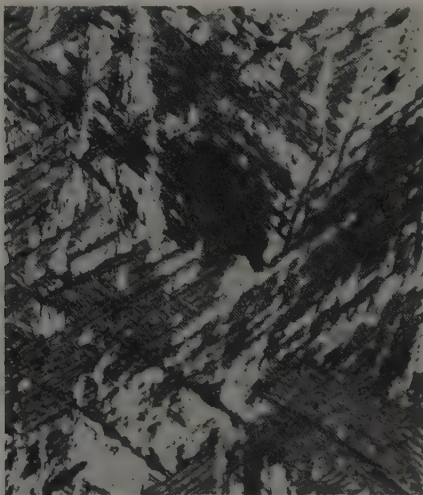


FIG. 11.—2.0 at.-% Iron Alloy, slowly cooled from 900° to 850° C., held for 16 hr. at 850° C., and quenched.



composition range. The slope of the  $\beta/(\alpha + \beta)$  boundary decreases with increasing copper concentration and, if this trend is maintained for copper concentrations greater than 5 at.-%, it would be reasonable to assume that the eutectoid composition lies in the neighbourhood of 10–12 at.-% copper.

Samples of each alloy used in this investigation have been quenched from 810° and 755° C. after heating at these temperatures for 16 and 136 hr., respectively. The types of microstructures obtained are indicated on Fig. 5 and are in agreement with the equilibrium diagram obtained by the hydrogen-pressure investigations. A study of these

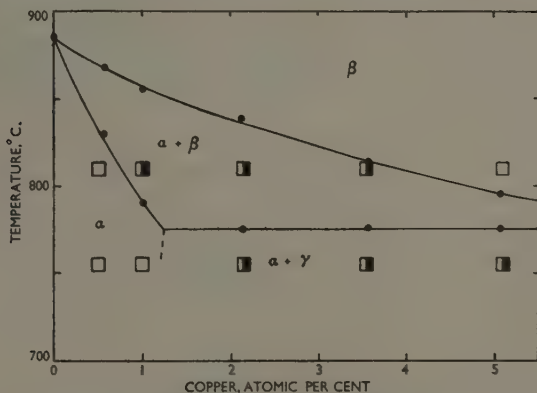


Fig. 5.—Portion of Titanium-Copper Equilibrium Diagram Obtained from Log  $p$  against  $1/T$  Curves.

- Single-phase structures (by micro-examination of quenched specimens).  
 ■ Two-phase " " " " "

microstructures suggests that it is not possible to suppress the transformation of the  $\beta$  phase by quenching until the copper concentration in this solution exceeds 5 at.-%. The decomposed  $\beta$  phase shows a Widmanstätten structure which etches darkly, whereas the primary grains of the  $\alpha$  phase remain unaffected by the etching reagent.

Figs. 6, 7, and 8 (Plate IX) illustrate three typical microstructures of quenched titanium-copper alloys which have been electrolytically polished in a perchloric acid-acetic acid bath and etched in an aqueous solution of hydrofluoric acid and hydrogen peroxide. Fig. 6 shows a 2 at.-% copper alloy which has been slowly cooled from the  $\beta$  phase and indicates the form of the primary crystals of the  $\alpha$  phase which have grown out of the original  $\beta$  phase. Fig. 7 shows the structure of a



1 at.-% alloy which is almost all in the  $\alpha$  form. The presence of a eutectoid transformation in this system can be deduced from Fig. 8, which shows the microstructure of a 5 at.-% alloy heavily deformed at 755° C. and held for 136 hr. at this temperature. The finely dispersed particles of the  $\gamma$  phase in a background of  $\alpha$  phase can be readily observed.

*Effect of Copper on the Hydrogen Solubility in the  $\beta$  Phase.*

The curves in Fig. 4 indicate that the addition of copper to titanium causes a change to occur in the position and gradient of the  $\log p$  against  $1/T$  curves for the  $\beta$  phase. As the copper content of the phase increases, the slope of the lines decreases, indicating a decrease in the numerical value of the negative heat of solution of molecular hydrogen in the alloy. Since the hydrogen concentration is constant, the gradient of the  $\log p$  against  $1/T$  curve may be seen from equation (1) to be given by the relationship :

$$\left( \frac{\partial \log p}{\partial \frac{1}{T}} \right) \frac{1}{c} = \frac{Q}{R}$$

and it is possible, therefore, to determine  $Q$  as a function of the copper content. When the value of  $Q$  for any particular curve is known, the corresponding quantity  $k$  may be evaluated.

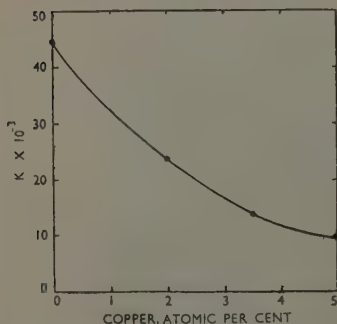


FIG. 12.—Values of  $k$  for Dilute Solutions of Hydrogen in  $\beta$  Phase of Titanium-Copper Alloys, as a Function of the Copper Content.

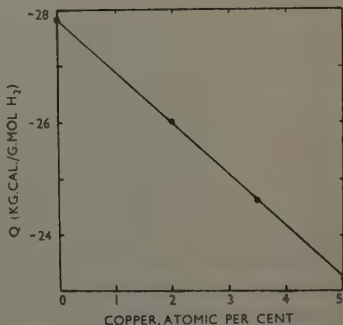


FIG. 13.—Heat of Solution of Hydrogen in  $\beta$  Phase of Titanium-Copper Alloys as a Function of the Copper Content.

Equation (1) is true, however, only if the laws of ideal dilute solutions are obeyed. Calculations of the changes in the quantities  $k$  and  $Q$  with variation of the copper content can be made only if the solution of

0.05 at.-% hydrogen in the alloys obeys these laws. Subsidiary experiments were carried out to check this point. For each alloy, the  $\log p$  against  $1/T$  curve in the  $\beta$  phase region was established for a series of hydrogen concentrations up to 5 at.-%. It was found that the values of  $k$  and  $Q$  for each alloy were independent of the hydrogen concentration over the range considered, and that the hydrogen pressure was exactly proportional to the square of the hydrogen concentration. Equation (1) may, therefore, be taken to give an accurate representation of the behaviour of dilute hydrogen solutions in the  $\beta$  phase of these copper alloys, and numerical values for  $k$  and  $Q$  may be obtained. The change in these quantities with copper concentration in the  $\beta$  phase are shown in Figs. 12 and 13. Both quantities are systematic functions of copper concentration, but whereas the value of  $Q$  decreases linearly with copper content, the relationship between  $k$  and copper content is more complicated.

Since the hydrogen equilibrium pressure exhibited by  $\beta$ -phase titanium-copper alloys is dependent on the particular values  $Q$  and  $k$  for each alloy, and these quantities vary independently with copper content, the variation of hydrogen equilibrium pressure with copper content will be complex. This explains the fact that the  $\log p$  against  $1/T$  curve for the  $\beta$  phase of the 5 at.-% copper alloy lies below that for the 3.5 at.-% alloy over the temperature range investigated.

#### V.—THE TITANIUM-IRON SYSTEM.

The titanium-iron system has been studied over the same composition and temperature range. The results obtained by hydrogen-pressure measurements, using 0.050 at.-% hydrogen dissolved in the alloys, are given in Fig. 14. The  $\log p$  against  $1/T$  curves for the titanium-iron alloys are similar to those for titanium-copper. They are linear at high temperatures and the temperature interval in which this linearity persists indicates the range of existence of the  $\beta$  phase. The discontinuities indicate the beginning of the two-phase ( $\alpha + \beta$ ) region, and occur at temperatures which decrease with increasing iron content. Thus iron, like copper, causes a lowering of the  $\alpha \rightleftharpoons \beta$  transformation temperature. In the ( $\alpha + \beta$ ) region the  $\log p$  against  $1/T$  curves at first behave in the manner indicated by the hypothetical case treated earlier, but at lower temperatures there is a reversal of curvatures and the curves for all the alloys converge and intersect at a point which lies very close to, if not on, the  $\log p$  against  $1/T$  curve for pure  $\alpha$ -titanium containing the same quantity of dissolved hydrogen. At temperatures below that at which the curves intersect, the hydrogen equilibrium pressure of the alloys lies above that for pure  $\alpha$ -titanium

by an amount which increases with the iron content. Since the curves of the alloys at temperatures below that at which they enter the  $(\alpha + \beta)$  region neither show a sharp discontinuity nor become linear, it would seem that the  $\alpha \rightleftharpoons \beta$  transformation is not completed in the temperature region examined.

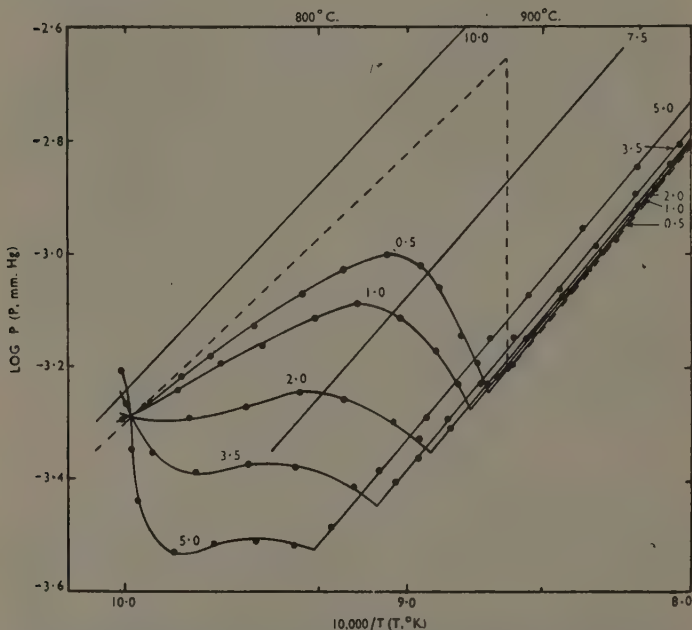


FIG. 14.—Log  $p$  against  $1/T$  Curves for a Series of Titanium-Iron Alloys. The figures on the curves give the iron content in at.-%. The broken line represents the log  $p$  against  $1/T$  curve for pure titanium containing the same amount of hydrogen.

The log  $p$  against  $1/T$  curves for  $\beta$ -phase alloys containing 7.5 and 10 at.-% iron are also indicated in Fig. 14. These larger additions of iron produce a marked increase in the hydrogen pressure at any temperature, the curve for the  $\beta$ -phase 10 at.-% alloy lying above that for pure  $\alpha$ -titanium. The effect, therefore, of increasing the iron content of the  $\beta$  phase is to decrease the hydrogen solubility in that phase. Since iron depresses the  $\beta/(\alpha + \beta)$  boundary, the  $\beta$  phase in equilibrium with the  $\alpha$  phase must become increasingly rich in iron as the tem-

perature decreases, and the hydrogen solubility in the  $\beta$  phase of a two-phase alloy will consequently decrease as the temperature falls. The change in curvature in the  $\log p$  against  $1/T$  curves in the  $(\alpha + \beta)$  region of alloys containing more than 1 at.-% iron at low temperatures is due to the effect of increasing amounts of iron on the hydrogen solubility in the  $\beta$  phase. At the temperature at which all the curves for the alloys intersect, the iron content of the  $\beta$  phase must have increased to a composition the hydrogen solubility for which is equal to that of the  $\alpha$  phase with which it is in equilibrium at that tempera-

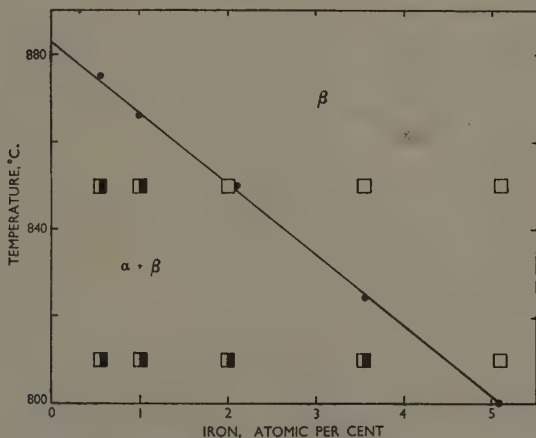


FIG. 15.—Portion of Titanium-Iron Equilibrium Diagram Obtained from  $\log p$  against  $1/T$  Curves.

- Single-phase structures (by micro-examination of quenched specimens).  
 ■ Two-phase " " " " " "

ture. Below this temperature, the iron content of the  $\beta$  phase will continue to increase while the alloys are still in the  $(\alpha + \beta)$  region. Since the hydrogen solubility in the  $\beta$  phase is now less than that for the  $\alpha$  phase, the order of the curves will be inverted. It is possible, therefore, to explain the form of the curves for the  $(\alpha + \beta)$  region of these iron alloys in terms of the change in hydrogen solubility in the  $\beta$  phase with increasing iron content.

By observing the discontinuities in the  $\log p$  against  $1/T$  curves for the iron alloys it is possible to construct only the  $\beta/(\alpha + \beta)$  boundary shown in Fig. 15. Within the limits of experimental error this boundary is a straight line. Since the alloy containing 0.5 at.-% iron remains in

the two-phase ( $\alpha + \beta$ ) condition at the lowest temperature for which measurements were made, the solubility of iron in the  $\alpha$  phase must be less than 0.5 at.-% at 725° C.

Microstructures of all the titanium-iron alloys have been examined after heating at 850° and 810° C. for 16 hr. and quenching. The types of structure obtained are indicated on Fig. 15 and are consistent with the form of the diagram obtained from hydrogen-pressure measurements. As in the case of the titanium-copper alloys it was not possible to retain the  $\beta$  phase until the iron content had reached 5 at.-%.

Figs. 9, 10, and 11 (Plate X) illustrate the structures obtained for alloys containing 0.5, 1, and 2 at.-% iron, respectively. The decomposed primary  $\beta$  phase, which etches darkly with a Widmanstätten structure, is present in the 0.5 at.-% alloy in appreciable amounts, con-

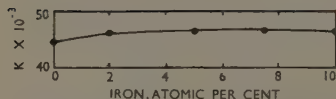


FIG. 16.—Values of  $k$  for Dilute Solutions of Hydrogen in  $\beta$  Phase of Titanium-Iron Alloys, as a Function of the Iron Content.

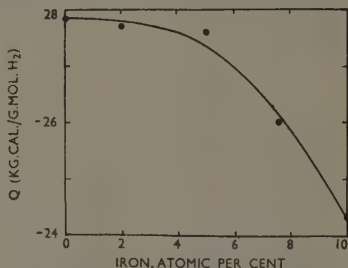


FIG. 17.—Heat of Solution of Hydrogen in  $\beta$  Phase of Titanium-Iron Alloys as a Function of the Iron Content.

firming that at 810° C. the solubility of iron in the  $\alpha$  phase is certainly less than 0.5 at.-%. Fig. 10 shows the structure at 850° C. of the 1 at.-% iron alloy containing roughly equal amounts of primary  $\alpha$  and  $\beta$  phases, while Fig. 11 indicates that at the same temperature the 2 at.-% alloy consisted completely of the  $\beta$  phase.

#### *Effect of Iron on the Hydrogen Solubility in the $\beta$ Phase.*

It has been shown, in exactly the same way as for the titanium-copper alloys, that equation (1) is valid for solutions of hydrogen in the  $\beta$  phase of titanium-iron alloys up to a hydrogen concentration of 5 at.-%, this being the maximum hydrogen concentration examined in these subsidiary experiments. The variations in the values of  $k$  and  $Q$  as functions of iron concentration in the  $\beta$  phase have been determined and are shown in Figs. 16 and 17, respectively. Up to 5 at.-% iron the value of  $Q$  does not change appreciably, but with higher iron contents

it decreases numerically. The value of  $k$  remains substantially constant over the whole composition range.

Since the values of  $k$  and  $Q$  for the  $\beta$  phase are known, equation (3) can be used to calculate the amount of  $\alpha$  phase present in each alloy at a series of temperatures. It is possible, therefore, to construct the  $\alpha/(\alpha + \beta)$  boundary from the known  $\beta/(\alpha + \beta)$  boundary. At temperatures between 882.5° and 800° C. the calculation gives values for the solubility of iron in  $\alpha$ -titanium within  $\pm 0.1$  at.-% of zero, from which it is concluded that the solubility of iron in the  $\alpha$  phase does not exceed 0.1 at.-% in this temperature range.

## VI.—DISCUSSION.

A study has been made of the behaviour of hydrogen when dissolved in a limited range of titanium-rich alloys in order to show as fully as possible the application of the hydrogen-pressure method to the elucidation of constitutional diagrams. The method has a number of advantages over many of the more conventional metallurgical techniques used for the study of equilibrium diagrams, especially those involving the extremely reactive metal titanium. The alloy specimens to be examined by the hydrogen-pressure method need be in no special form and only small quantities of material, about 0.5 g., are required. A further advantage of the method is that no connections have to be made to the specimen, as is necessary, for example, in the measurement of resistivity and thermoelectric power; the danger of contamination of the specimen by the material of the electrodes is thereby avoided. The specimen under examination can be maintained at any temperature for unlimited times, and it is possible, therefore, to be sure that the alloy is in a state of true equilibrium. The hydrogen-pressure method is, in this respect, superior to thermal analysis.

The determination of hydrogen equilibrium pressure requires only simple and inexpensive apparatus, and it is possible to replicate it easily so that a number of specimens can be examined at one time. In cases where prolonged periods are required for the attainment of metallurgical equilibrium, the simultaneous examination of a series of alloys results in a considerable saving in time. The author has used six specimen tubes in a single furnace with one bridge circuit for all the Pirani gauges, the reading for any gauge being obtained by the use of a selector switch.

The method would seem to be applicable to all alloys that contain an appreciable amount of a metal having a high hydrogen solubility, e.g. zirconium, vanadium, and tantalum. If the solubility of hydrogen in an alloy is low, it is necessary to decrease the internal volume of the apparatus and increase the size of the specimen, in order to keep the

amount of hydrogen required to set up the equilibrium pressure in the apparatus small in comparison with the quantity dissolved in the specimen. For very low hydrogen solubilities the practical difficulties involved set a limit to the usefulness of the method. In such cases it is possible, however, to follow the phase transformations by the direct determination of hydrogen solubility as has been shown by Potter and Lukens<sup>2</sup> in the case of manganese.

In the programme of work envisaged, it is hoped to continue the study of the effect of various addition elements on the  $\alpha \rightleftharpoons \beta$  transformation of titanium. Changes in the values of  $k$  and  $Q$  for the  $\beta$  phase of these alloys will also be investigated, since, apart from the purely utilitarian value of a knowledge of these quantities in the interpretation of the hydrogen equilibrium pressure curves, they possess a theoretical interest, and may throw some light on the electronic configuration of the alloys.

The solution of a molecule of hydrogen in a metal lattice may be considered to be a succession of discrete processes—the dissociation of the hydrogen molecule, the ionization of the resulting atoms, and the solution of the protons and electrons in the metal. Since the energy liberated by the solution of an electron in the metal is numerically equal to the work-function for that metal, the energy of solution of a proton in the metal can be calculated from a knowledge of  $Q$  and the work-function. The quantity  $k$  is not as easily visualized as  $Q$ , since it is related to the partition functions for the solutions of a proton and an electron in the metal lattice. Probably, however, the contribution made by the partition function of the proton would have the greater effect.<sup>3</sup> It is hoped that it will be possible to treat this subject more fully in another paper, when information on the effects of a greater range of addition elements on the values of  $k$  and  $Q$  for titanium-rich alloys is available.

#### ACKNOWLEDGEMENTS.

The work presented in this paper forms part of the research programme being carried out by the Physical Metallurgy Section of the Australian Commonwealth Scientific and Industrial Research Organization. The author would like to express his gratitude to Professor J. N. Greenwood of the Metallurgy Research Department, University of Melbourne, for his encouragement and for the laboratory facilities which have enabled this work to be undertaken.

#### REFERENCES.

1. A. D. McQuillan, *J. Inst. Metals*, 1950–51, **78**, 249.
2. E. V. Potter and H. C. Lukens, *Trans. Amer. Inst. Min. Met. Eng.*, 1947, **171**, 401.
3. R. H. Fowler and C. J. Smithells, *Proc. Roy. Soc.*, 1937, [A], **160**, 38.



# SOME NEW OBSERVATIONS ON THE MECHANISM OF FATIGUE IN METALS.\*

1299

By W. A. WOOD,<sup>†</sup> D.Sc., MEMBER, and A. K. HEAD,<sup>‡</sup> B.A., B.Sc.

## SYNOPSIS.

The response of the crystalline structure of a metal to static stressing has been compared by X-ray-diffraction methods with its response to cyclic, or fatigue, stressing. The essential difference is that static stressing produces an extensive and progressive disorientation of the internal structure of the grains, whereas under cyclic stressing this derangement is largely suppressed. The degree of suppression is shown to depend in part on the alternating character of the deformation under cyclic stress, though it depends also on the rate of alternation, there appearing to be a critical rate above which suppression of the disorientation sets in abruptly. For copper under alternating tension/compression, this critical rate lies between 300 and 400 cycles/min.

It is inferred from these observations that if a grain is subjected suddenly to a stress greater than the normal yield stress and then allowed to deform in its own time, there is a delay period before any appreciable plastic strain occurs. It would appear reasonable to assume also that this inhibition of unidirectional deformation at rates of cyclic stressing above the critical rate, in effect, transforms a normally ductile metal into a brittle medium, and thus accounts for some of the basic factors in the failure of metals by fatigue.

## I.—INTRODUCTION.

Two fundamental problems in the failure of metals by fatigue that have to be solved are, first, why a metal fails under repetition of a stress that would be too small to cause fracture by a single application; and secondly, why a metal that may be ductile under static stress appears to be embrittled by cyclic stressing, with the result that failure starts characteristically from a local cleavage crack.

In any attempt at an experimental solution to these problems, it is necessary as a preliminary step to establish the special modifications in atomic or crystalline structure of the metal that are brought about by cyclic as distinct from static stressing. Much work on these lines has already been done, in the first place by a study of the structural changes shown by the microscope. Such researches, carried out on polycrystalline metals by Ewing and Humfrey,<sup>1</sup> Stanton and Bairstow,<sup>2</sup> and Gough and Hanson,<sup>3</sup> and later on single metal crystals by Gough and his colleagues,<sup>4</sup> led to important advances that may be summarized briefly as follows:

\* Manuscript received 10 July 1950.

<sup>†</sup> Baillieu Laboratory, University of Melbourne, Australia.

<sup>‡</sup> Aeronautical Research Laboratories, Department of Supply and Development, Melbourne, Australia.

(i) Plastic deformation by both cyclic and static stressing takes place by the same basic mechanism of slip. In each case the slip follows similar crystallographic directions and is governed by the same law of maximum resolved shear.

(ii) In one half of a stress cycle, the slip occurs on one set of parallel atomic planes; in the reverse half, it is said to occur in the opposite direction but on other planes parallel to the first set. Therefore the density of the slip lines may increase under cyclic stressing as it does under the progressive unidirectional plastic flow produced by static stressing. Thus, internally a specimen may undergo cumulative deformation by slip under cyclic stressing, even though externally the reversals of the strain may leave the shape of the test specimen unchanged.

(iii) The cumulative plastic deformation indicated by an increasing density of slip lines is accompanied by strain-hardening in cyclic stressing as it is in static stressing. If the range of cyclic stress is too small to lead to fracture, the production of slip lines ceases after a certain number of cycles. Such considerations led Gough and Hanson to suggest that the fatigue fracture occurred when at some point of heavy deformation a certain limit of strain-hardening was exceeded. Later attempts to explain failure<sup>5</sup> on theoretical grounds have led essentially to the same conclusion.

(iv) In unsafe ranges of cyclic stress the fatigue fracture, in general, develops in regions of particularly dense slip. Thus failure is associated with heavy plastic deformation, as in the case of static stress.

These researches established that deformation and fracture, under cyclic stressing, were based on the same processes as under the more familiar static stressing. They tended, however, to emphasize the similarity in the changes in microstructure rather than the dissimilarity.

The crucial difference between the two cases has still to be found, but some advance in this direction resulted at a later date from a study of the microstructure by X-ray diffraction, first applied to the problem by Gough and Wood.<sup>6</sup> The X-ray technique differs from the metallographic in being particularly sensitive to disorientation and distortion of the atomic structure of the crystalline grain, as will be illustrated later in the present paper. Gough and Wood, in an examination of this process in mild steel, were able to demonstrate one major difference between the effects of static and cyclic stress. They showed that as the metal was progressively deformed to fracture under static stress this disorientation, or "fragmentation" as it was termed, spread to a striking extent throughout the material. Under alternating stress,

however, the disorientation was always much less; in fact, in a safe range of cyclic stress symmetrical about zero stress, i.e. one producing little residual plastic deformation, the effect was entirely suppressed. The incident X-ray beam used in diffraction experiments in practice covers about 1 or 2 mm.<sup>2</sup> of specimen and averages the effects over such an area. Gough and Wood concluded, therefore, that fatigue failure, if it did occur by an accumulation of effects similar to those produced by ordinary plastic deformation, must result from structural changes that were highly localized. A second major difference was discovered by Wood and Thorpe,<sup>7</sup> who subjected specimens of brass to alternating cycles of stress applied slowly by hand in the first place, and then to reversals applied at the rate of 2000 cycles/min., as commonly used in fatigue testing. They showed that the slow cycle produced a widespread disorientation of the grains similar to that caused by static stressing; but when the same stress cycle was applied at the high speed, this derangement of the structure was practically inhibited. They thus established the further point that not only the action of reversal but the *rate* of reversal of the stress produced a vital difference between the effects of static and cyclic stress.

Few further experimental developments of this type followed. The position has remained at the general conclusion that the changes in crystalline structure resulting from the two types of stressing are basically the same in kind but differ in degree and distribution. It is evident, however, that some aspect of this difference must play a vital part in determining the strength of a metal under cyclic stressing. The object of the present work has been to try and establish the crucial difference by suitable comparative experiments.

## II.—EXPERIMENTAL.

On the basis of previous experience the following special conditions of experiment were chosen.

First, an annealed non-ferrous metal (copper) was employed as the main test material, with aluminium being used for certain subsidiary tests. The reason for this choice was that the elastic range of these metals is low, and is almost certain to be exceeded at the peak of any useful stress cycle. In the first half of such a stress cycle, slowly applied, the metal will undergo plastic deformation, just as it would under the application of ordinary unidirectional static stress. Therefore the conditions are favourable for comparing the effects on the structure of a single plastic strain and, after the second half of the cycle, of a reversal of that strain. The further differences could then be examined between the respective effects of an increasing direct

stress or strain, and continued reversals of a fixed stress or strain. The solution to the fatigue problem might be expected to lie in the response of the crystalline structure to these two fundamentally different methods of attempting to produce cumulative internal deformation.

The second feature of the work was suggested by the observation of Wood and Thorpe that the crystalline structure was affected by the rate at which a cyclic strain was reversed. In order to pursue this point, a special machine was constructed that permitted a given stress cycle to be applied at any frequency from a few cycles/min. to approximately 700 cycles/min. Preliminary dynamic stress/strain tests were made to ensure that a given nominal stress was in fact applied to the specimen; it is hoped to describe such tests and the mechanical details of the machine in a separate paper. This machine was supplemented by a standard Haigh fatigue-testing machine operating at the more usual rate of 1800 cycles/min. In this way the significance of the speed effect could be investigated.

A third requirement was that the form of the stress cycle should be reasonably symmetrical about zero stress. Otherwise, a bias in tension or compression would superimpose on the cyclic strain a unidirectional plastic flow and thereby confuse the issue. This symmetry was satisfactorily achieved by the machine employed. The cycles were direct tension/compression, which was preferred to the other common stress systems, such as alternating torsion or bending, because of the more homogeneous nature of the associated deformation.

Finally, for the X-ray examination, it was necessary that after being machined to shape, the test specimens should be thoroughly annealed. This was desirable in order that the initial crystalline structure should be as perfect as possible, and free from the confusing effect of possible previous plastic deformation. Moreover, grains in this condition give sharp X-ray diffraction spots, changes in which are easily detected. The size of the grains relative to the incident X-ray beam was adjusted so that the individual reflection spots were well separated on the diffraction ring, again to simplify detection of the changes, since the chief of these—due to plastic deformation—is a circumferential spreading of the reflection spots. For the X-ray spectrometer employed, a suitable grain-size was 0.1 mm., and this was adopted as standard. The back-reflection X-ray technique was used, as other work had shown this to be the most sensitive to plastic deformation in the grains. Unless otherwise stated, the photographs reproduced show the (400) back-reflection rings of copper or (420) rings of aluminium, obtained with cobalt  $K\alpha$  radiation at a specimen-film distance of some 10 cm.

It will be evident that the above conditions define a case of what might be termed pure fatigue, as distinct from cyclic strain combined with ordinary unidirectional deformation. The latter more complex conditions are, of course, more usual in practice, but it is unlikely that their introduction will invalidate any fundamental principles observed in the special case of the pure fatigue.

### III.—RE-ORIENTATION EFFECT.

It is considered that the fundamental difference between the effects of cyclic and static stressing is brought out by the following basic experiments. The first shows how the effect on the atomic structure of progressive unidirectional strain differs from that produced by an equivalent cyclic strain. The second demonstrates that this difference is accentuated if the cycle is applied at a rapid rate of reversal. These effects appear to explain the difference observed by Gough and Wood in the condition of the material at fracture.

#### 1. *Comparison of the Disorientation Produced by Equivalent Direct and Reversed Strain.*

Two similar specimens of aluminium, in the form of tensile-test specimens with a parallel gauge-length  $2\frac{1}{4}$  in., and circular section  $\frac{5}{16}$  in. in dia., were prepared. Both specimens were extended by the same amount, namely 2%. One specimen was then subjected to a further 2% extension, while the other was compressed by 2% to its original dimensions. Thus, internally, both specimens underwent a virtual plastic strain of 4%. Externally, however, the strain was unidirectional in one specimen, whereas in the other it was reversed at the half-way value. The structural changes in the grains were examined at each stage by X-ray diffraction, with the following results.

The changes due to the first extension of 2% were, of course, similar in each specimen. The change of special relevance was a breakdown of the initial homogeneous structure of each grain into a mosaic of differently oriented regions, a feature discussed in other papers.<sup>8</sup> This disorientation is illustrated by the X-ray photographs reproduced as Figs. 1 and 2 (Plate XI), which correspond, respectively, to a specimen before and after the 2% extension. The sharpness of the reflection spots in the first photograph shows that the initial annealed grains possess a highly perfect and homogeneous structure. The second photograph shows that the small extension of 2% is sufficient to cause the reflections to undergo a marked diffusion and elongation along the



diffraction ring, indicating an extensive dissociation of the grains into elements that reflect over an appreciable angular range. This is the breakdown here termed "disorientation".

The subsequent changes in the two specimens differed in the following way. In the specimen extended by a further 2% the disorientation increased, as illustrated in Fig. 3 (Plate XI), obtained after 4% extension. But in the specimen compressed by 2% there was no increase; in fact, the structure tended, though imperfectly, to revert to the initial homogeneous orientation. This is clear from Fig. 4 (Plate XI), which refers to the same specimen as Fig. 2; this photograph shows that the reversal of the strain has caused no further elongation of the reflections, but, if anything, a contraction towards the initial sharp condition, an effect that could perhaps be described as "re-orientation".

Aluminium was purposely chosen for these first tests in order that the X-ray photographs should not be complicated by the effects of internal elastic strains or related distortion of the atomic lattice. Owing to the low strength of aluminium, such strains are small in magnitude and are known to produce minor diffusion only of the X-ray-diffraction pattern; this can therefore be neglected in comparison with the outstanding circumferential spreading of the X-ray reflections, and the corresponding drastic breakdown of the structure into macroscopic elements. The re-orientation effect was repeated, however, with copper, as well as with other aluminium specimens. It was established also for specimens of both metals subjected to reversed torsion and bending, in addition to reversed tension.

It is naturally to be expected that internal elastic stresses may be altered in sign or magnitude by reversing an external stress or strain; but it is less obvious that the larger-scale derangement under discussion should be at all reversible. The important feature brought out by these experiments, therefore, is that in cyclic plastic deformation the reversal of the strain in the second half of the cycle tends partially to restore the disorientation produced by the first half, whereas continued deformation in one direction produces progressive disorientation and breakdown of the structure.

It should be emphasized that the effects described were observed whatever point on the surface of the specimens was examined by the X-ray method, and etching tests indicated that they extended throughout the volume. All the structural changes mentioned in the paper similarly refer to changes occurring in the body of a specimen and are not special effects that might possibly take place locally in the vicinity of a fracture, should a fracture occur.

## 2. Comparison of Disorientation Produced by Slow and Rapid Cyclic Stress.

To determine how the disorientation process is affected by the speed at which the stress cycle is reversed, the following tests were applied.

Specimens of copper were prepared in the form of the standard fatigue specimen of circular section. A stress  $S$  was chosen of a value that would cause appreciable plastic deformation if applied slowly in tension or compression. The tensile yield strength of the annealed copper was approximately 2 tons/in.<sup>2</sup> and values of  $S$  employed were 3, 4, 5, 6, and 7 tons/in.<sup>2</sup>.

One specimen was subjected to slow cycles of  $\pm S$  in tension/compression at the slow rate of 10 cycles/min. After running for 10, 10<sup>2</sup>, and 10<sup>3</sup> cycles, the test was interrupted to allow of X-ray examination. In order to prevent excessive plastic flow in one direction or the other on first application of the stress, the amplitude of the stress cycle was built up in small increments until the peak  $\pm S$  was reached, and it was similarly removed in small decrements. The gradual application and removal of the cycle thus left the specimen with no significant external deformation, which might otherwise complicate the results.

An equivalent specimen was subjected to the same stress cycle in the Haigh machine running at the relatively rapid rate of 1800 cycles/min. This specimen also was examined by X-rays at suitable intervals.

A comparison of the behaviour of the two specimens established the effect of reversing an applied stress or strain cycle at low or high speeds. The experiment resembled that of Wood and Thorpe on brass, though in their work only one slow cycle was applied by hand, whereas in the present arrangement slow cycles could be applied up to any number and the cumulative effects of slow and rapid stress accordingly compared.

The results were as follows.

(i) A single, slow stress cycle produced a certain degree of re-orientation, as already discussed for a single reversal of strain, but, as in that case, the process was imperfect and in practice a distinct disorientation remained. With an increasing number of cycles a slight further deterioration occurred, but this was of a second order. The extent of the effect is illustrated for the case of  $S = \pm 5$  tons/in.<sup>2</sup> by Figs. 5 and 6 (Plate XI) and Fig. 7 (Plate XII), which show the X-ray patterns, respectively, before stressing and after 10<sup>2</sup> and 10<sup>3</sup> cycles. The breakdown is quite clear after each number of cycles, but there is no major increase between the successive stages.

(ii) When the same stress cycle was applied at high speed the test specimen showed practically no disorientation. This is clear from



Fig. 8 (Plate XII), which was obtained after subjecting a specimen to  $10^4$  cycles at  $\pm 5$  tons/in.<sup>2</sup> at 1800 cycles/min. The reflection spots are almost as sharp as those in Fig. 5, which was characteristic of the initial annealed state. There is some slight diffusion of the spots, which shows that the internal structure of the grains has been disturbed to some extent. This change, though small, is of some significance in relation to points discussed later, but it is quite evident from the photographs that its extent is negligible in comparison with that produced by the corresponding stress cycle applied at a slow rate. The same difference was equally marked with the other ranges of stress from 3 to 7 tons/in.<sup>2</sup>; also it was maintained whatever number of cycles was imposed. Therefore, in contrast with the effect of the slow cycles, that of the rapid cycles is largely to inhibit the disorientation throughout all stages of a test.

(iii) Of the conclusions to be deduced from the re-orientation and speed effects described, that which appears to be of most importance to the main object of the research is that when a polycrystalline metal is subjected to stress, a finite time is required before that stress can produce the change in the shape of a grain which is normally associated with plastic yield and which in practice results in a macroscopic internal breakdown and disorientation of the grain. It appears as if the boundary of a grain acted as a viscous "container" of higher strength than the interior, and this boundary gave way under stress only after a distinct interval of time. This inference is discussed more conveniently in Section V.

### *3. Cumulative Structural Changes Occurring Finally at Fracture.*

A comparison was made between the final structure of copper after fracture had been produced: (a) by continued repetition of a rapid stress cycle, (b) by a slow cycle, and (c) by progressive static deformation under increasing stress. This led to the interesting observation that under rapid cycles of a given stress, the cumulative disorientation and breakdown of the grains at fracture remained relatively small; and that under slow cycles of the same stress the breakdown, though more marked, was still not excessive. But at fracture under progressive unidirectional strain, the breakdown was of an altogether higher order of magnitude. The significant point emerging was that at fracture by progressive repetition of cyclic stress, rapid or slow, there is no accumulation of the internal breakdown and disorientation of the grains at all comparable with that produced by progressive unidirectional deformation.

The contrast is illustrated by Figs. 9, 10, and 11 (Plate XII).

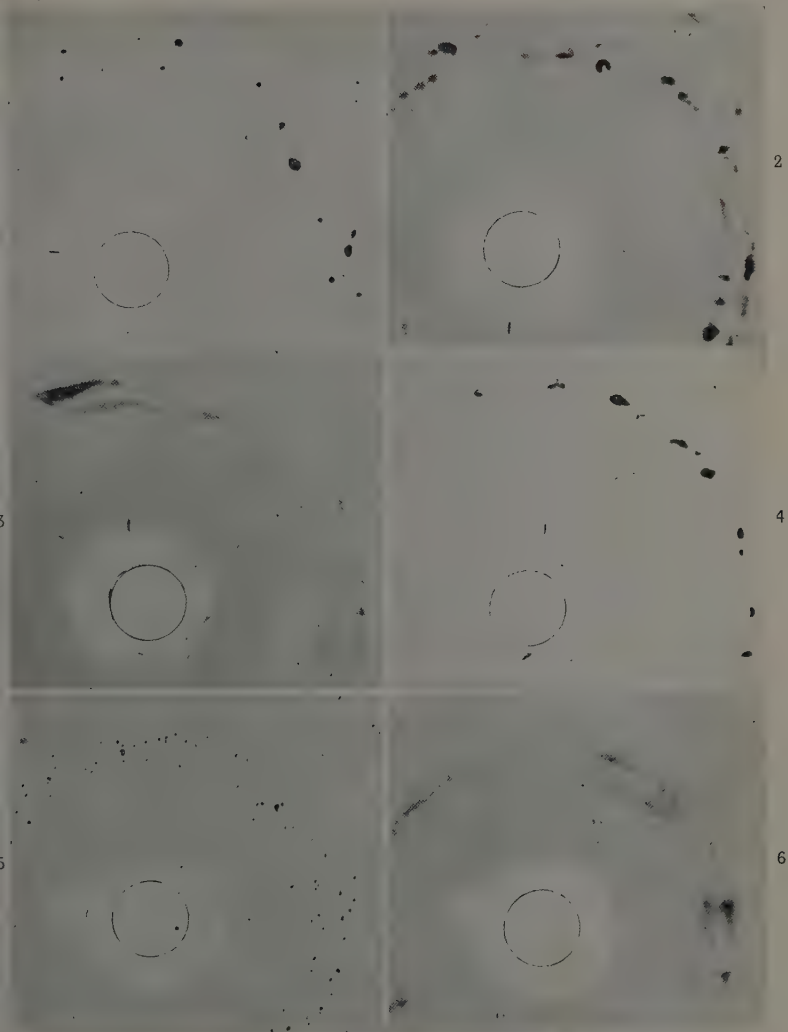


FIG. 1.—Aluminium (99.98% pure), initial annealed state.  
 FIG. 2.— „ after 2% extension.  
 FIG. 3.— „ after 4% extension.  
 FIG. 4.— „ after 2% extension, then 2% compression.  
 FIG. 5.—Copper (commercial H.C.), initial annealed state.  
 FIG. 6.— „ after  $10^2$  cycles  $\pm 5$  tons/in.<sup>2</sup> at 10 cycles/min.

[To face p. 96.]

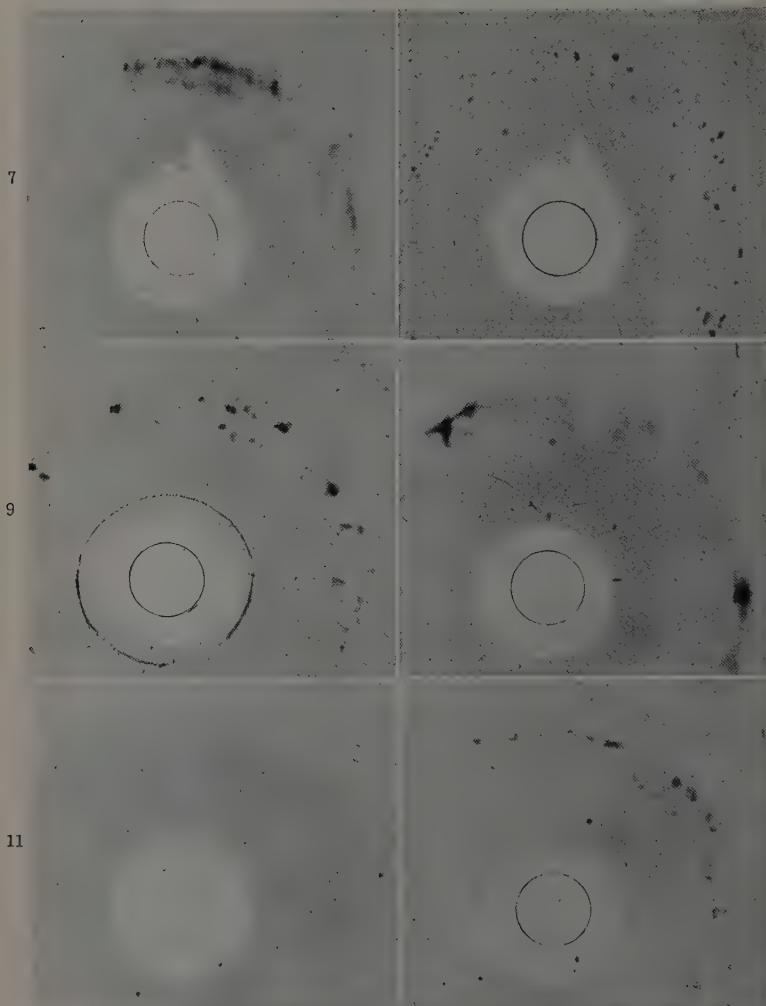


FIG. 7.—Copper, after  $10^3$  cycles  $\pm 5$  tons/in.<sup>2</sup> at 10 cycles/min.  
 FIG. 8.— „ after  $10^4$  cycles  $\pm 5$  tons/in.<sup>2</sup> at 1800 cycles/min.  
 FIG. 9.— „ as fractured by  $10^5$  cycles  $\pm 7$  tons/in.<sup>2</sup> at 1800 cycles/min.  
 FIG. 10.— „ as fractured by  $10^5$  cycles  $\pm 7$  tons/in.<sup>2</sup> at 150 cycles/min.  
 FIG. 11.— „ as fractured by static tensile loading.  
 FIG. 12.— „ after  $10^3$  cycles  $\pm 5$  tons/in.<sup>2</sup> at 100 cycles/min.

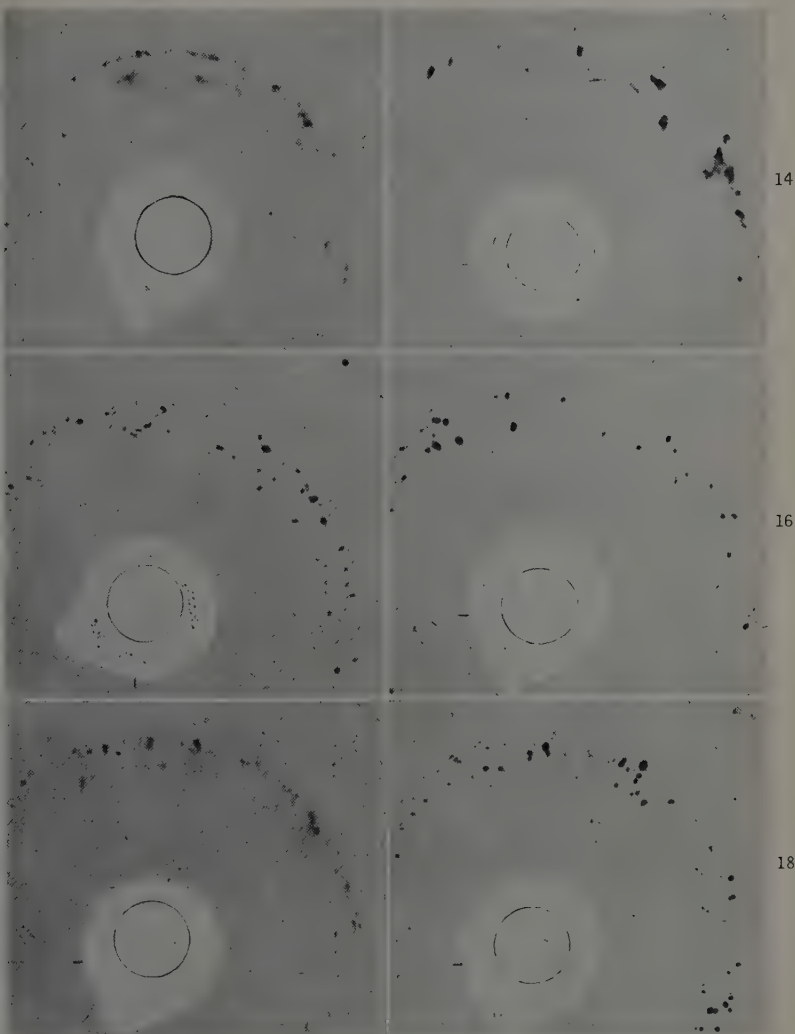


FIG. 13.—Copper, after  $10^2$  cycles  $\pm$  5 tons/in.<sup>2</sup> at 150 cycles/min.  
 FIG. 14.— " after  $10^2$  cycles  $\pm$  5 tons/in.<sup>2</sup> at 300 cycles/min.  
 FIG. 15.— " after  $10^2$  cycles  $\pm$  5 tons/in.<sup>2</sup> at 400 cycles/min.  
 FIG. 16.— " after  $10^2$  cycles  $\pm$  5 tons/in.<sup>2</sup> at 600 cycles/min.  
 FIG. 17.— " after  $10^2$  cycles  $\pm$  3 tons/in.<sup>2</sup> at 300 cycles/min.  
 FIG. 18.— " after  $10^2$  cycles  $\pm$  3 tons/in.<sup>2</sup> at 400 cycles/min.

19

21

23

- FIG. 19.—Copper, after  $10^2$  cycles  $\pm 6$  tons/in.<sup>2</sup> at 300 cycles/min.  
 FIG. 20.— " after  $10^2$  cycles  $\pm 6$  tons/in.<sup>2</sup> at 400 cycles/min.  
 FIG. 21.— " after  $10^2$  cycles  $\pm 7$  tons/in.<sup>2</sup> at 300 cycles/min.  
 FIG. 22.— " after  $10^2$  cycles  $\pm 7$  tons/in.<sup>2</sup> at 400 cycles/min.  
 FIG. 23.— " after  $10^4$  cycles  $\pm 5$  tons/in.<sup>2</sup> at 300 cycles/min.  
 FIG. 24.— " after  $10^4$  cycles  $\pm 5$  tons/in.<sup>2</sup> at 400 cycles/min.

Fig. 9 refers to a specimen fractured by approximately  $10^5$  cycles at  $\pm 7$  tons/in.<sup>2</sup> applied in the Haigh machine at 1800 cycles/min.; there is relatively little spreading of the X-ray reflection spots. Fig. 10, which relates to a specimen fractured at the same stress range but after about  $10^5$  cycles at 150 cycles/min., contains rather more evidence of breakdown. But Fig. 11, obtained after fracture under progressive tensile stress, clearly shows a major change; the breakdown has proceeded until the initial sharp reflections of the unstressed metal have been transformed into a weak continuous halo.

The breakdown of the grains under static stress is demonstrated particularly well by the X-ray examination of copper. It was partly for this reason that copper was chosen for the tests, for the effect of cyclic stressing in suppressing the breakdown normally associated with plastic deformation is thus established for an especially sensitive case.

It is clear that this suppression is a consequence of the "re-orientation" effect and the enhanced efficiency with which this re-orientation is maintained when a stress cycle is applied rapidly. It becomes increasingly probable, therefore, that these are the effects which underlie the characteristic differences in mechanical behaviour of a metal under static and fatigue stressing.

#### IV.—CRITICAL SPEED FOR SUPPRESSION OF DISORIENTATION.

It has been established that the disorientation produced by the same stress cycle is marked when it is applied at a low speed and very slight at a high speed. At some intermediate rate, therefore, a transitional condition should occur. When this aspect was investigated, the surprising observation was made that the transition took place quite abruptly in a relatively narrow band of frequencies. There appeared to be a fundamental critical speed of cyclic stressing below which the grains could change shape by the normal process of internal plastic flow, and above which this internal plastic flow was virtually suppressed. A further interesting point was that this speed was relatively low—much lower than the speed of elastic or plastic waves in metals.

In the experiments employed to study this effect, a given stress cycle,  $\pm S$ , was applied to a set of copper specimens at 10, 100, 150, 300, 400, or 600 cycles/min., each test being interrupted after  $10^2$ ,  $10^3$ , and  $10^4$  cycles to permit of X-ray examination. The procedure was then repeated for other sets of specimens at other stress ranges, until the values  $S = \pm 3, \pm 4, \pm 5, \pm 6$ , and  $\pm 7$  tons/in.<sup>2</sup> had been covered. The results may be summarized as follows.

(1) The critical rate for the annealed copper employed was between 300 and 400 cycles/min.

(2) The variation in the critical rate with stress was negligible within the ranges studied, although there was a tendency for the rate to drift to a somewhat higher value at the higher stress ranges.

(3) This transition of the grains from a disorientated structure to a homogeneous structure between 300 and 400 cycles/min. was equally marked whether comparison was made after a few cycles or after a large number of stress cycles; this corresponds with the earlier observation that at any frequency the main changes were established in the first few cycles.

These points are illustrated in Figs. 12-16 (Plates XII and XIII) for  $S = \pm 5$  tons/in.<sup>2</sup>. The condition of the structure after  $10^2$  cycles at rates from 100 to 600 cycles/min. is shown by the sequence of X-ray photographs. The spread and diffusion of the X-ray reflections, associated with breakdown of the grains, is marked for the rates up to and including 300 cycles/min., but at 400 and 600 cycles/min., the X-ray reflection spots remain almost as sharp as before stressing (cf. Figs. 15 and 16 with Fig. 5). The transition between 300 and 400 cycles/min. (Figs. 14 and 15) is quite distinctive.

To prove that this transition is not greatly dependent on the stress range of the cycle, the change from 300 to 400 cycles/min. is illustrated for  $S = \pm 3$  tons/in.<sup>2</sup> in Figs. 17 and 18 (Plate XIII); for  $S = \pm 6$  tons/in.<sup>2</sup> in Figs. 19 and 20 (Plate XIV); and for  $S = \pm 7$  tons/in.<sup>2</sup> in Figs. 21 and 22 (Plate XIV). Each pair shows the condition of the structure after  $10^2$  cycles. Again it is clear that 300-400 cycles/min. forms a critical frequency band in each case.

To demonstrate that the transition is equally marked whatever number of cycles is applied, the change from 300 to 400 cycles/min. is illustrated in Figs. 23 and 24 (Plate XIV) for  $10^4$  cycles at  $\pm 5$  tons/in.<sup>2</sup>. These may be compared with Figs. 14 and 15, showing the structure after  $10^2$  cycles.

From the results obtained it appears that if a stress is applied to copper in such a way that the peak value is reached in one-400th of a minute or less, and the stress then as quickly removed, a grain has not time to undergo a macroscopic change in shape, as it would have done under the same stress applied slowly. On the view already suggested, which regards a grain boundary as having a certain viscous strength, this would mean that the stress must be applied for longer than that time interval before the boundary will collapse, at least on a macroscopic scale. Therefore under these conditions, the copper will withstand a stress much greater than the static yield stress without undergoing any internal or external deformation comparable with ordinary static yield.



# V.—DISCUSSION.

The following points emerge as being of particular interest.

## (a) *Dynamic Overstrain.*

The amount of internal disorientation produced in an initially annealed grain deformed by slip at room temperature is roughly proportional to the unidirectional plastic strain imposed. The inhibition of disorientation by rapid cyclic stressing therefore suggests at once that the amplitude of the cyclic strain is small in comparison with a slow cycle. Actually, the tendency of rapid fatigue stressing to suppress plastic flow is well known. In fact, as shown by measurements made by Wood and Thorpe, after a sufficient number of cycles the dynamic

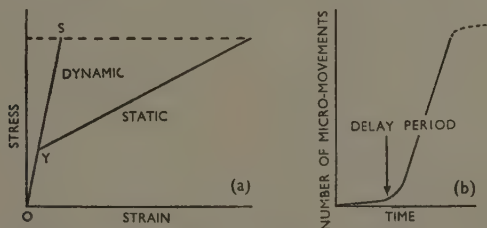


FIG. 25.—(a) Representation of “Dynamic” and “Static” Stress/Strain Curves on Application of Stress  $S$ . (b) Suggested Rate of Incidence of Slip or Micro-movements Following Sudden Application of Stress  $S$ . The rate will, of course, slow down as equilibrium between stress and strain is approached.

stress/strain curve tends to become an extension of the static elastic range. This point is illustrated in Fig. 25 (a). The dynamic stress/strain relation under the range  $\pm S$  tends to follow the line  $OYS$ , where  $Y$  is the static yield.

This “dynamic overstrain” is not a true extension of the primitive static elastic range because it results in strain-hardening. In the present tests it was found that after sufficient cycles of the stress range  $\pm S$ , the specimens strain-hardened by much the same amount for slow or rapid rates of application. Moreover, the increase in hardness was of the same order as that produced by the much greater “static overstrain” resulting from a static stress  $S$ .

Therefore the suppression of the disorientation by the rapid cyclic stress is probably due partly to the limitation of amplitude associated with the pseudo-elastic nature of the deformation. But in order to account for the strain-hardening, the dynamic overstrain must cause the grains to undergo the same degree of internal structural changes as

the much larger static overstrain produced by an equivalent static stress.

(b) *Delay Period for Static Overstrain.*

The implication of the critical-speed effect is as follows. If a grain is subjected suddenly to a particular stress  $S$  greater than the yield and then allowed to deform under the stress in its own time, there will be a delay period before the stress is followed by any appreciable plastic strain. It is evident that this is likely to be the crucial feature leading to the difference in behaviour of a metal under cyclic and static stress.

(c) *Tentative Interpretation.*

After the delay period following application of the stress  $S$ , a given grain will undergo a relatively large plastic strain as a result of a large number of internal micro-movements, each of which may be considered for simplicity to contribute equally to the overall strain and also to the strain-hardening. One micro-movement may be identical with the movement associated with one slip line. It is just possible, however, that the co-operation of a number of such small movements is required to produce one macro-slip movement of the type observed under the microscope, and it is useful, therefore, in the present argument, though not essential, to use the more general term micro-movement until more is known of the generation of slip, especially under cyclic stress.

It is suggested, first, that while each individual micro-movement may itself develop and propagate rapidly, the different movements do not occur simultaneously; and secondly, that the successive movements follow each other in a definite manner characterized by a rate that begins slowly and then accelerates as depicted in Fig. 25 (b) until, of course, equilibrium between stress and strain is established, when it will slow down again. This assumption, that the movements follow a cumulative or co-operative law, may be justified by a number of arguments, but at the moment it is put forward empirically as the concept most in keeping with the present results.

The main observations may be explained as follows. When a stress  $S$  is applied for a period longer than the delay period indicated in Fig. 25 (b), the micro-movements rapidly produce the macro-strains associated with unidirectional plastic flow. If the stress is applied for a shorter period, relatively few micro-movements occur; and if the stress is quickly reversed, again only few movements occur and these are opposite in direction to the first. It is clear that this latter condition would correspond to the case of rapid cyclic stressing; it would explain the pseudo-elastic nature of the dynamic overstrain, and a gradual increase of strain-hardening with repeated cycles, a process

that could be quite protracted. It could also account for suppression of the disorientation. For it has been shown that even with appreciable plastic strain, some degree of re-orientation results on reversing the strain. Therefore with the much smaller deformations involved in the rapid cyclic stressing, it is reasonable to expect a more perfect re-orientation after the first reversal, without any appreciable progressive disorientation after successive cycles.

It should perhaps be added that the curve in Fig. 25 (b), which describes the rate of appearance of the micro-deformations, is not one that would arise from any viscous feature of plastic strain. A time lag between stress and strain might suggest that such a feature is operative. But the properties of media that are partly elastic and partly viscous, which have been discussed fully by Zener,<sup>9</sup> are such as to lead to deformation that would respond to a stress at first rapidly and then slowly. This is the opposite of the requirements in the present case, which calls for a slow initial flow and then a relatively sudden acceleration. It is considered that, though ordinary viscous elements may be present, the controlling factor in producing the time lag here is rather the reaction of neighbouring grains to sudden deformation in any one grain. For no grain can deform appreciably until accommodation is provided by a whole series of grains, and it is unlikely that this accommodation will be immediately spontaneous. This reaction might be regarded as conferring on the boundary of a particular grain an enhanced strength, as already suggested, and, in view of the time lag, a certain viscosity. It is convenient to consider the effect from this point of view for purposes of calculation, but the correspondence would be purely formal.

#### (d) *Application to Fatigue Failure.*

It is hoped to treat this aspect more fully after the completion of other work, the main aim of the present paper being to indicate what appear to be the relevant differences in behaviour of the metallic structure under fatigue and static stressing. But it will be clear how the present observations may be applied. It may be anticipated that a crack will be initiated equally under cyclic or static stressing in the distorted or disoriented zones associated with the micro-deformations, but that the conditions for propagation will be quite different. For under slow or static stress, considerable plastic flow and disorientation of the structure is permissible at the head of the crack. But the suppression of this flow by the action of rapid cyclic stress, in the manner demonstrated, in effect transforms the metal to a brittle medium. In such a medium it is reasonable to suppose that the crack may be pro-

pagated with less loss of energy, and also with the cleavage appearance usually associated with a fatigue failure.

#### ACKNOWLEDGEMENTS.

The authors are greatly indebted for assistance in discussing and planning the experiments in this joint research to Professor J. N. Greenwood, University of Melbourne, and to Mr. H. A. Wills, Head of the Materials and Structures Division of the Aeronautical Research Laboratories, Australian Department of Supply. They wish also to express their thanks to Mr. Bruce Peggie of the latter Department for essential assistance with the mechanical tests.

#### REFERENCES.

1. J. A. Ewing and J. W. C. Humfrey, *Phil. Trans. Roy. Soc.*, 1903, [A], **200**, 241.
2. T. E. Stanton and L. Bairstow, *Proc. Inst. Civil Eng.*, 1906, **166**, 78.
3. H. J. Gough and D. Hanson, *Proc. Roy. Soc.*, 1923, [A], **104**, 539.
4. H. J. Gough, *Proc. Amer. Soc. Test. Mat.*, 1933, **33**, (II), 3.
5. E. Orowan, *Proc. Roy. Soc.*, 1939, [A], **171**, 79.
6. H. J. Gough and W. A. Wood, *Proc. Roy. Soc.*, 1936, [A], **154**, 510; *J. Roy. Aeronaut. Soc.*, 1936, **40**, 586.
7. W. A. Wood and P. L. Thorpe, *Proc. Roy. Soc.*, 1940, [A], **174**, 310.
8. W. A. Wood, *Proc. Roy. Soc.*, 1939, [A], **172**, 231.
9. C. Zener, "Elasticity and Anelasticity of Metals". Chicago: 1948 (University of Chicago Press).

# THE STABILITY OF THE $\text{Co}_2\text{Al}_9$ -TYPE STRUCTURE IN THE ALUMINIUM-RICH ALLOYS OF THE ALUMINIUM-IRON-COBALT-NICKEL SYSTEM.\*

By M. B. WALDRON,† B.Sc., Ph.D., A.I.M., JUNIOR MEMBER.

## SYNOPSIS.

In the aluminium-rich portion of the system aluminium-iron-cobalt-nickel, there exists a quaternary phase  $(\text{Fe}, \text{Co}, \text{Ni})_2\text{Al}_9$ , whose range of homogeneity includes the terminal compositions  $\text{Co}_2\text{Al}_9$  and  $\text{FeNiAl}_9$ ; electron : atom ( $e/a$ ) ratios of 2.12 and 2.16, respectively, can be assigned to these compositions, assuming that cobalt, iron, and nickel may accept respectively 1.71, 2.66, and 0.61 electrons per atom from the structure as a whole. The iron-rich boundary of the phase, which corresponds to the lower limit of the  $e/a$  ratio, starts as a straight line of constant  $e/a$  ratio 2.07 from the  $\text{Co}_2\text{Al}_9$  region, but changes direction sharply, when half the cobalt atoms have been replaced by iron and nickel atoms, and approaches linearly a value giving an  $e/a$  ratio of 2.14.

The lower limiting  $e/a$  ratio of a phase is determined by the point at which the depletion of electrons reduces the binding energy of the structure relatively to that of an alternative phase. Thus, compositions in the region of  $\text{Co}_2\text{Al}_9$  appear to be more stable than those in the region of  $\text{FeNiAl}_9$ , since  $\text{Co}_2\text{Al}_9$  permits solution of iron until the  $e/a$  ratio has been reduced from 2.12 to 2.07, compared with a reduction from 2.16 to 2.14 in the region of  $\text{FeNiAl}_9$ . Melting points are further indices of stability:  $\text{Co}_2\text{Al}_9$  melts at  $943^\circ\text{C}$ . and forms a eutectic with  $\text{FeAl}_3$  and the aluminium-rich solid solution;  $\text{FeNiAl}_9$  is formed peritectically from  $\text{FeAl}_3$  at  $809^\circ\text{C}$ .

An experimental technique has been devised which makes possible the determination of the composition of the quaternary phase at the point where the eutectic relationship with  $\text{FeAl}_3$  changes to the peritectic reaction. This is found to occur at the phase composition associated with the change in direction of the phase boundary and is an interesting verification of the dependence of the stability of this type of intermetallic compound on the  $e/a$  ratio. The experimental technique may prove useful in other systems in which it is necessary to investigate a peritectic reaction.

## I.—INTRODUCTION.

IN the course of an investigation of the ternary system aluminium-iron-nickel, Bradley and Taylor<sup>1</sup> identified the phase  $\text{FeNiAl}_9$  and showed by X-ray methods that it is isomorphous with the phase  $\text{Co}_2\text{Al}_9$  which occurs in the binary system aluminium-cobalt. Both these phases come into equilibrium with an aluminium-rich solid solution in the

\* Manuscript received 14 July 1950.

† Formerly in the Department of Metallurgy, University of Birmingham; now in the Metallurgy Division, Atomic Energy Research Establishment, Harwell, Berks.

respective alloy systems. Subsequent examination of the aluminium-iron-nickel<sup>2</sup> and aluminium-cobalt-nickel<sup>3</sup> systems by Raynor and Pfeil, and of the aluminium-cobalt-iron<sup>4</sup> system by Raynor and the present author, confirmed the existence of the  $\text{Co}_2\text{Al}_9$  type of structure in each system and showed that iron and nickel atoms were capable of replacing cobalt atoms in this structure, atom for atom.

In the two systems containing nickel, it was found that  $\text{Co}_2\text{Al}_9$  permitted the replacement of cobalt atoms by nickel until the electron : atom ratio had been increased from an initial value of 2.12 to one of 2.28, while similarly  $\text{FeNiAl}_9$  dissolved nickel until the electron : atom ratio had risen to 2.28. These electron : atom ratios have been computed assuming that the transitional metals, when alloyed with a metal of high valency, can absorb electrons into "atomic orbitals" to the following extent : <sup>5, 6, 7</sup>

	Fe	Co	Ni
Number of electrons	2.66	1.71	0.61

In the ternary system aluminium-cobalt-iron, however, it was found that  $\text{Co}_2\text{Al}_9$  could dissolve iron, at 600° C., until its electron : atom ratio was reduced from 2.12 to 2.07; whereas  $\text{FeNiAl}_9$  could dissolve only sufficient iron to lower its electron : atom ratio from a characteristic value of 2.16 to 2.14. This is in contrast to the extent to which these phases dissolve nickel.

The agreement between the electron : atom ratios corresponding to the maximum solution of nickel in the phases  $\text{Co}_2\text{Al}_9$  and  $\text{FeNiAl}_9$  is consistent with the ability of the Brillouin zone to accommodate an increase in the number of electrons per atom until the electronic energy begins to rise excessively. It has been demonstrated that the most probable Brillouin zone for the  $\text{Co}_2\text{Al}_9$  structure can, in fact, accommodate 2.28 electrons per atom before restriction of available energy states becomes very pronounced.<sup>8, 9</sup>

The solid solutions based on the phases  $\text{Co}_2\text{Al}_9$  and  $\text{FeNiAl}_9$  containing the maximum amount of iron, both come into equilibrium with the binary compound  $\text{FeAl}_3$ .  $\text{Co}_2\text{Al}_9$  is stable up to 943° C. and forms a eutectic system with  $\text{FeAl}_3$ , while  $\text{FeNiAl}_9$  is formed by a peritectic reaction from  $\text{FeAl}_3$  and liquid at the considerably lower temperature of 809° C. It is, therefore, of special significance that  $\text{Co}_2\text{Al}_9$ , which is more stable than  $\text{FeNiAl}_9$  with respect to  $\text{FeAl}_3$ , is capable of sustaining a correspondingly greater diminution of the electron : atom ratio by a substitutional solution of iron atoms in the structure. An examination of the quaternary system aluminium-iron-cobalt-nickel, recently published,<sup>10</sup> shows not only that the phases  $\text{Co}_2\text{Al}_9$  and  $\text{FeNiAl}_9$  have similar structures but also that they merge together to give a continuous



quaternary body denoted  $(\text{Fe}, \text{Co}, \text{Ni})_2\text{Al}_9$  such that, on an average, approximately two transitional metal atoms are combined with nine aluminium atoms. The range of homogeneity of this field gives rise to an  $\alpha + (\text{Fe}, \text{Co}, \text{Ni})_2\text{Al}_9$  field in the tetrahedral isothermal constitutional model for the quaternary system, the boundaries of which radiate as ruled surfaces from the aluminium apex, as shown diagrammatically in Fig. 1. Consequently, any section through the field parallel to the plane of the phase in the tetrahedral model is geometrically similar to the boundaries of the phase itself. Such a section, represented by the plane  $ABC$  in Fig. 1 and shown separately in Fig. 2, gives the form of

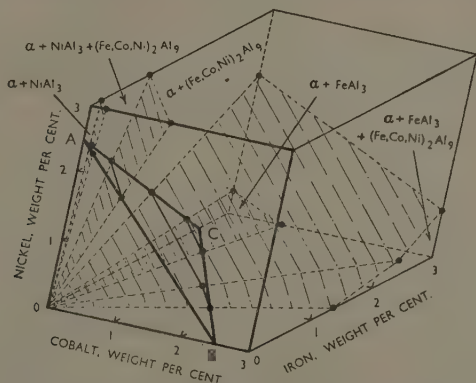


FIG. 1.—Diagrammatic Representation of the Quaternary Isothermal Constitutional Model of the System Al-Fe-Co-Ni.

the  $600^\circ\text{C}$ . isothermal section at 97.5 wt.-% aluminium. It will be seen that the nickel-rich boundary of the  $\alpha + (\text{Fe}, \text{Co}, \text{Ni})_2\text{Al}_9$  field is a straight line joining the intercepts, on the axes of the diagram, of the boundaries in the ternary systems. Thus, the corresponding boundary of the phase itself is characterized by a constant electron : atom ratio of 2.28, which marks the nickel-rich limit of the ternary phases based on  $\text{Co}_2\text{Al}_9$  and  $\text{FeNiAl}_9$ , and which agrees with the extent to which the most probable Brillouin zone may be filled.

The iron-rich boundary of the  $\alpha + (\text{Fe}, \text{Co}, \text{Ni})_2\text{Al}_9$  field in Fig. 2 is not a straight line of constant electron : atom ratio, by reason of differing electron : atom ratios connected with the limits of solution of iron in the ternary phases  $\text{Co}_2\text{Al}_9$  and  $\text{FeNiAl}_9$ . This boundary may be regarded as consisting of two linear branches. The direction in which it leaves the aluminium-cobalt-iron edge of the diagram is consistent



with cobalt atoms in the structure being replaced by iron and nickel in such proportions that an electron : atom ratio of 2.07 is maintained in the plane of the phase itself. After this initial portion, the boundary curves over a short range of compositions and appears to approach linearly the iron-rich composition of  $\text{FeNiAl}_9$  on the aluminium-iron-nickel edge of the diagram, with a steady increase of electron : atom ratio. The lower limit of the range of homogeneity of a phase, in terms of electron : atom ratio, is connected with the stability, or binding

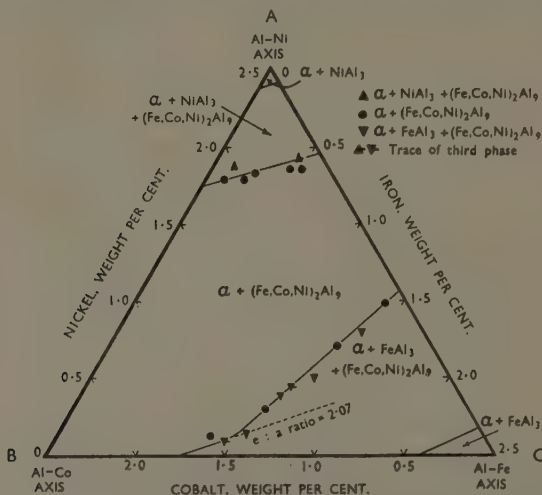


FIG. 2.—600° C. Isothermal Section of the System Al-Fe-Co-Ni at 97.5 wt.-% Aluminium. Corresponds to the plane ABC in Fig. 1.

energy, of the structure. The "relative valency effect", which Hume-Rothery<sup>11</sup> found of importance in the formation of substitutional solid solutions, indicates that it is more serious to decrease the number of valency electrons binding the structure together than to increase it.

It would seem, therefore, that the structure in which all the transitional-metal atomic sites are occupied by cobalt ( $\text{Co}_2\text{Al}_9$ ) is inherently more stable than the same structure having these sites occupied by iron and nickel, as their respective melting points suggest. A closer examination of the iron-rich boundary of the quaternary phase, which includes these two terminal compositions, shows that the change in direction of the boundary occurs in the region where half the cobalt atoms have been replaced by iron and nickel atoms.

The series of experiments described in this paper was devised and carried out to discover at what stage in the process of replacement of cobalt atoms by atoms of iron and nickel the eutectic relationship changes into a peritectic reaction.

## II.—EXPERIMENTAL PROCEDURE.

### 1. *Preparation of the Alloys.*

Alloys intended for microscopical examination only were prepared in quantities of 10 g. by melting the appropriate quantities of high-purity master alloys and super-pure aluminium in crucibles lined with a high-purity alundum cement, which had been shown to be satisfactory in previous experiments. As identification of primary separations was necessary throughout the work, the melt was thoroughly stirred and then cooled without further disturbance at a uniform rate of  $1.5^\circ \text{C./min.}$ , using a Foster Potentiometric Programme controller.

Alloys were also prepared in the same manner, in quantities of 50 g., for the electrolytic extraction of primary crystals using dilute hydrochloric acid, as previously described.<sup>12</sup> Clean, good-quality crystals were then sorted by hand from the treated residues and were analysed.

Sections of all alloys were examined micrographically after a standard preparation; this consisted of the usual treatment on emery papers and on Selvyt cloth using "Brasso" polish, followed by polishing with magnesia on blanket-felt to reduce relief of hard constituents, and a final polish with fine alumina on Selvyt cloth. The clearest distinction between  $(\text{Fe,Co,Ni})_2\text{Al}_9$  and  $\text{FeAl}_3$  is given by immersion for 45 sec. in cold 10% caustic soda solution which had been aged for 24 hr.  $(\text{Fe,Co,Ni})_2\text{Al}_9$  is coloured dark brown, while  $\text{FeAl}_3$  is unattacked.

### 2. *Identification of the Peritectic Reaction.*

Since alloys showing evidence of a peritectic reaction, by the presence of spines of one phase in primary crystals of another, are worthless for analytical experiments on extracted primary residues, a procedure was specially developed to relate the existence of a peritectic or eutectic reaction in an alloy to the composition of the  $(\text{Fe,Co,Ni})_2\text{Al}_9$  crystals separating in it.

For simplicity, a hypothetical binary system containing a typical peritectic reaction may be considered. The general form of the relevant part of the equilibrium diagram is that shown in Fig. 3. An alloy of composition (1), if slowly cooled, would deposit primary crystals of the phase X until the peritectic temperature was reached, when these crystals would react with the liquid to form crystals of the phase Y.

Since the reaction usually has not sufficient time to attain equilibrium, the microstructure would show primary crystals of  $Y$  containing untransformed  $X$ . For this reason, analysis of crystals of  $Y$  obtained from such an alloy would be unreliable. However, by changing the

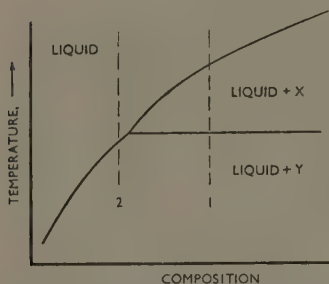


FIG. 3.—Hypothetical Binary System Containing Typical Peritectic Reaction.

alloy composition towards (2) the proportion of spines of  $X$  would be decreased, and crystals of  $Y$  extracted from alloy (2) itself, for instance, would be uncontaminated with  $X$ ; analysis of such crystals would give the true composition of the phase formed by the peritectic reaction.

In order to understand the process of primary separation in a ternary alloy system, it is necessary to consider the projection of the surfaces of primary

separation on the base of the conventional ternary model, as in Fig. 4, which is drawn for the aluminium-iron-nickel system. The diagram shows that there is a peritectic reaction along the line  $bc$ ,  $\text{FeAl}_3$  reacting with the liquid to give  $\text{FeNiAl}_9$ , and that at the point  $b$  the reaction becomes invariant owing to the simultaneous separation of the  $\alpha$ -solid solution, as indicated by the arrows on the phase-field

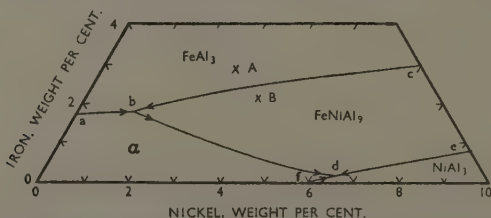


FIG. 4.—Projection of Surfaces of Primary Separation on Base of Ternary Model for System Al-Fe-Ni.

boundaries. Therefore, when an alloy of composition  $A$  cools, on reaching the  $\text{FeAl}_3$  surface of primary separation crystals of  $\text{FeAl}_3$  are deposited from the melt, and the composition of the remaining liquid shifts from  $A$  towards the line  $bc$  as the temperature continues to fall. When the composition of the melt has reached the boundary  $bc$ ,  $\text{FeNiAl}_9$  crystals begin to form by peritectic reaction of  $\text{FeAl}_3$  with the liquid,

and, under normal experimental conditions, the composition of the liquid moves across the surface  $cbde$  towards the line  $bd$ . This would again result in a microstructure containing reaction spines of  $\text{FeAl}_3$  within primary crystals of  $\text{FeNiAl}_9$ . However, changing the original

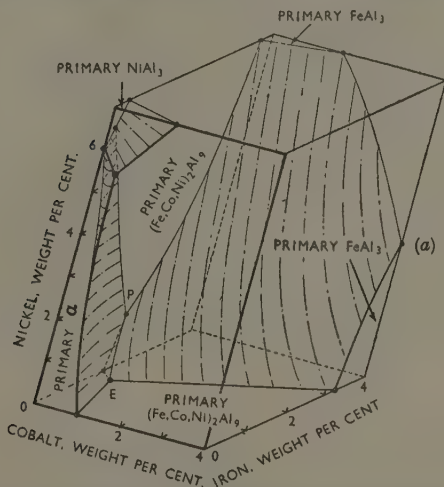


FIG. 5(a).—System Al-Fe-Co-Ni: Tetrahedral Model the faces of which are formed by the projections of the surfaces of primary separation on the bases of the ternary models.

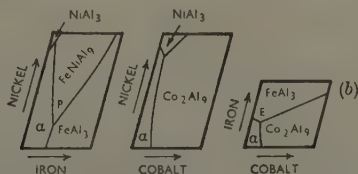


FIG. 5(b).—Projections of surfaces of primary separation in systems Al-Fe-Ni, Al-Co-Ni, and Al-Fe-Co.

alloy composition from  $A$  towards  $B$  results in a diminishing proportion of  $\text{FeAl}_3$  reaction spines, so that an alloy such as  $B$  would normally contain uncontaminated crystals of  $\text{FeNiAl}_9$ .

In the quaternary system aluminium-iron-cobalt-nickel it has already been shown that there is a continuous phase joining binary  $\text{Co}_2\text{Al}_9$  to ternary  $\text{FeNiAl}_9$ . It has also been mentioned that  $\text{Co}_2\text{Al}_9$  forms a eutectic with  $\text{FeAl}_3$ , while  $\text{FeNiAl}_9$  is formed peritectically from



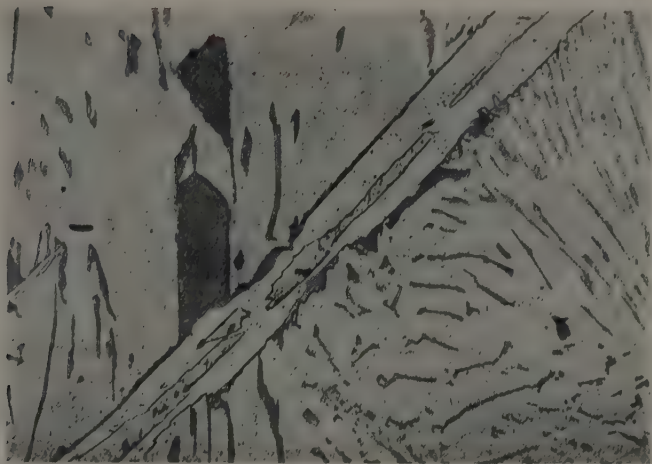


FIG. 7. Aluminum Alloy Containing Iron 5, Cobalt 0, Nickel 2.5%. 75.

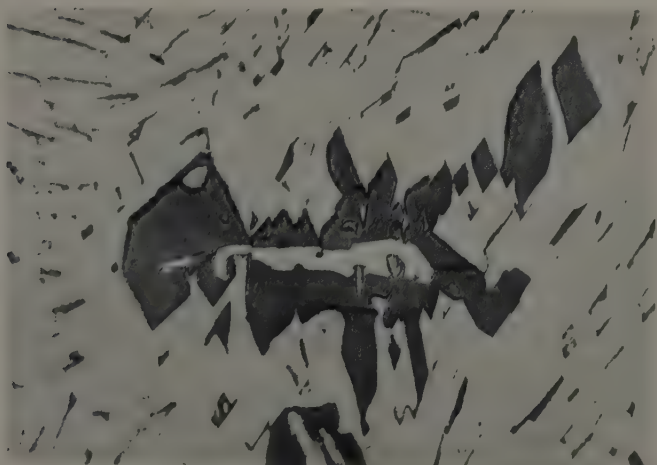


FIG. 8.—Aluminium Alloy Containing Iron 2.5, Cobalt 0, Nickel 2.5%.  $\times 75$ .

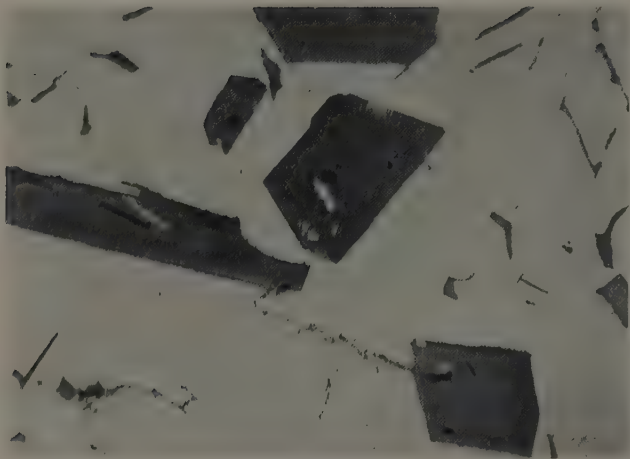


FIG. 9. - Aluminum Alloy Containing Iron 3, Cobalt 1.5, Nickel 0.5%.  $\times 75$ .

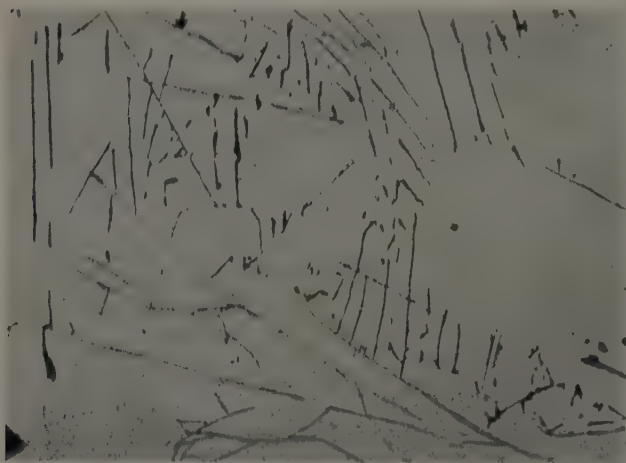


FIG. 10. - Aluminum Alloy Containing Iron 2.75, Cobalt 1.75, Nickel 0.5%.  
100.



mately constant percentage of cobalt. In a diagram such as Fig. 6, which represents the range of homogeneity of the phase in terms of the atomic proportion of cobalt, iron, and nickel present (aluminum being constant throughout), the residues extracted from such alloys would lie on lines of constant cobalt, parallel to the Fe-Ni axis of the diagram. An alloy such as *B* in Fig. 4 would deposit crystals of a composition lying on *bc* itself, in Fig. 6, very close to the point *c*.

Considering now a series of alloys containing a small fixed amount of cobalt with increasing nickel contents and decreasing iron contents, the microstructure would, at first, be expected to show primary  $\text{FeAl}_3$  crystals; then, with increasing nickel content,  $\text{FeAl}_3$  crystals would be rimmed with  $(\text{Fe},\text{Co},\text{Ni})_2\text{Al}_5$  and eventually samples containing pure primary crystals of  $(\text{Fe},\text{Co},\text{Ni})_2\text{Al}_5$  would be obtained. If such crystals were analysed and their compositions plotted in Fig. 6, they would lie on a line approximately parallel to *bc* and the sample nearest to *cd* would give a close indication of the composition of the crystals formed peritectically from  $\text{FeAl}_3$ . This process can be repeated with increasing cobalt contents until a series of alloys is obtained without evidence of peritectic reaction but exhibiting instead the features of a eutectiferous system. This series then provides a bracket, with the previous series, of the point at which the peritectic changes into a eutectic reaction. By analysing crystals of  $(\text{Fe},\text{Co},\text{Ni})_2\text{Al}_5$  extracted from that alloy in each series which is richest in iron but contains uncontaminated crystals, a number of points can be plotted near the boundary *cd*, each of which is one of a series associated with either a peritectic or a eutectic reaction.

### III. EXPERIMENTAL RESULTS.

In order to obtain the maximum yield of extracted residues from a 50-g. ingot, using the master alloys available, all alloys were prepared with 5% total alloy content. The first series contained no cobalt—thus being ternary aluminium-iron-nickel alloys—to ensure that the microscopical examination of the slow-cooled ingots would permit identification of the boundary between the primary  $\text{FeAl}_3$  and primary  $(\text{Fe},\text{Co},\text{Ni})_2\text{Al}_5$  fields, which were already known from Fig. 4. These experiments also provided reliable experience for the recognition of a peritectic reaction in the quaternary system. Alloys 3/0/2, 2.5/0/2.5, and 2/0/3 were therefore prepared.\* According to Fig. 4, the first and second alloys should contain primary crystals of  $\text{FeAl}_3$ , probably rimmed with  $(\text{Fe},\text{Co},\text{Ni})_2\text{Al}_5$ , while the third alloy should contain only primary crystals of  $(\text{Fe},\text{Co},\text{Ni})_2\text{Al}_5$  uncontaminated with  $\text{FeAl}_3$ . Microscopic examination of alloy 3/0/2 showed clearly  $\text{FeAl}_3$  crystals

\* Alloy 3/0/2 contains Fe 3%, Co 0%, Ni 2%, and so on.

surrounded by thin sheaths of the second phase. A typical field of this alloy is illustrated in Fig. 7 (Plate XV). Alloy 2.5/0/2.5 was found to contain principally  $(\text{Fe,Co,Ni})_2\text{Al}_9$  primary crystals, usually with substantial spines of untransformed  $\text{FeAl}_3$  from which the  $(\text{Fe,Co,Ni})_2\text{Al}_9$  particles had evidently grown. Fig. 8 (Plate XV) shows a cluster of the quaternary phase including a particle of  $\text{FeAl}_3$ ; the irregular outline of the  $(\text{Fe,Co,Ni})_2\text{Al}_9$  phase and the separation of extreme portions from the main part of it are typical indications of an incomplete peritectic transformation. The final alloy in this series contained primary particles of the  $(\text{Fe,Co,Ni})_2\text{Al}_9$  phase only, in full agreement with Fig. 4. These preliminary experiments demonstrate the use of the microscopic method to identify the peritectic reaction in this system and show that the results so obtained are in keeping with previous work on the ternary system aluminium-iron-nickel.

A second series of alloys was made containing 1% cobalt, as follows: 3.5/1.0/0.5, 3/1/1, 2.5/1.0/1.5, and 2/1/2. These alloys showed definite metallographic evidence of a peritectic reaction, and the first three contained  $\text{FeAl}_3$  primary crystals with rims of the quaternary phase, in a manner similar to that described for the previous series. In alloy 2/1/2, however, the primary crystals of the quaternary phase were completely free from spines of  $\text{FeAl}_3$ , so that a large ingot of the same composition was prepared for extraction of residues. The analysis of the extracted primary crystals is given in Table I and is plotted in Fig. 6.

TABLE I.—*Analysis of Extracted Primary Crystals.*

Alloy Composition, %			Analysis of Extracted Primary Crystals, wt.-%			Atomic Proportions			Type of Reaction
Fe	Co	Ni	Fe	Co	Ni	Fe	Co	Ni	
2	1	2	12.79	10.40	9.16	0.41	0.31	0.28	} Peritectic
0.5	1.0	4.0	6.83	11.66	16.16	0.21	0.33	0.46	
2.5	1.5	1.0	12.97	13.98	4.78	0.42	0.43	0.15	
2.75	1.75	0.5	12.30	17.63	2.56	0.40	0.53	0.08	Eutectic

To provide an indication of the way in which extracted residues from other alloys in this series would fall in the diagram, the composition of crystals from alloy 0.5/1.0/4.0 is also quoted in the table and inserted in the diagram. It will be noticed that both alloys contain 1% cobalt, and that although the total alloy content differs slightly, the crystals from each alloy contain similar proportions of cobalt.

Two alloys containing 1.5% cobalt were next prepared for microscopical examination, namely 3.0/1.5/0.5 and 2.5/1.5/1.0. These alloys were still within the region of the peritectic reaction, since the former

contained crystals of  $(\text{Fe},\text{Co},\text{Ni})_2\text{Al}_9$  with small reaction cores of  $\text{FeAl}_3$ . Fig. 9 (Plate XVI) shows an area of this alloy in which the small but definite reaction spines are clearly visible. In view of the critical appearance of this alloy, it was subjected to a very careful examination, and special attention was directed to the nature of the secondary separations, but no evidence of a ternary eutectic structure was found. As the second alloy of the series was entirely free from reaction spines, a 50-g. melt of this composition was prepared, and primary crystals of the quaternary phase were extracted for analysis. The alloy composition and crystal analysis are given in Table I and plotted in Fig. 6.

It was found necessary to prepare only two more alloys, 3.0/1.75/0.25 and 2.75/1.75/0.5, each containing 1.75% cobalt: in neither of these alloys were genuine reaction spines found. There frequently occurred particles of both  $\text{FeAl}_3$  and  $(\text{Fe},\text{Co},\text{Ni})_2\text{Al}_9$  growing side by side, with no evidence of a peritectic reaction between the two. From the microstructures it would appear that the  $(\text{Fe},\text{Co},\text{Ni})_2\text{Al}_9$  particles were existent before the  $\text{FeAl}_3$  particles grew. This behaviour is very characteristic of an alloy occurring close to a eutectic "valley", where it is probable that the separation of one phase causes a change in composition of the surrounding liquid so that further primary separation then takes place in the adjacent phase field, the process alternating until the solidus is reached. Some confusion may result from the way in which one of the phases in such a system may nucleate a primary separation of the other, for example, one particle of  $\text{FeAl}_3$  appearing embedded in a crystal of the quaternary phase. This process can be distinguished from traces of a peritectic reaction both by the regular outline of the inclusion and by the penetration of other particles of the quaternary phase into crystals of  $\text{FeAl}_3$ . In the peritectic case, however, it is usual to find the spines of  $\text{FeAl}_3$  in a discontinuous state, as in Fig. 9 (Plate XVI), where the original particle has been transformed to  $(\text{Fe},\text{Co},\text{Ni})_2\text{Al}_9$  and small fragments only are left. Further evidence of the existence of a ternary eutectic is found by an examination of the secondary separations in these alloys, which frequently occur in a characteristic intimate mixture of the two phases and the aluminium-rich solid solution. A typical example of this, in alloy 2.75/1.75/0.5, is shown at a high magnification in Fig. 10 (Plate XVI). In this photomicrograph there can be seen thin plates of  $\text{FeAl}_3$ , unattacked, among a finer separation of  $(\text{Fe},\text{Co},\text{Ni})_2\text{Al}_9$ , which is dark; presenting an appearance of a eutectic formed in an alloy that has been slowly cooled. Primary crystals of the quaternary phase were extracted from a 50-g. ingot of alloy 2.75/1.75/0.5, the analysis of which is included in Table I and plotted in Fig. 6.

## IV.—DISCUSSION OF RESULTS.

It has been shown in Section I that the varying stability of the quaternary phase  $(\text{Fe}, \text{Co}, \text{Ni})_2\text{Al}_9$  is of theoretical interest when considered in relation to the extent to which the electron : atom ratio can be varied, by the solution of iron and nickel, from the values associated with the ideal compositions  $\text{Co}_2\text{Al}_9$  and  $\text{FeNiAl}_9$ .

Previous investigations<sup>4, 10</sup> have shown that the nickel-rich boundary of the phase  $(\text{Fe}, \text{Co}, \text{Ni})_2\text{Al}_9$ , in equilibrium with the aluminium-rich solid solution, is marked by a constant electron : atom ratio of 2.28 throughout the whole range. This evidently is not affected by the differences in phase stability to which reference has been made, but is more probably governed by the extent to which the Brillouin zone characteristic of the structure may be filled. Calculation of the most probable Brillouin zone<sup>8, 9</sup> has shown that the inscribed sphere can hold 2.1 electrons per atom, in keeping with the ratio (2.12) characteristic of binary  $\text{Co}_2\text{Al}_9$ , and that when the Fermi surface corresponds to 2.28 electrons per atom, it encounters rapidly increasing restrictions on the number of possible energy states; this would lead to a steep rise in the electronic energy, causing the phase to be unstable. This circumstance becomes an overriding limitation on further increase of the electron : atom ratio; hence the nickel-rich boundary of the phase is marked by a constant electron : atom ratio of 2.28.

When, however, iron replaces cobalt and nickel in the structure the electron : atom ratio is decreased and the extent of solution is no longer limited by Brillouin-zone considerations. Instead, the number of electrons providing the bonding energy of the structure is being reduced, and this may be expected to affect the stability of the phase. A connection has been traced between the high stability of  $\text{Co}_2\text{Al}_9$  as compared with  $\text{FeNiAl}_9$ , and the considerable reduction of its electron : atom ratio from 2.12 to 2.07, whereas  $\text{FeNiAl}_9$  has an electron : atom ratio of 2.16 which can only be reduced to 2.14. This difference in stability is reflected by the eutectic relationship between  $\text{Co}_2\text{Al}_9$  and  $\text{FeAl}_3$ , on the one hand, and the peritectic transformation between  $\text{FeAl}_3$  and  $\text{FeNiAl}_9$ , on the other. Examination of the equilibrium relationships in the quaternary system has shown how the lower limit of the electron : atom ratio changed as the quaternary body was traversed from  $\text{Co}_2\text{Al}_9$  to  $\text{FeNiAl}_9$ . Hence it was considered desirable to find out how the eutectic relationship of  $\text{Co}_2\text{Al}_9$  with  $\text{FeAl}_3$  and the peritectic reaction of  $\text{FeNiAl}_9$  with  $\text{FeAl}_3$  become reconciled within this range.

The experiments described gave three compositions bordering on

the limits of the quaternary phase, which come into relation with the phase FeAl<sub>3</sub>. Two of these compositions are from a series of alloys in which (Fe,Co,Ni)<sub>2</sub>Al<sub>9</sub> is formed peritectically from FeAl<sub>3</sub> and the third from a series which is marked by a eutectic relationship and includes the same two phases. Since a comparison of the extracts from alloys 2/1/2 and 0.5/1.0/4.0 shows that crystals from further alloys of each series would lie approximately on lines of constant cobalt content in Fig. 6, it is clear that the point at which the peritectic reaction transforms into a peritectic system must be connected with a cobalt content in the quaternary phase intermediate between those of the extracted crystals from alloys 2.5/1.5/1.0 and 2.75/1.75/0.5. Reference to the diagram will show that at this stage half the transitional metal atoms are cobalt, the remainder being iron and nickel jointly.

It was mentioned in Section I that the iron-rich boundary of the quaternary phase at 600° C. changes direction at the point where cobalt atoms occupy half the transitional-metal sites. The boundary to the cobalt-rich side of this region maintains a constant electron : atom ratio of 2.07, while in the other direction the electron : atom ratio gradually approaches a value of 2.14. The present work shows that the phase is capable of maintaining the depressed value of the electron : atom ratio and of entering into a eutectic relationship with FeAl<sub>3</sub>, as long as half the transitional-metal atom sites in the structure are occupied by cobalt. A reduction in the proportion of cobalt atoms beyond this point, up to which the phase may still be regarded as characteristically Co<sub>2</sub>Al<sub>9</sub>, appears so to affect the inherent stability of the structure that it can neither maintain the same deficit of electrons nor retain a eutectic, rather than a peritectic, relation with FeAl<sub>3</sub>.

If it is legitimate to assume that the deficit of electrons which the phase maintains is an index of the variation of stability of the structure, and that the stability of the phase is reflected by its melting point, then it would appear that the melting point of (Fe,Co,Ni)<sub>2</sub>Al<sub>9</sub> is not depressed greatly by substitution of iron or nickel for cobalt atoms, until it enters into a peritectic relationship with FeAl<sub>3</sub>. It is difficult to examine this point experimentally.

The experimental results described in this paper suggest a significant coincidence between the change-over from a eutectic to a peritectic reaction and the form of the phase boundary. Evidently the stability of the Co<sub>2</sub>Al<sub>9</sub> structure becomes seriously affected when more than half the cobalt atoms are replaced by iron or nickel. It is not possible to decide at present what causes this to take place, but it would appear that replacement proceeds preferentially on certain planes until half the cobalt atoms have been involved, in such a way that the structure is



not seriously impaired. It has proved impracticable to investigate the structural changes by X-ray diffraction methods, because of the low symmetry of the monoclinic cell of Co<sub>2</sub>Al<sub>9</sub>, the corresponding complexity of the diffraction pattern, and the smallness of the changes in symmetry that are observed.

Considerable interest attaches to the study of the occurrence of the peritectic and eutectic reactions in this complex alloy system by a combined use of normal metallographic examination and of the analysis of extracted residues. This technique may well be applied to the determination of the limits of other peritectic reactions.

#### ACKNOWLEDGEMENTS.

The author's thanks are due to Professor D. Hanson, D.Sc., Director of the Department of Metallurgy, University of Birmingham, for his interest in the work and for the provision of laboratory facilities. Grateful acknowledgement is also due to Professor G. V. Raynor, D.Sc., for his supervision and encouragement, to Mr. A. Roberts for his care in the analytical work, and to Mr. G. Welsh for assistance with the experiments. The financial aid of the Department of Scientific and Industrial Research is much appreciated and the Director of the Atomic Energy Research Establishment is thanked for permitting the research to be completed.

#### REFERENCES.

1. A. J. Bradley and A. Taylor, *J. Inst. Metals*, 1940, **66**, 53.
2. G. V. Raynor and P. C. L. Pfeil, *J. Inst. Metals*, 1947, **73**, 397.
3. G. V. Raynor and P. C. L. Pfeil, *J. Inst. Metals*, 1947, **73**, 609.
4. G. V. Raynor and M. B. Waldron, *Proc. Roy. Soc.*, 1948, [A], **194**, 362.
5. G. V. Raynor, *J. Inst. Metals*, 1944, **70**, 531.
6. G. V. Raynor and K. Little, *J. Inst. Metals*, 1945, **71**, 493.
7. G. V. Raynor, *Phil. Mag.*, 1945, [vii], **36**, 770.
8. G. V. Raynor and M. B. Waldron, *Nature*, 1948, **162**, 565.
9. G. V. Raynor and M. B. Waldron, *Phil. Mag.*, 1949, [vii], **40**, 198.
10. G. V. Raynor and M. B. Waldron, *Proc. Roy. Soc.*, 1950, [A], **202**, 420.
11. W. Hummel-Rothery, "The Structure of Metals and Alloys", *Inst. Metals Monograph and Report Series*, No. 1, 1945, p. 66.
12. G. V. Raynor and D. W. Wakeman, *Proc. Roy. Soc.*, 1947, [A], **190**, 82.

## PRESIDENTIAL ADDRESS.\*

1301

By PROFESSOR A. J. MURPHY,† M.Sc., F.I.M.

I HAVE long since realized how fortunate I have been in finding satisfaction in the everyday work which has come my way : I have therefore lacked the stimulus of the divine discontent which causes men to strive to change their lot. But, even if I had been endowed with such a motive force, my aspirations would not have brought the Presidency of this Institute within their sights. I have seen sixteen successive occupants of this Chair, and never in my wildest dreams have I pictured myself joining their illustrious company. You will understand therefore that to-day's proceedings wear for me a certain air of unreality.

It would be a privilege to have one's name joined to a list containing any of my distinguished predecessors, but I must confess that it is a cause of very special pride for me to occupy for a while a place which long ago was adorned by Walter Rosenhain, my chief and guide for ten years, whose greatness we are marking to-day by the conferment of the first Rosenhain Medal. I should like to think that his shade, looking on to-day's proceedings, would approve, although I am certain that in that event he would add a salutary word on the dangers of being puffed up unduly by a temporary elevation to office.

I have been a member of this Institute since 1921—considerably more than a half of my life—and I owe to the Institute much of the knowledge of men and things which I have gathered, and I am indeed grateful for many occasions of interest and happiness experienced at its meetings. After an early introduction, sometime in the thirties, to my first love, the Publication Committee, I appear to have served sentences of shorter or longer duration on most of the committees to which your Council entrusts the greater part of its executive duties. It would be remarkable if in the course of this pilgrimage through the estate of our Institute I had not gained some rough idea of what members were hoping to find in it; in other words, if I have progressed—and seeing the dizzy height where I now stand and reflecting on the humble ground of a Student Member from which I started, it is impossible to deny that my net movement has been upwards—I trust that, in a somewhat unusual application of the phrase, I have climbed an educational

\* Delivered at the Annual General Meeting, London, 13 March 1951.

† Professor of Industrial Metallurgy, University of Birmingham.



ladder: I mean that climbing the ladder has been an educating experience for me.

One's life is not altogether contained within the ambit of the Institute's affairs, however, and during the times when I have been released for short periods from its committee meetings I have contrived to earn a living in three quite distinct metallurgical spheres: first in a Government research establishment, next in industry, and now in academic life. This has given me the opportunity to form an idea of what are the impressions made upon those concerned with non-ferrous metals in three different fields by the Institute and its activities. During the whole of the time covered by my experience, the Institute has been held in high esteem; in this country it has no rival, and all over the world its *Journal*, and especially its service for abstracting the scientific literature of non-ferrous metallurgy, have been acknowledged to be in the first rank. I have no reason to think that its reputation does not stand as high to-day as ever. This eminence has been maintained not by a policy of conservation and standing still, but by a constantly renewed self-examination and a willingness to make experiments where it appears that new developments offer the possibility of improved service.

#### THE INSTITUTE'S FUNCTIONS.

This is an appropriate moment to consider how well calculated these services are to meet the needs of to-day. We are living in an age of swiftly changing relationships in the economic, industrial, and social structure of our world, and it would be folly to assume that the Institute of Metals could afford to ignore these changes with any greater degree of impunity than, say, a commercial organization which depends for its well-being on satisfying a public demand.

As an Institute we have a two-fold responsibility of service: to our own members and to the community. On the principle that charity begins at home, let us first examine the needs of our members to-day.

I believe the Institute is performing most admirably its main service to members of providing a channel of communication for the discussion, on the highest level of impartial enquiry, of all matters concerned with the physical metallurgy of the non-ferrous metals. The Institute is functioning well as a learned society in this field, and its open discussions are well supported and maintained in the best traditions of scientific debate. I believe that the practical man, whose loyal wailings of neglect used to fill the air periodically, no longer feels that he receives less than a fair share of attention at our meetings; the successive symposia on different aspects of metallurgical production

have been enthusiastically received and well attended. On the other hand, it was a heartening experience at the meeting a year ago to see that members whose interests are related more to the theoretical and metal-physics side felt equally that the Institute provided the natural arena for their jousts, and I shall long remember how in a crowded meeting they insisted on extending the session by a half-day beyond that officially arranged, in order to allow a few more rounds in the X-Ray *versus* Microscope tournament.

### *Meetings.*

If there is less general satisfaction with the state of affairs in one direction, I think it is perhaps in connection with the expense involved in participating in the social activities of the Institute and particularly the Autumn Meetings. Here we are caught up in the strong economic currents which all of us are feeling in our private affairs as well as in company finances and university exchequers. Simply expressed, the cost of our main functions and of overseas meetings has risen to such an extent that large numbers of our members find it impossible to take part in these functions in the way they would like. For those who have to travel from a distance the cost of railway fares and two or three nights' hotels may be a heavy burden, and even the most economically devised luncheon for 200 or 300 people is very expensive compared with pre-war standards. When anything in the way of an evening dinner and dance in our old style is contemplated, the charge has to be proportionately heavier. With the strain on personal budgets which most of us are experiencing to-day, it is unfortunately true that the Autumn Meetings and social functions are deprived of the support of many who would have to bear the cost entirely from their private means. This strikes particularly hard at the younger members, members of staffs of research associations, and university people. There is a real dilemma, since on the one hand the prestige of the Institute demands a certain standard of accommodation and hospitality in its main functions, and on the other there is a substantial body of members who find it an increasing strain to join in them and in some cases have to forego that pleasure.

Without raising any hope of a completely satisfactory answer, it does appear that we might find a partial solution to the problem by some measure of decentralization, making fuller use of our excellent Local Section organization. It may be that we could profitably re-examine the scheme, of which we had a short experience before the war, for discussing some of the papers which have appeared in the monthly *Journal* at General Meetings organized for the purpose at centres away

from London. Special social gatherings at Local Sections might also be held from time to time, with appropriate financial support from the Council, invitations to participate being extended to the general membership of the Institute in other parts of the country. In these ways relief might be afforded from some part of the expense in travelling and hotels which attendance at a distant meeting involves.

As regards overseas meetings, in which the actual fares for travelling constitute so large a part of the cost, it is difficult to see what can be done to reduce expenditure. The high cost of rail, sea, and air travel is a most serious de-liberalizing influence. We must particularly regret that at the present time so very few of our members could afford the cost of a visit to America—an event for which all arrangements had been made in 1938, but which now has only a remote air of possibility. Perhaps an acceptable solace for those unable to make the journey to a foreign meeting would be to organize simultaneously discussions of papers in Britain, either in London or in a provincial centre. Constitutionally these would probably have to be counted as informal meetings, but they might nevertheless serve a useful purpose.

The Council and its appropriate committees will be giving earnest attention to these matters in the immediate future. The last thing they wish is to see a division develop between members who for one reason or another can afford to attend certain meetings and those who cannot. I would assure all members on whom this question of expenditure is pressing rather heavily that the most careful consideration will be afforded to any suggestion which offers a serious prospect of relieving the situation, while permitting the Institute to continue the pursuit of its traditional objects. I know that, in spite of all the difficulties, there are substantial numbers of members who are prepared to make some sacrifice to join in the functions and meetings of the Institute. I would urge them to continue to do so, and I would encourage others to follow their example. Interesting acquaintances and treasured friendships are made in thus rubbing shoulders with one's fellow members: and so far as technical meetings are concerned actual attendance enables the witness to catch the spirit of a debate and to understand its course in a way which cannot be provided by any written account.

#### *Publications.*

Publications constitute by far the most important activity of the Institute in terms of financial commitment and allocation of staff. In times of financial stress, therefore, this side of our affairs has to be watched carefully because on the one hand our accounts are very

sensitive to any increase in the cost of producing the *Journal* and, on the other, any economy in printing each paper leads to a worthwhile saving on the total sum of matter to be brought out during the year. It has been very pleasing to find that throughout all the discussions on this topic in Council and committees there has been complete unanimity on the necessity of maintaining our high standards of presentation and also on the desirability of publishing all papers submitted which are judged by the Publication Committee to be acceptable on grounds of merit and interest.

The Publication Committee, anxious always to follow these principles and at the same time mindful of the need for economy, has to be on guard against extravagance in such things as photographs, which are costly to reproduce. It is a fairly simple matter to indicate to an author when some reduction in the number of illustrations is possible and to suggest which might be omitted. When referees find the text to be unduly long, it is often rather difficult to suggest exactly where excision or abridgement might be achieved. With the best will in the world, moreover, an author not uncommonly is hard put to it to reduce an already written account, by, say, 20 per cent. I would ask authors, therefore, in their own interests as well as those of the Institute, to make a serious effort to effect the greatest condensation consistent with easy reading before submitting their manuscripts. There are few papers which would not actually be improved in clarity by an hour or two of the author's time being devoted to the removal of superfluous words and phrases.

Apart from a prolixity of style, two other causes of unnecessary length in papers often struck me when I was specially closely concerned with publications. One results from an author failing to realize that a document suitable as a report to a research committee may not be in the best form for a paper intended for presentation to the Institute. The research report is quite properly concerned in many cases to explain to the committee how the time of the investigator has been occupied, but this is of no interest to the reader of the paper in the *Journal* of the Institute. There is an understandable temptation to submit the report without alteration as the manuscript for an Institute paper, but the temptation should be resisted, and the text ought to be carefully re-examined before presentation to the Institute to see whether there are not opportunities for omission of some portions and abbreviation of others. The second cause of avoidable bulk is the inclination of an author to present his paper as a chronological account of his investigations. This may sometimes be the most effective treatment of the subject, but if the author would put himself in the position of the

reader he would more readily realize the advantage of a shorter account, omitting, or making only brief reference to, lines of experiment which proved to be unprofitable.

If authors would bear these points in mind and make a special effort to submit a manuscript shorn of all unnecessary trimmings, they would have the satisfaction not only of having produced a more easily assimilable account, but also of knowing that they had made a useful contribution towards keeping down the costs of the Institute's publications.

#### THE INDUSTRIAL ECONOMICS OF METALLURGY.

So far I have spoken of ways in which we might meet the present needs of our members and one or two directions in which we can help in the good housekeeping of the Institute. But these are, after all, only the domestic affairs of the Institute, and we should be sadly out of tune with the times if we were not conscious of our responsibilities as an Institute to the community at large. It appears to me that there is a clear opportunity for the Institute to perform a public service by devoting some attention to those aspects of metallurgical science and industry concerned with the resources of metals on which the non-ferrous metallurgical industry is based and with the most efficient utilization of those resources. In searching for a concise description of the subject I had in mind I thought of the title: "The Industrial Economics of Metallurgy". This name leaves me dissatisfied, but as I develop my theme I hope some of my audience may think of a better term.

This country has seen a most critical situation arise during recent months in connection with most of the non-ferrous metals of major importance. If I speak of the United Kingdom particularly, it is only because the details of developments here come so regularly and so forcibly to my notice. I am well aware that the circumstances and trends in other parts of the world are very similar.

We have seen the supply of copper and zinc in relation to demand become so precarious that drastic curtailment of releases of the metals has become necessary; manufacturers who, seeking an alternative, turn to aluminium find that even established users of the metal must contrive to reduce their consumption substantially below the rate recorded over a certain period in 1949. Lead is now so difficult to come by that motorists are warned to lock the bonnets which cover the precious batteries in their cars, and lead roofs are stripped by predatory citizens not, as formerly, for the silver content but simply for the value of the lead, while tin has settled down as a four-figure metal in £s per ton.



It may be said that so far as the metallic resources are represented by mineral ores they are more properly the affair of our sister institute, the Institution of Mining and Metallurgy, and I would not dispute this. But the most complete knowledge of the reserves of metal in the ground, of the rates of production, and of the economics of mining would still leave untouched factors of immense importance affecting the availability of metal for use by the metal-working industries.

An important factor in producing the present shortages has undoubtedly been the precautionary stockpiling which has been adopted as a part of their policy by so many states. If this were the only factor, or the greatly predominant factor, it would be serious enough, since the balance of our complex industry is so delicate that even a temporary diversion of raw materials can have devastating consequences for companies and individuals far outside the circle of concerns immediately involved. It might be that a stockpiling programme could be accommodated without grave dislocation, albeit certainly at the cost of much inconvenience, if a term could be set to the period of the stockpiling. It is not the practice, however, for stockpilers to announce the size of the stock which they aim to create, and the activity remains an influence of uncertain intensity and duration.

The most superficial study of statistics of production and consumption of the principal non-ferrous metals since the beginning of the century reveals a shifting of the balance between supply and demand which is producing a disequilibrium increasing in an exponential manner. Looking at the long-term trend and thinking of developments in decades rather than years, we see influences of an apparently permanent and potent nature compared with which stockpiling is merely a ripple in a powerful stream. The basic forces spring from three elements: first, the increasing population of the world; secondly, the essentially exhaustible, non-renewable characteristic of mineral resources; and thirdly, the world-wide demand for higher standards of living. The first and third forces, that is increasing numbers and expanding desires, have not the quality of inevitability of the second, but they appear to be essential features of civilization as we understand it, and unless we are to plunge deeply into philosophical and social-anthropological speculation we may regard them as permanent.

There is no need to quote large collections of statistics to depict the scale and rate of movement. The population of the world, which was 1009 millions in 1845, is now 2300 millions, and is increasing by 20 millions each year; that is, every  $2\frac{1}{2}$  years there is added to the human inhabitants of the globe a number equal to the present population of the United Kingdom. Over the same period the annual rate of pro-

duction and industrial application of iron and steel has increased five times as fast as the population; since 1880 the consumption of copper has increased tenfold and that of zinc fivefold. We see therefore that imposed on the increase in numbers of consumers is a steep rise in consumption per head. The effect of a movement towards a higher standard of living has been illustrated by the calculation that if the consumption of copper per head throughout the world rose to be one half of that in the United States, the tonnage of new copper required annually would be 10.9 millions, compared with the present world production of 2.4 million tons.

A situation like this presents a problem to all whose interests are related to those of metallurgical industry. In one way or another it affects all classes of our membership, and it does so by posing three questions :

- (1) What can we do to improve our supplies?
- (2) How can we make better use of what we have?
- (3) What substitutes can we use in place of the metals which have become difficult in supply?

The first takes us at once into the fields of prospecting and mining, extraction and refining. The Institution of Mining and Metallurgy has for long devoted much of its activities to these matters, and we may well be content to leave them in their hands, not overlooking our interest in some aspects of refining, such as the thermodynamics of metal-halide reactions, which are rather far removed from process metallurgy as ordinarily understood.

Making better use of what we have means in the first place an examination of the efficiency with which we employ our metals. Here it is not a question of mechanical efficiency, for instance, by economy of weight in aeronautical structures, but rather the avoidance of extravagance in the quality of metal used in particular applications. The criterion of quality which is relevant in this connection is the difficulty of replacement in stock and not necessarily the usual test of chemical purity, although the two are often synonymous. The use of a higher grade of a metal than the application, or the method of manufacture, technically demands, or the unnecessary use of one metal in place of another more freely available, and likely to remain so, is metallurgically inefficient.

There is another direction in which we must look if we are to secure the most effective outlay of our stores. This involves enquiry into the fate of all the metals which, once having been won from the earth, have survived in the metallic form or as compounds easily reduced once



again to metals. These comprise the great corpus of metals in current service in an infinity of forms and also the stock of metals which are temporarily out of active use, the worn-out or obsolete or redundant articles constituting old scrap and the surplus from manufacturing processes such as turnings, clippings, and furnace residues. This is the field of secondary metals, which has been relatively neglected by scientific metallurgy.

A variety of causes has probably been responsible for this neglect. One may well have been a reluctance of metallurgists to study the leavings and contaminated side-products of industry and society. Another deterrent has been provided by the complexity of many secondary metals and the difficulty in deducing the effects of the simultaneous presence in an alloy of several impurities, quite apart from the influence of non-metallic inclusions. Whatever the reasons for the lack of interest in secondary metals on the part of metallurgists, it is clear that this indifference cannot persist when we realize how great and vital a part secondary metals play in the economy of metallurgical industry. In copper 38% of the metal consumed in 1948 was of secondary derivation, in aluminium the proportion was 30%, in lead 45%, and in zinc 28%. We know that the steelmaking industry takes 55% of its metal input as scrap.

The third question to which I suggested we must address ourselves in the face of the growing crisis was: What substitutes can we use in place of the metals which have become difficult in supply? In one sense the answer in respect of any specified application is easily given: it calls only for an analysis of the properties essential to the performance of the service, a reference to the tabulated data for the classes of material offering a *prima facie* case for consideration, and then a selection in the light of availability. Even within such circumscribed terms of reference as these, the treatment of the problem may be rather involved; for one thing, where a usage has existed for a long time it is often by no means easy to deduce which characteristics of the metal are indispensable for the application and which are unimportant.

It is only dealing with the first stage of the problem of substitution if we confine ourselves to discussing interchangeability on the basis of equivalence or similarity of physical characteristics. We must pass from this step to consider the position as regards supplies of the technically acceptable substitute: will they be only temporarily easier and will they be exposed to risks of interruption or curtailment or to fluctuations in price to which the industry has not been accustomed and for which it is not organized? Is the alternative peculiarly sensitive to contamination, does it involve an unduly large ratio of metal cast to

finished product, will it demand troublesome changes in manipulative plant? Only after the patient unravelling of these and similar interwoven threads can the possibility and appropriateness of a substitute be assessed.

My object in making this very brief review of the subject of resources is to discuss what service this Institute can perform in this connection for its members and indeed for the community. In the course of our normal activities hitherto we have given little attention to these matters, although our rules do not exclude them explicitly or by implication from our interest and although they are of the liveliest concern to the great majority of our members in whatever capacity they have to deal with metals. Future readers of our *Journal* for the year of 1950 will find no reflection in our papers and discussions of the fact that the non-ferrous metals industry has entered a phase of crisis in its supplies of material which is likely to have a profound effect on its immediate fortunes and its ultimate pattern of development. I feel it is wrong that, as an Institute, we should give this impression of detachment from these problems which are of such vital interest to our members. It may be objected that questions of supply and demand are essentially the affair of the economist and therefore not properly brought before our Institute for discussions. But this is a territory in which economic considerations and technical metallurgical factors are most closely linked.

Think, for instance, of the factors which have to be taken into account in forming a sound judgment on the value in Britain of home-produced magnesium as a replacement for imported metals. There is the mineral resource in unlimited amount: magnesium chloride in the sea and dolomite in the Pennines, and electric power for electrolysis of the fused chloride is to be had. But the power is expensive in this country in relation to the cost in Canada and other countries with very large hydro-electric installations. Is there a point where the assurance of a supply of light metal produced at home would outweigh the disadvantage of a higher cost of production? As another example, in copper alloys we have the repercussions of the change in practice from cold rolling to hot rolling of 70:30 brass. While making possible a great acceleration of production, this demands a higher grade of purity of metal, and consequently the exclusion of some secondaries which could be used when cold rolling was the method used.

The examples could be multiplied by anybody who has had to assume a measure of responsibility for policy in a manufacturing concern using or producing semi-finished products of metallurgical industry. In each of these there is a metallurgical component inextricably involved with the economic: a proposal which may be attractive on broad economic

grounds may fall down on account of a technical metallurgical obstacle, or a scheme impeccable metallurgically may require for its achievement economic conditions not producible at the time.

I do not doubt there are learned societies and institutions where papers are received dealing with the economic side, but I know of none in which a metallurgist would feel at home in submitting his contributions for joint discussion with the man who would say his own approach was certainly that of the business executive.

Since writing this I have come across the following passage in Rosenhain's Presidential Address in 1928 \* :

" There is no function of this Institute which I value more highly than that of promoting interchange of ideas and experiences between practical men and between practical and scientific men who are interested in the same subject. The Institute has done much to break down barriers that formerly hampered the progress of the non-ferrous metals industry. Men, both practical and scientific, have come to know and understand one another better, and with increasing mutual knowledge has come that measure of confidence which is essential if men are to work together profitably. I only wish that it might be possible for that understanding and confidence to grow not only deeper as between the technical man in the works and the scientific man, but that it might grow wide enough to embrace also the business man—the man who, ultimately, controls finance, and therefore is the deciding factor in determining how far and how soon the results of research are to be utilized. Even in that difficult direction the Institute has done something, and will, I hope, do more in the future."

My suggestion is that this is a field in which—while most emphatically not contemplating any curtailment of the scientific activity on which its reputation as a learned society has been gained—our Institute can perform a valuable function by providing a forum where these aspects of metal-economics can be discussed. I am strongly encouraged to put forward this proposal by a study of the papers which were communicated to the conference organized by the United Nations Economic and Social Council at Lake Success in 1949. Under the title of " Conservation and Utilization of Resources ", the Conference cast a very wide net. In the sections dealing with metallic resources of the world there were several papers which would have fallen appropriately within the range I envisage being covered by this new activity of the Institute. I will quote some of the titles and authors of these papers, and I commend them to your attention if you are not already acquainted with them :

" The World Resources Situation ", by Fairfield Osborn.

" World Resources and World Population ", by Colin Clark.

" Critical Mineral Shortages ", by H. L. Keenleyside.

" Conservation of Mineral Resources ", by Donald H. McLaughlin.

\* *J. Inst. Metals*, 1928, 39, 28.

"The Accumulation and Conservation of Metals in Use", by Charles White Merrill.

"The Supply and Industrial Applications of Scrap Metals", by H. J. Miller.

A valuable report of the conference by Dr. H. Sutton appeared last year in the technical press.\*

Some of my friends may say that this would not be a new activity for the Institute, and I agree that it would certainly be within the declared aims and objects of the Institute, the two most important of which are: To promote the science and practice of non-ferrous metallurgy in all its branches; and to facilitate the exchange of ideas between members of the Institute and the community at large, by holding meetings and by the publication of literature, and in particular by the publication of a Journal dealing with the objects of the Institute.

If it is not a new activity, so much the better. In any case, if I find any support for the idea, I propose to arrange an informal meeting of members and non-members who might be interested to take part in a discussion of a paper prepared by somebody engaged in this line of enquiry or even on one or two of the papers from the United Nations conference to which I have already referred. In the event of such a meeting proving successful, not the least of the benefits which the Institute could receive might be some additions to its membership from circles concerned with non-ferrous metals who had not previously found the Institute devoting attention to the aspects of interest to them. But more important than this would be the prospect of making an appreciable contribution to the study, and perhaps the solution, of the gravest problem which has beset the non-ferrous metallurgical industry in the lifetime of our Institute.

We may rightly be proud of our past history, with its record of continuous progress; we may take satisfaction from our present membership, which has never been more numerous, and our status which has never been higher. The future of the Institute is in our own hands. If we keep clearly before us the aims and objects which were defined by the founders of the Institute, I believe the quality of our work will ensure the material support needed for its continuance, provided that we make that work known. If within the affairs of this organization we are ever watchful for new opportunities of service to metallurgical science and industry, we shall have the satisfaction of finding that in this way we are at the same time discharging our responsibilities to the community and strengthening the growing structure of our Institute.

\* *Metal Ind.*, 1950, 77, 3, 19, 35, 57.

SLIP AND POLYGONIZATION IN  
ALUMINIUM.\*

1302

By R. W. CAHN,† B.A., Ph.D., JUNIOR MEMBER.

## SYNOPSIS.

A method is described for making aluminium crystals of predetermined orientation from the melt. The development of slip lines during stretching of these crystals was studied in detail, with particular reference to cross slip (localized slip on planes other than the main octahedral plane subject to the maximum shear stress) and to deformation bands. While always maintaining the same slip direction as the principal slip, cross slip took place on several distinct planes, an octahedral one being the most common. The proportion of cross slip increased with the deformation and with rising temperature of deformation. Deformation bands were found to be associated with uneven elongation of adjacent parts of a crystal; their orientation changed systematically with increasing deformation, being initially normal to the slip direction. They were also formed in bicrystals and polycrystals and during deformation at elevated temperatures, but not in bent crystals. Annealing at high temperatures caused progressive polygonization within the bands; new grains formed by recrystallization tended to advance preferentially along the bands. Polygonization of the deformation bands was associated with a local rumpling of the free surface of the specimen. The formation of these markings was accelerated by the application of a tensile or compressive stress while annealing; this implies that polygonization is accelerated by an applied stress. Possible reasons for the occurrence of cross slip and deformation bands are discussed.

## I.—INTRODUCTION.

MOST metals undergo plastic deformation by slip, which ideally consists of the movement, relative to each other, of thin sheets or lamellæ within the individual grains, the planes of the lamellæ and the direction of motion having fixed crystallographic indices. The process is often compared to the shearing of a pack of cards. Slip does occur in this ideal form in some instances, as in single crystals of zinc or cadmium of suitable orientations when deformed in tension. More often, however, some deviation from ideal slip is encountered. The indices of slip plane and direction may vary within a single grain; or the lamellæ may not be flat, but bent either microscopically or on a larger scale.

Iron constitutes a well-known instance of simultaneous slip on planes of different indices (also known as pencil glide) in which (110), (112), and (123) planes all operate, though the slip direction is always [111].<sup>1</sup> The question of which is the preponderant plane appears to depend on temperature and on previous deformation. The resultant slip lines visible on the surface of a deformed crystal are wavy instead

\* Manuscript received 22 August 1950.

† Atomic Energy Research Establishment, Harwell, Berks.



of being straight. The change of slip plane with temperature is a common property of most body-centred cubic metals, and a systematic relationship between the preponderant slip plane and the temperature expressed as a function of the melting point has been established by Andrade and Tsien.<sup>2</sup> A recent study of silver chloride<sup>3</sup> has shown that the slip planes vary from grain to grain, though the slip direction is invariant. Face-centred cubic metals also deviate from ideal slip, though less markedly than do the body-centred cubic metals. The imperfection in this case takes the form of cross-slip, which has recently been examined in crystals of  $\alpha$ -brass by Maddin, Mathewson, and Hibbard.<sup>4</sup> The slip lines, corresponding to slip on (111) planes, are straight, but some of them go through sharp zig-zag steps where the slip plane is locally altered to (1 $\bar{1}$ 1). The two planes share a common [ $\bar{1}$ 01] slip direction. Slip lines of somewhat similar appearance were reported by Ogilvie and Boas<sup>5</sup> on aluminium.

Bending of the slip lamellæ always occurs, as a geometrical necessity, near the grip-ends of stretched single crystals. This is caused by the rotation of the crystal lattice relative to the axis of extension which occurs in the stretched portion, rotation being inhibited at the ends of the crystal by the grips. The portion of a single-crystal tensile specimen remote from the grips should in theory remain entirely unbent. X-ray evidence<sup>6, 7</sup> shows that zinc and cadmium crystals, even when extended by over 100%, retain an almost completely unbent lattice. However, this is not true for certain cubic metals, e.g. aluminium, iron, sodium, and potassium; X-ray Laue photographs of stretched crystals of these metals, taken after annealing, exhibit spotty asterisms.<sup>8, 9</sup> According to recent observations<sup>10, 11</sup> this is a sign that polygonization has taken place. Since polygonization can occur only where the lattice is bent, lattice curvatures must have been present in the extended crystals before they were annealed. The only recorded observation, known to the writer, of lattice curvature in stretched single crystals, is by Crusard,<sup>12</sup> who detected kinks or *pliages* in extended aluminium crystals. Collins and Mathewson<sup>13</sup> observed markings on aluminium crystals which were almost certainly deformation bands, though they did not recognize them as such. There is often much curvature in deformed polycrystalline specimens in which the most strongly bent regions have been called deformation bands. Barrett and Levenson<sup>14</sup> have investigated these in compressed aluminium; their existence was early recognized in iron, in which they were studied by Pfeil.<sup>15</sup> They are common in a number of other metals, and a résumé of the observations of their occurrence is given by Barrett.<sup>16</sup> The characteristic feature of deformation bands is that the lattice in them, or near their boundaries, becomes progressively more bent as deformation is continued; in the

extreme case the grains themselves may become aligned in one preferred texture, while the lattice in the body of the bands takes up another.<sup>17</sup>

Recently, Honeycombe<sup>7</sup> has studied deformation bands in aluminium by microscopic examination of diffraction spots recorded on film placed close to the specimen.

The present paper reports experiments with aluminium crystals, deformed mostly in tension, which cast some new light on both these types of slip imperfection. The experiments were begun with the aim of examining the recrystallization textures of the stretched crystals; the unrecrystallized crystals, however, showed features which were sufficiently interesting to warrant a separate study. The results on the recrystallization textures will form the subject of another paper.

## II.—EXPERIMENTAL METHODS.

### 1. *Making the Crystals.*

The crystals were made from the melt by a variant of the method introduced by Chalmers<sup>18</sup> for making tin crystals. They were in the form of plates, 20 mm. wide, 2 mm. thick, and 150 mm. in length. Plate blanks of the correct shape were milled out of ingots of super purity aluminium (99.99% approx. with iron and silicon as chief impurities). A blank was flame-welded to a seed crystal of the desired orientation, and placed in a graphite boat fitted with a graphite stop and lid in such a way that the blank was tightly enclosed on all sides. This prevented it from gathering into a large drop when molten. The boat was pushed far enough into a temperature-controlled tubular electric furnace for half the seed to become molten, and was then withdrawn at the rate of 5–8 cm./hr. The blank was invariably turned into a single crystal of the same orientation as the seed. X-ray photographs prepared from such crystals showed them to possess a macromosaic or lineage structure, which was confirmed by macro-etching. The angular range of orientation covered by this structure was about 2°.

The seed was made by determining the orientation of a number of unseeded cylindrical crystals till one was found the axis of which fell close to a desired point in an elementary triangle of the cubic stereographic projection, viz., the point *a* in triangle *ABD* of Fig. 2. This was rotated into the correct azimuth, bent slightly to correct the orientation, and fused to a blank which was then turned into a seed for repeated use. The orientations of all crystals were determined goniometrically after etching in the three-acid reagent recommended by Barrett and Levenson;<sup>19</sup> they were generally not more than 2–3° from the ideal orientation.



## 2. Orientation of Crystals.

The orientation chosen, shown in Fig. 1, had been decided upon originally for the texture experiments mentioned in Section I. A thin plate-shaped crystal was desirable because this would render visible a

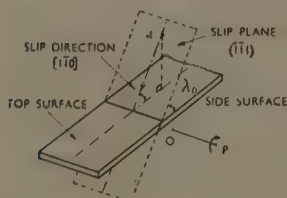


FIG. 1.—Orientation of Crystals.

large proportion of the grains formed by recrystallization. To minimize the distortion in the region of the grips, the axis of rotation operating in flexural glide had to be parallel to  $OP$  (Fig. 1). The angle  $\lambda_0$  was made  $49^\circ$  because a stereographic projection (Fig. 2) showed that the crystal could then be extended by as much as 40% and still slip on the

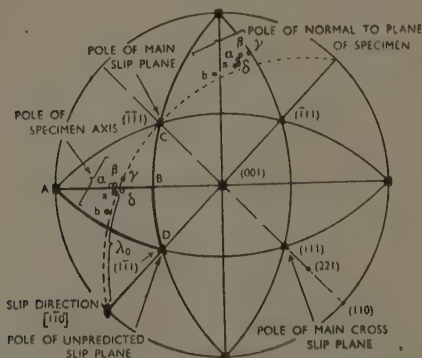


FIG. 2.—Cubic Stereographic Projection of the Orientations of Crystals and Deformation Bands.

## KEY.

$a$  Undeformed crystal.  
 $b$  Crystal extended 20%.

$\alpha, \beta, \gamma, \delta$  Deformation bands.  
 Angle between  $a$  and  $b = \phi$ .

axis is marked at  $a$  in the triangle  $ABD$ ; on extension it rotates towards  $[1\bar{1}0]$ , and as long as it does not cross the great circle  $AD$ , the crystal deforms by single slip. The pole of the normal to the crystal plate is also included in Fig. 2.

\* All indices refer to Fig. 2.

A series of specimens was also made of orientation as shown in Fig. 1, except that the angle  $\lambda_0$  was different for each specimen. This was done by growing a large flat crystal of orientation such that the  $[1\bar{1}0]$  slip direction lay in the plane of the crystal, and cutting the specimens out. Pieces from the crystal were also used for seeding a symmetrical bicrystal.

### 3. Specimen Preparation.

For the study of the nature of slip, smaller specimens, usually about  $10 \times 2 \times 50$  mm., were cut from the large crystals, and one top and one side surface of each specimen was ground flat to 000 emery paper. The narrow side surface was made as nearly as possible perpendicular to the top surface by holding the crystal in an appropriate jig during grinding. The whole crystal was then given a deep electrolytic polish in the perchloric acid ethyl alcohol bath introduced by de Sy and Haemers.<sup>20</sup>

All crystals were extended rapidly by a Hounsfield tensometer, at a rate of the order of 1% per second. Most of the extensions were carried out at room temperature, but one crystal was pulled immediately after cooling in liquid oxygen; others were pulled at 250° and 400° C., and some were annealed while under stress applied by suspending a small weight from them, or by a simple compression jig. Many of the specimens were annealed after extension in a temperature-controlled furnace and allowed to cool in the furnace.

### 4. Metallography.

Four methods of metallographic examination were employed: (a) The slip lines on the polished specimen were examined under the microscope. (b) The specimen was macro-etched with Barrett and Levenson's reagent and examined on a two-circle goniometer. (c) The specimen was reground and repolished and micro-etched in Lacombe and Beaujard's<sup>21</sup> reagent. This reagent produced much finer pits than Barrett and Levenson's mixture, and revealed discontinuities of structure. (d) The specimen was reground and repolished and extended again by 2.5%. The new slip lines acted analogously to a micro-etchant in revealing the orientation at each point. Methods (c) and (d) were used for annealed specimens.

In addition, Laue transmission photographs of some of the specimens were taken. The beam passed through the specimen normally to the top surface, and the diffraction pattern was registered on a cylindrical film of radius 3 cm.

It may be mentioned that crystals of the orientation described

above were also used for experiments on bending and polygonization; Figs. 17 and 18 (Plate XVIII) of the author's earlier paper<sup>10</sup> were made from such crystals, examined by method (c).

### III.—EXPERIMENTAL RESULTS.

#### 1. *Cross Slip.*

All extended crystals proved, on examination, to have slipped predominantly on the expected ( $\bar{1}\bar{1}1$ ) plane and in the  $[1\bar{1}0]$  direction (Fig. 2). This was clear both from the direction of the slip lines on the top and side surfaces, and from the observed rotation of the crystal axis towards the  $[1\bar{1}0]$  direction (Fig. 2). Furthermore, all specimens had marks of cross slip. This could be seen to best advantage on specimens deformed fairly weakly; Figs. 7, 8, and 9 (Plates XVII and XVIII) are of a specimen extended 7% at room temperature. Since



FIG. 3.—Nature of Cross Slip.



FIG. 4.—Intimate Cross Slip: (a) Low magnification. (b) High magnification.

the elements of cross slip have several different directions, it follows that cross slip took place on several different planes; the most common of these was  $(111)$ , the trace of which makes an angle of  $70^\circ$  with the trace of ( $\bar{1}\bar{1}1$ ). No sign of cross slip is visible on the side surface (Fig. 9). Theoretically, this surface is exactly parallel to the  $[1\bar{1}0]$  slip direction, and the slip lines should not be revealed. In practice, however, the surface generally lay  $2-3^\circ$  from this theoretical orientation, and slip lines could in fact be seen. The conclusion to be drawn from the appearance of the side surface was that all the cross slip planes shared  $[1\bar{1}0]$  as a common slip direction. The main ( $\bar{1}\bar{1}1$ ) slip "planes" have therefore become corrugated (Fig. 3). The analogy for slip in terms of a pack of cards is evidently inappropriate; it is better to compare it to the motion of the saddle of a lathe on its bed.

#### (a) *Unpredicted Slip.*

A few distinct slip lines appearing on Figs. 7 and 9 (Plates XVII and XVIII) and particularly on Figs. 20 and 21 (Plate XXI), correspond to slip on  $(1\bar{1}1)$  planes. These occurred in some places in all crystals, even in those very weakly extended. From their saw-toothed

appearance (Fig. 9) slip on  $(1\bar{1}1)$  must have preceded slip on the preponderant  $(\bar{1}\bar{1}1)$  plane. No trace of cross slip ever appeared on these unpredicted slip lines. The  $(1\bar{1}1)$  planes would be subject to the greatest shear stress only if the pole of the specimen axis lay within the triangle  $ABC$  (Fig. 2). The pole of the undeformed crystal lies in  $ABD$  quite close to  $AB$ , and it might be, therefore, that the near equality of shear stress on  $(\bar{1}\bar{1}1)$  and  $(1\bar{1}1)$  leads to a small amount of slip on the latter at the beginning of the extension. Against this there is the consideration that the same phenomenon was observed with some other crystals for which the pole of the specimen axis was well inside  $ABD$ .

### (b) *Prominent and Intimate Cross Slip.*

Figs. 11 and 12 (Plate XVIII) are high-power photomicrographs of cross-slip sites on the top surface of a specimen extended by 5%. The former shows what Maddin *et al.*<sup>4</sup> called "prominent" cross slip; the latter what they termed "intimate" cross slip. In Fig. 12 the multiple fine structure of slip lines in aluminium (recently discovered by Heidenreich and Shockley<sup>22</sup> by means of the electron microscope) can be clearly seen, as the individual fine slip elements do not all change from  $(\bar{1}\bar{1}1)$  to  $(111)$  planes at exactly the same spot. Moreover, in the prominent cross slip, the slip elements often weave a zig-zag pattern by repeatedly changing from one plane to the other, as they do in Fig. 11. The result of this is that at low magnifications, the direction of prominent cross slips is liable to be deceptive and the derived cross-slip plane may be the wrong one. In other specimens the cross slips appear curved (Fig. 23, Plate XXI); this is undoubtedly due to the incidence of such "zig-zag" cross slip.\*

The intimate cross-slip site shown in Fig. 12 (Plate XVIII) would appear, at low magnifications, as in Fig. 4 (a), with a gradual tapering of the slip lines where they run opposite each other, while the true nature of intimate cross slip as illustrated by the photomicrograph is sketched in Fig. 4 (b).

### (c) *Effect of Changing Temperature.*

It was found that different specimens which had been identically treated showed markedly different amounts of cross slip. Where there was less of it, a greater proportion was intimate. A low temperature of deformation favoured intimate cross slip, while the high temperatures tended to favour prominent cross slips (Figs. 20-23, Plate XXI).

\* The designations prominent, intimate, and zig-zag are introduced purely for convenience in description; it is not intended to imply that they refer to fundamentally different kinds of cross slips.

In the specimen pulled at 500° C. (Fig. 23), the cross slip was very prominent and predominantly wavy, which implied that there was much zig-zag cross slip. In spite of the disorderly appearance of the top surface of this specimen, the common  $[1\bar{1}0]$  slip direction was strictly maintained. This was deduced from the complete regularity of the slip lines on the side surface. The specimen differed from those pulled at other temperatures in that the cross slips connected together the separate main  $(\bar{1}\bar{1}1)$  lines in an intricate interlaced pattern rather like that of a railway marshalling yard. In the specimens deformed at lower temperatures the individual lines were less often joined together.

(d) *Effect of Increasing Extension.*

The specimens described up to now had been extended only by a few per cent. Further extension at room temperature considerably increased the amount of very intimate cross slip, with the result that the slip lines looked increasingly wobbly on the top surface but remained straight on the side surface. The predominant slip still took place strictly on  $(\bar{1}\bar{1}1)$ , as evidenced by the general direction of the slip traces on the top surface. Fig. 19 (Plate XX) illustrates the slip lines on a specimen which had been stretched 27%, repolished and re-extended by 2% (method (d)). The straightness of the main slip lines is well exemplified by this, and the intimate cross slip is also clearly discernible. This is on so fine a scale that much of it probably involves a few only of the many fine strands constituting each line, and the width of the cross slip is comparable with the total width of the compound slip line. This extreme form of intimate cross slip has also been observed by Brown<sup>23</sup> during his studies of aluminium crystals by the electron microscope.

(e) *Effect of Etch-pits on Slip.*

The following observation, made accidentally, may help to reveal the origin of cross slip. A specimen which had been micro-etched (method (c)) was extended by about 20% without being repolished. The slip lines on the top surface had characteristic cross slip steps (all corresponding to the  $(111)$  cross slip plane) wherever they approached an etch-pit; this cross slip was the more extensive the larger the pit, and was always on the same side of the pit. Behind each large pit there was also a slipless region, all the main slip lines having been bent aside by cross slip. The two phenomena can be clearly seen in Fig. 17 (Plate XX). The cross slip and slipless regions were on the side of each pit which, if a light-beam were imagined coming parallel to the slip direction from inside the crystal, would be in the shadow of the pit.

(f) *Indices of Cross-Slip Planes.*

To determine which cross-slip planes were the most common, a specimen was extended by 5%, and the carefully prepared top surface examined under the microscope at medium magnification, using a cross-wire eye-piece and a calibrated rotating stage. It was easy to determine the pole of any cross-slip plane from the angle its trace on the top surface made with the traces of the  $(\bar{1}\bar{1}1)$  planes, since it was already known that all cross-slip planes included the  $[\bar{1}\bar{1}0]$  slip direction. The locus of the poles of possible cross-slip planes is the great circle indicated by the broken line in Fig. 2. Only straight cross slips were examined, to avoid confusion with zig-zag cross slip, but nevertheless the shortness of most cross slips made very accurate determination of their directions difficult. The cross slips were grouped into families with approximately the same direction. The main operative planes were found to be  $(111)$ ,  $(001)$ , and  $(221)$ , the most common being  $(111)$ . There also appeared to be other operative planes lying between  $(111)$  and  $(110)$ , and in the vicinity of  $(001)$ . No cross-slip planes of orientation close to the main  $(\bar{1}\bar{1}1)$  slip plane were found, though it is true that they would be relatively difficult to detect.

(g) *Continuity of Slip Lines Across Grain Boundaries.*

Cross slip furnishes the explanation for the puzzling observation, first made by Lacombe and Beaujard,<sup>21</sup> of the continuity of slip lines across boundaries between grains of not very different orientations. This was checked by extending a coarse-grained specimen, which had been made by recrystallizing a strained single crystal and in which the orientation of all grains had been determined, so that boundaries between grains of neighbouring orientations could be selected for observation. Lacombe and Beaujard's finding was confirmed, and it was also found that the slip lines in one of the two neighbours, in particular, exhibited much cross slip (Fig. 24, Plate XXII). In some regions this went so far that, away from the boundary, the directions of the main and cross slip traces were interchanged (Fig. 25, Plate XXII). The difficulty raised by Lacombe and Beaujard's observation was that there was no reason why, in general, the rectilinear intersection of the slip planes in neighbouring grains should everywhere coincide with the boundary surface, which might have any shape. If cross slip occurs, the intersection, instead of being a straight line, becomes a serrated or stepped line (macroscopically, a skew curve) which can coincide with a boundary of any shape.

This does not obviate the difficulty that the slip directions in the neighbouring grains will in general be different. The local stresses



caused by the difference can be relieved by highly localized slip on some other plane. This was repeatedly observed, and is illustrated in Fig. 24 (Plate XXII) by the short line starting at the intersection of the slip lines in the two grains.

(h) *Cross and Unpredicted Slip in Bent Crystals.*

Some crystals were deformed by bending about the axis *OP* (Fig. 1); this was done primarily to study polygonization. It was noted, that in a crystal bent carefully and true about the intended axis, the incidence of cross slip was much less than in one bent skew (in which the crystal axis was a skew curve after bending). Unpredicted slip, as described above, took place in the same way and on the same plane as in extended crystals.

It may occasion surprise that cross slip is so clearly visible in many of the photomicrographs, in view of the fact that its occurrence in aluminium has been overlooked for years. This is due to the peculiarly favourable orientation of the top surface of the specimens, which showed up the cross slip with maximum contrast of direction. This contrast was much reduced on the oblique surfaces that were ground on some specimens.

## 2. *Deformation Bands.*

(a) *Macroscopic Appearance.*

When a flat polished specimen was extended by a few per cent., the top surface became somewhat crumpled, similarly to the surface of very shallow sea waves with sharp crests. The side surface, on the other hand, remained perfectly smooth, although when the extension exceeded 15–20%, a number of faint parallel striations could just be detected, which were approximately normal to the slip lines. These striations ran into the crests of the waves on the top surface. The inference to be drawn from the new appearance of the top surface was that the extension of the specimen took place inhomogeneously. To test this, several reference marks were made on the specimens, and the separate elongations of the several sections were measured. The elongations differed by up to 5% in different sections of the same specimen.

In the hope of making the striations more prominent, some of the extended specimens were repolished and macro-etched (method (a)). This treatment revealed clearly marked striations or bands on both surfaces, even of weakly extended specimens. Figs. 5 and 6 (Plate XVII) show them on the top and side surfaces respectively of a specimen stretched by 7%. The uniform direction and spacing of the bands

on the side surface, in particular, should be noted. On the top surface the bands were sometimes forked, and were less regular. They became still less regular if the crystal was further extended, repolished, and re-etched. This is illustrated by Fig. 10 (Plate XVIII) of a specimen extended by 20%. The enhanced contrast of the bands against the rest of the crystal in this specimen, as compared with the one less extended, is also evident.

(b) *Orientation of the Lattice in Deformation Bands.*

Some extended specimens, etched in this way, were examined on the two-circle goniometer, and the orientation of the lattice in the bands was found by noting the setting of the specimen when the reflections from the bands were at their brightest. This optimum setting could not be as sharply determined as that for the remainder of the crystal between the bands. It was observed that if a specimen was annealed for some time at about 450° C. before being etched, the optimum goniometer settings for the bands were better marked.

The orientation of the lattice of the undeformed crystal, the extended crystal, and four deformation bands in a specimen stretched by 20% is marked in Fig. 2. The accuracy for the first two orientations was about 1° while for the others it was only 3–4°. These orientations were typical of all specimens examined. Fig. 1 indicates that, within the experimental error, the lattice in the bands rotated by varying amounts relative to the rest of the crystal about the axis *OP*. This is also the axis of rotation for flexural glide near the grips, and the vector in the slip plane perpendicular to the slip directions. The sense of rotation was opposite in the two cases.

(c) *Orientation of Planes of Deformation Bands.*

These measurements were supplemented by a determination of the orientation of the bands themselves, as distinct from the orientation of the lattice in them. The bands were the traces in the top and side surfaces of roughly flat sheets going right through the specimen. In specimens extended by a few per cent. only, these sheets were invariably perpendicular to the  $[1\bar{1}0]$  slip direction (i.e. parallel to the (110) plane), within a few degrees. In more strongly extended specimens the sheets were no longer exactly perpendicular to  $[1\bar{1}0]$ , but were rotated from this position by an angle  $\theta$ . The amount of this rotation was correlated with the rotation  $\rho$  of the lattice in the bands relative to the lattice in the crystal matrix. The two angles are indicated in Fig. 34 and their values, for a specimen extended by 20%, are given in Table I. They were determined to an accuracy of about 3°, the inaccuracy in  $\theta$  being

due to the imperfect flatness of the bands. Within the experimental error the two rotations were equal, though the small but consistently positive difference always found between  $\theta$  and  $\rho$  may well be significant.

The conclusion is that the planes of the sheets were not parallel to rational crystallographic planes, except for weak extensions, but were rotated from the normal to the slip direction by a rotation equal to or slightly greater than the lattice rotation in the bands. The axis of rotation lay in the slip plane, normal to the slip direction. This conclusion was confirmed by the examination of unetched specimens. In these the deformation bands showed up under the microscope only on the side surfaces, because here the slip lines went through a

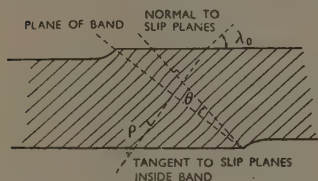


FIG. 34.—Angles in a Deformation Band.

bend in the bands. This did not occur on the top surfaces, which were parallel to  $OP$ , the axis of rotation (Fig. 1); the direction of the slip lines was not altered in the bands, and the only indication of bands was the slight difference in brightness caused by the local tilt of the surface.

Crussard<sup>12</sup> stated that the bands tended to align themselves parallel to a  $(351)$  plane and gave reasons why they should be particularly stable in this position. It is easily verified that the pole of  $(35\bar{1})$  lies

TABLE I.—Orientations of Several Deformation Bands.

Specimen extended 20%.

Band	Angle $\theta$	Angle $\rho$	Difference
<i>a</i>	$19\frac{1}{2}^\circ$	$15^\circ$	$4\frac{1}{2}^\circ$
<i>b</i>	$20\frac{1}{2}^\circ$	$19^\circ$	$1\frac{1}{2}^\circ$
<i>c</i>	$16^\circ$	$10^\circ$	$6^\circ$
<i>d</i>	$21^\circ$	$17\frac{1}{2}^\circ$	$3\frac{1}{2}^\circ$
<i>e</i>	$12\frac{1}{2}$ – $15^\circ$	$10^\circ$	$2\frac{1}{2}$ – $5\frac{1}{2}^\circ$

on the zone connecting the slip direction  $(1\bar{1}0)$  with the slip plane  $(\bar{1}\bar{1}\bar{1})$  at an angle of  $17^\circ$  from the former. Thus in crystals deformed sufficiently (about 30% for crystals of the orientation used here) the bands will coincide with the  $(35\bar{1})$  plane; but the coincidence is obviously fortuitous.

It should be noted that a band was occasionally found to have an orientation markedly different from that of its neighbours, or to fork, with one prong of the fork deviating markedly in direction. However, these bands were relatively rare.

(d) *Effect of Increasing Extension.*

Several bands can be seen in Fig. 14 (Plate XIX), which is the side surface of a specimen extended by 25%. Fig. 15 (a) (Plate XIX) is a portion of the same surface at higher magnification. Fig. 13 (Plate XIX) illustrates a deformation band in another crystal, extended by 20%. The bands were less easily detected in weakly extended specimens, because the curvature of the slip lines in them was weak, and there was no discontinuity in the lines where they passed through a band. When, however, extension was continued, many lines stopped in the bands and new ones started on the other side. Beyond about 20% extension, short fragments of slip lines corresponding to planes other than  $(\bar{1}\bar{1}1)$  or  $(111)$  appeared in and near the band (Fig. 15 (a)). They were found by construction to correspond to the other two octahedral slip planes,  $(\bar{1}11)$  and  $(1\bar{1}1)$ . As the extension was increased, the spacing of the main bands (those clearly revealed under the microscope or by macro-etching) remained remarkably constant at a mean value of 1 mm. along the specimen axis. Some very faint bands could be detected between the main bands after heavy deformation, but the fact remains that most of the bands were formed at the start and developed with increasing deformation.

(e) *Effect of Varying  $\lambda_0$ .*

All the experiments described were carried out with specimens of the standard orientation shown in Fig. 1. To test whether the initial orientation had any effect on the development of the bands, a series of crystals was made with different values of  $\lambda_0$  (Fig. 1). These were extended by amounts calculated for each value of  $\lambda_0$  to cause a lattice

TABLE II.—*Effect of Varying the Initial Orientation.*

Specimen	Angle $\lambda_0$	Extension, %	Angle $\theta$ (Mean)	Angle $\rho$ (Mean)
a	49°	14½	11°	10°
b	46°	16½	14°	13°
c	44°	18	12°	9°
d	41½°	20	14°	7°
e	39°	22	15°	9°

rotation  $\phi$  (Fig. 2) of 8°. (In fact,  $\phi$  proved to be 10°–11°.) The bands developed for all values, and the only systematic difference was that in the crystals with the smaller  $\lambda_0$  values, the bands were narrower. The quantitative data, averaged over several bands in each crystal, are given in Table II.

*(f) Other Factors.*

Experiments were also carried out with crystals of the standard orientation but of different thicknesses, up to 8 mm. The bands developed in the ordinary way, with approximately the same spacing as before. To test whether the presence of grain boundaries affected the development of the bands, a symmetrical bicrystal was made and extended by 9%. A portion of this bicrystal, unetched and photographed by oblique illumination, is shown in Fig. 16 (Plate XX). Apart from a narrow region in one of the grains, adjacent to the boundary, in which slip occurred on an unpredicted system, slip took place in both grains on those octahedral planes along which the resolved shear stress was the greatest. The deformation bands were formed in just the same way as in single crystals. Bands were also found in many grains of deformed coarse-grained specimens.

Deformation at high temperatures did not impede the development of bands. In the specimen stretched at 400° C. the bands were no different from those in the specimens pulled at room temperature.

Deformation bands of the kind observed seem to be associated with the particular type of deformation employed. No experiments in compression were carried out, but it was noted that no bands ever appeared in specimens deformed by pure bending, even when this was very severe (radius of curvature only 0.5 cm.).

Although no visible deformation bands were found in bent crystals, the bent regions near the gripped ends of a stretched crystal (where flexural glide had occurred) contained deformation bands similar to those in the remainder of the crystal.

### *3. The Effects of Annealing.*

*(a) X-Ray Examination.*

Study of the deformation bands soon made it appear probable that they were connected with the polygonization which has been reported in extended and annealed crystals (cf. Section I). To investigate this point, X-rays were used in the first place. Fig. 26 (Plate XXII) shows the Laue pattern obtained from a crystal stretched 7%. The set of asterisms in the photograph correspond to lattice curvatures with approximately the same axis of curvature as the deformation bands. For this reason alone it appears very probable that the bands were the cause of the asterisms. Honeycombe<sup>7</sup> has recently argued from the patchy appearance of the asterisms that they are due to deformation bands; the patchiness is believed to be associated with

slightly differing orientations in adjacent blocks of crystal matrix. The crystal was annealed at progressively higher temperatures and Laue photographs taken after each anneal. The asterisms were all progressively broken up; this was clearly seen after annealing at  $530^{\circ}\text{C}$ ., and the pattern after 36 hours' annealing at temperatures up to  $590^{\circ}\text{C}$ . is shown in Fig. 27 (Plate XXII). Similar experiments were carried out with more heavily deformed crystals. Very fine splitting of asterisms was detected with a crystal pulled by 15% after annealing for 16 hr. at  $440^{\circ}\text{C}$ . In general, the more heavily deformed crystals revealed polygonization less clearly than those lightly deformed. (The temperatures quoted may be compared with those given by Guinier and Tennevin<sup>24</sup> as being the lowest which would produce polygonization detectable by their sensitive X-ray method: about  $450^{\circ}\text{C}$ . for crystals stretched 5%,  $400^{\circ}\text{C}$ . for those stretched 10%.)

(b) *Microscopic Examination.*

On the hypothesis that asterisms are due to deformation bands, the fact that these asterisms became split up on annealing implies that polygonization took place within the deformation bands. Since this was expected to be visible under the microscope, the annealed crystals were examined metallographically. First they were examined after micro-etching (method (c) above). Fig. 28 (Plate XXIII) is a typical photograph of the side surface of one such crystal (a grain due to recrystallization appears on the right). The etch-pits tend to align themselves parallel to an oblique direction which is in fact parallel to the deformation bands. The crystal having been weakly extended, the fragmentary rows of etch-pits are consequently normal to the slip planes, which is a characteristic of polygonization boundaries. There are also a large number of short rows approximately parallel to the slip planes, delimiting small rectangular blocks, and an indication that these blocks lie on distinct bands which presumably correspond to the original deformation bands. When more heavily deformed crystals were examined by this method many of the etch-pits were still found to lie on short rows, but they appeared to be distributed at random in position and direction.

For these heavily deformed crystals another method (method (d)) was evolved. Slip lines were produced on the repolished surface by giving the crystal a weak extension, and these lines showed up well the boundaries formed by polygonization (Figs. 29 and 30, Plate XXIII). The slip lines generally entered each band with a sharp kink and left it in the same way (Fig. 29). This should be contrasted with the S-shaped bend of the slip lines in the unannealed crystal, and shows that



the gradual change of orientation characteristic of the unannealed bands has given way to two sharp changes of orientation. In some crystals this was so marked that a different family of slip planes operated within the bands (Fig. 30). The sharp change of orientation after polygonization is presumably the reason for the observed greater contrast between bands and matrix on an annealed and macro-etched crystal.



FIG. 35.—Polygonized Deformation Band. (Striations indicate lattice orientations.)

From a detailed examination of the crystals, it was clear that polygonization had actually given rise to a structure similar to that sketched in Fig. 35. The existence of numerous small blocks differing somewhat in orientation also explains the large number of spots into which the Laue asterisms from an annealed crystal are decomposed, even though the beam intersected only two or three major bands.

It must be presumed that at an earlier stage of polygonization, the blocks are far smaller and there are several across the width of each band; but at this stage method (d) would hardly reveal the small direction changes between the several blocks, and the bands would appear unpolygonized; this was in fact often observed.

### (c) *Recrystallization.*

An interesting observation was made on specimens in which recrystallization had begun, which happened at very variable temperatures and in an unpredictable fashion. Frequently, it was found that the newly formed grains grew preferentially along the deformation bands, ending in long narrow tongues; Fig. 18 (Plate XX) illustrates this very clearly. It should be emphasized that this occurred preferentially at thoroughly polygonized deformation bands, as in Fig. 18. A result of this type of growth was that often a large proportion of the new grains finished up with boundaries parallel to the original bands. Occasionally a new grain became very large, and sent tongues into all the deformation bands it reached in the course of its growth.

It was fairly commonly observed that new grains formed by recrystallization, on etching with Lacombe and Beaujard's reagent, exhibited a smaller density of etch-pits than did the unrecrystallized portion. Fig. 28 (Plate XXIII) shows a case in point. If the plausible view is taken that etch-pits are nucleated at points where there is a concentration of dislocations and therefore a high strain energy, this

observation can be explained, since the new grains would be expected to be structurally more perfect. The theory is reinforced by the observed concentration of etch-pits on polygonization boundaries, which are packed with dislocations.

(d) *Effect of Annealing on Shape of Specimen, and Effect of Stress.*

To test whether annealing affected the shape of a stretched crystal, several crystals, extended by 20–35%, were carefully reground, re-polished, and annealed for some hours at temperatures of 425°–435° C. In all samples the polished top surface after annealing showed countless fine ridges arranged in clusters running parallel to the direction the deformation bands had followed before repolishing. Many of the clusters were easily visible to the naked eye. The markings became stronger as annealing was continued, but became settled after some hours, and continued annealing caused little change in height or position of the ridges (as was confirmed by repeated examination of the same fields). Evidently, the ridges were the traces in the polished surface of the dislocation arrays which had formed as the deformation bands became polygonized. When the S-shaped variation of orientation through a band becomes a stepped variation as a result of polygonization, there must be some shift in position of the atoms lying in the band relative to those outside the bands. This point is amplified on p. 155.

Figs. 31 and 32 (Plate XXIV) are photomicrographs of a characteristic specimen. It will be seen that, in addition to the crowded clusters or ridges, there are numerous faint, narrow clusters. These were always found and are caused by weakly curved deformation bands which were not discernible in the crystal as stretched.

A further interesting observation resulted when some specimens were annealed while under the action of a small tensile stress (35–100 g./mm.<sup>2</sup>) applied by dead loading. Here the ridged structure developed much more rapidly. In one experiment, two specimens were cut from adjacent parts of the same crystal which had been stretched 20%, repolished, and suspended side by side in a furnace. One specimen was subjected to a stress of 100 g./mm.<sup>2</sup>, while the other was unstressed. The surface ridging along the deformation bands appeared strongly on the stressed specimen, while only a few were dimly visible on the other. Figs. 31, 32, and 33 (Plate XXIV) were all made from stressed specimens. Fig. 31, taken on an oblique surface, shows particularly well-developed ridge markings inside a deformation band. The slip bands in this figure were developed before annealing by a small extension; at places where such lines passed through a band on the side surface, their

appearance after annealing was as shown in Fig. 29 (Plate XXIII). In a second experiment two more specimens were cut from the same crystal and treated in exactly the same manner, except that the stress applied to one of the specimens was compressive. Again, the ridging was more marked on the specimen stressed in tension, but the difference was not so striking as in the previous experiment.

The markings on the stressed crystals had at first been assumed to be due to viscous slip at the sub-boundaries formed by polygonization. This assumption was reinforced by the marked viscous slip observed at the boundaries of grains formed by recrystallization near the grips during the anneal. However, viscous slip at the sub-boundaries, if it occurred at all, must have been very restricted, as was shown by the following experiment. A specimen was annealed for a long period without being stressed, and several fields were photographed under the microscope. Their appearance at high power was similar to that shown in Fig. 32 (Plate XXIV). The specimen was re-annealed under stress, and the same fields were photographed again; they had changed only in minor details. If extensive viscous flow had taken place, a distinct blackening of the markings would have appeared, as was the case at the grain boundaries previously mentioned. Nevertheless, it is considered to be an open question whether markings such as those seen in Fig. 33 were wholly or partly due to viscous slip. The displacement of a scratch at the thick marking in the middle of the photograph suggests that there has been viscous slip here.

#### IV.—DISCUSSION.

##### 1. *Cross Slip.*

Cross slip may be regarded as a defect superimposed on the ideal mechanism of plastic slip. In the same way, we may regard the "ideal" mechanism, as it operates in hexagonal metals, to be an imperfect version of homogeneous translation. By this is meant uniform slip on each individual atomic plane of a family. In actual fact, of course, large amounts of slip take place on a few individual planes; several such planes, close together, constitute a "slip zone" and give rise to visible slip lines. An explanation for the development of these zones has to be sought in terms of structural disturbances of some kind which impede the free motion of dislocations on a glide plane and, by causing them to pile up, so harden the vicinity of that plane that no more slip can take place there. We may suppose that there also exist types of structural disturbance which do not lead to seizing

up of this kind but instead deflect dislocations to a different plane. This can be appreciated more clearly if the motion of a dislocation is considered in detail. According to modern ideas,<sup>25</sup> dislocations exist in metals before the application of stress. They generally have curved fronts, and when they spread under the action of stress they will remain curved (i.e. they remain a complex of edge and screw types of dislocation). As the dislocation front spreads it will meet various obstacles. Some will hold up a portion of the front altogether, but sometimes the stress field surrounding an obstacle will deflect the dislocation front on to a slip plane of different index—a cross slip plane. The slip direction for this plane must remain the same as before, since this is a fixed vector for the dislocation. The width, or prominence, of the cross slip will be limited by the repulsion due to the stress field of the dislocations in a neighbouring slip zone, and would be expected to be greatest at the beginning of deformation, when the slip zones are widely spaced; this was in fact observed. Raising the temperature widens the cross slips and causes neighbouring slip zones to become more often connected by cross slips. Perhaps the greater mobility of dislocations at high temperature allows them to move more freely on cross-slip planes despite the fact that the resolved shear stress on the cross-slip planes is smaller than on the main slip plane.

It must be asked what kind of lattice disturbances can cause dislocations to be deflected. Isolated impurity atoms of sufficiently large or small atomic radius are one possibility. A second possible source of disturbance is the fine lamellar mosaic structure which appears to exist in all metals. The extensive evidence for the existence of such a structure has been collected together by Crussard and Guinier.<sup>26</sup> The planes of the lamellæ are parallel to (100) in cubic metals and to (0001) in hexagonal metals. The main slip plane in cubic metals is therefore intersected by the lamellæ and, whatever the nature of the discontinuities between these, they are able to interfere with the propagation of dislocations. In hexagonal metals there can be no such interference since the plane of the lamellæ is parallel to the slip plane. This is the theory put forward by Crussard,<sup>12</sup> and by Crussard and Guinier<sup>26</sup> to account for the greatly differing plastic behaviour of cubic and hexagonal metals. A third possible source of disturbance is provided by lineage boundaries, which generally exist in cast metals and certainly existed in the crystals used in this investigation. Such boundaries should have the same effect as ordinary grain boundaries of small orientation difference in promoting cross slip to cause the intersection of slip zones to coincide everywhere with the boundary [Section III, 1 (g)]. However, it is difficult to reconcile with this view the fact that cross

slip was found to occur to some extent when a coarse-grained specimen made by recrystallization was deformed, although there was probably no lineage. Crussard's and Honeycombe's crystals were also made by recrystallization.

We may now recall that cross slip was found to be peculiarly associated with etch-pits (Section III, 1 (e)). It can readily be understood why there were slipless regions in the "shadows" of etch-pits. In these regions, as can be verified by drawing a section, there is ideally no resolved shear stress on the main slip plane. The stress on the cross-slip plane (111), which makes a large angle with the main slip plane, remains almost unaltered. The result of this is the observed local deviation of main slip to the cross-slip plane behind each pit, leaving a slipless region. This is a vivid example of how a lattice disturbance (in this case a surface disturbance) can affect the stress distribution in such a way as to cause cross slip.

Maddin, Mathewson, and Hibbard<sup>4</sup> consider that cross slip is the mechanism by which restraints are accommodated at the places where the specimen is gripped. This can hardly be the explanation here, because the particular orientation chosen was such that slip on the main slip system could entirely accommodate this restraint; in any case, the incidence of cross slip was no greater near the grips than elsewhere. Nevertheless, the very variable incidence of cross slip may have been connected with inexact alignment of the grips and consequent non-axial straining. This idea is reinforced by the greater amount of cross slip seen on a skew-bent specimen as compared with one bent truly.

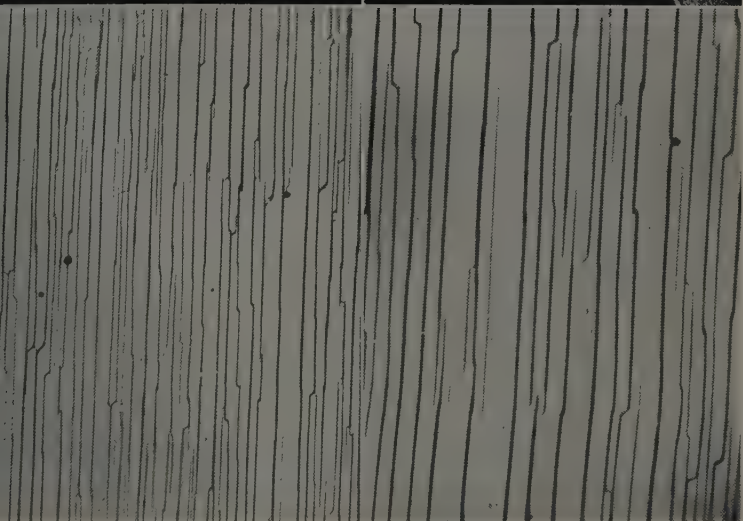
An attractive explanation is to hold the so-called "unpredicted slip" responsible for most of the cross slip. The unpredicted slip on (111), illustrated by Figs. 20 and 21 (Plate XXI), was itself always entirely devoid of any sign of cross slip. It is quite possible that the disturbances introduced into the lattice by this slip (disturbances which must be considerable in view of the fragmentary nature of the slip lines) are the places where dislocation of the main slip system are subsequently deflected on to the cross-slip planes. The unpredicted slip was only visible in patches, but it may have been too weak in most places to be visible at all. Apart from the question why unpredicted slip on (111) happens in the first place,\* this hypothesis would explain

\* Wu and Smoluchowski<sup>27</sup> have recently shown that the slip occurring first in *thin* aluminium crystals is that which provides a particularly short path through the crystal, irrespective of shear stress. It is not known which slip direction in the unpredicted slip plane (111) operated, but the direction [101] is one of the three possible directions, and this has a much shorter slip path than [110].





6



8

FIG. 5.—Crystal extended 7%. Top surface. Etched by method (b).  $\times 4$ .

FIG. 6.—Same Crystal. Side surface. Etched by method (b).  $\times 4$ .

FIG. 7.—Same Crystal. Top surface. Unetched.  $\times 180$ .

FIG. 8.—As Fig. 7.  $\times 320$ .



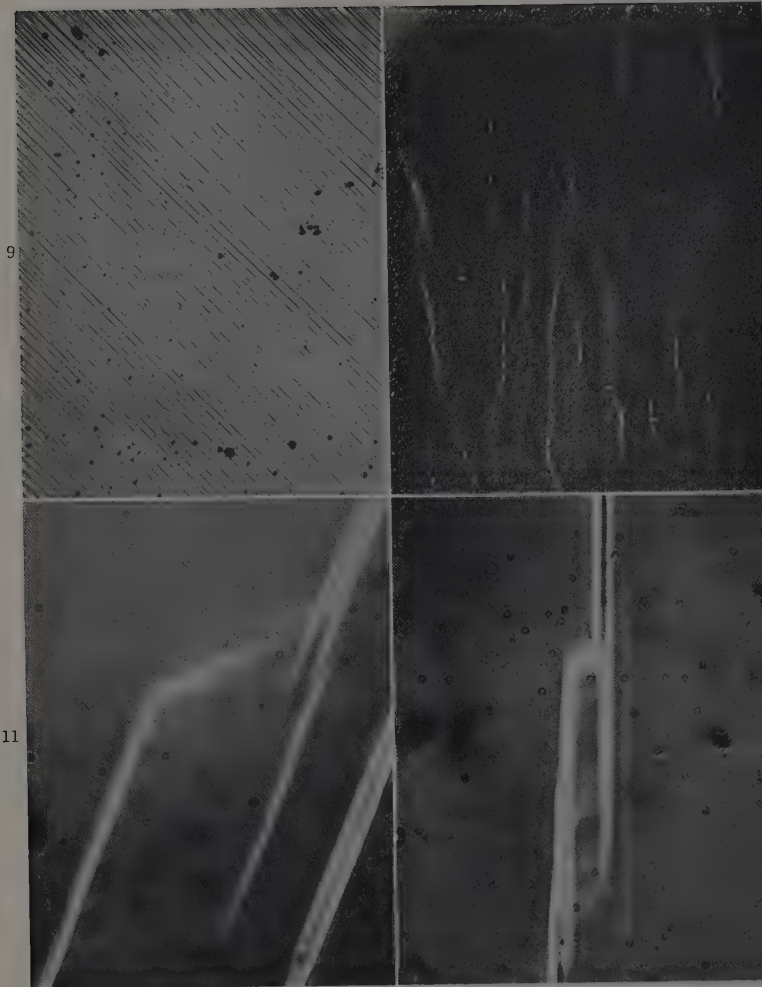
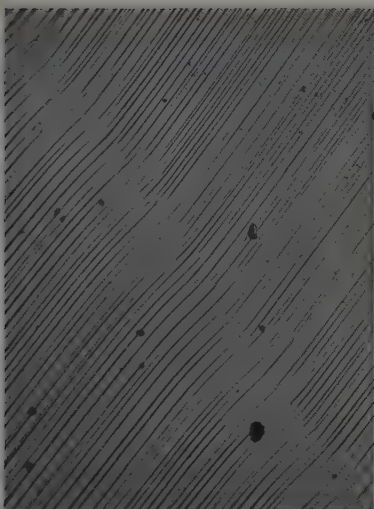

 FIG. 9.—Crystal extended 7%. Side surface. Unetched.  $\times 125$ .

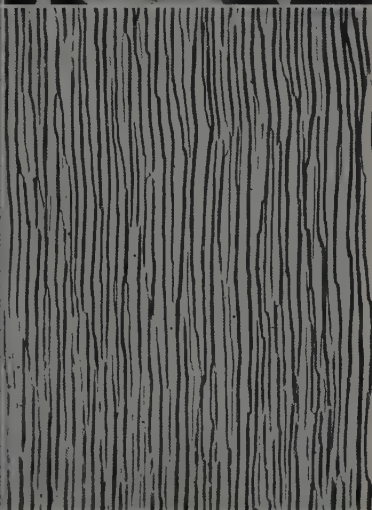
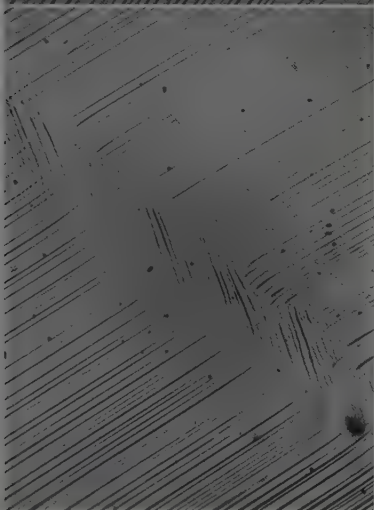
 FIG. 10.—Crystal extended 20%. Top surface. Etched by method (b).  $\times 11$ .

 FIG. 11.—Crystal extended 5%. Top surface, showing prominent cross slip. Unetched.  $\times 235$ .

 FIG. 12.—Crystal extended 5%. Top surface, showing intimate cross slip. Unetched.  $\times 235$ .



14



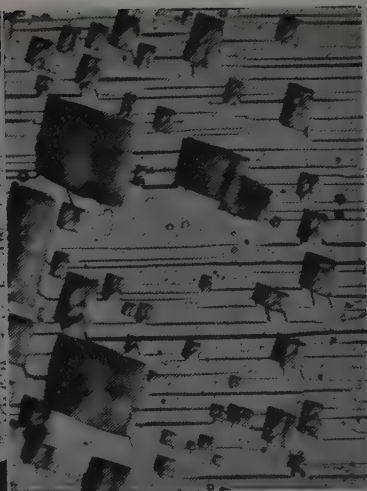
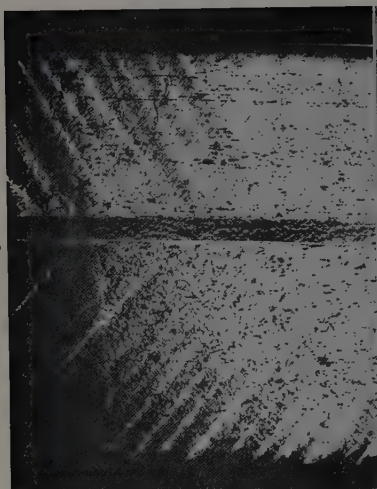
15b

FIG. 13.—Crystal extended 20%. Side surface, showing deformation band. Unetched.  $\times 250$ .

FIG. 14.—Crystal extended 25%. Side surface. Unetched.  $\times 32$ .

FIG. 15.—As Fig. 14. Side surface (a) and top surface (b). Unetched.  $\times 190$ .

16



18

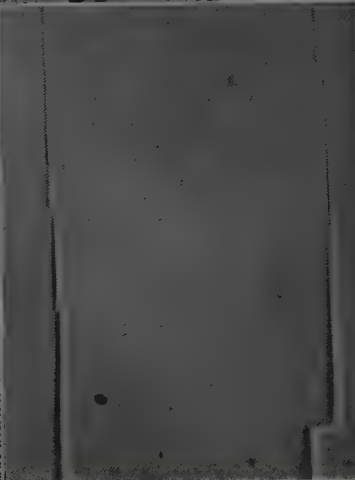
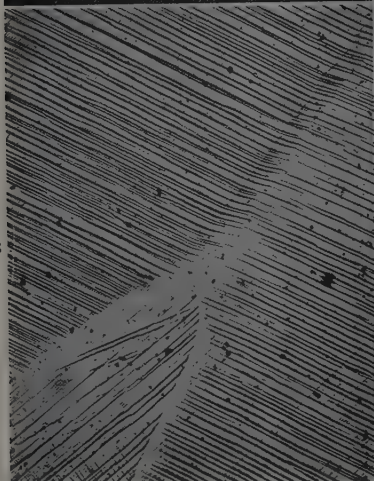


FIG. 16. Symmetrical Bicrystals, extended 9%. Unetched.  $\times 4$ .

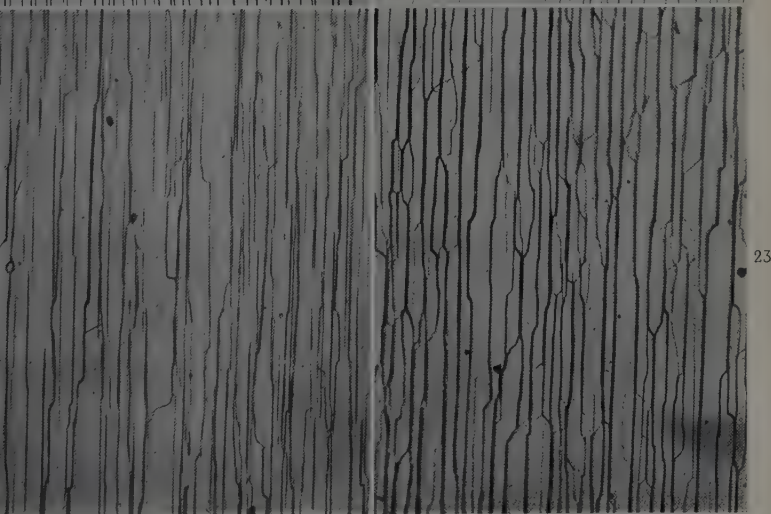
FIG. 17.—Etched Crystal extended 20%. Top surface. Unetched.  $\times 330$ .

FIG. 18.—Crystal extended 15%, annealed  $\frac{1}{2}$  hr. at  $450^{\circ}\text{C}$ . Side surface, showing new grain growing into polygonized deformation band. Prepared by method (d).  $\times 150$ .

FIG. 19.—Crystal extended 27%, annealed 2 hr. at  $450^{\circ}\text{C}$ . Top surface. Prepared by method (d).  $\times 1050$ .



21



23

FIG. 20. Crystal extended 6% after cooling in liquid oxygen. Top surface.  $\times 125$ .

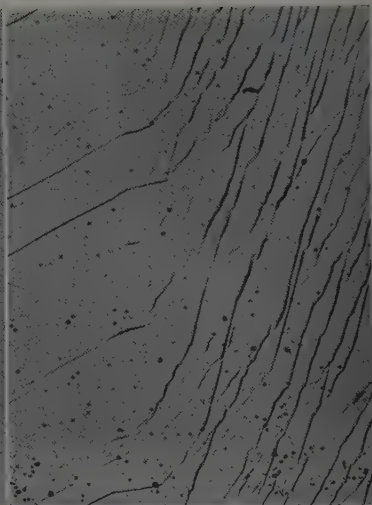
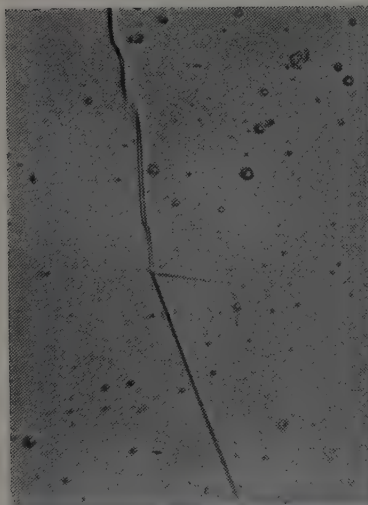
FIG. 21.—Crystal extended 7% at room temp. Top surface.  $\times 125$ .

FIG. 22.—Crystal extended 6% at 250° C. Top surface.  $\times 310$ .

FIG. 23.—Crystal extended 9% at 500° C. Top surface.  $\times 110$ .

All unetched.

24



26

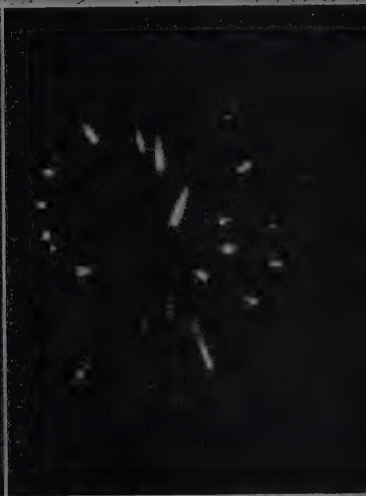


FIG. 24.—Slip Lines in Neighbouring Grains with small orientation difference. Unetched.  $\times 680$ .

FIG. 25.—Same Pair of Grains, another part of boundary. (Turned through  $90^\circ$  with respect to Fig. 24).  $\times 120$ .

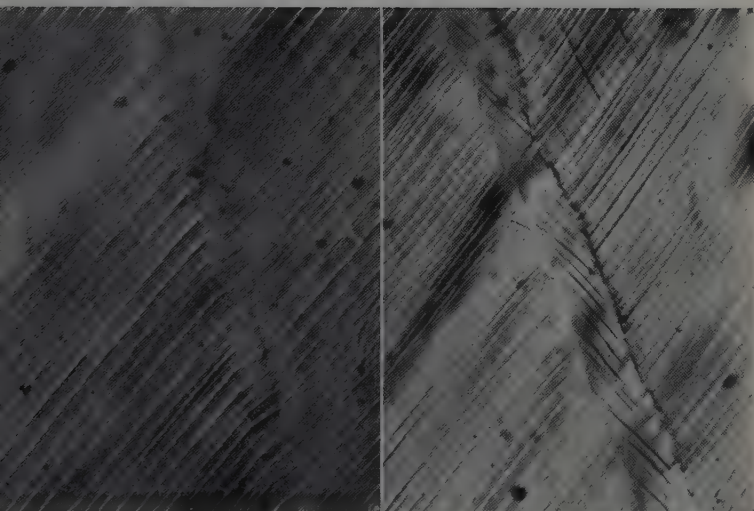
FIG. 26.—Crystal extended 7%, unannealed. Transmission Laue photograph.

FIG. 27.—Crystal extended 7%, annealed 36 hr. at temp. up to  $590^\circ\text{C}$ . Transmission Laue photograph.





28



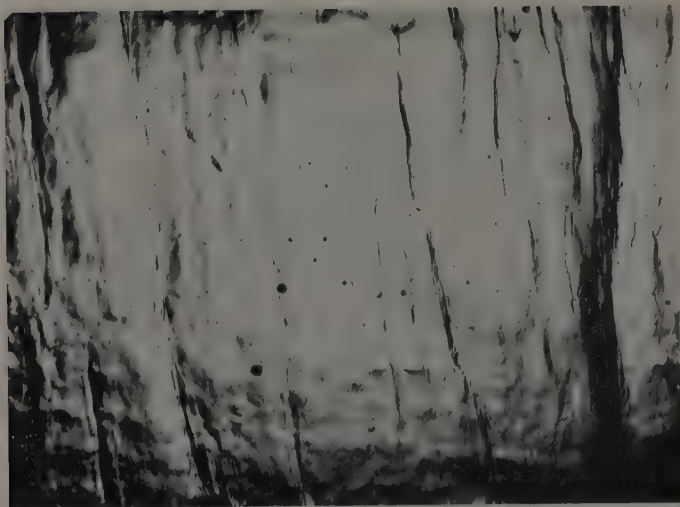
30

FIG. 28. Crystal extended 7%, annealed 36 hr. at temp. up to 590° C. Side surface. Etched by method (c).  $\times 70$ .

FIG. 29.—Crystal extended 31%, annealed 1 hr. at 450° C. Side surface, showing polygonized deformation band. Prepared by method (d).  $\times 260$ .

FIG. 30.—Same as Fig. 29. Another deformation band. Prepared by method (d).  $\times 200$ .





31



32



FIG. 31. — Crystal extended 35%, annealed 1 hr. at 450° C., repolished, suspended 16 hr. at 435° C. under tensile stress of 35 g./mm.<sup>2</sup>. Top surface, showing polygonized deformation bands.  $\times 32$ .

FIG. 32.—Same as Fig. 31.  $\times 200$ .

FIG. 33. — Crystal extended 26%, repolished, extended 1%, annealed 18 hr. at 425° C. unstressed, re annealed 21 hr. at 425° C. under tensile stress of 65 g./mm.<sup>2</sup>. Oblique surface  $\times 60$ .

why there is no cross slip associated with it, but only with subsequent slip on (111).

Even this explanation unfortunately has a difficulty. Greenland,<sup>28</sup> in experiments on the development of slip bands on mercury crystals strained in tension, found that the slip lines were very serrated if the crystal had been very carefully handled. If it was very lightly twisted before extension, the slip lines produced on subsequent extension were perfectly smooth (i.e. the exact opposite of what our line of argument would have predicted). This experiment emphasizes the influence of previous deformation on the nature of slip lines.

Mott and Frank<sup>29</sup> have a rather different picture of the origin of cross slip. They believe that dislocation loops on parallel but distinct planes spread independently till they are opposite each other; then the screw portions of the two loops are destroyed by the creation of a cross slip between them, converting them into a single loop with a step. On the basis of recent views<sup>30</sup> regarding the nature of slip lines, the two original loops are constantly being replaced from the same two sources of dislocations, and a repetition of the above process will soon generate a macroscopically visible cross slip.

From the preceding discussion the one thing that may safely be concluded is that no single cause is responsible for cross slip. The relative importance of the various possible causes can be determined only by further experiments in which the influence of variables such as orientation, surface condition, pre-strain, and temperature is studied in detail.

Cross slip in aluminium differs from that in brass, in which it is restricted to octahedral planes. The fact that there are numerous active cross-slip planes in aluminium is no doubt due to the near equality of the critical shear stresses on several lattice planes, as found by Burgers and Lebbink<sup>31</sup> during their experiments with aluminium crystals deformed in pure shear.

Finally, the distinction between cross slip and pencil glide (as it occurs in iron and silver chloride) should be explained. In pencil glide several slip planes operate together in such a way that the resultant slip line is either finely serrated or somewhat wavy; in other words, it could not be said of any one participating plane that it is the main plane, and of the others that they are cross-slip planes. The resultant apparent slip plane seems to be determined both by temperature and by the direction of stress relative to the crystal axes. During experiments (unpublished as yet) with  $\alpha$ -uranium, the author has found well-developed cross slips, the character of which varied with temperature in the same way as in aluminium.

## 2. Deformation Bands.

## (a) Discussion of Present Observations.

The development of deformation bands may be pictured by reference to Fig. 36. A crystal is sketched in the undeformed state and at two stages of extension. The hatching represents the main slip planes. For some reason to be determined, different sections of the crystal extend a given amount at slightly different stresses; for simplicity, only three such sections are drawn. Section *B* deforms first, and after it has stretched and rotated a little, section *A* and *C* follow; then the same sequence is repeated, and so on. In fact, at any stage the extensions of the different sections differ only by a few per cent, and the difference has been exaggerated for clarity in the sketch. (The slightly different directions of slip lines in neighbouring sections can be seen by

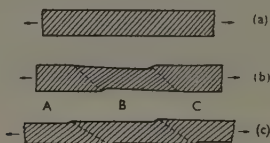


FIG. 36.—Stages in Development of Two Deformation Bands.

carefully studying Fig. 13, Plate XIX). At each yield, the lattice between neighbouring sections becomes bent. The bends are not straightened out when the neighbouring sections also yield, but are stored up cumulatively, developing the S-shaped lattice curvature in the bands. Since no study was made with very small extensions, it is not known whether this sub-division into sections begins at the very start of slip or only after one or two per cent of extension.

This picture is strongly supported by the data in Table I. The initial position of the boundary between neighbouring sections is always found to be normal to the slip direction. When section *A* has extended, the angle between the band and the slip lines in this section has become  $\sim (90 - \phi)$ , where  $\phi$  is the lattice rotation. When section *B* has also extended, the deformation band is inclined at an angle  $90 - \theta = 90 - \phi$  to the slip lines in *A* and *B*. Moreover, the range of lattice orientations within the bands (angle  $\rho$  in Fig. 34) is equal to  $\phi$ . Thus  $\theta$  and  $\rho$  should be equal if the proposed mechanism is correct and this was found to be approximately true (Table I).

It is understandable why the lattice curvature accumulates in the

band, once it has started to develop. The curvature in a band is very high, so that it must contain a large number of trapped dislocations. As slip proceeds in the adjacent sections, these dislocations are constantly added to, increasing the curvature. Once well started, the band acts as a highly efficient dislocation trap, as may be appreciated from the fact that many of the slip lines in a band are discontinuous. The efficiency of a band in this respect increases with its curvature; this is probably why a few bands develop strongly, while the majority remain very weak. The observed initial orientation of the bands at small extensions is readily understood in terms of the dislocation theory since an array of dislocations of one sign has minimum energy if oriented perpendicular to the slip direction. The dislocations present must be predominantly of one sign owing to the sharp curvature in the bands.

This does not explain why the crystal is divided into separate sections, or why the main resultant bands are so uniformly spaced. Thus the development of the bands is readily enough understood, but their genesis remains a mystery. An explanation at first appeared possible in terms of "geometrical softening", i.e. an increase of resolved shear stress as the crystal extends and the lattice rotates. Any portion of the crystal, once started, would then tend to go on slipping. The degree of softening depends on  $\lambda_0$  and on the rate of work-hardening. For  $\lambda_0 = 49^\circ$  there might be such softening for aluminium, but for  $\lambda_0 = 39^\circ$  calculation shows that, given the known rate of work-hardening of aluminium, there can be none. In fact, the development of bands was found to be independent of  $\lambda_0$  over the range  $39^\circ$ – $49^\circ$ , and this theory is therefore untenable.

A very recent study by Michaud<sup>32</sup> confirms the present results very well. The variation of "partial elongation" along a stretched single crystal was found to be considerable, and was correlated with a corresponding variation in lattice curvature, as revealed by X-rays.

#### (b) *Discussion of Recent Accounts of Kink Bands.*

Hess and Barrett<sup>33</sup> have published recently observations on the generation of *kink bands* in zinc which may be of assistance in interpreting the present observations. As originally discovered by Orowan,<sup>34</sup> if a cadmium or zinc crystal with its basal plane parallel to the specimen axis is subjected to axial compression, curious curvatures or *kinks* develop, which Orowan considered to be the result of a previously unknown type of plastic deformation, operating discontinuously. Hess and Barrett showed that in fact the kinks were a special kind of deforma-

tion bands (which do not normally develop to any great extent in hexagonal metals) and that they were formed by *gradual* rotation of the lattice. They were able to give a detailed interpretation of the observed orientation relationships and band positions on the following assumption:

"Kink-band formation is accounted for by assuming that pairs of dislocations are generated by buckling flexures . . . the positive dislocations aligning themselves in a plane and the negative in another plane (a configuration of minimum energy). These planes then move apart until stopped by defects or by opposing stresses in the adjoining segments of the rod. Successive planes of dislocations follow similar paths and build up continuously increasing angles of bend."

The main objection to this view is that the stresses needed to generate dislocation pairs are far greater than those applied in actual plastic deformation.<sup>35</sup> However, pre-existing dislocations of both signs could be substituted in this theory for newly generated ones, and the moving dislocation array may be imagined as sweeping up dislocations of the appropriate sign as it travels, and thereby increasing its own area.

It is proposed that the kind of deformation band discussed in the present paper be also known as "kink bands," to distinguish them from basically different types of deformation band which may occur, such as those in which a different slip system operates over a considerable width of band (e.g. the bands in iron described by Pfeil<sup>15</sup> were probably of this type). The justification for using the same name for the bands in aluminium as for those in zinc lies simply in their general similarity in appearance (two planes, close together, in which the lattice is bent opposite ways), a similarity which becomes more apparent when comparison is made with the polygonized bands in aluminium. Also, as will be seen later, the modes of formation may well be basically very similar.

Further striking observations on kinking in zinc have recently been reported by Jillson,<sup>36</sup> who lays emphasis on the individual bend plane, i.e. a plane perpendicular to the slip direction in which the lattice goes through a slight bend in one sense only. Two such bend planes, of opposite senses, constitute a kink band, and they apparently occur in zinc under a variety of conditions. They have also been found, well-marked, near the gripped end of a stretched crystal, and are associated with lenticular twin lamellæ, with impinging twin pairs, and with Brinell impressions. It is even stated that when a single crystal is bent, the curvature is not quite uniform and the crystal is in fact interspersed with bend planes (i.e. a form of incipient polygonization).

Jillson propounds a general hypothesis to the effect that "bendings

of the slip plane may be the more fundamental phenomenon, and the inhomogeneous shearing of slip may be merely a consequence". Briefly, his idea is that slip starts by a very gentle "rumpling" of the crystal (as shown in a greatly exaggerated fashion in Fig. 36 (b)) which will then "heal" again, producing in the process what is in effect a quantum of slip. This is pictured as repeatedly happening, the angles of bend involved being so small as to be invisible by ordinary methods. It is also stated that such bend planes as were observable were able to travel along the slip plane. The whole picture can be related to the results presented here. We may consider that at a very early stage of extension, the crystal has extended locally with the formation of bend planes, as in Fig. 37 (a). If the individual bend planes can indeed migrate, we may suppose the slipped sections to widen as a consequence of such

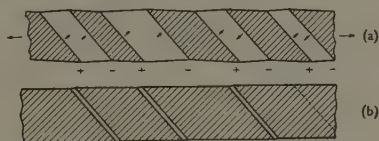


FIG. 37.—Creation of Kink Bands by Travelling Bend Planes. The hatched regions are those already passed by the bend planes. At the right, a pair of bend planes have annihilated each other. (The angles are greatly exaggerated.)

migration, as indicated by the arrows. (This differs from the ordinary concept of slip as being the result of the motion of dislocations across the slip plane, in that the dislocations, instead of travelling individually, move in a body; for a bend plane, being a place of small but sharp lattice rotation, must be the seat of dislocations in the same way as a polygonization boundary.) The process will continue till the bend planes finish up against one another (Fig. 37 (b)). They have then the choice of annihilating each other or of staying where they are. Jillson is of the opinion that in zinc they annihilate each other, and then the same cycle is repeated indefinitely. Conversely, if the bend planes remain where they are, a weak kink band has in effect been formed, and this is now locked in position. The newly-fledged kink band will consume any bend planes travelling into it at a later stage, so that large numbers of such planes remain close together, forming a gradual curvature. This appears to have happened with the aluminium crystals investigated here. The trapping of bend planes provides a mechanism for the observed progressive build-up of the kink bands. (This is merely an amplification of the mechanism illustrated in Fig. 36, not a new one.)

Slip by travel of bend planes will then continue between the kink



bands. Besides leading to the gradual intensification of the original kink' bands, it will involve the constant creation and destruction of very fine kink bands, as in Fig. 37 (b). This would account for the numerous fine kink bands revealed by annealing strongly extended crystals (as in Fig. 31).

The foregoing gives a detailed model of the generation and growth of kink bands but still leaves some points unexplained, one of which is the origin of the bend planes. A good reason why dislocations cannot be generated in pairs out of a perfect lattice has already been given.\* A bend plane can be conceived as starting from a small array of dislocations, either formed by chance or already present in the form of a particularly large mosaic boundary, and then growing in the way described. Again, it is not clear why at the beginning of straining bend planes form stable kink bands, while later on kink bands are formed and constantly destroyed again. Neither is the problem of the even spacing of the stable bands resolved.

If these basic questions can be resolved by future research, then it may be possible to evaluate fully the part played by bend planes and kink bands in slip.

One piece of evidence which has recently come to light has been left to last. It has been reported<sup>37</sup> that no kink bands detectable by ordinary micrographic means are formed when a tensile single-crystal specimen is oriented in such a way that duplex slip occurs from the beginning. This occurs if the pole of the specimen axis in Fig. 2 lies anywhere on  $AD$ . The resolved shear stresses on the  $(\bar{1}\bar{1}\bar{1})$  plane in the  $[1\bar{1}0]$  direction and on the  $(\bar{1}11)$  plane in the  $[0\bar{1}1]$  direction are then equal. (Chen<sup>38</sup> found that if the axis pole is near a pole of the form  $(111)$  or  $(110)$  there are no kink bands.) The pole of the axis travels towards  $(\bar{1}\bar{1}\bar{1})$  as extension proceeds. It should be noted that the axes of curvature for bend places, or kink bands if there were any, would differ for the two slip systems; they would be  $[112]$  and  $[211]$ , respectively. We can now understand why kink bands do not, in fact, form under these conditions. Any bend planes of the first slip system which tries to travel along its slip direction will soon meet a bend plane of the other slip system, and the lattice would be subjected to such contortions as a result of the different axes of curvature that it is difficult to believe that the bands could pass each other; if they do not, kink bands cannot develop. Alternatively, bend planes can only travel a very short way, and are easily annihilated by other bend planes

\* It is conceivable that the apex of a wedge-shaped region formed by two dislocation arrays of opposite signs (such as is often found in crystals kinked by compression) is a site of effective stress concentration sufficient to permit the creation of pairs of dislocations.

on the same slip system before their curvature has become strong enough for them to establish kink bands.

(c) *Influence of Kink Bands on Mechanical Properties.*

It is evident that the lattice distortion produced by kink bands must play an important part in determining the resistance to deformation. If it were possible to extend an aluminium crystal without generating kink bands, the corresponding curve of resolved shear stress and shear strain should be quite different from the normal parabolic shape. Kink bands can be largely avoided by choosing a crystal which will deform by duplex slip from the start (see preceding paragraph). With such crystals, Laloeuf and Crussard<sup>37</sup> obtained load/extension curves of abnormal shape, consisting of a short steep portion followed by a region of slow strain-hardening.

The most reliable way of assessing the effect of kink bands would be to deform a crystal in "pure shear" (i.e. shear applied along a (111) plane and  $[1\bar{1}0]$  direction); if carried out with proper precautions, this mode of deformation should lead to perfectly homogeneous slip without any lattice curvatures. The curve of shear stress and shear strain can be compared with the curve of resolved shear stress and shear strain for an extended crystal. Following earlier attempts<sup>31</sup> which failed to give perfectly homogeneous slip, Röhm and Kochendörfer<sup>39</sup> have succeeded in deforming long crystals in pure shear in a truly homogeneous fashion (as evidenced by the absence of asterism). The stress/strain curve was always a straight line which at all strains lay well below the corresponding curve for an extended crystal. It was argued that the difference between the two types of curve was due to the lattice distortion in the extended crystals. A way was also found to measure the "latent" hardening on each of those octahedral planes of an *extended* crystal which had not slipped. The results could be interpreted on the assumption that the lattice distortion in an extended crystal is arranged in parallel sheets (as is here shown to be the case). From the difference between the two types of stress/strain curves it can be concluded that the extra hardening due to the kink bands is the greatest for small strains; at a later stage the rate of strain-hardening becomes approximately equal for both modes of deformation.

It will be recalled that stretched zinc and cadmium crystals deform almost homogeneously<sup>7</sup>; it is striking that their stress/strain curves closely resemble those of aluminium deformed in pure shear. This emphasizes that the rectilinear curve is the basic relation of strain-hardening, which theoretical treatment should seek to explain. The latest such treatment<sup>40</sup> satisfies this requirement.

### 3. Surface Effects in the Polygonization of Kink Bands and the Effects of Stress.

The experiments described in Section III, 3 (d) are all readily explained in terms of the dislocation theory of polygonization. In Fig. 38 an unpolygonized kink band intersecting a polished surface is indicated by dotted lines. If we consider the ideal case of polygonization going to completion (i.e. two dislocation arrays  $AB$  and  $CD$  being formed, with no arrays between), we get the lattice arrangement indicated by the

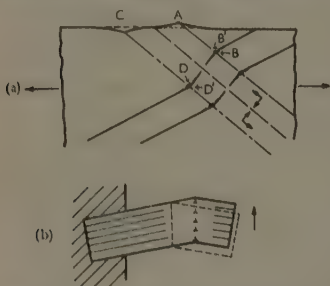


FIG. 38.—(a) Generation of Surface Ridges and Grooves of Polygonization in Kink Bands. (b) Migration of a Dislocation Array under the Action of Shear Stress. The dotted lines show the initial position, the solid lines the final position.

solid lines at  $B'D'$ . An atom which was at  $B$  before polygonization now lies at  $B'$ , and one originally at  $D$  moves to  $D'$ . This happens all along the deformation band, so that there must of necessity be a corresponding motion at the surface, producing a ridged hump at  $A$  and a sharp-bottomed groove at  $C$ .

In practice there are usually several dislocation arrays across each band, but sometimes the simple situation is found, particularly in "weak" kink bands. The band marked with an arrow in Fig. 31 (Plate XXIV) is a case in point.

The effect of stress on the rate of polygonization is readily understood when it is remembered that dislocations move easily under the action of stress. When polygonization takes place in the absence of stress, dislocations move towards the arrays solely under the action of the small attractive forces exerted on them by the arrays.<sup>35</sup> This process is bound to be slow, since they have to move through the stress field set up by other dislocations. An applied stress, so long as it has a shear component in the slip direction, will facilitate the motion of the dislocations against the stress field and so accelerate polygonization.

The stress should also help in another way. Consider a crystal under tensile stress, with an imagined slit along a partly polygonized kink band; the resolved stresses acting on each half of the band will be as indicated by the arrows in Fig. 38 (a). Now consider an imaginary crystal piece held and stressed as in Fig. 38 (b). The piece contains a dislocation array bisecting the slip planes in the two halves, i.e. a polygonization boundary of the usual sort. Under the action of the stress

the array will move to the right, thereby causing the right half of the piece to move in the direction of the applied stress. Each half of the split kink band in Fig. 38 (a) can be considered as a piece of this sort, "clamped" within the body of the crystal. The arrays will move towards the centre of the band under the action of a tensile stress, as easily verified by comparison with Fig. 38 (b). If the stress is compressive, the arrays will move the other way. In either case the moving arrays will sweep up dislocations as they move, and thereby accelerate polygonization. Since in this process the density of the array is increased, the corresponding hump on the free surface of the crystal will become progressively more marked.

The action of a small applied stress in accelerating the motion of dislocations at high temperatures has already been invoked by Greenough and Smith <sup>41</sup> to explain the ready polygonization of specimens subjected to creep, as made evident by the X-ray pattern. They showed up the marked effect of stress by comparing the patterns from two polycrystalline aluminium specimens which had both been stretched rapidly by a few per cent at room temperature, one then being annealed under a small stress while the other was annealed in the absence of stress. The X-ray pattern of the first specimen was much the more spotty. This experiment, and the author's present experiments, differ from ordinary creep experiments in that cold work preceded the creep. Nevertheless, it seems fair to say that the accumulated evidence confirms Greenough and Smith's ideas satisfactorily, and in particular leaves little doubt that the cellular structures described by Wood and his collaborators <sup>42, 43, 44</sup> were formed by a process closely similar to polygonization. The observations on ridge markings showed that viscous slip at polygonization boundaries was very limited and suggest that Wood was in error in attributing the entire deformation of his creep specimens to viscous slip at cell boundaries.

#### ACKNOWLEDGEMENTS.

The author would like to express his indebtedness to Mr. H. C. Sansom for his help in preparing specimens; to Mr. H. R. Haines and to Mr. S. D. Ford for their invaluable help with the photography; to Dr. H. M. Finnieston for his consistent encouragement; and to the Director, Atomic Energy Research Establishment, for permission to publish this paper.

#### REFERENCES.

1. G. I. Taylor and C. F. Elam, *Proc. Roy. Soc.*, 1926, [A], **112**, 337.  
H. Gough, *Proc. Roy. Soc.*, 1928, [A], **118**, 498.
2. E. N. da C. Andrade and L. C. Tsien, *Proc. Roy. Soc.*, 1937, [A], **163**, 1.
3. J. F. Nye, *Proc. Roy. Soc.*, 1949, [A], **198**, 190; **200**, 48.

# 158 Cahn : Slip and Polygonization in Aluminium

4. R. Maddin, C. H. Mathewson, and W. R. Hibbard, Jr., *Trans. Amer. Inst. Min. Met. Eng.*, 1948, **175**, 86; 1950, **185**, 527.
5. G. J. Ogilvie and W. Boas, *Trans. Amer. Inst. Min. Met. Eng.*, 1948, **175**, 102.
6. C. Crussard and F. Aubertin, *Métaux et Corrosion*, 1946, **21**, 45, 66.
7. R. W. K. Honeycombe, *Proc. Phys. Soc.*, 1950, [A], **63**, 672.
8. C. Crussard, *Rev. Mét.*, 1944, **41**, 111, 133.
9. E. N. da C. Andrade and Y. S. Chow, *Proc. Roy. Soc.*, 1940, [A], **175**, 290.
10. R. W. Cahn, *J. Inst. Metals*, 1949-50, **76**, 121.
11. A. Guinier and J. Tennevin, *Compt. rend.*, 1948, **226**, 1530.
12. C. Crussard, *Bull. Soc. Franç. Minéral.*, 1945, **68**, 174.
13. J. A. Collins and C. H. Mathewson, *Trans. Amer. Inst. Min. Met. Eng.*, 1940, **137**, 150.
14. C. S. Barrett and L. H. Levenson, *Trans. Amer. Inst. Min. Met. Eng.*, 1940, **137**, 112.
15. L. B. Pfeil, *Carnegie Schol. Mem., Iron Steel Inst.*, 1926, **15**, 319; 1927, **16**, 153.
16. C. S. Barrett, "Structure of Metals," p. 305. New York and London: 1943 (McGraw-Hill).
17. P. A. Beck and Hsun Hu, *Trans. Amer. Inst. Min. Met. Eng.*, 1949, **185**, 627.
18. B. Chalmers, *Proc. Roy. Soc.*, 1940, [A], **175**, 100.
19. C. S. Barrett and L. H. Levenson, *Trans. Amer. Inst. Min. Met. Eng.*, 1940, **137**, 76.
20. A. de Sy and H. Haemers, *Metal Progress*, 1948, **53**, 368.
21. P. Lacombe and L. Beaujard, *J. Inst. Metals*, 1948, **74**, 1.
22. R. D. Heidenreich and W. Shockley, *Phys. Soc. Rep. Conf. on Strength of Solids*, 1948, 57.
23. A. F. Brown, private communication.
24. A. Guinier and J. Tennevin, "Progress in Metal Physics," Vol. II. London: 1950 (Butterworth).
25. F. C. Frank, *Discussions Faraday Soc.*, 1949, (5), 48.
26. C. Crussard and A. Guinier, *Rev. Mét.*, 1949, **46**, 61.
27. T. L. Wu and R. Smoluchowski, *Phys. Rev.*, 1950, [ii], **78**, 468.
28. K. M. Greenland, *Proc. Roy. Soc.*, 1937, [A], **163**, 28.
29. N. F. Mott and F. C. Frank, private communication.
30. F. C. Frank and W. T. Read, Jr., *Phys. Rev.*, 1950, [ii], **79**, 722.
31. W. G. Burgers and F. J. Lebbink, *Rec. Trav. Chim.*, 1945, **64**, 321.
32. R. Michaud, *Pub. Sci. Tech. Ministère de l'Air*, 1950, (240).
33. J. B. Hess and C. S. Barrett, *Trans. Amer. Inst. Min. Met. Eng.*, 1949, **185**, 599.
34. E. Orowan, *Nature*, 1942, **149**, 643.
35. A. H. Cottrell, "Progress in Metal Physics," Vol. I., p. 88. London: 1949 (Butterworth).
36. D. C. Jillson, *Trans. Amer. Inst. Min. Met. Eng.*, 1950, **188**, 1009.
37. A. Laloeuf and C. Crussard, *Rev. Mét.*, 1951, **48**. (In the course of publication).
38. N. K. Chen, Dissertation, Yale University, 1950; quoted in *Trans. Amer. Inst. Min. Met. Eng.*, 1950, **188**, 1038, 1040.
39. F. Röhm and A. Kochendörfer, *Z. Metallkunde*, 1950, **41**, 265.
40. D. Kuhlmann, *Proc. Phys. Soc.*, 1951, [A], **64**, 140.
41. G. B. Greenough and E. M. Smith, *J. Inst. Metals*, 1950, **77**, 435.
42. G. R. Wilms and W. A. Wood, *J. Inst. Metals*, 1948-49, **75**, 693.
43. W. A. Wood and W. A. Rachinger, *J. Inst. Metals*, 1949-50, **76**, 237.
44. W. A. Wood and R. F. Scrutton, *J. Inst. Metals*, 1950, **77**, 423.

# THREE BASIC STAGES IN THE MECHAN-1303 ISM OF DEFORMATION OF METALS AT DIFFERENT TEMPERATURES AND STRAIN-RATES.\*

By W. A. WOOD,<sup>†</sup> D.Sc., MEMBER, G. R. WILMS,<sup>†</sup> M.Eng.Sc., and  
W. A. RACHINGER,<sup>‡</sup> M.Sc.

## SYNOPSIS.

In previous work it has been shown that as the temperature of deformation of aluminium is increased, or as the rate of strain at any one temperature is decreased, the familiar mechanism of slip is replaced progressively by a second mechanism which has been termed the "cell mechanism." In this, the deformation involves a dissociation of the grains into separate elements that increase in size with increase in temperature and decrease in strain-rate. It is shown in the present paper that by further reduction in the strain-rate at an elevated temperature, the cell mechanism is in turn superseded; this occurs when the cells become comparable in size with the grain itself. This third stage is termed "boundary micro-flow". The nature of the observations suggests that no other major change is likely to be observed as the rate of strain is further reduced. A short review is given of the position now reached, and the implications are discussed in relation to the mechanism of deformation, strain-hardening, and creep.

## I.—INTRODUCTION.

In recent work <sup>1, 2, 3</sup> the authors have compared the changes in micro-structure that occur when specimens of aluminium are extended at various temperatures and rates of strain, with the object of determining how the mechanism of deformation varies, especially when the conditions are such as to result in creep.

In the range of temperatures and strain-rates investigated, there are two mechanisms: (i) the familiar process of slip, and (ii) a process that supersedes the slip mechanism as the temperature of deformation is increased or the rate of strains decreased; this has been termed the cell mechanism.

The previous observations suggested that if the rates of strain at the higher temperatures were reduced below the values already studied, the cell mechanism would in turn be superseded, and further experiments have now confirmed this. The present paper describes the

\* Manuscript received 24 July 1950.

<sup>†</sup> Baillieu Laboratory, University of Melbourne, Australia.

<sup>‡</sup> Aeronautical Research Laboratories, Department of Supply and Development, Melbourne, Australia.



relevant results and shows that they do in fact establish the existence of a third mechanism.

At the same time, the nature of these later observations indicates that no further major change is likely to be revealed if the rates of deformation are still further reduced. The opportunity has therefore been taken of defining the three stages as they now appear and of reviewing the present state of knowledge.

## II.—FIRST STAGE—SLIP MECHANISM.

The fundamental feature of the first two stages is that the action of deformation causes a dissociation of the grains into elements that differ sufficiently in orientation to assume separate identities. The size of the elements in the sub-structure tends towards equilibrium with progressive deformation, the equilibrium being attained more rapidly at elevated temperatures. In the equilibrium condition, the elements become larger and more perfect as the temperature of deformation increases, or as the rate of strain at any one temperature decreases.

The slip mechanism is associated with deformation at the lower temperatures and higher rates of strain. It corresponds, therefore, to the most drastic dissociation of the grain. The following conclusions regarding the associated sub-structure have been reached after comparison of a large number of combined X-ray-diffraction and metallographic observations of the microstructure :

(i) The main elements of the sub-structure correspond with the blocks between the operative slip planes. The evidence for this is based on a systematic correspondence between the average spacing of the slip lines and the size of the elements shown by X-ray examination, as both are varied by altering the temperature and rate of deformation.

(ii) The slip process always produces a specific derangement that is attributed to the production of a disordered condition at the sub-boundaries between the elements of the sub-structure.<sup>3</sup> This effect is revealed by X-ray diffraction. Before deformation of an annealed specimen, the grains give rise to sharp X-ray reflection spots. After deformation, the reflections, when obtained by the appropriate technique, are seen as clusters of separate secondary reflection spots, which correspond to the disoriented elements formed in the initially homogeneous grains. The imperfection is indicated by a diffused spreading of these secondary reflections, mainly along the circumference of the diffraction ring. This characteristic was always found to accompany deformation by slip. That the imperfection is concentrated along the sub-boundaries, or slip planes, was suggested by the further observation

that the effect was systematically less when the slip lines were fewer and more widely spaced.

The disordered condition might be due to a distorted but continuous lattice connecting adjacent elements; or, so far as the X-ray effects are concerned, it could be caused equally well by material in a finer state of sub-division at the boundaries of the elements, a form of debris that in other work has been termed "crystallites". The latter interpretation is preferred for many reasons, but the distinction is immaterial in the present discussion.

(iii) The metallographic features of slip are well known, but it is important to recall that the effect in practice is the final result of the sharp displacement of a relatively large block of atoms; and that this displacement is through a large number of atomic spacings.

There was no evidence that increased magnification or resolving power of the microscope would reveal progressively smaller blocks or smaller displacements, i.e. "sub-microscopic slip", systematically filling in the spaces between the normal slip lines. In view of later observations, therefore, it will be convenient to class such relatively large displacements of atoms *en bloc* as "block movements". Evidently the change in shape of a grain by slip in a specimen undergoing deformation is mainly caused by internal block movements of this type.

### III.—SECOND STAGE—CELL MECHANISM.

As the temperature of deformation is increased, or the rate of strain at a given temperature is decreased, the slip lines become more widely spaced and irregular until finally they vanish. At the same time the elements of the associated sub-structures show an equivalent increase in size.<sup>2</sup> There is therefore a coarse sub-structure; and there is no trace of slip.

This stage defines the cell mechanism. The main features for a specimen deforming at a definite temperature and a definite rate are as follows:

(i) The internal structure of the elements is as perfect as that of the parent annealed grains, and this perfection is retained throughout deformation of the specimen. This follows from the observation that the separate X-ray secondary reflection spots are as sharp as the initial reflections from which they form and remain so.

(ii) There is a complete absence of the disordered material that characterizes the slip process. The sub-boundaries appear therefore to be comparable with ordinary annealed grain boundaries, which also show no disordering on a scale observable by X-ray diffraction. They would differ only in that the difference in orientation between neigh-

bouring elements is small, whereas that between adjacent grains may be many degrees.

The absence of the disordered material is indicated by the complete disappearance of the diffusion that is associated with the X-ray secondary reflections when slip is present.<sup>3</sup> It is significant that when there is no production of slip lines there is no detectable crystallite debris or related distortion.

(iii) The cells undergo relative displacement within the parent grains as the specimen is deformed. This is shown by the observation that as an initially polished specimen extends, the cell boundaries become observable as difference in level of the surface. In addition relative displacements occur in the secondary X-ray reflections from the sub-structure. Moreover, if markings are placed on the surface, discontinuous displacements occur at the sub-boundaries during the deformation. Thus, to some extent, the change in shape of a grain by the cell mechanism may take place by internal block movements (of the cells relatively to each other).

#### IV.—THIRD STAGE—BOUNDARY MICRO-FLOW.

In the cell mechanism it is found that, in agreement with the general rule, the size of the sub-structure increases systematically with the temperature of deformation or with a decrease in rate of strain. It follows that a stage will be reached when the size of the element approaches that of the grain itself. At this stage, the grain evidently cannot change shape by sub-division and internal block movements. This defines the third stage. There is no trace of a sub-structure and no trace of slip. The evidence is based on the experiments which will now be described.

##### 1. *Experimental Conditions.*

The test material, as in the previous work, was aluminium of 99.98% purity, from which annealed, flat tensile specimens were prepared with a standardized grain-size of 0.1–0.2 mm.

The previous work had shown that with a strain-rate of 0.1% per hr., the slip process predominates at temperatures up to about 200° C. and the cell mechanism from approximately 250° to 350° C. It was found in the present experiments that the critical increase in size of the cells could be obtained at working temperatures of 250°–350° C. if the strain-rate was reduced to 0.01% per hr. or less.

These lower strain-rates were obtained by two methods. In the first, a machine was employed that forcibly stretched a specimen at a constant rate of strain. In the second, advantage was taken of the

fact that between 250° and 350° C. aluminium deforms continuously under a constant load. In this case the different rates of strain were the secondary creep rates produced by various loads as in ordinary creep testing. It was interesting to note that for a given temperature and strain-rate, the changes in microstructure were essentially the same whichever method was used.

The microstructure was examined, as in the previous work, by both metallographic and X-ray methods. For the former, specimens were electropolished before deformation and then examined by the microscope after cooling at various stages of the extension, the same fields being kept under observation. For the X-ray tests, the back-reflection method was used, since it was found to be the most sensitive to the effects being studied. The conditions were such that with a stationary specimen the initial sharp reflection spots from the individual grain were well separated on the diffraction rings, so that changes in the character of the individual reflections could be followed as far as possible.

When any one grain breaks up into a sub-structure, the only elements that reflect are those in which the reflecting planes continue to make the same Bragg angle with the incident beam. In many of the X-ray tests, therefore, a modified technique was employed in order to record other elements. The specimen was oscillated to give the variously inclined elements an opportunity to reflect; at the same time, the back-reflection film holder was oscillated in synchronism to ensure that the additional reflections should not be superimposed on each other. If dissociation of the grain occurred, a cloud of secondary reflections appeared on the photographic film; as a result of this scatter it was possible to examine individual reflections under higher dispersion than with the standard back-reflection technique.

## *2. Transition from Second to Third Stage.*

The condition of the microstructure that defines the third stage is best shown by a set of photographs illustrating the transition from the second or cell mechanism.

Fig. 1 (Plate XXV) is a stationary X-ray back-reflection photograph from a specimen before extension, and illustrates the standard initial condition. The sharpness and discrete nature of the reflection spots indicate that the corresponding grains are relatively perfect and of homogeneous orientation.

Fig. 2 (Plate XXV) illustrates the change that occurs when the cell structure is formed, in this case after 7% creep elongation of a specimen in 290 hr. under a load of 500 lb./in.<sup>2</sup> at 250° C. The relevant

feature is the dispersion of the initial single reflection spots into groups of secondary reflection spots and the scatter of these spots along the diffraction ring, as discussed in detail in previous papers. Each grain in this specimen has evidently formed a sub-structure of differently oriented elements that are still small enough to produce numerous secondary reflections.

Fig. 3 (Plate XXV) shows the first signs of transition. This is a specimen that extended 7% at 350° C. in 14 hr. under a load of 350 lb./in.<sup>2</sup>. There are fewer secondary reflections, and these tend to concentrate around the parent reflection spots. The sub-structure is therefore larger, but the range of orientations less than in the previous case. Both Fig. 2 and Fig. 3 represent essentially the equilibrium condition.

With progressive reduction of the strain rate at 350° C. the secondary reflection spots were found to become fewer and fewer, till finally none were formed. The original reflections from the annealed grains remained apparently unchanged. This typified the third stage, when there was no noticeable dissociation of the grains. Fig. 4 (Plate XXV) illustrates this final stage and was obtained from a specimen after an extension of 8% at 350° C. in 764 hr. under the load of 150 lb./in.<sup>2</sup>. It is at once evident that this X-ray photograph is indistinguishable in nature from the initial photograph (Fig. 1). Examination of this specimen was made also after 1640 hr., when it had extended by 57%, but throughout all this extension no dispersion of the initial reflections into secondary reflections could be observed.

Other experiments were carried out in which X-ray reflections were examined in more detail at smaller successive intervals of extension. The synchronous back-reflection technique was found especially useful for this. Two typical photographs are reproduced in Fig. 5 (a) and (b) (Plate XXVI), which refer to a specimen before and after extension by 3% at 350° C. in the constant strain-rate machine operating at 0.01% per hr. Fig. 5 (a) shows that with this technique the  $\alpha_1\alpha_2$  doublets are recorded in a very distinct manner from a large number of grains, while Fig. 5 (b) shows quite clearly that the doublets are just as well defined after extension. There is no break-up of the initial reflections which indicates that the grains must preserve a surprising degree of internal homogeneity. This lack of change is typical of the third stage.

The absence of internal movements in the grain was confirmed also by metallographic examination, which revealed no sign of slip lines or the systematic markings associated with a cell structure. This is illustrated by the photomicrographs in Fig. 6 (a) and (b) (Plate XXVI), which correspond to the X-ray photographs of Fig. 5 (a) and (b).

## X-RAY BACK-REFLECTION PHOTOGRAPHS OF ALUMINIUM.

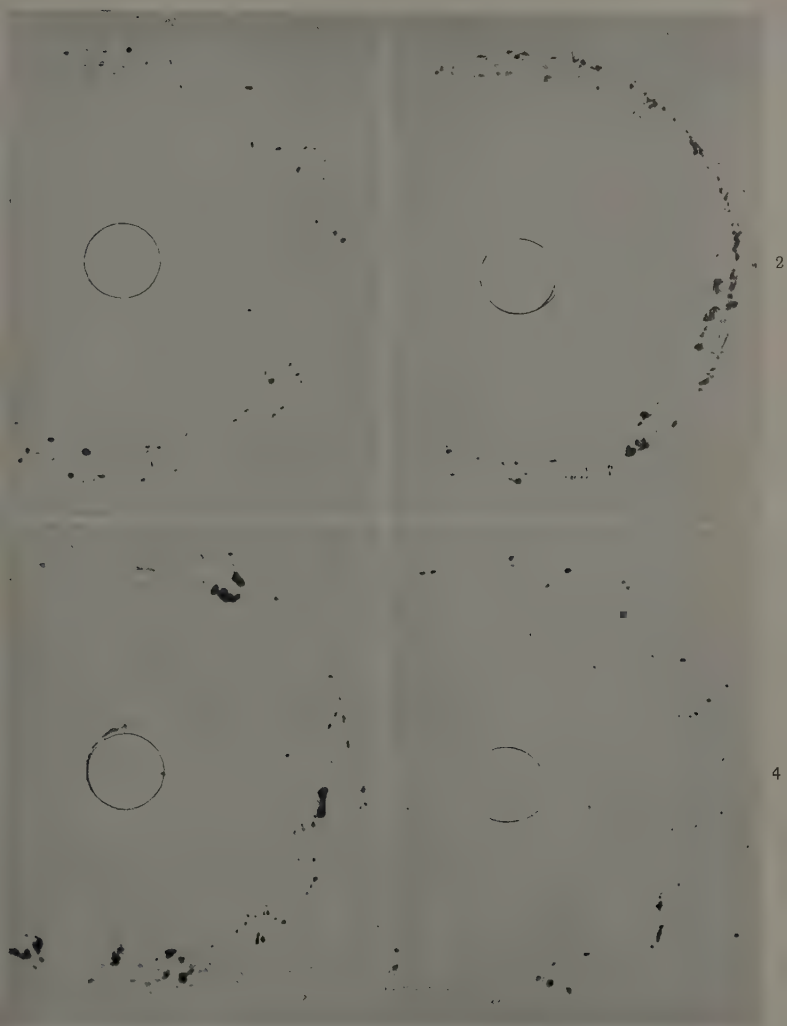


FIG. 1.—Initial Annealed Condition of Specimens.  
 FIG. 2.—After 7% Creep in 290 hr. at 250° C. under load of 500 lb./in.<sup>2</sup>. Break-up of grains.  
 FIG. 3.—After 7% Creep in 14 hr. at 350° C. under load of 350 lb./in.<sup>2</sup>. Less break-up.  
 FIG. 4.—After 8% Creep in 764 hr. at 350° C. under load of 150 lb./in.<sup>2</sup>. No break-up.



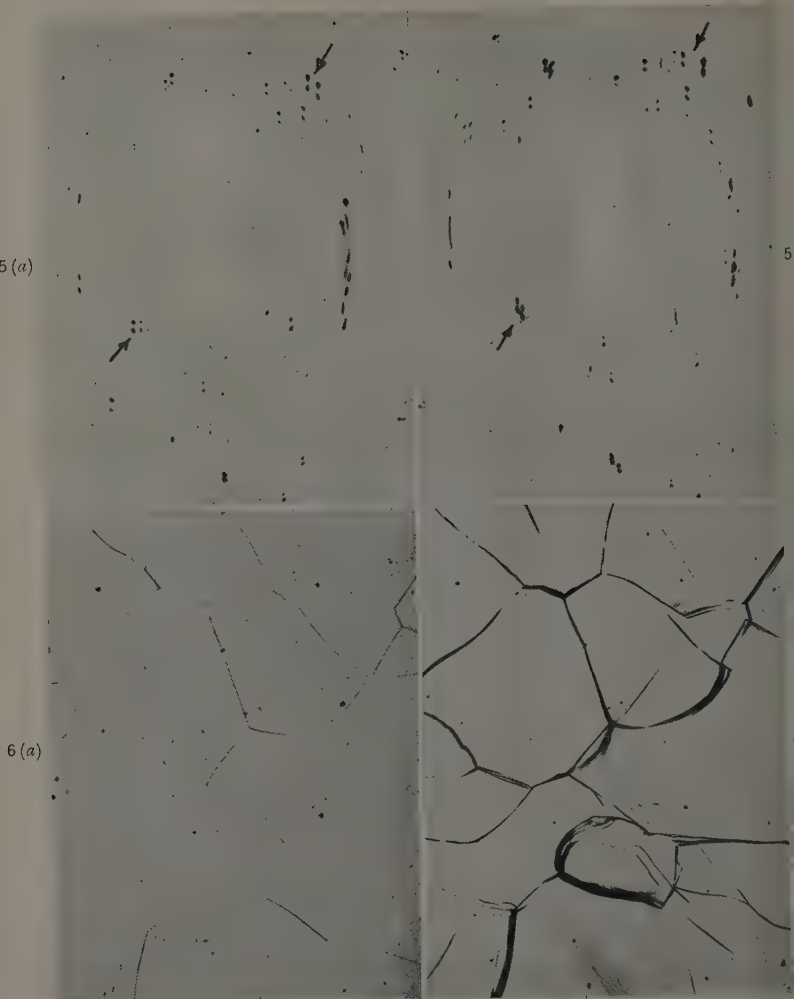


FIG. 5 (a) and (b).—X-Ray Back-Reflection Photographs of Aluminium Before (a) and After (b) 3% Extension at 0.01% per hr. at 350° C. X-ray reflections remain single sharp spots. No break-up of grains.

FIG. 6 (a) and (b).—Photomicrographs Before (a) and After (b) Extension. Conditions as for Fig. 5. Note absence of slip lines or cell formations.  $\times 100$ .

The synchronous technique also brought out the interesting point that the relative orientation of neighbouring grains may change slightly during this stage of deformation. Photographs at successive intervals of extension were obtained as nearly as possible from the same small area on a specimen. The reflections from many of the same grains then continued to appear in the photographs. It was noticed that during deformation these reflections became displaced relatively to each other, thus proving this point. An example occurs in the groups of spots indicated by arrows in Fig. 5.

Further experiments were carried out which showed that the grains did not appear as homogeneous entities merely because they were being replaced by recrystallized grains. Thus, when X-ray photographs were taken of the same area on a specimen at successive small increments of extension, it was possible within experimental limits to repeat the same reflection spots. The same grains therefore persisted. If at the successive stages specimens were re-polished and re-etched, it was clear that after allowing for boundary migrations the original grains were still there. Moreover, the creep/time curve was a straight line in these ranges of deformation; whereas it is known that, in general, recrystallization reveals itself by a distinct change in slope.

Thus the third stage is one in which considerable deformation of the grains may occur without internal block movements.

### *3. Interpretation as Boundary Micro-Flow.*

In view of the results just reported, it will be convenient, as a contrast with block movement, to use the term "micro-movement" to describe a movement that is too localized to disturb appreciably the internal homogeneity of the grain. The movement might result, for instance, from reorganization of a distorted group of atoms, or from the drift of single atoms or of very small groups of atoms.

The contrast might be emphasized by recalling that any block movement requires the action of a dislocation, which in its simplest form is a line of faults perpendicular to the direction of movement, a line that might be regarded crudely as a roller facilitating movement of one large block of atoms over another. But the micro-movement would merely require a disordering of the lattice about one point only. The results clearly suggest that the characteristic of the third stage is that the grain may deform entirely by micro-movements.

Other results indicated a concentration of such micro-movements at grain boundaries. It was also found that the range of temperatures and strain-rates over which any one of the three stages predominated

depended on the grain-size. An increase in grain-size affected the response of the microstructure in much the same way as a decrease in the temperature of deformation, or increase in the rate of strain, i.e. it postponed the third stage. In effect the increase in grain-size reduced the contribution of the micro-movements to the deformation. It was concluded, therefore, that the micro-movements took place mainly at grain boundaries or sub-boundaries. Consequently, to emphasize that micro-movements are involved, the third stage might appropriately be described as "boundary micro-flow".

A further property, especially relevant to creep, was that within limits of measurement the micro-flow was not accompanied by strain-hardening. This aspect was investigated by utilizing the machine for constant strain, which contained, in series with the specimen, an elastic weigh-bar that indicated the resistance to deformation during a test. It was always found that at the temperatures and strain-rates at which deformation proceeded by the mechanism of micro-flow, no increase in strength over that of the initial annealed condition of the specimen could be observed. Strain-hardening would presumably result from this mechanism only if the local lattice faults became exhausted. But elongations of 100% and upwards were obtained without strain-hardening. Therefore, in aluminium at any rate, exhaustion is not a factor of any consequence. Presumably the absence of strain-hardening indicates that the original lattice structure is never seriously deranged.

This last result is in keeping with the view that the micro-flow involves merely a local reorganization of a distorted lattice structure, the energy for which could be supplied mainly by thermal activation. The process then becomes analogous to viscous flow, which has been treated by many writers. It is easy to show <sup>4</sup> that if the average activation energy is  $A$ , the rate of flow at a temperature  $T$  and under a stress  $S$  becomes proportional to :

$$(S/kT) \exp (-A/kT)$$

This is Newtonian flow, with the rate proportional to the stress, and it could arise equally in crystalline or non-crystalline matter at a sufficiently high temperature.

Many other authors have found it necessary to postulate some form of micro-movement, principally at grain boundaries. The work of Zener <sup>5</sup> and of Kê <sup>4</sup> on internal damping is of especial interest in this connection, as well as the earlier conclusions of Rosenhain. But the present approach, in which the known forms of block movement are progressively and systematically eliminated, provides a particularly direct argument.

## V.—DISCUSSION OF RESULTS.

It is desired to submit as the principal proposition that these and the previous results provide for the first time a unified picture of the process of deformation over a whole range of temperatures and strain-rates. This is illustrated briefly below for some of the aspects of deformation particularly studied in the present experiments.

*1. The Three Stages of Deformation.*

Consider the conditions for the suggested micro-flow. First, the temperature must exceed a certain value, for although a thermally activated movement may occur at any temperature, the exponential factor in the formula means that the probability will increase rapidly above a particular temperature. The second requirement is a number of distorted centres at which a micro-movement may be generated; in effect the number will be related to the area of the original grain-boundary surfaces and any sub-boundary surfaces formed during the deformation.

With these considerations in mind, it is possible to understand the observed variation in the mechanism of deformation, as the rate of strain is varied at a given temperature. First, if the rate of strain is very small, the associated changes in shape, rotations, and other adjustments of the grains can be produced by micro-movements alone. There is no need for internal block movements. The mechanism of boundary micro-flow therefore predominates, the unit of block movement, if any, being the grain itself. Next, if the rate of strain is increased, a stage will be reached when micro-movements alone cannot cope with the imposed rate of deformation and block movements of whole groups of atoms within each grain are required. The unit of block movement is at first the cell, giving the stage of the cell mechanism. Later, as the rate of strain is further increased, the dissociation of the grain becomes more drastic; the blocks are also accompanied by disordered material at the sub-boundaries, and the movements occur in a characteristically pronounced and regular manner. The unit of block movement is then the element bounded by the slip planes, and possibly the crystallites. This constitutes the slip mechanism. Thus on this view it is possible to visualize a logical sequence in the development of the three main stages observed in these researches.

It is possible also to understand why the sub-structure should tend to a state of equilibrium with progressive deformation. For the gradual disintegration of the grain multiplies the misfitting sub-boundaries and thus provides more centres for potential micro-move-

ments. Therefore the action itself of progressive deformation tends to produce conditions favourable for reversion to boundary micro-flow. Evidently a final equilibrium in this respect will be reached more readily the higher the temperature or the lower the rate of deformation, as in fact was observed.

## 2. *Strength and Strain-Hardening.*

The above considerations also provide a logical basis for following the variation in the strength of a metal with temperature and rate of strain. The common factor is the nature of the sub-structure formed by the deformation, by which strength is necessarily measured. For the observations indicate that the strength varies inversely as the size of the elements in the sub-structure produced in the grains.<sup>2</sup>

Such a relation is reasonable on general grounds, since it is to be expected that a grain will offer more resistance when it has to deform by the movement of atoms *en bloc*. More energy is required to produce deformation as the blocks become smaller, because of the multiplication of sub-boundary surfaces. To a first approximation this energy will be proportional to the area of the new misfitting surfaces. If  $L$  is the average size of the elements, the energy will be roughly proportional to  $1/L$ , since there will be  $1/L^3$  elements per unit volume and the area of each will vary as  $L^2$ .

The strength will therefore be least when the process of boundary micro-flow predominates. At this stage the elements are virtually identical with the original grains. Moreover, since the grains do not dissociate in this process, there is no appreciable strain-hardening. This agrees with observation.

Next, as the rate of strain at a given temperature is increased the strength should appear greater because of the formation of a smaller and smaller sub-structure. Further, it will be greater the lower the temperature of deformation for the same reason. The strength  $S$  of the cell mechanism, the coarser form of dissociation, was found to be in good agreement<sup>2</sup> with a relation similar to that proposed by Bragg<sup>6</sup>:

$$S = Ed/L = C/L,$$

where  $E$  is Young's modulus and  $d$  the atomic spacing. Also in accordance with this view, it was observed that strain-hardening occurred while the grains were breaking down, but ceased when the sub-structure reached a state of equilibrium.

Finally, when the slip mechanism predominates, the above relation will become more complex because, on the present interpretation of the observations, the sub-structure contains not only the main elements

bounded by the slip planes but also the small crystallites or disordered material at the sub-boundaries. If the average size of the latter is  $l$ , then the relation becomes :

$$S = xC/L + yC/l,$$

where  $x$  and  $y$  are the proportions of material in each state. It is possible to test this relation only after heavy cold deformation, when the second factor  $y$  may be expected to predominate. It has been shown in this case that  $l$  tends to a lower limiting size, which can be estimated. If this size is substituted, the second factor should then give values for  $S$  that are of the same order as the ultimate strength of the metal. This result has in fact been obtained in previous tests.<sup>7</sup>

It is interesting to note that this interpretation of the sub-structure associated with slip would imply that the slip markings should possess a fine structure. Such a condition has now been observed in special cases by electron microscopy,<sup>8</sup> and has in fact been confirmed in similar preliminary experiments on specimens used in the present work.

### 3. Application to Creep.

On the above views, creep should occur when the sub-structures resulting from the initial loading of the specimen settle down to an equilibrium condition, for then there should be no progressive strain-hardening. This criterion definitely appears to hold in creep tests made on the aluminium used in the present work. The actual mechanism of the creep in all probability is mainly by micro-movements, since, as already suggested, it is these which make the equilibrium possible. The rate of creep, however, will depend primarily on the number of sub-boundaries created during the initial dissociation and remaining after exposure to the working temperature. It is considered that the unsatisfactory nature of current mathematical theories of creep lies in the fact that the changing microstructure of the metal is not taken into account. The criterion suggested by structural considerations involves a sufficiently high temperature to activate micro-movements and sufficient sub-boundaries to provide enough centres of distortion for micro-movements, the result being an equilibrium condition of the structure that leads to deformation without appreciable strain-hardening.

It may be added that aluminium is of special interest because it appears to deform in a particularly homogeneous manner. As a result, the three stages under consideration are well defined, and so are the ranges of temperature and strain-rate over which the separate stages predominate. Moreover, the three stages are compressed on the time scale, so that they can be covered in reasonably short-term tests. How-



ever, this state of affairs is not likely to be general, and in other metals it is possible that deformation may be irregular, so that one grain may be deforming at one time at a rate that necessitates slip, while at another time it may be deforming at a rate in which boundary micro-flow is entirely operative. Such metals would show, in addition, a tendency to recrystallize and even strain-harden locally because of the disordered material produced by the occasional slip movements. With some metals it is also possible that considerable dissociation of a grain may be necessary, even to the production of slip, before sufficient internal misfitting boundaries, and therefore sufficient potential centres of micro-flow, are created to permit an equilibrium condition of steady creep. These more complex cases can be understood, however, only when the underlying principles are obtained from a study of such metals as aluminium which behave in a simple and systematic fashion.

In conclusion, it may be of interest to consider the results in relation to certain more general issues. First, it is well known that the creep properties of a specimen are affected by the grain-size. This would follow at once from the above discussion, for the number of centres at which micro-flow can originate will depend on the area of the grain boundaries. The present results also show how the mechanism of deformation itself should vary with grain-size. Thus, for aluminium, it is evident that a particular temperature and rate of strain can be chosen at which a specimen with a sufficiently fine grain-size will deform by boundary micro-flow only. If, however, the grain-size is increased, a point will be reached when the grain must break down internally in order to adjust itself to the imposed rate of strain, first deforming by the cell mechanism and finally, if the grain-size is very large, by the slip mechanism. This would explain the observation of Hanson and Wheeler<sup>9</sup> that slip appeared in the creep of single aluminium crystals and also the recent results of Calnan and Burns<sup>10</sup> on impure coarse-grained aggregates.

Secondly, it has become usual to analyse creep curves into two components, "transient" and "steady-state" creep, following the work of Andrade.<sup>11</sup> The present results indicate that the former might correspond to the preliminary breaking-down of the grains before the establishment of an equilibrium state of the microstructure; the latter condition would then correspond to the "steady-state" creep. The results indicate that the general mode of deformation varies so markedly with the rate of strain, however, that it is uncertain how far this correspondence can safely be carried. They also suggest that generalizations from the mathematical analysis of creep curves might easily be carried too far.

Finally, it is considered that the present results give no support to the hypothesis of polygonization as postulated by Cahn<sup>12</sup> and others to explain "recovery" effects, nor to the suggestion by Crussard<sup>13</sup> and recently by Greenough and Smith<sup>14</sup> that polygonization might explain the earlier observation of the present authors on the dissociation of the grains during creep. In effect, polygonization envisages an intermediate distorted state of special significance before dissociation of the grain. The dissociation is then attributed to the effect of heat on this state. If the heat were insufficient, the grain could exist indefinitely in the distorted state. The present authors, on the contrary, consider that on deformation there is immediate dissociation of the grain into disoriented elements at any temperature, and that this is the direct effect of the deformation.

The effect of heat alone on a previously deformed grain may, in the authors' experience, cause partial absorption of the finer debris into the coarser elements or a partial growth of the elements, but only to a minor degree; and incidentally such absorption and growth would explain quite simply the X-ray evidence usually advanced in support of polygonization. Also, the various elements in the sub-structure may be in a state of elastic strain, and the effect of heat in general will relieve these strains; but this again is regarded as a secondary matter. The minor effect of heat in both these respects is easily shown by contrasting the final sub-structure in the grains of aluminium deformed at room temperature and then heated, with that produced when deformation and heating are concurrent, as in the creep conditions which lead to the cell structure.<sup>3</sup> The latter can be produced with a much greater order of size and higher degree of perfection than is possible by the "recovery" process, and it can be formed without the slightest indication of any intermediate disordered state.

Considerations such as these, and the knowledge that the cell size produced at a given temperature in a specimen can be systematically varied, increased, or decreased according to the rate of strain, have led to the present conclusion that any dissociation of the grain on deformation is direct and, for all practical purposes, instantaneous. There must, of course, be a momentary local distortion of the lattice along the plane which becomes a sub-boundary, and these disturbances necessitate the assumption that there are regions of weakness or dislocations in the lattice. The authors consider, however, that these regions are always sufficiently numerous to allow the grain to break down into either a coarse sub-structure, as in the cell formation, or a fine sub-structure, as in slip, according to the conditions of deformation; and that this change can occur without the elaborate preliminary mechan-

isms or intermediate metastable states postulated by polygonization. As already suggested, at the higher temperatures and lower strain-rates in a fine-grained aggregate there is no need for any breaking-down because of the active boundary micro-flow. At the lower temperatures and faster strain-rates, internal breakdown is necessary. This will occur with minimum expenditure of energy by utilizing as few as possible of the dislocations or weak regions in the lattice and thus forming as few misfitting sub-boundaries as possible. In this way, on a general view of weaknesses and dislocations in a lattice, it seems possible to give a more natural explanation of the direct formation of a sub-structure by deformation and of the variation of the size of the sub-structure with the temperature and rate of the deformation.

#### ACKNOWLEDGEMENTS.

The authors wish to thank Professor J. N. Greenwood, University of Melbourne, for his interest and continuous encouragement. They are also greatly indebted to Mr. H. A. Wills, Head of the Structures and Materials Section of the Aeronautical Research Laboratories, Department of Supply, with whom the researches were jointly undertaken, for arrangements enabling one of us (W.A.R.) to participate full time.

#### REFERENCES.

1. G. R. Wilms and W. A. Wood, *J. Inst. Metals*, 1948-49, **75**, 693.
2. W. A. Wood and W. A. Rachinger, *J. Inst. Metals*, 1949-50, **76**, 237.
3. W. A. Wood and R. F. Scrutton, *J. Inst. Metals*, 1950, **77**, 423.
4. T. S. Kê, *J. Appl. Physics*, 1949, **20**, 274.
5. C. Zener, "Elasticity and Anelasticity of Metals", Chicago: 1948 (University of Chicago Press).
6. W. L. Bragg, *Nature*, 1942, **149**, 511.
7. W. A. Wood and W. A. Rachinger, *J. Inst. Metals*, 1949, **75**, 571.
8. A. F. Brown, *Metallurgical Applications of the Electron Microscope* (*Inst. Metals Monograph No. 8*), 1950, 103.
9. D. Hanson and M. A. Wheeler, *J. Inst. Metals*, 1931, **45**, 229.
10. E. A. Calnan and B. D. Burns, *J. Inst. Metals*, 1950, **77**, 445.
11. E. N. da C. Andrade, *Proc. Roy. Soc.*, 1914, [A], **90**, 329.
12. R. W. Cahn, *J. Inst. Metals*, 1949-50, **76**, 121.
13. C. Crussard, *J. Inst. Metals*, 1948-49, **75**, 1125 (discussion).
14. G. B. Greenough and E. M. Smith, *J. Inst. Metals*, 1950, **77**, 435.

# THE CONSTITUTION OF TITANIUM-RICH ALLOYS OF IRON AND TITANIUM.\*

By H. W. WÖRNER,† M.Sc., MEMBER.

## SYNOPSIS.

Metallographic and X-ray methods have been employed to establish the general outline of the constitutional diagram for the titanium-rich portion of the titanium-iron system. The results of the investigation indicate that addition of iron causes a depression of both the freezing point and the  $\alpha \rightleftharpoons \beta$  transformation temperature of titanium. From the melting point of titanium, the liquidus and solidus fall steeply to a eutectic horizontal at 1060° C., the eutectic composition being at 29 at.-% iron. This eutectic consists of an intermetallic phase (FeTi), possessing a body-centred cubic structure, and a solid solution of iron in the high-temperature ( $\beta$ ) form of titanium. The maximum iron content of the  $\beta$ -solid solution is approximately 22 at.-% at the eutectic temperature. At lower temperatures, the  $\beta$ -solid solution field tapers to a eutectoid point at 15.5 at.-% iron, the temperature being approximately 600° C. The eutectoid transformation, which is very sluggish, yields FeTi and  $\alpha$ -titanium containing less than 0.8 at.-% iron in solid solution.

## I.—INTRODUCTION.

IRON-RICH alloys of titanium and iron have been investigated by Lamort,<sup>1</sup> Witte and Wallbaum,<sup>2</sup> Tofaute and Büttinghaus,<sup>3</sup> and Wallbaum,<sup>4</sup> but no systematic study of titanium-rich alloys appears to have been reported in the literature. Recently, Craighead, Simmons, and Eastwood<sup>5</sup> have reported on the microstructure and some mechanical properties of a few alloys in the range 0.5–2% iron.

The present paper deals with an exploratory investigation of alloys in the range from almost pure titanium to the first intermetallic phase (FeTi) in the titanium-iron system. The primary aim was to establish the general features of the constitutional diagram in the titanium-rich region of the system. Melting ranges have been determined only approximately, but careful attention has been given to the effects of iron on the allotropic transformation ( $\alpha \rightleftharpoons \beta$ ) in titanium. The  $\alpha$ , or low-temperature form, possesses a close-packed hexagonal structure, and the  $\beta$ , or high-temperature form, a body-centred cubic structure. The transformation temperature is close to 883° C. in refined titanium. The author would like to make it quite clear that he does not claim to

\* Manuscript received 31 August 1950.

† Senior Research Officer, Physical Metallurgy Section, Commonwealth Scientific and Industrial Research Organization, Baillieu Laboratory, University of Melbourne, Australia.

have established the equilibrium diagram for the pure binary titanium-iron system. When the investigation was initiated, supplies of high-purity titanium were not available, and titanium produced by the Kroll process was used as the basis metal. The comparatively low degree of purity of the basis metal should therefore be borne in mind when the results of the present investigation are considered. In this connection, it is important to realize that whereas the  $\alpha \rightleftharpoons \beta$  transformation occurs almost isothermally at 882°–884° C. in high-purity titanium, it occurs over a broad range of temperature (860°–970° C.) in the "Kroll" product. Thus it has proved impossible to establish precisely the boundaries between the  $\alpha$ ,  $\alpha + \beta$ , and  $\beta$  fields, particularly at low concentrations of iron. However, it is reasonable to expect that the constitutional diagram reported probably bears some general resemblance to the true titanium-iron phase diagram, and the work described provides a foundation for the further investigation of alloys of commercial purity.

Other objectives of the work were: (a) to ascertain whether the alloys were amenable to simple fabrication techniques, and (b) to determine their mechanical properties and the possibility of varying their strength by heat-treatment. These aspects of the investigation will be reported in a later paper.

## II.—EXPERIMENTAL METHODS AND RESULTS.

### 1. *Metals Used for Making the Alloys.*

It has been mentioned in the introduction that the titanium was made by the Kroll process, in which titanium tetrachloride is reduced by magnesium. Unfortunately, the "Kroll" titanium was a complex dilute alloy containing the following impurities:

Impurity	H <sub>2</sub>	O <sub>2</sub>	N <sub>2</sub>	C	Mg	Fe	Si
Approx. content, at.-%	12	0.6	0.3	0.4	0.5	0.2	0.1

The oxygen content was determined by a vacuum-fusion method in the National Physical Laboratory, Teddington, England. The nitrogen was estimated by a method similar to the Kjeldahl technique as applied to steels. The iron was determined by a colorimetric method developed by Corbett.<sup>6</sup> A combustion method was employed to ascertain the carbon content. The hydrogen and magnesium were expelled during the preparation of the alloys (cf. later section).

Carbonyl iron made by the General Aniline Works, New Jersey, was used as the alloying metal. Apart from traces of hydrogen and oxygen, both of which were eliminated by heating the iron *in vacuo* before using, the only important impurity was carbon (approx. 0.1

at.-%), while the only metallic impurity detected by spectrographic testing was a faint trace of nickel.

## 2, Method of Preparing the Alloys.

Small specimens weighing less than 10 g. were made by melting together small pieces of the two metals, which had previously been consolidated by arc melting in argon. Large specimens weighing up to 50 g. were made from powders by the following method. The weighed powders were mixed as well as possible by hand, and the mixture pressed into  $\frac{1}{4}$ -in. square-section bars. These were heated *in vacuo* to 1000° C. until the pressure was reduced to  $10^{-4}$  mm. mercury. This achieved two desirable aims: (1) the volatile impurities hydrogen and magnesium were almost completely eliminated from the metals, and (2) the powders sintered to form coherent bars which were convenient for loading on to the melting hearth in the subsequent arc-melting operation.

Melting was affected in the type of inert-atmosphere arc furnace described by Kroll.<sup>7</sup> There was no detectable contamination of the alloys with copper and tungsten, despite the fact that the specimens rested on a water-cooled copper hearth during the melting and that a tungsten electrode was used.

In the as-melted condition, alloys containing 5–20 at.-% iron appeared to be cored solid solutions, which suggested that there was a considerable interval between the liquidus and solidus in this composition range. Therefore, all alloys intended for metallographic and X-ray examination were homogenized by heat-treatment. The specimens of alloys which were amenable to hot working (i.e. those with 0.8–7 at.-% iron) were forged and swaged at about 700° C. and heated to 1000° C. for 30–40 hr. in a double-walled fused silica annealing furnace provided with an argon atmosphere. Alloys containing more than 9 at.-% iron could not be appreciably hot-worked owing to a marked tendency to intergranular cracking. These were homogenized by heating to 1000°–1030° C. in the argon-atmosphere furnace for about 70 hr. This treatment eliminated micro-coring. However, alloys with 14–20 at.-% iron exhibited macroscopic coring or segregation unless the specimens were limited to approximately 5–8 g. in weight. Apparently the small specimens chilled so rapidly that there was little opportunity for any but fine microscopic coring to occur. The segregation in large specimens was so serious that it was decided to use only homogenized 5-g. samples in attempts to locate the boundaries of the  $\beta$  phase field in the range 14–20 at.-% iron.

All the alloys containing 0.8–20 at.-% iron were analysed. Analysis



of specimens with iron contents of less than 15 at.-% was considered to be especially necessary because these alloys had fairly high melting ranges and they suffered losses by fuming and spitting during arc melting. Nominal compositions were accepted for most alloys in the range 25-50 at.-% iron as within these limits, the melting ranges were comparatively low and there was no appreciable spitting or fuming during melting. Consequently, the weights of the small ingots or buttons

TABLE I.—*Composition of Alloys.*

Alloy	Iron Content, wt.-%	Iron Content, at.-%
AHS . . . . .	0.95	0.81
AML . . . . .	1.06	0.92
AHT . . . . .	2.03	1.75
ABW 13 . . . . .	2.05	1.77
AMM . . . . .	2.06	1.78
AMJ . . . . .	3.08	2.70
AHU . . . . .	3.79	3.30
AMK . . . . .	4.07	3.50
AHV . . . . .	5.90	5.20
AIT . . . . .	8.7	7.6
AIU . . . . .	9.5	8.25
AIV . . . . .	12.0	10.5
AIW . . . . .	13.5	11.8
AJA . . . . .	16.2	14.2
AJB . . . . .	18.5	16.3
AJC . . . . .	20.4	18.0
AJD . . . . .	22.5	20.0
AKC . . . . .	27.8 *	24.9
AKD . . . . .	31.4 *	28.3
AKE . . . . .	34.0 *	30.7
AKF . . . . .	35.8 *	32.4
AKG . . . . .	44.0 *	40.3
AKH . . . . .	53.7 *	49.9

\* Nominal composition.

equalled the sum of the weights of the respective component metals, indicating that it was reasonable to adopt the nominal compositions.

The compositions of the alloys employed in this investigation are listed in Table I.

### 3. *Solidification Ranges.*

No attempt was made to determine melting or freezing ranges by the usual type of thermal analysis since liquid titanium and titanium-rich alloys rapidly react with refractories. However, some freezing ranges were determined very approximately by following the cooling of arc-melted specimens with a disappearing-filament optical pyrometer. The pyrometer had been checked at the freezing point of iron,

and emissivity corrections were based on the emission coefficients of titanium determined by Went and reported by van Arkel.<sup>8</sup> The results obtained do not indicate the equilibrium liquidus/solidus range because the rate of cooling was too high (100°–200° C./min.), and it is almost certain that undercooling occurred. In addition, since the as-melted alloys in the range 6–20 at.-% iron were cored solid solutions, it is evident that the completion of solidification would occur at a temperature below that of the true solidus for any composition within these limits. Nevertheless, the results are of some practical value and are reported in Table II.

TABLE II.—*Freezing Ranges and Solidus Temperatures.*

Iron Content, at.-%	Freezing Range,* °C.	Solidus,† °C.
8.25	1450–1250	...
11.8	1350–1130	1100
18.0	1250–1060	Between 1080 and 1100
20.0	...	" 1060 " 1070
24.9	...	" 1050 " 1060
30.7	...	" 1050 " 1060
		(Completely molten at 1070)
32.4	...	Between 1050 and 1060
40.3	...	" 1050 " 1060
49.9	Approx. 1250	...

\* Estimated by following the solidification of arc-melted specimens with a disappearing-filament optical pyrometer. Cooling rate 100°–200° C./min.

† Determined by observing specimens heated to successively higher temperatures.

Some solidus points of alloys in the range 18–40 at.-% iron were determined by simply heating specimens to successively higher temperatures and ascertaining, by visual and microscopic means, when the first signs of melting appeared. There was scarcely any need to use a microscope with alloys containing 30.7 and 32.4 at.-% iron. Visible beads of molten material appeared on the surface of these alloys when heated to 1060° C., while there were no signs of melting if the alloys were heated only to 1050° C. These results, together with those for specimens containing 18, 20, 24.9, and 40.3 at.-% iron, are also given in Table II.

#### 4. *Eutectic Horizontal.*

The constancy of the solidus temperature (between 1050° and 1060° C.) for alloys containing 24.9–40.3 at.-% iron indicates either a eutectic or peritectic horizontal extending from a point between 20 and 25 at.-% iron to some point between 40 and 50 at.-% iron. That it is a eutectic horizontal was shown by (a) the higher freezing ranges of

alloys on either side of this composition range, and (b) the almost isothermal melting of the 28.3 at.-% iron alloy. Furthermore, the microstructures of as-melted alloys in the range 25–40 at.-% iron were of the type to be expected in a eutectic system. A specimen of the 25 at.-% iron alloy exhibited primary crystals set in a matrix of a finely dispersed mixture of phases. The 28.3 and 30.7 at.-% iron alloys consisted almost entirely of this fine mixture of phases, while the 32.4 and 40.3 at.-% iron alloys contained, in addition to this fine mixture, dendritic primary crystals different from those seen in the 25 at.-% alloy. Careful observations indicated that the shape and etching properties of the primary crystals in the 28.3 and 30.7 at.-% iron alloys were significantly different, and it was concluded that the eutectic composition was approximately 29 at.-% iron. The microstructure of the eutectic is illustrated in Fig. 2 (Plate XXVII).

### *5. Establishing Phase Regions in Solid Alloys.*

The results of Debye-Scherrer X-ray-diffraction experiments have been combined with the microscopical examination of heat-treated specimens to ascertain the phase fields in the solid alloys. In the early stages of the investigation it was discovered that the addition of iron to titanium lowered the  $\alpha \rightleftharpoons \beta$  transformation temperature range. It was also found that by rapid cooling from the appropriate temperature, the solid solutions of iron in the high-temperature or  $\beta$  form of titanium could be retained as long as the iron content was 3.5 at.-% or more. This fact proved to be of great value in establishing the boundaries of the  $\beta$ -solid-solution field by both methods.

In most of the heat-treatments the specimens were heated up into the  $\beta$ -solid-solution field, cooled, either slowly or rapidly, to any desired temperature, and maintained there for a prolonged period to permit an approach to equilibrium conditions. Finally, the specimens had to be chilled to room temperature in an attempt to retain the conditions established by the prolonged heating. This quench presented an experimental difficulty because the prolonged heating had to be conducted in a vacuum to prevent contamination of the specimens with atmospheric gases. To overcome this difficulty, the following procedure was developed. The specimens were cooled as rapidly as possible in the silica vacuum envelope by removing the furnace and directing a stream of cold air on to the silica tube. They were then removed from the vacuum envelope and very rapidly reheated to their original temperatures by complete immersion in liquid tin. After 10–15 minutes' heating, the specimens were removed and immediately quenched in cold water. As a result of many observations, it was concluded that

the brief heating in tin served to cause resolution of any fine precipitate which may have formed during the cooling in the vacuum envelope. A thin surface-layer contaminated with oxygen and tin was present after heat-treatment in the liquid tin, but this was removed by grinding or filing.

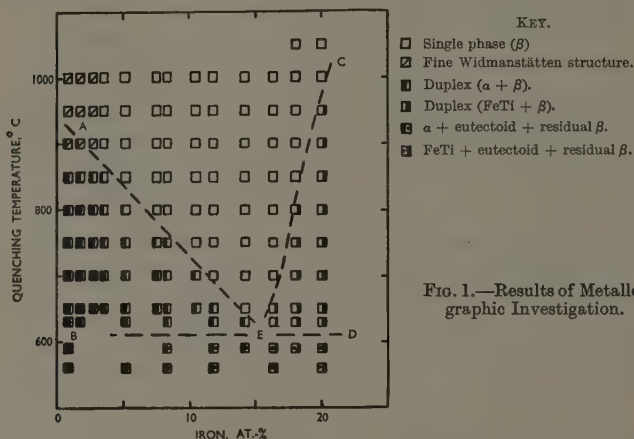
Both small block specimens and powdered samples have been employed for X-ray-diffraction experiments on alloys quenched from 800° C. or higher. Powders were used for most of the experiments which involved temperatures below 800° C. All alloys containing more than 25 at.-% iron were very brittle at normal temperature, and could be pulverized by grinding in a tungsten carbide percussion mortar. Other alloys were filed to produce powdered samples for X-ray-diffraction work. These powders were prepared from block specimens which had previously been heat-treated as required. To provide protection against contamination with atmospheric gases during repetition of the heat-treatment, the powder samples were sealed off in small evacuated receptacles of Pyrex glass or silica glass, the choice of material depending on the temperature of the subsequent heating. In many cases, a portion of the powder adjacent to the silica or Pyrex tended to frit to the walls of the receptacle. Whenever this happened, the particles of powder adhering to the receptacle were not dislodged during removal of the heat-treated powder. It should be noted here that the small receptacles did not crack during water-quenching operations and, hence, the specimens did not come into direct contact with the cooling water. Although this was advantageous in that superficial contamination was averted, it reduced the cooling rate during the quench. To check whether the reduced cooling rate was adequate, some results of Debye-Scherrer experiments on powders heat-treated as described above were compared with those obtained by using water-quenched block specimens. No differences were detected in the number and approximate proportions of identified phases. For any particular phase there were slight differences in lattice parameters such as could be explained by the effects of locked-up stresses in quenched block specimens.

#### 6. *Metallographic Investigation in the Range 0.8-20 at.-% Iron.*

The essential microstructural features of alloys quenched from various temperatures are graphically presented in Fig. 1, and some typical microstructures are illustrated in Figs. 2-11 (Plates XXVII and XXVIII). It is to be emphasized that these illustrations indicate equilibrium structures only down to approximately 600° C. Attainment of equilibrium during any given heat-treatment was tested by ascertaining

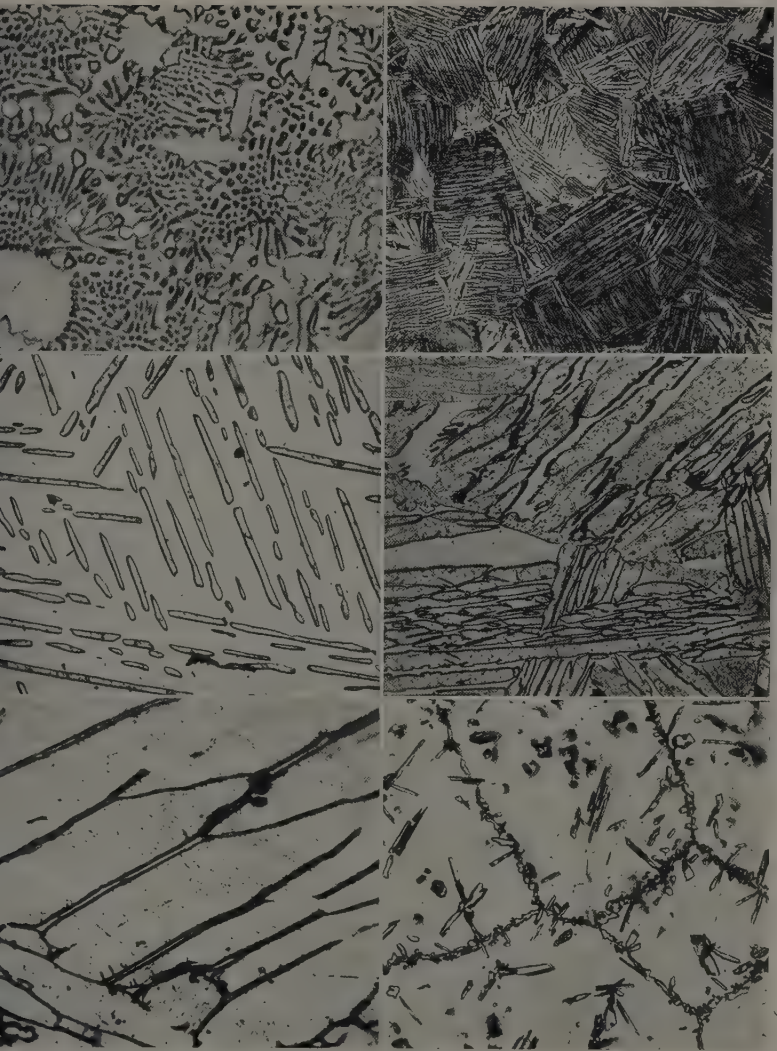
whether or not any further microstructural changes occurred on repeating the heat-treatment. There was ample evidence that below 600° C., the phase changes proceeded so slowly that equilibrium conditions would have been attained only by heating periods of perhaps several weeks. However, the structural changes developed at such a rate that the effects of several days' heating at temperatures in the range 600°–550° C. were quite apparent. This aspect of the investigation will be referred to again on p. 185.

Perhaps the most prominent feature of the observations recorded in Fig. 1 is the existence of a single-phase field which extends from low



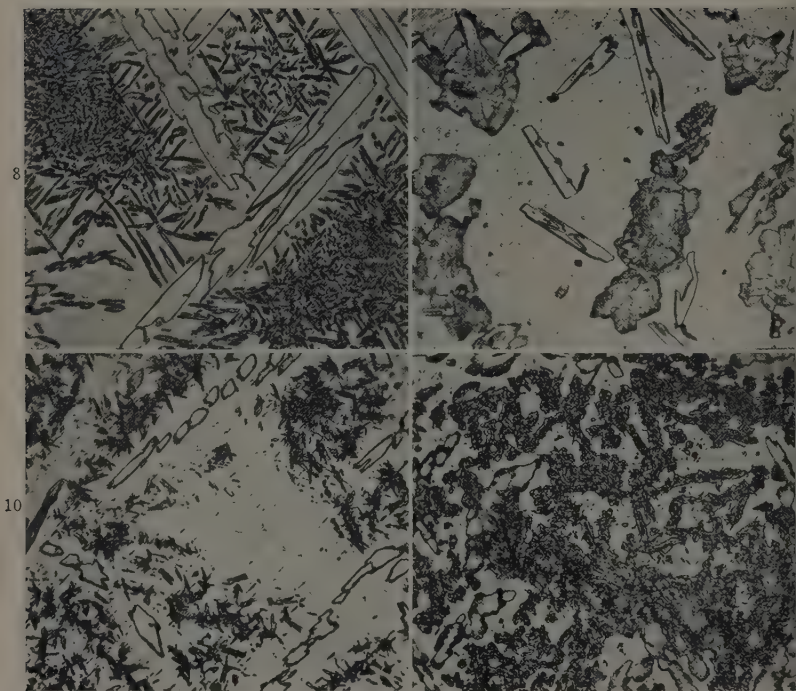
iron contents to approximately 20 at.-% at 900°–1050° C., but which tapers down to a point (*E*) at approximately 16 at.-% iron and 600°–630° C. Very fine Widmanstätten structures were observed in alloys of low iron content quenched from temperatures above 900° C. These structures, which are typified in Fig. 3 (Plate XXVII), are interpreted as evidence of a rapid breakdown, during quenching, of single-phase structures that existed at the elevated temperatures. Basic titanium exhibits the same fine Widmanstätten texture when quenched from 950° C. or higher and indicates that  $\beta$ -titanium is not retained even by water-quenching. It is considered that iron forms a solid solution with  $\beta$ -titanium and that if the solution contains not more than 3 at.-% iron, it tends to transform rapidly during a water-quench, just as pure titanium does. With increasing iron content from 0.8 to 2.7 at.-%,





- g. 2.—28.3 At.-% Iron Alloy, as melted. Eutectic + primary  $\beta$ .  $\times 1000$ .  
 g. 3.—0.8 At.-% Iron Alloy, Water-Quenched from  $950^{\circ}\text{C}$ . Fine Widmanstätten structure due to rapid  $\beta \rightarrow \alpha$  transformation.  $\times 150$ .  
 g. 4.—3.5 At.-% Iron Alloy, cooled slowly from  $1000^{\circ}$  to  $850^{\circ}\text{C}$ , then water-quenched. Needles of  $\alpha$  in matrix of  $\beta$ .  $\times 150$ .  
 g. 5.—3.5 At.-% Iron Alloy, cooled very slowly from  $1000^{\circ}$  to  $650^{\circ}\text{C}$ , then water-quenched. Mixture of  $\alpha$  (darker) and  $\beta$ . Heavily etched in aq. 1% HF solution.  $\times 150$ .  
 g. 6.—0.8 At.-% Iron Alloy, cooled very slowly from  $1000^{\circ}$  to  $650^{\circ}\text{C}$ , then water-quenched. Films of  $\beta$  phase in  $\alpha$ . Etched in aq. 1% HF solution.  $\times 150$ .  
 g. 7.—20.0 At.-% Iron Alloy, cooled very slowly from  $1000^{\circ}$  to  $750^{\circ}\text{C}$ , then water-quenched. FeTi along grain boundaries and within grains of  $\beta$ .  $\times 120$ .





- FIG. 8. 11.8 At.-% Iron Alloy, cooled very slowly from  $800^{\circ}$  to  $560^{\circ}$  C., maintained at  $560^{\circ}$  C. for 10 days, then water-quenched. Large elongated crystals of  $\alpha$  in matrix of eutectoid + residual  $\beta$ .  $\times 450$ .
- FIG. 9.—18.0 At.-% Iron Alloy, cooled very slowly from  $1000^{\circ}$  to  $590^{\circ}$  C., maintained at  $590^{\circ}$  C. for 7 days, then water-quenched. Matrix of  $\beta$  containing large crystals of FeTi and irregularly shaped areas of fine eutectoid.  $\times 350$ .
- FIG. 10. 16.3 At.-% Iron Alloy, cooled very slowly from  $800^{\circ}$  to  $560^{\circ}$  C., maintained at  $560^{\circ}$  C. for 7 days, then water-quenched. Matrix of  $\beta$  containing some large crystals of FeTi and scattered regions of fine eutectoid.  $\times 400$ .
- FIG. 11.—Same as Fig. 9, except that specimen had been heated for an additional 16 days at  $560^{\circ}$  C. Note increase in amount of eutectoid.  $\times 400$ .

Etching reagent: cold aq. solution containing 1 wt.-% HF and 0.5 wt.-%  $\text{H}_2\text{O}_2$ , except where otherwise stated.

the fine Widmanstätten pattern became less marked, and it was practically absent in water-quenched 3.3 and 3.5 at.-% iron alloys. There was no evidence of this type of structure in water-quenched alloys containing 5.2–20 at.-% iron. It was concluded that in this composition range, the  $\beta$  titanium-iron solid solutions could be retained by water-quenching. This was confirmed by X-ray-diffraction evidence, the details of which will be presented in Section II, 7. As a matter of metallographic interest it might be mentioned that the  $\beta$  solid solution retained by quenching was much less reactive during etching than pure titanium.

In the field *AEB* in Fig. 1, the two-phase structures showed coarse Widmanstätten patterns (Figs. 4 and 5, Plate XXVII). The phase which formed in Widmanstätten fashion from the parent  $\beta$  solid solution behaved, on etching, in very much the same way as the basic titanium in the slowly cooled or  $\alpha$  form. It was later confirmed by X-ray-diffraction experiments that this phase had in fact the  $\alpha$ -titanium structure so that the triangle *AEB* can be designated as the ( $\alpha + \beta$ ) field.

The solid solubility of iron in  $\alpha$ -titanium appears to be less than 0.8 at.-% from 850° to 600° C., because the 0.8 at.-% iron alloy was duplex after prolonged heating at all temperatures in this range just stated (Fig. 6, Plate XXVII).

In the field *CED* (Fig. 1), the phase which formed from the parent  $\beta$  solid solution did not show a marked Widmanstätten pattern. At most temperatures and compositions it appeared at grain boundaries of the original  $\beta$  solution and in small clusters within the  $\beta$ -grains (Fig. 7, Plate XXVII). Unlike the  $\alpha$  phase, the phase formed below the boundary *CE* etched even more slowly than the  $\beta$  solution. It has been established, partly on the basis of etching characteristics, but chiefly by Debye-Scherrer X-ray-diffraction experiments (see below), that this phase in the field *CED* is the intermetallic phase FeTi or has a composition very close to it. The phase FeTi and a  $\beta$  solid solution containing about 22 at.-% iron are the constituents of the eutectic already referred to in Section II, 4.

Alloys which have been brought to equilibrium just above the line *BD* and subsequently heated at temperatures just below *BD* show evidence of a very slow breakdown of the  $\beta$  solid solution into a finely dispersed mixture of phases. As is illustrated in Figs. 8, 9, 10, and 11 (Plate XXVIII), the formation of this fine mixture does not develop uniformly throughout the  $\beta$  phase, but rather does it occur in isolated regions. The number and size of these regions increase slowly with longer heating periods at any temperature between 600° and 540° C.

(cf. Figs. 10 and 11). The sluggishness of the change is evident from the fact that 10–20 days' heating at various temperatures in the range  $540^{\circ}$ – $600^{\circ}$  C. has failed to cause complete breakdown of the  $\beta$  solution. There are some indications that the rate of the phase change is greater at  $550^{\circ}$ – $570^{\circ}$  C. than it is at either higher or lower temperatures. At  $500^{\circ}$  C. and lower, the change is still in its very early stages even after 10 days' heating.

These observations can be interpreted in terms of a sluggish eutectoid decomposition of the  $\beta$  titanium–iron solid solution represented by the point *E* in Fig. 1. In Section II, 7, it will be shown that X-ray-diffraction experiments confirmed this interpretation.

The actual form and shape of the eutectoid regions seemed to be influenced by the temperature of formation and also by the phase already present before the eutectoid decomposition. When formed at  $590^{\circ}$ – $600^{\circ}$  C. in alloys containing appreciable quantities of FeTi crystals, the eutectoid tended to appear in irregularly-shaped, but fairly well-defined regions such as those shown in Fig. 9. However, the eutectoid regions depicted in Figs. 8, 10, and 11 are more typical of those observed in alloys close to, or on the low-iron side, of the eutectoid composition. Lower temperatures ( $550^{\circ}$ – $570^{\circ}$  C.) also favoured the formation of the type of eutectoid structures illustrated in Figs. 8, 10, and 11.

### 7. *X-Ray-Diffraction Investigations.*

The results of Debye–Scherrer experiments were used partly for the identification of phases present in heat-treated alloys and partly for determining the boundaries of the  $\beta$ -solid-solution<sub>0</sub> field at temperatures between  $1050^{\circ}$  and  $600^{\circ}$  C. Most of the experiments were carried out with an 11.46-cm.-dia. camera. Both copper  $K_{\alpha}$  and cobalt  $K_{\alpha}$  radiation were employed, although the latter was preferred because it produced diffraction patterns with a more marked contrast between the lines and background.

Fig. 12 presents the results of experiments with heat-treated specimens which identified the phases present in detectable quantities. These results fit into a constitutional diagram which resembles that derived from the metallographic investigation. Since the X-ray-diffraction technique does not reveal the presence of phases present in very small amount, the boundaries between the  $\beta$  field and the  $(\alpha + \beta)$  and  $(\beta + \text{FeTi})$  fields in Fig. 12 naturally tend to be lower than those in Fig. 1.

The lattice parameters of the  $\alpha$ -phase in both  $(\alpha + \beta)$  and  $(\alpha + \beta + \text{FeTi})$  mixtures were practically identical with those of the basis titan-

ium. This fact, which is evident from the data in Table III, agrees with the observation made in dealing with the metallographic investigation (p. 179), that the solid solubility of iron in  $\alpha$ -titanium is quite low.

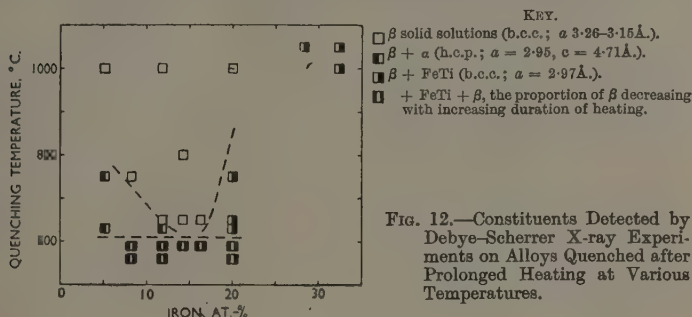


FIG. 12.—Constituents Detected by Debye-Scherrer X-ray Experiments on Alloys Quenched after Prolonged Heating at Various Temperatures.

The phase FeTi, which was found to have a body-centred cubic structure, has been produced in the following ways :

(1) By making a specimen containing almost exactly 50 at.-% iron. This specimen, AKH in Table I, was single phase in the as-melted condition and after prolonged heating at 600° and 650° C.

TABLE III.—*Lattice Parameters of Annealed Basis Titanium and the  $\alpha$  Phase in Titanium-Iron Alloys.*

Iron Content, at.-%	Treatment	Parameters, $\text{\AA}$ .	
		$a$	$c$
0.2 (Basis metal)	Annealed at 800° C.	2.95	4.71
0.8	96 hr. at 650° C.	2.95	4.72
5.2	96 " 650° C.	2.95	4.70
5.2	96 " 750° C.	2.95	4.71
8.25	170 " 590° C.	2.95	4.70
18.0	170 " 560° C.	2.95	4.72

(2) As a constituent of as-melted alloys in the composition range covered by the eutectic horizontal.

(3) As a constituent formed from iron-rich  $\beta$  solid solutions during cooling from between 1060° and 600° C.

(4) As a constituent formed during prolonged heating in the ( $\alpha + \beta + \text{FeTi}$ ) field below 600° C.

No matter what the origin of the FeTi was, its lattice parameter was, within the limits of measurement employed, always the same,

namely,  $a = 2.97 \pm 0.005 \text{ \AA}$ . This suggests that if there is a solid solution field based on FeTi, the boundary between it and the  $(\beta + \text{FeTi})$  field must be (a) close to the stoichiometric composition FeTi, and (b) nearly vertical from the eutectic temperature down to about  $600^\circ \text{C}$ .

When water-quenched from  $1000^\circ \text{C}$ ., alloys containing 5–20 at.-% iron were found to be homogeneous and to have a body-centred cubic structure, the value of  $a$  varying with iron content as shown by the full-line curve in Fig. 13. This curve also accommodates values of  $a$  for the 14.2 at.-% iron alloy quenched from both  $800^\circ$  and  $650^\circ \text{C}$ ., and the 16.3 at.-% iron alloy quenched from  $800^\circ \text{C}$ . It was confirmed

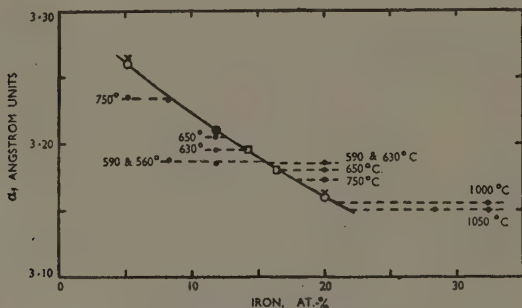


FIG. 13.—Lattice Parameter/Composition Relations for  $\beta$  Phase.

KEY.

- Powder specimens, quenched from  $1000^\circ \text{C}$ .
- × Block specimens, quenched from  $1000^\circ \text{C}$ .
- Powder specimens, quenched from  $800$  and  $650^\circ \text{C}$ .
- Powder specimens, quenched from temperatures indicated on graph ( $^\circ \text{C}$ ).

microscopically that these latter specimens were homogeneous. Values of  $a$  determined from experiments on quenched block specimens tended to be slightly higher than those obtained from powder samples. This could be attributed to locked-up stresses generated in block specimens during the quenching operation.

The parameters of the  $\beta$  constituent in duplex alloys have been plotted in Fig. 13, which serves to indicate the boundaries between the  $\beta$  field and the  $(\alpha + \beta)$  and  $(\beta + \text{FeTi})$  fields, respectively, at various temperatures. These points are plotted in Fig. 14, from which it is evident that the  $\beta$  field tapers to a point lying between 15 and 16 at.-% iron and at a temperature just above  $600^\circ \text{C}$ . Fig. 13 includes the parameters of the  $\beta$  phase present in some alloys in the  $(\alpha + \beta + \text{FeTi})$  regions, i.e. those heated for several days at  $560^\circ$  and  $590^\circ \text{C}$ . The practically constant value of  $a$  in this region indicates a fixed iron content

of 15.5 at.-% in the  $\beta$  constituent of the three-phase alloys. It is recorded graphically in Fig. 14 by the small crosses.

It is important to note that the proportions of  $\alpha$  and FeTi in the ( $\alpha + \beta + \text{FeTi}$ ) mixtures appeared to increase with increasing duration of heating in the range 550°–590° C. For example, after 2 days at 560° C. an alloy with 16.3 at.-% iron was found to contain just sufficient of the  $\alpha$  and FeTi phases to give very weak X-ray diffraction lines. After 7 days' heating at the same temperature, the diffraction lines from the  $\alpha$  and FeTi constituents had become readily detectable. An

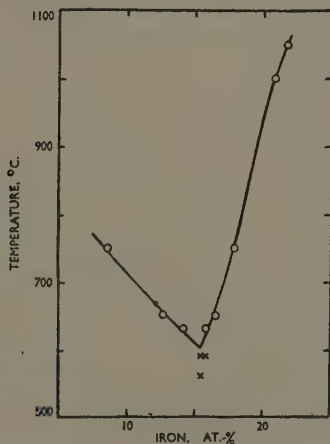


FIG. 14.—Boundaries of  $\beta$  Field Deduced from Fig. 13. The crosses represent the composition of the  $\beta$  constituent in ( $\alpha + \beta + \text{FeTi}$ ) mixtures.

additional 7 days' heating at 560° C. produced a further increase in the intensities of these lines as compared with those from the  $\beta$  phase. These effects could be partly due to coarsening of very fine particles which may have precipitated early in the heating period. However, it was significant that the increase in intensities of the  $\alpha$  and FeTi lines accompanied an increase in the proportions of the fine phase mixture illustrated in Figs. 10 and 11 (Plate XXVIII).

### III.—CONSTITUTIONAL DIAGRAM AND DISCUSSION.

On the basis of all the results presented in this paper, a constitutional diagram (Fig. 15) has been constructed covering the range from titanium up to FeTi.



It should be recalled that, apart from the eutectic horizontal, the liquidus/solidus region has been studied in only an approximate, exploratory fashion. The experimentally determined solidification ranges recorded in Table II lie below those suggested by the dotted boundaries of the (liq. +  $\beta$ ) field in Fig. 15. The reasons for this will be evident from the discussion in Section II, 3.

Wallbaum <sup>4</sup> has reported that the melting point of a phase designated FeTi is greater than 1600° C., and that there is a eutectic horizontal

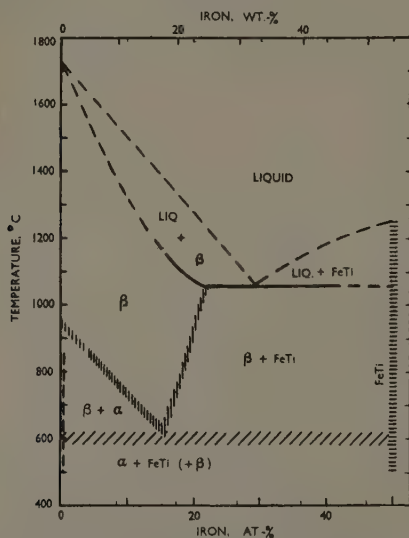


FIG. 15.—Constitutional Diagram Based on Metallographic and X-Ray Investigations.

at about 1580° C. extending from FeTi to a phase FeTi<sub>2</sub>. The present investigation revealed (a) that the melting point of FeTi (approximately 1250° C.) is much lower than the figure reported by Wallbaum, and (b) no evidence of the existence of an intermetallic phase FeTi<sub>2</sub>. Unfortunately, it has not been possible to consult Wallbaum's original article, but it is recorded in abstracts that he employed thermal analysis, and this suggests that his high-titanium specimens may have been seriously contaminated by contact with a refractory crucible.

When all the evidence from X-ray-diffraction experiments and from metallographic studies is considered together, it seems reasonably

certain that at temperatures below 600° C., the  $\beta$  titanium-iron solid solution with 15.5 at.-% iron decomposes by a eutectoid transformation into a mixture of titanium containing less than 0.8 at.-% iron in solid solution and the intermetallic phase FeTi. This phase change is a very sluggish one and might well explain why it has not been possible to produce alloys consisting entirely of the  $(\alpha + \text{FeTi})$  mixture. However, it should be remembered that the constitutional diagram resulting from this investigation does not pertain to a true binary system. There were appreciable quantities of impurities in the alloys studied; hence we are actually concerned with a section through a multi-component system. The effect of the impurities in broadening the  $\alpha \rightleftharpoons \beta$  transformation range in the basis titanium has already been mentioned, and it is possible that the impurities preclude a simple isothermal  $\beta \rightarrow \alpha + \text{FeTi}$  transformation. Even under equilibrium conditions, this change may occur over a range of temperature in alloys of the purity employed in this investigation. Because of this possibility and in view of the sluggishness of the transformation, no sharp eutectoid horizontal has been indicated in Fig. 15; a broad, shaded band has been drawn instead. For the same reasons, the area below the shaded band has been denoted  $\alpha + \text{FeTi} (+ \beta)$ .

One of the most interesting observations made during this investigation is the marked difference between the capacities of  $\alpha$ - and  $\beta$ -titanium to retain iron in solid solution. At present it is difficult to explain this in terms of the theory of alloys. As a matter of interest, it may be noted that the metallic radius of iron is about 14% smaller than that of titanium. Hence, from the standpoint of Hume-Rothery's simple atomic-size rule pertaining to substitutional solid solutions, this pair of metals is in the borderline class. It is evident that in considering the primary titanium-iron solid solutions from a theoretical aspect, considerable importance would have to be given to other factors such as ionic radii, relative volumes per valency electron, and variations of electron distribution among the outer or valency bands.

While a theoretical discussion of the constitutional diagram would be premature at present, it may be appropriate to mention some practical ideas based on a knowledge of the diagram. Alloys containing more than 3.5 at.-% iron may be retained in the  $\beta$  form by quenching from the appropriate temperatures as deduced from Fig. 15. If the quenched alloys are reheated into the  $\alpha + \text{FeTi} (+ \beta)$  field, there will be a tendency for the  $\beta$  solution to decompose into the phases stable at low temperatures. This tendency might well be expected to produce some effects on the mechanical properties of the alloy. In other words, it would seem that the quenched  $\beta$  solid solutions might possibly be

strengthened by heating to some temperature below 600° C. for an appropriate period. This type of effect has been sought for, and obtained, and will be dealt with in a later paper.

#### ACKNOWLEDGEMENTS.

The investigation described in this paper formed part of the programme of the Physical Metallurgy Section, Commonwealth Scientific and Industrial Research Organization, Australia. The work was conducted in the Baillieu Laboratory, University of Melbourne. The author gratefully acknowledges his indebtedness to Professor J. Neill Greenwood and the staff of the Baillieu Laboratory with whom he was able to discuss the investigation from time to time.

The titanium used in making the alloys was kindly provided by the United States Bureau of Mines. Most of the analyses were carried out by Mr. J. A. Corbett, while Mr. J. D. Martin rendered valuable assistance in the metallographic work.

#### REFERENCES.

1. J. Lamort, *Ferrum*, 1914, **11**, 225.
2. H. Witte and H. J. Wallbaum, *Z. Metallkunde*, 1938, **30**, 100.
3. W. Tofaute and A. Büttinghaus, *Arch. Eisenhüttenwesen*, 1938, **12**, 33.
4. H. J. Wallbaum, *Arch. Eisenhüttenwesen*, 1941, **14**, 521.
5. C. M. Craighead, O. W. Simmons, and L. W. Eastwood, *Trans. Amer. Inst. Min. Met. Eng.* (in *J. Metals*), 1950, **188**, 485.
6. J. A. Corbett, *Analyst*, 1950, **75**, 475.
7. W. J. Kroll, *Trans. Electrochem. Soc.*, 1940, **78**, 35.
8. A. E. van Arkel, "Reine Metalle", p. 187. Berlin : 1939 (Julius Springer).

# THE EFFECT OF MOULD MATERIAL AND 1305 ALLOYING ELEMENTS ON METAL/MOULD REACTION IN COPPER-BASE ALLOYS.\*

By N. B. RUTHERFORD,† B.Sc., A.I.M., MEMBER.

(Communication from The British Non-Ferrous Metals Research Association.)

## SYNOPSIS.

When a metal is cast in a sand or other mould in which a steam atmosphere is generated, it reacts with the steam and may absorb hydrogen during the reaction. The term "metal/mould reaction" is used to describe this effect.

The results are described of experiments to determine the influence of different mould materials on the mould reaction in phosphor bronze containing 10% tin and 0.5% phosphorus. The effects of variations in the moisture content and permeability of natural and synthetic sands were examined, as well as the effect of adding mineral- and vegetable-oil, cereal, resin, and cellulose-derivative core binders; mould reaction of varying intensity occurred in all cases. A sprayed mould coating of blacking was found to increase mould reaction when applied to a high-permeability synthetic sand, but to have only a small effect with a low-permeability natural sand. The protection afforded by a coating of aluminium paint varied considerably, but an aluminium-magnesium alloy paint coating prevented reaction with both naturally bonded sand and various core sands. Individual additions were made of bituminous coal, sulphur, ammonium bifluoride, and boric acid to a clay-bonded synthetic sand; of these, the bifluoride produced a high degree of inhibition and the boric acid may have had a very slight inhibiting effect.

The influence of various minor alloying additions on the mould reaction in certain copper-base alloys was also studied. Silicon was found to inhibit mould reaction in lead-free gun-metal containing 0.1% phosphorus, as it does in phosphor bronze. Lead gun-metals containing 0.03% silicon or more yielded castings with poor surfaces and with increased porosity which is attributed to the incidence of mould reaction. In phosphor bronze, mould reaction was inhibited by additions of 0.1% aluminium, 0.5% chromium, 0.1% vanadium, 0.1% boron, and possibly by small amounts (0.01%) of calcium. Running practice would probably need to be modified if additions of aluminium or chromium were adopted on a production scale, and perhaps with vanadium and boron also, because of the formation of tenacious oxide skins. Mould reaction in phosphor bronze was intensified by the addition of 0.5% iron or manganese, or 0.2% magnesium, while additions of 0.5% nickel, 0.1% beryllium, or small amounts of barium or sodium had no effect.

A number of theoretical considerations are discussed.

\* Manuscript received 25 July 1950. The work described in this paper was made available to members of the B.N.F.M.R.A. in a confidential report issued in 1948.

† Research Investigator, British Non-Ferrous Metals Research Association, London.

## I.—INTRODUCTION.

EARLIER work<sup>1-4</sup> carried out by the British Non-Ferrous Metals Research Association has shown that a reaction occurs when certain alloys containing highly oxidizable elements, such as phosphorus in tin bronze or magnesium in aluminium alloys, are cast into sand moulds. The water (combined or free) in the mould is reduced by the element, and atomic hydrogen is liberated at the surface of the casting. Some of this hydrogen is absorbed at the surface and dissolved in the metal. During solidification, a proportion of this dissolved gas is rejected from solution and forms small gas-holes or increases the amount of interdendritic porosity above that which would otherwise have formed from freezing shrinkage only. The term "metal/mould reaction" is used in describing these effects. There is reason to believe<sup>1</sup> that if the oxide film formed on the casting surface in the initial stages of the reaction is impermeable to the reactive element(s), the reaction is stifled and very little gas absorption occurs. On the other hand, if the film is permeable to the atoms of the reactive element(s), the reaction proceeds vigorously and much gas is absorbed. The rate of gas absorption at various stages of cooling in the mould is unknown, but the possibility exists that the expected decrease in this rate with fall of temperature will be partly countered by an increase in the concentration of the reactive element in the residual liquid formed during solidification.

The previous work had shown that the following copper-base alloys absorb gas when sand cast:

(a) Phosphor bronze containing 10% tin and more than about 0.2% phosphorus<sup>3</sup>;

(b) 88 : 10 : 2 and 88 : 8 : 4 Gun-metals and 85 : 5 : 5 : 5 leaded gun-metal, each containing more than about 0.03% residual phosphorus.<sup>1,3</sup> The increased reactivity of these alloys as compared with phosphor bronze is presumably due to their zinc content.

The porosity caused by mould reaction in these alloys reduces the density and tensile properties of well-fed castings, but in inadequately-fed castings the effects may be beneficial. A redistribution of porosity may occur such that the pressure-tightness of the castings is improved and the tensile strength of poorly-fed parts is raised.<sup>1,3,4</sup>

The work that has established these facts has also indicated some means of controlling the reaction. With higher pouring temperatures or residual phosphorus contents the porosity resulting from the reaction is greater.<sup>3,4</sup> It is not reduced by oven-drying green-sand moulds<sup>3</sup>—in fact a slight increase is probable<sup>2,5</sup>—but removal of free and combined

water by baking at 950° C. will suppress the reaction.<sup>3, 5</sup> In phosphor bronze the reaction can be inhibited by the addition of 0.3–0.5% silicon to the metal.<sup>3</sup>

The object of the work described in the present paper was to extend the information available on certain variables that may stimulate the reaction or that may assist in inhibiting or preventing it. The main aspects studied were: (1) the relative extents of mould reaction in phosphor bronzes cast in green and dry clay-bonded sands, with and without various additions and surface washes, and in core sands bonded with a variety of commonly used binders; (2) the effects of various additions to phosphor bronzes, gun-metals, and leaded gun-metals on the extent of the reaction, including experiments on the influence of the simultaneous presence of lead and silicon in copper-base alloys. (It is well known in industry that leaded bronzes contaminated with silicon have coarsely dendritic fractures and poor mechanical properties.)

## II.—EXPERIMENTAL TECHNIQUE.

### 1. *Materials.*

Melts were made from virgin metals of the purity indicated in Table I. Phosphorus, chromium, vanadium, boron, titanium, and zirconium were added as pure copper-base hardeners containing 10–30% of the

TABLE I.—*Materials Used.*

Material	Purity, %	Typical Impurities, %
Cathode copper	99.998	0.001 Ag; 0.0007 S; 0.0001 Ni; trace Pb.
Refined stick tin	99.827	0.065 Pb; 0.028 Sb; 0.022 Cu; 0.025 As; 0.013 Bi; 0.005 Fe; 0.013 Ni; 0.002 Ag.
Phosphor copper containing 15% phosphorus	...	0.04 As; 0.004 Ni and Ag; 0.001 Sb and Sn and Fe; 0.0006 Bi; trace Pb and Si. "
Ingot zinc	99.99+	Not detected: Co, Mn, Zn, Te.
Ingot lead	99.99+	...

element; other minor additions to the various melts were made as the pure metals. Spectrographic examination was used to confirm that the hardeners were not seriously contaminated with other elements.

### 2. *Melting Practice.*

Melting was carried out in gas-injector furnaces of 120- and 60-lb.-copper capacities, using clay-graphite crucibles. Precautions were



taken to prevent contamination of the melt by the crucible and furnace tools, this being especially important in the work described in Section III, 2.

The copper was melted, superheated, and alloyed, and the melt was then degassed with a vigorous stream of nitrogen maintained for 5-7 min.<sup>6</sup> The small additions of phosphor copper to gun-metal, and the other minor additions, were made just before pouring, but the phosphor copper additions to phosphor bronze were made before degassing to avoid the risk of regassing the metal.

Pouring began at 1100° C. for phosphor bronze, unless otherwise stated, and at 1150° C. for lead-free and leaded gun-metals. The

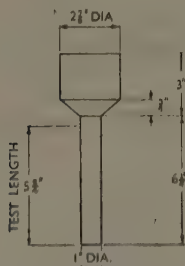


FIG. 1.—1-in.-dia. Test-Bar (D.T.D.-type), as cast; yield approx. 20%.

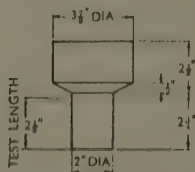


FIG. 2.—2-in.-dia. Test-Bar, as cast; yield approx. 20%.

pouring temperature was measured to within  $\pm 5^\circ$  C. by immersion of a sheathed Chromel/Alumel thermocouple; pouring took 1-3 min. per melt and 5-10 sec. per test-bar (Figs. 1 and 2).

### 3. Moulds.

Particulars of the moulding materials are given in Table II.

In determining whether mould reaction has occurred in a particular casting it is desirable to compare it with a similar one poured into a non-reactive mould (see Section II, 4 (b) below). The complete dehydration of a sand mould by baking at 950° C.<sup>3, 5</sup> is a slow process and even with care results in fragile and friable moulds giving castings with very poor surface finish. During the present work the non-reactive moulds used were made from sillimanite bonded with silica deposited during the hydrolysis of ethyl silicate; this type of mould is thoroughly baked at 1000° C. during production. The moulds were re-dried at 200°-300° C. just before use.

#### 4. *Assessment of Results.*

##### (a) *Test-Bars.*

Cylindrical castings 1 in. and 2 in. in dia., with ample superposed feeders (Figs. 1 and 2), were used for the examination of the amount of porosity arising from mould reaction in well-fed castings of two sizes of section.

##### (b) *Examination of Test-Bars.*

Samples for analysis were taken from the middle casting of each melt.

The appearance of the castings was noted, and the extent of mould reaction was assessed from the amount of porosity they contained. The porosity was determined from :

(i) Density measurements accurate to better than 1 part in 1000; and

(ii) Maximum densities calculated from the formula :

$$\text{Maximum density} = 8.93 - (0.1 \times \% \text{ phosphorus}) - \\ (0.013 \times \% \text{ zinc}) + (0.025 \times \% \text{ lead}).^*$$

Sand castings in the alloys examined inevitably contain small amounts of porosity due to freezing shrinkage,<sup>3</sup> and the main function of the castings made in non-reactive moulds was to verify that the melts were adequately degassed before pouring. This was assumed if the porosity in these castings was of the low order expected from earlier work<sup>3</sup>; the extent of mould reaction was then measured by the total voids in the castings made in reactive moulds. In the present work the porosity in 1-in.- and 2-in.-dia. bars made in sillimanite moulds from thoroughly degassed metal was found to be of the order of 1% and 1.5% respectively (see Table II); the figure for the 1-in. bars agrees well with earlier work.<sup>3</sup> † There is, nevertheless, a variation of the order of  $\pm 0.5\%$  voids in the results for the "blank" castings, which may be due to (a) incomplete degassing, (b) variations in conditions of freezing leading to variations in the amount of shrinkage porosity, or (c) a combination of these factors. Whatever the cause, it is clear that, particularly when comparing castings from different heats, variations in porosity of the order of 0.5% cannot be regarded as significant.

\* This formula is based on previous B.N.F.M.R.A. work and information from other sources,<sup>7,8</sup> and its validity has previously been shown.<sup>1,3,4</sup> In the work described in Section III, 2, no allowance was made for the effect on maximum density of the small amounts of the various addition elements. Additions of tin to copper have little effect on the density.<sup>9</sup>

† 2-in.-dia. castings were not used in the earlier work.

## III.—RESULTS AND DISCUSSION.

1. *Effect of Mould Material (see Table II and Fig. 3).*(a) *General.*

With the exception of a single heat of gun-metal, these tests were made on phosphor bronze containing 10% tin. An examination of the figures in Table II shows that, for this phosphor bronze, the 2-in.-dia. bars were generally less porous than the 1-in.-dia. bars. In each heat the 1-in. bars were cast first. Apparently, therefore, the drop in temperature during pouring, which was of the order of 30°–50° C., together with the higher ratio of volume to surface area for the larger castings, more than counteracted the increase in porosity expected because the slower rate of solidification of the larger bars allows more time for mould reaction to occur.

(b) *Moulding Sands.*

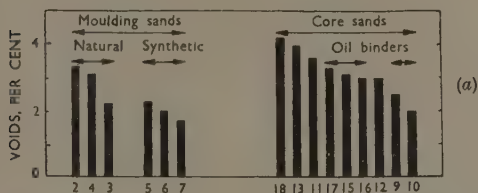
Lines 2, 3, and 4 of Table II, in conjunction with Fig. 3, confirm the view<sup>3</sup> that gas absorption can result from reduction of combined water, and that the moisture in a green-sand mould exerts a chilling effect which tends to suppress the reaction.<sup>5</sup> Thus, castings made in natural sand were more porous when the moulds were dried at 180° C., or contained only 4% moisture, than when the moulds contained 8% moisture. There was little difference between the results from the dried moulds and the moulds made from sand containing 4% moisture. Similarly, with a silica sand bonded with Western bentonite there was little difference between the results from dried moulds and from green moulds made from sand containing 3% moisture (lines 5 and 6).<sup>\*</sup> It thus seems, as might be expected, that the moisture content of a sand has to be above a certain level before it exerts a chilling effect sufficient to reduce the amount of mould-reaction porosity in the final casting.

Reduction of the permeability of the bentonite-bonded synthetic moulding sand from 147 to 71 A.F.S. No. had little effect on the amount of reaction (lines 5 and 7).

Less reaction occurred with the synthetic than with the natural sand, an effect that has been noted by other workers<sup>5</sup> when casting 85 : 5 : 5 : 5 gun-metal.

An incidental check was made, during the work described later, on the effect of the age of the bond; single castings from melts NUY3 and NUZ1 (Table IV) were made in completely new Mansfield sand and the remainder in well-used floor sand. No difference was found in their densities.

<sup>\*</sup> Experiments with an aluminium–10% magnesium alloy gave increased porosity in dried moulds, whether the mould was of Mansfield sand or of silica-bentonite.<sup>2</sup>

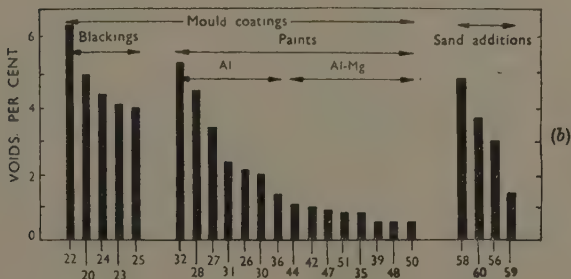


MOULDING SANDS.

CORE SANDS (PARISH'S BASE).

2. Mansfield, 4% moisture.
3. " 8% dried 180° C.
4. " 8% dried 180° C.
5. Parish's, 5% bentonite, 8% moisture.
6. " 8% dried 180° C.
7. As No. 5 + 15% silica powder.

9. 2% linseed oil.
10. 1% " 1% mineral oil.
11. 4% dextrin.
12. 1% proprietary binder A, 2% dextrin.
13. 1.3% " B.
15. 1.2% linseed oil, 0.8% proprietary binder C.
16. 1.2% " 0.8% " D.
17. 2% proprietary binder E.
18. 3.6% " F.



MOULD COATINGS.

- |   |                                     |
|---|-------------------------------------|
| 20. Parish's coated with blacking (iii).              | 30. Mansfield coated with Al paint. |
| 22. " " " (iii), air dried.                           | 31. " " " " " dried 180° C.         |
| 23. Mansfield " " " (i).                              | 32. " " " " " " "                   |
| 24. " " " " (ii).                                     | 35. " " " " Al-Mg paint.            |
| 25. " " " " (iii).                                    | 36. " " " " Al paint.               |
| 26. Mansfield coated with Al paint.                   | 39. " " " " Al-Mg paint.            |
| 27. " " " " " "                                       | 42. " " " " " "                     |
| 28. " " " " " dried 180° C.                           | 44. " " " " " "                     |
| 47. Parish's + 2% linseed oil.                        | } coated with Al-Mg paint.          |
| 48. " + 3.5% proprietary binder F.                    |                                     |
| 50. " + 4% dextrin.                                   |                                     |
| 51. " + 1.2% linseed oil + 0.8% proprietary binder D. |                                     |

ADDITIONS TO PARISH'S SAND.

56. 5% bituminous coal.
58. 5% flowers of sulphur.
59. 5% ammonium bifluoride.
60. 6% boric acid.

FIG. 3.—Mean Values of Porosity from Table II, Plotted to Show Relative Effect of Various Moulding Materials (a) and Mould Coatings and Additions to the Moulding Sand (b).

TABLE II.—*Effect of Mould Material on Metal/Mould Reaction in Phosphor Bronze and Gun-Metal.*

Line Ref. No.	Mould Details					Porosity in Castings, %		Line Ref. No.		
	Material	Type of Bond	Drying Treatment	Moisture, %	Permeability, A.P.S. No.	Green Compression Strength (A.F.S.), lb./in. <sup>2</sup>	Dry Compression Strength (A.F.S.), lb./in. <sup>2</sup>		1-in. Section	2-in. Section
A.—MOULDING SANDS										
<i>Melt HXJ 500 * (9.48% Sn, 0.49% P).</i>										
1	Sillimanite-silica	Silica	See text (p. 192)	...	...	...	...	0.7	1.7	1
2	Mansfield red	Inherent clay	Used green	4.0	...	5.4	...	3.7	2.8	2
3	"	"	16 hr., 180° C.	8.0	19	4.9	...	2.3	2.8	3
4	"	"	Used green	...	40	...	271	3.3	2.8	4
5	Parish's No. 1 washed silica + 5% Western bentonite	Added bentonite	Used green	2.8	147	2.7	...	2.8	1.7	5
6	"	"	16 hr., 180° C.	...	185	...	...	1.5	2.6	6
7	Parish's No. 1 washed silica + 15% of 180-mesh silica powder	"	Used green	...	71	2.5	...	2.3	1.1	7
B.—CORE SANDS										
<i>Melt HXJ 501 * (9.98% Sn, 0.66% P).</i>										
8	Sillimanite-silica	Silica	See text	...	...	...	...	1.1	1.8	8
9	Parish's + 2% linseed oil + 2% water	Seed oil	2 hr., 220° C.	...	255	...	521	2.4	2.5	9
10	Parish's + 1% linseed oil + 1% mineral oil + 2% water	Seed/mineral oil	"	...	266	...	723	1.8	2.1	10
11	Parish's + 4% dextrin + 0.8% water	Cereal	2 hr., 160° C.	...	145	...	723	3.8	3.3	11
12	Parish's + 1% proprietary binder A + 2% dextrin + 2% water	Urea formaldehyde resin/cereal	"	...	358	...	86	3.5	2.4	12
13	Parish's + 7.3% (proprietary binder B: water::1:4.6)	Cellulose glycollic acid + Na <sub>2</sub> SO <sub>4</sub> + NaCl	2 hr., 180° C.	...	265	...	41	4.5	3.5	13
<i>Melt HXJ 502 * (10.44% Sn, 0.48% P).</i>										
14	Sillimanite-silica	Silica	See text	...	...	...	...	...	2.3	14
15	Parish's + 1.2% linseed oil + 0.8% proprietary binder C + 0.7% water	Seed oil/petroleum aromatic extract	2.5 hr., 190° C.	...	170	...	637	3.5	2.6	15
16	Parish's + 1.2% linseed oil + 0.8% proprietary binder D + 0.7% water	"	"	...	200	...	846	3.2	2.8	16
17	Parish's + 2% proprietary binder E	Oil	"	...	135	...	1111	3.8	2.8	17
18	Parish's + 3.5% proprietary binder F	Resin	"	...	180	...	1364	5.3	3.1	18





TABLE II.—*continued.*

Mould Details										Line Ref. No.
Material	Type of Bond	Drying Treatment	Mois- ture, %	Perme- ability, A.F.S., No.	Green Com- pression Strength (A.F.S.), lb./in. <sup>2</sup>	Dry Com- pression Strength (A.F.S.), lb./in. <sup>2</sup>	Porosity in Castings, %			
							1-in. Section	2-in. Section		
C.—MOULD COATINGS (continued)										
Melt H X J 523 (10% + Sn, 0.43% P).	Seed oil Resin Silica Cereal Seed oil/petroleum aromatic extract sprayed with Al-Mg paint	3 hr., 225° C.	...	...	...	...	...	1-0	47	
47 Parish's + 2% linseed oil + 2% water, sprayed with Al-Mg paint		2-5 hr., 190° C.	...	...	...	...	...	0-6	48	
48 Parish's + 3-5% proprietary binder P, sprayed with Al-Mg paint.		See text	...	...	...	...	...	2-1	49	
49 Sillimanite-silica		2-5 hr., 180° C.	...	...	...	...	...	0-6	50	
50 Parish's + 4% dextrin + 0-8% water, sprayed with Al-Mg paint		2-5 hr., 200° C.	...	...	...	...	...	0-9	51	
51 Parish's + 1-2% linseed oil + 0-8% proprietary binder D + 0-7% water, sprayed with Al-Mg paint			...	...	...	...				
Melt J Z L 270 (7-19% Sn, 3-9% Zn, 0-07% P).	... Silica or MgO Inherent clay	Used green	5-0	...	...	...	...	0-6	52	
52 Mansfield sprayed with Al-Mg paint		See text	...	...	...	...	...	0-7	53	
53 Sillimanite		Used green	5-0	...	...	...	...	2-0	54	
54 Mansfield										
D.—ADDITIONS TO THE SAND										
Melt H X J 502* (10-44% Sn, 0-48% P).	Silica Added bentonite	See text	...	...	...	...	...	2-3	55	
55 Sillimanite-silica		Used green	3	...	...	...	...	2-1	56	
56 Parish's + 5% bentonite + 5% bituminous coal										
Melt H X J 516 (10-29% Sn, 0-63% P).	Inherent clay Bentonite " " " Silica	Used green	...	...	...	...	...	5-8	57	
57 Mansfield		"	...	...	...	...	...	5-2	58	
58 Parish's + 5% bentonite + 5% flowers of sulphur		"	...	...	...	...	...	1-3	59	
59 Parish's + 5% bentonite + 5% NH <sub>4</sub> HF <sub>2</sub>		"	...	...	...	...	...	4-5	60	
60 Parish's + 5% bentonite + 6% boric acid		"	...	...	...	...	...	...	0-9	61
61 Sillimanite-silica	See text	...	...	...	...	...	...			

(c) *Core Sands.*

Mould reaction of an order of severity similar to, or slightly higher than, that experienced with the moulding sands occurred with all the core sands. It is noticeable, however, that the sands bonded with oil (lines 9, 10, 15, 16, 17, Table II), whether seed or mineral, produced less porosity than the remainder (excepting one resin).<sup>\*</sup> Hudson also noted <sup>10</sup> that properly dried cores bonded with a linseed oil-dextrin mixture gave "minimum gassing" with phosphor bronze. Reaction with the core sands is presumably due to reduction of combined water and of water released by oxidation of the organic binders. It is also possible that hydrocarbons evolved from the binders are cracked at the metal surface, in which case some of the nascent hydrogen liberated might be absorbed by the casting.

(d) *Mould Coatings.*

A suspension of plumbago in oil or water is frequently used in industry as a mould coating to improve the surface finish of the casting and to facilitate fettling. It is therefore worthy of note that a coating of plumbago in water stimulated metal/mould reaction (lines 20, 22, 23, 24, 25, Table II), especially when applied to a medium-grained sand with a narrow range of grain-sizes and a permeability of about 150 A.F.S. No. (lines 20 and 22), i.e. a relatively open sand to which such coatings might well be applied in practice. The additional moisture on the surface of the black-washed mould might be expected to reduce reaction by exerting a chilling effect, as noted above (Section III, 1 (b)); and, in fact, overnight air-drying of a sprayed mould did cause increased porosity (cf. lines 20 and 22). The results with the black washes are surprising at first sight, for it might be expected <sup>11</sup> that the steam formed in the mould during pouring would react with the carbon at the prevailing temperatures and that the hydrogen liberated would associate to the molecular form before it came in contact with the metal; little gas absorption would then occur (cf. aluminium paint below). It may be that the final products of reaction between the alloy and steam in the absence of blacking—probably phosphates formed from initial oxidation of phosphorus and tin and/or copper <sup>1</sup>—provide partial protection against absorption of hydrogen, but that the

<sup>\*</sup> A comparison of the present results with those obtained on aluminium-10% magnesium alloy cast in similar moulds shows a difference in the orders of reactivity of the core sands. Thus, with the light alloy, the most reactive core was that bonded with a linseed oil/mineral oil mixture and the least reactive that bonded with a proprietary oil (proprietary binder *E* of Table II). Of the remainder, cereal, plain linseed oil, cellulose glycollic acid, and the resins produced more porosity than ordinary moulding sands.<sup>2</sup>

presence of a high concentration of carbon at the casting surface prevents the oxidation of copper and tin and the formation of phosphates,\* and thus leaves the casting with a surface through which hydrogen can be freely absorbed.

The use of a mould coating suggested by Walker<sup>12</sup> as an alternative to blacking has been shown<sup>1</sup> to increase the reaction beyond that occurring in an uncoated mould; the coating solution consists of a suspension of a proprietary mould paint (said to contain silica flour, bentonite, talc, dextrin, and a little plumbago) in shellac dissolved in methylated spirits.

Earlier work<sup>1</sup> had indicated that mould reaction was inhibited if the mould was coated with aluminium paint and, in much of the work described in later sections, "blank" test-bars were made in such moulds. Many of these castings showed unexpectedly high voids and in further experiments bars were cast from the same melts in these moulds and in silica-bonded sillimanite moulds. The results (Table II, lines 27-34, 36-38) indicate that the inhibiting effect of the paint was frequently incomplete; the pouring temperature seems to have had some bearing on this (cf. lines 27 and 30, 28 and 31; the bars were poured in the order given in Table II and mould reaction decreased with the fall in pouring temperature occurring during casting). In subsequent work it has been found that the paint affords no protection to castings of lead-free gun-metal.<sup>15</sup>

It is possible that such inhibition as is afforded by the paint is a result of one or both of the following processes: (i) the formation on the surface of the casting of an alumina film which is impermeable to phosphorus and thus stifles the reaction, and (ii) a sacrificial action in which the aluminium reacts with the water and liberates atomic hydrogen, which—not being in immediate proximity to the metal surface, as is assumed in the reaction of water with the phosphorus in the casting—associates and forms a blanket of molecular hydrogen, which is known to dissolve relatively slowly. Of these, the second process was considered the more likely, since no sign of alumina films was visible on cast surfaces, and spectrographic analysis detected no aluminium in metal that had been repeatedly remelted and poured into aluminium-sprayed moulds.<sup>1</sup> This view suggested that inhibition might be more complete if a material were used that would react with the water more vigorously and, in particular, for longer times than the aluminium, bearing in mind that the reaction might be rapidly stifled

\* The free energies of formation of the oxides at 1100° C.<sup>13, 14</sup> support this explanation.  $\Delta G^\circ_{1373}$ : CO, 111; H<sub>2</sub>O, 82; P<sub>2</sub>O<sub>5</sub>, 80; SnO<sub>2</sub>, 73; SnO, 68; Cu<sub>2</sub>O, 38 kg.cal./mole of oxygen.

by the alumina films formed on the particles of aluminium in the paint. Some support for this theory is provided by the results given in lines 27 and 28 and 30 and 31 (Table II); sprayed moulds proved more reactive after drying at 180° C. than when green, a fact that could be explained by increased passivity of the aluminium caused by the formation of alumina during drying.

An aluminium-35% magnesium alloy was therefore reduced to 100-mesh powder by grinding, and sprayed on moulds in the same resinous carrier as that used for the aluminium paint. The first result obtained showed that the aluminium-magnesium paint produced a high degree of inhibition (cf. lines 35, 36, and 38). Four further melts were made, and the results from these (lines 39-54) not only confirmed that the paint prevented reaction between phosphor bronze and Mansfield sand, but also showed that it was equally effective with various core sands and with 88 : 8 : 4 gun-metal containing nominally 0.1% phosphorus. In some later experiments it has been shown that 85 : 5 : 5 : 5 leaded gun-metal containing nominally 0.1% phosphorus is similarly protected.<sup>15</sup>\*

Castings made in moulds dressed with either aluminium or aluminium-magnesium paint are covered with a black sand layer on stripping, due, presumably, to deposition of carbon from the liquid component of the paint; there is less burning-on of sand, however, and the castings clean easily and then show a good surface.

#### (e) *Additions to the Sand.*

In contrast to the stimulating effect of the high concentration of carbon at the casting surface provided by a mould coat of blacking (see Section III, 1 (d)), an addition of bituminous coal to Parish's sand had little effect on the extent of metal/mould reaction (cf. lines 20, 22, and 56, with 5, Table II).

Sulphur in the sand is known<sup>1</sup> to intensify mould reaction in an aluminium-10% magnesium alloy, whereas the presence of 6% boric acid will prevent it, at least in 2-in.-dia. sections.<sup>2</sup> Addition of sulphur or boric acid to the sand had no marked influence on mould reaction in phosphor bronze (lines 58 and 60), though the boric acid may have effected slight inhibition. The castings from the sulphur sand had a very poor surface.

The most interesting result produced by additions to the sand was that caused by 5% ammonium bifluoride, which prevents reaction in

\* The paint used in these experiments, which was made at the request of the B.N.F.M.R.A., is available commercially; it consists of 200-mesh aluminium-45% magnesium powder in the resinous carrier mentioned in the text.

the light alloy.<sup>1</sup> The top surfaces of the feeder heads of phosphor bronze castings made in this sand did not show the usual covering of "cauliflower" oxide (see Fig. 4 (b), Plate XXIX) and the cast faces were quite free from sand and were of a deep red-gold colour. The appearance of the castings suggested that the ammonium bifluoride might have inhibited mould reaction, and the density determinations confirmed this (Table II, line 59). In the case of the light alloy, the inhibition has been ascribed to the formation of impermeable films of the more stable magnesium fluoride in preference to relatively permeable films of the less stable magnesia.<sup>1</sup> If the fluorides of phosphorus are more stable than the oxides, the phosphorus in the bronze might form volatile fluorides instead of reducing the steam. Alternatively, protection might be afforded by a blanket of volatilized ammonium bifluoride.

An undesirable feature of this method of inhibiting metal/mould reaction is that volumes of white fumes, probably containing hydrogen fluoride, are evolved during casting.

## 2. *Effect of Additions to Copper-Base Alloys.*

The results to be described were obtained using green moulds made from Mansfield red sand containing 4-5% moisture.

### (a) *Silicon and Lead in Gun-Metals.*

Silicon has been shown to inhibit mould reaction in phosphor bronze.<sup>3</sup> In the present work, additions of 0.1% and 0.5% silicon were made to 88:8:4 gun-metal containing 0.1% phosphorus, to see whether silicon was similarly effective with this alloy. The results (lines 1-9, Table III) indicate that silicon does inhibit reaction in this gun-metal. The surprising feature is that the silicon appears to be more effective in the larger sections than in the smaller; whereas 0.1% silicon was a sufficient addition with the 2-in.-dia. bars, even 0.5% did not completely inhibit reaction in the 1-in. bars. This unexpected result cannot readily be explained by the lower pouring temperature of the 2-in. bars (they were again cast after the 1-in. bars), for in the absence of silicon they proved much more porous than the 1-in. bars (lines 1-3, Table III). With 0.5% silicon a tenacious oxide skin, similar to that on aluminium bronze was present on the molten alloy and on the heads of the castings (Fig. 5 (a), Plate XXX).<sup>4</sup>

The effect of silicon contamination of leaded gun-metal was examined by adding up to 0.1% silicon (nominal) to a "phosphorus-free" 85:5:5:5 alloy. The cleanliness of the molten metal appeared to improve with increasing silicon content, but castings poured from

TABLE III.—The Effect of Lead and Silicon on Mould Reaction in Copper-Base Alloys.

Line Ref. No.	Melt No.	Analysed Composition					Mould Material*	Porosity in Castings, %		Remarks	Line Ref. No.	
		Cu, %	Sn, %	Zn, % (diff.)	Pb, %	P, %		Si, %	1-in. Section			2-in. Section
A.—INHIBITION OF LEAD-FREE GUN-METAL WITH SILICON												
1	JZL 268	88.1	7.99	3.9	...	0.063	...	{ M S M S M M S M M	2.6	4.4	{ No silicon addition; normal melt and castings. Normal melt and castings. Melt covered by tenacious skin. No dross formed on heads.	1
2									0.9	1.6		2
3									2.1	3.9		3
4	JZL 258	88.4	8.65	2.7	...	0.089	0.12	{ S M M S M M	1.3	1.4	{ Normal melt and castings.	4
5									3.1	0.9		5
6									2.5	0.9		6
7	JZL 258	86.7	9.33	3.4	...	0.087	0.49	{ S M M	2.0	1.3	{ Melt covered by tenacious skin. No dross formed on heads.	7
8									2.6	1.2		8
9									2.7	1.2		9
B.—ALLOWABLE SILICON CONTAMINATION IN LEADED GUN-METAL												
10	NTY	85.0	4.98	5.3	4.71	Not detected	0.006	{ M	1.2	2.8	{ Clean castings (Fig. 5(b), Plate XXX).	10
12	1/4							{ M	1.1	2.8		12
13	NTY	85.9	4.87	4.9	4.31	"	0.009	{ M	0.9	1.9		13
15	1/10							{ M	0.8	1.8	{ Castings covered with white film; a number of small surface inclusions present. Heads mainly smooth (Fig. 5(c), Plate XXX).	15
16	NTY	85.5	5.28	4.4	4.79	0.0007	0.03	{ M	2.2	3.4		16
18	2/4							{ M	3.2	3.3		18
19	NTY	85.1	5.38	4.5	4.95	0.0007	0.07	{ M	3.0	4.0		19
21	2/10							{ M	3.3	3.7		21

\* M = Green Mansfield sand mould. S = Sillimanite-silica mould.



metal containing 0.03% silicon or more were coated with a non-adherent white film and had a number of small but rather deep surface inclusions (Fig. 5 (c), Plate XXX). At the same silicon content a noticeable increase in the amount of porosity in the castings occurred (Table III, Section B). Since copper will take over 4% silicon into solution,<sup>16</sup> it is unlikely that there is a sudden change in the mode of solidification of the experimental castings to which the increased porosity might be attributed, and it therefore seems probable that this porosity is caused by mould reaction. Thus, the known deleterious effect on the mechanical properties of leaded gun-metal caused by contamination of the alloy with small amounts of silicon may be attributed, at least partly, to increased porosity arising from mould reaction. It was thought that the incidence of mould reaction might be due to the formation at the surface of the casting of lead silicate. Lead silicate is a thin fluid at the temperature of pouring and, with its good solvent powers, might be expected to leave the surface of the casting largely free to absorb hydrogen. However, an X-ray examination of the white powder scraped from the cold castings failed to reveal the presence of any lead; the powder consisted mainly of zinc oxide, with some silica as  $\alpha$ -quartz and traces of cupric oxide, stannic oxide, and zinc silicate.

(b) *Other Elements in Phosphor Bronze (10% Sn, 0.5% P).*

In industrial practice it is often possible to use the metal/mould reaction to improve the soundness of otherwise inadequately-fed parts of castings<sup>1</sup>; in other cases the reaction must be avoided if satisfactory castings are to be obtained. It is therefore most desirable to know which alloying elements stimulate and which stifle the reaction.

According to the theory outlined in Section I, the effects of small additions of other elements to phosphor bronze will be determined by their effect on the film formed at the surface of the casting. If this film is a simple oxide of the most reactive element in the alloy, it should be possible to predict the effect of a given element by considering: (i) the affinity of the element for oxygen at the prevailing temperatures (800°–1100° C.); and (ii) the nature of the oxide of the element, particularly the ratio between the volume of the oxide and the volume of the metal from which it is formed (the Pilling-Bedworth ratio); provided that this ratio is greater than unity the oxide film formed on the pure metal is dense and, compared to the porous films found when the ratio is less than unity, relatively impermeable.<sup>17</sup>

In fact, it is likely that the film formed on the surface of the casting is a complex one, and predictions on the basis of the above theory may then be invalid. Further, the reactive element is present only in



FIG. 4.—“As-Stripped” Heads of Phosphor Bronze Castings (10% Tin, 0.5% Phosphorus, Showing (a) and (b) Effects of Additions to Moulding Sand, and (c)-(l) Effects of Small Additions of Other Elements to Bronze.

a	Cast in boric acid sand.	g	Bronze without additions.
b	Cast in ammonium hydroxide sand.	h	0.05% manganese added to bronze.
c	0.1% aluminium added to bronze.	i	0.05% magnesium "
d	0.1% beryllium "	j	0.05% iron "
e	0.05% chromium "		
f	0.1% zirconium "		

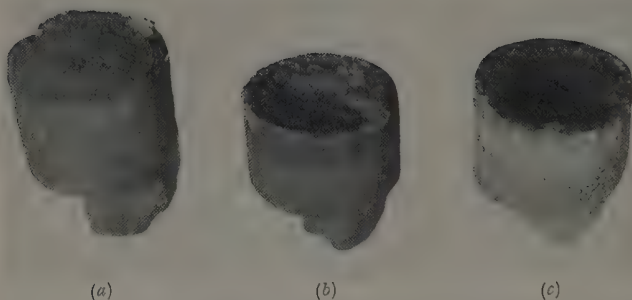


FIG. 5.—“ As-Stripped ” Heads of Gun-Metal Castings, Showing Effect of Small Amounts of Silicon.

- (a) 88 : 8 : 4 gun-metal + 0.5% silicon.  
 (b) Normal 85 : 5 : 5 gun-metal.  
 (c)     "         "         "         + 0.1% silicon.

TABLE IV.—*Effect of Small Amounts of Added Elements on Metal/Mould Reaction in Phosphor Bronze\* Cast into Green Mansfield Sand Moulds.*

Melt No.	Composition, %			Porosity in Castings, %			Remarks
	Nominal	Analysed		1-in. Section	2-in. Section	Mean	
	Added Element	Added Element	P				
GROUP A: ELEMENTS EXPECTED TO INHIBIT MOULD REACTION ( $-\Delta G^{\circ}_{1373}$ (Oxide) $> -\Delta G^{\circ}_{1373}$ ( $P_2O_5$ or $H_2O$ ) and Filling-Bedworth ratio $> 1$ ).							
NUX2	0.01 Al	0.01 Al	0.58	4.0 3.8	2.8 2.6	3.3	Small amount of dross formed on melt surface, but no continuous skin. Castings of normal appearance.
NUX3	0.10 Al	0.09 Al	0.52	1.3 1.6	1.9 1.9	1.7	Skin formed over melt when aluminium added. No "cauliflower" oxide on surfaces of heads of castings. Cast surfaces clean except for a few oxide laps near tops of heads (see Fig. 4(c), Plate XXIX).
NUK1	0.01 Be	N.A.	0.58	2.6 2.7	2.1 2.2	2.4	Melt and castings normal.
NUK2	0.10 Be	0.10 Be	0.57	3.1 2.9	3.7 3.3	3.2	As for NUX3. Castings silver-gold colour (Fig. 4(d)).
NUK3	0.10 Be	N.A.	0.52	3.0 2.8	3.3 3.3	3.1	As for NUK2.
NUK4	0.10 Be	N.A.	0.60	2.3	2.9 3.1	2.7	As for NUK2.
NXS1	0.09 B	0.01 B	0.48	0.9 1.0	1.3 2.7	1.5	Tenacious skin formed over melt when boron added; pouring stream fairly clean. Heads smooth; some small oxide folds.
NUY2	0.05 Cr	0.02 Cr	0.53	4.2 3.1	3.5 2.3	3.5	Melt and castings normal.
NUY3	0.50 Cr	0.32 Cr	0.51	0.5 0.5	0.9 1.6	0.9	As for NUX3, but more laps in heads. Castings silver-green in appearance (Fig. 4(e)).
NVD1	0.50 Fe	0.46 Fe	0.42	5.2 4.8	6.4 6.4	5.7	Tin sweat on heads of castings. Small explosion in one casting when head nearly solid (4.8% voids) (Fig. 4(f)).
NUZ1	0.50 Mn	0.35 Mn	0.52	6.5 6.2	5.8 5.8	6.1	Severe tin sweat on heads of castings. Oxide on heads but not of the "cauliflower" type (Fig. 4(h)).
NXR1	0.10 V	0.005 V approx.	0.47	0.6 0.6	0.7 0.8	0.7	Skin formed over melt when vanadium added; broke up into pouring stream. Some "cauliflower" oxide on heads and some small folds.
NXP1	0.10 Ti	0.024 Ti	0.46	3.6 3.8	2.9 2.5	3.2	Light skin formed on melt when titanium added. Castings normal.
NVE1	0.01 Zr	N.A.	0.48	2.2 2.0	2.8 2.3	2.3	Tendency towards formation of skin on melt. Castings normal but slightly less oxide on heads.
NVE2	0.10 Zr	0.04 Zr	0.37	1.1 0.9	3.2 2.5	1.9	Skin formed over melt when zirconium added. Tops of heads oxidized but smooth (Fig. 4(f)).

TABLE IV.—*continued.*

Melt No.	Composition, %			Porosity in Castings, %			Remarks
	Nominal	Analysed		1-in. Section	2-in. Section	Mean	
		Added Element	Added Element				
GROUP B: ELEMENTS EXPECTED TO INTENSIFY MOULD REACTION (- $\Delta G^{\circ}_{1972}$ (oxide) > - $\Delta G^{\circ}_{1972}$ ( $P_2O_5$ or $H_2O$ ) and Pilling-Bedworth ratio < 1).							
NVH1	0.08 Ba	†	0.48	1.9 1.3	2.6 3.0	2.2	Non-continuous dross formed on melt surface when barium added, but part gradually dissolved; remainder skimmed off. Castings normal.
NVG2	0.01 Ca	†	0.48	1.4 1.6	2.2 2.2	1.9	Some fluffy dross formed on addition of calcium skimmed off. Castings normal.
NVG1	0.10 Ca	†	0.44	3.8 3.5	3.2 2.9	3.3	Fluffy dross formed on addition of calcium. Castings normal.
NUB1	0.05 Mg See footnote †	0.008 Mg	0.48	2.2 2.1	2.1 2.1	2.4	Normal. Couple contaminated during use and casting temperature probably about 1060° C. according to subsequent check.
NVF1	0.10 Na	†	0.52	3.5 3.2	4.8 4.0	3.9	Tin sweat on head of one casting; edges of this head and of one other free from black oxide.
GROUP C: ELEMENTS NOT EXPECTED TO AFFECT MOULD REACTION (- $\Delta G^{\circ}_{1972}$ (oxide) < - $\Delta G^{\circ}_{1972}$ ( $P_2O_5$ or $H_2O$ ) and Pilling-Bedworth ratio < 1).							
NVO1	0.50 Ni	0.61 Ni	0.56	4.0 2.9	4.6 2.9	3.6	Normal.

N.A. = Not analysed.

\* Containing nominally 10% tin and 0.5% phosphorus.

† Spectrographic comparison indicated (i) that the relative amounts of calcium and barium present were in accord with the nominal additions; and (ii) that there was about 10 times as much sodium present as in a normal melt.

‡ Alloys with additions of 0.2 or 0.5% magnesium reacted vigorously (see Fig. 4 (i), Plate XXIX), the castings being grossly unsound and having a soft oxide layer about  $\frac{1}{8}$  in. thick. Earlier tests<sup>1</sup> with 0.2% magnesium added gave results comparable with that in Table IV for an alloy with 0.05% magnesium added.

relatively small amounts and in solution; therefore its activity may be less than unity. In addition, it is conceivable that any other element present may cause mould reaction because it diffuses more rapidly than the most reactive element through whatever film is formed initially on the casting.

For lack of a better basis, however, the probable effects of individual additions of numerous elements have been classified into three groups on the above lines, some account being taken of melting point and volatility, but not of the (largely unknown) activities of the elements in copper-base solutions. The amounts of porosity found in castings poured from phosphor bronze heats containing small additions of ele-





the amounts of porosity in the 1-in. and 2-in. bar castings were more nearly equal than in the test described in Section III, 1. Consequently, the figures for the two bars have been averaged before comparison on the above basis.

The results in Table IV show that the basis on which the elements had been grouped was unsound. For example, silicon,<sup>3</sup> aluminium, chromium, vanadium, and boron (see Table IV) had an inhibiting effect, as predicted, but zinc,<sup>1,3,4</sup> manganese,<sup>1</sup> and iron stimulated the reaction instead of inhibiting it. Again, beryllium, titanium, and zirconium exercised no effect, whereas inhibition was expected (the low figure for voids in the castings containing 0.1% zirconium is no doubt a result of the lower phosphorus content of these castings compared with the others). Of the elements predicted as stimulating the reaction, magnesium had the expected effect when more than 0.2% (nominal) was present (see footnote to Table IV), but barium, calcium, and sodium did not. In fact, barium and small amounts of calcium may have had a slight inhibiting influence, though in the aluminium-magnesium alloys they appear to be deleterious.<sup>1,2</sup> Of the elements unlikely to affect the reaction, only lead and nickel have been examined. In earlier work lead had no effect (cf. leaded and lead-free gun-metals<sup>1,3,4</sup>) and nickel contents greater than 2% produced a small inhibiting influence.<sup>1</sup> The 0.5% nickel addition made in the present work had no effect; the influence of lead was not re-examined.

The surfaces of the castings containing aluminium, beryllium, chromium, vanadium, and boron were very smooth, and exhibited tenacious oxide films. With one exception, beryllium, this was associated with inhibition. Small folds of oxide were evident on the heads of the castings, and special running techniques would probably be required in practice in order to avoid entrapped oxide.

The result with beryllium was a little unexpected, especially as small additions of this element to the aluminium-10% magnesium alloy were known to confer protection from mould reaction.<sup>1,2</sup> However, a repetition of the melt containing 0.1% beryllium produced confirmatory results (melt NUK3, Table IV). It was thought that the beryllium addition might be introducing gas into the melt, but a further heat in which the beryllium was added before instead of after degassing gave similar figures (melt NUK4, Table IV). Since the film on molten aluminium-10% magnesium alloy containing 0.1% beryllium is known to contain beryllia,<sup>1</sup> it is not unreasonable to assume that this is also present in the film on castings of the alloy and, further, that the different appearance of bronze melts and castings with and without additions of beryllium is caused by the absence or presence of beryllia. The ionic

radius of  $P^{5+}$  (0.3–0.4 Å.) is similar to that of  $Be^{++}$  (0.34 Å.), but that of  $Mg^{++}$  (0.78 Å.) is twice that of  $Be^{++}$  and, on this ground, phosphorus might be expected to replace beryllium in a lattice with relative ease.\* It seems therefore that the difference between the protection against metal/mould reaction afforded by the addition of beryllium to the light alloy and to the bronze might be ascribed to greatly varying rates of diffusion of magnesium or phosphorus through the films formed on the melts and castings.

#### IV.—CONCLUSIONS.

The conclusions to be drawn from the work reported above may be summarized as follows :

(1) Reaction will occur between the metal and the mould when phosphor bronze is poured into natural and synthetic moulding sands or core sands bonded with vegetable or mineral oils, cereals, synthetic resins, or cellulose glycollic acid.

(2) The use of a mould coating of plumbago and water on a high-permeability synthetic moulding sand is likely to intensify the reaction.

(3) A mould coating of aluminium paint produces a variable degree of inhibition. Excellent protection is afforded by a coating of aluminium–magnesium alloy paint on various moulding and core sands, for castings both of phosphor bronze and of gun-metal containing residual phosphorus in excess of 0.03%.

(4) Metal/mould reaction may be almost completely inhibited in phosphor bronze by the addition of 5% ammonium bifluoride to a synthetic moulding sand.

(5) The addition of 0.5% silicon to 88 : 8 : 4 gun-metal containing 0.1% phosphorus will inhibit mould reaction.

(6) More than 0.02% silicon in 85 : 5 : 5 : 5 leaded gun-metal is undesirable ; mould reaction is promoted and the surface of the castings is badly affected.

(7) Nominal additions of 0.1% aluminium, 0.5% chromium, 0.1% vanadium, 0.1% boron, and possibly small amounts (0.01%) of calcium, will inhibit mould reaction in 10% tin bronze containing 0.5% phosphorus. It is probable that pouring and moulding practice would require modification if additions of aluminium and chromium and, possibly, vanadium and boron were used commercially.

(8) Nominal additions of 0.5% iron or manganese, or 0.2% magnesium, will intensify the reaction.

(9) The reaction is unaffected by small additions of nickel, beryllium, titanium, zirconium, barium, or sodium.

\* These ionic radii are for six-fold co-ordination.<sup>18</sup>

## ACKNOWLEDGEMENTS.

The author is indebted to the Director and Council of the British Non-Ferrous Metals Research Association for permission to publish this paper, and to Dr. A. G. Quarrell, Mr. W. A. Baker, and other members of the Association's staff for helpful discussion.

## REFERENCES.

1. B.N.F.M.R.A. confidential reports.
2. B. W. Peck, *B.N.F.M.R.A. Research Rep.* No. R.R.A. 806, 1948.
3. W. A. Baker, F. C. Child, and W. H. Glaisher, *J. Inst. Metals*, 1944, **70**, 373.
4. W. H. Glaisher, *J. Inst. Metals*, 1949-50, **76**, (4), 377.
5. L. W. Eastwood and J. G. Kura, *Foundry*, 1947, **75**, (10), 86.
6. W. A. Baker and F. C. Child, *J. Inst. Metals*, 1944, **70**, 349.
7. D. Hanson, S. L. Archbutt, and Grace W. Ford, *J. Inst. Metals*, 1930, **43**, 41.
8. E. A. Owen and Ll. Pickup, *J. Inst. Metals*, 1934, **55**, 215.
9. N. P. Allen and S. M. Puddephat, *J. Inst. Metals*, 1935, **57**, 79.
10. F. Hudson, *Foundry*, 1948, **76**, (3), 86.
11. H. J. T. Ellingham, *J. Soc. Chem. Ind.*, 1944, **63**, 125.
12. K. E. Walker, *Found. Trade J.*, 1943, **69**, 30.
13. F. D. Richardson and J. H. E. Jeffes, *J. Iron Steel Inst.*, 1948, **160**, 261.
14. U.S. National Bureau of Standards, "Selected Values of Chemical Thermodynamic Properties." Washington, D.C. : 1949 (U.S. Government Printing Office).
15. N. B. Rutherford, *B.N.F.M.R.A. Research Rep.* No. R.R.A. 804, 1948.
16. C. J. Smithells, "Metals Reference Book," p. 314. London : 1949 (Butterworths Scientific Publications).
17. N. B. Pilling and R. E. Bedworth, *J. Inst. Metals*, 1923, **29**, 529.
18. R. C. Evans, "An Introduction to Crystal Chemistry," p. 171. Cambridge : 1939 (University Press).

# THE INTERMETALLIC COMPOUNDS IN THE 1306 ALLOYS OF ALUMINIUM AND SILICON WITH CHROMIUM, MANGANESE, IRON, COBALT, AND NICKEL.\*

By J. N. PRATT,† B.Sc., Ph.D., and PROFESSOR G. V. RAYNOR,‡ M.A., D.Sc.,  
MEMBER OF COUNCIL.

## SYNOPSIS.

In further examination of the alloying behaviour of transitional metals in aluminium-rich alloys, a study has been made of the intermetallic compounds which occur in the ternary aluminium-rich alloys of aluminium and silicon with transitional metals of the first long period. Pure samples of the compounds have been extracted from suitably heat-treated alloys, and submitted to chemical analysis and metallographic X-ray examination. The following ternary compounds have been characterized:

(i)  $\alpha(\text{MnSi})$ , with a range of homogeneity from 29% manganese and 8.5% silicon to 27% manganese and 12.5% silicon.

(ii)  $\beta(\text{MnSi})$ , with compositions lying in the range 37–33.7% manganese and 5–7.7% silicon.

(iii)  $\alpha(\text{FeSi})$ , containing approximately 32.5% iron and 8.5–10.5% silicon.

(iv)  $\beta(\text{FeSi})$ , with approximately 27% iron and 13.8–15% silicon.

(v)  $\alpha(\text{CrSi})$ , containing approximately 30.5% chromium and 17.5% silicon.

(vi)  $\beta(\text{CrSi})$ , a compound, based on  $\text{CrSi}_2$ , containing approximately 45% chromium and 42% silicon.

No ternary compounds occur in the aluminium-cobalt-silicon and aluminium-nickel-silicon systems, but  $\text{Co}_2\text{Al}_3$  dissolves appreciable amounts of silicon. The solubility of silicon in  $\text{NiAl}_3$  is restricted.

Determinations have been made of the projections of the surfaces of primary separation on to the base of the equilibrium model for the systems aluminium-silicon and aluminium-chromium-silicon. In the latter, considerable differences from the diagram proposed by Mondolfo ("Metallography of Aluminium Alloys," New York: 1943) were observed. In both systems the results were checked by annealing experiments in the solid state.

## I.—INTRODUCTION.

IN recent years, the constitutions of a number of aluminium-rich ternary alloys containing one or two transitional metals of the first long period as solutes have been studied. This work was undertaken to gain information of the alloying behaviour of transitional metals present in relatively small amounts in association with a solvent metal of high valency. The main conclusions from the work already carried out<sup>1</sup> are that, when associated with an excess of a metal of high valency

\* Manuscript received 25 July 1950.

† Research Fellow, University of Birmingham.

‡ Professor of Metal Physics, University of Birmingham.

(e.g. aluminium), transitional metals tend to absorb electrons supplied to the structure as a whole by the solvent atoms. In addition, the binary and ternary intermetallic compounds formed in aluminium-rich alloys have many of the characteristics of electron compounds, in so far as their compositions, and to some extent their crystal structures, depend upon the establishment of definite electron : atom ratios, if these are calculated on the assumption that the number of electrons accepted by the transitional metal atom is closely similar to the number of vacancies for electrons in the "atomic orbitals" postulated by the Pauling hypothesis concerning the electronic structure of transitional metals.<sup>2</sup> The numbers of electrons accepted per atom are thus somewhat greater than would be expected from strict application of the band theory of transitional metals.<sup>3</sup>

By the application of these ideas, interesting regularities between the equilibrium diagrams of several aluminium-base ternary and quaternary alloy systems have been observed. During this work, aluminium-rich systems were examined which contained two transitional metals, or in which one solute was a transitional metal and the other a non-transitional metal of valency not greater than two. It was of interest, therefore, to examine cases in which one solute was a transitional metal, and the other a quadrivalent element. Of the quadrivalent elements, silicon appeared to be the most suitable for theoretical reasons; this choice had the additional advantage that information would be obtained on the compositions and general characteristics of the intermetallic compounds occurring in certain technically important aluminium-rich alloys.

Accordingly, a detailed examination was made of the alloys of aluminium and silicon with chromium, manganese, iron, cobalt, and nickel, with particular emphasis on the characterization of the intermetallic compounds formed. Wherever possible, pure samples of the compounds were extracted for examination, and micrographic and X-ray studies have been carried out where necessary.

## II.—PREVIOUS WORK ON THE ALLOY SYSTEMS.

A considerable amount of metallographic and thermal work has been carried out on some of the alloys considered in this paper, and may be summarized as follows :

### 1. *The Binary Systems.*

The equilibrium diagrams of the binary alloys relevant to the present work are reproduced as Figs. 1-6. All are well established, and little comment is necessary, except in relation to the phases  $\text{FeAl}_3$  and  $\text{Co}_2\text{Al}_9$ . According to the X-ray work of Bradley and Taylor,<sup>9</sup>  $\text{FeAl}_3$  decomposes on slow cooling into  $\text{Fe}_2\text{Al}_5$  and  $\text{Fe}_2\text{Al}_7$ . The trans-

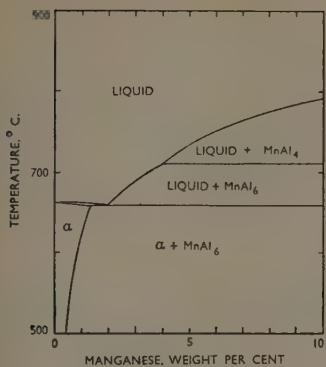


FIG. 1.—Al-Mn.<sup>4, 5, 6</sup>

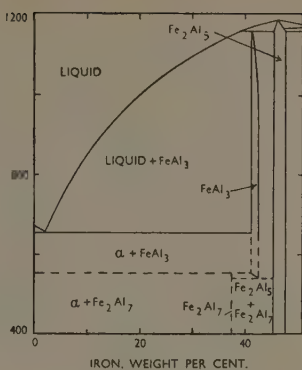


FIG. 2.—Al-Fe.<sup>7-10</sup>

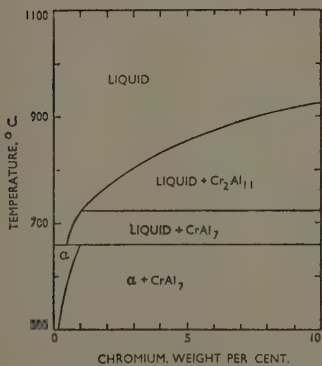


FIG. 3.—Al-Cr.<sup>11-15</sup>

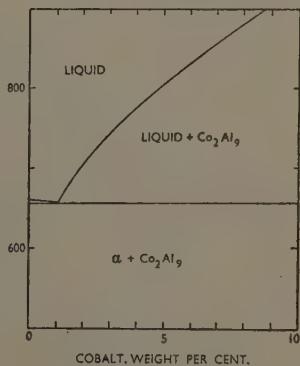


FIG. 4.—Al-Co.<sup>16</sup>

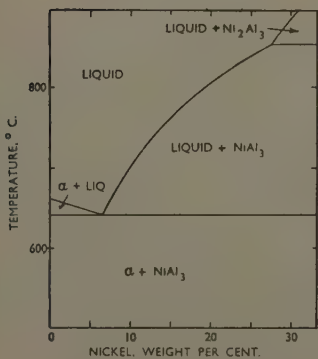


FIG. 5.—Al-Ni.<sup>17-19</sup>

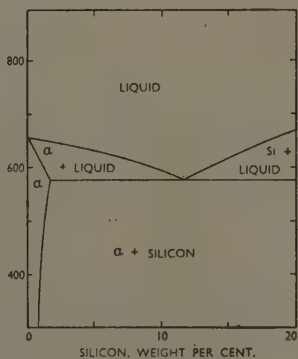


FIG. 6.—Al-Si.

FIGS. 1-6.—Equilibrium Diagrams of Aluminium-Rich Alloys.



formation temperature, though below  $600^{\circ}\text{C.}$ , is not accurately known, and is indicated by broken lines in Fig. 2. In the case of  $\text{Co}_2\text{Al}_9$ , careful analysis of extracted crystals <sup>1(c)</sup> shows that this phase contains slightly more cobalt than the formula indicates; the recent crystallographic work of Douglas,<sup>20</sup> however, makes it clear that the compound is based essentially upon the ratio  $9\text{Al} : 2\text{Co}$ .

## 2. The Ternary Systems.

### (a) Aluminium-Manganese-Silicon.

This system has been investigated by Bückle<sup>21</sup> and by Phillips<sup>22</sup> and is of some complexity. The projections of the liquidus surfaces due to the two workers are given in Figs. 7 and 8. In addition to the binary phases, Bückle reports three ternary phases: *T*, a phase of variable composition containing approximately 40% manganese and 15% silicon, and *X* and *Y* which were not examined in detail, although it was suggested that *X* might be a solid solution of silicon in  $\text{MnAl}_3$ . Phillips reports two ternary phases, denoted  $\alpha(\text{MnSi})$  and  $\beta(\text{MnSi})$ , which correspond respectively with Bückle's *T* and *X*.  $\alpha(\text{MnSi})$ , which comes into equilibrium with the primary solid solution, may be formed peritectically from  $\text{MnAl}_3$  or from  $\beta(\text{MnSi})$ , and forms a ternary eutectic with aluminium and silicon.  $\beta(\text{MnSi})$  reacts peritectically with the liquid to give  $\text{MnAl}_3$  or  $\alpha(\text{MnSi})$ , but there is no peritectic change of  $\beta(\text{MnSi})$  into  $\text{MnAl}_3$  as suggested by Bückle; the relationship is of the eutectic type, and it is, therefore, improbable that  $\beta(\text{MnSi})$  is based upon any of the binary aluminium-manganese compounds.

Apart from Bückle's estimate of the composition of  $\alpha(\text{MnSi})$ , the only information with regard to composition is given by Phragmén,<sup>23</sup> who isolated a phase containing 26.6% manganese and 8.0% silicon. Under the conditions of his experiments, this phase should also be  $\alpha(\text{MnSi})$ , so that considerable difference of opinion is shown.\*

### (b) Aluminium-Iron-Silicon.

A considerable amount of work has been carried out on these alloys, and confusion existed, at the beginning of this research, as to the nature of the ternary compounds formed. The most reliable projection of the liquidus surfaces is due to Phillips and Varley<sup>24</sup> (Fig. 9). Two ternary compounds exist within the composition range studied;  $\alpha(\text{FeSi})$  is formed peritectically from  $\text{FeAl}_3$ , and in turn reacts with the liquid to produce  $\beta(\text{FeSi})$ . This work is in general agreement with the earlier researches of Gwyer and Phillips,<sup>25</sup> who also found two other ternary compounds which occur at silicon contents greater than that corresponding to the ternary eutectic and are, therefore, of no direct concern to the

\* The work of Phragmén was not published until the present work had been completed.

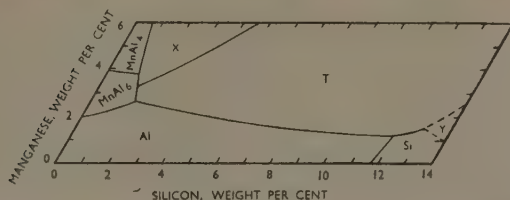


FIG. 7.—The Surfaces of Primary Separation in the Aluminium-Manganese-Silicon System (*Buckle*).

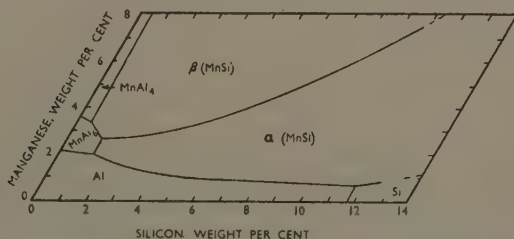


FIG. 8.—The Surfaces of Primary Separation in the Aluminium-Manganese-Silicon System (*Phillips*).

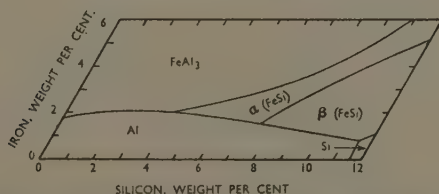


FIG. 9.—The Surfaces of Primary Separation in the Aluminium-Iron-Silicon System (*Phillips and Varley*).

present work. Their compound  $\beta$  (corresponding to the  $\alpha(\text{FeSi})$  of Phillips and Varley) was estimated to contain 18% silicon and from 25% to 42.5% iron. The presence of these two ternary compounds was also established by Dix and Heath,<sup>26</sup> who gave the compositions as :

	Iron, %	Silicon, %
$\alpha(\text{FeSi})$ . . . . .	30	8
$\beta(\text{FeSi})$ . . . . .	27	15

Fink and Van Horn<sup>27</sup> have stated that, whereas  $\beta(\text{FeSi})$  gives a characteristic X-ray-diffraction pattern,  $\alpha(\text{FeSi})$  gives a pattern which is very similar to that of  $\text{FeAl}_3$ ; they therefore considered  $\alpha(\text{FeSi})$  to

be a solid solution of silicon in  $\text{FeAl}_3$ . Phillips and Varley, however, have shown that  $\text{FeAl}_3$  and  $\alpha(\text{FeSi})$  have dissimilar properties and that a thermal effect is associated with the formation of the latter from the former; it seems likely, therefore, that  $\alpha(\text{FeSi})$  is a true ternary compound. The close similarity of diffraction patterns does not preclude the existence of two distinct phases; for example, the patterns given by  $\text{CrAl}_7$  and  $\text{Cr}_2\text{Al}_{11}$  are almost identical, while those of  $\text{Fe}_2\text{Al}_5$  and  $\text{Fe}_2\text{Al}_7$  are also difficult to distinguish.

Phragmén<sup>23</sup> has isolated compounds which would appear to be respectively  $\alpha(\text{FeSi})$  and  $\beta(\text{FeSi})$ ; their chemical compositions were:

	Iron, %	Silicon, %
$\alpha(\text{FeSi})$ . . . . .	31.9	5.57
$\beta(\text{FeSi})$ . . . . .	27	13.5

Other investigators have reported widely different "formulæ" for these compounds upon which no reliance can be placed. It is of interest to note, however, that work on the quaternary aluminium-manganese-iron-silicon system has shown that  $\alpha(\text{MnSi})$  and  $\alpha(\text{FeSi})$  form a complete series of solid solutions with each other.<sup>23, 24</sup>

The general evidence from the previous work indicates the existence of two distinct ternary compounds,  $\alpha(\text{FeSi})$  and  $\beta(\text{FeSi})$ , but at the outset of the work, these had not been satisfactorily characterized.

(c) *Aluminium-Cobalt-Silicon.*

The only previous work available is that of Mondolfo,<sup>28</sup> who superficially examined the aluminium-rich alloys, and found that only  $\text{Co}_2\text{Al}_9$  and silicon enter into equilibrium with the primary solid solution, with which they form a ternary eutectic at 0.7% cobalt, 13% silicon, 575° C. The relevant diagram is given in Fig. 10.

(d) *Aluminium-Chromium-Silicon.*

Mondolfo<sup>28</sup> has found, again by a superficial examination, that there are two ternary compounds, and has published the equilibrium diagram shown in Fig. 11. It is suggested that  $\alpha(\text{CrSi})$  corresponds with  $\text{CrSiAl}_6$ , while  $\beta(\text{CrSi})$  is approximately  $\text{CrSi}_2\text{Al}_4$ . Aluminium, silicon, and  $\alpha(\text{CrSi})$  form a ternary eutectic with each other.

(e) *Aluminium-Nickel-Silicon.*

The aluminium-rich alloys of this system have been examined by Weisse<sup>29</sup> and by Phillips<sup>30</sup>; the surfaces of primary separation are reproduced as Fig. 12. The only constituents are aluminium, silicon, and  $\text{NiAl}_3$ ; these crystallize from the melt as a ternary eutectic which, according to the accurate work of Phillips, lies at 4.9% nickel, 10.98% silicon, and 567° C. No ternary compounds have been reported.

From the brief descriptions of the ternary systems, it will be appre-

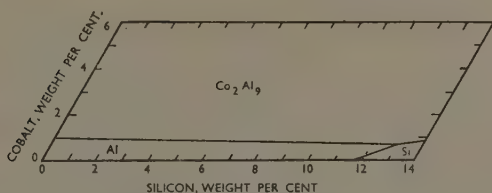


FIG. 10.—The Surfaces of Primary Separation in the Aluminium-Cobalt-Silicon System (*Mondolfo*).

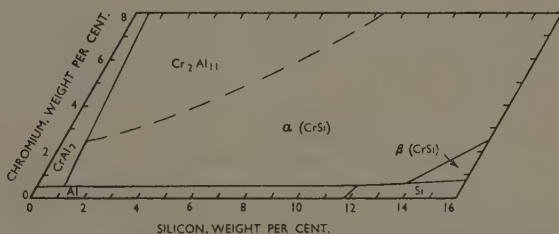


FIG. 11.—The Surfaces of Primary Separation in the Aluminium-Chromium-Silicon System (*Mondolfo*).

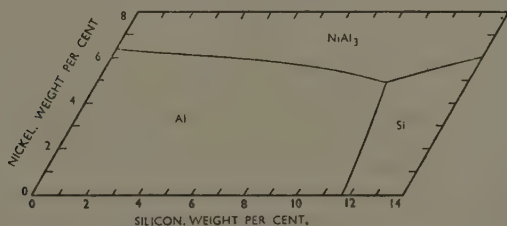


FIG. 12.—The Surfaces of Primary Separation in the Aluminium-Nickel-Silicon System (*Weisse and Phillips*).

ciated that considerable confusion existed at the outset of this research with regard to the nature of the phases which occur.

### III.—EXPERIMENTAL METHODS.

#### 1. Materials Used.

Throughout the work, alloys were prepared from super-pure aluminium, obtained from The British Aluminium Company, Ltd., and binary master alloys. The latter were made from pure materials; several were kindly presented by The British Aluminium Company,

while others were made in the authors' laboratory. The impurity contents of these alloys were very low, and details are given in Table I:

TABLE I.—*Impurity Contents of Master Alloys.*

Alloy	Mn, %	Fe, %	Cr, %	Co, %	Ni, %	Si, %	Cu, %	Ca, %	Remarks
AlMn	5.20	...	...	...	...	...	...	...	
AlMn	9.90	0.0025	...	...	...	0.0025	0.0025	...	
AlFe	...	5.70	...	...	...	0.0035	0.0035	...	
AlFe	0.0015	5.85	...	...	...	0.0015	0.0015	...	
AlCr	...	...	8.66	...	...	...	...	...	
AlCr	0.0005	0.005	10.40	...	...	0.009	<0.0005	...	
AlCo	0.006	0.014	...	4.85	...	0.0065	0.0045	...	
AlNi	...	...	...	...	9.94	...	...	...	
AlSi	...	...	...	...	...	23.31	...	...	Prepared from super-pure Al and 99.98% pure Si.
AlSi	0.002	0.05	...	...	...	17.50	0.003	0.060	
AlSi	0.006	0.17	...	...	...	19.40	0.006	...	Used only for exploratory experiments.

## 2. Experimental Techniques.

The general experimental methods used in the present work were closely similar to those previously employed.<sup>1</sup> Melting was carried out in vertical electric crucible furnaces, using crucibles lined with an alumina-fluorspar mixture. Alloys for metallographic work were cast into cold copper moulds, and annealing was carried out in horizontal resistance furnaces controlled by temperature regulators; specimens were sealed in evacuated glass capsules to avoid composition changes due to selective oxidation or volatilization, but in general no alumina sheath was used to separate the alloys from the glass, since contamination by silicon was not important for the alloys studied. At the end of annealing experiments, all alloys were rapidly quenched into cold water. Temperatures were measured with an accurately calibrated platinum/platinum-rhodium thermocouple.

In general, specimens of intermetallic compounds were isolated from slowly cooled alloys. For this purpose, alloys of chosen composition were prepared in quantities of 50–60 g., well stirred with alumina stirrers, and cooled at a rate of 0.75° C./min.; during the cooling, the furnace was controlled by a potentiometric programme controller, a heavy copper furnace lining being used to minimize temperature fluctuations. The primary crystals deposited frequently grew to a conveniently large size for subsequent examination. If the compound which separated underwent no peritectic changes on cooling, the ingots were cooled to room temperature; if, however, peritectic reactions intervened, the cooling was stopped at a temperature slightly above that of the reaction. The temperature was then held constant for an hour, and the semi-liquid alloy subsequently quenched in cold water. In this way it was possible to suppress the reaction and to obtain uncontaminated samples of the

compounds. When cold, ingots were sectioned; one half was examined micrographically, and the other half was used for the extraction of the compound present.

Crystals of intermetallic compounds were separated from the slowly cooled ingots by the electrolytic extraction method previously described.<sup>1(a)</sup> The electrolyte was normally a 7.5% aqueous hydrochloric acid solution, and a current density of 0.1 amp./in.<sup>2</sup> at 8 V. was employed. The crystals, freed from the matrix by anodic solution of the latter, fell to the bottom of the electrolytic cell, and were, at the completion of the extraction, well washed, treated with 50% nitric acid to dissolve possible adhering matrix particles, again washed with water and with alcohol, and finally dried. The residue was then examined under a low-power binocular microscope; in most cases the residue was homogeneous, and the best-formed crystals were easily picked out using forceps. In some cases crystals of more than one form were observed, but since the types were readily distinguishable, they could be separated by hand-sorting. Occasionally crystals were observed to be contaminated with adhering fine silicon particles; these were removed by carefully brushing each crystal with a camel-hair brush. Throughout the research, care was taken to select only sound, uncontaminated crystals, illustrations of which are referred to in Section IV.

Polishing techniques for the metallographic examination were developed to avoid undue differences in level between the hard compound particles and the relatively softer matrix. Etching techniques proved to be unreliable in certain cases, so that X-ray methods were extensively used for the identification of compounds. Samples of crystals were crushed to a fine powder in an agate mortar, and mounted with Canada balsam on hairs or fine glass fibres. Specimens were exposed to iron  $K_{\alpha}$  radiation from a Metropolitan-Vickers demountable X-ray unit in a 9- or 19-cm. Debye-Scherrer camera of the van Arkel type.

The compositions of the intermetallic compounds prepared were established by the chemical analysis of carefully selected samples extracted from the slowly cooled ingots. The analyses were carried out by Messrs. A. Roberts and A. J. Hawkes of the authors' laboratory, or by Messrs. Johnson, Matthey and Company Ltd. The results from the two laboratories were consistent.

In the next section, individual alloys are referred to in terms of their compositions. Thus, an alloy containing 2% of a transitional metal and 10% of silicon is referred to as "alloy 2/10"; in general, the figures refer to intended, and not analysed, compositions. In order to avoid confusion with certain ternary compounds, for which Phillips's nomenclature has been adopted, the symbol Al has been employed to indicate the aluminium-rich solid solution in compiling tables of results.



## IV.—EXPERIMENTAL RESULTS.

In the experimental work, attention was directed primarily towards the isolation and study of the ternary compounds which occur in the aluminium-manganese-silicon and aluminium-iron-silicon systems. As results accumulated, it became necessary also to examine the aluminium-silicon alloys with chromium, cobalt, and nickel. Because of the previous metallographic work, it was possible to proceed without further investigation to the isolation of suitable samples of  $\alpha(\text{MnSi})$ ,  $\beta(\text{MnSi})$ ,  $\alpha(\text{FeSi})$ , and  $\beta(\text{FeSi})$ . The information with regard to the systems containing chromium and cobalt was, however, too meagre for a similar approach, and preliminary experiments with slowly cooled ingots and annealed alloys were necessary. In the case of the aluminium-nickel-silicon system, experiments were carried out to check the previous work and to investigate the solid solubility of silicon in  $\text{NiAl}_3$ .

1. *The Aluminium-Manganese-Silicon System.*(a) *Metallography.*

In the slowly cooled alloys, the matrix consisted of the aluminium-rich solid solution. Free silicon was readily identifiable because of its dark blue-grey colour, and its characteristic form (rhomboidal masses when primary, but script-like when secondary). The other constituents observed were :

(i)  $\text{MnAl}_6$ . This occurred as hollow silver-grey needles, formed peritectically from  $\beta(\text{MnSi})$  in certain alloys.

(ii)  $\alpha(\text{MnSi})$ . When primary, this phase crystallized as regular polyhedral prisms, frequently of a pronounced cubic form; when secondary, the form was script-like. In all cases the colour was grey.

(iii)  $\beta(\text{MnSi})$ . There is considerable variation in the habit of this phase. At low silicon contents primary particles occur as thin polyhedral plates; at high silicon contents, well-formed needles are deposited; at intermediate contents the primary crystals are small regular prisms.

The first and last types appear in microsections as blue-grey needles.

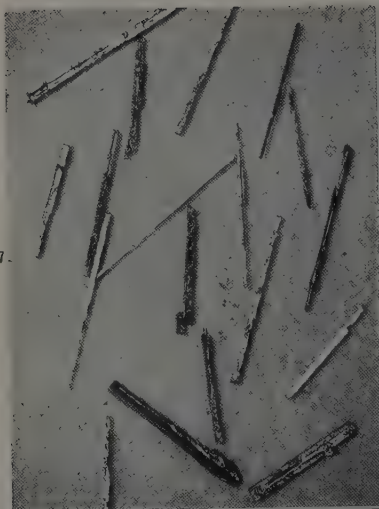
(b) *The Compound  $\alpha(\text{MnSi})$ .*

Initial slow-cooling experiments of alloys lying in the  $\alpha(\text{MnSi})$  primary field of Fig. 8 gave primary crystals which were too fine for successful extraction. In later work, therefore, the cooling process was halted at a temperature a few degrees above that at which secondary separations occur for a period of the order of an hour. Cooling was then resumed, and in the cold ingots crystals of a size suitable for extraction were metallographically observed. Thirteen alloys were examined,



FIG. 13.—Crystals of  $\alpha(\text{MnSi})$ .  $\times 12$ .  
 FIG. 14.—Crystals of  $\beta(\text{MnSi})$ . Thin plates.  $\times 7$ .  
 FIG. 15.—Crystals of  $\beta(\text{MnSi})$ . Equi-axed prisms.  $\times 7$ .  
 FIG. 16.—Crystals of  $\beta(\text{MnSi})$ . Long prisms.  $\times 7$ .

17.



19.

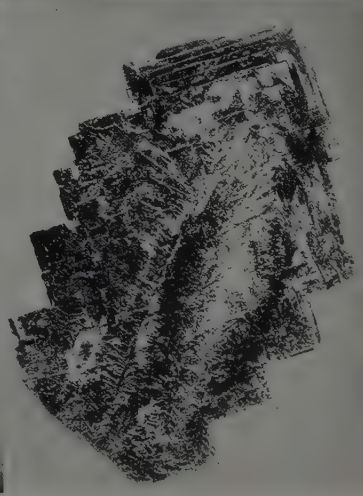
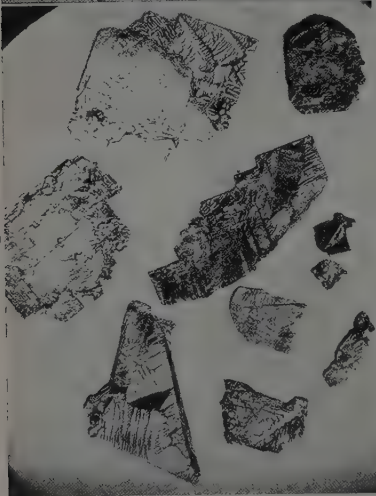


FIG. 17.—Crystals of  $\text{MnAl}_3$ .  $\times 7$ .  
 FIG. 18.—Crystals of  $\alpha(\text{FeSi})$ .  $\times 10$ .  
 FIG. 19.—Crystals of  $\beta(\text{FeSi})$ .  $\times 3$ .  
 FIG. 20.—Large Crystal of  $\beta(\text{FeSi})$ .  $\times 4$ .

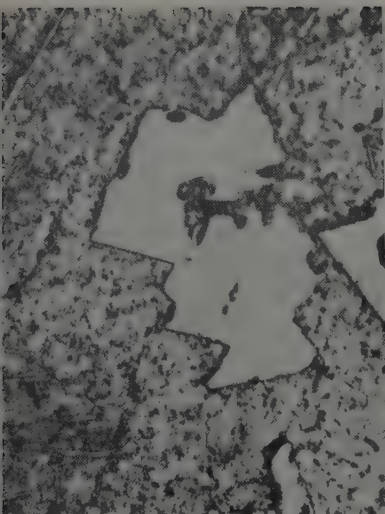


FIG. 21.—Primary Crystals of  $\alpha(\text{CrSi})$  in Slowly Cooled Ingot.  $\times 70$ .

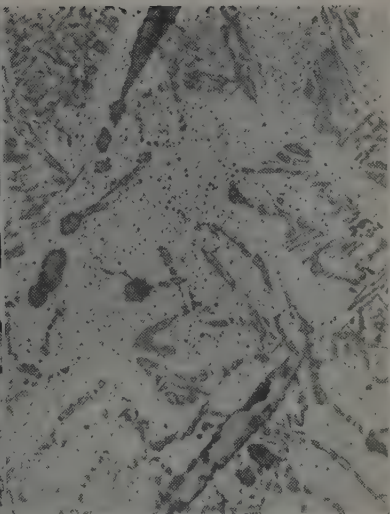


FIG. 22.—Primary Crystals of  $\beta(\text{CrSi})$  in Slowly Cooled Ingot.  $\times 70$ .

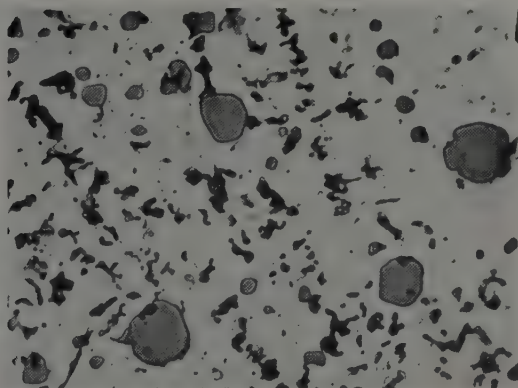
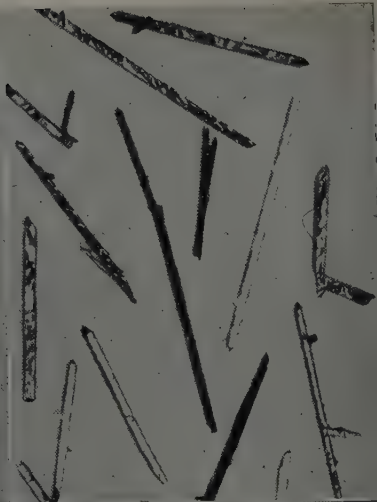


FIG. 23.—Three-Phase Microstructure: Al (light) + Si (half-tone) +  $\alpha(\text{CrSi})$  (dark).  $\times 500$ .

24



26

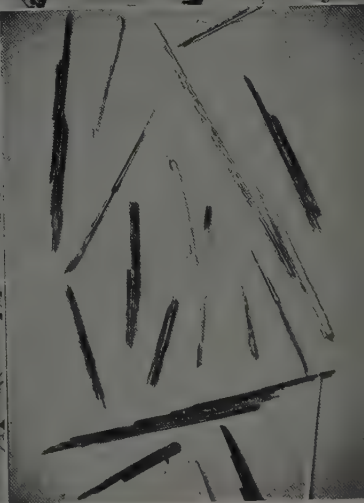
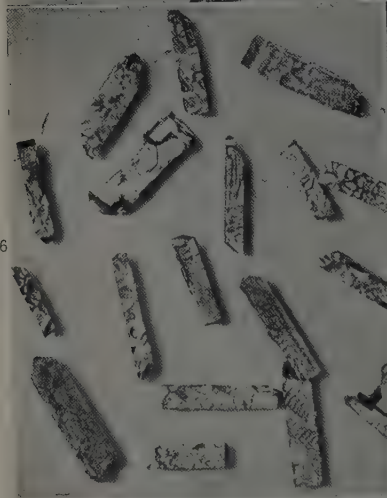


FIG. 24.—Crystals of  $\alpha(\text{CrSi})$ .  $\times 7$ .  
 FIG. 25.—Crystals of  $\beta(\text{CrSi})$ .  $\times 7$ .  
 FIG. 26.—Crystals of  $\text{Co}_2\text{Al}_9$ .  $\times 6$ .  
 FIG. 27.—Crystals of  $\text{NiAl}_3$ .  $\times 3$ .

and the results are summarized in Table II. In all cases satisfactory residues were obtained by electrolytic extraction, an example being shown in Fig. 13 (Plate XXXI). In addition to these crystals, the residues from the three alloys least rich in silicon contained quantities of silver-coloured dendrites and smaller angular dendrites which were

 TABLE II.—*Aluminium-Manganese-Silicon Alloys.*

Alloy	Microstructure	Remarks	Compound Extracted	Composition of Compound Extracted	
				Mn, %	Si, %
2/2	Al + $\alpha$ (MnSi) script	Delayed slow cool	...	...	...
2/3	Al + $\alpha$ (MnSi) script + Si	Delayed slow cool	$\alpha$ (MnSi)	28.72	8.4
2/4	Al + $\alpha$ (MnSi) + Si	Delayed slow cool	$\alpha$ (MnSi)	29.25	8.91
2/5				29.11	9.85
2/6				27.93	9.91
3/5				29.32	9.01
3/6				28.65	10.09
2/10		Direct slow cool		26.35	10.97
2/12				27.60	10.76
2/14				27.74	11.36
2/16				27.25	12.72
2/18				27.00	12.20
3/0.75		25.50	10.88		
5/1	Al + plates + MnAl <sub>6</sub>	Quenched from 655° C.	...	...	...
6/1			...	...	...
6/1 (repeat)	Al + plates	Quenched from 690° C.	$\beta$ (MnSi)	35.17	4.84
6/1A	Al + plates + MnAl <sub>6</sub>	Quenched from 690° C.	$\beta$ (MnSi)	44.87	3.9
6/1.5	Al + plates	Quenched from 670° C.	$\beta$ (MnSi)	36.81	4.82
6/2		" " 660° C.		36.67	5.48
6/2.5		" " 670° C.		36.95	5.62
6/3		" " 665° C.		27.75	5.90
6/3 (repeat)		" " 670° C.		35.32	6.18
6/4		" " 690° C.		37.15	6.47
5/5		" " 680° C.		32.66	7.53
6/5		" " 700° C.		35.90	6.94
6/6		" " 700° C.		33.41	7.73
6/7.5		" " 700° C.		34.30	7.66

dark in colour. The diffraction patterns proved these to consist of aluminium-rich solid solution and a mixture of secondary  $\alpha$ (MnSi) and silicon respectively; the diffraction pattern of the  $\alpha$ (MnSi) crystals was complex and characteristic, and quite different from those of aluminium, silicon, or the binary compounds of the aluminium-manganese system.

### (c) *The Compound $\beta$ (MnSi).*

Initially the alloys 5/1, 5/5, 6/1, 6/2, 6/3, 6/6, and 6/7.5 were cooled and quenched from above the temperature of the peritectic reaction, micro-examination being used to confirm the absence of peritectic rims round the primary particles. Alloys 5/1 and 6/1 contained many needles of MnAl<sub>6</sub> after quenching from 655° C.; a further alloy (6/1A) was thus made and quenched from 690° C. after which treatment only



traces of  $\text{MnAl}_6$  were observed. In the remaining alloys the peritectic was successfully suppressed, and clean  $\beta(\text{MnSi})$  crystals were observed. The analysed compositions of the extracted crystals are summarized in Table II. It appeared possible at this stage that two distinct compounds might be involved, one relatively rich in manganese (e.g. alloy 6/1A) and corresponding to Bückle's *X* compound, and the other less rich in manganese and corresponding to Phillips'  $\beta(\text{MnSi})$ . Alloys with intermediate compositions 6/1.5, 6/2.5, 6/4, and 6/5 were then examined, and alloys 6/1 and 6/3, which had given the samples of most extreme composition, were duplicated. The results for these alloys in agreement with the majority of the analyses, and are also given in Table II. With the exception of the original results from alloys 6/1 and 6/3 all the analyses fall into a single group; it is likely that the wide divergence of composition shown by these two samples is caused by contamination resulting from some imperfection in the early technique, and the results have been rejected in favour of the more consistent results given by the subsequent duplicates.

The differences in habit of the  $\beta(\text{MnSi})$  crystals revealed by the microscope was more strikingly demonstrated by the extracted residues, although a general similarity of form existed. Samples from individual alloys were uniform. The thin, somewhat irregular plates (Fig. 14, Plate XXXI) occurred in alloys 6/1, 6/1.5, 6/2, 6/2.5, and 6/3, but tended to increase in thickness with increasing silicon content until, in 6/3 and 6/4, the more equi-axed prisms of Fig. 15 (Plate XXXI) were obtained. Alloys 5/5, 6/5, 6/6, and 6/7.5 all contained the long prisms seen in Fig. 16 (Plate XXXI); in cross-section these showed irregular hexagonal outlines similar to the largest crystal faces of the plate- and prism-type crystals.

In view of these differences in habit, X-ray diffraction patterns were obtained from all the  $\beta(\text{MnSi})$  samples extracted. All samples gave a similar pattern, so that, in spite of the changes in habit, only one compound is involved. This conclusion has been confirmed by single-crystal photographs which were kindly taken at the Cavendish Laboratory, Cambridge. The diffraction pattern is complex, and easily differentiated from those of  $\alpha(\text{MnSi})$  or the binary compounds  $\text{MnAl}_4$  and  $\text{MnAl}_6$ .

#### (d) *The Compound $\text{MnAl}_6$ .*

Attempts to obtain satisfactory  $\text{MnAl}_6$  crystals by cooling alloys lying in the appropriate field of primary separation in Fig. 8 and quenching from above the peritectic temperature were not successful, owing to the relatively small slope of the liquidus surface. An excellent small sample of needles (Fig. 17, Plate XXXII) was, however, obtained by hand sorting of the residue from alloy 5/1. The chemical analysis of this

sample showed that no silicon was present. The compound  $\text{MnAl}_3$  is, therefore, incapable of dissolving silicon.

In this system both the ternary compounds are of variable composition, but  $\alpha(\text{MnSi})$  contains much less manganese and silicon than was estimated by Bückle, while it is slightly richer in both solutes than reported by Phragmén. The wide range of compositions found for  $\beta(\text{MnSi})$  has been shown by X-ray examination to correspond with a single ternary phase, and the existence of the ternary compounds  $X$  and  $Y$  (Fig. 7) as reported by Bückle has not been confirmed.

## 2. The Aluminium-Iron-Silicon System.

### (a) *Metallography.*

The constituents observed, in addition to aluminium and silicon, were :

(i)  $\text{FeAl}_3$ . This phase occurred as blue-grey needles.

(ii)  $\alpha(\text{FeSi})$ . The ternary compound appeared as regular polyhedral prisms, very similar to  $\alpha(\text{MnSi})$ . On quenching a semi-liquid alloy, small needles of this phase were frequently observed. The colour was also blue-grey.

(iii)  $\beta(\text{FeSi})$ . This phase occurred as large thin plates, which appeared in microsections to be long, well-formed needles lighter in colour than  $\alpha(\text{FeSi})$ .

### (b) *The Compound $\alpha(\text{FeSi})$ .*

$\alpha(\text{FeSi})$  is the primary constituent for a relatively narrow band of composition (Fig. 9). It was, therefore, difficult to prepare a sufficiently wide selection of alloys for characterization of the compound. The alloys investigated are summarized in Table III. The four alloys quenched from  $615^\circ$ – $620^\circ$  C. gave clean, well-formed crystals in a matrix having a fine quenched structure; the type of extract obtained is shown in Fig. 18 (Plate XXXII). Alloys 2/6 and 2/7 were so near to the  $\text{Al}/\alpha(\text{FeSi})$  eutectic valley that no peritectic rimming of  $\alpha(\text{FeSi})$  by  $\beta(\text{FeSi})$  would be expected; these alloys were slowly cooled, annealed in the semi-liquid region, and then cooled to room temperature. The crystals obtained, in both initial and duplicate experiments, were too small for adequate sorting for analysis. X-ray examination of a small hand-sorted sample, however, proved these crystals to be  $\alpha(\text{FeSi})$ . As previously reported,<sup>27</sup> the diffraction pattern obtained is similar to that of  $\text{FeAl}_3$ .

### (c) *The Compound $\beta(\text{FeSi})$ .*

Seven alloys lying in the field of primary separation of this compound were examined, using the delayed slow-cooling technique. Micro-examination showed that the primary crystals appeared in the

form of long grey needles; secondary compound and free silicon were also present. In addition, alloys 3/10 and 3/11 contained small amounts of equi-axed  $\alpha(\text{FeSi})$ , which was not, however, peritectically rimmed.

TABLE III.—*Aluminium-Iron-Silicon Alloys.*

Alloy	Microstructure	Remarks	Compound Extracted	Composition of Compound Extracted	
				Fe, %	Si, %
2/6 2/7	} Al + $\alpha(\text{FeSi})$ script	Delayed slow cool	{ ...	...	...
2-75/7 2-75/7-5 3/8 3-5/8-5				...	...
2-75/7 2-75/7-5 3/8 3-5/8-5	} Al + $\alpha(\text{FeSi})$	Quenched from 615° C.	$\alpha(\text{FeSi})$ {	32-45	8-41
				32-53	8-7
				32-52	8-7
				32-59	8-92
2/9 2/10 2/11 2/12	} Al + $\beta(\text{FeSi})$ + Si	Delayed slow cool	$\beta(\text{FeSi})$ {	27-18	13-82
				26-97	14-82
				26-87	14-70
				26-65	14-93
3/10 3/11 3/11	} Al + $\beta(\text{FeSi})$ + $\alpha(\text{FeSi})$ + Si	Delayed slow cool	{ $\alpha(\text{FeSi})$ $\alpha(\text{FeSi})$ $\beta(\text{FeSi})$	32-69	9-95
				32-12	10-32
				27-21	14-90
1-5/11	Al + $\beta(\text{FeSi})$ + Si	Delayed slow cool	$\beta(\text{FeSi})$	27-30	14-49
4/1 4/3 4/5 4/6	} Al + $\text{FeAl}_3$	Quenched from 650° C.	{ ...	...	...
				...	...
				...	...
				...	...

On extraction, the crystals were found to consist of large flat plates (Fig. 19, Plate XXXII), hand-sorting of which was easy, so that pure samples were readily obtained. Analysis and X-ray examination showed that the crystals from all samples corresponded to a single distinct ternary compound of variable composition. Alloy 3/10 did not give enough  $\beta(\text{FeSi})$  crystals for analysis, but the equi-axed crystals were proved to be  $\alpha(\text{FeSi})$  by analysis and by X-ray examination. Alloy 3/11 gave similar indications.

Several alloys were found to give exceptionally large crystals, as illustrated in Fig. 20 (Plate XXXII). Though somewhat irregular in shape, they were, in general, single crystals, and not agglomerations of smaller plates. Specimens of this type may be of use in the investigation of the physical and mechanical properties of such compounds by either mechanical or acoustical methods, and preliminary experiments towards this end are in progress.

#### (d) The Compound $\text{FeAl}_3$ .

The extracts obtained from the alloys listed in Table III were not suitable for chemical analysis, as the crystals were small and of poor quality.

The samples extracted from as wide a range of compositions as possible, therefore, confirm the presence of two ternary compounds of variable composition.  $\alpha(\text{FeSi})$  contains much less silicon than suggested by Gwyer and Phillips, but the almost constant iron content lies very near the centre of the range they proposed. The compositions of both compounds are in agreement with the less extensive work and approximate estimates of Dix and Heath.

### 3. The Aluminium-Chromium-Silicon System.

#### (a) The Form of the Surfaces of Primary Separation.

In view of the limited nature of the information available with regard to this system, the surfaces of primary separation were investigated by

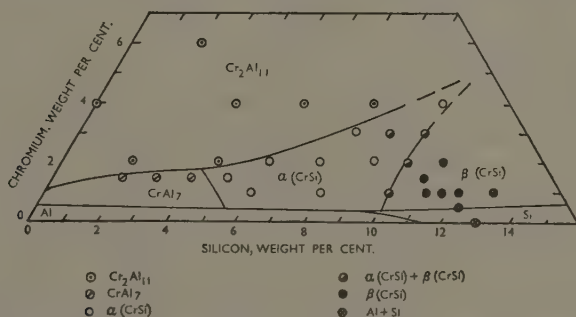


FIG. 28.—The Surfaces of Primary Separation in the Aluminium-Chromium-Silicon System.

metallographic examination of slowly cooled alloys. The results are summarized in Fig. 28, which shows that two ternary compounds  $\alpha(\text{CrSi})$  and  $\beta(\text{CrSi})$  may occur in the aluminium-rich alloys. Alloys which lay in the primary  $\text{Cr}_2\text{Al}_{11}$  field were readily recognized by the cores of this material, which, in both binary aluminium-chromium and the ternary alloys, appeared pink in the unetched state and pale brown on swabbing with 0.5% aqueous hydrofluoric acid. The material surrounding the cores was identified, according to composition, as either  $\text{CrAl}_7$  (grey and inert to etching) or a new phase, which was strongly attacked and coloured dark brown by hydrofluoric acid. Alloys in the primary  $\text{CrAl}_7$  field showed primary crystals of  $\text{CrAl}_7$ , which, as the silicon content increased, became progressively more heavily rimmed with the dark-etching phase, into which it therefore transforms peritectically. The dark-etching phase formed the primary particles in the field labelled  $\alpha(\text{CrSi})$ ; a small amount of crystals extracted from

alloy 2/6 gave a diffraction pattern quite different from that of aluminium, silicon, or the two aluminium-chromium compounds, indicating that the phase is to be regarded as a ternary compound. In the field labelled  $\beta(\text{CrSi})$  an entirely new phase, resistant to attack by etching reagents, and crystallizing as needles, was observed. These crystals, on extraction, proved to correspond with a diffraction pattern somewhat similar to that of  $\alpha(\text{CrSi})$ , but with easily recognizable differences. Alloys 1/10, 2/10, and 3/10, on slow cooling, deposited both types of primary crystal; this was proved both by etching and by the X-ray examination of extracted residues. These alloys thus lie very close to a boundary separating the regions of primary separation of  $\alpha(\text{CrSi})$  and  $\beta(\text{CrSi})$ . All boundaries in Fig. 28 have been drawn in accordance with the relative amounts of the various phases present. Typical microsections are shown in Figs. 21 and 22 (Plate XXXIII).

Several alloys with silicon contents between 6% and 12% showed patches of ternary eutectic; the constituents were aluminium, silicon, and a third phase, which, owing to the fineness of the structure, could not be definitely recognized as  $\alpha(\text{CrSi})$  or  $\beta(\text{CrSi})$ . From the slow-cooling experiments alone, therefore, it was impossible to decide whether the boundary between  $\alpha(\text{CrSi})$  and  $\beta(\text{CrSi})$  cut the  $\alpha(\text{CrSi})/\text{Al}$  boundary or a boundary between  $\beta(\text{CrSi})$  and silicon. Accordingly, six alloys with compositions lying on the line joining compositions 0/12 and 2/10 were chill cast and annealed for 16 days at a temperature of 559° C., the temperature of the eutectic having been established by annealing and quenching experiments as between 570° and 580° C. The microstructures of alloys 0/12 and 0.25/11.75 were (Al + Si); the remaining alloys showed the presence, in addition to the primary solid solution, of silicon and the dark-etching  $\alpha(\text{CrSi})$  (Fig. 23, Plate XXXIII). The eutectic reaction therefore involves aluminium, silicon and  $\alpha(\text{CrSi})$ ; this result has been utilized in drawing Fig. 28, which differs considerably from the diagram proposed by Mondolfo (Fig. 11).

(b) *The Compounds  $\alpha(\text{CrSi})$  and  $\beta(\text{CrSi})$ .*

Ten alloys containing 1% chromium and 6–20% silicon were prepared for the extraction of primary crystals. Since these alloys lay near the boundaries adjacent to the regions of primary separation of aluminium and silicon, the risk of peritectic rimming or contamination of one compound with the other on slow cooling was very small. This was confirmed by microscopic examination. Specimens were therefore cooled continuously to room temperature. Typical crystals of  $\alpha(\text{CrSi})$  and  $\beta(\text{CrSi})$  are shown in Figs. 24 and 25 (Plate XXXIV), and the results are summarized in Table IV. The samples from alloy 1/9, used for identification purposes at an early stage in the work, were very small,

and little reliance can be placed on the results obtained from these residues. The remaining results, however, indicate clearly that the crystals correspond with two distinct compounds, one of which contains a high proportion of chromium.

TABLE IV.—*Aluminium-Chromium-Silicon Alloys.*

Alloy	Microstructure	Remarks	Compound Extracted	Composition of Compound Extracted	
				Cr, %	Si, %
1/6 1/8	$\text{Al} + \alpha(\text{CrSi}) + \text{Si}$	...	$\alpha(\text{CrSi})$	30.73	17.34
				30.53	17.84
1/9	$\text{Al} + \alpha(\text{CrSi}) + \beta(\text{CrSi}) + \text{Si}$	Very small analytical sample	$\alpha(\text{CrSi})$	22.93	18.02
1/9		Very small analytical sample	$\beta(\text{CrSi})$	28.91	31.42
1/10		...	$\alpha(\text{CrSi})$	30.35	17.28
1/11 1/12 1/13 1/16 1/18	$\text{Al} + \beta(\text{CrSi}) + \text{Si}$	...	$\beta(\text{CrSi})$	46.96	42.24
		...		46.37	42.46
		...		40.57	41.55
		...		39.80	46.02
		Too few crystals for analysis	...	...	...
1/20		Too few crystals for analysis	...	...	...

(c) *Equilibrium in the Solid State at 550° C.*

The form of the surfaces of primary separation renders it difficult to prepare a wide range of alloys for the isolation of  $\alpha(\text{CrSi})$ . Accord-

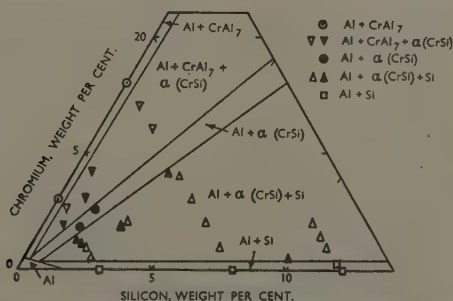


FIG. 29.—The 550° C. Isothermal of the Aluminium-Chromium-Silicon System.

ingly, further information with regard to the range of homogeneity of this compound was obtained by annealing a series of chill-cast alloys for 21 days at 550° C. The results are shown in Fig. 29 in which



analysed critical alloys are distinguished by black symbols. These experiments indicate that the ternary compound  $\alpha(\text{CrSi})$  has a somewhat wider range of homogeneity than suggested by the figures in Table IV. The results summarized in Fig. 29 also show that the solubility of silicon in  $\text{CrAl}_7$  is restricted, as expected in the presence of a stable ternary compound. No trace of  $\beta(\text{CrSi})$  was observed in any of the annealed microsections, confirming that this compound does not enter into equilibrium with the aluminium-rich solid solution.

#### 4. The Aluminium-Cobalt-Silicon System.

##### (a) The Form of the Surfaces of Primary Separation.

As in the case of the aluminium-chromium-silicon system, the surfaces of primary separation were determined by examination of

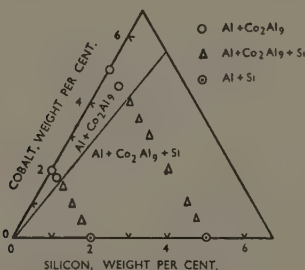


FIG. 30.—The 536° C. Isothermal of the Aluminium-Cobalt-Silicon System.

slowly cooled alloys. The results of eighteen experiments were in good general agreement with Mondolfo's diagram (Fig. 10), and no further diagram is therefore reproduced. No ternary compound was observed in the microsections, and no constituents were encountered except the aluminium-rich solid solution, silicon, and  $\text{Co}_2\text{Al}_9$ . These identifications were checked by the X-ray examination of extracted residues. It was observed that the habit of the  $\text{Co}_2\text{Al}_9$  crystals was not constant; two forms were observed, one which occurred as large plate-like crystals, and the other which separated as small rounded crystals. However, the diffraction patterns of the two forms, which frequently occurred in the same alloy, were identical. The lattice spacings of the  $\text{Co}_2\text{Al}_9$  specimens extracted from different alloys were not constant; solid solubility of silicon in  $\text{Co}_2\text{Al}_9$  was therefore indicated.

##### (b) Equilibrium in the Solid State at 536° C.

The experiments with the slowly cooled alloys were supplemented by the microscopic examination of twelve chill-cast alloys annealed for

21 days at 536° C. The results are shown in Fig. 30. The only constituents observed were the aluminium-rich solid solution,  $\text{Co}_2\text{Al}_9$ , and silicon, in agreement with the previous experiments. The diagram indicates that  $\text{Co}_2\text{Al}_9$  can dissolve an appreciable amount of silicon, but insufficient alloys were used to define accurately the  $(\text{Al} + \text{Co}_2\text{Al}_9 + \text{Si})$  boundary, and therefore to estimate the maximum solubility of silicon in the compound. Since the  $\text{Co}_2\text{Al}_9$  primary surface is extensive (Fig. 10), it was considered that this limiting solubility could be more accurately obtained by the analysis of extracted crystals.

(c) *The Solubility of Silicon in  $\text{Co}_2\text{Al}_9$ .*

Four alloys, containing 2% cobalt and 8–14% silicon, were slowly cooled, and good-quality crystals of  $\text{Co}_2\text{Al}_9$  were extracted (Fig. 26, Plate XXXIV). The analysed compositions of these crystals are given in Table V. These values represent replacement of cobalt by silicon,

TABLE V.—*Composition of  $\text{Co}_2\text{Al}_9$  Crystals.*

Alloy	Composition of Crystals	
	Co, %	Si, %
2/8	30.9	2.98
2/10	30.25	3.46
2/12	29.59	3.89
2/14	32.49	5.31

atom for atom, up to approximately 4.5 at.-%; above this limit, however, atom-for-atom replacement ceases, and both silicon and cobalt contents increase so that the arrangement approximating to  $(\text{CoSi})_2\text{Al}_9$  is no longer preserved.

5. *The Aluminium-Nickel-Silicon System.*

Since all previous workers agree that no ternary compounds occur in the aluminium-rich alloys of this system, the present experiments were confined to an examination of the solubility of silicon in  $\text{NiAl}_3$ . Three alloys were slowly cooled and good-quality crystals were extracted (Fig. 27, Plate XXXIV). Their analysed compositions are given in Table VI; their diffraction patterns were identical with that of  $\text{NiAl}_3$ . These results indicate that the solubility of silicon in  $\text{NiAl}_3$  is restricted to little more than 0.6 at.-%. Although only three alloys were examined, it is very probable that the true limit of solid solubility has been observed, since three almost identical values have been obtained; any

greater solubility would have been revealed by the present range of alloys.

TABLE VI.—Composition of  $NiAl_3$  Crystals.

Alloy	Composition of Crystals	
	Ni, %	Si, %
7/3	41.58	0.45
7/6	41.58	0.51
6/8	41.40	0.46

### V.—SUMMARY AND DISCUSSION.

Experiments have been carried out to isolate the ternary compounds likely to occur in the aluminium-rich alloys of aluminium and silicon with manganese, iron, and chromium. The compounds examined may be considered in turn:

(i)  $\alpha(MnSi)$ .—This compound, crystallizing as almost cubic polyhedra, has a range of compositions extending from 29% manganese and 8.5% silicon to 27% manganese and 12.5% silicon. The composition suggested by Bückle<sup>21</sup> (40% manganese, 15% silicon) is therefore not confirmed, but it may be noted that the composition given by Phragmén<sup>23</sup> (26.6% manganese, 8.0% silicon) is in reasonable agreement with the more extensive investigation reported in the present paper. According to Phragmén, the phase has a cubic crystal structure, with  $a$  (the side of the unit cell) = 12.625 Å. The analysed compositions do not correspond with a simple atomic arrangement, but the structure may be ideally based upon the composition  $Mn_3Si_5Al_{21}$ .

(ii)  $\beta(MnSi)$ .—The compositions of this phase lie in the region 37% manganese and 5–7.7% silicon. The compound is based on a hexagonal cell, and the structure appears to be very similar to that of  $Co_2Al_5$ .<sup>31</sup> It is of interest to note that the analysed compositions of the alloys are grouped about the composition required for the "formula"  $(MnSi)_2Al_5$ .

(iii)  $\alpha(FeSi)$ .—This phase, which separates from the melt in polyhedra of a similar form to those of  $\alpha(MnSi)$ , contains approximately 32.5% iron and 8.5–10.5% silicon. There is much less silicon present than was suggested by Gwyer and Phillips,<sup>25</sup> but the present work is in fair agreement with the estimate made by Dix and Heath.<sup>26</sup> The iron content agrees with that proposed by Phragmén (31.9%), but his estimate of 5.57% silicon appears to be definitely low. The crystal structure of the phase is cubic,<sup>23</sup> with  $a$  = 12.52 Å., and it is reported<sup>23, 24</sup> that it forms a continuous series of solid solutions with  $\alpha(MnSi)$ .

(iv)  $\beta(\text{FeSi})$ .—The homogeneity range of this phase is 13.8–15% silicon at approximately 27% iron, in reasonable agreement with the previous work of Dix and Heath,<sup>26</sup> and of Phragmén,<sup>23</sup> who suggested that the ideal composition was  $\text{Al}_9\text{Fe}_2\text{Si}_2$ . The crystal structure is monoclinic.

(v)  $\alpha(\text{CrSi})$ .—According to the present work, this phase contains approximately 30.5% chromium and 17.5% silicon, in marked contrast to the suggestion of Mondolfo<sup>28</sup> that it is based upon  $\text{CrSiAl}_6$  (21.5% chromium, 11.6% silicon). The annealing work in the solid state shows that the range of homogeneity is wider than that indicated by the analysis of extracted crystals, and extends up to 21% silicon. The compound appears to approach an ideal atomic arrangement corresponding to  $\text{CrSiAl}_3$ . The crystal structure is cubic, with face-centred symmetry.<sup>31</sup>

(vi)  $\beta(\text{CrSi})$ .—This compound has approximately 45% chromium and 42% silicon, again in contrast to Mondolfo's suggestion that the "formula" of the compound is  $\text{CrSi}_2\text{Al}_4$  (24.07% chromium, 25.98% silicon). The X-ray work by Robinson<sup>31</sup> suggests that  $\beta(\text{CrSi})$  may be a solid solution of aluminium in  $\text{CrSi}_2$ .

No ternary compound is found in aluminium-cobalt-silicon alloys, but  $\text{Co}_2\text{Al}_9$  dissolves silicon to an appreciable extent. This behaviour is in accordance with the previous observation that solution of a third metal in a binary compound of aluminium and a transitional metal is only appreciable in the absence of ternary compounds. When a ternary compound is present, the homogeneity ranges of the binary compounds in the ternary diagram tend to be limited; thus, in the present work, the solubilities of silicon in  $\text{MnAl}_6$  and  $\text{CrAl}_7$  were found to be very restricted.  $\text{NiAl}_3$ , however, in spite of the absence of a ternary compound in the aluminium-nickel-silicon system, dissolves very little silicon, and the reason for this behaviour is not understood.

Examination of the compositions and crystal structures of these compounds in terms of electron : atom ratios, calculated according to the assumption that the transitional metal atoms may accept electrons from the structure as a whole, is of theoretical interest. This subject is discussed in a separate publication.<sup>32</sup>

#### ACKNOWLEDGEMENTS.

This research was carried out in the Metallurgy Department of the University of Birmingham, under the general direction of Professor D. Hanson, to whom the authors' thanks are due for his interest and support. The authors must also acknowledge the valuable assistance of

Mr. G. Welsh in the experimental work, and the analytical work of Messrs. Johnson, Matthey and Company, Ltd., and Mr. A. J. Hawkes of the authors' Department.

The authors express their gratitude to the Department of Scientific and Industrial Research, the Royal Society, the Chemical Society, and Imperial Chemical Industries, Ltd., for generous financial assistance.

## REFERENCES.

1. The following papers report relevant previous work on the theory of transitional metals in alloys :
  - (a) G. V. Raynor and D. W. Wakeman, *Proc. Roy. Soc.*, 1947, [A], **190**, 82.
  - (b) G. V. Raynor and M. B. Waldron, *Proc. Roy. Soc.*, 1948, [A], **194**, 362.
  - (c) G. V. Raynor and P. C. L. Pfeil, *J. Inst. Metals*, 1947, **73**, 609.
  - (d) G. V. Raynor and P. C. L. Pfeil, *Proc. Roy. Soc.*, 1949, [A], **197**, 321.
2. L. Pauling, *Phys. Rev.*, 1938, [ii], **54**, 899.
3. N. F. Mott and H. Jones, "The Theory of the Properties of Metals and Alloys." London : 1938 (Oxford University Press).
4. E. H. Dix, Jr., W. L. Fink, and L. A. Willey, *Trans. Amer. Inst. Min. Met. Eng.*, 1933, **104**, 335.
5. H. W. L. Phillips, *J. Inst. Metals*, 1943, **69**, 275.
6. E. Butchers and W. Hume-Rothery, *J. Inst. Metals*, 1945, **71**, 87.
7. A. G. C. Gwyer and H. W. L. Phillips, *J. Inst. Metals*, 1927, **38**, 29.
8. H. W. L. Phillips, *J. Inst. Metals*, 1941, **67**, 275.
9. A. J. Bradley and A. Taylor, *Proc. Roy. Soc.*, 1938, [A], **166**, 353.
10. J. K. Edgar, *Trans. Amer. Inst. Min. Met. Eng.*, 1949, **180**, 225.
11. A. J. Bradley and S. S. Lu, *J. Inst. Metals*, 1937, **60**, 319.
12. W. L. Fink and H. R. Freche, *Trans. Amer. Inst. Min. Met. Eng.*, 1933, **104**, 325.
13. W. Koch and H. Winterhager, *Metallwirtschaft*, 1938, **17**, 1159.
14. G. V. Raynor and K. Little, *J. Inst. Metals*, 1945, **71**, 481.
15. M. Gotō and G. Dōgane, *Nippon Kōgyō Kwai Shi*, 1927, **43**, 931.
16. W. L. Fink and H. R. Freche, *Trans. Amer. Inst. Min. Met. Eng.*, 1932, **99**, 141.
17. W. L. Fink and L. A. Willey, *Trans. Amer. Inst. Min. Met. Eng.*, 1934, **111**, 293.
18. W. O. Alexander and N. B. Vaughan, *J. Inst. Metals*, 1937, **61**, 247.
19. H. W. L. Phillips, *J. Inst. Metals*, 1942, **68**, 28.
20. A. M. B. Douglas, *Acta Cryst.*, 1950, **3**, 19.
21. H. Bückle, *Aluminium Arch.*, 1938, (13).
22. H. W. L. Phillips, *J. Inst. Metals*, 1943, **69**, 291.
23. G. Phragmén, *J. Inst. Metals*, 1950, **77**, 489.
24. H. W. L. Phillips and P. C. Varley, *J. Inst. Metals*, 1943, **69**, 318.
25. A. G. C. Gwyer and H. W. L. Phillips, *J. Inst. Metals*, 1927, **38**, 44.
26. E. H. Dix, Jr., and A. C. Heath, Jr., *Trans. Amer. Inst. Min. Met. Eng., Inst. Metal Div.*, 1928, 164.
27. W. L. Fink and K. R. Van Horn, *Trans. Amer. Inst. Min. Met. Eng., Inst. Metals Div.*, 1931, 383.
28. L. F. Mondolfo, "Metallography of Aluminium Alloys." New York : 1943 (John Wiley and Sons, Inc.).
29. E. Weisse, *Aluminium Arch.*, 1939, (26).
30. H. W. L. Phillips, *J. Inst. Metals*, 1942, **68**, 30.
31. K. Robinson, private communication.
32. J. N. Pratt and G. V. Raynor, *Proc. Roy. Soc.*, 1951, [A], **205**, 103.

# THE VARIATION WITH STRAIN-RATE OF 1307 THE MECHANISM OF DEFORMATION OF A LEAD-THALLIUM ALLOY.\*

By R. C. GIFKINS,† B.Sc., A.I.M.

## SYNOPSIS.

Recent papers by Wood and his co-workers (e.g. *J. Inst. Metals*, 1951, 79, 159) have shown that the deformation of high-purity aluminium takes place by three mechanisms which depend systematically on the temperature and rate of straining. The present paper describes similar changes in mechanism that occur when a single-phase lead-thallium alloy of high purity is deformed at room temperature. At high rates of strain, deformation occurs almost entirely by slip within the grains, the shapes of which change in conformity with the extension of the aggregate. As the strain rate is decreased the slip lines become less regular and more widely spaced, and at this stage deformation takes place partly by the formation of these slip zones and by "micro-flow" within them, and partly by "boundary micro-flow". At still lower strain-rates, deformation proceeds almost entirely by "boundary micro-flow", and consequently the grains remain comparatively undisturbed, except in the neighbourhood of the boundaries. These stages of deformation found in the lead-thallium alloy are discussed and correlated with those which have been described for aluminium.

## I.—INTRODUCTION.

THE present paper describes observations on the deformation of a lead-thallium alloy, specimens of which were strained at various rates at room temperature; the highest rate of straining used was that of a tensile test and the slowest was that of a creep test lasting several months. Particular attention has been directed to microscopical and X-ray-diffraction evidence of the mechanism of deformation and its relation to the strain-rate.

A series of papers on the deformation of metals, with particular reference to creep, have been published recently by Wood and his associates<sup>1-4</sup> and a fifth paper, by Wood, Wilms, and Rachinger,<sup>5</sup> has extended and reviewed this work. Based on experiments with high-purity aluminium, evidence has been put forward by these authors for three stages of metal deformation at different temperatures and strain-rates. It is shown that at ordinary temperatures and fairly high strain-rates deformation takes place by slip, but that as the temperature of deformation is increased, or the rate of deformation at a given temperature is decreased, slip is progressively replaced by what has been described as a "cell" mechanism, whereby the metal

\* Manuscript received 20 September 1950.

† Baillieu Laboratory, University of Melbourne, Australia.



grains break up into a relatively coarse sub-structure. On further reduction of the strain-rate at elevated temperatures, it is found that the size of these "cells" becomes larger until they can be identified with the original grains, and deformation then takes place by movement at the grain boundaries; this process has been termed "boundary micro-flow". These ideas have been developed from observations of the microstructure of electropolished specimens and from X-ray back-reflection photographs taken during tests at various temperatures and strain-rates.

Slip has been found to be associated with diffuseness of the original sharp X-ray reflections, and when the amount of slip is great complete rings are eventually produced. It has been suggested that this spreading of the reflections around the ring is caused by the corresponding spread of orientation of crystallites in the slip zones rather than to bending of the lattice in these regions.<sup>1</sup> The "cell" structure has been observed with the optical microscope and identified on the X-ray photographs with the secondary reflections into which the original reflections split.<sup>2</sup> "Boundary micro-flow" is associated with the absence of slip lines or "cell" structure when the specimens are examined under the microscope, and the original sharp reflections on the X-ray photograph remain unchanged during deformation.<sup>5</sup>

Since the evidence for the mechanism of deformation that has been described was obtained in work on aluminium, the author thought that it would be of interest to extend the scope of some creep tests which were being made with lead and its alloys, in order to examine the mechanism of deformation of lead. As the pure lead being used recrystallized under stress at fairly low strains, and the initial grain-size was relatively coarse, it was decided that systematic observations could be more readily made with one of a group of lead-thallium alloys which were being studied. Of these alloys, one containing 2.48 at.-% (2.45 wt.-%) thallium was selected for the experiments, since this amount is well below the limit of solid solubility of thallium in lead (54 at.-% at 20° C.).

The results that are presented show the influence of the rate of straining on the microstructure and on the corresponding X-ray back-reflection patterns of specimens of the lead-thallium alloy.

## II.—MATERIAL AND EXPERIMENTAL TECHNIQUE.

The alloy used was made from high-purity lead (0.0008% total impurities in a batch analysis for ten common impurities), and thallium which contained spectroscopically determined traces of calcium and cadmium. The alloy was melted in a graphite crucible in an apparatus evacuated to about  $10^{-2}$  mm. Hg, and after scrubbing the alloy with hydrogen at 550° C., the apparatus was re-evacuated and the alloy cast

in an iron mould within the evacuated chamber. The cast alloy was cold worked, annealed in a similar vacuum for two days at  $250^{\circ}\text{C}$ . in order to homogenize it, and then extruded at room temperature from an experimental direct press. The extruded bar was prevented from curling during extrusion by passing it vertically downwards through a close-fitting guide, and great care was exercised subsequently when handling the specimens to ensure that no strain was introduced by accidental bending. The specimens were 5-in. lengths cut from this extruded bar, which had a cross-section  $\frac{1}{2} \times \frac{1}{8}$  in.

The specimens were annealed for  $2\frac{1}{2}$  hr. at  $100^{\circ}\text{C}$ . in air and then polished in a mixture of acetic acid and hydrogen peroxide. Etching was confined to short periods in a solution kept below  $15^{\circ}\text{C}$ ., so that no distortion was introduced into the structure by thermal effects from the highly exothermic reaction. Before obtaining a final polish it was found necessary to etch away about 0.001 in. from the surface of the specimens in order to remove a layer formed during extrusion; this layer was in a condition that gave rise to an X-ray back-reflection pattern of sharp reflections, which corresponded to the observed grain-size, and which was superimposed on a continuous ring. As sharp reflections are a prerequisite for systematic observation, this deep-etching technique was adopted. The surface effect on extruded lead and the etching technique for the preparation of the specimens is described more fully elsewhere.<sup>6</sup> The grain-size of the annealed specimens was about 0.1 mm., although there was considerable variation both locally and between areas; these variations can be seen in the photomicrographs described in the next section. The photographs might be interpreted as indicative of specimens of different grain-size, but it is to be emphasized that the specimens had a similar range of grain-sizes and the behaviour of the grains at the extremes of this range has not been overlooked.

The specimens were held by serrated grips tightened with bolts and spring washers, and were strained by axially arranged direct loading in a room maintained at  $70^{\circ} \pm 3^{\circ}\text{F}$ . ( $21^{\circ} \pm 1.5^{\circ}\text{C}$ .). Extensions were measured on a 2-in. gauge-length by a travelling microscope.

The X-ray back-reflection photographs were taken using unfiltered cobalt *K* radiation and a film-to-specimen distance of 4.5 cm., by which the (511,333) $\alpha_1\alpha_2$  doublet and the (600,442) and (531)  $\beta$  reflections were recorded. The observations in this paper are confined to the doublet, which is the strongest of the rings.

### III.—RESULTS OF VARYING THE STRAIN-RATE.

Loads giving initial stresses of 300, 500, 1000, 1500, and 2000 lb./in.<sup>2</sup> were applied to a series of annealed and polished specimens, and the

loads were removed in order to take photomicrographs and X-ray photographs when extensions of 4 and 10% had been reached; similar observations were also made on two of the specimens after larger extensions, and the microstructures of all the specimens were frequently examined, using the travelling microscope by which extensions were measured.

### 1. Strain/Time Curves.

Fig. 1 records the strain/time curves for all tests except that at 2000 lb./in.<sup>2</sup>, at which extension was too rapid to be plotted on this scale. For the specimen under a load of 2000 lb./in.<sup>2</sup> the initial exten-

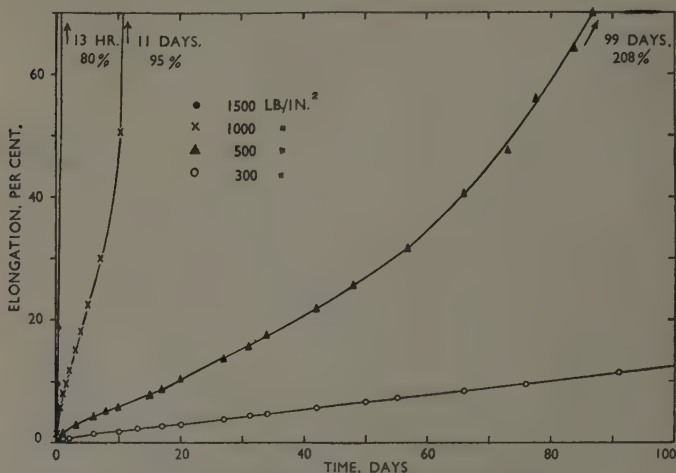


FIG. 1.—Strain/Time Curves for Lead-Thallium Alloy.

sion of 9.6% occurred after 1 min., during which loading and unloading each took 20 sec. and the full load was maintained for the remainder of the time; after 8 min. the extension was 18.4%, and after 11 min. 47.5%. The tests at 1500 and 500 lb./in.<sup>2</sup> were repeated, and the agreement between the corresponding strain/time curves was good.

In Table I the initial stress and average rate of strain between 4% and 10% extensions are given in the first two columns while the third column shows the extension immediately after loading, and the last column the extension when rupture occurred. The test at 300 lb./in.<sup>2</sup> had not reached the stage of fracture when these results were recorded, and the specimen under 2000 lb./in.<sup>2</sup> load fractured at the grips after 58% extension.

X-RAY BACK-REFLECTION PHOTOGRAPHS OF LEAD-THALLIUM ALLOY.

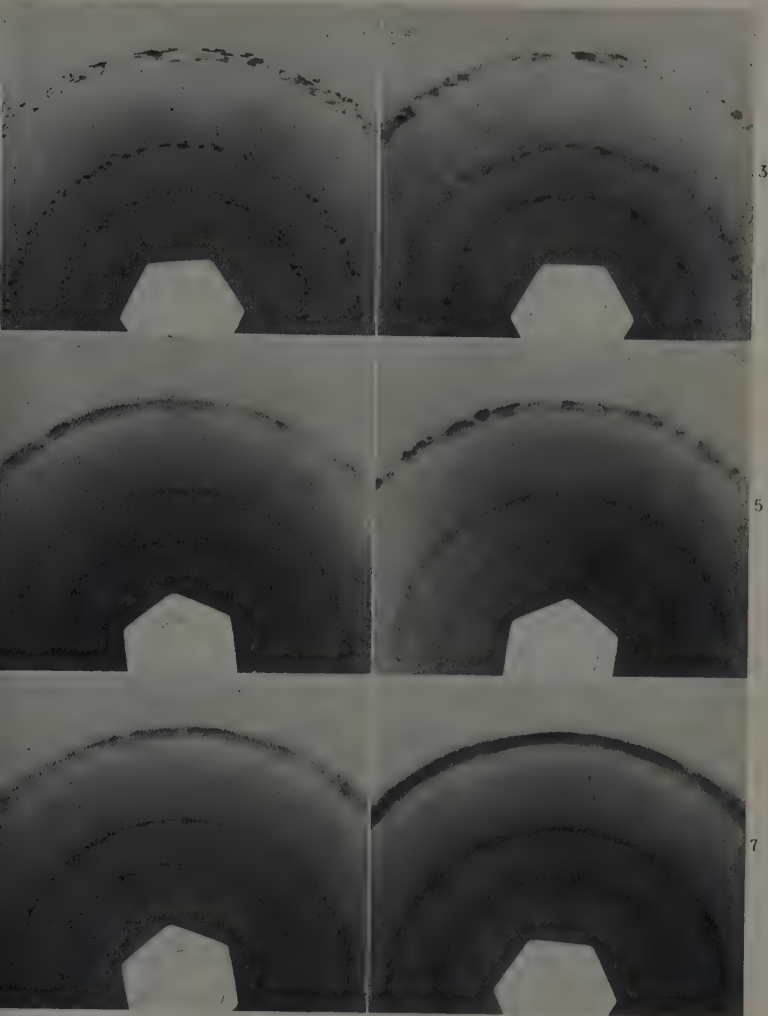


FIG. 2.—Annealed Specimen.

FIG. 3.—Specimen Under 300 lb./in.<sup>2</sup> Load After 4% Extension. (29 days.)

FIG. 4.—Specimen Under 1500 lb./in.<sup>2</sup> Load After 4½% Extension. (On Loading.)

FIG. 5.—Specimen Under 300 lb./in.<sup>2</sup> Load After 10% Extension. (79 days.)

FIG. 6.—Specimen Under 1000 lb./in.<sup>2</sup> Load After 10% Extension. (36 hr.)

FIG. 7.—Specimen Under 2000 lb. in.<sup>2</sup> Load After 9½% Extension. (On Loading.)

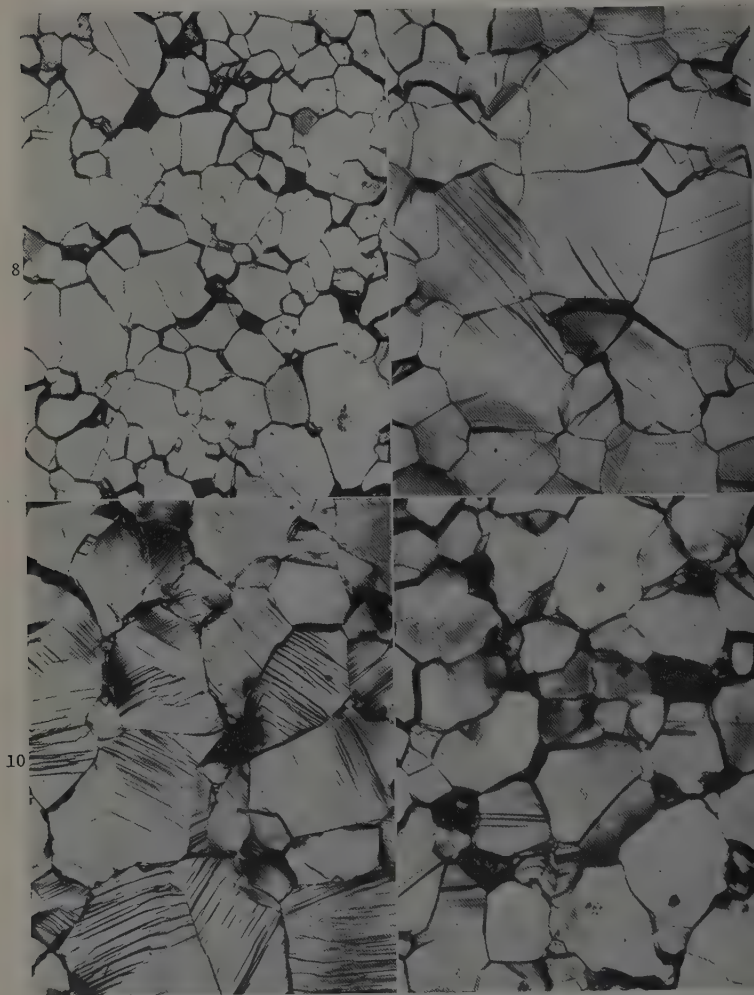
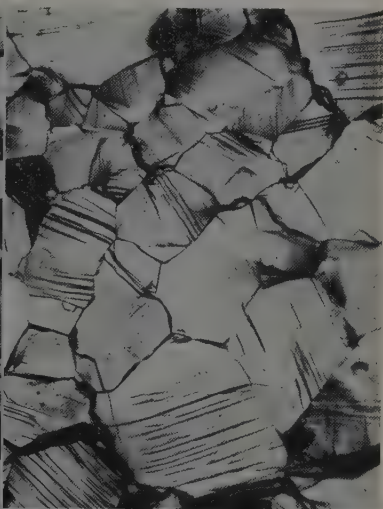
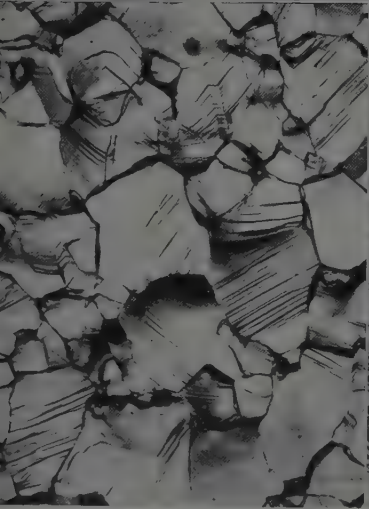


FIG. 8.—Specimen Under 300 lb./in.<sup>2</sup> Load After 4% Extension. (29 days.)  
 FIG. 9.—Specimen Under 500 lb./in.<sup>2</sup> Load After 4% Extension. (5½ days.)  
 FIG. 10.—Specimen Under 1500 lb./in.<sup>2</sup> Load After 4½% Extension. (On Loading.)  
 FIG. 11.—Specimen Under 300 lb./in.<sup>2</sup> Load After 10% Extension. (79 days.)

The direction of the applied stress is parallel to the long edge of all the photomicrographs.

PHOTOMICROGRAPHS OF LEAD-THALLIUM ALLOY.  $\times 150$ .

13



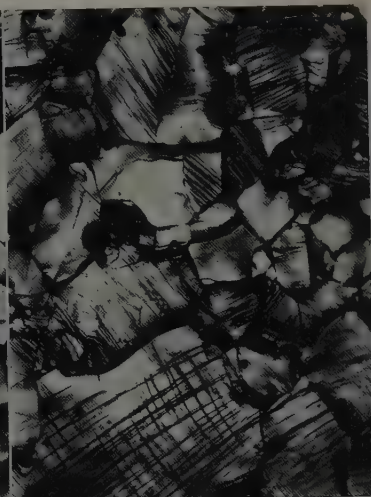
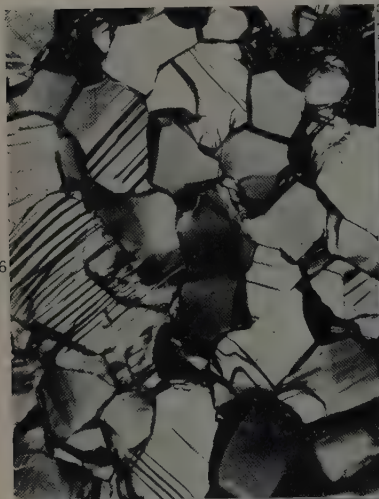
15

FIG. 12.—Specimen Under 500 lb./in.<sup>2</sup> Load After 10% Extension. (20 days.)FIG. 13.—Specimen Under 1000 lb./in.<sup>2</sup> Load After 10% Extension. (36 hr.)FIG. 14.—Specimen Under 1500 lb./in.<sup>2</sup> Load After 10% Extension. (5 hr.)FIG. 15.—Specimen Under 2000 lb./in.<sup>2</sup> Load After 9½% Extension. (On Loading.)

The direction of the applied stress is parallel to the long edge of all the photomicrographs.



16



18



FIG. 16.—Specimen Under 500 lb./in.<sup>2</sup> Load After 20% Extension. (39 days.)

FIG. 17.—Specimen Under 2000 lb./in.<sup>2</sup> Load After 20% Extension. (9 min.)

FIG. 18.—Specimen Under 500 lb./in.<sup>2</sup> Load After 50% Extension. (75 days.)

FIG. 19.—Specimen Under 2000 lb./in.<sup>2</sup> Load After 50% Extension. (11 min.)

The direction of the applied stress is parallel to the long edge of all the photomicrographs.

An examination of Fig. 1 and Table I shows that the tests ranged from a typical creep test of a specimen loaded under 300 lb./in.<sup>2</sup> to the rapid extension of the specimen stressed to 2000 lb./in.<sup>2</sup> Excluding

TABLE I.—*Extensions and Strain-Rates for Various Stresses.*

Initial Stress, lb./in. <sup>2</sup>	Strain-Rate between 4 and 10%, mm./mm./day	Initial Extension, %	Final Extension at rupture, %
300	$1 \times 10^{-3}$	0.12	Test not complete
500	$4.3 \times 10^{-3}$	0.47	208
1000	$46.0 \times 10^{-3}$	1.5	95
1500	$970 \times 10^{-3}$	4.45	80
2000	almost instantaneous	9.6	(58)

the latter, the range of strain-rates is of the order of a thousand-fold. The specimens loaded to 300 and 500 lb./in.<sup>2</sup> developed minimum creep rates after short periods of primary creep, and this was maintained under the lower stress up to 100 days (when observations for this paper were concluded), but under 500 lb./in.<sup>2</sup> the specimen passed into an extended tertiary stage after about 10% extension. The curve for the specimen under a load of 1000 lb./in.<sup>2</sup> is typical of that class of creep tests in which the minimum creep rate is replaced by a point of inflection, and with the specimen under 1500 lb./in.<sup>2</sup> load the point of inflection occurred soon after loading, so that the strain rate increased continuously from this point. The rate of straining for the first 10% extension of the specimen loaded to 2000 lb./in.<sup>2</sup>, was comparatively high and subsequently was such that it extended about 50% in 12 min.

## 2. Specimens Strained Up to 4% Extension.

Considering the X-ray back-reflection photographs taken on the specimens when an extension of 4% was reached, a progressive change was apparent as the strain-rate increased. With a stress of 300 lb./in.<sup>2</sup> the original sharp reflections remained fairly well separated though a little diffused, and as the strain-rate increased the broadening of the reflections continued until with a stress of 1500 lb./in.<sup>2</sup> a complete ring with local diffuse spots was obtained. In this last test the strain-rate was high, as the extension of 4.5% resulted immediately after loading. The extent of these changes is illustrated by Figs. 2, 3, and 4 (Plate XXXV) which are the X-ray patterns from an annealed specimen, and after about 4% extension under a load of 300 and 1500 lb./in.<sup>2</sup>, respectively.

A parallel change in microstructure was also observed.

(a) Under the lowest stress (300 lb./in.<sup>2</sup>) slip was not seen below 4% extension, the main effect being broadening and some migration of boundaries (Fig. 8, Plate XXXVI). Owing to tarnishing of much of this

specimen during the test, photographs had to be confined to areas which happened to have a finer grain-size than that generally found, but it was still possible to observe the tarnished areas, and the behaviour of the larger grains was not different from those shown. Some markings, which appear like broad slip in Fig. 8, are actually twin boundaries that become apparent soon after loading. Twins have been observed also on the annealed specimens before straining, and the author does not believe that those shown are the result of straining during the test.

(b) Under 500 lb./in.<sup>2</sup> slip lines were observed after 2% extension, and at 4% most grains, especially the larger ones, had developed fairly widely spaced slip lines (Fig. 9, Plate XXXVI); broadening of the boundaries also occurred immediately after loading and increased rapidly until slip was seen.

(c) Under 1000 lb./in.<sup>2</sup> grain-boundary broadening and slip were both observed immediately after loading, and slip lines were visible in most grains at 3% extension; at 4% extension slip was apparent in all but a few grains.

(d) Under 1500 lb./in.<sup>2</sup> numerous slip lines were seen as soon as the load was applied and thickening of the grain boundaries was more noticeable in those boundaries across the specimen, i.e., at right angles to the direction of loading (Fig. 10, Plate XXXVI).

Thus it was found that during the initial 4% extension the amount of slip observed increased with increasing strain-rate and the grain-boundary broadening became less marked. The corresponding X-ray pattern exhibited a parallel change from slightly diffused spots to a continuous ring in which local denser areas were present.

### 3. *Specimens Strained to 10% Extension.*

The tendencies which have just been described became more evident as the total strain increased and the observations after 10% extension can be taken as typical. Figs. 5, 6, and 7 (Plate XXXV) are the X-ray back-reflection patterns for the specimens under loads of 300, 1000, and 2000 lb./in.<sup>2</sup>, respectively, when 10% extension had been reached. They show that, although at the lowest stress the original reflections are diffused, they are still distinguishable, whereas under 1000 lb./in.<sup>2</sup> only traces of these reflections are discernible in the continuous ring and in the case of the specimen loaded to 2000 lb./in.<sup>2</sup> continuous rings, which resolve the doublet, are present.

The microstructures at this extension also follow the pattern for the 4% strain. Slip was seen only in isolated grains in the specimen stressed at 300 lb./in., but considerable movement at the grain boundaries was evident by their broadening (see Fig. 11, Plate XXXVI). Figs. 12, 13, 14, and 15 (Plate XXXVII) are the structures of specimens

loaded under 500, 1000, 1500, and 2000 lb./in.<sup>2</sup>, respectively, and show that the number of slip lines becomes greater, the spacing of these lines smaller, and the movement at the boundaries less as the strain-rate is increased.

#### 4. Specimens Strained to Above 10% Extension.

With increasing total strain the difference between the structures of the specimens extended at the two limiting strain-rates became more marked, although the specimen under a load of 300 lb./in.<sup>2</sup> was not available for comparison, since it had not extended much beyond 10% at the time of writing. Figs. 16 and 17 (Plate XXXVIII) illustrate the microstructures of the specimens loaded under 500 and 2000 lb./in.<sup>2</sup>, respectively, when they had extended 20%, and they show that the number of slip lines formed at the higher stress is much greater than at the lower. The X-ray photograph for the specimen subjected to 2000 lb./in.<sup>2</sup> stress was similar to Fig. 7 (Plate XXXV), except that sufficient broadening had occurred to make the doublet no longer resolved, but in the corresponding X-ray photograph for the specimen under 500 lb./in.<sup>2</sup> load, broadly diffuse reflections were superimposed on a continuous ring.

A more striking difference between the microstructures of these two specimens was apparent at 50% extension, and is illustrated by Figs. 18 and 19 (Plate XXXVIII). Many of the original grains of the specimen under 500 lb./in.<sup>2</sup> are still relatively undistorted, although they are separated by regions in which so much movement, of the surface at least, has taken place, that light has been scattered away from the microscope objective. In the specimen under 2000 lb./in.<sup>2</sup>, however, a large number of grains have been elongated in conformity with the general extension and they have remained in contact without the intergranular upheaval which seems to be associated with the lower stress, but the grains themselves are heavily marked by systems of slip lines and surface rumpling. At this extension the X-ray back-reflection photograph for the specimen under 500 lb./in.<sup>2</sup> load showed almost continuous rings which had not broadened to the extent of those for the specimen under 2000 lb./in.<sup>2</sup> load, but which showed only faint remnants of the original reflections. A comparison of the times taken to reach 50% extension for these two specimens, i.e. 11 min. and 75 days, respectively, emphasizes the effect of strain-rate on the mode of deformation.

The extension when fracture occurred, recorded in the last column of Table I, increased markedly as the strain-rate decreased, a particularly high elongation being obtained on the specimen subjected to 500 lb./in.<sup>2</sup> load. The fractures of specimens loaded to 500, 1000, and 1500 lb./in.<sup>2</sup> were all of a ductile knife-edged type.

## IV.—DISCUSSION.

The main result of the present investigation is the discovery that decreasing the strain-rate when testing, at room temperature, a lead-thallium alloy containing 2.45% thallium, produces systematic changes in the microstructure and X-ray reflections which, although corresponding fundamentally to those found in aluminium by Wood and his associates, are different from them.

The lower melting point of the alloy, compared with aluminium, can be assumed to indicate a higher atomic mobility, so that testing the alloy at room temperature might be expected to be equivalent to testing aluminium at 200° C. or perhaps higher. The specimen loaded under 1000 lb./in.<sup>2</sup> was strained at a similar rate to that used for the aluminium specimens for Figs. 3*x* and 3*m* (Plate XCIV), at room temperature, in Wilms and Wood's paper<sup>2</sup> and for Figs. 17 and 18 (Plate XXX), at 150° C., in Wood and Rachinger's paper.<sup>3</sup> If the present Figs. 6 and 13 are compared with these, it will be seen there is a rough equivalence between the amount of slip and the diffuseness of reflections, which suggests that testing at room temperature for the alloy is comparable with testing at 150° C. for aluminium.

However, comparison of the sequence of mechanisms for the alloy with that for aluminium at 150°–250° C. indicates that the lead-thallium alloy deforms by slip at high rates of strain and by "boundary micro-flow" at low rates, but that the intermediate "cell" mechanism is not immediately apparent. Also, even at the slowest rate of straining slip is not entirely absent in the lead-thallium alloy, although the comparative perfection of the X-ray reflections shows that the main mechanism of deformation must be attributed to boundary micro-flow. This slip might be the result of non-uniformity of stress from grain to grain, causing the rate of strain to be high enough, at times, to bring about slip in some grains, but falling to the value for boundary micro-flow generally, as suggested by Wood, Wilms, and Rachinger.<sup>5</sup> Interlocking of major irregularities of the grains when some boundary micro-flow has taken place might be the possible source of stress magnification which provides the energy for slip in isolated grains. It may also be that the distribution of thallium in the alloy has some influence on the variable incidence of slip, despite the high solubility of thallium in lead, the small gap between liquidus and solidus for the alloy, and the homogenizing treatment given to the alloy.

At first sight it might appear that the cell mechanism was absent in the tests with the lead-thallium alloy, but the widely spaced and somewhat irregular slip lines which became increasingly marked as the strain-rate decreased indicate how the extremes of slip and boundary micro-flow were bridged. Although such irregular slip could be seen on the



specimen loaded under 1500 lb./in.<sup>2</sup> (Fig. 14, Plate XXXVII), it became predominant only at relatively low rates of strain such as appeared in the specimen under 500 lb./in.<sup>2</sup> load. Fig. 12 (Plate XXXVII) shows several grains where the slip has resulted in the formation of large, fairly regular blocks. Once the grains have broken up by slip into such blocks, boundary micro-flow can take place in the zones between them in the same way as in the cell sub-boundaries that have been observed in aluminium. The diffusion of X-ray reflections associated with deformation at the slower rates in the lead-thallium alloy suggests that the blocks formed by slip differ in orientation sufficiently to give a zone capable of sustaining flow, although the change in orientation from block to block is not as great as that between the cells in aluminium, from which discrete secondary reflections are obtained on the X-ray photograph.

The mechanisms can be envisaged qualitatively from considerations of the grain-boundary model proposed by Mott <sup>7</sup> and based on the work of Kê, who has himself subsequently put forward evidence for a similar model.<sup>8</sup> The main difference between the two models appears to be in the type of elementary atomic movement postulated. Mott assumes regions or "islands" of good fit alternating with regions of bad fit between boundary atoms and neighbouring grains, and bases his theory on disordering at the surface of the islands; whereas Kê founds his analysis on the disordered regions which are assumed to consist of numbers of "imperfection units". However, the general model is similar and is discussed by King and Chalmers,<sup>9</sup> who show how it can explain boundary movement in creep. At temperatures sufficiently high to cause local disordering, it can be shown that boundary movement takes place at a rate proportional to the stress, and appreciable deformation of an aggregate is brought about if sufficient time is allowed. Any small irregularities of the grains which have interlocked are broken down by stress magnification, and viscous flow is maintained. In the lead-thallium alloy it appears that the size of the "islands" of good fit at room temperature is such that the activation energy for flow is relatively low, and thus at slow rates of strain all deformation can take place by boundary micro-flow. However, at higher rates of strain, the time is not sufficient for the grain boundaries to sustain deformation by flow alone, and local stresses cause slip which results in large, fairly regular blocks within the grains. Thereby new disordered regions are created, between the blocks, and deformation can continue to take place by boundary micro-flow in these regions, as well as in the grain boundaries. In aluminium, at a comparable temperature of about 200° C., it may be that there are already disordered regions, such as dislocations, within the grains, so that when relaxation by boundary micro-flow does



not take place fast enough, energy is diverted to activate flow within the grains on boundaries which link up existing defects and produce grain-like cells, rather than to initiate slip and the formation of the blocks such as have been observed in the lead-thallium alloy.

The elongation of individual grains in the specimen strained at a high rate to 50% extension indicates how multiple slip has produced deformation conforming to that of the aggregate, in the manner postulated by Taylor<sup>10</sup>; while the relative concentration of movement to the grain boundaries of the specimen loaded under 500 lb./in.<sup>2</sup>, and strained to the same amount at a much lower rate, confirms the suggestion that the slip mechanism is replaced by boundary micro-flow at this strain-rate.

Thus, in the lead-thallium alloy deformed at room temperature, deformation at high rates of strain takes place mostly by slip, but as the strain-rate decreases the slip lines become more widely spaced and less regular, and deformation then proceeds by boundary micro-flow. At first, some of this flow is in the zones between the blocks created by the irregular slip and corresponds to the stage of cell formation in aluminium, but at still lower rates of strain most of the deformation is by flow in the grain boundaries. These results were obtained with arbitrarily imposed conditions of temperature, grain-size, and composition. For a fuller understanding of the mechanisms and their correlation with those found in high-purity aluminium, it will be necessary to study the influence of these variables and possibly to attempt the determination of the activation energies associated with the various stages of deformation.

#### ACKNOWLEDGEMENTS.

The work reported in this paper formed part of the programme of research by the Physical Metallurgy Section of the Commonwealth Scientific and Industrial Research Organization and was carried out at the Baillieu Laboratory under the general direction of Professor J. Neill Greenwood, whose knowledge and experience of the creep of lead was particularly valuable in the investigation; the advice and help of Dr. W. A. Wood on X-ray diffraction and in general discussion is also gratefully acknowledged.

#### REFERENCES.

1. W. A. Wood and W. A. Rachinger, *J. Inst. Metals*, 1948-49, **75**, 571.
2. G. R. Wilms and W. A. Wood, *J. Inst. Metals*, 1948-49, **75**, 693.
3. W. A. Wood and W. A. Rachinger, *J. Inst. Metals*, 1949-50, **76**, 237.
4. W. A. Wood and R. F. Scrutton, *J. Inst. Metals*, 1950, **77**, 423.
5. W. A. Wood, G. R. Wilms, and W. A. Rachinger, *J. Inst. Metals*, 1951, **79**, (3), 159.
6. R. C. Gifkins and H. C. Coe, *Metallurgia*, 1951, **43**, 47.
7. N. F. Mott, *Proc. Phys. Soc.*, 1948, **60**, 391.
8. T. S. Kê, *J. Appl. Physics*, 1949, **20**, 274.
9. R. King and B. Chalmers, "Progress in Metal Physics", Vol. I, p. 148. London: 1949 (Butterworths Scientific Publications).
10. G. I. Taylor, *J. Inst. Metals*, 1938, **62**, 307.

# COPPER-NICKEL-IRON ALLOYS RESISTANT TO SEA-WATER CORROSION.\*

By G. L. BAILEY,† M.Sc., F.I.M., MEMBER OF COUNCIL.

(Communication from the British Non-Ferrous Metals Research Association.)

## SYNOPSIS.

The paper describes the development of copper alloys containing 5-10% nickel and 1-2% iron as materials easily worked by the copper-smith and resistant to corrosion by moving sea-water. In the earlier sections an account is given of the origin of the investigation, including a description of the work carried out some years before the war on the effect of small additions of iron and manganese on the resistance of 70 : 30 copper-nickel alloy to sea-water corrosion. As a result of the evidence revealed by this work of the beneficial effects of iron additions, the corrosion-resistance of copper-nickel alloys low in nickel and with various iron contents has been explored. The experimental work comprised mainly tests of resistance to impingement attack in moving sea-water containing air bubbles, and included the observation of corrosion at shielded areas under conditions of rapid water movement. These tests were supplemented by an examination of the resistance to attack under deposits in stagnant conditions. This exploratory work showed that the addition of iron in amounts of the order of 1-2% greatly improved the resistance to corrosion of alloys of low nickel content and pointed to the excellent performance of the alloys containing 5-10% nickel. The resistance to corrosion has been shown to be affected by the heat-treatment given, and the results of a preliminary investigation of the structure of the copper-rich alloys are described in Appendix I.

In view of the importance of providing alloys for use in sea-water-carrying pipes in H.M. ships which would be more resistant to corrosion than is copper (which is normally used for this purpose), an examination has also been made of the mechanical and working properties of these alloys. This examination, the results of which are given in Appendix II, has shown the materials to be readily workable, both hot and cold, provided certain precautions are taken in heat-treatment. The results are given of a full study of the effect of heat-treatment on the corrosion-resistance of the alloys in the selected range, and finally a comparison is made of selected copper-nickel-iron alloys with standard materials used in condenser systems.

## I.—INTRODUCTION.

THE corrosion of condenser tubes was first extensively studied by the investigators working under the Corrosion Research Committee of the Institute of Metals set up in 1910. During the twenty years of that Committee's work eight reports were published, together with papers

\* Manuscript received 4 October 1950. The work described in this paper was made available to members of the British Non-Ferrous Metals Research Association in a confidential research report issued in October 1950.

† Director, British Non-Ferrous Metals Research Association, London.

summarizing the practical recommendations made. In 1930 the work of this Committee was taken over by the British Non-Ferrous Metals Research Association and has since continued without intermission. The most far-reaching developments during this second period have been the experimental proof of the beneficial effects of iron and manganese additions on the corrosion-resistance of the 70:30 copper-nickel alloy and the development of the use of the aluminium-brass condenser tube, which was introduced in 1928. This provided, at a lower cost, resistance to corrosion little inferior to that of the 70:30 cupro-nickel tube.

The work of the Institute of Metals Corrosion Committee established the main types of corrosion occurring in a condenser tube. These were described by May in 1937 in a paper<sup>1</sup> which also discussed the practical causes of corrosion and its control. The whole question of corrosion in cooling-water systems, the effect of design on the intensity of corrosive attack, and the relative behaviour of standard materials has been fully discussed in a more recent paper by Slater, Kenworthy, and May.<sup>2</sup> These papers provide the background for the present work, and should be referred to by those interested in the subject. The main picture they present can be briefly summarized as follows:

The problem of dezincification of  $\alpha$ -brasses, which was one of the first to be tackled, was solved many years ago by the addition of arsenic, but the arsenical 70:30 and 70:29:1 brasses proved insufficiently resistant to impingement attack. By 1939, however, the position had been reached in which the use of 70:30 cupro-nickel with suitable iron and manganese contents<sup>3</sup> or of aluminium brass<sup>4, 5</sup> met the requirements for condenser-tube alloys in existing conditions of service. This was confirmed by war-time experience, which showed that "the condenser tube problem may be considered as virtually solved," but that "severe corrosion was liable to occur in other parts of the cooling systems in H.M. ships".<sup>2</sup> The main difficulty was the impingement attack of copper used for trunking, fire mains, &c., by moving sea-water. Designers did much to reduce impingement attack in copper piping by avoiding undue turbulence, but the need was for "better alloys for sheet and piping which have to be shaped and bent to form".<sup>2</sup> Moreover, designers of condensers were looking ahead and were contemplating "much higher water speeds and even better alloys".<sup>2</sup> Even with the condenser-tube alloys that were resistant to impingement attack, rapid pitting, particularly with aluminium brass, was occasionally encountered and appeared to be related to the pollution of the sea-water. The fact that sea-water varies widely in its corrosive properties according to the extent to which it is contaminated by

effluents or by the products of bacterial metabolism is extremely important in considering both the service behaviour of copper alloys and the laboratory testing of materials for resistance to sea-water corrosion. The types of contaminants and their general effects have been discussed by Slater, Kenworthy, and May<sup>2</sup> and particularly by Rogers.<sup>7</sup>

The present paper describes the development of alloys designed to meet the requirements summarized above.\* After a brief discussion of the types of attack occurring in practice and the methods of laboratory testing employed, the initial experiments on the effect of the addition of iron and manganese to the 70% copper-30% nickel alloys are described (Section IV). The benefits that resulted from moderate iron additions, particularly as regards freedom from impingement attack, suggested that corresponding advantages might result from the addition of suitable amounts of this element to alloys of lower nickel contents. Preliminary tests were then made on alloys having a wide range of compositions, and the results (which are described in Section V) showed that alloys containing 5-10% nickel and 1-2% iron were outstandingly attractive. A fuller programme of work on the properties and treatment of alloys within this range is then described (Section VI), followed by a comparison of these alloys with standard materials and a general discussion of the conclusions reached.

## II.—TYPES OF CORROSION ATTACK.

Although previous references to fuller discussions of the subject have been given, the following brief notes describing the main types of attack that occur are included in this paper for the convenience of the reader.

(i) *Impingement attack* or "corrosion-erosion" is due to the erosion of the protective film by the impingement of the water followed by corrosion of the exposed anodic areas. Its severity increases with increasing amounts of entangled air and with higher water speeds and is materially affected by the presence of corrosion accelerators referred to below.

(ii) *Deposit attack* takes place under deposits of foreign matter or of loose corrosion products which have formed on the surface of the metal. This is most likely to occur in the presence of solid matter in the

\* The British Patent Application<sup>a</sup> covering these alloys was filed in March 1939. The specification was regarded as confidential, and publication was accordingly delayed until May 1946. In the meantime, however, the existence and properties of these alloys became known in confidence within a wide circle in the United Kingdom, the Dominions, and the United States of America.

circulating water, with low water speeds, or when the system is lying idle.

(iii) *Pitting* is associated with some form of highly localized breakdown of a protective film on the surface of the metal, such as the formation and breaking of a small blister in the film. If a metal does not possess the necessary film-forming properties or if the healing of an injury is impeded in any way, serious local attack or pitting is likely to occur. The rate of such pitting can vary over a wide range; abnormally rapid pitting tends to occur in waters containing traces of hydrogen sulphide or of certain other sulphur compounds produced in most cases by the action of bacteria growing in the water.<sup>7</sup> In some cases colonies of certain other bacteria can grow on the surface of the tubes and liberate corrosive substances directly in contact with the metal, giving another type of severe pitting.<sup>9</sup>

### III.—METHODS OF CORROSION TESTING.

The resistance of materials to impingement attack is assessed in the laboratory mainly by means of a jet-impingement test which has been described in the Eighth Report to the Corrosion Research Committee of the Institute of Metals.<sup>5</sup> Recent modifications in design are described by May and Stacpoole,<sup>6</sup> and its use is fully discussed by Slater, Kenworthy, and May.<sup>2</sup> Most of the tests for resistance to impingement attack described in the present paper have been made in this apparatus, in which 12 or 24 specimens are subjected simultaneously to jets of water containing usually 3% by volume of entangled air and impinging on the metal surface at a speed of 15 ft./sec. The sea-water (about 10 gal. in each unit) is recirculated throughout each test, which lasts 4 weeks.

In the early work confirmation of the results of the jet-tests was obtained by tests of tubes in an experimental condenser. In this apparatus sea-water containing air bubbles was pumped at 8 ft./sec. through tubes 12 ft. long. The sea-water capacity of this system was 300 gal. This was changed once during any one run—after the first week. In this respect, therefore, as well as the absence of any heat transfer, the conditions were not identical with those in a condenser in service.

Resistance of materials to deposit attack is determined by allowing a deposit of sand to lie on a specimen immersed in stagnant sea-water, sometimes at 40° C. to accelerate the test.

No specific test for resistance to pitting is known. Pitting is liable to develop in either the jet- or the deposit-tests, and all specimens

were examined for pits, particularly at areas partially shielded from the sea-water.

The behaviour of a particular batch of sea-water samples cannot be forecast with accuracy, as the nature of the various contaminants is not sufficiently well known for close control of their action. It is necessary, therefore, in testing the resistance of alloys to marine corrosion to make a large number of tests on any one material in different samples of sea-water. Some general measure of the corrosive character of each sample of sea-water towards copper is obtained by the technique described by Rogers.<sup>10</sup> This test has been used in most of the present work, and provides a useful indication of the contamination. The best quantitative significance of a particular test result is that afforded by the behaviour of a standard alloy in each test, and check specimens were for this reason included in most runs.

#### IV.—EFFECT OF IRON AND MANGANESE ON RESISTANCE OF 70 : 30 CUPRO-NICKEL TO CORROSION.

##### 1. *Additions of up to 1% Iron.*

In investigating the suggestion that variations in the behaviour in service of the early 70 : 30 cupro-nickel tubes were due to variations in the iron and manganese contents, a number of 70% copper-30% nickel alloys was prepared in the form of sheet or tube with iron contents varying from 0.04 to 1% and with manganese from 0.33 to 2%. Jet-tests were carried out on these materials with both 2 and 4% admixed air. The results showed a rapid increase in the resistance of the alloys to impingement attack as the iron content increased to 0.3%. At higher iron contents resistance to impingement attack in these tests was almost complete.

Manganese had much less effect on resistance to impingement attack, but there was some evidence of its beneficial effect at lower iron contents. With iron contents in excess of 0.3% there was no evidence of any effect of manganese. Tests in the experimental condenser of a series of tubes varying in manganese content from 0.4 to 2.4% and in iron from 0.09 to 0.47% gave the results shown in Table I.

These results are of particular interest in that they show both the beneficial effect of increasing iron with any one particular manganese content and the advantage of increasing the manganese when the iron content is low. The benefits of increasing iron are obvious from Table I. The benefits of increasing manganese are shown by comparing tubes 11A, A, and 6. These contain respectively 0.18, 0.2,



and 0.15% iron, while the manganese contents are 0.5, 1.0, and 2.4%. Impingement attack was severe on the low-manganese alloy, slight with 1% manganese, and very slight with 2.4%. It is clear that the small differences in the iron contents of these three samples have been more than nullified by the beneficial effect of increasing the manganese.

TABLE I.—*Experimental Condenser Tests on 70 : 30 Cupro-Nickel Tubes with Varying Iron and Manganese Contents.*

Tube Mark	Minor Additions		Impingement Attack	Severe Pitting
	Mn, %	Fe, %		
9A	2.4	0.41	Negligible	Nil
6	2.4	0.15	Very slight	Nil
12	2.4	0.10	Severe	One severe pit in each half
10	1.1	0.37	Nil	Nil
5A	1.2	0.24	Slight	A few moderately bad pits
4	1.2	0.09	Severe	Many severe pits with intercrystalline attack
3B	0.5	0.47	Nil	Nil
3A	0.4	0.28	Very slight	Nil
11A	0.5	0.18	Severe	One or two with slight attack
1	0.5	0.13	Severe	One or two moderately bad pits
A	1.0	0.2	Slight	Nil
B	0.3	0.04	Very severe	Several severe pits

Other tests showed that the resistance to deposit attack, like the resistance to impingement attack, was improved by the addition of iron up to about 0.3%, but was little influenced by further increase up to 1%.

Reviewing these results generally, it was recommended<sup>3</sup> that the iron content of 70 : 30 cupro-nickel tubes should be not less than 0.3% and not more than 1%, with manganese between 0.25 and 2%. To avoid the minimum of both iron and manganese in one alloy, it was recommended that the iron content plus one-fifth of the manganese content should together be not less than 0.5%. On this basis the minimum iron content (0.3%) would require a manganese content of 1%, and an iron content of 0.5% and over would only require the minimum manganese content, i.e. 0.25%.

The beneficial effect of iron in the 70 : 30 cupro-nickel was confirmed by Tracy and Hungerford,<sup>11(a)</sup> who, using a rotating radial-strip test in synthetic sea-water (made from sea salt), recommended 0.5% iron as the optimum for this alloy. A later paper by LaQue and Mason<sup>12</sup>

discusses the information resulting from the many tests carried out at Kure Beach, N.C., in different types of apparatus and again shows that 0.5% iron produces something approaching the optimum resistance to attack in the 70 : 30 alloy. In the discussion of the paper by Tracy and Hungerford, LaQue <sup>11(b)</sup> also discussed the work at Kure Beach, and called special attention to the great beneficial effect resulting from the addition of 0.2% iron to the 70 : 30 alloy, with a more gradual effect thereafter.

(2) *Effect of Large Iron Additions (up to 32%).*

Experiments were next carried out to determine the upper limit of useful iron additions to 70 : 30 cupro-nickel. For this work two series of alloys with the same constant copper : nickel ratio were prepared, the first by additions of from 0.25 to 32% iron to a 70 : 30 copper-nickel stock alloy, and the second by additions of from 2 to 10% iron. The manganese contents of the first and second series were approximately 0.7 and 1.0%, respectively, and ingots  $1\frac{3}{4}$  in. square were in each case chill cast. In the first series these were cold rolled (with intermediate annealing at 700° C.) to strip 0.08 in. thick, while in the second series they were first reduced 25% under the power hammer at 700° C. and then cold rolled to 0.08 in., again with intermediate annealing at 700° C. In the first series the alloys containing 8, 16, and 32% iron cracked in the initial cold rolling, although it was possible to select some uncracked material for testing.

Samples of alloys of all these compositions were submitted to jet-and deposit-tests. In all cases alloys with more than 0.5% iron were virtually free from impingement attack at the jet, although the conditions were such as to produce fairly severe attack in a check 70 : 30 alloy of low iron content (0.04%). Alloys of the first series containing 4% or more of iron showed a small amount of pitting and blistering of the scale, and those with 16 and 32% iron rusted; but alloys of the second series showed no attack at the jet in any of three separate runs, though the low-iron check alloy was attacked to depths from 25 to 40 mils \* in each run.

With more than 2% iron some attack occurred in the crevices between the specimen and the ebonite holder at the extreme ends of the specimen where it is tied to the holder with sulphur-free rubber bands (see Fig. 8, Plate XXXIX). With 4% and more iron this attack was accompanied by some disintegration of the alloy surface. This, however, did not seem to increase greatly the depth of the pitting which

\* 1 mil = 0.001 in. = 0.025 mm.

occurred in these crevices and which varied from about 6 to 10 mils in all the jet-test runs of the second series of alloys, irrespective of iron content. This type of attack at shielded areas where oxygen concentration is lower than elsewhere is believed to be accelerated by intense depolarization by air-bubble impingement of the cathodic area adjacent to the point of attack, so that the attack at the shielded area is raised to a high level of activity. It is in a sense, therefore, evidence of susceptibility to a rather severe form of deposit attack. The only indication that such conditions are important in practice is the apparently abnormal rate of deposit attack sometimes observed under obstructions of foreign matter which have lodged in the tubes, thereby causing local turbulence as well as setting up deposit attack.

Deposit-tests under stagnant conditions showed that alloys containing up to 2% iron were highly resistant to attack, but that those with more than 4% iron, although showing little total attack, suffered some surface disintegration at the corroded areas. This suggests some similarity to the more serious attack of these high-iron alloys at shielded areas in the jet-test.

The general conclusions to be drawn from this section of the work on 70 : 30 copper-nickel alloys are that under the conditions of testing so far employed :

(i) Alloys that contain from about 0.3 to 4% iron are resistant to impingement attack. No differentiation between iron contents within this range is possible without more severe conditions of testing.

(ii) The effect of manganese is to supplement that of iron, particularly at lower iron contents, but its beneficial effects on impingement-resistance are of minor importance compared with those of iron.

(iii) Alloys that contain more than 4% iron show some pitting at the jet and blistering of the scale, suggesting that this is the upper limit for optimum resistance to impingement attack.

(iv) Under conditions favourable to deposit attack, particularly where adjacent cathodic areas are depolarized by moving aerated water, alloys with 2% and more of iron are liable to pitting, which, under the worst conditions, may be fairly rapid and extensive. With iron contents of 4% or more this pitting is accompanied by some surface disintegration.

(v) Having regard to resistance to pitting, deposit, and impingement attack, it appears that the optimum iron content for general resistance to corrosion is about 0.5-1%. Whether more severe testing conditions would show sufficient improvement in impingement attack in alloys of high iron content to offset the increasing danger of attack at shielded areas cannot be stated.

V.—EXPLORATION OF THE EFFECT OF IRON ADDITIONS ON THE CORROSION-RESISTANCE OF COPPER-NICKEL ALLOYS CONTAINING LESS THAN 30% NICKEL.

1. *Preliminary Experiments on Alloys Containing 4% Iron.*

In parallel with the experiments described in the preceding section, three alloys were made and tested containing 4% iron with nickel contents of 10, 20, and 23%. An alloy with the same iron content but with 30% nickel was tested simultaneously for comparison. All these alloys contained 0.7–1% manganese, and were made at the same time and in the same way as the second series of high-iron 70 : 30 copper-nickel alloys described in the preceding section. These lower-nickel alloys were tested in the same three runs of the jet-test as were used for the second series of 70 : 30 copper-nickel alloys and none showed any attack whatever at the jet. They were all, however, pitted to some extent at the shielded areas where the specimens were held against the ebonite holder. The alloy with 20% nickel was attacked at this point to a depth of about 10 mils, but the 10% nickel alloy showed attack to a depth of only 2 mils, which was less than on any of the 70 : 30 alloys.

Deposit-tests under stagnant conditions suggested that the alloy which contained only 10% nickel suffered more general attack, with the formation of more copper salts, than did the other alloys, but no conclusions could be drawn from these tests, as the results were destroyed by enemy action in 1940.

2. *Properties of Alloys Containing 3–30% Nickel and 1–9% Iron.*

The results of the preliminary experiments described above suggested the possibility of developing cupro-nickels with nickel contents of the order of 10% and with high resistance to impingement and deposit attack in sea-water, provided the alloys contained iron in substantial amounts. A series of alloys was accordingly prepared with a range of composition sufficiently wide to explore the whole field of low-nickel high-iron cupro-nickels. The preparation of the alloys and the results of corrosion tests on them are described in the following paragraphs of this section, and for convenience reference is made to the structure of the alloys and to the effects of heat-treatment and to their mechanical and working properties. These subjects are discussed more fully in Appendices I and II respectively.

(a) *Materials.*

The alloys were prepared from cathode copper, Mond nickel pellets, and wrought iron. Manganese, where used as a deoxidizer, was added

as the commercially pure metal. Ingots  $9 \times 4\frac{1}{2} \times 1$  in. were cast, annealed at  $900^{\circ}\text{C}$ . for 2 hr., hot rolled to 0.25 in. (75% reduction), annealed at  $850^{\circ}\text{C}$ . for 2 hr., quenched, and cold rolled to 0.08 in. (68% reduction) without further annealing. This heat-treatment (which is fully discussed in the next section) appeared in some preliminary experiments to confer the optimum resistance to corrosion on alloys of any composition, and it was adopted in the early stages of the investigations on the basis of empirical observations only.

The compositions of the alloys prepared are shown in Fig. 1, to which should be added three alloys containing 9% iron with 10, 15, and 20%

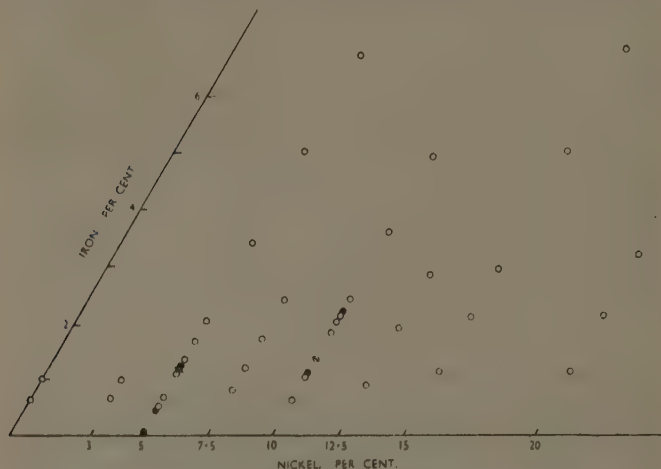


FIG. 1.—Compositions of Alloys Tested in a Preliminary Survey.

KEY.

- Alloys containing 0.5–0.7% manganese.
- Compositions free from manganese but containing 0.01–0.03% phosphorus.
- Compositions containing 0.4% manganese and 0.03% phosphorus.

nickel, respectively, and the standard 70:30 compositions with low and medium iron contents and 1 and 2% iron. It can be seen from this figure that most of these alloys contained only manganese as a deoxidizer. Alloys of five compositions were made up in the 5–10% nickel range, deoxidized with phosphorus and free from manganese, and two manganese-bearing alloys were also deoxidized with phosphorus.

Two alloys in the as-cast state and samples of commercial tubes from  $\frac{5}{8}$  to 3 in. dia, manufactured by member firms of the Association

were also tested. The compositions and other details of these will be referred to in the appropriate places in the text.

(b) *Structure of the Alloys and Effect of Heat-Treatment.*

The alloys in the cast condition were, in most cases, of duplex structure containing an iron-rich second phase (pale blue in colour) in a matrix of solid solution which, in the cast condition, was heavily cored. Long-time annealing at temperatures of 850° C. and upwards appeared necessary to dissolve the second phase, and subsequent heat-treatment at temperatures of the order of 600° C. resulted in the decomposition of this solid-solution phase. The work carried out in investigating these changes is fully described in Appendix I (p. 277). It must be remembered that this work was incidental to the programme of corrosion testing and does not purport to constitute a comprehensive metallographic study. The main conclusions are summarized by the following \* :

(i) Annealing for a further 2 hr. at 900° C. followed by quenching led to the formation of a single solid solution of which the iron content reached a maximum of 3% in the alloy containing 5% nickel and 4.5% in the alloy containing 20% nickel.

(ii) Re-annealing alloys in the above condition for 2 hr. at 600° C. caused a microscopically visible precipitation of the second phase in alloys of all compositions with more than about 2% iron, but where the iron content was less than 2% there was in general no second phase visible under the microscope. The electron microscope, however, revealed clearly that the alloy containing, for example, 5% nickel and 1.2% iron precipitated after this treatment a second phase presumed to be richer in iron and nickel.

(iii) The particle size of the second phase increased with time of annealing and became visible on careful examination under the optical microscope after about 8 hr. at 600° C. It was clearly defined by slow cooling from 900° to 600° C. at the rate of 1° C./min.

(iv) The precipitation of this second phase after 2 hours' heating at 600° C. is accompanied by hardness changes which are of a minor order only (approximately 10–30 Vickers numbers).

(v) If the high-temperature heat-treatment has sufficed to ensure uniformity in composition of the solid solution, precipitation when it occurs is uniformly distributed. Where, however, solid solution is effected without homogenization, precipitation of the second phase on low-temperature heat-treatment is liable to occur only in those areas

\* Unless otherwise stated the heat-treatments were applied to material rolled in accordance with the schedule described in the preceding section.



of initially higher iron content. Hence such precipitation is likely to be related to the dendritic pattern of the initial solidification.

(vi) The precipitation of this second phase is accompanied by a marked increase in magnetic permeability.

(vii) The discrepancy between these findings and the diagram published by Bradley, Cox, and Goldschmidt,<sup>13</sup> who showed an extensive field of uniform solid solution covering most of the compositions in Fig. 1, is due to the fact that the second phase appears to be a solid solution richer in nickel and iron than the solution with which it is in equilibrium, though of almost identical lattice parameter.

### (c) Results of Corrosion Tests.

(i) *Impingement Attack.*—A general survey of the resistance of these alloys to impingement attack was made by carrying out a series of jet-tests on considerable numbers of specimens. Where initial tests showed poor resistance, few further tests were done; the more resistant alloys were tested in many different waters. Most samples were tested as cold rolled after quenching from 850° C., and a number after re-annealing at 600° C. for 2 hr. Twenty-four jet-test runs were carried out in this preliminary survey, which included 362 different specimens. In most of the runs check specimens of 70% copper-30% nickel alloys, *A* and *B* of Table I (0.2 and 0.04% iron respectively), were included to provide a measure of the severity of the conditions.

The work described in this report was largely carried out during the early years of the war, when water samples could not be collected from the open sea. Hence, most were drawn from inshore positions off the coast of North Wales and in a few instances from Plymouth, and the corrosive properties of these different batches varied widely. In three runs the water was taken from Colwyn Bay or aquarium tanks at Plymouth. These waters proved to be extremely corrosive, nearly all alloys showing attack at the jet and at shielded areas. With alloys of all compositions the film of corrosion product was brown, becoming thinner as the nickel content increased from 5 to 20%.

In two later runs water from the Colwyn Bay tanks was decontaminated by circulating it over initially clean copper for two days before use. Water so treated produced no attack on any alloy. In the decontaminated waters (as with synthetic solutions or deep-sea waters) the film of corrosion product was transparent on alloys of higher nickel content and only lightly coloured on the alloys of lower nickel content. With waters of average corrosive properties the corrosion film formed on quenched alloys was generally golden brown in colour and as contamination increased the films became thicker and darker.

With one exception, the waters taken off the beach and used without treatment were moderately corrosive, attacking some alloys slightly and none really seriously. The exceptional batch proved highly corrosive. In several runs iron was introduced into the water during the test in the belief that the presence of iron corrosion products in the water materially reduced its corrosive characteristics. In others small amounts (3 p.p.m.) of cystine were added with the intention of increasing the amount of the attack. Neither of these additions appeared to have any marked effect.

In eight of the later runs the corrosive characteristics of the water were examined during the course of the test by measuring the copper corrosion index (C.C.I.).<sup>10</sup> In seven of these cases the initial figure varied from 5 to 7 and generally rose to 13 or 15 at the end of the test. In the eighth case, where the amount of attack of all alloys was more severe, the copper corrosion index was initially 12 and rose only to 15 during the test.

The variation in the C.C.I. figures and the differences in the amount of attack on the same alloys in different runs all confirm the early observations concerning the wide variations in corrosive properties of different batches of natural sea-water due to the presence of minor contaminants. Pending further and more precise control of the corrosive properties of the sea-water, the policy which has been adopted throughout this work of testing each alloy in a sufficiently wide variety of waters to represent inshore, harbour, and ocean conditions and the inclusion in each run of a sample of standard material of known behaviour, seemed to be the only safe procedure.

It is not proposed to give the detailed results of all the tests carried out in this section of the work. The outstanding indications of these experiments can be summarized as follows :

(1) Resistance to impingement attack increased (a) with increasing nickel content, and (b) with increasing iron content up to an optimum value which varied with the nickel content.

(2) Alloys containing 7.5–30% nickel were virtually immune from impingement attack under these conditions of testing if they were of the appropriate iron content.

(3) With nickel contents of 12% and over, attack at shielded areas (see Fig. 8, Plate XXXIX) was considerable in alloys containing iron in amounts of the order of 1% or more.

(4) Iron contents up to 1% had little effect on the resistance to impingement attack of pure copper, but were markedly beneficial in alloys containing 3% nickel.

(5) The lowest nickel content to give really high resistance to

impingement attack was 5%. The behaviour of this alloy was very sensitive to iron content. All the results of tests on alloys containing 5% nickel, 107 specimens in all, are summarized in Fig. 2, where the depth of attack at the jet is plotted against the iron content. The small figures alongside each point on the curves indicate the number of individual specimens, the results of which were averaged to give the point shown. For the 79 specimens tested after quenching from 850° C. and cold rolling, it will be seen that the optimum resistance was

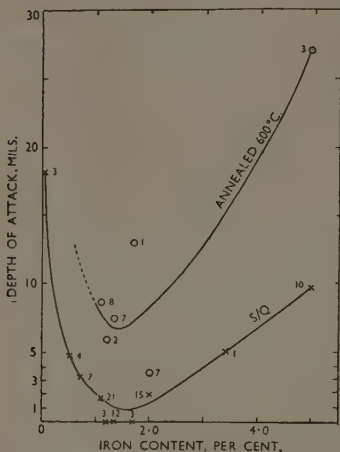


FIG. 2.—Effect of Iron Content on the Resistance to Impingement Attack of 5% Cupro-Nickels. (S/Q = Final heat-treatment involves quenching from 850° C.)

reached at iron contents between 1 and 2%, over which range the average depth of attack at the jet on 54 specimens was less than 2 mils. Markedly increased attack was shown on average by 25 separate specimens of alloys outside this iron range.

Fig. 2 also shows the average depths of attack on 28 specimens tested after annealing at 600° C. Here again the optimum resistance was obtained with between 1 and 2% iron, but the resistance had been reduced by annealing, the average attack over this iron range being 8 mils. Annealing at 600° C. also tended to cause a change in the colour of the film of corrosion product from golden brown to black. The amount of attack on specimens so annealed appeared to vary less

consistently with composition than was the case with the quenched strips, but this may be owing to the fewer results available for annealed alloys. While there was a marked reduction in resistance after annealing at 600° C., in nearly all tests the alloys containing 5% nickel and 1.2–1.7% iron behaved better than did 70 : 30 cupro-nickel of low iron content.

(6) Alloys containing 7.5% nickel with four iron contents (from 0.8 to 2.4%) were tested in only two jet-test runs. In one run of 22 specimens, some quenched and some annealed at 600° C., there was virtually no attack at shielded areas or at the jet in any specimen, although the low-iron 70 : 30 cupro-nickel check alloy was attacked at

the jet to a depth of 8 mils. In the second run the alloy of lowest iron content (1.2%) showed attack at the jet varying from 3 to 6 mils, while the alloys containing 1.7 and 2.4% iron were substantially resistant.

(7) For alloys containing 10% nickel the variation in behaviour with different iron contents is summarized in Fig. 3. This contains the average results of 80 tests on the material in the quenched and cold-rolled condition. The optimum resistance to impingement attack was reached between 1.3 and 2.5% iron: 52 specimens within this range showed no attack at the jet, while the 28 tests on specimens with lower or higher iron contents showed on the average marked attack. Twenty-three specimens of alloys containing 10% nickel with seven different iron contents were tested after annealing at 600° C. This treatment produced much less effect than in the case of the alloys with 5% nickel, the only alloy to show a serious increase in attack being that with 5% iron. The colour of the film of corrosion product again turned to black on all annealed specimens. As the iron content of the alloys with 10% nickel exceeded 2.4% attack at shielded areas, such as is illustrated in Fig. 8 (Plate XXXIX), occurred to some degree.

(8) Alloys of higher nickel content behaved as follows :

12.5% *Nickel* : 18 specimens with 3 different iron contents varying from 1 to 3% showed no significant attack at the jet in any test, but shielded-area attack occurred in all alloys.

15% *Nickel* : 17 specimens with 6 different iron contents varying from 1 to 9% were tested in abnormally corrosive aquarium-water and were either deeply attacked at the jet (up to 30 mils penetration) or were coated with heavy, thick scale which had blistered and which, therefore, could only have provided a temporary protection. Attack at shielded areas was severe in all specimens, particularly where the heavy scale had stifled attack at the jet.

20% *Nickel* : 27 specimens with 6 different iron contents varying from 1 to 9% showed severe attack at the shielded areas in all types

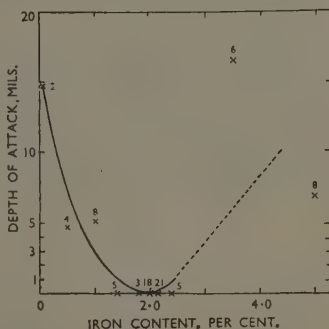


FIG. 3.—Effect of Iron Content on the Resistance to Impingement Attack of 10% Cupro-Nickels Quenched from 850° C.

of water. In corrosive aquarium-water alloys with iron contents exceeding 3% also showed severe attack at the jet.

30% *Nickel*: 23 specimens with 4 different iron contents varying from 0.04 to 2% were tested. A few specimens with 1 and 2% iron showed no attack at the jet in any test, but shielded-area attack was severe. Other samples with either 0.04 or 0.2% iron (commercial tubes with unknown thermal treatment) were used as standard check specimens. Of the alloy containing 0.04% iron 12 specimens in 8 different waters showed an average attack of 15 mils. Six specimens of the 0.2% iron alloy were unattacked at the jet and suffered only slight attack at shielded areas.

Reviewing these results broadly, the optimum corrosion-resistance in the low-nickel range was offered by the copper-10% nickel-2% iron alloys. On material containing 5% nickel and about 1.5% iron in the quenched condition the results were nearly as good, but there was more deterioration on annealing at 600° C. The alloy of intermediate nickel content (7.5%) showed excellent corrosion-resistance with an iron content of about 1.7%, but insufficient tests have been carried out to permit a close comparison with the alloys containing 5 and 10% nickel. Alloys of higher nickel content were highly resistant to impingement attack except when substantially iron-free, but with iron contents of 1% or more they tended to suffer shielded-area attack.

These results are substantially supported by those of Tracy and Hungerford,<sup>11(a)</sup> who, working with a solution of sea-salt, recommended iron contents of 1.0 and 0.75% for the alloys containing 5 and 10% nickel, respectively, contents markedly lower than those suggested by the work just described.

A preliminary exploration of the effect of heat-treatment on the corrosion-resistance of alloys containing 5% nickel, 1.35% iron and 10% nickel, 2% iron was made in two jet-test runs. Samples of material cold rolled to 68% reduction after quenching from 850° C. of each of these compositions were examined in the following conditions:

- (a) Reheated to 900° C. and quenched.
- (b)-(d) Reheated to 900° C., furnace cooled (at 2.5° C./min.) to (b) 800° C., (c) 700° C., and (d) 600° C., and quenched.
- (e)-(h) Reheated to 900° C., quenched, and re-annealed at 600° C. for (e) 5 min., (f) 30 min., (g) 2 hr., and (h) 24 hr., followed by air cooling.
- (j) Reheated to 900° C., quenched, and re-annealed at 700° C. for 2 hr., followed by air cooling.
- (k) Reheated to 900° C., furnace cooled to 600° C., and air cooled.

In neither of the two runs did the alloys with 10% nickel and 2% iron show any significant attack at the jet in any condition of heat-



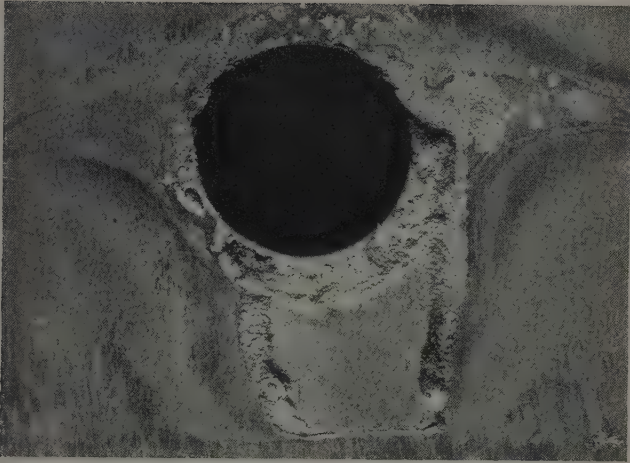


FIG. 8.—Typical Form of Attack at Shielded Areas of the Jet-Test Specimens.  
× 8.



FIG. 9.—Longitudinal Section of Copper (above) and Copper-5% Nickel-1% Iron Alloy Tubes After Testing for One Month in Flowing Aerated Sea-Water.



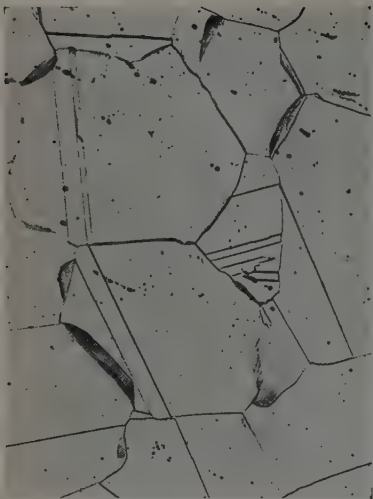


FIG. 10.—Typical Precipitation Resulting from Reheating an Alloy of Comparatively High Iron Content.  $\times 500$ .



FIG. 11.—Precipitation from Segregated Areas of High Iron Content after Reheating.  $\times 500$ .

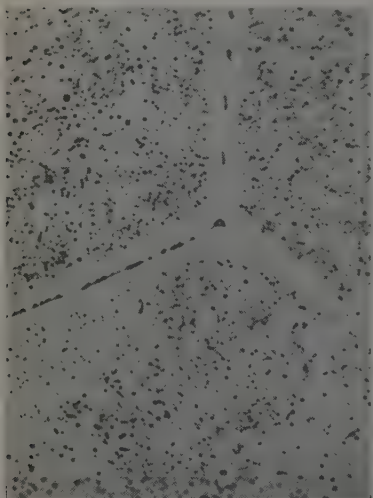


FIG. 12.—Structure of a Copper-5% Nickel-1.3% Iron Alloy Slowly Cooled from 900° to 600° C.  $\times 2000$ .



FIG. 13.—Structure of a Copper 5% Nickel-1.3% Iron Alloy Quenched from 900° C. and Re-annealed at 600° C. for 8 hr.  $\times 1000$ .

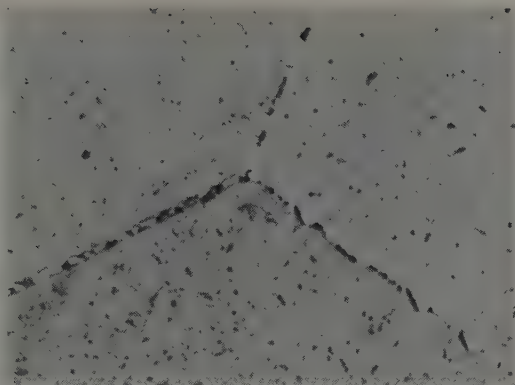


FIG. 14.—Structure of a Copper-10% Nickel-2% Iron Alloy Quenched from 900° C. and Re-annealed at 600° C. for 32 hr.  $\times 2500$ .

ELECTRON MICROGRAPHS OF A COPPER-5% NICKEL-1.3% IRON ALLOY.



FIG. 15.—Slowly Cooled to 700° C.  $\times 6000$ .

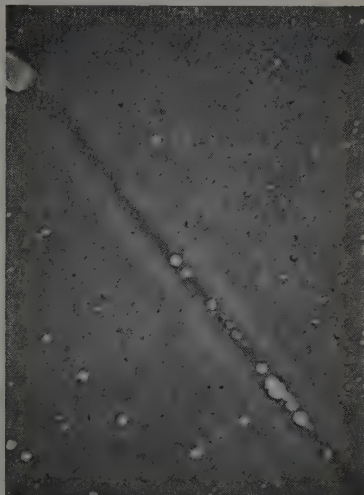


FIG. 16.—Slowly Cooled to 600° C.  $\times 7500$ .

ELECTRON MICROGRAPHS OF A COPPER-5% NICKEL-1.3% IRON ALLOY.

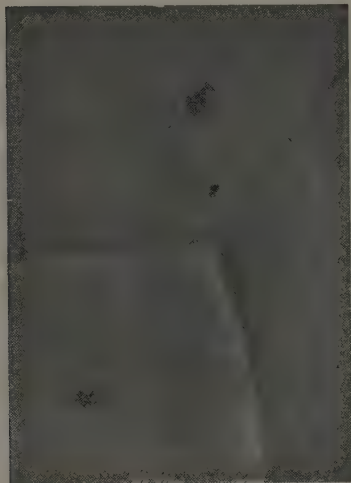


FIG. 17.—Quenched from 900° C.  $\times 6000$ .

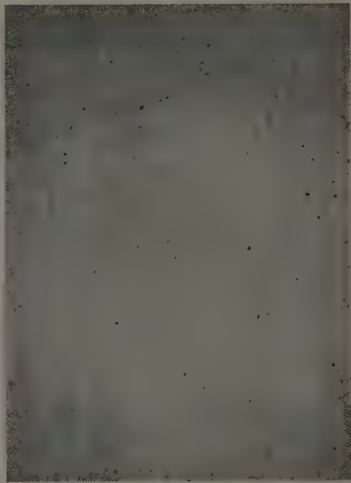


FIG. 18.—Quenched from 900° C. and Re-annealed at 600° C. for 2 hr.  $\times 6000$ .

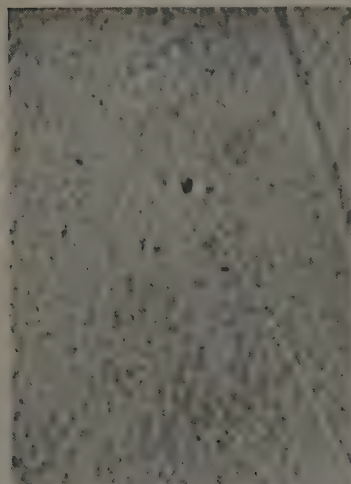


FIG. 19.—Quenched from 900 C. and Re-annealed at 600° C. for 2 hr. Replica gold shadowed.  $\times 11,000$ .



FIG. 20.—Quenched from 900° C. and Re-annealed at 600° C. for 4 hr. Replica gold-palladium shadowed.  $\times 11,000$ .

treatment, but all specimens heat-treated at temperatures below 700° C. (except those reheated to 600° C. for 5 min. only) formed a dark scale. No specimen was attacked at shielded areas. The alloy containing 5% nickel and 1.35% iron showed differences varying from complete resistance in the specimens quenched from 900° and 800° C., to attack at the jet to a depth of about 6.5 mils in specimens furnace cooled to 600° C. before quenching or reheating to 600° C. for 24 hr. Reheating for 5 min. at 600° C. had little effect. All the specimens showing attack were covered with a darker scale than those that were resistant; again there was no attack at shielded areas. Comparison of specimens (d) and (k) showed no apparent effect of the rate of cooling from 600° C.

(ii) *Deposit Attack*.—Duplicate specimens of alloys of each composition were tested for resistance to deposit attack under stagnant conditions. All alloys with less than 5% nickel suffered attack and those with 5% nickel and less than 0.5% iron were attacked quite severely under the deposit. Copper-5% nickel alloys with 0.5-2% iron were highly resistant to attack, but the one with 3.4% iron was severely attacked. The copper-10% nickel alloys were all resistant with the exception of that containing 3.5% iron. In the higher-nickel range most alloys containing 15-20% nickel showed fairly severe attack.

It is interesting to note that under the conditions of rapid movement and high aeration of the jet-test the lower-nickel alloys which suffered deposit attack under stagnant conditions suffered impingement attack over a wide area at the jet, but were not attacked at shielded areas. The alloys containing 5 and 10% nickel and of moderate iron content proved resistant to deposit attack under stagnant conditions and to impingement and shielded-area attack in the jet-test. The high-iron alloys of these nickel contents, however, and most of the alloys of higher nickel content were more or less attacked in the deposit-test and were consistently attacked at shielded areas in the jet-test. In the relatively few cases where these resistant alloys were attacked at the jet in these tests the area undergoing attack was extremely small.

It should be remembered that for the higher-nickel alloys the iron contents tested were unusually high. There is no suggestion that the low-nickel alloys are more resistant to corrosion than the 70 : 30 cupro-nickel containing 0.2-0.5% iron, or that the 80 : 20 alloy might not be improved by some iron addition below 1%.

#### (d) *Preliminary Tests on Industrial Tubes.*

During the course of this preliminary work two member firms of the Association manufactured several series of tubes from alloys containing

5% nickel with ten different iron contents varying from 0.7 to 2.15%, and 10% nickel with seven different iron contents varying from 1.7 to 2.25%. All the alloys but two contained 0.4–0.8% manganese. The two exceptions, containing 5% nickel and 1.4% iron, and 10% nickel and 2.3% iron, were phosphorus-deoxidized only. Tube diameters varied from the  $\frac{5}{8}$  in. of condenser tubes to 3-in. pipes. Most of the billets of both series are understood to have been heated to 950° C. for 16 hr. before extrusion, and with one of each series the extruded shell was heated to 920° C. and quenched in water before further drawing, which was carried out without re-annealing.

Sixteen specimens of the first two tubes of experimental industrial manufacture, containing 5% nickel and 1% iron, were included in three runs with laboratory-prepared alloys. In none of these runs was the attack on any material severe, and these tubes behaved comparably with the laboratory alloys except that in one run the as-received tubes were attacked to a depth of 10–12 mils compared with 6–7 mils for the tubes made from laboratory alloys. The remainder of the industrial tubes (54 specimens) were tested in three special runs in all of which a fairly highly contaminated North Wales sea-water (C.C.I. figures up to about 14) was used; 70:30 cupro-nickel checks were attacked to depths of up to 30 mils. In all these runs the only specimens which showed attack exceeding 3 mils were two samples containing 5% nickel and 0.7 and 2.1% iron respectively and, somewhat surprisingly, one specimen only of a copper-10% nickel-2.1% iron tube which was pitted to a depth of 24 mils. None of the alloys containing 5% nickel showed any attack at shielded areas, but in two runs the alloys with 10% nickel, both quenched and annealed showed this attack, in one of them to a surprising degree. This was the test in sea-water with the highest initial C.C.I. of the series. Nearly all the copper-10% nickel alloys in this run formed a dark film which was blistered, but there is insufficient evidence to judge whether this unusually severe attack at shielded areas in the specimens was caused by the condition of the water or that of the tubes. One interesting feature of these results is that the two tubes which were free from manganese and contained 5 and 10% nickel behaved in all respects as the manganese-bearing tubes of corresponding iron content.

Some of the first experimental tubes made from an alloy containing 5% nickel, 1.1% iron, and 0.6% manganese\* were submitted by the Admiralty to a special test in which sea-water carrying air bubbles

\* In making these tubes a cast billet was heated to 750° C. for 12 hr. then raised to 850° C. and extruded, subsequently annealed at 850° C. for 2 hr. and then drawn to size with intermediate annealings at 675° C.

was run through 1-in.-dia. pipes with a knee bend. The water pressure (due to gravity) was such as to give an actual speed through the pipes of 10–14 ft./sec. The injected-air content was of the order of 4–5% by volume. Under these conditions tests were carried out on pipes of this alloy and of ordinary copper for one month, at the end of which time one of the copper pipes was perforated at the knee. Photographs of the sectioned pipes are shown in Fig. 9 (Plate XXXIX), from which it will be seen that the attack on the copper–nickel–iron alloy was relatively insignificant while that on the copper was severe at the points of maximum impingement.

(e) *Mechanical and Working Properties.*

In order to examine the suitability of these materials for copper-smithing work, tests were carried out which are fully described in Appendix II. In tensile properties the alloys containing 5% nickel and 1.1–1.8% iron were slightly harder and less ductile than copper, while this trend was still more marked with copper–10% nickel–2% iron alloy. Drop-hammer forging tests showed a reduction in length of standard cylinders at 600° C. of 10–20% less than that of copper, while at 800° C. the copper–nickel–iron alloys showed a reduction in length which was again 10–20% smaller than that of copper and 20–25% less than that of 60 : 40 brass at this temperature.

Flanging, bending, and similar tests showed satisfactory working properties, the slightly greater toughness of these alloys proving no serious disadvantage. In some conditions of hot bending, however, tubes of the alloys cracked, though tubes which had presumably been annealed between cold draws at temperatures which resulted in a duplex structure were satisfactorily hot worked at temperatures up to 700° C. If the temperature of reheating exceeded 750° C., the second phase redissolved and such tubes (or tubes initially of single-phase structure) cracked on hot working at 600°–700° C. owing to structural changes at the grain boundaries which are described in Appendix I. Copper-smithing tests carried out in H.M. Dockyards gave results as satisfactory as those made in the Association's workshops. Welding by both oxy-acetylene and metallic arc techniques proved successful.

(f) *Conclusions.*

Reviewing these preliminary results broadly, the outstanding observation was the excellent resistance to sea-water corrosion, under both stagnant and impingement conditions, of the alloys containing 5–10% nickel and 1–2% iron, the behaviour of which was comparable with that of alloys of high nickel and lower iron contents. Increasing



the iron content markedly improved the resistance to impingement attack, while increasing the nickel content resulted in the formation of a thinner and strongly protective film. Alloys with over 10% nickel, however, in the presence of sufficient iron to give resistance to impingement, seemed to be liable to attack at shielded areas in moving aerated water.

The presence of coarse segregations or large undissolved particles of the iron-rich second phase largely destroyed the corrosion-resistance and thus imposed an upper limit on the desirable iron content. Below this limit the maximum resistance to impingement attack was reached by quenching the alloys from a temperature in excess of 800° C. The extremely fine state of division of the precipitate of the second phase resulting from heating these quenched alloys at about 600° C. resulted in a marked but not serious deterioration in corrosion-resistance. The presence of this second phase, even in a finely divided state, could be clearly detected because it resulted in a dark appearance of the film of corrosion product which formed on the surface in the jet-test. Specimens that did not have this second phase owing to their having been quenched from a high temperature formed golden or almost transparent and extremely thin films.

The copper-smithing tests carried out in H.M. Dockyards and the work on mechanical and working properties reported in Appendix II all suggested that the alloys containing 5% nickel and 1.2-1.4% iron offer that combination of corrosion-resistance and workability that was being sought. On the other hand a still higher corrosion-resistance appeared to be offered by the alloy containing 10% nickel and 2% iron, a degree of resistance which suggests the potential value of this alloy as a condenser tube, although its greater cost and the greater difficulty in working make it less attractive for the copper-smith.

#### VI.—PROPERTIES AND HEAT-TREATMENT OF ALLOYS CONTAINING 5-10% NICKEL AND 1-2% IRON.

While the information in the preceding section focused attention on alloys within the above range of compositions possessing the optimum combination of corrosion-resistance with good working properties, there remained considerable uncertainty as to the extent to which corrosion-resistance was affected by heat-treatment. Further work was undertaken, therefore, to provide fuller information on the benefits of heat-treatment on corrosion-resistance, particularly of high-temperature solution-treatment before breaking down and of subsequent lower-temperature heat-treatment of the finished product. This work is

described in the following sections, together with some examination of the effect of minor constituents, particularly phosphorus and manganese, and the effects of welding on corrosion behaviour.

### 1. *Effect of Solution-Treatment Before Hot-Working.*

As has been suggested earlier, it was thought desirable from the early experimental work to ensure if possible solid solution of the iron-rich constituent, which could only be effected by quenching from above 800° C. Failing this, if subsequent low-temperature annealing proved necessary, it was thought to be an advantage to ensure by a long-time high-temperature solution-treatment that the iron was sufficiently evenly distributed to produce a uniformly disseminated precipitate rather than a localized precipitate from an iron-rich area. It is notoriously difficult to eliminate coring from the copper-nickel alloys, and in order to achieve this it appeared necessary to heat-treat for some hours at temperatures of the order of 900° C. Since such a treatment of the relatively thin section of a tube or an extruded shell would be likely to cause distortion and both surface and sub-scale oxidation, the soaking of billets or ingots for a long time before hot working appeared an effective alternative. The necessity for this high-temperature solution-treatment and its effect on subsequent behaviour was therefore examined by comparing tube and strip made from billets and ingots soaked at 950° C. for 16 hr. with materials not so treated. The experiments carried out and the observations made are recorded for convenience in separate sections according to the type of casting from which the materials were prepared.

#### (a) *Tubes and Strips Made From Tube Billets.*

Billets of alloys containing 5% nickel and 1.5% iron, 7.5% nickel and 1.7% iron, and 10% nickel and 2% iron, each containing 0.3–0.5% manganese and 0.02–0.03% phosphorus, were poured at 1200°–1250° C. in moulds 18 in. long by 5½ in. dia. After cropping, each billet was cut into two 7-in. lengths for extrusion, and a slice 1 in. thick from the mid-section was retained for rolling. One 7-in. length was annealed for 16 hr. at about 950° C. and quenched in water. This billet and the 7-in. length which had not been so heat-treated were then extruded at 860° C., the tube shells air cooled, and subsequently drawn cold to ⅝ in. dia. in 7 passes with two intermediate anneals at 800° C. The central slice cut from each billet was divided diametrically and one half solution heat-treated at 950° C. for 16 hr. Both halves were then hot rolled at 860° C. to 0.25 in. thickness and cold rolled to 0.08 in. without intermediate annealing.

Samples of the tubes were tested in five different runs in the jet-test. In three of these there was no appreciable attack on any specimen of these alloys, nor on the low-iron 70 : 30 cupro-nickel tube used as a check. In the other runs the 70 : 30 tubes containing 0.04% iron were attacked to depths of 10 and 15 mils, respectively. The attack on the experimental materials did not exceed 4 mils, with the exception of one length of the alloy tube containing 10% nickel which in one run underwent irregular and unusual attack to a depth of 6 mils. The duplicate specimen was not attacked.

TABLE II.—*Tests on Copper-Nickel-Iron Alloy Tubes and Strips (80 mils Thick) Made With and Without an Initial Solution Heat-Treatment (S.T.) at 950° C. for 16 Hr.*

Alloy	Material and Condition	C.C.I. of Sea-Water					
		12.2	12.6-12.4	12.6	13.2	15.2-10.7	28.3-22.3
		Depth of Attack at Jet, mils					
5% Ni, 1.5% Fe	Tube S.T.	8	14	10	7	14	25
	„ not S.T.	8	25	10	7	15	*
	Strip S.T.	8	7	9	5	10	28
	„ not S.T.	9	32	10	7	11	32
7.5% Ni, 1.7% Fe	Tube S.T.	<1	8	4	2	6	10
	„ not S.T.	2	13	4	<1	7	14
	Strip S.T.	<1	4	2	1	2	14
	„ not S.T.	3	8	9	2	10	*
10% Ni, 2% Fe	Tube S.T.	Nil	6	Nil	Nil	Nil	*
	„ not S.T.	„	*	„	„	„	18
	Strip S.T.	„	<1	„	„	„	49
	„ not S.T.	1	3	<1	„	8	*

\* Perforated.

The manufacturer who kindly made these tubes provided for test at the same time a tube of an alloy containing 5% nickel and 1.2% iron from his current manufacture. This, like the experimental materials, was not attacked in three of the runs; in one of the others it suffered slight attack comparable with the experimental alloys of similar composition and in the last and most severe run, in which the 70 : 30 check specimen was attacked to a depth of 15 mils, this commercial tube was attacked to a depth of 6 mils only. These results reveal no difference in behaviour after initial solution heat-treatment, suggesting either that uniform distribution of the iron constituent is not

necessary or that the intermediate annealings at 800° C. between the stages of cold drawing had been sufficient to produce a uniform structure.

Fuller information was obtained by testing samples of each of the tubes and of the strips rolled from the same billets in six different runs, the results of which are shown in Table II. These runs contained no check specimens, and the C.C.I. figures for the waters used were high.

In the 18 samples of tube, with and without initial heat-treatment, significant differences were shown in only four cases; in three of these the unsoaked tubes were more severely attacked, and the soaked one in the fourth. In the case of the strips the initial soaking had been beneficial in all the six cases in which significant differences were found. The only consistent difference in the degree of attack on tubes and strips appeared to be in the slightly superior behaviour of the strips when both had been made from initially soaked material.

#### (b) *Strips Made from Small Ingots.*

In parallel with the work just described, the influence of wide variations in production treatments was studied on a series of  $9 \times 4\frac{1}{2} \times 1$ -in. rolling slabs made in the laboratory. One slab was sand cast and another chill cast in each of the following compositions: 5% nickel with both 1 and 1.5% iron, 7.5% nickel with 1.8% iron, and 10% nickel with 2% iron. All these materials contained 0.5–0.6% manganese and approximately 0.015% phosphorus. Chill- and sand-cast slabs were prepared, to provide evidence of the effect of as-cast grain-size on subsequent response to heat-treatment. No consequent differences were observed, and in the following discussion no distinction is made between sand- and chill-cast materials.

Strips were rolled in accordance with the schedule set out in Fig. 4. This provided from the two ingots of each composition eight lengths of strip in different conditions designed to throw light not only on the effect of initial solution heat-treatment but also of rolling temperature and of solution-treatment subsequent to rolling. Samples of the 16 strips of each composition thus obtained were tested in duplicate runs, which also included two 70 : 30 cupro-nickel (0.04% iron) check specimens. In only one of these eight runs was the attack produced on the check specimen severe and even in this case few of the specimens in any condition of heat-treatment were attacked to a depth exceeding 4 mils. The only results which call for comment as indicating any significant effect of soaking at high temperatures are that the alloy containing 10% nickel and 2% iron hot rolled at 700° C. without any previous soaking showed more attack than is usual with that alloy.

The depth of attack at the jet in this case ranged from 1 to 6 mils, compared with 7 mils for the 70 : 30 (0.04% iron) cupro-nickel check.

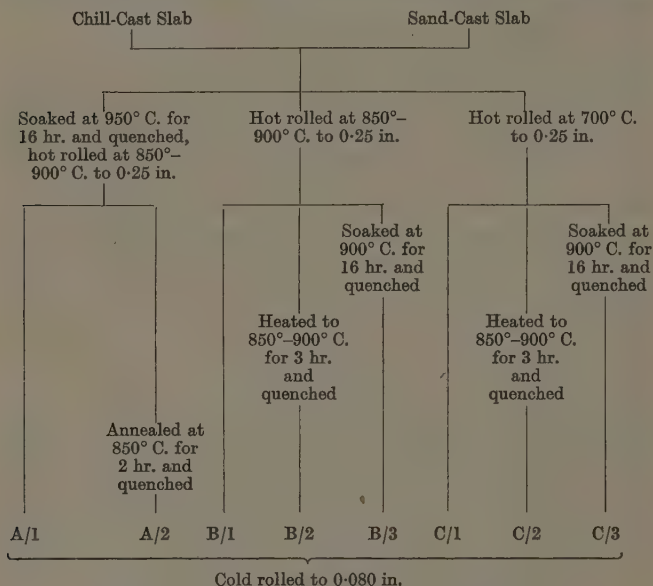


FIG. 4.—Production Schedules for Strip Specimens.

The following general conclusions were drawn from these results :

(i) The corrosion-resistance of copper-nickel-iron alloy tube which had been extruded at about 860° C. and given two intermediate anneals at 800° C. during drawing, was not significantly improved by a soak at 950° C. before extrusion. This was true of alloys containing 5, 7.5, or 10% nickel. There was little evidence of coring, even if no initial soak were given.

(ii) Whenever the amount of the attack was sufficient to reveal differences, strips of all compositions produced by hot and subsequent cold rolling without intermediate annealing showed improved corrosion-resistance when the billet slices from which they were prepared had been soaked at 950° C. for 16 hr. before hot rolling.

(iii) Strips prepared from billet slices soaked at 950° C. showed slightly better corrosion-resistance than tubes made from the corresponding soaked billets. The reason for this may be that the cooling

from the rolling temperature of 850°–900° C. occurring during rolling of small slabs was more rapid than the cooling of the tubes from the intermediate annealing temperature of 800° C.

(iv) While the strips cold rolled after hot rolling at 860° C. without any soaking were worse in corrosion-resistance than the strips prepared from billets soaked at 950° C., the tube samples showed no such difference. It is suggested that the annealing of the tubes at 800° C. between draws had had an effect on the structure similar to that of the previous soaking.

(v) The alloy containing 10% nickel was relatively unsatisfactory when hot rolled at only 700° C., but apart from this only minor differences in corrosion-resistance resulted from the various heat-treatments during production.

## 2. Effect of Subsequent Heat-Treatment.

The results of the exploratory tests described in Section V.2 illustrate the effect of heat-treatment on the corrosion-resistance of these alloys, particularly calling attention to the reduction in corrosion-resistance resulting from annealing the alloys with 5% nickel in the neighbourhood of 600° C. (Fig. 2). A fuller investigation has been made of the degree of deterioration resulting from this annealing, using alloys containing 5, 7.5, and 10% nickel.

Strips of alloys containing 5% nickel and 1.2% iron, hot rolled at 700° C., were tested in the conditions shown, with the results recorded in Table III. The waters used in these three runs were unusually corrosive, the low-iron 70 : 30 cupro-nickel check alloy being completely penetrated in each. The fact that the water A was slightly contaminated with hydrogen sulphide was established by the preparation therefrom of a culture of *Vibrio desulphuricans*. This bacterium reduces sulphate to sulphide, and the extremely heavy and irregular attack on all materials is consistent with experience of waters containing traces of hydrogen sulphide. The thick film of corrosion product which has afforded temporary protection to some specimens probably gives a misleading impression of the resistance in this particular experiment of the material as rolled at 700° C.

The other two runs, in which contamination, although severe, was less abnormal, showed a beneficial effect of heating to 950° C. and quenching and a marked deterioration on subsequent reheating for 30 min. at 600° C.

Similar tests were carried out on strip hot rolled at 700° C. from an alloy containing 10% nickel and 2% iron. This was tested in two comparatively clean waters (C.C.I. 6.6 and 5.6 respectively) and all



TABLE III.—*Attack at the Jet of Alloy Strip Specimens (80 mils Thick) Containing 5% Nickel and 1.2% Iron After Various Heat-Treatments.*

Heat-Treatment		Attack at Jet, mils		
		Sea-Water A Contaminated with H <sub>2</sub> S	Sea-water B C.C.I. = 16.4	Sea-Water C C.C.I. = 12.2
<i>a</i>	Hot rolled 700° C.	32 31	Penetrated "	17 17
<i>b</i>	Heated to 950° C. and quenched	Penetrated	8	6
<i>c</i>	As ( <i>b</i> ), reheated to 600° C. for 30 min.	Penetrated "	Penetrated "	26 24
<i>d</i>	As ( <i>a</i> ), annealed 2 hr. at 950° C. and quenched	Penetrated 33	<1 <1	<1 7
<i>e</i>	As ( <i>d</i> ), reheated to 600° C. for 30 min.	Penetrated 15	25 27	16 25
<i>f</i>	70 : 30 (0.04% iron) cupro-nickel	Penetrated	Penetrated	Penetrated

specimens resisted attack whatever the condition of heat-treatment. Strips of the copper-5% nickel-1.5% iron alloy prepared by each of the eight different rolling schedules illustrated in Fig. 4 were heat-treated at 600° C. for 30 min. and tested in these and in the original conditions.

In one run (C.C.I. 6.2-10.2) none of the as-rolled materials was attacked to a depth greater than 1 mil, while in all cases after annealing

TABLE IV.—*Depth of Attack on Quenched and Annealed Specimens Containing 5% Nickel and 1.3% Iron under Strictly Comparable Conditions.*

Condition	Group		
	1 (No attack)	2 (Attack < 2 mils)	3 (Attack > 2 mils)
Quenched from 850° C. :			
Mean . . . . .	Nil	1.1	5.5
Standard error . . . . .	...	±1.0	±3.0
No. of samples . . . . .	7	10	5
Range . . . . .	0-0	0-2.8	0.4-7.9
Annealed at 600° C. :			
Mean . . . . .	2.4	4.3	14.2
Standard error . . . . .	±2.2	±1.0	±8.5
No. of samples . . . . .	15	13	5
Range . . . . .	0-6.3	2.4-5.9	5.1-25.2

at 600° C. the attack was increased to 2.5–5 mils. The depth of attack on 70 : 30 cupro-nickel (0.04% iron) was 6 mils. In a second run specimens annealed at 600° C. were compared only with the 70 : 30 check alloy, the depths of attack on two specimens of which were 6 and 8 mils respectively. The copper–nickel–iron alloy specimens .42 (soaked at 950° C. before hot rolling and at 850° C. before cold rolling) were attacked to a depth of 4 and 5 mils respectively. All the 14 other samples of this alloy were uniformly attacked in this run to a depth of 7.5–9 mils. Thus, in this particular test, the copper–5% nickel–1.5% iron alloy annealed at 600° C. behaved no better than the 70 : 30 (0.04% iron) cupro-nickel.

In one run copper–7.5% nickel and copper–10% nickel alloy tubes (of the same batches as those reported on in Table II) were tested with and without annealing at 600° C. for 30 min. The 70 : 30 check was attacked to a depth of 6 mils, but the tubes were virtually unattacked, although the specimens annealed at 600° C. were slightly more "marked" than those which had not been so treated.

Fig. 5 summarizes the comparative behaviour of alloys containing 5% nickel and 1.1–1.35% iron in various conditions of heat-treatment when tested in waters of different corrosive properties.\*

The lower curve shows the amount of attack on a number of specimens quenched from 850° C., arbitrarily grouped in three classes according to the amount of attack. Those showing no attack were put in Group 1, those showing attack up to 2 mils in Group 2, and those showing attack of over 2 mils in Group 3. The upper curve shows the depth of attack in the same waters on specimens annealed at 600° C. Results are only incorporated in this figure when specimens of the same composition in the two conditions of heat-treatment have been compared in the same water. The average results with the standard error of mean, the number of observations, and the range of each group are shown in Table IV.

These results confirm quantitatively the wide differences in corrosive

\* Tests carried out in artificially contaminated sea-waters are excluded from this summary, as are those in sea-waters A and B of Table III. Sea-water A was clearly abnormal in its behaviour, and the results with sea-water B are possibly unduly favourable to the quenched material.

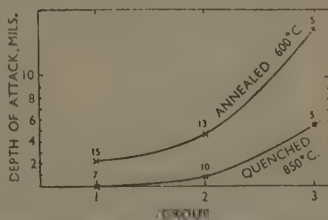


FIG. 5.—Effect of Contamination of Water on Impingement Attack on Copper–Nickel–Iron Alloys Containing 5% Ni, and 1.1–1.3% Fe in Different States of Heat-Treatment.

properties of ten different batches of natural sea-water and emphasize once more the dangers of testing a particular alloy in one or two batches of sea-water only and drawing from these results general conclusions about the behaviour of material under all conditions of service.

The conclusions drawn from this section of the work are as follows :

(i) Reheating to 600° C. for 30 min. caused some deterioration in the corrosion-resistance of all the materials tested. The deterioration was insignificant in the copper-10% nickel alloy, but was marked in the copper-5% nickel alloys. The deterioration is increasingly serious as the pollution of the water increases.

(ii) Even after reheating to 600° C. the resistance of the copper-5% nickel alloys to impingement attack was never worse than that of 70 : 30 cupro-nickel of low-iron content (0.04%).

(iii) The resistance to impingement attack of the copper-5% nickel alloy after final annealing at 600° C. for 30 min. was virtually constant whatever manufacturing schedule was employed.

### 3. *Effect of Minor Constituents on Corrosion-Resistance.*

As has been stated in the earlier part of this paper, nearly all the alloys tested contained manganese, and the results obtained have been discussed on the assumption that manganese exerted no major effect on the structure or corrosion-resistance of these materials. Relatively few of the alloys made in the laboratory contained phosphorus as well as manganese, but some comparisons have been made of copper-nickel-iron alloys containing 0.5-0.75% manganese with similar compositions (a) free from manganese but containing about 0.02% phosphorus, and (b) containing this amount of phosphorus in addition to the manganese. The compositions compared are shown in Table V.

Samples of groups *A* to *F* were tested simultaneously in the same waters. A careful study of the results obtained shows no difference in attack at the jet or elsewhere that could be attributed to differences in manganese and phosphorus contents. The results were few, however, and the amount of attack occurring on an alloy of any one composition in these particular runs was slight. Had they been tested in more corrosive waters, differences might have been revealed, but the evidence available suggests that the resistance of these alloys is not markedly dependent on the manganese or phosphorus content within the limits shown.

The alloys of group *H* (Table V) were made from both sand- and chill-cast slabs by the procedure illustrated in Fig. 4. The alloy of each composition therefore provided 16 samples in different conditions. Each group was tested together with the 70 : 30 (0.04% iron) cupro-

nickel check in every case, in separate jet-test units, the conditions for the three tests being as nearly identical as possible. The copper-5% nickel-1.5% iron alloys containing (a) 0.65% manganese and no

TABLE V.—*Compositions of Alloys with Varying Manganese and Phosphorus Contents.*

Alloy	Nickel, %	Iron, %	Manganese, %	Phosphorus, %	
<i>A</i>	5.0	0.54 0.49	0.70 Nil	Nil 0.017	
<i>B</i>		1.20 1.23	0.40 Nil	Nil 0.016	
<i>C</i>		1.46 1.46 1.43	0.70 0.50 0.03	0.03 Nil 0.04	
<i>D</i>		10.0	1.04 1.10	0.75 Nil	Nil 0.025
<i>E</i>			1.43 1.36	0.47 0.75	0.033 Nil
<i>F</i>			2.11 2.18	0.72 Nil	Nil 0.015
<i>G</i>	5.0		1.3 1.3 1.3	0.5 0.6 0.5	0.02 0.03 0.06
<i>H</i>		1.5 1.5 1.4	0.6 0.65 Nil	0.015 Nil 0.007	

phosphorus and (b) 0.007% phosphorus and no manganese gave results in very close agreement with those obtained on the alloy containing 0.6% manganese and 0.015% phosphorus.

Finally, alloys of group *G* (Table V), in the cold-rolled condition after quenching from 900° C., were tested to provide information on the effect of varying phosphorus contents. In the same run copper-5% nickel alloys containing lower and higher iron contents, with and without about 0.02% phosphorus, were also tested.

The water used in this run was sufficiently corrosive to attack the 70 : 30 cupro-nickel check to a depth of 4 mils. The alloys containing 1% iron were more severely corroded, but the alloys containing 1.3% iron with 0.02 and 0.03% phosphorus underwent no measurable attack. When the phosphorus was increased to 0.06%, however, the depth of attack increased to 5 mils, suggesting that this higher phosphorus content had neutralized to some extent the beneficial effect of the

increasing iron content. As far as conclusions can be drawn from this single experiment, it would appear that there is no advantage and may be some disadvantage in increasing the phosphorus content of these alloys above 0.03%.

#### 4. *Effect of Welding.*

##### (a) *Tests on Cast Materials.*

As a preliminary to the examination of the corrosion-resistance of welded joints in these alloys, tests were carried out in two different waters on samples of cast alloys containing 5% nickel with 1% iron and 10% nickel with 2% iron. In both these runs the 70:30 low-iron cupro-nickel tube was attacked at the jet to a depth of 23 mils. In one run, only chill-cast specimens of the two compositions were included, and with neither composition was there any attack at the jet. In the other run both chill- and sand-cast specimens were tested. Again the chill-cast specimen was unattacked, but the sand-cast specimen showed attack at the jet to a depth of 30-50 mils. In both cases the attack resulted in a marked etch effect in which the dendrites were clearly visible, suggesting that the corrosion was associated with segregation accompanying the coarse grain.

##### (b) *Tests on Welds.*

Specimens of welds in sheet and tube of alloys containing 5% nickel with 1.3 and 1.5% iron and 10% nickel with 2% iron, the quality and mechanical properties of which are referred to in Appendix II, were tested under conditions of general impingement. Samples  $1\frac{1}{8}$  in. long by  $\frac{1}{2}$  in. wide were cut transversely to the directions of welding, with the weld in the centre. To avoid testing these alloys in such restricted conditions of impingement that the jet would affect only the cast or the wrought material, the whole surface of these  $1\frac{1}{8} \times \frac{1}{2}$ -in. strips was subjected to impingement conditions. They were mounted on the periphery of a disc which was rotated in a bath of sea-water under conditions involving the entraining of much air and a peripheral speed of the order of 15 ft./sec. It is difficult to compare quantitatively the results of this test with those of the jet-test, but it was clear from these results that a small amount of impingement attack occurred in most specimens with no preferential attack at the weld except in one or two cases where the weld metal was porous.

This limited evidence on the behaviour of welded joints is in line with the few tests described of cast materials and suggests that where the mass of weld metal is small and the rate of cooling therefore rapid, welding does not involve any danger of serious deterioration in corro-

sion-resistance. The considerable attack on sand-cast specimens suggests that welds in thick specimens, where the rate of cooling is slow, might suffer severe corrosion.

#### VII.—COMPARISON OF 5 AND 10% NICKEL ALLOYS WITH STANDARD CONDENSER MATERIALS.

During most of this work comparison has been made with the low-iron 70 : 30 cupro-nickel. In some jet-test runs (15 ft./sec. with 3% air) other materials used in cooling-water systems have been included, but only four runs contained arsenical copper, Admiralty brass, aluminium brass, and the copper-5% nickel alloys with different heat-treatments. In these runs attack on aluminium brass and the copper-5% nickel alloys in the quenched condition was nil, on the copper-5% nickel alloy reheated to 600° C. it averaged 2 mils in depth, while Admiralty brass and copper were attacked to average depths of 9 and 13 mils, respectively.

More comprehensive information on this comparison is provided by more recent work, in which the standard alloys listed in Table VI were

TABLE VI.—*Comparison of Different Alloys in Jet-Tests at 15 ft./sec. (1.5-5% Air by Volume).*

Material	Range of Depths of Attack, mils	Average Depth, mils	No. of Runs (2 specimens in each)
Arsenical copper . . . . .	4-25	14	5
Admiralty brass * (70 : 29 : 1) . . . . .	5-20	14	8
Aluminium brass (76 : 22 : 2) . . . . .	0-26 †	2	8
70 : 30 cupro-nickel (0.04% iron) . . . . .	0-13	4	8
70 : 30 cupro-nickel (0.2% iron) . . . . .	0- 5	1	8
Copper-5% nickel-1.5% iron ‡ . . . . .	0- 4	1	8
Copper-5% nickel-1.5% iron, reheated at 600° C. for 30 minutes . . . . .	1-12	6	5
Copper-10% nickel-2% iron ‡ . . . . .	0	0	8

\* Admiralty brass was tested in a different series of runs from the other materials in this table.

† One specimen 26 mils; no other greater than 1 mil.

‡ Commercial tubes made as described in Section VI. 1 (a).

tested together in some eight different runs with copper-5% nickel-1.5% iron and copper-10% nickel-2% iron alloys in the conditions shown. The superiority of the high-iron 70 : 30 cupro-nickel and the copper-10% nickel-2% iron alloy is clearly shown. The copper-5% nickel-1.5% iron alloy in the quenched condition is virtually as good as these, but it deteriorates on annealing to a position roughly equal to that of the low-iron 70 : 30 cupro-nickel. Arsenical copper and



Admiralty brass are markedly inferior to any of the other materials. Fifteen specimens of the aluminium brass resisted excellently, but the sixteenth was deeply attacked in a run containing 5% of air—a confirmation of the liability of this alloy to occasional deep attack when conditions are severe.

#### VIII.—SUMMARY AND DISCUSSION OF RESULTS.

The more outstanding observations recorded in this paper can be briefly summarized as follows :

(1) The resistance to corrosion of 70 : 30 cupro-nickel by moving aerated sea-water is greatly increased by the presence of 0.3–1% iron.

(2) Iron contents of 1% or more in 70 : 30 cupro-nickel increase the tendency of this alloy to local pitting at areas shielded from oxygen.

(3) Alloys of low nickel content (5–10%) are greatly inferior to the 70 : 30 alloy if the iron content is below 1%.

(4) The addition of 1.3–2% iron to these low-nickel alloys confers on them a resistance to corrosion of the same order as that of the 70 : 30 alloy containing 0.3–0.5% iron.

(5) Alloys containing 5–10% nickel and 1–2% iron offer their optimum resistance to sea-water corrosion when quenched from temperatures of the order of 850°–950° C. This resistance is reduced, particularly in contaminated waters, by annealing at or slowly cooling to temperatures of the order of 600° C.

(6) The reduction in corrosion-resistance accompanying these heat-treatments is due to the separation of a second solid solution richer in nickel and iron.

(7) Optimum corrosion-resistance is not compatible with hot workability, since breakdown of the corrosion-resistant structure on heating to 600°–700° C. during hot working develops a liability to cracking.

(8) The corrosion-resistance of the alloys as normally manufactured in tube form is in normal circumstances not sufficiently below the optimum to justify the troublesome steps necessary to ensure the best possible results.

(9) The alloys containing 5–10% nickel and 1–2% iron can be readily cold worked whatever the heat-treatment or structure, and hot worked if suitable precautions are taken in manufacture.

The corrosion-resistance of the alloys and the appearance of the films of corrosion product formed on their surfaces vary considerably with the condition of heat-treatment. Optimum resistance is offered after solution heat-treatment and quenching from about 900° C., in which condition the alloys normally form a thin, golden-brown film

of corrosion product when water contamination is slight. If the alloys are annealed at 600° C., or slowly cooled to temperatures of this order, and then tested in waters of similar contamination, they normally form a thin, black film. These changes in colour of the film of corrosion product are paralleled by changes in the magnetic susceptibility of the alloy, which is relatively high when the film of corrosion product is black and very low when the film is golden or colourless. Where the water is heavily contaminated, the film of corrosion product is in both conditions thicker and darker than in the clean waters. This thick film can occasionally be protective, but frequently tends to break down locally with rapid attack of the underlying metal at the point of failure. The tendency of such a thick film to form increases not only with the contamination of the water, but also with the amount of second phase present in the structure, whether due to excessive iron content or to heat-treatment which precipitates this phase from the lower-iron alloys.

Incidental to the main programme of corrosion testing, a considerable amount of work has been carried out to throw light on the composition and properties of the films formed on these alloys under different conditions and to elucidate the somewhat surprisingly beneficial effects which iron additions have on their corrosion-resistance.

It is clear from the test results and from electrochemical measurements carried out on a number of different alloys that the film of corrosion product is strongly cathodic to the basis metal. The thick, dark film formed in contaminated waters is very similar in appearance and in electrical characteristics to that formed in an initially clean sea-water to which cystine has been added. The change in potential of a copper-5% nickel-1% iron alloy in this case has been found to be rapid and large, particularly when the basis metal has been annealed at 600° C. For example, in one such test, within a few hours of adding cystine, the potential became more cathodic by 150 mV. A similar test on the same alloy in the quenched condition resulted in a change in potential of only 60 mV. and a much more rapid return to the original condition.

Various attempts have been made to examine the composition of the protective films of corrosion product formed in relatively clean sea-waters, particularly to detect the differences between the light and dark films formed respectively on quenched and annealed specimens. Examination of these films by X-rays after scraping from the basis metal showed that the copper-5% nickel-1.5% iron alloys had a cuprous oxide film when quenched, but when annealed the black film formed contained no crystalline cuprous oxide. This film was, in fact, identical with the black film formed on the copper-10% nickel-2% iron alloy after annealing at 600° C., though this alloy showed no

crystalline cuprous oxide in the film in either the quenched or the annealed conditions. Attempts were made to investigate the compositions of the films using the electrolytic-reduction method described by Miley and Evans.<sup>14</sup> By this method, Price and Thomas<sup>15</sup> found that each of the four principal constituents in the tarnish film on silver-copper alloys could be reduced at a different and characteristic potential. In this way it was hoped to be able to estimate the amounts of copper, nickel, and iron oxides in the film on copper-nickel-iron alloys, but no success was obtained, as no well-defined potential steps occurred during the reduction process.

On reviewing the results broadly, it is clear that the addition of iron to the cupro-nickel renders the film of corrosion product formed on the alloy surface in aerated sea-water more protective. For its beneficial effects to be exploited to the full, the iron should be in solid solution and, under conditions of uniform aeration, any one copper-nickel alloy achieves its highest corrosion-resistance when it contains as much iron as is possible without the appearance of a second constituent in the structure. With the appearance of a second iron-rich phase, or on the breakdown of the initial solid solution by a subsequent heat-treatment, the film formed is less resistant, the deterioration increasing with growing aggregation of the second phase.

As is usual in the case of protective films, improvement in the resistance of the film is accompanied by increased concentration of attack at any point at which film breakdown for any reason occurs. Such attack, in the case of these alloys, takes the form of local pitting and a local deficiency of oxygen seems to be one of the causes of breakdown of the film. Thus, at areas shielded from access of oxygen, the otherwise highly protective film formed on an alloy of fairly high iron content is liable to break down, with the occurrence of rapid and serious pitting.

This observation is in line with American experience of these alloys as recently recorded by Lynes,<sup>16</sup> but the implication in his paper that in the absence of oxygen iron is a positive disadvantage is not borne out by our experience. Thus, alloys in which as much iron as possible is in solution may possess a high resistance to attack in the presence of a uniform oxygen supply, but may suffer severely from pitting in areas where oxygen access is reduced. The optimum iron content for all-round corrosion-resistance is therefore not necessarily the highest iron content that can be obtained in solid solution. Where more severely contaminated waters are encountered, it seems even more important, if maximum corrosion-resistance is to be obtained, to ensure that the iron content is in solution. The consequences of a breakdown of this

solution are more serious with severe contamination, and the general impression is that contamination is more effective in increasing the attack on an alloy with a free second phase, however finely divided this may be, than on alloys which have been quenched from 950° C. There is evidence that the contaminant enters into the composition of the film of corrosion product with results which are hardly beneficial, and that it does so more readily if the alloy contains a second phase. No explanation can be offered for these effects, however, since no satisfactory and reliable information is available on the types of film formed in clean and contaminated waters.

## APPENDIX I.

### THE STRUCTURE OF COPPER-NICKEL-IRON ALLOYS.

Published information on the copper-rich alloys of this ternary system is meagre. Köster and Dannöhl<sup>17</sup> showed a solubility of iron in copper-nickel-iron alloys of only 1% with nickel contents up to 70%, but they offer no evidence for the shape of the  $\alpha$ -phase field at compositions below 30% nickel. The most recent and comprehensive study of the system is that first referred to by Bradley and Bragg<sup>18</sup> and later described in greater detail by Bradley, Cox, and Goldschmidt.<sup>13</sup> These investigators determined the equilibrium solubility curve of the  $\alpha$ -phase at several temperatures above 750° C., having first mapped a phase diagram for a range of slowly cooled alloys representative of the complete system. This preliminary diagram was plotted from X-ray observations upon filings annealed at 900° C. and cooled at the rate of 20° C./hr. after lump-annealing for more than 24 hr. at temperatures above 1000° C.

Although Bradley, Cox, and Goldschmidt remark that the copper-rich corner of the diagram, beyond 80% copper, was not fully investigated, their phase diagram for the slowly cooled alloys shows an iron solubility rising from nil in pure copper to about 13% at 4% nickel, and thereafter falling to 3% at 30% nickel. The phase boundary found in the copper-rich corner of the 750° C. section, plotted from observations on filed materials, annealed for 24 hr., and quenched, is closely similar in shape.

The alloys employed in the investigations described in the present paper had compositions lying within this single-phase field, and their condition of heat-treatment was usually such that, in view of the observations of Bradley and his collaborators, they could be expected to have a single-phase structure. Yet different specimens of identical

composition showed sharp variations in corrosion-resistance and hot-working properties which were found to depend critically upon heat-treatment. The work described in this Appendix was undertaken to throw light on these variations. In doing so, it showed also that there is room for further study of the copper-rich corner of the ternary diagram.

### 1. The Properties of the Alloys.

#### (a) Alloys Examined.

The alloys of the compositions shown in Fig. 1, prepared in accordance with the procedure described previously in this paper, were subjected to an exploratory examination. Short lengths of each strip

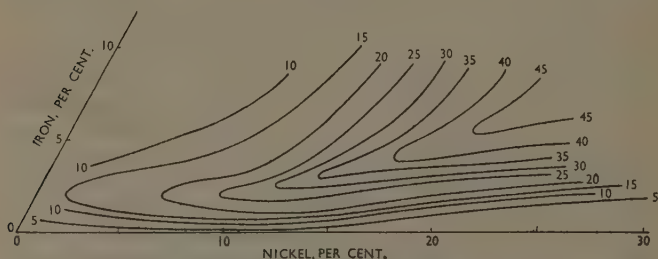


FIG. 6.—Contours of Increase in Hardness of Alloys on Reheating for 2 hr. at 600° C. after Quenching from 900° C.

were annealed for 2 hr. at 900° C., quenched, and subsequently reheated at 500°, 600°, and 700° C. for periods up to 32 hr. The hardness of all specimens was measured and a number were examined microscopically. The two alloys of greatest interest on account of their corrosion-resistance, namely copper-5% nickel-1.3% iron and copper-10% nickel-2% iron, were subjected to more extensive examination, which included observation with the electron microscope and a study of the changes in magnetic permeability accompanying heat-treatment.

#### (b) Hardness Changes.

The alloys were in the softest condition after quenching from 900° C. Reheating for 2 hr. at 600° C. resulted in hardening, the extent of which is plotted in Fig. 6. At this temperature, 2 hr. was in most cases sufficient to bring about the maximum hardening and reheating for longer periods, up to 32 hr., had little further effect. Annealing at

500° C. resulted in similar increases of hardness, which occurred rather more slowly, and, in general, reheating at 700° C. produced smaller hardness changes.

(c) *Structure.*

Microscopic examination at high magnification of all alloys as quenched from 900° C. showed a single phase except for alloys containing more than about 5% iron. After reheating for 2 hr. at 600° C., precipitation was observed in alloys with more than about 2% iron. The second phase present in quenched alloys containing more than 5% iron was blue in colour and was presumed to be iron-rich. Where this phase had completely dissolved on annealing at 900° C. and a second constituent was observed only after reheating at 600° C., it took the form shown in Fig. 10 or Fig. 11 (Plate XL). It is presumed that Fig. 10 shows precipitation from a supersaturated solid solution, whereas Fig. 11 shows precipitation from iron-rich regions in a non-homogeneous solid solution, which correspond to iron-rich segregates in the original casting.

These observations are not more fully discussed, since a subsequent study of the two alloys of most interest showed the occurrence of significant changes on a scale so fine that the light microscope is not fully effective for their observation. These changes were investigated in the alloys containing 5% nickel with 1.3% iron and 10% nickel with 2% iron. The two alloys were in the form of strip which had been annealed at over 850° C. for some hours before and during cold working, and were obtained in the following heat-treated conditions:

(i) Quenched from 900° C. after annealing a further 2 hr. at that temperature.

(ii) Slowly cooled from 900° C. (1° C./min.) to 800°, 700°, and 600° C., and quenched.

(iii) As (i), but reheated to 600° C. for times from 1 hr. to 256 hr.

It will be noted that the slowly cooled specimens were cooled at three times the rate used by Bradley, Cox, and Goldschmidt.

Examination at high magnification with the light microscope showed that the two specimens quenched from 900° C. and those cooled to 800° C. before quenching all appeared to be homogeneous, twinned  $\alpha$ -solid solutions. Slow cooling to 700° C. produced a small amount of a second phase, particularly clearly shown at the grain boundaries but also distributed in a fine state of division throughout the grains. Slow cooling to 600° C. showed the same structure in a more fully developed form (Fig. 12, Plate XL). The presence of a band which is relatively free from particles of the precipitated phase will be noted, occurring on



either side of the larger particles of precipitate formed in the grain boundaries. These larger particles also appeared blue in colour.

Specimens reheated for 2 hr. at  $600^{\circ}\text{C}$ . appeared unchanged on microscopic examination. A small change was detected after reheating for 4 hr. and was more clearly defined after annealing for 8 hr. (Fig. 13, Plate XL). The grain boundaries contain small particles of precipitate, between groups of which there are narrow zones which appear lighter than the adjacent grains themselves. The structure of the grain boundaries of these alloys after treatment of this nature is more clearly seen in Fig. 14 (Plate XLI) which shows the copper-10% nickel-2% iron alloy as quenched from  $900^{\circ}\text{C}$ . and re-annealed at  $600^{\circ}\text{C}$ . for 32 hr. This micrograph provides evidence of the presence in the boundary of a zone which is believed to be impoverished in nickel and iron.

The structures which have been described are visible with the light microscope only when the magnification used is so great that diffraction effects make their detailed appreciation difficult. Further evidence was provided by submission of the specimens of copper-5% nickel alloy to examination by means of the electron microscope, using the plastic-film replica technique. The structure of the specimen quenched from  $900^{\circ}\text{C}$ . appeared to be entirely single-phase. After slow cooling to  $700^{\circ}\text{C}$ ., clear evidence was found (Fig. 15, Plate XLI) of the presence of rounded areas of a second phase, which were larger in the grain boundaries than in the grains. A similar and more fully developed structure was observed in the specimen slowly cooled to  $600^{\circ}\text{C}$ . (Fig. 16, Plate XLI), and showed clearly the precipitate-free band at the grain boundaries which was referred to in describing Fig. 12.

The structure observed in the specimen which had been reheated at  $600^{\circ}\text{C}$ . for 2 hr. showed no evidence of precipitation either at the grain boundaries or within the grains, in line with the results of optical examination. However, comparison of Fig. 17 (Plate XLII), from the specimen quenched at  $900^{\circ}\text{C}$ ., with Fig. 18 (Plate XLII) shows there is evidence for a change of structure in the mottled appearance which characterizes Fig. 18. This effect was investigated by "shadowing" the surface of the plastic replicas with gold or gold-palladium alloy, which enhances the contrast and definition obtained.

Shadowed replicas of specimens quenched from  $900^{\circ}\text{C}$ . showed no more roughness, when examined at about 12,000 diameters, than was obtained by using a glass slide control. When shadowed in the same way, the replica of the specimen reheated for 2 hr. at  $600^{\circ}\text{C}$ . appeared typically as in Fig. 19 (Plate XLII), which was prepared from a very lightly etched surface. It is clear from this examination that quenching

after annealing for some hours at 900° C. results in a uniform solid solution, whereas reheating the quenched alloy at 600° C. for 2 hr. is sufficient to initiate decomposition of this solid solution in a way that the light microscope is unable to detect.

The progression of this change is made clear by Fig. 20 (Plate XLII), which shows the structure of the specimen reheated for 4 hr. The replica was shadowed with gold-palladium alloy, which, in contrast to gold, does not aggregate appreciably. The photograph shows adjacent grains, one of which has a striated surface while the other has a nodular form of roughness. At the boundary between the two are three rounded particles which are thought to be of stable second phase. These particles lie within a broad band at the boundary that probably corresponds to the light-etching zones in Fig. 13 (Plate XL). From a study of Fig. 20 and a number of similar micrographs it is considered that the etching reagent selectively removes material from both sides of the grain boundary, so forming an abnormally wide, shallow groove. Etching appears to proceed most rapidly where striations meet the boundary at right angles so that, as in Fig. 20, the grooves may be asymmetrical in cross-section.

These observations lend support to the belief that the grain-boundary surfaces are flanked by thin zones of material impoverished in iron and nickel. Presumably atoms of these two elements diffuse comparatively readily in the interface between adjacent grains, until they contribute to the nucleation and growth in the grain boundary of particles of  $\alpha'$  phase. More iron and nickel atoms diffuse from the matrix to the boundary, this process occurring most readily along the direction of the striations. Concentration gradients are thus established in directions normal to the boundary surfaces and these give rise to the observed etching effects.

It may be noted that the form of segregation into two phases appears to be rod-like rather than lamellar, since, although the right-hand grain of Fig. 20 has a striated appearance, the adjacent grain has a nodular appearance which cannot correspond to any section through lamellæ.

#### (d) *Magnetic Properties.*

It is mentioned in the paper that the changes in corrosion-resistance that occur on heat-treatment are accompanied by changes in magnetic properties. These magnetic changes were measured using a crude form of balanced-coil magnetometer. Values obtained for the initial permeability of the two alloys in different conditions of heat-treatment are given in Table VII and Fig. 7.

Table VII shows that both alloys, when slowly cooled to tempera-



(e) *Curie Point.*

The Curie point was also affected by heat-treatment, and a comparison in these two alloys of the effects of slow cooling and of quenching and re-annealing is shown in the first two columns of Table VIII. The figure numbers shown in parentheses refer to the illustrations, where available, of microstructures of the copper-5% nickel alloy.

The specimens annealed for 2 hr. at 600° C. were unstable, and the temperature of the Curie point tended to rise during the experiments for its determination. The more stable structure resulting from slow cooling corresponded with a markedly higher Curie point.

(f) *Electrical Resistivity.*

The resistivity at 20° C. of the two alloys in different conditions of heat-treatment are also recorded in Table VIII. That the resistivity

TABLE VIII.—*Changes of Curie Point and of Electrical Resistivity After Heat-Treatment.*

Heat-Treatment	Curie Point		Resistivity, $\mu\Omega/\text{cm.}^3$	
	5% Ni- 1.3% Fe Alloy	10% Ni- 2% Fe Alloy	5% Ni- 1.3% Fe Alloy	10% Ni- 2% Fe Alloy
Quenched from 900° C.	...	...	13.9 (Fig. 17)	19.9
Slowly cooled (1° C./min.) from 900° C. to 600° C. and quenched.	260° C. (Figs. 12 and 16)	517° C.	13.2 (Figs. 12 and 16)	18.7
Quenched from 900° C., re-annealed at 600° C. for 2 hr., and quenched.	160° C. (Figs. 18 and 19)	275° C.	11.8 (Figs. 18 and 19)	17.8

should be highest after quenching from 900° C. is not surprising, but that the unstable material showing incipient breakdown of the solid solution should have a lower resistivity than the more stable structure of the fully separated type shown in Fig. 12 was unexpected.

## 2. Discussion of Results.

The microscopically observed structural changes described in this Appendix amply show that many of the alloys investigated from the corrosion point of view and, in particular the copper-5% nickel-1.3% iron alloy and the copper-10% nickel-2% iron alloy, undergo substantial decomposition into two phases, presumed to be  $\alpha$  and  $\alpha'$ ,

on slowly cooling from 900° C. to temperatures below 700° C. That this should have been missed by Bradley and his collaborators, who employed even slower rates of cooling, must be attributed to the insensitivity of the X-ray method in this particular case. The insensitivity is understandable, since both the  $\alpha$  and  $\alpha'$  phases have the face-centred-cubic structure and, though their compositions may differ widely, the corresponding lattice parameters may lie close together. Bradley, Cox, and Goldschmidt's phase diagram for slowly cooled alloys is seriously in error, for they show an iron solubility at 5% nickel content which must exceed the limiting value by at least ten times.

It is also clear from the electron-microscopical and magnetic observations that marked changes occur on reheating at 600° C., even for short times. The nature of these changes is not at once evident, though they are presumably connected with the precipitation of the  $\alpha'$  phase, since there is no direct evidence of precipitation except at the grain boundaries, and even here it is not observed until after several hours. It seems likely, however, that the transformation  $\alpha \rightarrow \alpha + \alpha'$  in these alloys may very closely resemble that first noted by Bradley and Bragg<sup>18</sup> in an alloy of approximate composition  $\text{Cu}_4\text{Ni}_3\text{Fe}$ . From examination of X-ray photographs of specimens cooled at 30° C./hr. from above 800° C., Bradley and Bragg concluded that the transformation had not proceeded to completion. In their particular example they proposed that the grains of the originally homogeneous solid solution remained intact and that within each there were families of lamellæ, alternately rich in copper and iron, lying parallel to the cube faces of the original face-centred cubic structure. Each lamella was several hundred atoms wide and about fifty atoms thick. Adjacent lamellæ cohered, so that the lattice parameters of the copper-rich and copper-poor lamellæ were the same in the plane of the lamellæ. In a direction normal to this plane, the copper-rich lamellæ had a parameter differing from that of the copper-poor regions, both structures being tetragonal.

Later work by Daniel and Lipson<sup>19,20</sup> and by Hargreaves<sup>21</sup> on quenched and reheated alloys of compositions similar to that studied by Bradley and Bragg, have thrown light on the way in which the regions of differing concentration form, grow, and ultimately break away to give a stable two-phase structure. The transformation is invariably accompanied by the formation of regions of concentration periodicity.

The appearance of Fig. 20 suggests that the processes of precipitation encountered in the low-iron alloys may resemble those which have been studied in alloys of much greater iron and nickel content. This view receives support from an inspection of the magnetic curves of

Fig. 7, in which the occurrence of a maximum could reasonably be connected with the formation and break-away of plates of the second phase. The changes with heat-treatment in the Curie point and in the electrical resistivity are in some respects surprising and are recorded for future reference.

The bearing of the results of the investigations described in this Appendix upon the variation with heat-treatment of the corrosion-resistance of the low-iron alloys will at once be evident. It is none the less remarkable that the formation of dark corrosion films in sea-water is observed upon alloys at a stage in which the beginnings of precipitation can be seen directly only by examining shadowed replicas in the electron microscope.

## APPENDIX II.

### MECHANICAL AND WORKING PROPERTIES OF THE COPPER-NICKEL-IRON ALLOYS.

Since one of the main interests in the development of these alloys has been their use by the copper-smith, some tests have been made of their workability and suitability for installation in sea-water piping systems in place of copper. These tests have sufficed to show that the alloys are mechanically suitable for copper-smithing and can be worked where necessary into complicated shapes. This Appendix describes the tests that have been carried out, confined mainly to alloys containing 5% nickel and 1.1–1.8% iron and to a lesser extent to alloys containing 10% nickel and 2% iron. Evidence which the tests presented of hot embrittlement of alloys under certain conditions is discussed, and the conditions for the avoidance of this embrittlement are established.

#### 1. *Mechanical Properties.*

Rod and strip materials were prepared from  $1\frac{3}{4}$ -in. square bar and 1-in. thick ingots, respectively. The castings were annealed for 2 hr. at 950° C., quenched, then hot rolled at 850° C., and finally cold rolled to  $\frac{3}{4}$ -in.-dia. rod and 0.08-in.-thick strip, respectively.

##### (a) *Tensile Tests at Room Temperature.*

The compositions and the results of tensile tests carried out on the rolled strips are reported in Table IX, each test result being the average of triplicate determinations. Only with the slowly cooled copper-10% nickel-2% iron alloy do the properties differ widely from those of copper.



TABLE IX.—*Tensile Properties of Copper-Nickel-Iron Alloys.*

Composition, %				Material Heated 2 hr. at 950° C., Followed by :			
				Furnace Cooling		Quenching	
Ni	Fe	Mn	P	U.T.S., tons./in. <sup>2</sup>	Elongation, %	U.T.S., tons./in. <sup>2</sup>	Elongation, %
5.14	1.11	0.57	0.03	16.1	31	16.6	39
5.01	1.29	0.59	0.03	16.0	30	16.8	31
5.04	1.30	0.50	0.07	16.0	41	19.6	29
5.12	1.41	0.55	0.04	15.6	32	17.8	31
5.02	1.51	0.55	0.04	15.8	32	18.0	31
5.05	1.63	0.53	0.04	15.6	30	17.6	33
5.03	1.59	0.54	0.06	15.5	28	16.6	29
5.08	1.79	0.54	0.04	15.7	30	17.4	31
10.28	2.07	0.46	0.04	20.5	22	16.6	33
10.06	2.08	0.62	0.03	20.3	21	17.9	33

(b) *Hardness.*

Vickers hardness determinations were made on a large number of alloys in many different conditions of heat-treatment. A few typical results are given in Table X. These show the marked effect of iron in

TABLE X.—*Diamond Pyramid Hardness of Typical Copper-Nickel-Iron Alloys.*

Composition, %			Cold Rolled after Quenching from 900° C.	Annealed at 900° C. for 2 hr.		
Cu	Ni	Fe		Quenched	Slowly Cooled	Quenched, Re-annealed at 600° C. for 2 hr.
95.2	3.1	1.1	141	63	...	77
93.7	5.1	0.54	141	53	59	61
93.3	5.0	1.1	143	53	64	61
93.2	4.9	1.35	148	57	...	65
91.7	5.5	2.0	150	57	75	69
89.0	5.2	5.1	157	83	90	90
87.6	10.6	1.0	155	59	64	72
87.4	9.9	2.0	152	65	...	90
85.4	10.3	3.6	170	79	84	100
82.5	15.6	1.1	169	67	89	78
82.2	14.9	2.1	171	74	125	99
77.4	20.6	1.1	175	78	86	80
77.1	20.0	2.1	179	78	128	98

increasing the hardness of slowly cooled materials, particularly when the nickel content is higher, but the relatively small effect of iron and nickel contents on the hardness after quenching from 900° C. Re-

annealing of the quenched alloys at 600° C. causes an increase in hardness which is more marked as the iron content increases.

(c) *Drop-Hammer Forging Tests.*

Cylinders  $\frac{5}{8}$  in. in dia. by  $\frac{5}{8}$  in. high were subjected to the blow of a falling weight of roughly 650 ft.lb. at room temperature and at 50° C. intervals in the range 600°–800° C. Cylinders of tough-pitch and phosphorus-deoxidized coppers and of 60:40 brass were tested for comparison. Table XI shows the observed reductions in height. The

TABLE XI.—*Percentage Reductions in Height of  $\frac{5}{8}$ -in. Cylinders Forged with a 650-ft.lb. Blow.*

Material	20° C.	600° C.	800° C.
Copper	50	67	76
Copper containing 5% nickel and 1.1–1.8% iron	41–45	55–61	65–68
Copper containing 10% nickel and 2% iron	39–42	53–58	62–63
60:40 brass	...	43	85

figures for copper are the average for duplicate tests on both high-conductivity and phosphorus-deoxidized coppers, between which there was no significant difference. The figures for the copper–5% nickel alloys show the lowest and highest recorded values obtained on all the 8 alloys whose compositions are given in Table IX, each tested in both the quenched and the slowly cooled condition.

## 2. *Working Properties.*

Workshop copper-smithing tests were carried out in the Association's laboratories on commercial tubes made from three alloys containing 5% nickel and 1–1.5% iron. Bend tests under workshop conditions were also made on a variety of commercial tubes of alloys containing 5–10% nickel in different conditions of heat-treatment.

(a) *Flanging Tests.*

Simple flanging operations, followed in some cases by turning the flange back parallel to the tube, were performed satisfactorily on each tube with no more than the slight cracking which occurred in similar operations on commercial copper tubes. The 5% alloy was stated to be somewhat tougher than copper, but the difference was considered of little practical significance.

*(b) Bend Tests.*

A series of commercial tubes with diameters of  $\frac{5}{8}$  in. and 1 in. from two sources and made of alloys containing 5% nickel with 1.5–2% iron and 10% nickel with 1.7–2.25% iron, were bent under workshop conditions. Cold bending after annealing at 850° C. and quenching was satisfactory with all alloys although the copper–10% nickel–2% iron alloy tubes proved to be much stiffer than the copper–5% nickel–1.5% iron alloy tube. Hot bending, however, resulted in cracking where the tube was heated to a temperature of over 750° C. before hot working.

*3. Occurrence and Causes of Cracking.*

A detailed laboratory investigation of the conditions leading to cracking of these alloys in hot working showed :

(a) The cracking was intercrystalline and was associated with the presence of minute separate particles of a grain-boundary constituent. The amount of this constituent was of the same order in alloys with markedly different iron contents, e.g. 0.5–1.5%, and was in all cases small.

(b) This constituent went into solution above about 800° C., but was reprecipitated at temperatures in the neighbourhood of 600° C.

(c) Reheating quenched material for a minute or so at 600° C. did not cause brittleness, but increasing the heating time caused grain-boundary precipitation and cracking. Susceptibility to cracking reached a maximum in 50–60 min. Increasing the time still further up to 16 hr. resulted in a progressive slow decrease in the extent of cracking, varying slightly with different samples. In the bar-impact tests, which are more sensitive to embrittlement than most industrial working operations, a marked fall in impact value was shown on testing at 600° C. after annealing at this temperature for 15 min. There was little further change with heating times at 600° C. up to 16 hr., but with three different materials there was an indication of an increase in the notched-bar value as the heating time was very prolonged.

(d) Alloys containing 5% nickel in a brittle condition showed an abrupt drop in impact value at 400° C. to a minimum at 600°–700° C., the extent of this fall increasing with the iron content. After passing the minimum the impact value rose to figures such as would be expected from a ductile alloy.

(e) A few tests on copper–nickel and copper–iron alloys showed that cracking only occurred when all three elements were present.

(f) Tubes of commercial manufacture, which are cold worked and

intermediately annealed at about 700° C. during fabrication, do not crack if they are heated to 600° C. and severely hot worked at that temperature. However, these, like rod and tube materials made from laboratory casts, crack during hot working at 600° C. if the material is heat-treated at, and quickly cooled from, a high temperature, e.g. 900° C., before working at 600° C.

(g) On the assumption that embrittlement was due to a small amount of impurity or addition element efforts were made to identify the constituent responsible, but they proved unsuccessful.

The work described in Appendix I has shown that the precipitate is the  $\alpha'$  phase of the copper-nickel-iron system. It tends to aggregate more readily at the grain boundary than within the grains, leaving thin films of the  $\alpha$  solution impoverished in nickel and iron which are precipitated in the  $\alpha'$  phase. This interpretation of the microstructure lends no support to the impurity theory suggested in (g) above, but provides the alternative explanation that the grain-boundary weakness is due to extremely thin intercrystalline films of the  $\alpha$ -solid-solution denuded of nickel and iron by the formation of the precipitate phase  $\alpha'$ . If the properties of this film were such as to cause intercrystalline weakness (cf. Perryman and Blade<sup>22</sup>), observation (c) would be explained by the relatively slow formation at 600° C. of the films of impoverished solution, while observation (f) is explained by the prior precipitation of  $\alpha'$  on the earlier annealings and the subsequent breaking-up of the films of  $\alpha$  solution during the cold-working and annealing operations, resulting in a material which is stable when reheated to 600° C. for hot working.

#### 4. Copper-Smithing Tests in H.M. Dockyards.

From time to time tests have been carried out in H.M. Dockyards, and the Admiralty has courteously passed its copper-smiths' observations to the Association. In 1943 some copper-5% nickel-1% iron alloy tubes of 3 in. dia. were made by rotary piercing and of 1 in. dia. by extrusion, with subsequent drawing in each case (wall thicknesses 10 and 12 S.W.G., respectively). These were subjected to tests designed to cover the operations likely to occur in practice. Hot bending, cold bending, hot and cold forming, brazing, and flame welding were successfully performed. The copper-5% nickel-1% iron alloy was reported to be tougher than copper, but no difficulty was experienced in any of the operations. Flame welding was carried out with an efficiency, as shown by a tensile test on a butt weld, of 82%.

On the other hand, a later series of tests on some 1-in.-bore tubes

(14 S.W.G. wall thickness) of copper-5% nickel-1.5% iron, copper-5% nickel-2% iron, and copper-10% nickel-2% iron alloys gave less satisfactory results in that the copper-smiths appear to have had considerable trouble in making bends without frequent reheating. Before a specification was finally settled, therefore, 1-, 3½-, and 5-in.-dia. tubes (16, 14, and 12 S.W.G., respectively) of alloys containing 5% nickel and 1, 1.2, and 1.4% iron were specially prepared for copper-smithing tests. Hot and cold bending proved completely satisfactory on the alloys containing 1.0 and 1.2% iron, but that containing 1.4% iron was found to be rather too difficult for severe cold deformation. The general conclusion drawn was that all the alloys were satisfactory from the copper-smithing point of view, although that containing 1.4% iron proved more difficult to work than those containing 1 and 1.2% iron. The Admiralty commented in 1948 that the copper-5% nickel-1% iron alloy had by then been installed on a considerable scale in H.M. ships and that this work had been carried out with the same facility as when using copper.

### 5. *Welding.*

In addition to the preliminary flame-welding trial reported above, 10-gauge sheet of copper-5% nickel-1% iron alloy was arc welded in H.M. Dockyards with coated electrodes of similar composition. Butt and fillet welds were prepared, and from the butt welds tensile and bend test-pieces were cut. The ultimate tensile strength of the weld was 16.5 compared with 17.1 tons/in.<sup>2</sup> for the annealed sheet with an elongation of 14%. Of three bend test-pieces, two bent through 180° without cracks but the third cracked at 64° bend. The fillet-weld specimen withstood considerable deformation before fracture. It was concluded from the limited number of welds made that metallic arc welding of this sheet was applicable to the fabrication and repair of pipes and trunking in this alloy.

Welds on a number of sheet and strip materials of 12-14 S.W.G. thickness were made in the Association's laboratory with an oxy-acetylene flame, using filler rods of the same compositions as the basis materials. The alloys so tested contained 5% nickel with 1.2-1.5% iron and 10% nickel with 2% iron. Most alloys contained 0.01-0.03% phosphorus, but one copper-5% nickel and one copper-10% nickel alloy free from phosphorus were welded for comparison. All the welds were satisfactory, fractures occurring in the basis metal in most cases. The copper-10% nickel alloys were somewhat easier to weld than the copper-5% nickel alloy, and the presence of 0.01% phosphorus was

a marked advantage. Increasing the phosphorus content to 0.04% made the weld metal too fluid for easy working. Under the particular conditions used there was no cracking at the weld in any composition.

#### ACKNOWLEDGEMENTS.

This paper describes the results of researches carried out over twelve years. The detailed results have been reported to the Association's members during this time in some eight reports which carry in all the names of eight investigators, some of whom have now left the Association's staff. The author, who with his colleague, Mr. R. May, has been associated with this work throughout, acknowledges particularly his indebtedness to his former colleague, Mr. E. A. G. Liddiard, for his contribution to the early stages of the work, and to Mr. T. Howard Rogers who has been responsible for the bulk of the experimental work. To the many others who have contributed by the supervision or the execution of particular items in the research programme, the author tenders his grateful thanks.

The Admiralty, through the Non-Ferrous Sub-Committee of the Admiralty Corrosion Committee, kindly carried out tests on the working properties of the alloys and investigated their corrosion-resistance under service conditions. The results of their experiments have been made available and their co-operation in both carrying out tests and in allowing results to be quoted in this paper is freely acknowledged.

Thanks are also due to those manufacturers, members of the Research Association, who have made the production of these alloys possible by their manufacturing trials, and to the Council of the British Non-Ferrous Metals Research Association for permission to publish this paper.

#### REFERENCES.

1. R. May, *Trans. Inst. Marine Eng.*, 1937, **49**, 171.
2. I. G. Slater, L. Kenworthy, and R. May, *J. Inst. Metals*, 1950, **77**, 309.
3. British Non-Ferrous Metals Research Association. B.N.F.M.R.A. Rep. **D31**, 1939.
4. British Patent No. **308,647**, (1927).
5. R. May, *J. Inst. Metals*, 1928, **40**, 141.
6. R. May and R. W. de Vere Stacpoole, *J. Inst. Metals*, 1950, **77**, 331.
7. T. H. Rogers, *J. Inst. Metals*, 1948-49, **75**, 19.
8. British Patents Nos. **577,065** (1939), and **578,283** (1943).
9. R. Grant, E. Bate, and W. H. Myers, *Inst. Eng. Australia, Sydney Div.*, **1921**, Paper No. 8.
10. T. H. Rogers, *J. Inst. Metals*, 1949-50, **76**, 597.
- 11(a). A. W. Tracy and R. L. Hungerford, *Proc. Amer. Soc. Test. Mat.*, 1945, **45**, 591.
- 11(b). F. L. LaQue, *ibid.*, p. 613.
12. F. L. LaQue and J. F. Mason, *Proc. Amer. Petroleum Inst.*, 1950, **30M**, [III], 103.
13. A. J. Bradley, W. F. Cox, and H. J. Goldschmidt, *J. Inst. Metals*, 1941, **67**, 189.



14. H. A. Miley and U. R. Evans, *J. Chem. Soc.*, **1937**, 1295.
15. L. E. Price and G. J. Thomas, *Trans. Electrochem. Soc.*, 1939, **76**, 329.
16. W. Lynes, *Power*, 1949, **93**, 84.
17. W. Köster and W. Dannöhl, *Z. Metallkunde*, 1935, **27**, 220.
18. A. J. Bradley and W. L. Bragg, *J. Iron Steel Inst.*, 1940, **141**, 70P.
19. V. Daniel and H. Lipson, *Proc. Roy. Soc.*, 1943, [A], **181**, 368.
20. V. Daniel and H. Lipson, *Proc. Roy. Soc.*, 1944, [A], **182**, 378.
21. M. E. Hargreaves, *Acta Cryst.*, 1949, **2**, 259.
22. E. C. W. Perryman and J. C. Blade, *J. Inst. Metals*, 1950, **77**, 263.

# OBSERVATIONS ON SOME WROUGHT ALUMINIUM-ZINC-MAGNESIUM ALLOYS.\*

1309

By MAURICE COOK,† D.Sc., Ph.D., F.I.M., MEMBER, R. CHADWICK,‡  
M.A., F.I.M., MEMBER, and N. B. MUIR,§ B.Sc., A.I.M.

## SYNOPSIS.

High-strength aluminium-zinc-magnesium wrought alloys containing up to 12% zinc, 3.5% magnesium, and 3% copper, as well as chromium, manganese, iron, and silicon in amounts of less than 1% each, have been investigated with the object of establishing the most suitable range of compositions for bulk manufacture. Macro- and microstructures, mechanical properties, resistance to corrosion, and thermal treatments were studied on materials produced on an experimental scale. In addition, the freezing characteristics of the alloys were investigated to ascertain compositions with small eutectic contents and, hence, desirable casting properties. As a result of these studies limiting compositions were established for alloys which possessed optimum mechanical properties and corrosion-resistance, together with the desired freezing characteristics.

A comparison was then made, under manufacturing conditions, of the casting and extrusion characteristics of two alloys with similar mechanical properties in the wrought condition, the one having a small and the other a large eutectic content. The superiority of the former, from the point of view of casting and working, was confirmed. This alloy contained nominally 6.5% zinc, 1.8% magnesium, 1.5% copper, 0.25% manganese, and 0.25% chromium, and further observations on the effect of different heat-treatment procedures were made on an alloy of similar composition produced on a manufacturing scale in the form of rolled sheet. On this material the effects of cold work and secondary heat-treatment were also investigated to establish conditions for developing maximum corrosion-resistance compatible with high strength and a reasonable measure of ductility.

## I.—INTRODUCTION.

WROUGHT aluminium alloys containing 4–10% zinc and 1–4% magnesium have a marked capacity for age-hardening, and by the addition of small amounts of other elements such as copper, manganese, and chromium, alloys with attractive properties can be produced. In spite of the large volume of published work dealing with both fundamental and *ad hoc* investigations of various alloys of this type, and the not inconsiderable scale on which some of them have been manufactured, opinions differ concerning the optimum ranges of composition. The present paper describes briefly the results of work which has been

\* Manuscript received 31 January 1951.

† Director, Imperial Chemical Industries, Ltd., Metals Division, Birmingham.

‡ Assistant Research Manager, Imperial Chemical Industries, Ltd., Metals Division, Birmingham.

§ Technical Officer, Imperial Chemical Industries, Ltd., Metals Division, Birmingham.

carried out on the relation of composition to structure, age-hardening characteristics, mechanical properties, and corrosion-resistance, as well as on other aspects of a more practical and technological character.

## II.—PREVIOUS WORK.

Published information on wrought aluminium-zinc-magnesium alloys relates mainly to alloys prepared under laboratory conditions. Ternary alloys of high purity have been investigated by Hérenghuel and Chaudron,<sup>1,2</sup> who showed that the improvement in mechanical properties associated with increase in zinc and magnesium content is progressive up to a combined total of about 9% of these two elements, above which both strength and ductility are affected by brittleness which develops on age-hardening and the fracture becomes intergranular. A subsequent paper by Hérenghuel<sup>3</sup> indicates that alloys of commercial purity containing copper, chromium, and manganese are much less affected by this type of brittleness in the higher ranges of zinc and magnesium contents, although ductility may be quite low even when fracture is of the normal intragranular type. Hansen,<sup>4,5</sup> Siebel,<sup>6</sup> and their collaborators and others<sup>7,8,9</sup> have studied the properties of commercially pure alloys containing up to about 0.5% copper, primarily with a view to developing substitutes for the copper-bearing heat-treatable alloys, with preferred compositions falling within the range 4–6% zinc and 2–3.5% magnesium. Other commercially pure alloys have been investigated by Vachet<sup>10</sup> and by Mott and Thompson.<sup>11,12</sup>

The effect of copper on the properties of aluminium-zinc-magnesium alloys has been investigated by several workers,<sup>6,8,10,13,14</sup> and the evidence indicates that the presence of this element is generally beneficial. According to Hansen,<sup>5</sup> Petri,<sup>13</sup> and Bungardt,<sup>15</sup> and their collaborators, small additions of manganese have a hardening and strengthening effect, but Vachet<sup>10</sup> suggests that this element may be wholly or partly replaced by chromium with an improvement in corrosion-resistance. The effect of the silicon normally present as impurity has received attention, and it has been shown that tensile strength falls off as the silicon content increases,<sup>4,8,12</sup> although opinions differ as to the permissible maximum amount of this element.

Solution heat-treatment conditions for aluminium-zinc-magnesium alloys are generally regarded as being less critical than they are in some other aluminium age-hardening systems. Hansen, Mühlenbruch, and Seemann<sup>4</sup> have reported that the solution heat-treatment range for alloys with 4.5% zinc and 2% magnesium extends from 380° to 520° C., while the corresponding range for alloys much richer in zinc has been stated by Vachet<sup>10</sup> to be 435°–480° C. Feldman<sup>16</sup> and others<sup>3,4,10,15</sup>

have studied the age-hardening characteristics at room and elevated temperatures. Natural age-hardening is appreciable, but may not be complete even after a period of six months. Artificial age-hardening produces a greater increase in hardness, while prolonged heating at temperatures in excess of 100° C. results in ultimate softening.

The work of Köster<sup>17</sup> and Fink and Willey<sup>18</sup> on the constitution of the ternary aluminium-zinc-magnesium system has been augmented by Hume-Rothery and his colleagues,<sup>19-24</sup> who have examined the quaternary systems aluminium-zinc-magnesium-manganese and aluminium-zinc-magnesium-copper, thereby providing data of great assistance in determining the structure of the more complex alloys.

### III.—THE NATURE AND SCOPE OF THE WORK.

The present work relates to investigations into various aspects of the metallurgy of alloys based on the aluminium-zinc-magnesium system. It was undertaken with the object of establishing a composition or range of compositions suitable for the manufacture of alloys in wrought forms such as sheet and extrusions, which possess the maximum possible strength consistent with an adequate measure of ductility and good corrosion-resistance in the heat-treated condition.

The alloys dealt with contained up to 12% zinc, 3.5% magnesium, and 3% copper, as well as chromium, manganese, iron, and silicon, all in amounts of less than 1%. The effect on the mechanical properties and corrosion-resistance of varying each element separately within this range was determined on alloys prepared under laboratory conditions, using small ingots in which a high degree of uniformity could be achieved. The optimum range of composition for these two properties was thus established.

Wrought heat-treatable alloys of this type, however, have proved particularly difficult to make on a manufacturing scale, and it has been a common experience that alloys which possess attractive qualities when made on a pilot scale have proved disappointing when bulk production has been attempted. In the present investigation, therefore, the effect of composition on such important metallurgical factors as freedom from segregation and casting defects in large ingots, as well as the facility with which subsequent processing can be carried out on a modern plant, have also been considered. Production difficulties appear to be associated with the long freezing range and high eutectic content of many of these alloys. Hence a study was made of thermal freezing characteristics over the defined composition field, in which the major elements zinc, magnesium, and copper were mainly concerned, in order to establish a range of alloys in which the low-melting eutectic was

present in only small amounts or was entirely absent. It was found that such alloys could be cast and worked with comparative ease, and after comparing the solidification characteristics and mechanical properties of two types of alloys, made on a production scale, one having a very small and the other a much larger eutectic content, further detailed work was carried out on the heat-treatment and cold-working characteristics of a typical alloy falling within the narrower range of compositions and possessing both optimum mechanical properties and the requisite low eutectic content.

In studying the general relationship between structure and properties, an examination was made of the macrostructure of all the ingots for rolling or extrusion, and of the microstructure of the cast and wrought products, as well as of various samples after corrosion testing. In order to provide the reader with the salient and essential results of this aspect of the investigation, and to unify and shorten the treatment, it is dealt with separately before the other descriptive matter.

Stress-corrosion properties are not referred to, since it is the intention to deal with them in another paper. It should, however, be mentioned that the good resistance to unstressed corrosion of the typical alloy referred to above was accompanied by equally good stress-corrosion behaviour, the rate of corrosion being unaffected by stresses of up to 90% of the proof stress.

#### IV.—THE MACRO- AND MICROSTRUCTURE OF CAST AND WROUGHT ALLOYS.

All ingots prepared for hot working by rolling or extrusion were sectioned transversely for examination of the macrostructure. The small Durville-cast ingots were examined at the upper end after cutting away the feeder head down to sound metal, and the large ingots for processing on works plant were examined half-way along the length.

Micro-examination was carried out on a representative range of alloys in the cast condition to determine the nature and distribution of the phases comprising the eutectic constituent, and also of the other intermetallic compounds separating at earlier stages in solidification. The progress of breakdown and absorption of the included particles was assessed by micro-examination of some of these same alloys at various later stages of working. In order to confirm the identity of the various phases present in both cast and wrought alloys, many of the slowly cooled ingots used in connection with the thermal studies of solidification were also examined. The present observations on microstructure have not been extended to include systematic work on the constitution of the alloys, since this is outside the scope of the investigation.

Of the numerous micro-sections prepared in connection with the different aspects of the investigation, only a few have been selected for reproduction, but all the most important structural features which significantly affect the workability or properties of the alloys are shown in the four macro-sections, Figs. 1-4 (Plate XLIII), and ten micro-sections, Figs. 5-14 (Plates XLIV and XLV).

Over the whole range of alloys investigated differences of composition, apart from the chromium content, affected the macrostructures to only a slight extent. As shown in Figs. 1-3 (Plate XLIII) the presence of chromium coarsens the structure. By exercising careful control over mould and metal temperatures, however, all the alloys cast in the form of 7-lb. ingots were produced with a fine grain suitable for hot rolling, except the alloy containing 0.55% chromium, which cracked slightly in the early stages of breaking down. In large ingots for hot rolling or extrusion, in which 0.25% chromium was normally present, some additional means of controlling the grain-size were found to be desirable, and an addition of 0.05% titanium proved effective. The powerful grain-refining action of this element is indicated by its effect on the macro-section of the 7-lb. ingot illustrated in Fig. 4 (Plate XLIII).

The more highly alloyed members of the various series, which were of chief interest in connection with the present investigation, contained a greater amount of eutectic than is indicated by the equilibrium relationship. In the small chill castings the structure of the eutectic was generally extremely fine, and the separate constituents could not be identified with certainty. In the slowly cooled alloys prepared in connection with the thermal investigation, however, the various constituents were readily identified. Typical examples are illustrated in Figs. 5 and 6 (Plate XLIV).

The aluminium-zinc-magnesium alloy system has a eutectic valley between the area of separation of primary  $\alpha$  solid solution and that of the  $T(\text{Al}_2\text{Mg}_3\text{Zn}_3)$  and  $M(\text{MgZn}_2)$  phases, with a pseudo-binary eutectic solidifying at  $489^\circ\text{C}$ . The aluminium-copper-magnesium system has many similar features, both the  $T$ -phase ( $\text{Al}_6\text{Mg}_4\text{Cu}$ ), and the  $X$ - or  $M$ -phase ( $\text{AlCuMg}$ ), being isomorphous with their counterparts in the aluminium-zinc-magnesium system. In the complex alloys concerned in the present investigation, a sharp eutectic solidification occurs at temperatures between  $465^\circ$  and  $475^\circ\text{C}$ ., depending on composition, and the  $T$ - and  $M$ -phases can be identified in the eutectic, as indicated in Figs. 5 and 6. It can, therefore, be assumed that the equilibrium in these more complex alloys departs but little from that of the ternary aluminium-zinc-magnesium alloys. With more than 2% copper,



however, the eutectic arrest is not sharp, but occurs over a temperature range of a few degrees, which may be associated with the observation that with more than 1% copper an additional phase,  $S(\text{Al}_2\text{CuMg})$  of the aluminium-copper-magnesium system, is present. In the alloy illustrated in Fig. 6 the period of thermal arrest in cooling through the eutectic temperature was five times that of the alloy illustrated in Fig. 5, which is in good agreement with the relative amounts of eutectic revealed in the micro-sections.

The unsaturated  $\alpha$  solid solution is capable of reacting with the eutectic constituent at temperatures either above or a little below the eutectic melting point. The lower temperatures are preferred in ingots which are required for fabrication by rolling or extrusion, since any treatment carried out on the partially liquid ingots may lead to cracking or other damage. A large proportion of the eutectic can be taken into solution by prolonged soaking at  $450^\circ\text{C}.$ , and the process is continued to some extent in subsequent hot working. A high degree of saturation of the  $\alpha$  solid solution is essential in order to obtain the maximum age-hardening capacity, and the extent to which this is effected depends upon fine dispersion of the eutectic in the cast structure. Fig. 7 (Plate XLIV) shows a typical example of the dispersion in an ingot made by the direct-chill continuous-casting process, and Fig. 8 (Plate XLIV) the microstructure of rod extruded from this same billet, which indicates the uniform distribution of unabsorbed particles, mainly iron- and manganese-bearing complexes, with very little residual eutectic.

In addition to the primary and eutectic phases arising mainly from the presence of the major alloying elements zinc, magnesium, and copper, intermetallic compounds are formed by the minor constituents manganese, iron, chromium, and silicon, most of which separate at an early stage in solidification and are readily distinguishable from the eutectic components. In Figs. 9-12 (Plate XLV) the more important constituents are illustrated in micro-sections of slowly cooled alloys, in which they tend to be present in massive segregated forms.

Manganese and iron were present in all the alloys to the extent of at least 0.2% each, and the complex insoluble compounds which these elements form with aluminium and silicon could always be detected. The microstructure of a cast alloy containing 0.4% iron and 0.4% manganese (Fig. 9) shows the complex  $\text{Al}(\text{Fe},\text{Mn})\text{Si}$  phase in Chinese script form, and a smaller quantity of  $\text{Al}_6(\text{Fe},\text{Mn})$  in typical rhombic form. Fig. 10 shows the effect of greater amounts of manganese and iron, which give rise to a larger proportion of the  $\text{Al}_6(\text{Fe},\text{Mn})$  phase.

In alloys with 0.2% manganese and 0.2% iron particles of  $\text{Mg}_2\text{Si}$

could be detected with as little as 0.17% silicon, and with further silicon additions the amount of this compound increased proportionately. Fig. 11 shows an area of rather high eutectic concentration in an alloy of 0.75% silicon content, in which dark-etching  $Mg_2Si$  is present together with small amounts of the  $Al(Fe,Mn)Si$  phase, which is grey and appears in partial relief. The larger additions of chromium tend to form massive segregates of  $Al_7Cr$ , a typical example of the mode of occurrence of this compound being shown in Fig. 12.

All the compounds referred to above are insoluble, and in hot and cold rolling they are elongated and fragmented into the form of stringers, the main effect of which is to diminish ductility, especially in bend tests where the axis of the bend is in the rolling direction. Fig. 13 (Plate XLV) illustrates a pronounced stringer formation in an alloy containing 0.8% iron and 0.8% manganese, in which the fragmented particles are mainly  $Al_6(Fe,Mn)$ . This and the other major insoluble constituents  $Al(Fe,Mn)Si$  and  $Mg_2Si$  are, however, relatively less deleterious in their effect than  $Al_7Cr$ , which, as shown in Fig. 14 (Plate XLV), is heavily segregated during hot rolling into continuous stringers and gives rise to local rupturing of the matrix alloy in the subsequent cold-rolling operations.

#### V.—THE EFFECT OF ZINC, MAGNESIUM, COPPER, MANGANESE, IRON, SILICON, AND CHROMIUM ON THE MECHANICAL PROPERTIES AND CORROSION-RESISTANCE.

##### 1. *Experimental Procedure.*

The compositions of the alloys for the systematic survey of the effect of composition on mechanical properties and corrosion-resistance in the wrought condition are detailed in Table I. These were made up from commercially pure metal and hardeners, melted in a gas-fired furnace, degassed by passing a rapid stream of chlorine for 3 min., and cast, at 700° C., in a Durville machine, into ingots measuring  $9 \times 4\frac{1}{2} \times 1\frac{1}{4}$  in., and weighing 7 lb. The ingots were soaked at 450° C. for 24 hr. and hot rolled from just below this temperature, without intermediate reheating, down to a thickness of 0.4 in., after which they were pickled, scratch-brushed, and processed by a series of cold-rolling reductions of not less than 50%, with intermediate anneals at 400° C., to sheet of 0.1 in. and 0.050 in. thickness required for the determination of the mechanical properties and corrosion-resistance.

To ensure that optimum mechanical properties were obtained with every alloy, it was first necessary to investigate the heat-treatment characteristics of each separately. This assessment, which was based

TABLE I.—*Composition of Alloys for Systematic Evaluation of Mechanical Properties.*

SERIES 1.— <i>Alloys with Varying Zinc and Magnesium Contents, about 0.02% Copper and 0.01% Titanium.</i>								
Nominal Contents		Chemical Determinations						
Zn, %	Mg, %	Zn, %	Mg, %	Mn, %	Cr, %	Fe, %	Si, %	
...	1.6	<0.05	1.65	0.23	<0.01	0.23	0.16	
...	3.5	<0.05	3.45	0.23	<0.01	0.22	0.16	
1.0	1.0	1.09	0.96	0.23	0.18	0.13	0.14	
1.0	2.5	1.14	2.64	0.25	0.21	0.14	0.13	
2.5	0.5	2.42	0.59	0.27	0.29	0.14	0.15	
2.5	1.0	2.65	1.05	0.25	0.29	0.21	0.15	
2.5	1.5	2.60	1.60	0.27	0.26	0.29	0.14	
3.0	2.5	2.94	2.53	0.23	0.21	0.13	0.14	
3.0	3.5	3.05	3.30	0.24	0.22	0.15	0.14	
4.0	1.25	3.84	1.25	0.26	0.21	0.20	0.22	
4.25	3.5	4.20	3.58	0.20	0.18	0.21	0.14	
4.5	2.5	4.64	2.50	0.24	0.23	0.14	0.15	
5.0	0.5	4.85	0.52	0.25	0.28	0.13	0.17	
5.0	1.0	5.13	1.07	0.25	0.28	0.23	0.15	
5.0	1.5	5.06	1.59	0.26	0.22	0.23	0.12	
6.0	2.5	6.12	2.50	0.58	0.27	0.24	0.15	
6.75	3.5	6.75	3.53	0.21	0.18	0.22	0.16	
7.0	2.25	7.10	2.25	0.25	0.24	0.22	0.11	
7.0	2.5	6.95	2.59	0.57	0.27	0.24	0.13	
7.5	0.5	7.39	0.56	0.28	0.27	0.14	0.17	
7.5	1.0	7.49	1.07	0.27	0.27	0.23	0.13	
7.5	1.5	7.49	1.57	0.26	0.27	0.22	0.12	
7.5	2.0	7.36	1.86	0.27	0.21	0.17	0.29	
8.0	2.5	7.74	2.40	0.52	0.25	0.23	0.12	
10.0	0.5	10.03	0.59	0.24	0.20	0.13	0.15	
10.0	1.0	10.04	1.04	0.24	0.23	0.11	0.13	
12.0	1.25	11.70	1.20	0.27	0.21	0.18	0.27	
SERIES 2.— <i>Alloys with Varying Zinc and Copper Contents, and about 0.01% Titanium.</i>								
Nominal Contents		Chemical Determinations						
Zn, %	Cu, %	Zn, %	Mg, %	Cu, %	Mn, %	Cr, %	Fe, %	Si, %
6.0	...	6.12	2.50	0.07	0.58	0.27	0.24	0.15
6.0	1.0	5.97	2.43	1.10	0.40	0.36	0.23	0.14
6.0	2.0	6.11	2.51	2.08	0.58	0.26	0.21	0.19
6.0	3.0	6.14	2.53	3.00	0.58	0.27	0.21	0.18
7.0	...	6.95	2.55	0.05	0.57	0.27	0.24	0.13
7.0	1.0	6.95	2.45	1.00	0.58	0.27	0.22	0.15
7.0	2.0	7.10	2.46	2.06	0.54	0.24	0.29	0.19
7.0	3.0	6.96	2.52	3.15	0.57	0.26	0.19	0.11
8.0	...	7.94	2.45	0.05	0.52	0.25	0.23	0.12
8.0	1.0	8.15	2.44	0.91	0.56	0.32	0.22	0.11
8.0	2.0	8.16	2.56	2.09	0.56	0.27	0.30	0.19
8.0	3.0	8.20	2.42	3.11	0.58	0.28	0.25	0.13

TABLE I (continued).

SERIES 3.—Alloys with Varying Iron and Manganese Contents, about 0.01% Chromium, and about 0.01% Titanium.							
Nominal Contents		Chemical Determinations					
Mn, %	Fe, %	Zn, %	Mg, %	Cu, %	Mn, %	Fe, %	Si, %
0.2	0.2	5.97	2.30	1.91	0.20	0.25	0.13
0.4	0.2	6.10	2.32	1.97	0.39	0.22	0.25
0.8	0.2	5.91	2.23	2.07	0.81	0.23	0.20
0.2	0.4	5.93	2.29	1.94	0.23	0.44	0.16
0.4	0.4	5.95	2.28	1.95	0.42	0.42	0.16
0.8	0.4	5.99	2.25	2.04	0.83	0.44	0.13
0.2	0.8	6.15	2.21	2.00	0.22	0.74	0.15
0.4	0.8	6.15	2.20	1.90	0.44	0.81	0.17
0.8	0.8	5.98	2.27	2.05	0.86	0.82	0.20
SERIES 4.—Alloys with Varying Silicon Content, about 0.01% Chromium, and about 0.01% Titanium.							
Nominal Content	Chemical Determinations						
Si, %	Zn, %	Mg, %	Cu, %	Mn, %	Fe, %	Si, %	
0.2	5.90	2.29	1.94	0.20	0.19	0.17	
0.4	5.93	2.21	1.88	0.20	0.19	0.37	
0.8	5.93	2.20	1.92	0.22	0.19	0.76	
SERIES 5.—Alloys with Varying Chromium Content, and about 0.01% Titanium.							
Nominal Content	Chemical Determinations						
Cr, %	Zn, %	Mg, %	Cu, %	Mn, %	Cr, %	Fe, %	Si, %
...	5.90	2.29	1.89	0.20	0.01	0.19	0.17
0.25	5.90	2.20	1.82	0.20	0.27	0.23	0.23
0.5	5.93	2.22	1.95	0.23	0.55	0.22	0.22

mainly on hardness measurements, involved quenching specimens from temperatures ranging up to 500° C. and subsequently ageing over a lower range of temperatures. The results obtained with the various alloys showed that, in general, hardness increased with the temperature of quenching provided the solidus temperature was not exceeded; but, on the other hand, the advantage obtained by raising the heat-treatment temperature in the more lightly alloyed members of the series was slight, and a standard quenching temperature of 460° C., which avoided incipient melting in all the alloys investigated, was

adopted. In ageing experiments on typical alloys at 90°–180° C. it was found that both maximum hardness and the time required to reach maximum hardness increased with decrease in ageing temperature within this range, although at temperatures below about 110° C. the time to attain maximum hardness was impracticably long. The results of more comprehensive ageing experiments on a selected alloy over the same range of temperatures, employing a fixed ageing period of 18 hr., i.e. about the maximum which is commercially practicable, are referred to later in the paper. The optimum temperature of 125° C., which was found to give the best combination of mechanical properties and corrosion-resistance in this alloy, was adopted in the standard ageing treatment for the whole series, and resulted in only slight deviations from optimum strength in a few of the alloys.

The assessment of mechanical properties was based mainly on the determinations of the 0.1% proof stress, ultimate tensile strength, and elongation on test-pieces of 0.050 in. thickness and 2-in. gauge-length conforming to British Standard 485. Corrosion-resistance was assessed by the fall in ultimate tensile strength sustained after a short period of immersion in a solution containing 3% sodium chloride and 0.3% by weight of hydrogen peroxide, which is a standard corroding medium for the accelerated testing of aluminium alloys, and is intended to simulate prolonged exposure to marine atmospheric conditions. The testing procedure was rigidly standardized, each tensile test-piece, the surface area of which was about 60 cm.<sup>2</sup>, being immersed in a separate jar containing 300 ml. of corroding medium for a period of 24 hr., any temperature rise in individual tests being prevented by the external water cooling of all the jars. At the conclusion of this period the test-pieces were washed and dried, and pulled with as little delay as possible.

Elongation provides a useful indication of ductility so long as the alloys are relatively homogeneous, but this property is affected only slightly by stringers of brittle intermetallic inclusions which have, however, a pronounced effect on bending. Tensile tests were, therefore, supplemented by bend tests on all the alloys of Series 3, 4, and 5 (Table I), some of which contained stringers associated with the higher manganese, iron, and chromium contents. The bend test involved the determination of the minimum radius ( $R$ ) over which sheet of thickness ( $T$ ) could be bent through 180° without surface rupture. Strips cut from 0.1-in.-thick sheet, in a direction transverse to that of final rolling, were fully softened by slow cooling from the annealing temperature of 400° C. These were bent on a compression machine between a steel punch, the nose of which was accurately ground to the required contour, and a pad of hard rubber, which provided uniform

pressure over the whole of the stretched surface. The use on separate test-pieces of punches of progressively smaller radius gives the minimum value of  $R$  and thence the  $R/T$  value, which is the usually accepted method of expressing this property.

The effects on mechanical properties and corrosion-resistance of zinc, magnesium, copper, manganese, iron, silicon, and chromium are discussed in the succeeding sections. The results, illustrated by graphs in Figs. 19-24, relate to sheet solution heat-treated at  $460^{\circ}\text{C}$ . and artificially aged for 18 hr. at  $125^{\circ}\text{C}$ . in test-piece form.

## 2. Effect of Zinc and Magnesium.

The effect, on the mechanical properties in the fully heat-treated condition, of zinc contents ranging from 1 to 12%, and magnesium contents from 0.5 to 3.5%, was determined on a series of 22 alloys with nominal manganese and chromium contents of 0.25% each and on three alloys with a somewhat higher manganese content. Values of the 0.1% proof stress, ultimate tensile strength, and elongation for these 25 ternary alloys and for two binary aluminium-magnesium alloys are given in Figs. 19, 20, and 21, respectively, in which curves of equal proof stress, tensile strength, and elongation are shown.

For a given zinc content the values of proof stress and ultimate tensile strength increase sharply with increase in magnesium until the proportions of the two elements correspond approximately to the compound  $\text{MgZn}_2$ , when further increase of magnesium is accompanied by less pronounced improvements in strength, and as the addition of magnesium is continued its effect tends to fall off asymptotically. By comparison, for a constant magnesium content, increase in the proportion of zinc is accompanied by an approximately uniform increase in 0.1% proof stress and ultimate tensile strength over the whole range of compositions. The elongation appears to reach a definite minimum as the magnesium content is progressively increased, and to increase again when the magnesium content exceeds the proportion required to form  $\text{MgZn}_2$ .

It is evident that a very wide range of mechanical properties can be obtained by varying the zinc and magnesium contents, and for any defined values of strength or ductility the composition can be varied in accordance with the curves plotted in Figs. 19-21. However, it will be noted that with alloys in which the magnesium content is less than that required to form  $\text{MgZn}_2$ , i.e. alloys below the  $\text{MgZn}_2$  line in Figs. 19-21, small variations in magnesium give rise to disproportionately large changes in mechanical properties, a fact which points to difficulties in the precise control of properties of alloys in this compositional zone.



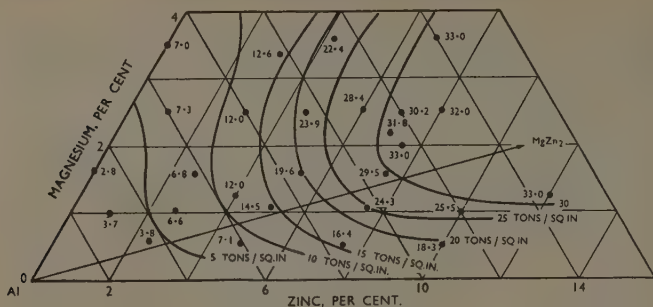


FIG. 19.—0.1% Proof Stress.

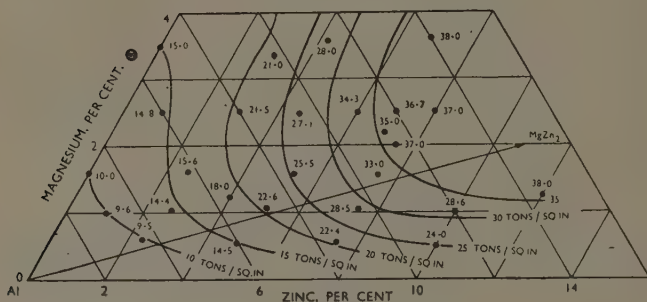


FIG. 20.—Ultimate Tensile Strength.

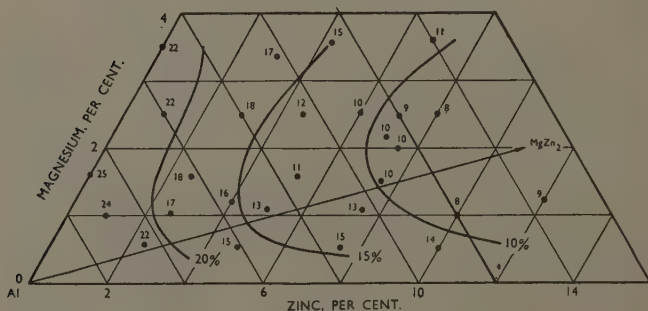


FIG. 21.—Elongation on 2 in.

FIGS. 19-21.—Tensile Properties of Alloys with Varying Zinc and Magnesium Contents. [Table I, series I.]

High magnesium contents in relation to zinc result in no improvement in mechanical properties, and the optimum range of compositions lies within an area in which the zinc content is at least equal to, and preferably not more than four times greater than, the magnesium content. Any increase in proof stress and tensile strength is, as usual, at the expense of ductility, and even when the primary consideration is the maximum possible strength, some measure of ductility is usually desired. On the assumption that a minimum acceptable value for this property is 10%, expressed in terms of elongation on 2 in., the maximum proof stress would be approximately 30 tons/in.<sup>2</sup> and the tensile strength 35 tons/in.<sup>2</sup>, properties of this order being attained in alloys with zinc contents between 6 and 7% and magnesium contents between 1.5 and 4.0%.

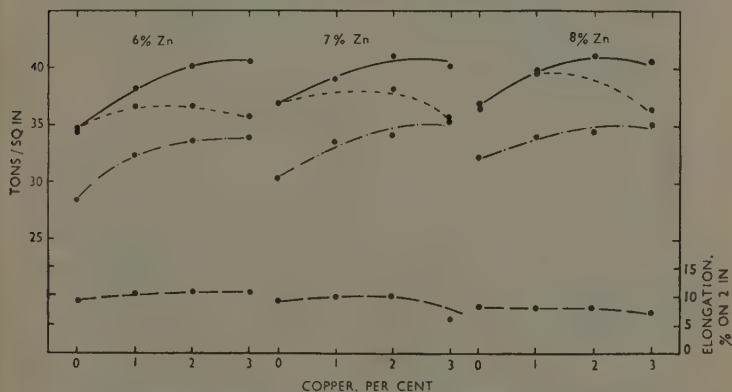


FIG. 22.—Mechanical Properties and Corrosion-Resistance of Alloys with Varying Zinc and Copper Contents. [Table I, series 2.]

KEY.  
 — Ultimate tensile strength.  
 - - - Ultimate tensile strength after corrosion test.  
 - · - · - 0.1% Proof stress.  
 - - - - Elongation.

### 3. Effect of Copper.

The effect of copper in amounts ranging from 0 to 3% was studied in alloys containing 6, 7, and 8% zinc with 2.5% magnesium, 0.5% manganese, and 0.25% chromium. Graphs showing 0.1% proof stress, ultimate tensile strength, and percentage elongation are reproduced in Fig. 22, together with ultimate tensile strength values after immersion for 24 hr. in the standard salt/peroxide corrosion-testing medium.

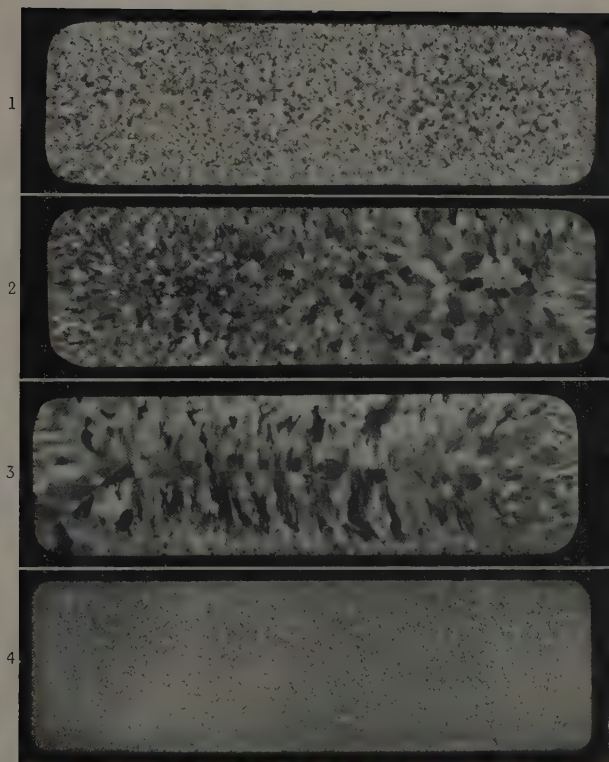
With all three zinc contents, additions of copper up to 2% cause a progressive increase in the 0.1% proof stress and ultimate tensile strength, but little further advantage accrues by increasing this element to 3%. This is to be expected from the constitution of the alloys as determined by Strawbridge, Hume-Rothery, and Little,<sup>23</sup> who indicated that the maximum solid solubility of copper at 460° C. in alloys containing 6–8% zinc and 2.5% magnesium is in the range 1.5–2%. Elongation values are about 10% in all the 6% zinc alloys, and in the 7% alloys with up to 2% copper. In the three 8% zinc alloys and in the 7% zinc–3% copper alloy, elongation values are about 7%, and are thus lower than the minimum referred to.

The curves for ultimate tensile strength before and after salt/peroxide test indicate that, irrespective of zinc content, the corrosion-resistance is progressively diminished by copper. This deleterious effect of copper is, however, relatively slight in amounts up to 1%, though thereafter it rapidly increases in significance.

#### 4. *Effect of Manganese and Iron.*

The effect on the mechanical properties and corrosion-resistance of increasing the iron content up to 0.8% from the level of about 0.2% in which it is normally present, and of similar additions of manganese, is shown in Figs. 23 and 24. In alloys with 0.2, 0.4, or 0.8% iron, the proof stress is not appreciably affected by varying the manganese, but with all three iron contents tensile strength is a maximum with 0.4% manganese and thereafter diminishes, while the elongation values decrease progressively with increase of manganese content. Corrosion-resistance, on the other hand, is improved by manganese, especially in the alloys of low iron content. Proof stress, tensile strength, elongation values, and resistance to corrosion are all diminished as the iron content is increased, and the detrimental effect of this element is greater in alloys with high than in alloys with low manganese content.

Limiting 180° bend tests on annealed sheet indicate that an increase in either iron or manganese is accompanied by a progressive deterioration in bending properties, the effects being approximately equal and additive, so that a plot of limiting  $R/T$  ratios against iron + manganese content reveals an approximately straight-line relationship (Fig. 24). The reduced formability is attributable to unabsorbed constituents present in the form of stringers, the appearance of which in the micro-structure of rolled alloys has already been described. Two intermetallic compounds are involved,  $Al_6(Fe,Mn)$  predominating in alloys of high manganese content (Fig. 13, Plate XLV) and  $Al(Fe,Mn)Si$  in alloys low in manganese.



FIGS. 1-4.—Macro-Sections of 7-lb. Ingots, Illustrating the Effect of Chromium Additions.

FIG. 1.—No Chromium.

FIG. 2.—0.25% Chromium.

FIG. 3.—0.5% Chromium.

FIG. 4.—0.25% Chromium, 0.05% Titanium.

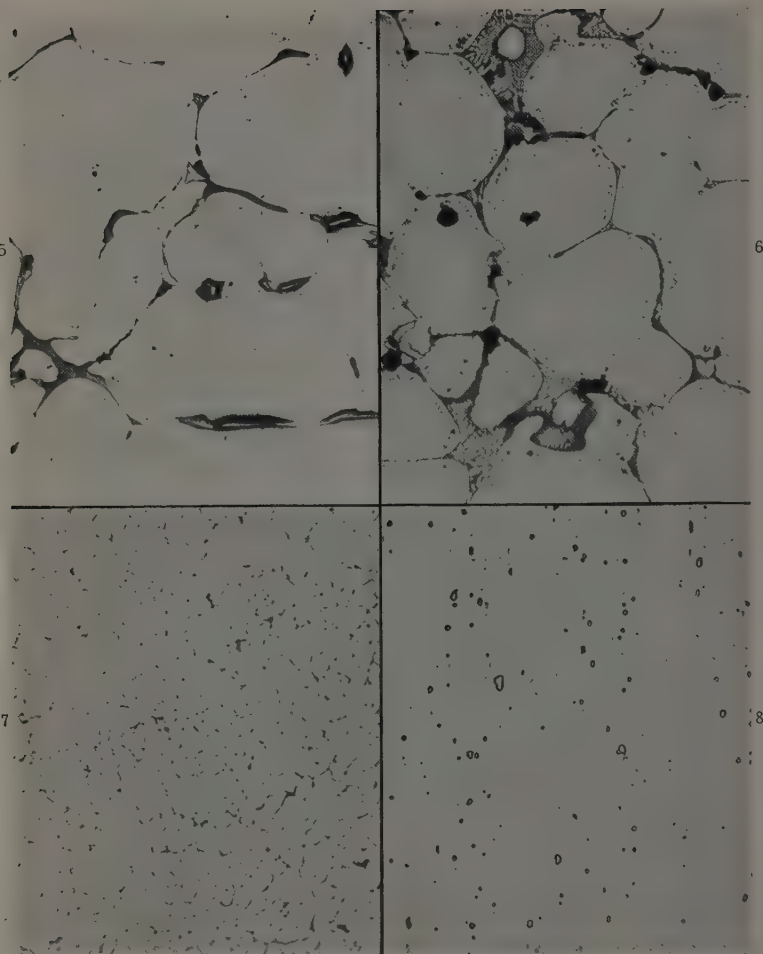


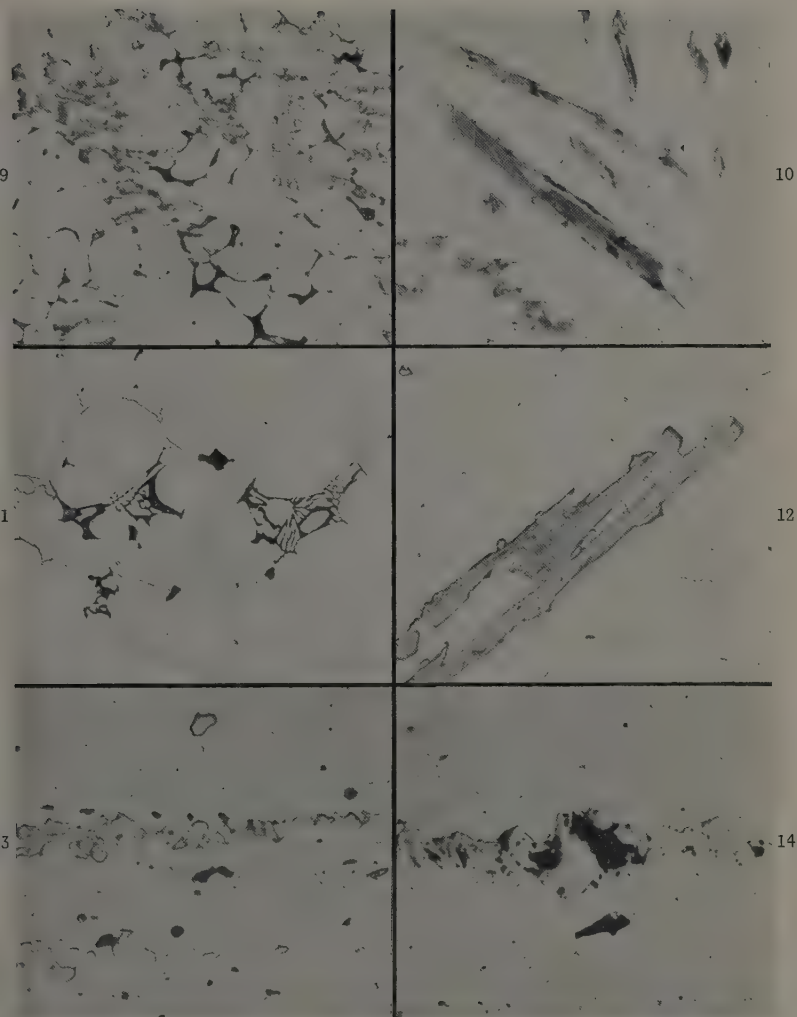
FIG. 5.—Alloy Containing 7.5% Zn, 1.5% Mg, 1.5% Cu, 0.25% Mn. Slowly Cooled. Eutectic arrest 0.5 min. S—dark grey; M—grey; T—black, very small amount.  $\times 50$ .

FIG. 6.—Alloy Containing 7.5% Zn, 2.5% Mg, 2.5% Cu, 0.25% Mn. Slowly Cooled. Eutectic arrest 2.5 min. S—dark grey, major constituent; M—light grey, very small amount; T—black.  $\times 50$ .

FIG. 7.—Direct-Chill-Cast 7-in.-dia. Billet of Alloy Containing 6.6% Zn, 1.8% Mg, 1.6% Cu, 0.2% Mn, 0.2% Cr.  $\times 50$ .

FIG. 8.—Longitudinal Micro-section of a 14-in.-dia. Rod Extruded from Alloy Billet shown in Fig. 7.  $\times 250$ .

All etched in 0.5% HF.



FIGS. 9-14. Microstructures of Cast and Wrought Al 6% Zn-2.25% Mg 2% Cu Alloys Showing Some of the Compounds Associated with Fe, Mn, Si, and Cr Additions.

FIG. 9.—0.4% Fe, 0.4% Mn, 0.15% Si. As cast.  $\text{Al}(\text{Fe,Mn})\text{Si}$ , Chinese script;  $\text{Al}_6(\text{Fe,Mn})$ , grey rhombic crystals.

FIG. 10.—0.8% Fe, 0.8% Mn, 0.15% Si. As cast.  $\text{Al}_6(\text{Fe,Mn})$ , dark grey rhombic crystals.

FIG. 11.—0.2% Fe, 0.2% Mn, 0.75% Si. As cast.  $\text{Mg}_2\text{Si}$ , black;  $\text{Al}(\text{Fe,Mn})\text{Si}$ , light grey, slightly in relief.

FIG. 12.—0.2% Fe, 0.2% Mn, 0.15% Si, 0.5% Cr. As cast.  $\text{Al}_7\text{Cr}$ , massive grey needles.

FIG. 13.—As Fig. 10. Hot and cold rolled to 0.1 in. Stringer of fragmented  $\text{Al}_6(\text{Fe,Mn})$ .

FIG. 14.—As Fig. 12. Hot and cold rolled to 0.1 in. Partly fragmented  $\text{Al}_7\text{Cr}$ .

All etched in 0.5% HF. Figs. 9-12,  $\times 50$ ; Figs. 13 and 14,  $\times 250$ .



15



16



17



18



FIGS. 15-18.—Longitudinal Sections of 0.05-in.-Thick Sheet After Immersion in Salt/Peroxide Solution.

FIG. 15.—Chromium-free alloy after 24 hours' immersion.  $\times 250$ .

FIG. 16.—Chromium-bearing alloy after 5 days' immersion.  $\times 250$ .

FIG. 17.—Chromium-bearing alloy artificially aged and cold rolled 30% (Table IV, condition (b)) after 5 days' immersion.  $\times 250$ .

FIG. 18.—As Fig. 17, re-heat-treated for 2 hr. at  $125^{\circ}\text{C}$ . (Table IV, condition (c)) after 5 days' immersion.  $\times 250$ .

The evidence indicates that on every count iron should be kept to a minimum, while the reduced ductility and formability associated with manganese contents as high as 0.8% outweighs the accompanying improvement in corrosion-resistance. On balance, 0.4% would seem to be about the maximum useful amount of this element.

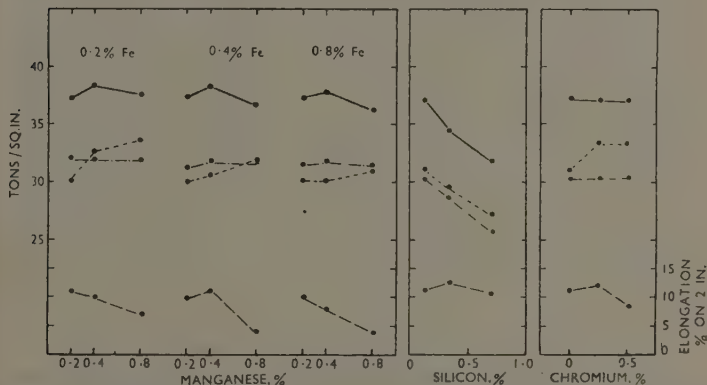


FIG. 23.—Mechanical Properties and Corrosion-Resistance of Alloys with Varying Manganese, Iron, Silicon, and Chromium Contents. [Table I, series 3, 4, and 5.] Key as for Fig. 22.

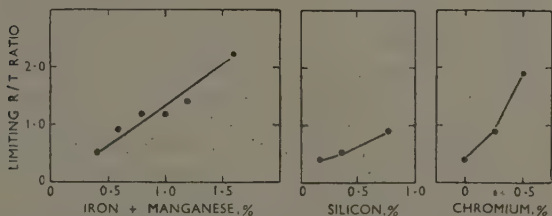


FIG. 24.—Bending Properties of 0.1-in.-Thick Alloy Sheet, Annealed and Slowly Cooled, with Varying Manganese, Iron, Silicon, and Chromium Contents. [Table I, series 3, 4, and 5.]

### 5. Effect of Silicon.

The effect of silicon up to 0.75% on an alloy containing 6% zinc, 2.25% magnesium, 2% copper, 0.2% iron, and 0.2% manganese is to decrease progressively the 0.1% proof stress and tensile strength, and with the maximum content of 0.75% the values for both properties are lower by some 5 tons/in.<sup>2</sup> than they are in the basis alloy (Fig. 23) of

which the silicon content is 0.17%. Elongation, on the other hand, is little affected, and the loss of strength due to corrosion was constant over the range of silicon additions studied. The reduction in strength is almost certainly due to the formation of  $\text{Mg}_2\text{Si}$ , which reduces the amount of magnesium available for age-hardening in the aluminium-zinc-magnesium system. The compound  $\text{Mg}_2\text{Si}$  can, itself, give rise to age-hardening in aluminium alloys, but the optimum temperatures for both solution heat-treatment and precipitation are considerably higher than those applicable to the alloys investigated. The bending properties of the alloy deteriorate with increasing silicon (Fig. 24), but it is clear that the element is less harmful in this respect than either manganese or iron. This is explained by the fine and even distribution of intermetallic compounds normally associated with a high silicon content. Thus it would seem that silicon reduces both strength and ductility without contributing any apparent benefits in respect of other properties, and it is, therefore, evident that this element should be held to the lowest possible limits.

#### 6. *Effect of Chromium.*

Chromium additions of 0.25 and 0.5% were made to an alloy of the same basic composition as that used in the silicon series, and the experimental data are plotted in Figs. 23 and 24. Ultimate tensile strength and 0.1% proof stress are much the same in all three alloys, but elongation is reduced in the 0.5% chromium alloy. Corrosion-resistance, on the other hand, is substantially increased by 0.25% chromium, the improvement being maintained, but not enhanced, with 0.5% chromium. In the chromium-free alloy deep localized surface pitting is accompanied by intercrystalline attack spreading from the base of pits (Fig. 15, Plate XLVI). By contrast, the chromium-containing alloys suffer only mild surface corrosion, even when the period of exposure to the corroding media is substantially increased (Fig. 16, Plate XLVI).

Formability is affected (Fig. 24) to a much greater extent than elongation, and the reduced bending properties with increasing chromium content can be attributed, as already mentioned, to the presence of stringer formations associated with the breakdown of the chromium-rich segregates present in the casting (Figs. 12 and 14, Plate XLV). It is clear, therefore, that although the presence of a small amount of chromium, such as 0.25%, is most desirable for improving corrosion-resistance, larger quantities would appear to be detrimental from several points of view.

## VI.—SOLIDIFICATION CHARACTERISTICS.

As in other types of heat-treatable aluminium alloys, the highly saturated solid solutions are the ideal basis for wrought aluminium-zinc-magnesium alloys and these can be obtained only indirectly, for the single-phase liquid alloy solidifies to a cored primary solid solution with dispersed eutectic constituents, and a homogeneous single phase can be obtained only by subsequent diffusion. In the aluminium-zinc-magnesium system it is particularly difficult to achieve homogeneity in the higher ranges of solid solution which are theoretically possible, because of the degree of segregation which arises from the long interval between primary and eutectic solidification, and the large proportion of eutectic resulting from the non-equilibrium conditions of freezing.

The extent of segregation and heterogeneity is determined by the rate of cooling and therefore by ingot size, and in the investigations which have been described in Section V, dealing with the effect of composition on the mechanical properties and resistance to corrosion, the attainment of the homogeneous condition in most alloys was made possible by the use of small ingots. As the ingot size is increased, the rate of cooling diminishes and the extent of segregation is such as to preclude the possibility of obtaining a completely homogeneous structure in many of the alloys even after prolonged heating.

With large ingots a long freezing range gives rise to other difficulties in casting, such as tearing on cooling through the liquid-solid stage, and the movement of liquid eutectic in the ingot arising from local strains and from gas evolution. In a typical high-strength aluminium-zinc-magnesium alloy, such as, for example, one containing 7.5% zinc and 2.5% magnesium, freezing begins at 640° C. and is completed by solidification of the eutectic at 470° C. This freezing range of 170° C. is possibly greater in relation to the casting temperature than that of any other alloy manufactured industrially. It is interesting to note, however, that in describing experiments with a 50:50 copper-iron alloy, in which the freezing range of 350° C. bears about the same relation to the casting temperature as in the aluminium-zinc-magnesium alloys, Smith and Palmer<sup>25</sup> drew attention to the extreme care necessary in mould preparation to avoid hot tearing and other damage during solidification.

The thermal studies had as their object the determination of the relationship between composition and duration of eutectic arrest. In these, 500 g. of an alloy of known composition were melted and thermal-arrest curves were established. The metal was then remelted and its composition modified by the addition of a known amount of one of the

alloying elements. The thermal analysis was repeated, and thereafter further additions and cooling-curve determinations were made. In this way as many as six cooling-curve determinations were sometimes made before it was necessary to resort to fresh basis material, and, in all, the freezing characteristics of about 126 different compositions were surveyed.

In order to ensure uniformity of temperature in the sample during the period when thermal observations were being made, and to facilitate the detection of small thermal arrests, a slow rate of cooling was employed—the temperature fall from 700° to 300° C. occupied 3 hr. As

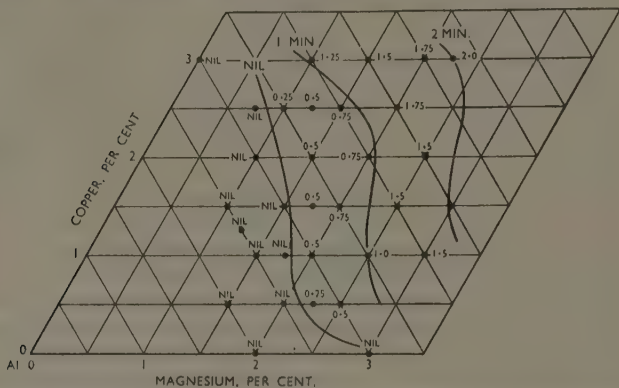


FIG. 25.—Thermal-Arrest Contours for Alloys Containing 4% Zinc and Varying Magnesium and Copper Contents.

the issue involved was the duration of the eutectic arrest, and not the precise determination of the temperature of eutectic and other thermal points, the cooling curves were obtained by direct plots with a potentiometer recorder which had an accuracy of about  $\pm 2^\circ$  C.

The alloys were of similar purity to those used in the study of mechanical properties, and the main series of experiments, in which zinc, magnesium, and copper contents were varied, was carried out on over a hundred alloys, all of which contained 0.25% manganese, 0.20% iron, and 0.15% silicon. The alloy compositions are plotted in three separate diagrams (Figs. 25, 26, and 27), for zinc contents of 4, 7.5, and 12% respectively, in which the co-ordinates are copper and magnesium contents, and the figures inserted against each plotted composition are the eutectic periods in minutes. The arrests were sharply defined

in all except the alloys with 3% or more of copper, in which freezing took place over a range of 5° C. or so. The arrest temperatures over the

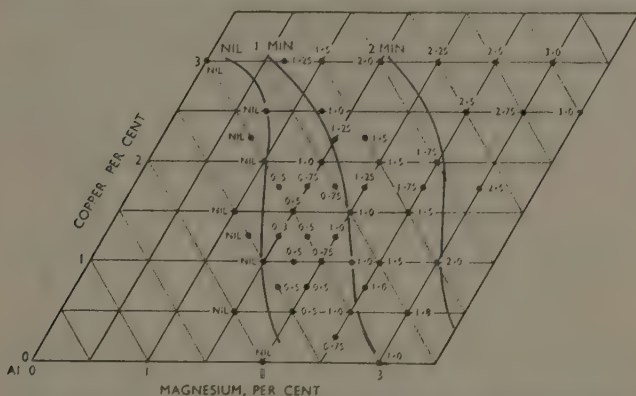


FIG. 26.—Thermal-Arrest Contours for Alloys Containing 7.5% Zinc and Varying Magnesium and Copper Contents.

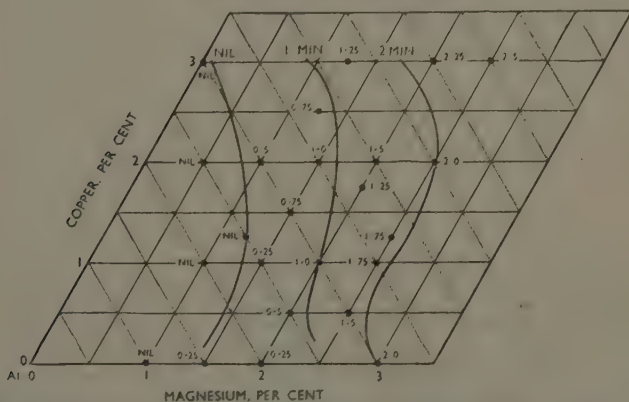


FIG. 27.—Thermal-Arrest Contours for Alloys Containing 12% Zinc and Varying Magnesium and Copper Contents.

whole series of alloys varied from about 480° C. in the 4% zinc alloys to 460° C. in the 12% zinc alloys, magnesium and copper having but little effect.

The results of experiments carried out on alloys containing 7.5% zinc, in which manganese and silicon were varied as well as copper and



magnesium, are reported in Table II. They indicate that manganese affects neither the temperature nor the magnitude of the eutectic arrest appreciably, but that with increased silicon an additional arrest occurs at some 80° C. above the final eutectic temperature.

The effect of zinc, magnesium, and copper can be most readily appreciated by reference to the curves interpolated in Figs. 25, 26, and 27, which indicate approximately the compositions of alloys with eutectic arrest periods of 1 and 2 min. and also the compositions at which the eutectic just ceases to be detected by thermal analysis. Zinc

TABLE II.—*Effect of Varying Manganese and Silicon Contents on the Cooling-Curve Eutectic Arrests in Alloys Containing 7.5% Zinc.*

Alloy Composition				Arrest (a)		Arrest (b)	
Mg, %	Cu, %	Mn, %	Si, %	Temperature, °C.	Duration, min.	Temperature, °C.	Duration, min.
1.5	1.5	...	0.02	...	...	473	0.5
1.5	1.5	...	1.0	540	0.5	...	...
1.5	1.5	0.25	0.2	...	...	472	0.5
1.5	1.5	0.25	1.0	540	0.5	...	...
1.5	1.5	0.8	0.02	...	...	474	0.5
2.5	1.5	0.25	0.02	...	...	472	2.0
2.5	1.5	0.25	0.2	540	V. slight	470	2.0
2.5	1.5	0.25	1.0	543	0.5	470	1.5
2.75	2.75	...	0.02	...	...	468	3.0
2.75	2.75	...	1.0	550	1.0	463	2.0
2.75	2.75	0.25	1.0	550	1.0	460	2.0
2.75	2.75	0.8	0.02	...	...	470	3.0

has the smallest effect on the magnitude of the arrest. For example, in alloys of 2% copper and 2% magnesium content, arrests corresponding to zinc contents of 4, 7.5, and 12%, are 0.75, 1.5, and 1.5 min. respectively; whereas in the alloy with 7.5% zinc a small variation in either the copper or magnesium content from 2% has quite a large effect on the magnitude of the arrest.

Both in casting and in subsequent rolling and extrusion operations, considerable advantage accrues from restricting the copper and magnesium contents so that the eutectic arrest on solidification is either small or absent. It is not, however, essential to confine compositions to those with a zero eutectic arrest, which unduly limits the tensile strength obtainable in the wrought material, and alloys with about a half-minute eutectic arrest can be quite readily cast and produced in wrought forms with good mechanical properties and with a high degree

of uniformity as the microstructure illustrated in Fig. 8 (Plate XLIV) clearly indicates. To facilitate a comparison between the range of composition of alloys of which the mechanical properties and resistance to corrosion have been determined, and those with a half-minute

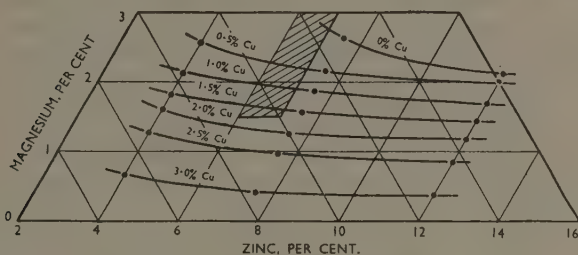


FIG. 28.—Limits of Compositions for Alloys with 30-Sec. Eutectic Arrest. The shaded area shows the limits for the optimum mechanical properties.

eutectic arrest period, the data expressed in Figs. 25, 26, and 27 are replotted in Fig. 28 with the same co-ordinates as in Figs. 19, 20, and 21. In this plot each curve represents the composition of alloys with constant copper contents of 0, 1, 2%, &c., and a half-minute arrest period. The composition limits previously defined for alloys with optimum strength and corrosion-resistance and with a minimum elongation value of 10% are indicated by the shaded area in this figure.

A further replot, with copper and magnesium as co-ordinates, of the compositions which fulfil the two requirements of optimum mechanical properties and a half-minute freezing arrest (Fig. 29), shows the compositions of alloys with 6 and 7% zinc contents corresponding respectively to the left- and right-hand edges of the shaded area in Fig. 28. These curves can be taken as indicating the composition limits of high-strength alloys suitable for manufacture on a bulk scale. It is evident that the zinc content may be varied between 6 and 7% without appreciably affecting the optimum proportions of copper and magnesium, but that these two latter elements can be varied only in inverse relation

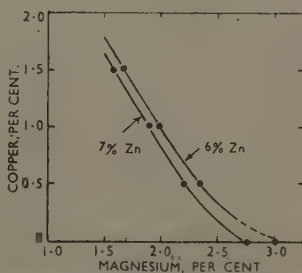


FIG. 29.—Relation Between Copper and Magnesium in Alloys of High Strength and Low Eutectic Content.

to each other. The maximum permissible amount of copper is 1.75%, and the corresponding magnesium content is 1.5%, while if copper is absent magnesium may be increased to a maximum of 3%.

#### VII.—THE CASTING AND PROCESSING OF LARGE INGOTS.

Some of the reasons for choosing an alloy with a short eutectic arrest rather than a long one have already been enumerated, and the extent to which they are confirmed in practice can be demonstrated by quoting data on two alloys produced as extruded rod (Table III). Both were

TABLE III.—*Composition, Extrusion Conditions, and Mechanical Properties of Alloys with Short and Long Eutectic Arrests.*

	Alloy A : Short Eutectic Arrest						Alloy B : Long Eutectic Arrest		
	Zn 6.5%	Mg 1.7%	Cu 1.5%	Zn 6.6%	Mg 1.8%	Cu 1.6%	Zn 6.0%	Mg 2.4%	Cu 2.3%
Method of casting	Tilting cast-iron mould.			Semi-continuous process (direct water sprays).			Tilting cast-iron mould.		
Eutectic arrest, min.	0.5			0.5			1.75		
Billet dimensions, in.	7½ dia. × 15			6½ dia. × 15			7½ dia. × 15		
Extruded rod, diameter, in.	1⅜			1½			1⅜		
Extrusion temperature, °C.	425			440			435		
Max. ram pressure, lb./in. <sup>2</sup>	3200			2900			2800		
Extrusion speed,* { (a)	14.5			40.0			3.0		
ft./min. { (b)	12.5			22.0			2.7		
0.1% Proof stress, tons/in. <sup>2</sup>	35.5			36.7			39.1		
Ultimate tensile strength, tons/in. <sup>2</sup>	39.7			41.4			43.2		
Elongation on 4√A, %	12			9.5			7		

\* (a) Maximum speed of extrusion; (b) Extrusion speed of material on which mechanical properties were determined.

within the defined range of compositions having optimum mechanical properties, the one, alloy A, being also within the range of low eutectic contents shown in Fig. 29, and the other, alloy B, having a eutectic arrest period of 1.75 min. Billets of alloy A were cast by two different methods, i.e. by direct pouring into a tilting cast-iron mould, and by the semi-continuous direct-chill process, in which water sprays impinge on the solidifying billet itself, causing very rapid freezing and producing the fine structure which is illustrated in Fig. 7 (Plate XLIV). The alloy B could not be cast satisfactorily, however, by the direct-chill process because of its unsuitable solidification characteristics, which, as

already stated, greatly increase the tendency to cracking and tearing, and therefore only billets poured into iron moulds were used.

All billets were homogenized by heating for 24 hr. at 460° C. before extrusion and were inserted in the press container at temperatures of 420°–440° C., extrusion being carried out under the conditions stated in Table III. In the extrusion of the first billet of each alloy the ram speed was progressively increased until the product showed signs of peripheral cracking, whereupon the speed was again reduced until cracking ceased. This process was repeated two or three times on a single billet in order to provide a reliable comparison of the hot-working properties of the three materials and also to establish appropriate speeds for extruding the remaining billets into rod for mechanical testing.

In addition to the advantages in casting associated with alloys of low eutectic content, these alloys can, as the figures in Table III show, be extruded at appreciably greater speeds than alloys of high eutectic content, and extrusion speeds can be realized that are comparable with those for aluminium-copper-magnesium alloys. Mechanical properties were determined on the extruded rod after solution heat-treatment at 460° C. for  $\frac{1}{2}$  hr., followed by ageing for 18 hr. at 125° C., and the values quoted are the mean of determinations on specimens taken at different positions along the length of the rod. Although the 0.1% proof stress and ultimate tensile strength values for alloy *B* are, by virtue of its higher alloy content, slightly greater than those for alloy *A*, the differences are not large, and, moreover, they are only realized at the expense of a substantial reduction in elongation value and, as already noted, in the rate of extrusion.

While these experiments clearly indicate the advantage of working within the limits of composition defined by Fig. 29, these should not be regarded as absolute limits outside which no useful commercial alloy can be obtained. Thus, if an elongation of less than 10% on 2 in. is acceptable, the strength can be increased by increasing the zinc content. If, however, relatively small ingots or billets are used and low rates of working adopted, the increase in strength can alternatively be achieved by raising the magnesium or copper contents, but even so the eutectic content should not be greater than that indicated as giving a one-minute eutectic arrest.<sup>26</sup>

#### VIII.—HEAT-TREATMENT AND COLD WORKING.

Alloys in the optimum range of composition defined by the curves in Fig. 29 can be readily rolled or extruded, and further experimental work was carried out on the heat-treatment of material produced on a manufacturing scale to establish the necessary conditions for obtaining

maximum possible strength and corrosion-resistance. The investigations were carried out on sheet, since this is less liable to variations in structure and mechanical properties than extruded rod, and it was rolled from slabs produced by the direct-chill continuous-casting process. The alloy was of the preferred or optimum composition, similar to alloy *A* in Table III, and contained 6.75% zinc, 1.75% magnesium, 1.5% copper, 0.25% manganese, 0.25% chromium, 0.2% iron, and 0.15% silicon.

### 1. Age-Hardening Characteristics.

The process of age-hardening at room and elevated temperatures was studied in specimens 0.05 in. thick, which were solution heat-treated for  $\frac{1}{2}$  hr. at 460° C., quenched, and naturally aged for increasing periods up to a maximum of 6 months, or artificially aged for 18 hr. at temperatures ranging from 90° to 180° C.

The properties developed by room-temperature age-hardening are shown in Fig. 30. Elongation values are substantially unaffected, but hardness, proof stress, and tensile strength increase progressively over the whole period, the 0.1% proof stress rising from 7 to 21 tons/in.<sup>2</sup>, and the ultimate tensile strength from 19 to 33 tons/in.<sup>2</sup>, and it is apparent that age-hardening is not complete after the lapse of six months.

The properties developed by age-hardening at elevated temperatures for a standard 18-hr. period are illustrated in Fig. 31. Maximum hardness and tensile-strength values are attained over a relatively wide range of temperatures between 90° and 120° C., while by contrast the 0.1% proof stress values show a more sharply defined maximum at 125°–135° C., and elongation values fall progressively with temperature.

In order to differentiate between the corrosion-resistance of specimens subjected to different ageing treatments, it was necessary to employ a 5-day immersion test in the standard salt/peroxide solution, the activity of which was maintained by daily renewal. At the end of 5 days loss of strength was considerable in the room-temperature-aged material and in specimens aged at 90° C., but the corrosion diminished with increase in temperature of ageing and loss in strength was slight at temperatures in the range 120°–130° C. From microscopic examination of corroded specimens it was clear that the temperature of ageing was affecting the nature as well as the degree of attack, intercrystalline penetration occurring in samples aged at 90°–100° C., while only localized pitting attack was apparent in material aged at temperatures of 120° C. and upwards. According to Saulnier,<sup>27</sup> the phases that precipitate on age-hardening below 125° C. are  $\text{Al}_2\text{Cu}$  and

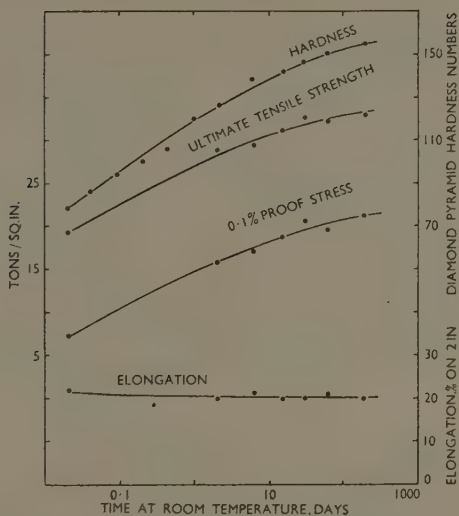


FIG. 30.—Effect of Room-Temperature Ageing on the Mechanical Properties of Solution Heat-Treated 0.05-in.-Thick Sheet.

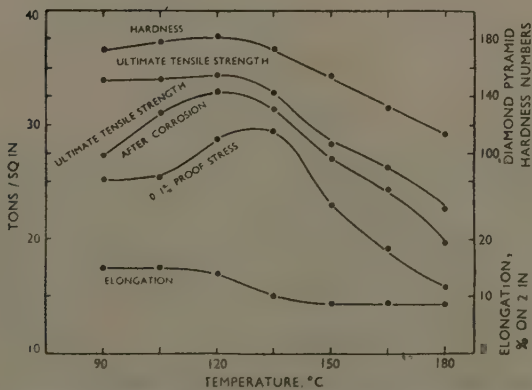


FIG. 31.—Effect of Artificial Ageing for 18 hr. at Elevated Temperatures on the Mechanical Properties and Corrosion-Resistance of 0.05-in.-Thick Sheet.



$\text{Al}_2\text{CuMg}$ , while above this temperature the main age-hardening constituent is  $\text{MgZn}_2$ . From surface-potential data it would seem that grain-boundary precipitation of either of the copper-bearing phases might be expected to have a more harmful effect than precipitation of  $\text{MgZn}_2$ , and Saulnier's observations might, therefore, offer a satisfactory explanation of the observed behaviour. It is clear, however, that artificial ageing at temperatures below  $120^\circ\text{C}$ . should be avoided, and the optimum combination of proof stress, tensile strength, and corrosion-resistance is obtained by ageing within the range  $125^\circ\text{--}130^\circ\text{C}$ .

## 2. Effect of Cold Work and Secondary Heat-Treatment.

As in other heat-treatable alloys, cold working before ageing has a relatively slight effect on the mechanical properties that can be obtained by subsequent artificial ageing, although the temperature of age-

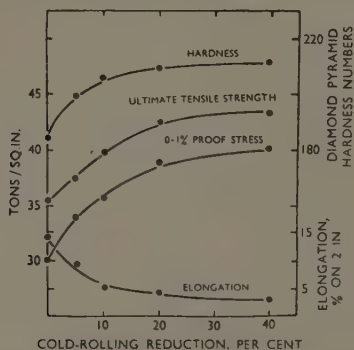


FIG. 32.—Effect of Cold Rolling on the Mechanical Properties of Artificially Aged Sheet.

hardening is lowered and the extent to which age-hardening occurs at room temperature may be increased. The extent to which properties are affected by cold working subsequent to heat-treatment has been studied on the same alloy as that used in investigating age-hardening characteristics (p. 316). Sheet with a thickness of 0.1 in. was quenched, artificially aged for 18 hr. at  $125^\circ\text{C}$ ., and cold rolled with reductions of up to a total of 40% in thickness, beyond which cracking occurred. The mechanical properties of material so treated are plotted in Fig. 32, which shows the progressive increase in hardness, 0.1% proof stress, and tensile strength, and the corresponding decrease in elongation. Most of the hardening and strengthening occurs with reductions of up

to 20%. The resistance to corrosion of the heat-treated material was diminished by cold rolling, the form of attack changing from the slight surface roughening of the kind illustrated in Fig. 16 (Plate XLVI), to penetration along shear planes (Fig. 17, Plate XLVI). Resistance to corrosion of the cold-rolled alloy was improved by subsequent, or secondary, heat-treatment at temperatures up to 180° C. Precipitation and softening in the rolled stock occurred more rapidly than in material hardened only by heat-treatment. After 2 hr. at 150° C., for example, the hardness fell below that of the heat-treated alloy before rolling. The effect of a 2-hr. secondary heat-treatment at 125° C., which was judged to be about the optimum in respect of both residual strength and corrosion-resistance,<sup>28</sup> is shown in Table IV, which records proper-

TABLE IV.—*Mechanical Properties and Corrosion-Resistance of Quenched and Artificially Aged 0.05-in.-Thick Sheet After Cold Rolling and Secondary Heat-Treatment.*

Condition of Sheet	0.1% Proof Stress, tons/in. <sup>2</sup>	U.T.S., tons/in. <sup>2</sup>	Elongation on 2 in., %	Diamond Pyramid Hardness No.	After 5 Days' Immersion in Salt/Peroxide Solution		
					U.T.S., tons/in. <sup>2</sup>	Elongation on 2 in., %	Loss in Strength, %
(a) Artificially aged.	30.3	37.1	16	187	36.3	13.5	2.2
(b) Artificially aged and cold rolled to 31% reduction.	38.9	44.5	5	211	41.3	2.5	7.0
(c) Aged, cold rolled, and re-heated for 2 hr. at 125° C.	37.6	42.0	6	202	40.5	5	3.5

ties at each of the three successive stages, i.e. (a) fully heat-treated, (b) fully heat-treated and cold rolled, and (c) fully heat-treated, rolled, and aged at 125° C. In the last condition the alloy has appreciably improved mechanical properties, and the corrosion-resistance is only slightly inferior to that of the original heat-treated alloy. The form of corrosion in the accelerated test was pitting with some slight ex-foliation as illustrated in Fig. 18 (Plate XLVI).

#### ACKNOWLEDGEMENTS.

The authors' thanks are due to Mr. G. H. Blenkarn and several other of their colleagues for help in connection with various aspects of the work described in this paper.

## REFERENCES.

1. J. Hérenghuel and G. Chaudron, *Compt. rend.*, 1939, **209**, 109.
2. J. Hérenghuel and G. Chaudron, *Métaux et Corrosion*, 1941, **16**, 33, 49.
3. J. Hérenghuel, *Rev. Mét.*, 1947, **44**, 77.
4. M. Hansen, A. Mühlenbruch, and H. J. Seemann, *Metallwirtschaft*, 1940, **19**, 535.
5. M. Hansen, A. Mühlenbruch, and H. J. Seemann, *Aluminium*, 1940, **22**, 442.
6. G. Siebel and H. Vosskübler, *Metallwirtschaft*, 1940, **19**, 1167.
7. W. Bungardt and G. Schmitberger, *Metallwirtschaft*, 1941, **20**, 719.
8. W. Bungardt and H. Gröber, *Metallwirtschaft*, 1944, **23**, 392.
9. P. Brenner and W. Feldman, *Z. Metallkunde*, 1940, **32**, 290.
10. P. Vachot, *Rev. Aluminium*, 1947, (134), 189; (135), 225.
11. B. W. Mott and J. Thompson, *Metal Treatment*, 1947-8, **14**, 227.
12. B. W. Mott and J. Thompson, *Metal Treatment*, 1948, **15**, 33, 91.
13. H. G. Petri, G. Siebel, and H. Vosskübler, *Aluminium*, 1942, **24**, 385.
14. K. L. Dreyer and H. J. Seemann, *Aluminium*, 1944, **26**, 76.
15. W. Bungardt and V. Hauk, *Metallforschung*, 1947, **2**, 161.
16. W. Feldman, *Metallwirtschaft*, 1941, **20**, 501.
17. W. Köster and W. Wolf, *Z. Metallkunde*, 1936, **28**, 155.  
W. Köster and W. Dullenkopf, *Z. Metallkunde*, 1936, **28**, 309, 363.
18. W. L. Fink and L. A. Willey, *Trans. Amer. Inst. Min. Met. Eng.*, 1937, **124**, 78.
19. E. Butchers, G. V. Raynor, and W. Hume-Rothery, *J. Inst. Metals*, 1943, **69**, 209.
20. G. V. Raynor and W. Hume-Rothery, *ibid.*, 415.
21. A. T. Little, G. V. Raynor, and W. Hume-Rothery, *ibid.*, 423.
22. A. T. Little, G. V. Raynor, and W. Hume-Rothery, *ibid.*, 467.
23. D. J. Strawbridge, W. Hume-Rothery, and A. T. Little, *J. Inst. Metals*, 1948, **74**, 191.
24. H. J. Axon and W. Hume-Rothery, *ibid.*, 315.
25. C. S. Smith and E. W. Palmer, *Trans. Amer. Inst. Min. Met. Eng.*, (in *J. Metals*), 1950, **188**, 1486.
26. British Patent No. **598,192**.
27. A. Saulnier, *Compt. rend.*, 1948, **226**, 181.
28. British Patent No. **621,336**.

# THE AGEING CHARACTERISTICS OF BINARY 1310 ALUMINIUM-COPPER ALLOYS.\*

By H. K. HARDY,† Ph.D., M.Sc., A.R.S.M., A.I.M., MEMBER.

## SYNOPSIS.

Hardness/ageing-time curves have been obtained on aluminium alloys containing 2.0-4.5% copper at temperatures between 30° and 240° C. Ageing at 30° C. gave an increase in hardness to a constant value. Ageing at 130° C. caused an initial rise in hardness, which then remained at a constant value for a short time in alloys with 3.5-4.5% copper. This was followed by a second rise to peak hardness. The time to attain this peak hardness was independent of composition in the range 3.0-4.5% copper. Single-stage ageing curves were obtained at higher ageing temperatures.

The results have been analysed in terms of hardness/concentration, time/concentration, and temperature/time relationships for various parts of the ageing curves. The maximum attainable hardness was reached when the two-stage ageing curve was operative. A branched curve was obtained for the temperature/incubation value relationships.

The results are discussed with reference to a recent thermodynamic analysis of the decomposition of supersaturated solid solutions (H. K. Hardy, *J. Inst. Metals*, 1950, **77**, 457). The conditions for alloy systems with a negative heat of solution (E. Schell, *Z. Metallkunde*, 1950, **41**, 44) have been applied, and it is thought that the G.P. (Guinier-Preston) zones [1] and [2] originate in ordering reactions. The G.P. zones [1] correspond to partially ordered aggregates and the G.P. zones [2] to fully ordered regions.

The initial rise in hardness is due to the formation of G.P. zones [1]. The single-stage ageing curve at higher temperatures is associated with the formation of G.P. zones [2] directly from the matrix by a process of nucleation and growth. The higher peak hardness reached with the two-stage ageing curve is believed to be due to effects from G.P. zones [1] and [2], present simultaneously. The latter may have formed by an allotropic change or may have arisen in the matrix between the G.P. zones [1].

The free energy/compositional/structural relationships, the growth law of the G.P. zones, calculations of the diffusion coefficients from the sizes of the G.P. zones, and the slope of reciprocal rate curves are discussed in Appendixes.

## I.—INTRODUCTION.

IN spite of the amount of work carried out since Wilm's discovery of age-hardening,<sup>1</sup> there is no complete agreement on the mechanism of the ageing process. The aluminium-copper system is of fundamental importance, not only on account of the complexity it exhibits, but also because it is the basis of many alloys of technical importance.

A detailed examination of the ageing characteristics of aluminium alloys of different copper contents was thought to afford the most promising starting point for a new investigation. This type of study

\* Manuscript received 6 September 1950.

† Head of Physical Metallurgy Section, Fulmer Research Institute, Stoke Poges, Bucks.

has previously received less attention than other aspects of the subject, but allows a comparison to be made of the ageing processes for various degrees of supersaturation. It is intended that metallographic and single-crystal X-ray examinations shall subsequently be allied to this approach.

The work described in the present paper, which forms part of a general investigation into the ageing processes of aluminium-copper alloys, had the following objectives:

(1) To investigate the ageing curves at different temperatures for alloys of various copper contents.

(2) To deduce possible ageing processes for different degrees of supersaturation.

(3) To obtain data for suitable ageing treatments for subsequent metallographic and single-crystal X-ray investigations, designed to yield experimental evidence and to test the hypotheses put forward.

(4) To set up ageing curves for binary aluminium-copper alloys for future comparison with those for alloys containing additional elements.

## II.—PREVIOUS WORK.

Detailed reviews of the process of precipitation from a supersaturated solution are already extant.<sup>2-4</sup> These render a general account unnecessary at this stage, and reference will be made only to work directly relevant to the present research.

Hunsicker<sup>5</sup> obtained hardness/ageing curves on high-purity aluminium alloys with 1-4.5% copper. His specimens were cold-water quenched and aged at room temperature, or were quenched in boiling water and aged at room temperature or at 150° C. The ageing curves were continued for periods up to 90 days in each case. The chief purpose of this work was to compare the ageing curves of ternary aluminium-4.5% copper alloys containing 0.15-1.05% iron, with those of the binary aluminium-copper alloys. The results were not intended to elucidate the ageing processes in binary aluminium-copper alloys, but it will be shown later that they confirm an important aspect of the present work.

A series of papers by Gayler culminated in two important studies of the aluminium-4% copper alloy.<sup>6,7</sup> The first represents the most intensive investigation yet made of the ageing characteristics of a single alloy, and hardness/ageing curves were obtained at numerous temperatures between 0° and 450° C. Gayler and Parkhuse showed very clearly in this paper that the hardening process occurred in two stages over a certain range of ageing temperatures: an initial rise in hardness was followed by a period of constant hardness, which preceded a second rise to the peak hardness value before softening occurred. The experi-

mental methods and ageing temperatures chosen for the present research were largely based on the results of this work. The second paper <sup>7</sup> represented a detailed metallographic study of the ageing process.

Descriptive theories of the precipitation process have been critically discussed in an earlier paper.<sup>8</sup> Guinier <sup>9, 10</sup> and Preston <sup>11, 12</sup> suggested independently, on the basis of single-crystal X-ray examinations, that the first stage in the decomposition of supersaturated aluminium-copper alloys was by the segregation of small plate-like clusters of solute atoms parallel to the (100) planes of the matrix. These have previously been termed Guinier-Preston (G.P.) zones [1].<sup>8</sup> Later work on an aluminium-5.22% copper alloy by Guinier,<sup>13</sup> using a modified X-ray technique, showed that these were replaced by regions possessing an ordered arrangement of copper and aluminium atoms, designated G.P. zones [2].<sup>8</sup> At a later stage in the ageing process the latter are transformed into the  $\theta'$  intermediate precipitate, which is the forerunner of the stable  $\theta$  ( $\text{CuAl}_2$ ) precipitate.<sup>14</sup>

An alternative view has been that the G.P. zones are actually very small regions possessing the structure of  $\theta'$ . But very recently Guinier <sup>15</sup> has been able to show that the structure of the G.P. zones [2] differs from that of  $\theta'$  and he has designated this structure  $\theta''$ .

The lattice of the precipitate (or G.P. zone) remains continuous with that of the matrix as long as the particles are small and, in this condition, the precipitate is said to be "coherent". The coherency stresses due to a slight dis-register between the lattices of the precipitate and of the matrix increase as the particle grows, and it will break away from the matrix when these can no longer be withstood. The formation of an interface facilitates internal structural rearrangements of the precipitate to a more stable form. Non-coherent particles of precipitate may cause hardening by slip interference, but the coherency strains are now regarded as more efficient in blocking the movement of dislocations.

Gayler and Parkhouse <sup>6</sup> associated the initial rise in hardness with the formation of the G.P. zones [1], the second rise being thought to be due to the formation of  $\theta'$ . However, the later metallographic work of Gayler <sup>7</sup> showed that the precipitate after ageing to maximum hardness at 130° C. was a copper-rich region with etching characteristics different from those of  $\theta'$ . In view of Guinier's work, this was assumed to be the G.P. zones [2].<sup>16</sup>

Gayler interpreted the flat portion of the ageing curves, between the initial rise and the second increase to the peak hardness, as being due to a balance between the growth of submicroscopic G.P. zones to a critical size and their precipitation to allow relief of strain, together with the formation of associated submicroscopic crystallites of the



aluminium solid solution of equilibrium concentration.<sup>7</sup> This view has been criticized by the present author on the grounds that "precipitation" of the G.P. zones to allow relief of strain would have to be accompanied by a loss of coherency with the matrix, and this would not occur without the formation of a new phase.<sup>8</sup> It was suggested that the flat portion on the hardness/ageing curve represented the time for the small G.P. zones [1] to re-dissolve and to re-deposit on the larger G.P. zones [1], which transformed to the G.P. zone [2] when a critical size had been exceeded. This view will be discussed later in the light of the results of the present investigation.

### III.—EXPERIMENTAL METHODS.

Hardness testing was adopted as offering the simplest method of dealing with a large number of specimens, as well as revealing clearly the different stages in the ageing process.<sup>6</sup> The disadvantage of this method is that the hardness value is not a fundamental property of the material. Furthermore, the results give the hardness of the surface of the specimen, and this may differ from that of the bulk material. It was advisable to average a fairly large number of readings, and the ease of operation of the Vickers pyramidal-diamond tester more than compensated for the inherent disadvantages. This was particularly appropriate when it is realized that the number of specimens envisaged<sup>17</sup> was so great that the heat-treatment and hardness-testing schedules were put on a routine basis.

The ageing temperatures chosen by reference to the work of Gayler and Parkhouse,<sup>6</sup> were such that the lowest temperature would clearly show the two stages and the highest temperature would give essentially a single stage for the aluminium-4.0% copper alloy. Ageing curves were also obtained close to room temperature.

#### 1. *Preparation of the Alloys.*

The materials used were of the highest available purity. The aluminium (99.99%) was obtained from The British Aluminium Co., Ltd. Some of the alloys were melted in high-purity graphite crucibles and others in sillimanite crucibles lined with alumina. Preliminary tests showed that these techniques caused no appreciable reduction in metal purity. A high-frequency furnace was used in all cases. The aluminium-copper hardener was granulated by pouring into water in order to obtain uniformity of composition.

The melts were chlorine-degassed through an alumina tube. The billets were water-chill cast by pouring into a 1½-in.-dia. cylindrical thin sheet steel container and allowing water in an annular space between

this and an outer container to rise at such a rate that directional solidification occurred from the bottom of the ingot.

The melt analyses all fell within  $\pm 0.1\%$  of the required copper content. Test analyses showed that the billets were of uniform composition. The iron and silicon contents were always less than  $0.01\%$ .

### 2. Forging.

It had been noted previously that the response to low-temperature ageing of specimens made from normal chill-cast billets <sup>6</sup> was affected by the forging technique used. A preliminary investigation did not provide strong confirmation of this effect, but the alloys were cold forged in order to ensure the greatest possible reproducibility of working conditions. The cast billets were scalped to 1.1 in. dia. and 8 in. long and annealed for 48 hr. at  $250^{\circ}\text{C}$ . These were cold forged to 0.52 in. square, annealed 24 hr. at  $495^{\circ}\text{C}$ ., and air-cooled, followed by 24 hr. at  $250^{\circ}\text{C}$ . The square bars were then flattened on one face to 0.22 in. thick and  $1-1\frac{1}{4}$  in. wide.

### 3. Specimen Preparation.

It was desired to carry out the hardness tests on a surface well away from that of the original cast billet, in order to reduce the possible chance of errors due to inverse segregation. Preliminary work showed it to be essential to keep to a minimum the handling of the specimens after solution heat-treatment. It was found that the cold work due to a hacksaw cut could affect a depth of  $\frac{1}{4}$  in. in the case of material freshly quenched. The specimens were therefore prepared as fully as possible before heat-treatment. Satisfactory results were obtained with the method used, which was well suited to deal with large numbers of specimens.

Half-inch lengths were marked off on one side of the strips and stamped individually for identification; 0.050 in. was machined from the opposite surface and the specimens were cut and drilled so that they could be suspended by 0.028-in.-dia. wire. The machined surfaces were ground to 0 emery paper. The specimens then only required grinding on 00 emery paper before hardness testing after heat-treatment.

### 4. Heat-Treatment.

Salt-bath heat-treatment was adopted in order to obtain a fine grain-size. The specimens were solution heat-treated for not less than 48 hr. at  $520^{\circ}\text{C}$ ., except that a temperature of  $530^{\circ}\text{C}$ . was used for the aluminium-4.5% copper alloy. This was followed by quenching in water at  $20^{\circ}\pm 1^{\circ}\text{C}$ . Metallographic examination showed that these treatments gave complete solution of the  $\text{CuAl}_2$  particles.

The quenched specimens were dried by rinsing in acetone and aged

at 30°, 130°, 165°, 190°, and 220° C. The aluminium-4.0% copper alloy only was aged at 240° C. The time between quenching and insertion in the ageing furnace was less than 5 min. The 30° and 165° C. treatments were carried out in oil baths. Circulating-air furnaces were used at 130°, 190°, and 220° C. A salt bath was employed at 240° C. The useful volume of the furnaces was chosen so that the overall temperature fluctuations did not exceed  $\pm 1\frac{1}{2}^{\circ}$  C. The times taken by the specimens to reach a temperature 2° C. lower than that of the furnace were 4 min., 6 min., 5 min., 5 min., and 1.5 min. for the 130°, 165°, 190°, 220°, and 240° C. furnaces, respectively. These times were allowed for in plotting the hardness curves. Spectrographic analysis showed no changes in the composition at the surface during heat-treatment.

### 5. Hardness Testing.

Five Vickers pyramidal-diamond hardness tests were made on each specimen after ageing. The complete hardness range was readily covered with the 10-kg. load. Duplicate specimens were used for the early parts of the ageing curves. Specimens that had been aged for very short times were re-solution treated. Where specimens had been aged for somewhat longer times one was put back into the furnace for further, generally very long-time, ageing. The other specimen was placed in a refrigerator at  $-10^{\circ}$  C. to be stored until a convenient opportunity arose for metallographic examination.

The results have been slightly weighted in that hardness readings which fell well away from the test-piece average were neglected.

### 6. Terminology of Ageing Curves.

The terms used to describe the different parts of the ageing curves are shown diagrammatically in Fig. 1. The upper curve has been termed a "two-stage ageing curve", and the lower "a single-stage ageing curve".

An incubation value has been adopted to indicate the time to the beginning of ageing. As normally assessed, the incubation period ( $t_p$ , Fig. 2), is greatly influenced by grain boundaries and may therefore not be fully characteristic of the alloy, even if the scatter of results did not preclude its ready assessment. The time to the maximum rate of hardening is probably a safer measure of the general incubation period of the alloy as a whole, but suffers from the same drawback that it cannot be closely defined on the ageing curves. For these reasons an "incubation value" ( $t_v$ ) was obtained by extrapolating the curve for the rise in hardness back to the hardness value possessed during the incubation period. This could be carried out fairly readily, as the curve for the initial rise of hardness normally followed a straight line

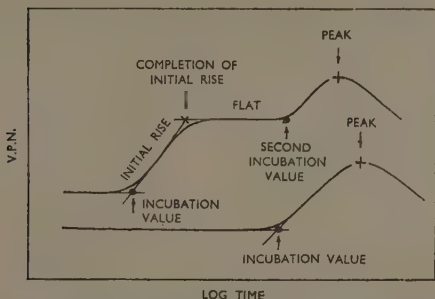


FIG. 1.—Diagrammatic Illustration of the Terms Used to Indicate Various Positions on the Ageing Curves.

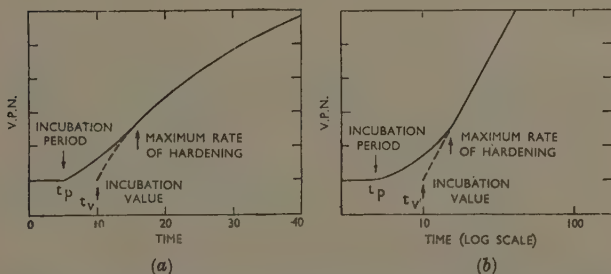


FIG. 2.—Relation Between the Incubation Period, Incubation Value, and Position of Maximum Hardening Rate for Identical Ageing Curves Plotted (a) Against Time and (b) Against Log Time.

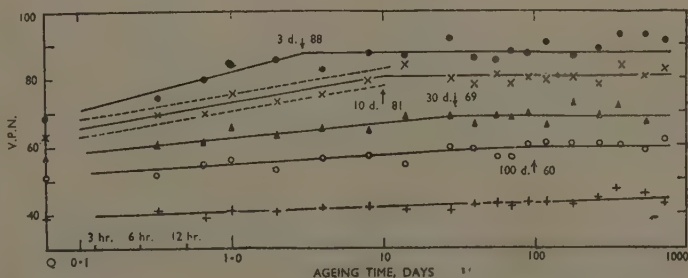


FIG. 3.—Hardness Curves for Aluminium-Copper Alloys Aged at 30°C. Each point represents the average of five impressions on each of two specimens, except that the quenched values represent the average of five impressions on each of eight specimens. (For key see Fig. 4.)

when plotted logarithmically. As shown in Fig. 2, the incubation value fell between the incubation period and the time to the maximum rate of hardening.

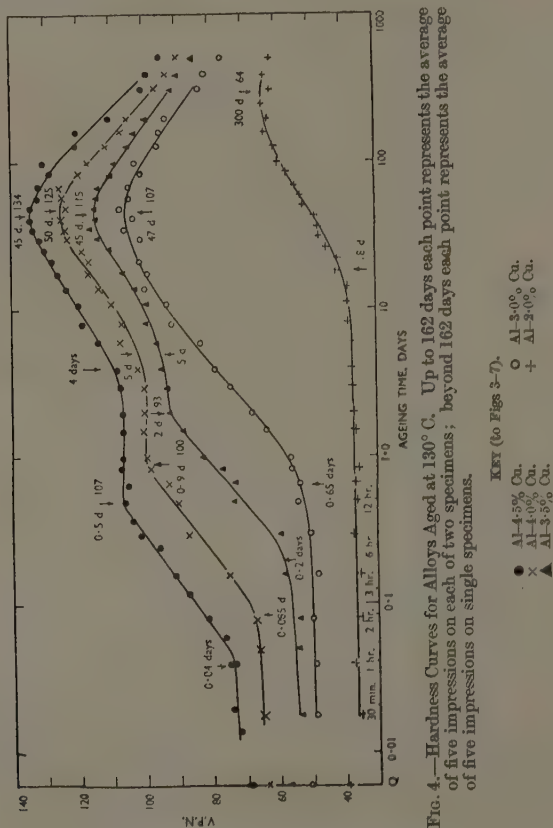


FIG. 4.—Hardness Curves for Alloys Aged at 130° C. Up to 162 days each point represents the average of five impressions on each of two specimens; beyond 162 days each point represents the average of five impressions on single specimens.

KEY (to Figs 3-7).

- Al-4.5% Cu.
- × Al-4.0% Cu.
- ▲ Al-3.5% Cu.
- Al-3.0% Cu.
- + Al-2.0% Cu.

#### IV.—HARDNESS/AGEING CURVES.

Hardness/ageing curves at 30°, 130°, 165°, 190°, 220°, and 240° C., are given in Figs. 3-8, respectively.

##### (a) Ageing at 30° C. (Fig. 3).

The incubation value was of the order of 0.05 day for all the alloys. The constancy of this value may have resulted from the strains intro-

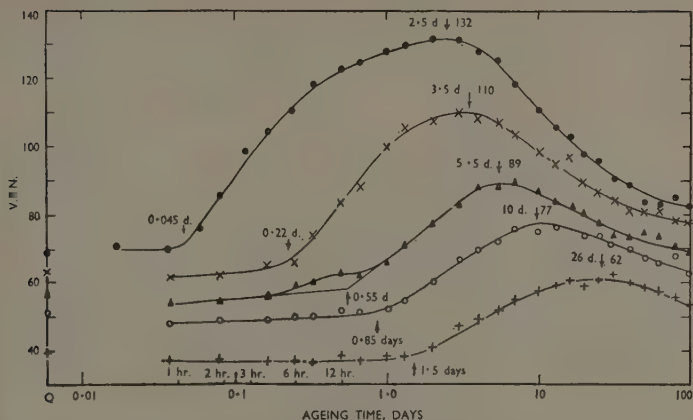


FIG. 5.—Hardness Curves for Alloys Aged at 165° C. Up to 7 days each point represents the average of five impressions on each of two specimens; beyond 7 days each point represents the average of five impressions on single specimens. (For key see Fig. 4.)

duced by the quenching operation, as the hardness measurements were made on the surface of the specimens.

Within the limits of experimental error, the ageing curves could be represented as two straight lines intersecting at the completion of the initial rise. Ageing beyond this point gave no further hardness

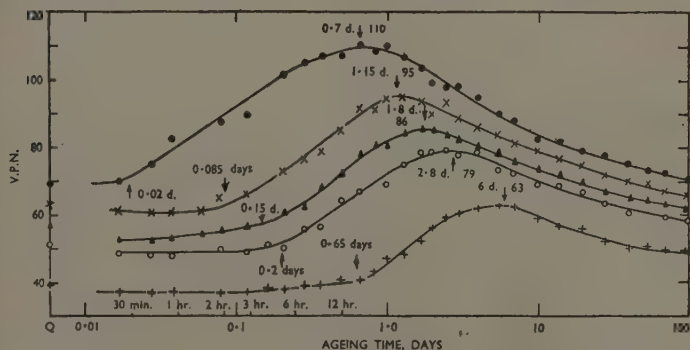


FIG. 6.—Hardness Curves for Alloys Aged at 190° C. Up to 28 days each point represents the average of five impressions on each of two specimens; beyond 28 days each point represents the average of five impressions on single specimens. (For key see Fig. 4.)



increment. The rate of hardening of the aluminium-4.0% copper alloy was less than that observed by Gayler and Parkhouse at the same temperature,<sup>6</sup> but was more in accordance with the results of Hunsicker.<sup>5</sup>

(b) *Ageing at 130° C. (Fig. 4).*

At very short ageing times most of the alloys showed a slight drop in hardness from the values of the quenched specimens, and this may be associated with relief of quenching strains. The incubation values became progressively longer for alloys of lower supersaturation. The initial rise for the alloys with 3-4.5% copper can be represented as straight lines of approximately constant slope against the logarithmic time base. The end of the initial rise was followed by a period of nearly constant hardness for the alloys with 3.5-4.5% copper. The second incubation value, which preceded the rise to peak hardness, occurred after very similar ageing times for these alloys.

The time to peak hardness was substantially independent of composition over the range 3-4.5% copper. The aluminium-2.0% copper alloy showed only a single-stage rise to a peak hardness value at a much longer ageing time.

The curve for the aluminium-4.0% copper alloy confirmed the two-stage ageing curves observed by Gayler and Parkhouse.<sup>6</sup> The second incubation value and peak hardness occurred after very similar times in both cases. The time to the completion of the initial rise was longer in the present instance, in agreement with the slower rate of ageing noted at 30° C.

(c) *Ageing at 165° C. (Fig. 5).*

Slight softening occurred after very short ageing times. The incubation values lengthened with decrease of copper content. The aluminium-3.5% copper alloy showed a very small initial rise which was almost within the limits of the experimental error. The logarithmic rate of hardening was appreciably greater for the 4.5% and 4.0% copper alloys than for the remainder. The curves increased continuously to the peak values in all cases, but the curve for the aluminium-4.5% copper alloy was very similar in general appearance to that of the aluminium-3.0% copper alloy aged at 130° C.

(d) *Ageing at 190° C. (Fig. 6).*

A slight initial drop in hardness was obtained, as noted previously. The hardness curves increased smoothly from the incubation values to the peak hardnesses. Gayler and Parkhouse<sup>6</sup> had noted a small initial

rise for the 4% copper alloy. A similar effect was not observed, except possibly for one point off the curve at 0.08 days.

(e) Ageing at 220° C. (Fig. 7).

The hardness curves showed single-stage ageing passing through peak hardness values.

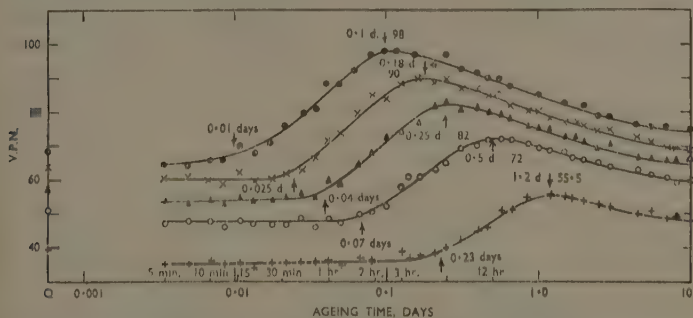


FIG. 7.—Hardness Curves for Alloys Aged at 220° C. Each point represents the average of five impressions on each of two specimens. (For key see Fig. 4.)

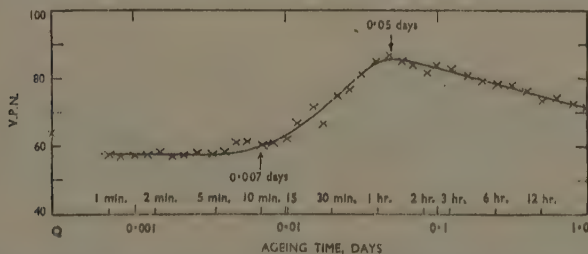


FIG. 8.—Hardness Curve for an Aluminium-4.0% Copper Alloy Aged at 240° C. Each point represents the average of five impressions on each of two specimens.

(f) Ageing at 240° C. (Fig. 8).

Only the 4% copper alloy was examined at this temperature and gave a smooth ageing curve.

### V.—ANALYSIS OF RESULTS.

The relation between atomic and weight percentage is almost linear over the range aluminium-2.0% copper to aluminium-4.5% copper, so that relations derived against weight percentages are also valid for atomic percentages.

## 1. Concentration/Hardness Relationships.

Hardness values after various periods of time at 30° C. and the completion of the initial rise at 130° C. are shown in Fig. 9. The results on the quenched alloys exhibited a linear relationship with concentration over the range examined. The shape of the curves for the other ageing periods at 30° C. was a function of the extent to which the ageing process had been completed. The hardness values after the completion of the initial rise at 130° C. were appreciably higher than those attained at 30° C.

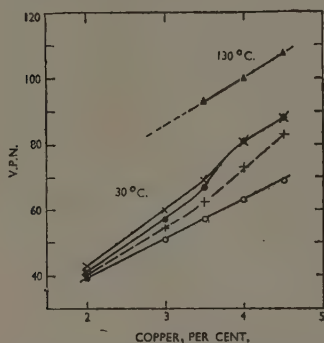


FIG. 9.—Hardness Values of Aluminium-Copper Alloys After Different Periods of Time at 30° C. and the Completion of the Initial Rise at 130° C.

KEY.

- ▲ 130° C. × 100 days.
- 10 days, + 1 day at 30° C.
- Quenched.

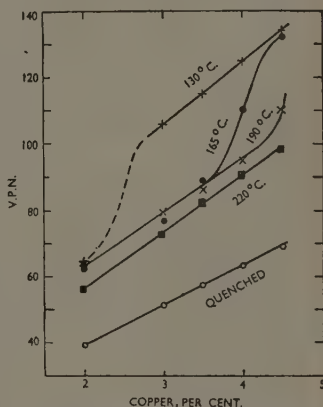


FIG. 10.—Quenched and Peak Hardness Values of Alloys Aged at Different Temperatures.

The peak hardness values at different ageing temperatures have been plotted against concentration in Fig. 10, and fall clearly into two groups. A linear relationship exists between the peak hardness at 130° C. and concentration over the range 3–4.5% copper. This forms the upper group of results to which belongs the aluminium-4.5% copper alloy aged at 165° C.

The lower group of results is made up by the peak hardness values at 220° C., at 190° C. over the range 2–4% copper, at 165° C. over the range 2–3.5% copper, and the 2% copper alloy at 130° C. The aluminium-4% copper alloy aged at 165° C. and the aluminium-4.5% copper alloy aged at 190° C. fall into an intermediate category (Fig. 10).

A similar relationship may be derived for the peak hardness values

of Hunsicker's alloys quenched in boiling water and aged at  $150^{\circ}\text{C}.$ <sup>5</sup> (see Fig. 11). Hunsicker originally drew a smooth inflected curve through these results from which the points at 2.5 and 3% copper were appreciably offset to opposite sides. His quenched values also bore a relationship to concentration which was very nearly linear.

Comparison of Fig. 10 with the ageing curves (Figs. 3-8), shows that the higher group of peak hardness values is to be associated with the two-stage ageing curves and the lower group of peak hardness values with the single-stage ageing curves. The intermediate values represent conditions under which both types of ageing curve are obtained simultaneously to a greater or lesser extent. The aluminium-3.0% copper alloy aged at  $130^{\circ}\text{C}.$  (Fig. 4), and the aluminium-4.5% copper alloy aged at  $165^{\circ}\text{C}.$  (Fig. 5), belong to the upper group and represent cases where the occurrence of the flat has been prevented.

The single-stage ageing curve is favoured by high ageing temperatures and low degrees of supersaturation; the two-stage ageing curve by a lower ageing temperature and high degrees of supersaturation.

The relation between concentration and the increment from the quenched to peak hardness values for the single-stage ageing curves is shown in Fig. 12. The relation for the hardness increment from the flat to the peak at  $130^{\circ}\text{C}.$  was of a similar form, but displaced to higher concentrations.

## 2. Concentration/Rate of Hardening Relationships.

Alloys of different concentrations of copper which give ageing curves of equal slope when plotted logarithmically may possess very different maximum rates of hardening. Approximate values have been derived from the ageing curves for the maximum rate of hardening (Fig. 2) during the initial rise at  $30^{\circ}$  and  $130^{\circ}\text{C}.$  It will be noted from Fig. 13 that this increased rapidly with increasing supersaturation. The maximum rate was much greater at  $130^{\circ}\text{C}.$  than at  $30^{\circ}\text{C}.$  for alloys with more than 3% copper. The curves in Fig. 13 fell close to a straight line when the logarithm of the maximum rate was plotted against concentration.

## 3. Concentration/Time Relationships.

The logarithm of the time to the completion of the initial rise shows a linear relation with concentration over the range investigated (Fig. 14). If the curves may be extrapolated, the aluminium-2.0% copper alloy should complete its initial rise after approximately 1000 days at  $30^{\circ}\text{C}.$

The times required for the attainment of peak hardness have been

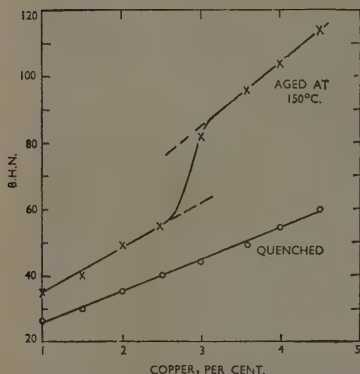


FIG. 11.—Quenched and Peak Hardness Values of Alloys Quenched in Boiling Water and Aged at 150° C., drawn from Fig. 3 of Hunsicker.<sup>5</sup>

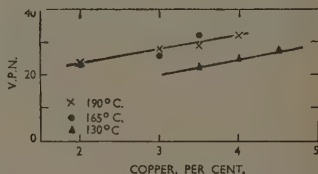


FIG. 12.—Increment between Quenched and Peak Hardness Values for Alloys Showing a Single-Stage Ageing Curve at 165° and 190° C. The increment between the hardness at the completion of the initial rise and the peak value is also shown for alloys aged at 130° C.

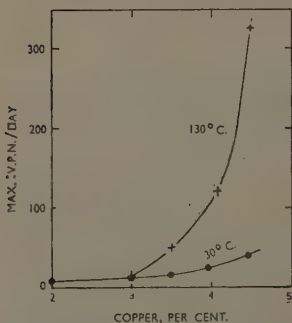


FIG. 13.—Maximum Rate of Hardening During the Initial Rise at 30° and 130° C. The values have been derived from the ageing curves and are only approximate.

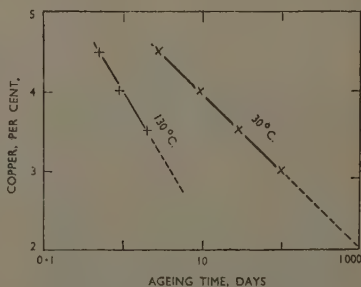


FIG. 14.—Time to the Completion of the Initial Rise for Alloys Aged at 30° and 130° C.

plotted against composition in Fig. 15. A linear relation existed between the logarithm of the time to peak hardness at 220° C. and the concentration. This also applied to alloys containing 2-4% copper aged at 190° C. The point for the aluminium-4.5% copper alloy aged at 190° C. fell to the right of this line. Similar effects were found at 165° C., where the points for the aluminium-4.5% copper alloy and, possibly, also the aluminium-4.0% copper alloy were displaced from the average line through the other points. The times to reach peak hardness at 130° C. were independent of concentration over the range 3-4.5% copper. Any real variation at this temperature would certainly be less than the experimental error in its determination. Comparison with Fig. 10 shows that the times to reach the peak hardness reflect the relationships between the peak hardness value and the concentration. The ageing times to the peak hardness tended to become independent of composition when the two-stage ageing curve was operative.

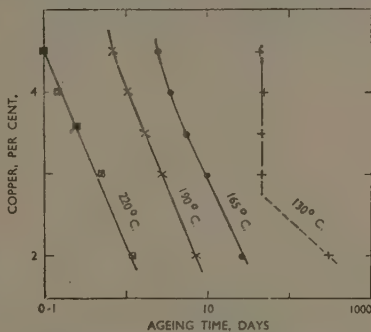


FIG. 15.—Time to Peak Hardness for Alloys Aged at 130°, 165°, 190°, and 220° C.

#### 4. Temperature/Time Relationships for the Aluminium-4.0% Copper Alloy.

Before discussing the present work it is necessary to study the results of Gayler and Parkhouse,<sup>6</sup> as they investigated the aluminium-4% copper alloy at numerous ageing temperatures. The results are given in Fig. 16, where the logarithm of the times to various parts of the ageing curves are plotted against the reciprocal of the absolute temperature. Gayler and Parkhouse found a smooth curve for the completion of the initial rise. The times taken to reach peak hardness fell on a straight line, although it may be noted that the point at 250° C. lay somewhat to one side and the point at 350° C. was also slightly to the other side of this line.

The incubation values and the second incubation values have been derived from the ageing curves of Gayler and Parkhouse and added to Fig. 16. The incubation values could only be assessed for ageing temperatures between 100° and 250° C. It was thought probable that



the values at low temperatures might be unduly influenced by quenching strains, while hardness measurements do not form a suitable means of following the changes at very high ageing temperatures. The curves for the incubation values between 100° and 250° C. show two branches which cross at approximately 172° C. Gayler and Parkhouse had found indications of a two-stage ageing curve at 190° C., which would imply

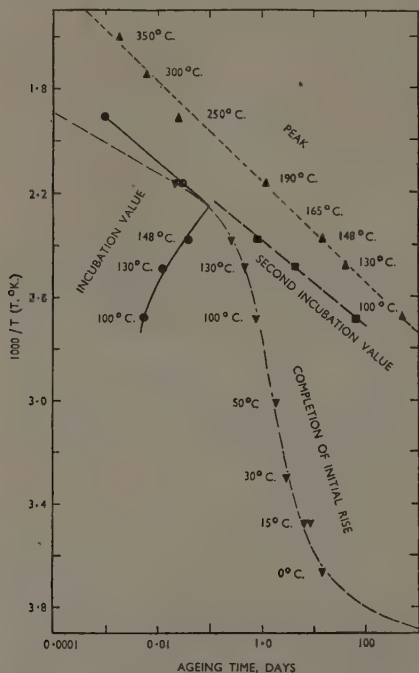


FIG. 16.—Temperature/Time Relationships for the Ageing Curves of an Aluminium-4% Copper Alloy. (Gayler and Parkhouse.<sup>6</sup>)

KEY.

- ▼ Completion of initial rise (due to Gayler and Parkhouse).
- ▲ Peak hardness (due to Gayler and Parkhouse).
- Incubation value (plotted from Gayler and Parkhouse).
- Second incubation value (plotted from Gayler and Parkhouse).

an inflected curve for the first incubation value between 148° and 190° C. However, this point at 190° C. has been neglected, since only a single-stage ageing curve was found in the present work.

The second incubation values could not be determined accurately, but the results fell on a straight line which was nearly an extrapolation of the incubation values at 190° and 250° C.

The results of the present work on the aluminium-4.0% copper alloy are given in Fig. 17. The line joining the points for the completion of the initial rise at 30° and 130° C. is parallel to the curve in Fig. 16,

but displaced to slightly longer times. The times to attain peak hardness at 130°, 165°, 190°, and 220° C. fall on or very close to the straight line chosen by Gayler and Parkhouse. The value at 240° C. lies to the left of this line, confirming the point obtained by these workers <sup>6</sup> at 250° C. This suggests that the time to attain peak hardness between 220° and 350° C. is better represented by the curved line shown in Fig. 17, which has been drawn with due regard to the experimental points at 250°, 300°, and 350° C. in Fig. 16. A branched curve was

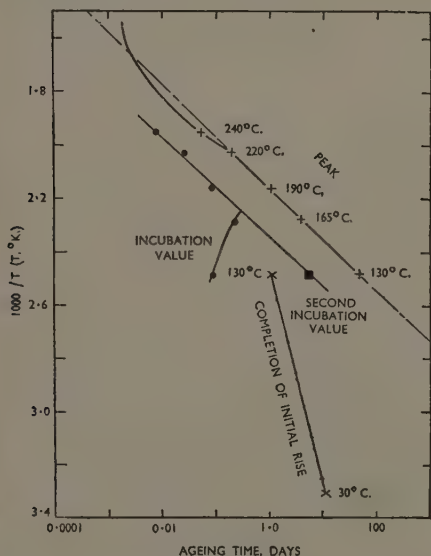


FIG. 17.—Temperature/Time Relationships for Ageing Curves of an Aluminium-4.0% Copper Alloy. (Hardy: present investigation.)

KEY.

- Incubation value.
- Second incubation value.
- x Completion of initial rise.
- + Peak hardness.

also obtained for the incubation values between 130° and 240° C. and has been drawn to intersect at 172° C., by analogy with Fig. 16.

##### 5. Temperature/Incubation-Value Relationships.

The incubation values have been plotted against the reciprocal of the absolute temperature in Fig. 18. The results for the aluminium-4.0% copper alloy indicate two branches with a junction point at 172° C. Comparison with Figs. 4 and 10 shows that the lower branch of the curve for the aluminium-4.0% copper alloy in Fig. 17 is in the temperature range associated with the two-stage ageing curve. The upper branch of the curve in Fig. 17 is in the temperature range of the

single-stage ageing curve. The junction point corresponds to a temperature at which the two types of ageing curve overlap, as may be judged from Fig. 10.

These relationships were used in drawing the curves for the other alloys in Fig. 18. It may be seen from Fig. 10 that the junction point between the single-stage and two-stage type of ageing curves is below 165° C. for the aluminium-3.5% copper and aluminium-3.0% copper alloys. Therefore, these alloys may not unreasonably be expected to possess the types of curves shown in Fig. 18. The junction point for the aluminium-4.5% copper alloy would be in excess of 165° C. accord-

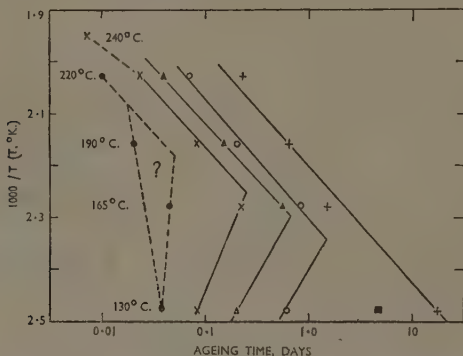


FIG. 18.—Temperature/Incubation Value Relationships.

KEY.

Incubation value: ● 4.5%; × 4.0%; ▲ 3.5%; ○ 3.0%; + 2.0% copper.  
Second incubation value: ■ (average of 4.5, 4.0, and 3.0% copper alloys).

ing to Fig. 10. However, the scatter of results prevents a clear choice of curve in Fig. 18.

The aluminium-2.0% copper alloy gave a single-stage ageing curve at all temperatures, and the incubation values have been represented by a straight line in Fig. 18.

It may be noted that the second incubation value at 130° C. lies very close to an extrapolation from the upper branch of the curve for the aluminium-3.5% copper alloy.

#### 6. Temperature/Time-to-Peak-Hardness Relationships.

It will be seen from the results in Fig. 19 that the straight-line relationship found by Gayler and Parkhouse<sup>6</sup> for the aluminium-4% copper alloy over the range 100°–190° C. did not apply to the other

alloys. The failure of this simple relationship arose from the common time to peak hardness at 130° C., and it is not unlikely that this would be repeated at 100° C. The times for the aluminium-4.5% copper and the aluminium-3.0% copper alloy deviated in opposite directions from the common point at 130° C., so that the linear relation found for the aluminium-4% copper alloy must be regarded as fortuitous.

The results on the aluminium-2.0% copper alloy fell on a straight line very nearly parallel to the straight-line part of the curve for the aluminium-4% copper alloy.

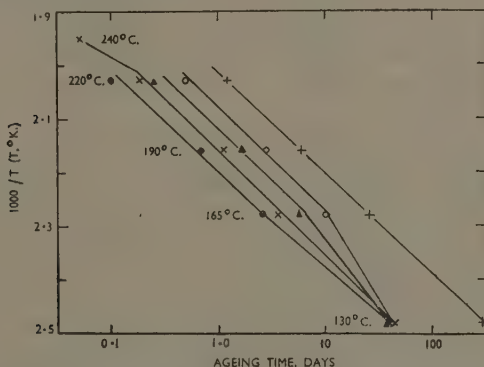


FIG. 19.—Temperature/Time-to-Peak-Hardness Relationships.

KEY.

Time to peak: ● 4.5%; × 4.0%; ▲ 3.5%; ○ 3.0%; + 2.0% copper.

## VI.—BASES OF A DESCRIPTIVE THEORY OF AGEING.

### 1. Thermodynamic Relationships.

The mode and rate of decomposition is determined by the free energy/compositional/structural relationships within the supersaturated solid solution and between the alloy phases. Methods of decomposition to be expected for alloys quenched to various parts of a hypothetical free energy/composition curve have been analysed in an earlier paper.<sup>18</sup> Very similar conclusions were reached independently by Laurent.<sup>19</sup> It was tacitly assumed<sup>18</sup> that an inflected free energy/composition curve \* for the solid solution could occur in alloy systems that also possessed intermetallic compounds. If the model of a "regular" solution † be adopted as an approximation to real metallic solutions, an

\* An inflected relationship shows both convex and concave regions.

† A regular solution is defined as possessing the entropy of an ideal solution.

inflected free energy/composition curve can be obtained only when the heat of solution is positive (Appendix I, p. 355). This implies that the two sorts of atoms will tend to keep apart and not form intermetallic compounds. Alloy systems that possess intermetallic compounds generally have a negative heat of solution which cannot, of itself, give rise to an inflected free energy/composition curve. Other factors, such as differences in atomic sizes, play a part in determining the nature of the free energy/composition curve, but are not amenable to a simple treatment. The first stage of decomposition in systems with an inflected free energy/composition curve is the formation of segregates.<sup>18</sup> This cannot apply when the free energy/composition curve is always convex to the composition axis, and Scheil<sup>20</sup> has suggested that ordering reactions provide the alternative mechanism for systems with a negative heat of solution.

The previous thermodynamic analysis applies directly to alloys with a positive heat of solution where segregates of the second component are formed within the matrix and are replaced during ageing by the more stable second solid solution, e.g. aluminium-zinc alloys.<sup>21-23</sup> The analysis also applies directly to alloys with a negative heat of solution that possess an inflected free energy/composition curve. The conception of a regular solution with a convex free energy/composition curve for alloys with a negative heat of solution, represents the more general case which has to be adopted because the more complicated models have not been worked out in detail (Appendix I). The previous thermodynamic analysis applies here provided that an alternative criterion is used, namely, that the source of the first decomposition product resides in order-disorder reactions. An account of the thermodynamic treatment leading to this model<sup>20</sup> is given in Appendix I.

Possible modes of decomposition for supersaturated solid solutions in a system with a negative heat of solution may be described in terms of Fig. 20. The free energy/composition curves of the solid solution, of the ordered phase, and of the precipitate are all convex to the  $x$  axis, so that  $\partial^2 F / \partial x^2$  is positive in each case. The free energy/degree-of-order curve may be convex or concave (as in Fig. 20) to the degree-of-order axis. Scheil,<sup>20</sup> to whom this model is due, regards the latter case as the more significant, but this refinement does not seem to be fully necessary. It is important to notice that the limit of the attainable degree of order varies with the composition. The atomic arrangement in the quenched alloy may show evidence of short-range order, but even if statistically uniform, it will contain a large number of small regions of higher concentration than the mean.<sup>24</sup> Regions of the alloy of composition such as  $x_7$  will be capable of undergoing ordering reactions

within the parent lattice with no appreciable change in concentration (Appendix I). The only activation energy required would be that for diffusion. There may be a tendency for this process to slow up when the degree of order reaches the point of inflection at  $s_7$  in Fig. 20 (b), but in any event full order cannot be attained by this composition. Such regions will be termed partially ordered aggregates. The concentration of the matrix in metastable equilibrium with these regions will

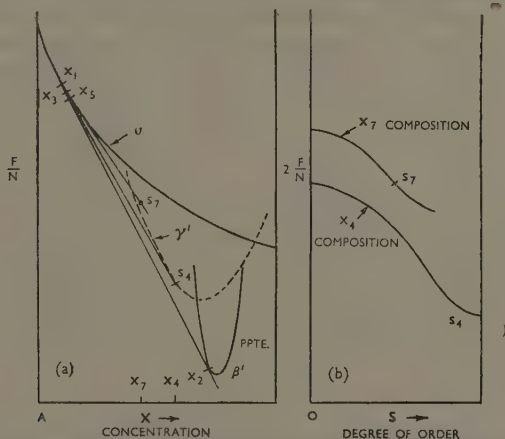


FIG. 20.—Free Energy/Compositional/Structural Relationships for Precipitation in a Hypothetical System with a Negative Heat of Solution. (See Appendix I, p. 355.)

$\alpha$  is the free energy/composition curve for the solid solution.

$\gamma'$  " " " " for an ordered solid solution.

$\beta'$  " " " " for an intermediate precipitation.

be given, for example, by the tangent from  $s_7$  in Fig. 20 (a) to the free-energy curve of the solid solution, i.e. at  $x_5$ .

Alloys of somewhat lower concentration could also form partially ordered aggregates, but an additional activation energy would be required to promote the initial segregation.<sup>18</sup> The partially ordered aggregates would grow by downhill diffusion until the matrix had tended to the appropriate composition (e.g. such as  $x_5$  in Fig. 20 (a)). The final partially ordered aggregates may be expected to show a fairly wide range of composition and degree of order. (Appendix I).

The partially ordered aggregates may be capable of transforming to fully ordered regions when a critical size has been reached,<sup>18</sup> provided that the process is structurally continuous and that they have attained





segregates.<sup>18, 23</sup> The first decomposition products have essentially similar thermodynamic properties in both the models for the systems with either a negative or positive heat of solution.

It is very tempting to make the curves of the solid solution and of the ordered phase in Fig. 20 continuous by an inflected region. This would be completely intuitive, since no formal model predicts this shape, although it is not theoretically impossible (see Appendix I). In this case the first decomposition product would show both segregation and partial ordering. The segregation would probably not go beyond the second inflection point (such as  $x_7$  in Fig. 21).

Although the exact free energy/compositional/structural relationships cannot be deduced explicitly, it is possible to hope that the results of the present thermodynamic analysis may be applicable to the ageing of aluminium-copper alloys. It seems very reasonable to include ordering reactions as a source of ageing phenomena in alloys with a negative heat of solution. It is clear from Raynor's survey<sup>25</sup> of electron compounds that frequently no sharp distinction can be made between a solid solution with long-range order and an intermetallic compound with metallic bonding. Many of the stable<sup>26</sup> and metastable<sup>27</sup> intermediate phases in the copper-aluminium system probably show superlattice formation, although atomic-size relationships may also be important, as in the case of  $\text{CuAl}_2$ .<sup>25</sup>

## 2. Reciprocal-Rate Curves.

The probabilities of the formation of a partially ordered aggregate and of a fully ordered region (or precipitate) are, respectively, proportional to :

$$e^{-(Q+W)/RT} \text{ and } e^{-(Q+A)/RT}$$

where  $Q$  is the activation energy for diffusion,  $W$  is the activation energy for segregation to initiate a partially ordered aggregate,  $A$  is the activation energy for the nucleation of a fully ordered region,  $R$  is the gas constant, and  $T$  is the absolute temperature.<sup>18</sup>  $W$  will go from zero to infinity as the supersaturation is reduced.  $A$  will probably go from a finite value (due to interfacial-energy terms) to infinity as the supersaturation is reduced.

Thus, the time for the formation of a partially ordered aggregate may be written :

$$t_1 = C_1 e^{(Q+W)/RT} \quad . \quad . \quad . \quad . \quad . \quad (1)$$

and for the formation of a fully ordered region :

$$t_2 = C_2 e^{(Q+A)/RT} \quad . \quad . \quad . \quad . \quad . \quad (2)$$

where  $C_1$  and  $C_2$  are constants.

The initial decomposition will be by the process with the higher probability. The logarithm of the measured time to the beginning of decomposition by the formation of partially ordered aggregates will give a straight line of slope  $Q/R$  when plotted against  $1/T$ , as long as  $W$  is very small compared with  $Q$ . The curve will deviate from a straight line as  $W$  increases, owing to the decrease of supersaturation at higher ageing temperatures. This is shown in Fig. 22, and a point will be reached at which the probabilities of decomposition by both methods will be equal, i.e.  $t_1 = t_2$ . A break is to be expected in the direction of the reciprocal-rate curve when the higher ageing temperature, and consequently lower supersaturation, favours the second mode of decomposition.<sup>18</sup> An excellent example of this type of effect is given by the bainite reaction in alloy steels.<sup>28, 29</sup>

### 3. Structural Changes.

Knowledge of the structural changes in aluminium-copper alloys after relatively short ageing times is due entirely to the single-crystal work of Guinier<sup>9, 10</sup> and of Preston,<sup>11, 12</sup> to which reference has already

been made. The initial decomposition product has been termed G.P. zones [1]<sup>8</sup> and consists of copper-rich planes parallel to the (100) plane of the matrix. This is shown diagrammatically in Fig. 23 (a).

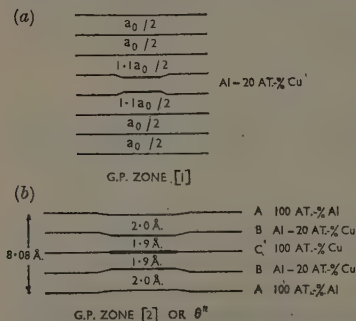


FIG. 23.—The Structure of G.P. Zones [1] and [2]. The sequence of planes *ABCB* is repeated through the thickness of the zone. (After Guinier.)

of a superlattice, and Guinier uses the term "surstructure" to denote this decomposition product.<sup>13</sup> More recently, Guinier<sup>15</sup> has prepared specimens containing G.P. zones [2] of a large size and has been able to measure their lattice spacing (Fig. 23 (b)). Guinier's work, whereby the G.P. zones [2] (or  $\theta''$  as he now terms the product) were detected, was largely confined to the aluminium-5.22% copper alloy,

The formation of the G.P. zones [2] marks a further stage in the ageing process. These regions are also copper-rich, but possess a preferred arrangement of copper and aluminium atoms (Fig. 23 (b)). The lattice-diffraction effects associated with these zones are very similar to those

the term "surstructure" to denote this decomposition product.<sup>13</sup> More recently, Guinier<sup>15</sup> has prepared specimens containing G.P. zones [2] of a large size and has been able to measure their lattice spacing (Fig. 23 (b)). Guinier's work, whereby the G.P. zones [2] (or  $\theta''$  as he now terms the product) were detected, was largely confined to the aluminium-5.22% copper alloy,

so that it is not possible to make a direct comparison with the present results. Guinier's ageing times and temperatures were rather scattered, but it appears that the G.P. zones [1] are replaced by the G.P. zones [2] over the range of ageing temperatures in which his alloy may be expected to show the two-stage ageing curve. G.P. zones [1] were not observed at high ageing temperatures, but it was not clear whether the G.P. zones [2] were formed directly from the matrix. The first-formed precipitate at higher ageing temperatures was  $\theta'$ , whilst  $\theta$  was also formed directly from the matrix at still higher temperatures.

The details of the changes up to the peak hardness at low ageing temperatures are submicroscopic. However, Gayler<sup>7</sup> has confirmed that the precipitate up to peak hardness at 130° C. is a copper-rich region other than  $\theta'$  or  $\theta$ . This precipitate was associated with a "light phenomenon"<sup>6,7</sup> which Gayler thought to be a recrystallized region of equilibrium concentration.

#### 4. Factors Requiring Explanation.

A quantitative theory of the ageing processes in aluminium-copper alloys is not yet possible, but any complete descriptive theory must be capable of accounting for the following factors which arose in the analysis of the experimental results (Section V):

(1) The two branches of the curve relating temperature and incubation values (Figs. 16, 17, and 18).

(2) The rapid rise in the rate of hardening with increasing supersaturation (Fig. 13).

(3) The dependence on the ageing temperature of the hardness at the completion of the initial rise, i.e. the higher hardness on ageing at 130° C. compared with 30° C. (Fig. 9).

(4) The differentiation between the single-stage and two-stage types of ageing curves (Figs. 4-8).

(5) The temperature and concentration dependence of the change from the two-stage to the single-stage type of ageing curve (Figs. 10 and 18).

(6) The increased peak-hardness value observed when the two-stage ageing curve is operative (Fig. 10).

(7) The relative independence of the second incubation value from variation with composition (Fig. 4).

(8) The constant time to peak hardness over a wide range of composition with the two-stage ageing curves (Figs. 4, 15, and 16).

## VII.—DESCRIPTIVE THEORY OF AGEING FOR ALUMINIUM-COPPER ALLOYS.

It is not yet possible to determine experimentally the free energy/compositional/structural relationships. However, the correlation between the effects observed experimentally and the mode of decomposition derived analytically is very encouraging. The hypothesis will be adopted that the system possesses free-energy relationships with properties essentially similar to those proposed in Section VI. The ageing of aluminium-copper alloys will therefore be described in terms of the thermodynamic model. It must be remembered that the ageing curves have been obtained by hardness measurement on the surface of the specimens and will be influenced by the quenching strains.

The first stages of the ageing process are viewed as ordering reactions. The G.P. zones [1] then correspond to the partially ordered aggregates and the G.P. zones [2] are taken to be the fully ordered regions. It has already been noted that the structure of the latter is very similar to that of a superlattice. The structure of the intermediate precipitate,  $\theta'$ , is viewed as showing evidence of the relative sizes of the atoms, which is more clearly demonstrated by the equilibrium precipitate  $\theta$ .

It is unnecessary to assume that full structural continuity exists between the different decomposition products. It is known that  $\theta$  can be formed from  $\theta'$ , but experimental evidence is lacking as to whether an individual G.P. zone [1]  $\rightarrow$  G.P. zone [2]  $\rightarrow \theta'$ . The possibility that these form from one another by allotropic changes is not ruled out, but it is implicit in the theoretical argument that each of the decomposition products is capable of being formed directly from the matrix.

*1. The Initial Rise.*

It is generally accepted that the initial rise is associated with the formation of G.P. zones [1]. When the degree of supersaturation is very high, this will occur by internal rearrangements of groups of atoms of suitable compositions to form partially ordered aggregates. No true incubation period is to be expected for partially ordered aggregates formed from fluctuations existing after quenching. This may well apply to alloys of high copper content aged at 30° C., although the quenching strains will have a considerable influence on this process.

There will be a smaller number of fluctuations in the quenched alloy of suitable composition for ordering at 130° C. than at 30° C. The majority of the G.P. zones [1] probably require an initial activation energy for their formation, since the degree of supersaturation will be

somewhat lower than at 30° C. It may be noted that the incubation values at 130° C. lengthen with decreasing supersaturation. Once the G.P. zones [1] have been formed, their further growth will occur by normal downhill diffusion. These effects would be expected to give rise to a smaller number of larger aggregates than in the case examined in the previous paragraph. It is known from Guinier's work that the size of the G.P. zone [1] increases with increasing ageing temperature and this fact could easily account for the hardness values obtained at the completion of the initial rise at 130° C. being higher than those at 30° C. (Fig. 9). A greater rate of ageing follows automatically from a higher degree of supersaturation (Fig. 13).

The equation of the family of straight lines for the initial rise at 130° C. is (Appendix II, p. 359) :

$$\frac{H - H_v}{H_f - H_v} = m \ln t - m \ln t_v \quad . \quad . \quad . \quad (3)$$

where  $H$  is the hardness at time  $t$ ,  $H_v$  is the hardness at the time of the incubation value  $t_v$ ,  $H_f$  is the hardness at the completion of the initial rise, and  $m^{-1} = \ln t_f/t_v$ . The value of  $m$  was found to be independent of concentration over the range 3.5–4.5% copper. The value of  $m$  will vary with temperature, but it is not possible to account for its constancy with change in concentration. This, together with the equality of the slope of the straight lines, was taken to indicate that the same process was occurring in each alloy.

There is apparently no physical model that predicts a straight-line relationship between the fraction transformed and the logarithm of the time (equation (3)). The model usually taken leads to :

$$\ln \ln \frac{H_f - H_v}{H_f - H} = p \ln t - p \ln \tau \quad . \quad . \quad . \quad (4)$$

where  $p$  is a constant and  $\tau$  is a time constant. This gives the inflected curve for the initial rise in Fig. 24, which falls within the limits of the experimental error. Details of the calculations and the physical significance of  $p$  are given in Appendix II. The experimental value of  $p$  is 1.5,\* which corresponds theoretically to the formation of spheres. The G.P. zones [1] take the form of platelets for which  $p$  should be 2.5, provided that their radius can be set proportional to the time of growth as opposed to the square root of this value which applies to their thickness and also to the radius of spherical particles.<sup>30, 31</sup> The conditions at the edge of a growing platelet are not easily defined and the growth law may differ from those of the interstitial alloys studied by Wert.<sup>31</sup>

The thickness of the G.P. zone [1] at the completion of the initial rise has been calculated using a formula due to Zener<sup>30</sup> (Appendix II),

\* See note on p. 354.



with an appropriate value for the diffusion coefficient (Appendix III, p. 363). This gives a thickness of 8 Å. at the completion of the initial rise and is substantially independent of concentration over the range 3.5–4.5% copper.

It will be shown later that in view of the temperature range there is, surprisingly, very little difference between the diffusion coefficients at 30° and 130° C., calculated from the sizes of the G.P. zones [1]. It is apparent from Fig. 14 that the rates of reaction have a different concentration dependence at the two ageing temperatures. These effects may arise because the quenching strains have a larger influence on the ageing process at the lower temperature.

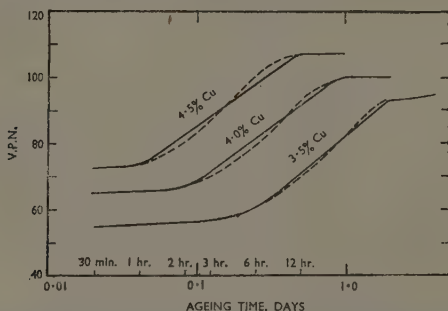


FIG. 24.—The Initial Rise for Alloys Aged at 130° C. (from Fig. 4). The infected curves (dashed) are for the calculated course of the reaction, assuming the normal model for a phase transformation in solids. (See Appendix II, p. 360.)

## 2. Single-Stage Ageing Curves.

The single-stage ageing curve at higher temperatures and correspondingly lower degrees of supersaturation is believed to be due to the formation of the G.P. zones [2] (fully ordered regions) directly from the matrix by a process of nucleation and growth. This does not preclude the formation of a small proportion of G.P. zones [1] at the lower ageing temperatures, but this is not the dominant process.

The present work does not allow a distinction to be made between ageing effects due to the G.P. zones [2] and those arising from  $\theta'$  when it replaces the former metastable phase.  $\theta'$  will be the initial decomposition product at sufficiently low degrees of supersaturation.

## 3. Reciprocal-Rate Curves for the Incubation Values.

The distinction between the initial decomposition by the formation of G.P. zones [1] and by the formation of G.P. zones [2] accounts for

the two branches on the reciprocal-rate curves relating the temperature and incubation values (Figs. 16, 17, and 18). The lower branch represents the formation of the initial G.P. zones [1] under conditions of a fairly high activation energy. The upper branch represents the formation of G.P. zones [2] directly from the matrix, in a temperature range where their probability of formation is greater than that of the G.P. zones [1] (equations (1) and (2), p. 343). The lowering of the tem-

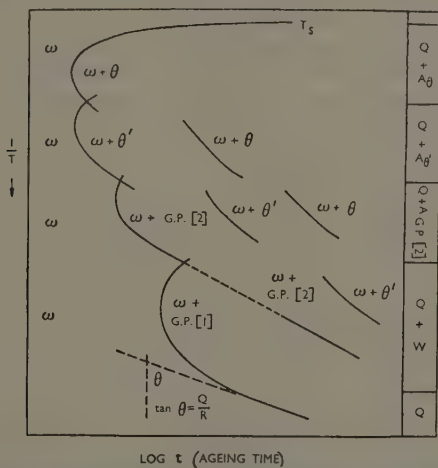


FIG. 25.—Diagrammatic Representation of the Ageing Process/Time Relationships for an Aluminium-Copper Alloy Quenched and Aged at Different Temperatures.  $\omega$  represents the solid solution at all degrees of saturation, the final product is  $\omega + \theta$  ( $\text{CuAl}_2$ ). The right-hand column gives the activation energies for the initial decomposition product.  $Q$  is the activation energy for diffusion,  $W$  is the activation energy for segregation needed to form the partially ordered aggregates, and  $A_\theta$ , &c., is the activation energy for a stable nucleus of the new phase.<sup>18</sup>

perature of the intersection point between the two branches with decreasing supersaturation is readily explained by a shift within the free energy/compositional/structural relationships.

Similar effects may occur when  $\theta'$ , and subsequently  $\theta$ , become the initial stages in the decomposition. The ageing processes consequent on this view are shown diagrammatically in Fig. 25, in which the initial stages have been represented as a series of interpenetrating C-curves. It is difficult to detect the separate curves experimentally when they run into one another at a very obtuse angle. This accounts for the inability to distinguish the C-curves for the G.P. zones [2] from those for  $\theta'$  in

the present work. The results on the aluminium-2% copper alloy could possibly be represented as C-curves in place of the straight line in Fig. 18.

Only the initial rise will be completed at temperatures well below the intersection point of the two branches in the curves for the temperature/incubation value relationships (Figs. 16, 17, and 18). The alloy will then remain permanently in a metastable condition. At temperatures close to the intersection point both modes of decomposition will occur simultaneously. The aluminium-4% copper alloy aged at 165° C. and the aluminium-3% copper alloy aged at 130° C. are examples of the type of ageing curves obtained under conditions where both processes are occurring together. The small initial rise at temperatures higher than the intersection point, as in the aluminium-3.5% copper alloy at 165° C. and in the aluminium-4% copper alloy of Gayler and Parkhouse <sup>6</sup> at 190° C., are only just outside the limits of the experimental accuracy. These may represent cases where the compositional fluctuations in the quenched alloy are unusually large, so that some G.P. zones [1] are formed.

#### 4. *Two-Stage Ageing Curves.*

The initial rise at temperatures such as 130° C. is followed by a flat portion of relatively constant hardness which precedes a second rise to the peak hardness. The structure on the flat portion of the ageing curve is visualized as consisting of G.P. zones [1] in a matrix of solid solution of metastable equilibrium concentration. This concentration will be approximately the same for all alloy compositions, but their G.P. zones [1] may or may not differ in number and in size. The higher peak hardness with the two-stage ageing (Fig. 10) is believed to be due to the simultaneous presence of G.P. zones [1] and G.P. zones [2]. This may be expected to occur in one or all of the following ways:

(1) The transfer from G.P. zone [1] to G.P. zone [2] takes place by an allotropic change when a critical size <sup>18</sup> and composition have been reached.

(2) The G.P. zones [2] are nucleated directly from the matrix, as occurs at higher ageing temperatures, but between the G.P. zones [1] already present.

(3) The G.P. zones [2] are nucleated by recrystallization due to lattice strains around the largest G.P. zones [1].

The first process requires that the composition of the G.P. zones [1] shall be easily adjustable to that of the G.P. zones [2]. This would probably be unlikely on the thermodynamic model adopted, although the composition of the G.P. zones [1] may change as they grow in size

by downhill diffusion. This process could only predict a constant incubation value for the rise to peak hardness and a constant time to peak hardness (Figs. 4 and 15) if the important dimensions of the G.P. zones [1] were of the same size in alloys of different compositions. This requirement may be met (Appendix II) in relation to the thickness at the completion of the initial rise. The first process would also require that the coherent lattice strain associated with a new G.P. zone [2] should be greater than that of the G.P. zone [1] from which it had been formed. In assessing this, allowance would have to be made for the subsequent rapid growth of the new G.P. zone [2] due to an associated reduction in the metastable equilibrium concentration of the matrix.

Alloys of higher copper content would be expected to contain a greater number of G.P. zones [1], from which a greater number of G.P. zones [2] would be formed. This could explain the concentration dependence of the hardness increment during the rise to peak hardness at 130° C. (Fig. 12). The flat on the ageing curve would represent the time for the G.P. zones [1] to increase to the critical size<sup>8</sup> in the important dimensions, and also to attain the correct composition. A major difficulty in accepting the first process is to explain why this should take longer in alloys of higher copper content, which have the longer flat portion, and why the hardness remains constant during this period.

The second process predicts directly that the second incubation value and the time to reach peak hardness should be substantially independent of composition, as required by Figs. 4 and 15. This follows because the matrix in which the G.P. zones [2] are forming is of approximately the same composition in all alloys. The flat on the ageing curve represents part of the incubation period, thus accounting for its constant hardness. It may be noted that the second incubation value lies very close to an extrapolation of the upper branches of the temperature/incubation value relationships (Figs. 16, 17, and 18).

The third process would predict a constant second incubation value and a constant time to peak hardness only if the recrystallization occurred after a constant time in all alloys. As with the first process, it is difficult to see why this should be independent of composition and also why the extra lattice strain around the G.P. zones [2], which is necessary to account for the higher hardness, does not cause further recrystallization. Some softening might be expected during the period occupied by the flat portion of the curve. An experimental observation which also militates against this process is that a single crystal of an aluminium-4% copper alloy aged for 70 days at 130° C. remained a single crystal when re-solution heat-treated.

The present experimental work does not allow a clear choice to be made between these alternatives and all processes may take place simultaneously. Forms of two-stage ageing curves also occur in Duralumin,<sup>32</sup> aluminium-zinc alloys,<sup>22, 33</sup> and aluminium-silver alloys.<sup>34</sup> The two latter systems are known to show pre-precipitation effects.<sup>13, 21</sup> It would be of considerable interest to investigate the concentration dependence of the time to reach peak hardness for two-stage ageing curves in systems other than aluminium-copper.

### 5. *Peak Hardness.*

The hardness is not an absolute property of the alloy and is a function both of the hardening due to coherent lattice strains and the softening due to depletion of solute.<sup>8</sup> Peak hardness corresponds to the maximum effective lattice strain and is followed by softening. This may be aided by the formation of a new decomposition product, such as  $\theta'$ , which may be only partially coherent with the matrix,<sup>8</sup> and thus help to relieve the lattice strain, although particle-size effects also play an important part.

### 6. *Re-Solution Effects.*

Irrespective of the manner in which the G.P. zones [2] arise on ageing at 130° C., the remaining G.P. zones [1] will be forced to re-dissolve in an effort to maintain the matrix composition at the value required for their stability.<sup>18</sup> Consider, for example, an alloy aged to contain partially ordered aggregates of free energy ( $s_7$  in Fig 20) in which a fully ordered region of free energy,  $s_4$ , is formed. The metastable matrix concentration is  $x_5$  in the first case and  $x_3$  in the latter. Downhill diffusion towards the fully ordered region will lower the matrix concentration from  $x_5$  towards  $x_3$ . Any partially ordered aggregates which happen to lie within the volume affected will no longer be in contact with a matrix of composition  $x_5$  and will thus be forced to re-dissolve. Similar effects are to be expected whenever a more stable decomposition product is formed amongst particles in metastable equilibrium with the matrix.

The re-solution of the G.P. zones [1] around the G.P. zones [2] may well be the explanation of Gayler's "light phenomenon".<sup>6, 7</sup> The etching behaviour would be changed from a dark-etching region containing G.P. zones [1] to a light-etching solid solution of lower concentration containing a few large particles of the G.P. zones [2]. Perryman and Blade<sup>22</sup> have recently shown the light phenomenon to exist in aluminium-zinc alloys. The first stage in the decomposition of these alloys is believed to be the formation of spherical clusters of zinc atoms,<sup>21</sup>

which is most probably a segregation process<sup>18</sup> (Appendix I). Their re-resolution on the formation of the next more stable phase would also be expected to lead to a "light phenomenon".<sup>23</sup>

Re-resolution effects may also occur when an intermediate precipitate transfers to a more stable form. If one of the ageing processes produced sufficient lattice strain to lead to fragmentation and recrystallization of the matrix, this would provide an excellent opportunity for the formation of the next more stable phase. These two factors may be used to explain the observation of Geisler, Barrett, and Mehl<sup>35</sup> that the transfer from  $\gamma'$  to  $\gamma$  in an aluminium-20% silver alloy was accompanied by recrystallization with no simple orientation relation between the precipitates (see Fig. 2 of ref. 8).

It has been suggested earlier<sup>8</sup> that whether the lattice strain is sufficiently great to cause recrystallization accounts for the metallographic difference between continuous and discontinuous precipitation. Discontinuous precipitation with the co-existence of old and new solid solutions, as shown in the Debye-Scherrer pattern, may also occur in the absence of recrystallization. It is probable that the re-resolution of a less stable product tends to hold constant the lattice parameter of the old solid solution. Only a small proportion of the matrix will have parameters between this value and that of the new solid solution around the particles of the next more stable precipitate.

The present experimental work does not enable any deductions to be drawn as to whether the ageing process in aluminium-copper alloys is continuous or discontinuous. Neither is it known experimentally whether relief of strain or recrystallization effects play any part in the ageing processes. The "light phenomenon" is certainly associated with movement of grain boundaries.<sup>6, 7, 22</sup> It is not known whether its intracrystalline existence is also to be associated with recrystallization as well as with re-resolution but, as described above, this seems unlikely.

Well-marked reversion effects are known to occur in aluminium-copper alloys. A metastable decomposition product formed on ageing at one temperature may be unstable when the alloy is raised to a suitable higher temperature. The effects obtained will depend partly on the scale of the alloy structure and reversion to a greater or lesser extent will also occur with somewhat coarser structures.<sup>36</sup>

### 7. Diffusion Coefficient and Activation Energy.

It is of interest to calculate the diffusion coefficient for the formation of the G.P. zones [1] from the sizes assigned to them by Guinier.<sup>10, 37</sup> This has been done in Appendix III (p. 363), and gives a value, appropriate to 30° C., of approximately  $10^{-13}$  cm.<sup>2</sup>/day, whereas the value



obtained by extrapolation from measurements at high temperatures is  $10^{-20}$  cm.<sup>2</sup>/day.<sup>38</sup> Very similar results have been reported by Jagodzinski and Laves,<sup>39</sup> who pointed out that no ageing would occur if the extrapolated value applied. The discrepancy at 150° C. is smaller, the calculated value being  $10^{-11}$  cm.<sup>2</sup>/day and the extrapolated value  $10^{-13}$  cm.<sup>2</sup>/day (Table III, Appendix III). The temperature dependence of the values calculated from the G.P. zones is remarkably small.

The activation energy calculated from the straight-line relationship between the time to reach peak hardness and the reciprocal of the absolute temperature <sup>6</sup> (Fig. 16) is 24,000 cal./g.-atom.<sup>40</sup> This is less than the experimentally measured activation energy for diffusion at high temperatures, which may be taken as 34,000 cal./g.-atom.<sup>38</sup> Jetter and Mehl<sup>41</sup> regard this type of difference as common to most ageing systems. In Appendix IV (p. 364) the conditions are examined under which the activation energy deduced from the reciprocal-rate curves could be less than the activation energy for diffusion. This is theoretically possible, but would lengthen the time required for the reaction. The calculated diffusion coefficients are, however, several orders of magnitude lower than that obtained by extrapolation, and this militates against any hypothesis which lengthens the reaction time. It seems more likely that the activation energy for diffusion at low temperatures is actually lower than that measured at high temperatures. This would require a change in the mode of atomic interchange, and it is possible that dislocations play a larger part as the temperature is decreased. Nevertheless the activation energy derived from the reciprocal-rate curve may still be less than that for diffusion at the same temperature.

*Note Added in Proof.*

Hardness and dilatation curves for an aluminium-4% copper alloy aged at different temperatures have recently been published by Lankes and Wassermann.<sup>73</sup> Their results showed that the initial rise in hardness was associated with a contraction. This also occurred, although more slowly, when the alloy had been given a reversion treatment which would have relieved the quenching stresses. The single-stage ageing curves were associated with an expansion. The change from contraction to expansion at intermediate ageing temperatures commenced during the second rise in hardness. The results confirm the deduction in the present work that a distinction can be drawn between the G.P. zones [1] and [2].

The inflected expansion curve at 200° C. has been analysed according to equations (4) and (11) and gave a straight line of slope  $p = 1.5$  over

the range 10-90% transformation. The G.P. zones [2] evidently obey the same growth law as the G.P. zones [1] which had the same value of  $p$  (see Section VII and Appendix II).

## APPENDIX I.

### FREE ENERGY/COMPOSITIONAL/STRUCTURAL RELATIONSHIPS.

The free-energy change due to the formation of one mole of solution from the pure components is given by :

$$\Delta F = \Delta H - T\Delta S \quad . \quad . \quad . \quad . \quad . \quad (5)$$

where  $\Delta H$  is the change in heat content and  $\Delta S$  is the change in entropy. By applying the conceptions of "regular" solutions,<sup>42, 43</sup> this may be written :

$$\Delta F = Vx(1 - x) + RT[x \ln x + (1 - x) \ln (1 - x)] \quad . \quad . \quad (6)$$

where  $V$  is the integral molar heat of solution,  $x$  the atomic fraction,  $R$  the gas constant, and  $T$  the absolute temperature.

By considering the internal energy as a function solely of the interaction energies of nearest neighbours in the atomic assembly,<sup>44</sup> it is readily shown that :<sup>45</sup>

$$V = zNv \quad . \quad . \quad . \quad . \quad . \quad . \quad (7)$$

where  $z$  is the co-ordination number,  $N$  Avogadro's number, and  $v = v_{AB} - \frac{1}{2}(v_{AA} + v_{BB})$ ; where  $v_{AA}$ , &c., are the interaction energies between pairs of neighbouring atoms;  $v$ , and hence  $V$ , may be either positive, zero, or negative.

If  $v$ , and hence  $V$ , be positive, the interaction energy between unlike atoms is greater than that between like atoms. An inflected free energy/composition curve results (Fig. 26 (a)) and leads to an immiscibility gap between two terminal solid solutions.

If  $v$  be zero, equation (6) reduces to that for an ideal solution in which the free-energy change is completely defined by the change in the positional entropy ( $\Delta S$  in Figs. 26 (a) and (b)).

The free energy/composition curve is always convex to the composition axis when  $v$  is negative (Fig. 26 (b)). This in itself would give rise to an uninterrupted series of solid solutions, but these may be replaced by the formation of intermetallic compounds.

Unfortunately this treatment represents an over-simplification, since the simple theory of regular solutions applies only when the atoms do not differ greatly in size. Differences in atomic diameter are well known to limit the extent of solid-solubility formation<sup>46</sup> and can lead to an immiscibility gap even when the heat of solution is zero.<sup>47</sup> They also have an important influence on the thermodynamic properties of liquid

solutions.<sup>48</sup> The simple theory of regular solutions also neglects volume changes and additional terms for the vibrational entropy of solutions.<sup>48, 49</sup> These factors cannot easily be allowed for and it is preferable to use the regular-solution hypothesis, though bearing in mind the limitations which arise from the original assumptions.

The regular-solution hypothesis has been adopted in the following discussion, as more rigorous treatments are not available for the present problem. Possible free energy/compositional/structural relationships of real solutions, which cannot be treated on this basis, are mentioned in the last paragraph of this Appendix.

In the previous thermodynamic treatment<sup>18</sup> of a hypothetical system it was tacitly assumed that an inflected free energy/composition

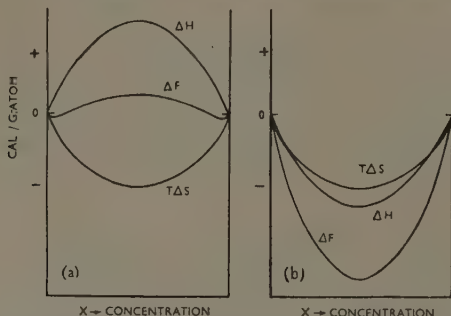


FIG. 26.—Free Energy/Composition Curves for the Formation of Solution with (a) a Positive and (b) a Negative Heat of Solution, for the case where the integral molar heat of solution  $V = 3.5 RT$ .  $T\Delta S$  should strictly be  $-T\Delta S$ .

curve existed together with an intermetallic compound. An examination of the collected data,<sup>50, 51</sup> mostly on liquid systems, showed that a positive heat of solution\* was associated with alloys possessing terminal solid solutions but no intermetallic compounds. Systems with a negative heat of solution in the liquid state generally possessed intermetallic compounds in the solid state. This is, of course, in agreement with the view that like atoms tend to segregate together in systems with a positive value of  $v$ , while unlike atoms segregate together when  $v$  is negative.

Thus, the presence of intermetallic compounds is strong, but not necessarily conclusive, evidence<sup>54</sup> that a given system has a negative heat of solution. Nevertheless, it may be generally accepted that an inflected free energy/composition curve resulting from a positive heat

\* A thermodynamically positive heat of solution is negative in thermochemistry.

of solution is only obtained in systems with terminal solid solutions and no intermetallic compounds. This would apply to aluminium-zinc alloys,<sup>23, 52</sup> but not to aluminium-copper alloys, which have a negative heat of solution.<sup>53, 55</sup> Aluminium-zinc alloys would be expected to undergo segregation of like atoms as the first stage in the decomposition of a highly supersaturated solid solution,<sup>21, 23</sup> but this would not apply to aluminium-copper alloys.

This difficulty has been pointed out by Scheil,<sup>20</sup> who put forward an important alternative hypothesis, which accounts for the single-phase decomposition of alloys with a negative heat of solution by an ordering reaction.

Several attempts have been made to calculate phase diagrams applicable to systems (notably gold-copper) showing order-disorder reactions. Both Easthope<sup>56, 57</sup> and Shockley<sup>58</sup> have found that a narrow two-phase ordered and disordered region could exist at very low concentrations, provided that the temperature was sufficiently low. Cowley's treatment<sup>59</sup> differed considerably, but also predicts a narrow two-phase region extending to low concentrations.

Scheil considered the *AB* type of ordering and set up an equation

for the potential energy as a function of the concentrations of the incorrectly ordered *A* and incorrectly ordered *B* atoms. He deduced that the potential-energy surface was saddle-shaped and calculated the projection on the base plane of the boundary between the hyperbolic and elliptical regions (this corresponds to the locus of the points of inflection). These calculations have been repeated and the results are shown in Fig. 27. The extent of the hyperbolic region increases as the temperature is lowered. Sections through the free-energy surface have been calculated and are shown in Fig. 28. Sections parallel to the composition axis are always convex towards the basal plane, while sections perpendicular to the composition axis show a slightly inflected curve, with the point of inflection at the limit of the hyperbolic region. These relations have been confirmed mathematically.<sup>60</sup>

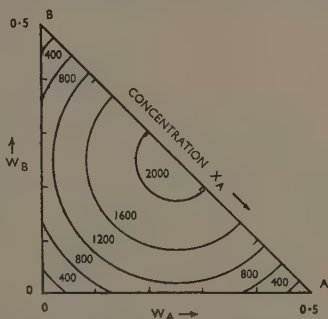


FIG. 27.—The Locus of Points of Inflection on the Free Energy Compositional/Degree of Order Surface of Scheil's<sup>20</sup> Model for a system showing the *AB* type of ordering.  $W_A$  and  $W_B$  are the fractions of wrongly ordered *A* and *B* atoms, respectively, and the hypotenuse of the triangle is the composition axis. The numbers are values of  $RT$ .

An inflected free energy/degree-of-order curve, not very dissimilar from that in Fig. 28, was also given by one of the models examined by Bragg and Williams.<sup>61</sup> Scheil chose his energy constants in such a way that an inflected curve was obtained. In his view the first stage in the decomposition of a supersaturated solid solution would be by the ordering of groups of atoms in the region where the free energy/degree-of-order curve is concave and up to the limits of the hyperbolic region.

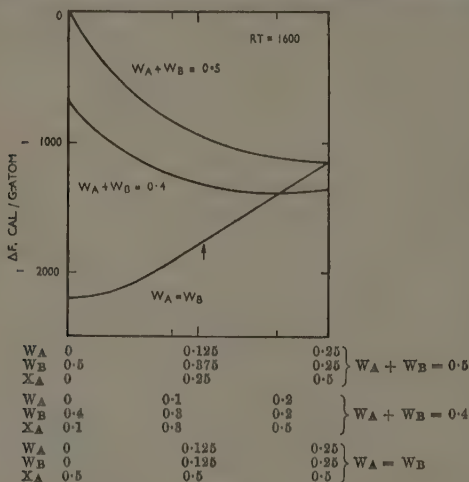


FIG. 28.

FIG. 28.—Sections through the Free Energy/Compositional/Degree-of-Order Surface Erected on the Triangular Base of Fig. 27.  $W_A$  and  $W_B$  are the fractions of wrongly ordered  $A$  and  $B$  atoms, respectively.  $X_A$  is the concentration of  $A$  atoms.

However, it seems unnecessary to draw a distinction between convex and concave parts of the free energy/degree-of-order curve such as must be made in the case of the free energy/composition curve. More significance is given in the present paper to the fact that a limited degree of ordering may occur at quite low concentrations.

As would be expected from the regular-solution assumptions, the free energy/composition curves of the solid solution and ordered phases are always convex to the composition axis in the above treatments. That this need not necessarily apply to real binary solutions may be deduced from certain ternary phase diagrams. For example, the copper-nickel-aluminium diagram<sup>62</sup> contains a phase field at high

temperatures extending from  $\beta$  ( $\text{Cu}_3\text{Al}$ ) to  $\text{NiAl}$  with a critical temperature of  $760^\circ\text{C}$ . A similar effect occurs in iron-nickel-aluminium alloys, where body-centred cubic iron forms a continuous series of solid solutions with  $\text{NiAl}$  above  $1200^\circ\text{C}$ .<sup>63</sup> These effects must be associated with inflected free energy/compositional curves even though the binary alloys in these systems show negative heats of solution. Thus it is not impossible that a more rigorous treatment might show an inflected free energy/composition curve for certain binary systems which undergo ordering reactions. Nevertheless, the models resulting from the regular-solution hypothesis have been adopted in the paper, as their theoretical background is well established.

## APPENDIX II.

### GROWTH OF THE G.P. ZONES DURING THE INITIAL RISE.

It was noted that the curves in Fig. 4 (p. 328) for the initial rise of the alloys with 3.5, 4.0, or 4.5% copper were very similar in general appearance and could be represented by straight lines within the limits of the experimental error. The general equation of the straight-line portion is :

$$\frac{H - H_v}{H_f - H_v} = \frac{\ln t/t_v}{\ln t_f/t_v} \quad . \quad . \quad . \quad . \quad . \quad . \quad (8)$$

or :

$$\frac{H - H_v}{H_f - H_v} = m \ln t - m \ln t_v = u = \frac{c_0 - c}{c_0 - c_f} \quad . \quad . \quad (9)$$

where  $m^{-1} = \ln t_f/t_v$ ,  $H_v$  is the hardness at the time of the incubation value  $t_v$ ,  $H_f$  the hardness at the completion of the initial rise at time  $t_f$ , and  $H$  the hardness at time  $t$ .

It may be assumed that this part of the decomposition process goes to completion between  $t_v$  and  $t_f$ . It will be further assumed that the ratio of the hardness increment to the total change in hardness may be taken as giving the fraction,  $u$ , to which the process has proceeded and that this is a simple function of the depletion of solute.  $c_0$  and  $c_f$  are the initial and final concentrations and  $c$  is the average concentration at time  $t$ . Values of  $m$  have been calculated from Fig. 4 and are given in Table I. These show that  $m$  is almost independent of composition over the range investigated.

A straight-line relation has also been observed between the hardness and the logarithm of the tempering time for several steels.<sup>64-67</sup> Although the softening has been represented mathematically,<sup>67</sup> no physical models appear to have been put forward which predict



hardness changes proportional to the logarithm of the time. The possibility that the experimental results in Fig. 4 could be represented in an alternative manner was therefore investigated.

TABLE I.—Values of  $m$ .

Alloy	$t_f$ , days	$t_v$ , days	$t_f/t_v$	$m = (\ln t_f/t_v)^{-1}$
Al-3.5% Cu . .	2	0.2	10	0.43
Al-4.0% Cu . .	0.9	0.085	10.5	0.43
Al-4.5% Cu . .	0.5	0.04	12.5	0.40

Several analyses have been made of the rates of transformation for reactions such as recrystallization and the  $\gamma \rightarrow$  pearlite change in steels.<sup>68-71</sup> These may be applied to precipitation, as long as it is realized that the fraction transformed really signifies the fraction of the alloy, around the particle of precipitate, depleted in solute. The fraction of precipitate,  $u$ , or the fraction transformed may reasonably be set as:

$$u = 1 - \exp\left[-\left(\frac{t}{\tau}\right)^p\right] = \frac{c_0 - c_f}{c_0 - c_v} \quad . \quad . \quad . \quad (10)$$

where  $t$  is the time,  $\tau$  is a time constant, and  $p$  is a constant. This equation may be re-written:

$$\begin{aligned} \ln \ln \frac{1}{1-u} &= p \ln t - p \ln \tau \\ &= \ln \ln \frac{c_0 - c_f}{c_0 - c_v} = \ln \ln \frac{H_f - H_v}{H_f - H} \quad . \quad . \quad (11) \end{aligned}$$

from which  $\tau$  is seen to be the time at which:

$$u = \frac{c_0 - 1}{c_0} \doteq 0.63$$

Values of  $H$  have been read from the straight lines for the initial rise in Fig. 4 and used to calculate  $u$  according to the relation in equation (9). These have been plotted as  $\log \log \frac{1}{1-u}$  against  $\log t$  to give the inflected curves in Fig. 29. The best straight line was drawn through these curves and had a slope of  $p = 1.5$ . Values read from these straight lines were used to calculate the theoretical hardness corresponding to the transformation process of equation (11). These values have been plotted to give the inflected curves in Fig. 24 (p. 348) which also fall within the limits of the experimental error. Whether the initial rise is represented by an inflected curve or a straight line is thus a matter of choice.

If all the particles of a given shape begin to grow at the same time, the law of growth for the entire process is the same as that for the individual particles.<sup>72</sup> Zener<sup>30</sup> suggested that the physical significance of  $p$  (equations (10) and (11)) could be interpreted in terms of the geometrical shape of the particle.

Zener<sup>30</sup> has given the size of a particle growing in an infinite matrix as :

$$l \propto \delta [D(t - t_0)]^{1/2} \quad . \quad . \quad . \quad . \quad . \quad . \quad (12)$$

where  $l$  is the growth co-ordinate of a particle growing for time  $(t - t_0)$ ,

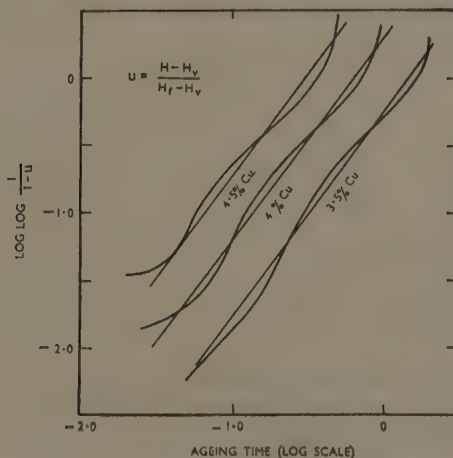


FIG. 20.—Curves for the Initial Rises at 130°C. (Fig. 4) Replotted According to Equation (11).  $u$  is the fraction to which the decomposition process has proceeded.

$\delta$  is a function of the concentrations and of the shape of the particle, and  $D$  is the diffusion coefficient. The proportionality factor for this equation does not vary greatly from unity. The growth co-ordinate  $l$  depends on the shape of the particle and may be half the thickness of a thin disc, the radius of a long cylinder, or the radius of a sphere.

Since Wert<sup>31</sup> takes the radius of a disc as being proportional to the time of growth, the volume of a disc or sphere may be set as :<sup>30, 31, 72</sup>

$$V_{\text{disc}} \propto (t - t_0)^{5/2} \quad V_{\text{sphere}} \propto (t - t_0)^{3/2} \quad . \quad . \quad . \quad . \quad (13)$$

Wert<sup>31</sup> studied the precipitation of nitrogen or carbon from pure iron. Plotting the results according to equation (11) gave straight lines of slope 2.5 and 1.5, respectively. This was interpreted in terms

of equations (11) and (13) to mean that the particles of precipitate were discs in the case of iron-nitrogen alloys or spheres in the case of iron-carbon alloys.

The initial decomposition product in aluminium-copper alloys is known to take the form of platelets. Following Wert, the growth law for their volume should give  $p = 2.5$ , whereas experimental results from the hardness curves for the initial rise indicate a value of  $p = 1.5$  (Fig. 29).<sup>\*</sup> It may be that the conditions for the radial growth of the G.P. zones are not those appropriate to the alloys studied by Wert, or that the process obeys some law expressed by equation (9) and not that of equation (11).

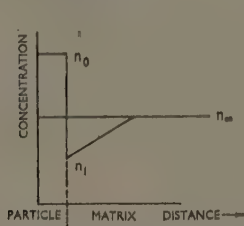


FIG. 30.—Diagrammatic Representation of the Concentration Distribution at a Growing Particle.<sup>20</sup>

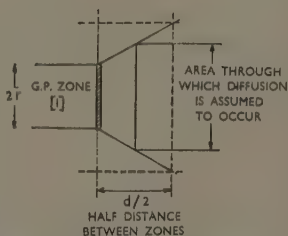


FIG. 31.—Model for Calculation of Diffusion Coefficient Associated with G.P. Zones [1].

It is, however, of interest to calculate the growth co-ordinate,  $l$ , in equation (12), for the half-thickness of the G.P. zones [1]. The coefficient  $\delta_1$  for discs is given by :

$$\delta_1 = \frac{n_\infty - n_1}{(n_0 - n_1)^{1/2}(n_0 - n_\infty)^{1/2}} \quad \dots \quad (14)$$

where  $n_1$ ,  $n_0$ , and  $n_\infty$  are the concentrations shown in Fig. 30.

If the concentration in contact with the zones growing by downhill diffusion at 130° C. be taken as 2 wt.-% copper and  $n_0$  be taken as

TABLE II.—Values of  $\delta_1(t_f - t_v)^{1/2}$ .

Alloy	$\delta_1$	$t_f - t_v$ , days	$(t_f - t_v)^{1/2}$	$\delta_1(t_f - t_v)^{1/2}$
Al-3.5% Cu . .	0.032	1.8	1.34	$4.3 \times 10^{-2}$
Al-4.0% Cu . .	0.045	0.815	0.9	$4.05 \times 10^{-2}$
Al-4.5% Cu . .	0.059	0.46	0.68	$4.0 \times 10^{-2}$

20 at.-% copper,<sup>13</sup> the values of  $\delta_1(t_f - t_v)^{1/2}$  are as given in Table II. The similarity of these values suggests that the G.P. zones [1] have a

<sup>\*</sup> See note on p. 354.

relatively constant thickness at the completion of the initial rise at 130° C. for alloys containing 3.5–4.5% copper.

By putting a value of  $D = 10^{-12}$  cm.<sup>2</sup>/day (Appendix III, below) into equation (12), together with values from Table II, a thickness of 8 Å. is obtained for the G.P. zones [1], which is of the right order of magnitude.

### APPENDIX III.

#### CALCULATION OF DIFFUSION COEFFICIENTS.

Guinier<sup>10,37</sup> gives the diameter of the G.P. zones [1] for an aluminium-5.2% copper alloy aged at room temperature as 45 Å., and 250 Å. after 50 min. at 150° C. Hunsicker's ageing curves<sup>5</sup> suggest that the latter treatment would not take the alloy beyond the flat on the curve. This example would, therefore, be comparable with the present alloys aged at 130° C.

It will be assumed that each zone consists of 100 at.-% copper and is two atom-layers thick at room temperature and four atom-layers thick at 150° C. It will also be assumed that half the copper is present in the G.P. zones [1]. The distance between the G.P. zones is now readily calculable from a knowledge of the copper concentration of the alloy.

Diffusion is assumed to occur under the conditions shown in Fig. 31 and is calculated according to :

$$P = D \frac{\Delta c}{\Delta y} \quad . \quad . \quad . \quad . \quad . \quad . \quad (15)$$

where  $P$  is the permeability or the flux of copper atoms/unit area/unit time/unit concentration gradient,  $D$  is the diffusion coefficient, and  $\frac{\Delta c}{\Delta y}$  is the concentration gradient along the  $y$  axis with  $c$  measured in copper atoms/unit volume.  $\Delta c$  has been placed as 2.6 wt.-% converted to the appropriate units in accordance with the assumption of downhill diffusion and  $\Delta y$  put equal to half the distance between the zones to give the mean diffusion gradient over the whole time interval (Fig. 31).

The results are given in Table III, and are compared with values of  $D$  at 30° C. and 150° C. calculated by extrapolation from the measured value at 504° C.<sup>38</sup> The relatively small temperature dependence of the calculated values may imply that different modes of decomposition have occurred in the two cases. However, the uncertainty in the experimental values assumed to apply to the G.P. zones precludes any definite conclusion being drawn. Fairly similar values of  $D$  have also been given by Jagodzinski and Laves,<sup>39</sup> quoting unpublished work of Intrau, but the method of calculation was not described.

The value of the diffusion coefficient calculated by extrapolation from higher temperatures is so low that no ageing would be obtained at room temperature if this value applied to the decomposition processes.

TABLE III.—*Calculation of the Diffusion Coefficient for the Growth of G.P. Zones [1] in an Aluminium-5.2% Copper Alloy by Downhill Diffusion.*

	Ageing at 30° C.	Ageing at 150° C.
Ageing time . . . .	1 day (from Fig. 14)	50 min.
Dia. of G.P. zone . . . .	45 Å.	250 Å.
Assumed thickness . . . .	2 atom-layers	4 atom-layers
Atoms/zone assumed 100% copper . . . .	390	24,000
Distance between zones assuming half copper remains in matrix . . . .	80 Å.	320 Å.
Area through which diffusion assumed to occur . . . .	3600 Å <sup>2</sup>	81,000 Å <sup>2</sup>
Copper atoms transferred to each side of zone, atoms/cm. <sup>2</sup> /day/unit gradient . . . .	$\frac{390}{2} \cdot \frac{10.6}{3600}$	$\frac{6}{5} \cdot 24 \cdot \frac{24,000}{2} \cdot \frac{10.6}{81,000}$
$\frac{\Delta c}{\Delta y}$ copper atoms/cm. <sup>3</sup> /cm. . . .	$\frac{10^8}{40} \cdot \frac{1.25}{10^3} \cdot \frac{10^{24}}{16}$	$\frac{10^8}{160} \cdot \frac{1.25}{10^3} \cdot \frac{10^{24}}{16}$
$D_{calc.}$ cm. <sup>2</sup> /day . . . .	$2.8 \times 10^{-13}$	$9 \times 10^{-11}$
$D$ by extrapolation from experiment <sup>§</sup> , cm. <sup>2</sup> /day . . . .	$4.6 \times 10^{-20}$	$4.2 \times 10^{-13}$

The diffusion coefficient as normally obtained is the product of the probability for a place exchange multiplied by a factor based on the free energy/composition gradient.<sup>18</sup> In an ideal solution the latter has the value of unity. The value of the diffusion coefficient calculated from the G.P. zones [1] contains both these terms. The driving force for diffusion should always be expressed as the free-energy gradient and not as the composition gradient. Part of the discrepancy between the values of the diffusion coefficient calculated by the different methods undoubtedly lies in the thermodynamic factor, but the difference is so great that this is probably not the whole explanation.

#### APPENDIX IV.

##### SLOPE OF RECIPROCAL-RATE CURVES.

The value of the activation energy for a precipitation process as derived from the reciprocal-rate curves is frequently less than the activation energy for diffusion as measured at higher temperatures.<sup>41</sup> It is intended to examine the conditions which could bring this about and yet retain the same value of the activation energy for diffusion.

The general equation for the time of initial decomposition is given by:<sup>18</sup>

$$\ln t = c + \frac{Q}{RT} + \frac{\alpha}{RT} \quad . \quad . \quad . \quad . \quad . \quad (16)$$

where  $c$  is a constant,  $Q$  is the activation energy for diffusion,  $\alpha$  is an additional activation energy required by the particular process,  $R$  is the gas constant, and  $T$  is the absolute temperature.

This predicts a straight line of slope  $Q/R$  when  $\ln t$  is plotted against  $1/T$ , as long as  $\alpha$  is very small compared with  $Q$ . The slope of equation (16) is given by:

$$\frac{\partial \ln t}{\partial (1/T)} = \frac{Q}{R} + \frac{\alpha}{R} + \frac{1}{RT} \frac{\partial \alpha}{\partial (1/T)} \quad . \quad . \quad . \quad . \quad (17)$$

Since  $\alpha$  increases with increasing temperature,<sup>18</sup> the last term in this equation is negative. When  $\alpha$  is not negligibly small the experimentally determined slope will be less than  $Q/R$  provided that:

$$\frac{\alpha}{R} < \frac{1}{RT} \frac{\partial \alpha}{\partial (1/T)} \quad . \quad . \quad . \quad . \quad . \quad (18)$$

This relation has been recognized previously by Jetter and Mehl,<sup>41</sup> who suggested that equation (17) should give an approximately straight line at low ageing temperatures. This may be extended to cover an appreciable range of temperature by placing the last two terms in equation (17) equal to a constant, so that:

$$\frac{\alpha}{R} + \frac{1}{RT} \frac{\partial \alpha}{\partial (1/T)} = -K_1 \quad . \quad . \quad . \quad . \quad (19)$$

By integrating:

$$\frac{\alpha}{RT} = -K_1 \left( \frac{1}{T} \right) + K_2$$

and:

$$\frac{\alpha}{R} = K_2 T - K_1 \quad . \quad . \quad . \quad . \quad . \quad (20)$$

A straight line of slope less than  $Q$  is also to be expected over a range of temperature where the additional activation energy can be represented by an expression similar to equation (20), even when  $\alpha$  is large, provided that relation (18) holds.

Consider the straight lines in Fig. 32 corresponding to the equations:

$$\ln t = c + \frac{Q}{RT} \quad . \quad . \quad . \quad . \quad . \quad (21)$$

$$\ln t' = c' + \frac{Q'}{RT} = c + \frac{Q}{RT} + \frac{\alpha}{RT} \quad . \quad . \quad . \quad (22)$$



Comparison of equations 21 and 22 shows that :

$$\frac{\alpha}{RT} = \ln \frac{t'}{t} \quad . \quad . \quad . \quad . \quad . \quad . \quad (23)$$

and the angle marked  $X$  in Fig. 32 is equal to  $\tan^{-1} \frac{\alpha}{R}$  where this value of  $\alpha$  is appropriate to  $T_1$ .

$\ln t' - \ln t$  goes from nil to  $c' - c$  over the range  $\frac{1}{T} = \frac{1}{T_0}$  to  $\frac{1}{T} = 0$ .

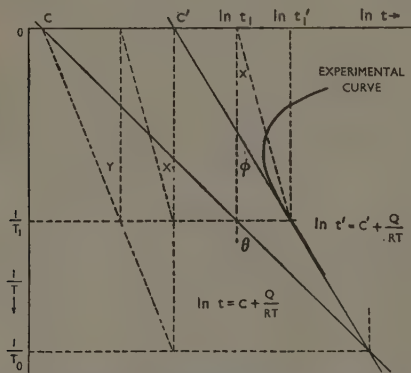


FIG. 32.—Relations Between an Experimentally Determined Activation Energy,  $Q'$ , and the Activation Energy for Diffusion,  $Q$ . The straight lines may be regarded as having been extrapolated in both directions from the temperature ranges examined.

$$\tan \theta = \frac{Q}{R}; \quad \tan \phi = \frac{Q'}{R}; \quad \tan X = \frac{\alpha}{R}; \quad \tan Y = \frac{\beta}{R} = \frac{Q - Q'}{R}$$

Comparison with Fig. 32 shows that :

$$\ln \frac{t'}{t} = (c' - c) \left(1 - \frac{T_0}{T}\right) = \frac{\alpha}{RT} \quad . \quad . \quad . \quad . \quad (24)$$

so that  $K_2 = (c' - c)$  and  $K_1 = T_0(c' - c)$  in equation (20) and  $\alpha$  is positive as long as  $T > T_0$  or  $\frac{1}{T} < \frac{1}{T_0}$ .

At  $T_0$ ,  $t' = t$  and  $\frac{\alpha}{RT} = 0$ , hence from equations (21) and (22) :

$$c' - c = \frac{Q - Q'}{RT_0} = \frac{\beta}{RT_0} \quad . \quad . \quad . \quad . \quad (25)$$

Comparison of equations (24) and (25) shows that :

$$\frac{\alpha}{RT} = \frac{\beta}{RT_0} \left(1 - \frac{T_0}{T}\right)$$

hence :

$$\frac{\alpha}{R} = \frac{Q - Q'}{RT_0} \cdot (T - T_0) \quad . \quad . \quad . \quad . \quad (26)$$

Angle  $Y$  in Fig. 32 has a value of  $\tan^{-1} \frac{\beta}{R} = \tan^{-1} \frac{Q - Q'}{R}$ .

$Q'$ ,  $c'$ , and  $Q$  may be taken as known, but  $\alpha$  could not be calculated unless either  $c$  or  $T_0$  could be determined. However, an estimate for the order of magnitude of  $\alpha$  may be made from equation (26) with an assumed value of  $T_0$ . If  $Q - Q' = 10,000$  cal./g.-atom and  $T_0 = 200^\circ$ , then  $\alpha = 15,000$  cal./g.-atom at  $T = 500^\circ$  and  $\alpha = 7500$  cal./g.-atom at  $T = 350^\circ$ .

The model examined above gives the conditions (equations (20) and (25)) under which a straight-line relation with a slope less than  $Q/R$  would be given by the reciprocal-rate curve. These conditions may be fulfilled at high ageing temperatures when the activation energy for diffusion is known from experimental measurements. It is implicit in this argument that the time for the initiation of the precipitation process shall be appreciably longer than that for diffusion (Fig. 32). It is quite evident from Appendix III that decomposition according to the extrapolated diffusion rate would require an impossibly long time at low ageing temperatures. The requirements of the present model would also lengthen this time. It must, therefore, be concluded that a lower activation energy exists for diffusion at low temperatures than that at the elevated temperatures at which diffusion measurements are normally carried out. Nevertheless the activation energy derived from the reciprocal-rate curve may still be less than that for diffusion at the same temperature.

#### ACKNOWLEDGEMENTS.

The author and the Fulmer Research Institute thank the Chief Scientist, Ministry of Supply, for permission to publish this paper. The author's thanks are also due to his colleagues who contributed to the experimental work and to Dr. A. H. Sully for helpful discussion.

## REFERENCES.

1. A. Wilm, *Metallurgie*, 1911, **8**, 225.
2. R. F. Mehl and L. K. Jetter, *Age-Hardening of Metals* (*Amer. Soc. Metals*), 1940, 342.
3. H. K. Hardy, *Light Metals*, 1944, **7**, 328, 383.
4. G. C. Smith, "Progress in Metal Physics", Vol. I, p. 163. London: 1949 (Butterworths Scientific Publications).
5. H. Y. Hunsicker, *Age-Hardening of Metals* (*Amer. Soc. Metals*), 1940, 56.
6. M. L. V. Gayler and R. Parkhouse, *J. Inst. Metals*, 1940, **66**, 67.
7. M. L. V. Gayler, *J. Inst. Metals*, 1946, **72**, 243.
8. H. K. Hardy, *J. Inst. Metals*, 1948-49, **75**, 707.
9. A. Guinier, *Nature*, 1938, **142**, 569.
10. A. Guinier, *Compt. rend.*, 1938, **206**, 1641.  
J. Calvet, P. Jacquet, and A. Guinier, *Compt. rend.*, 1938, **206**, 1972.
11. G. D. Preston, *Proc. Roy. Soc.*, 1938, [A], **167**, 526.
12. G. D. Preston, *Phil. Mag.*, 1938, [vii], **26**, 855.
13. A. Guinier, *J. Phys. Radium*, 1942, [viii], **3**, 124; *Bull. Lab. d'Essais*, 1946, (21).
14. G. Wassermann and J. Weerts, *Metallwirtschaft*, 1935, **14**, 605.
15. A. Guinier, *Compt. rend.*, 1950, **231**, 655.
16. A. Guinier, *J. Inst. Metals*, 1946, **72**, 686 (discussion).
17. H. K. Hardy, unpublished work.
18. H. K. Hardy, *J. Inst. Metals*, 1950, **77**, 457.
19. P. Laurent, *Rev. Mét.*, 1950, **47**, 835.
20. E. Scheil, *Z. Metallkunde*, 1950, **41**, 41.
21. A. Guinier, *Métaux, Corrosion, Usure*, 1943, **18**, 209; *Bull. Lab. d'Essais*, 1947, (23).
22. E. C. W. Perryman and J. C. Blade, *J. Inst. Metals*, 1950, **77**, 263.
23. H. K. Hardy, *J. Inst. Metals*, 1950, **77**, 637 (discussion).
24. W. L. Fink and D. W. Smith, *Trans. Amer. Inst. Min. Met. Eng.*, 1940, **137**, 95.
25. G. V. Raynor, "Progress in Metal Physics", Vol. I, p. 1. London: 1949 (Butterworths Scientific Publications).
26. G. V. Raynor, *Inst. Metals: Annotated Equilib. Diag. Series No. 4*, 1944.
27. G. Wassermann, *Metallwirtschaft*, 1934, **13**, 133.
28. T. Lyman and A. R. Troiano, *Trans. Amer. Soc. Metals*, 1946, **37**, 402.
29. A. Hultgren, *Trans. Amer. Soc. Metals*, 1947, **39**, 915.
30. C. Zener, *J. Appl. Physics*, 1949, **20**, 950.
31. C. A. Wert, *J. Appl. Physics*, 1949, **20**, 943.
32. M. Cohen, *Trans. Amer. Inst. Min. Met. Eng.*, 1939, **133**, 95.
33. W. L. Finlay and W. R. Hibbard, Jr., *Trans. Amer. Inst. Min. Met. Eng.*, 1949, **180**, 255.
34. W. Köster, *Z. Metallkunde*, 1950, **41**, 71.
35. A. H. Geisler, C. S. Barrett, and R. F. Mehl, *Trans. Amer. Inst. Min. Met. Eng.*, 1943, **152**, 182.
36. H. Auer, *Z. Naturforsch.*, 1949, [A], **4**, 533.
37. A. Guinier, *Ann. Physique*, 1939, [xi], **12**, 161.
38. R. F. Mehl, F. N. Rhines, and K. A. v. den Steinen, *Metals and Alloys*, 1941, **13**, (1), 41.
39. H. Jagodzinski and F. Laves, *Z. Metallkunde*, 1949, **40**, 296.
40. F. R. N. Nabarro, *J. Inst. Metals*, 1940, **66**, 312 (discussion).
41. L. K. Jetter and R. F. Mehl, *Trans. Amer. Inst. Min. Met. Eng.*, 1943, **152**, 166.
42. J. H. Hildebrand, *Proc. Nat. Acad. Sci.*, 1927, **13**, 267; and *J. Amer. Chem. Soc.*, 1929, **51**, 66.
43. R. H. Fowler and E. A. Guggenheim, "Statistical Thermodynamics", p. 356. Cambridge: 1949 (University Press).
44. H. A. Bethe, *Proc. Roy. Soc.*, 1935, [A], **150**, 552.
45. R. Becker, *Z. Metallkunde*, 1937, **29**, 245.
46. W. Hume-Rothery, "The Structure of Metals and Alloys" (*Inst. Metals Monograph and Rep. Series No. 1*), 1949, 59.

47. A. W. Lawson, *J. Chem. Physics*, 1947, **15**, 831.
48. O. J. Kleppa, *J. Amer. Chem. Soc.*, 1949, **71**, 3275; 1950, **72**, 3346; 1951, **73**, 385.
49. C. Zener, *Thermodynamics in Physical Metallurgy* (Amer. Soc. Metals), 1950, 16.
50. O. Kubaschewski, *Z. Elektrochem.*, 1942, **48**, 559, 646.
51. F. Weibke and O. Kubaschewski, "Thermochemie der Legierungen", Berlin : 1943 (Springer Verlag).
52. F. Weibke and O. Kubaschewski, *ibid.*, p. 149.
53. F. Weibke and O. Kubaschewski, *ibid.*, p. 139.
54. E. Scheil, *Z. Elektrochem.*, 1943, **49**, 242.
55. G. Grube and P. Hantelmann, *Z. Elektrochem.*, 1942, **48**, 399.
56. C. E. Easthope, *Proc. Camb. Phil. Soc.*, 1937, **33**, 502.
57. C. E. Easthope, *Proc. Camb. Phil. Soc.*, 1938, **34**, 68.
58. W. Shockley, *J. Chem. Physics*, 1938, **6**, 130.
59. J. M. Cowley, *Phys. Rev.*, 1950, [ii], **77**, 669.
60. E. Scheil, private communication.
61. W. L. Bragg and E. J. Williams, *Proc. Roy. Soc.*, 1935, [A], **151**, 540.
62. W. O. Alexander, *J. Inst. Metals*, 1938, **63**, 163.
63. S. Kiuti, *Tōkyō Teikoku-Daigaku Kōku Kenkyūzō Hōkoku* (Rep. Aeronaut. Res. Inst. Tōkyō Imp. Univ.), 1940, **15**, 601.
64. C. R. Austin and B. S. Norris, *Trans. Amer. Soc. Metals*, 1938, **26**, 788.
65. E. C. Bain, "Functions of the Alloying Elements in Steel". Cleveland, O. : 1939 (American Society for Metals).
66. E. H. Engel, *Trans. Amer. Soc. Metals*, 1939, **27**, 1.
67. J. H. Hollomon and L. D. Jaffe, *Trans. Amer. Inst. Min. Met. Eng.*, 1945, **162**, 223.
68. W. A. Johnson and R. F. Mehl, *Trans. Amer. Inst. Min. Met. Eng.*, 1939, **135**, 416.
69. U. R. Evans, *Trans. Faraday Soc.*, 1945, **41**, 365.
70. M. Avrami, *J. Chem. Physics*, 1940, **8**, 212.
71. M. Cook and T. Ll. Richards, *J. Inst. Metals*, 1947, **73**, 1.
72. C. A. Wert, *Thermodynamics in Physical Metallurgy* (Amer. Soc. Metals), 1950, 178.
73. J. C. Lankes and G. Wassermann, *Z. Metallkunde*, 1950, **41**, 381.



# THE TITANIUM-HYDROGEN SYSTEM FOR 1311 MAGNESIUM-REDUCED TITANIUM.\*

By A. D. McQUILLAN,† Ph.D., B.Sc.

## SYNOPSIS.

As an extension of recent work in which the author has shown that the allotropic  $\alpha \rightleftharpoons \beta$  transformation occurring in titanium metal is much affected by the impurities present in material produced by the magnesium reduction of titanium tetrachloride (*J. Inst. Metals*, 1950-51, **78**, 249), the constitutional diagram of the titanium-hydrogen system has been studied using magnesium-reduced titanium, and the results are compared with those obtained for the same system when van Arkel titanium was used. It has been found that the system magnesium-reduced titanium-hydrogen cannot be treated as a simple binary, but must be considered as a section through a multi-component system. The results obtained in the study of systems of magnesium-reduced titanium with other metals are likely to be affected in the same way.

## I.—INTRODUCTION.

It has been shown by the author<sup>1</sup> that the impurities normally present in magnesium-reduced titanium prepared by the Kroll process cause the  $\alpha \rightleftharpoons \beta$  transformation to occur over a temperature interval of 850°-955° C. Analysis of the Kroll material gives: O 0.35, C 0.40, N 0.14, Si 0.07, Mg 0.25, Fe 0.17, Mn 0.02, Co 0.02 at.-%. It would seem reasonable, therefore, to expect that these impurities would also have a profound effect on the form of any constitutional diagram obtained for a titanium system in which magnesium-reduced, Kroll titanium has been used. As the cost of producing titanium by the van Arkel method is very high, it is to be expected that much of the work being carried out on titanium will be done on Kroll titanium and that any commercially useful titanium alloys will be based on this material. A comparison between the constitutional diagram determined for a particular system using van Arkel titanium and that obtained for the same system when magnesium-reduced titanium is used would be a useful guide for all workers in this field, since it would indicate the extent of the departure from ideal behaviour to be expected in alloys made from the less pure metal.

\* Manuscript received 28 August 1950.

† Formerly Senior Research Officer, Physical Metallurgy Section, Commonwealth Scientific and Industrial Research Organization, Baillieu Laboratory, University of Melbourne, Australia.



## II.—EXPERIMENTAL METHOD.

The titanium-hydrogen system has already been studied by the author using van Arkel titanium.<sup>2</sup> This system may be studied rapidly and conveniently, since alloys are easily prepared by dissolving gaseous hydrogen in the metal, and the constitutional diagram may be deduced from the experimentally determined pressure-temperature-concentration relationships of the gaseous hydrogen in equilibrium with the metal-hydrogen solutions. The system has now been re-examined using Kroll titanium, and the constitutional diagram obtained has been compared with that previously established for van Arkel material.

The titanium specimens used in these experiments were prepared from powder supplied by the U.S. Bureau of Mines and consisted of blocks, weighing approximately 0.5 g., cut from a melted ingot. The ingot was prepared by melting a powder compact, which had been heated for 8 hr. at 1000° C. at a pressure of  $10^{-5}$  mm. mercury in order to remove all volatile impurities, in an arc furnace. The argon atmosphere of the arc furnace was purified before melting the compact by maintaining a separate piece of titanium in a molten condition in the furnace for 20 min. Details of the construction and operation of an argon arc furnace substantially the same as that used in this laboratory have been described by Geach and Summers-Smith.<sup>3</sup>

The experimental method and apparatus used for determining the titanium-hydrogen system has already been described.<sup>2</sup> Essentially, the method consists in dissolving known amounts of purified hydrogen in a titanium specimen contained in a closed system of known volume, and measuring the change in hydrogen pressure in the system as a function of specimen temperature. The region of the constitutional diagram which may be investigated in this way is limited by three factors: (1) the permeability of the silica specimen tube to atmospheric gases above 950° C., (2) the limitation of the hydrogen pressure to a maximum of one atmosphere because of the glass apparatus, and (3) the low-temperature limit set by the time required for equilibrium to be obtained in the alloys. When pure titanium was used for this investigation, hydrogen equilibrium pressures could be measured at temperatures down to 450° C. For Kroll titanium the lowest temperature that could be conveniently investigated in a reasonable time was controlled by the rates of diffusion of the impurities in the metal and was found to be 550° C. The rates of diffusion of the impurity elements had a further effect in that the times required for the attainment of equilibrium in two-phase regions of the system were much longer than the equivalent times required when using pure titanium. In spite of the restricted

region of the diagram that could be conveniently investigated, the results obtained when compared with those for pure titanium show that a system based on magnesium-reduced titanium deviates markedly from the form to be expected for a binary system.

### III.—THE PRESSURE-CONCENTRATION-TEMPERATURE RELATIONSHIPS.

The pressure temperature and pressure-concentration relationships for solution of hydrogen in Kroll titanium are illustrated in Figs. 1

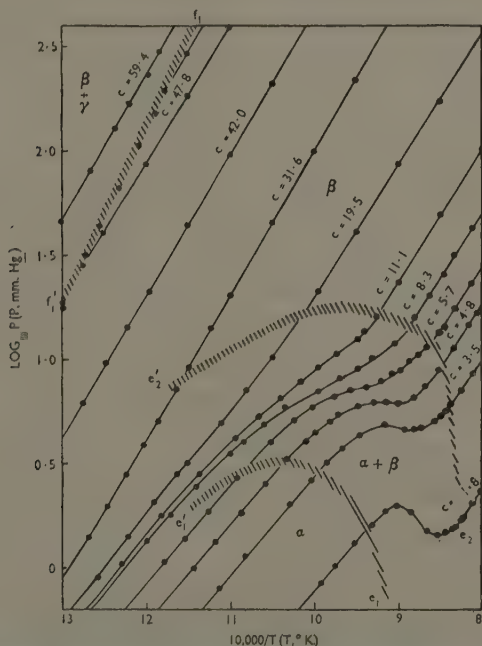


FIG. 1.—Pressure/Temperature Curves for a Range of Concentrations of Hydrogen in Magnesium-Reduced Titanium.  $c$  = at.-% hydrogen.

and 2, in which the pressure and concentration have been plotted logarithmically and the temperature expressed in terms of the reciprocal absolute temperature. In any region of the constitutional diagram of the condensed phases in which an alloy is single-phase, the hydrogen

pressure  $p$  at constant hydrogen concentration  $c$  is related to the temperature  $T$  by the relation :

$$\left( \frac{\partial \log p}{\partial \frac{1}{T}} \right)_c = \frac{Q}{R} \quad . \quad . \quad . \quad . \quad (1)$$

where  $Q$  is the heat of solution of molecular hydrogen in the particular phase of the alloy and  $R$  is the gas constant. The value of  $Q$  will, over the temperature range covered in this investigation, be substantially independent of temperature, but will in general change with the concentration of dissolved hydrogen in any phase and will be different for different phases. The curve of  $\log p$  against  $1/T$  for an alloy of given hydrogen concentration would, therefore, from equation (1) be expected to be linear in a single-phase region. It will be seen in Fig. 1 that for alloys containing up to 31.6 at.-% hydrogen the curves are all linear at high temperatures; this part of the diagram corresponds to the solid solution based on the body-centred cubic  $\beta$ -form of titanium. The effect of the impurities on the curves for this region is to cause a constant increase in the logarithm of the hydrogen equilibrium pressure at any temperature and concentration compared with the corresponding pressure in the pure titanium system. As would be expected, therefore, the impurities produce a reduction in the solubility of hydrogen in the  $\beta$ -alloys. After passing through a curved region, the curves for hydrogen concentrations below 5.7 at.-% become linear again at lower temperatures when the alloys enter the single-phase region corresponding to the solid solution based on hexagonal close-packed  $\alpha$ -titanium. The effect of the impurities in this region is again to produce a decrease in the hydrogen solubility compared with that for pure alloys. Fig. 1 shows that the heat of solution  $Q$  for the  $\alpha$  phase is numerically smaller than that for the  $\beta$  solid solution. The curves for alloys containing between 8.3 and 31.6 at.-% hydrogen remain curved at the lowest temperatures investigated, and it must be assumed that these alloys do not leave the two-phase ( $\alpha + \beta$ ) region. The shape of the curves of  $\log p$  against  $1/T$  in the ( $\alpha + \beta$ ) region is determined by the distribution of hydrogen between the two co-existing phases, which is a function of the hydrogen solubility and the relative amounts of the two phases. Since these factors will vary with temperature, the curves will be, in general, non-linear.

The lines  $e_1e_1'$  and  $e_2e_2'$  in Fig. 1 denote the limits of the  $\alpha$ - and  $\beta$ -solutions and are shown as shaded areas to indicate the region of uncertainty. Fig. 2 shows the isothermal  $\log p/\log c$  curves which have been derived for a series of temperatures from the curves of  $\log p$

against  $1/T$  in Fig. 1. The limits of  $\alpha$  and  $\beta$  solutions obtained in Fig. 1 are again shown as shaded areas in Fig. 2. For  $\alpha$  solutions at all hydrogen concentrations at which they exist and for  $\beta$  solutions up to a hydrogen concentration of about 10 at.-%, the  $\log p/\log c$  curves are linear and have a gradient of exactly two, indicating that the hydrogen goes into solution in the titanium in the form of atoms. At higher concentrations of hydrogen in  $\beta$  solution, the  $\log p/\log c$  curves are no longer linear, the gradient of the curves increasing with hydrogen concentration until, at low temperatures and hydrogen concentrations of approximately 50 at.-%, the  $\log p/\log c$  curves are almost parallel to the  $\log p$  axis. In this region the  $\beta$  solution is approaching saturation, and the rapid increase of pressure with concentration indicates the difficulty experienced by further hydrogen atoms in entering the metal lattice. This behaviour follows the same pattern as that observed for solutions of hydrogen in pure titanium and has been more fully discussed in the paper describing that work.<sup>2</sup> A statistical-mechanical explanation of the  $\log p/\log c$  curves for  $\beta$  solutions can be formulated, using a few reasonable assumptions, and this will be the subject of a future paper.

It follows directly from the phase rule that the vapour pressure of either component in a two-phase region of a binary system at a given temperature must be independent of the relative concentration of the two components. In the titanium-hydrogen system for pure titanium, the  $\log p/\log c$  curves in the  $(\alpha + \beta)$  region were in accordance with this, and lay parallel to the concentration axis within close limits. In the system with magnesium-reduced titanium, as can be seen from Fig. 2, this is no longer the case, the curves for this region having become S-shaped in form. The system thus shows a marked deviation from the behaviour to be expected from a true binary system. The pressure-concentration-temperature relations cannot, therefore, be used for a determination of the free-energy relationships as was the case for the pure titanium system. This deviation from true binary behaviour is also observable in Fig. 1, in which the lines  $e_1e_1'$  and  $e_2e_2'$  would coincide if the hydrogen pressure were independent of concentration in the  $(\alpha + \beta)$  region. The distance between these lines is, therefore, a measure of the deviation from ideal behaviour, and in the case of the  $(\alpha + \beta)$  region the deviation is extensive.

In Fig. 2, the  $\log p/\log c$  curves for temperatures of 560° and 596° C. ( $10^4/T = 12$  and 11.5) show a discontinuity in slope at hydrogen concentrations of about 50 at.-%. This discontinuity must correspond to the beginning of the two-phase region, in which the  $\beta$ -solid solution is in equilibrium with the face-centred cubic  $\gamma$ -phase, and which was

marked in the case of the system with van Arkel titanium by the  $\log p/\log c$  curves turning abruptly to become parallel to the concentration axis. As a result of the presence of the impurities in the magnesium-reduced titanium, the  $\log p/\log c$  curves are not now independent of concentration in the two-phase region, and it is difficult to fix its beginning accurately. It is unfortunate that owing to the greater hydrogen equilibrium pressures encountered with alloys of

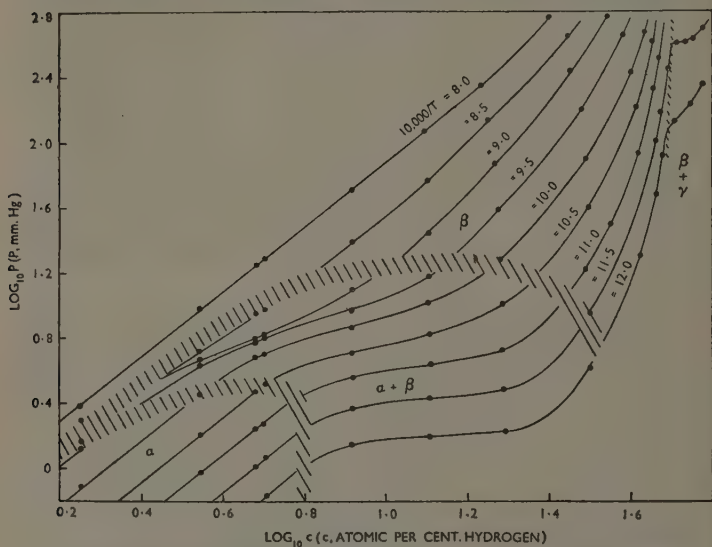


FIG. 2.—Isothermal Pressure/Concentration Curves for Solutions of Hydrogen in Magnesium-Reduced Titanium.

magnesium-reduced titanium, the pressures in equilibrium with most of the  $(\beta + \gamma)$  alloys are above one atmosphere, and it is not possible to obtain much evidence on the  $(\beta + \gamma)$  region. The region investigated lies in the small temperature range  $550^{\circ}$ – $600^{\circ}$  C., the upper limit of this range being imposed by pressure considerations and the lower one by the slowness with which equilibrium conditions can be attained. In this region the  $\log p/\log c$  curves for the  $\beta$  solution which can co-exist with the  $\gamma$  phase show that the  $\beta$  solution is almost completely saturated, and comparison with the results for pure titanium shows that the impurities have no appreciable effect on the limiting hydrogen concentration. The  $\beta/(\beta + \gamma)$  boundary is, therefore, unaffected by the

presence of impurities. No evidence on the homogeneous  $\gamma$  phase could be obtained in this system, since the rate of diffusion of impurities at temperatures at which the equilibrium pressure was less than one atmosphere was too slow for equilibrium conditions to be reached in periods up to a number of days.

#### IV.—THE CONSTITUTIONAL DIAGRAM.

The  $\alpha/(\alpha + \beta)$  and  $\beta/(\alpha + \beta)$  phase boundaries for the system titanium-hydrogen, using Kroll titanium, may be obtained by plotting the concentration-temperature relations along lines  $e_1e_1'$  and  $e_2e_2'$  in Fig. 1. These boundaries are shown in Fig. 3 and are represented by shaded regions indicating the extent of the uncertainty in their determination. The equivalent boundaries for the titanium-hydrogen system using van Arkel titanium have been indicated in Fig. 3 for comparison.

The  $\alpha \rightleftharpoons \beta$  transformation in pure titanium occurs at  $882^\circ \pm 1^\circ \text{C.}$  and in Kroll titanium over a range from  $850^\circ$  to  $955^\circ \text{C.}$ <sup>1</sup> This is illustrated in Figs. 4-9 (Plate XLVII) which show the microstructures of specimens of Kroll titanium heated for half an hour at progressively increasing temperatures in the transformation range. The original  $\beta$ -titanium has decomposed on quenching, giving a pronounced Widmannstätten pattern that enables it to be distinguished from the primary  $\alpha$  grains, which are unaffected by the etchant. The microstructures are in excellent agreement with the author's previous results. The effect of the impurities is, therefore, to depress the beginning of the transformation by  $32^\circ \text{C.}$  and elevate the end of the transformation by  $73^\circ \text{C.}$  Fig. 3 shows that this tendency is maintained in the  $(\alpha - \beta)$  region of the diagram in the whole concentration region over which it has been examined. The  $\alpha$  ( $\alpha + \beta$ ) boundary for impure titanium lies below the corresponding boundary for pure titanium, and the  $\beta$  ( $\alpha + \beta$ ) boundary above that for the pure system. The  $\beta$  ( $\beta - \gamma$ ) boundary

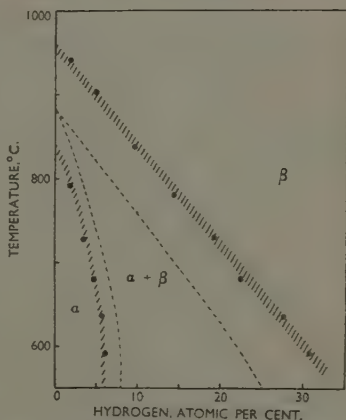


FIG. 3.—Portion of the Constitutional Diagram of Hydrogen with Magnesium-Reduced Titanium.

--- Corresponding Boundaries for Pure Titanium.



over the limited temperature range examined is almost parallel to the temperature axis of the constitutional diagram and occurs at 50 at.-% hydrogen in the range 560°–600° C. It coincides almost exactly with the corresponding boundary found for the pure titanium system.

#### V.—CONCLUSION.

It has been shown that the impurities normally present in Kroll titanium, as at present available, are of sufficient quantity and of such a nature as to cause large deviations from true binary behaviour in the ( $\alpha + \beta$ ) region of the titanium-hydrogen system. Preliminary, and as yet unpublished, investigations carried out in this laboratory have shown that this is also true for the binary systems of titanium with copper, iron, and chromium. Any system containing Kroll titanium must, therefore, be regarded as a section through a multi-component system.

In the titanium-hydrogen system with magnesium-reduced titanium it has not been possible to investigate the eutectoid horizontal which occurs in the pure system at about 325° C. In view of the effect of the impurities on the ( $\alpha + \beta$ ) region, it is, however, to be expected that the eutectoid line would be replaced by a three-phase ( $\alpha + \beta + \gamma$ ) region. Information on this point could be found by studying the titanium-copper system, which, when pure, has a eutectoid horizontal at 776° C.<sup>4</sup> and is, therefore, at a sufficiently high temperature for equilibrium conditions to be readily obtained.

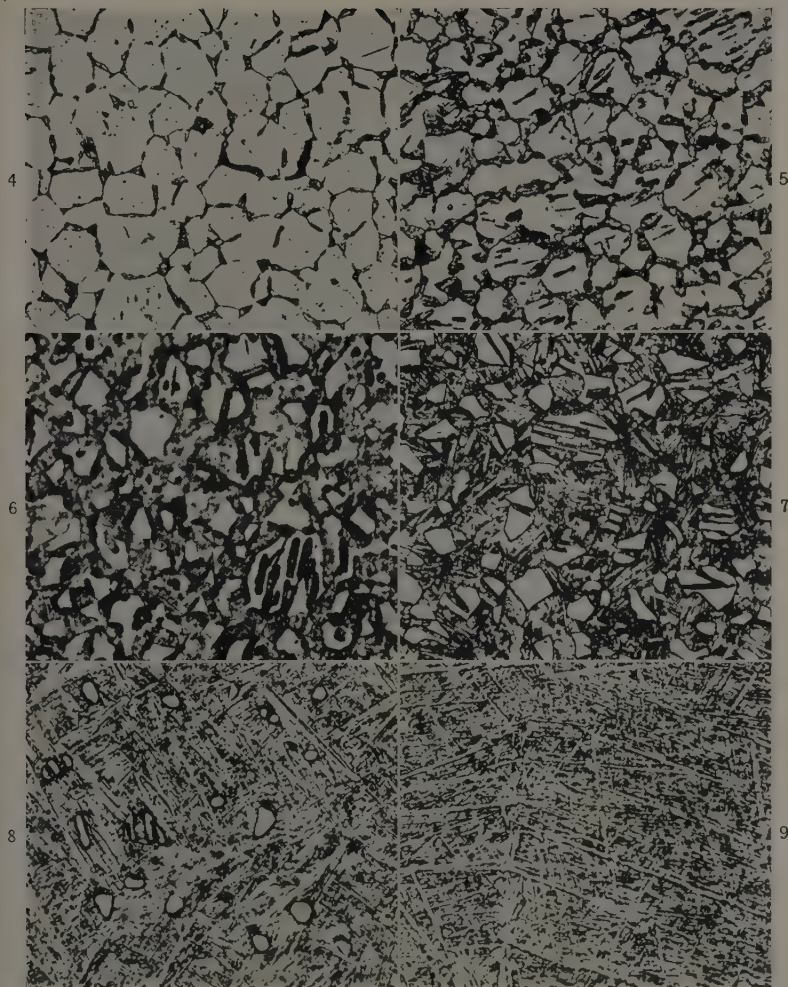
The broadening of the ( $\alpha + \beta$ ) region at lower and higher temperatures suggests that some of the impurities present in Kroll titanium must elevate, while others depress, the  $\alpha \rightleftharpoons \beta$  transformation in titanium. It has been shown in a previous paper<sup>4</sup> that iron depresses the transformation, and unpublished work of this laboratory has shown that additions of oxygen produce a marked elevation in the transformation temperature. Since both these elements are present in Kroll titanium, its behaviour is not surprising.

#### ACKNOWLEDGEMENT.

The work presented in this paper forms part of a theoretical and experimental study of titanium and its alloys being carried out by the Physical Metallurgy Section of the Commonwealth Scientific and Industrial Research Organization at the Baillieu Laboratory, University of Melbourne.

#### REFERENCES.

1. A. D. McQuillan, *J. Inst. Metals*, 1950–51, **78**, 249.
2. A. D. McQuillan, *Proc. Roy. Soc.*, 1950, [A], **204**, 309.
3. G. A. Geach and D. Summers-Smith, *Metallurgia*, 1950, **42**, 153.
4. A. D. McQuillan, *J. Inst. Metals*, 1951, **79**, (2), 73.



FIGS. 4-9.—Magnesium-Reduced Titanium Quenched from the Transformation Region after  $\frac{1}{2}$  hr. at the Temperature Indicated.  $\times 200$ .

FIG. 4.—864° C.  
FIG. 5.—888° C.

FIG. 6.—901° C.  
FIG. 7.—917° C.

FIG. 8.—950° C.  
FIG. 9.—965° C.



# A PROVISIONAL CONSTITUTIONAL DIAGRAM<sup>1312</sup> OF THE CHROMIUM-TITANIUM SYSTEM.\*

By (MRS.) M. K. McQUILLAN,† M.A., MEMBER.

## SYNOPSIS.

The chromium-titanium system has been studied by quenching methods over the whole range of compositions, and the general nature of the system established. At temperatures between 1360° and 1400° C. the elements appear to be completely soluble in one another, but on quenching the solution breaks up to form a compound,  $\text{Cr}_3\text{Ti}_2$ , and a body-centred cubic solid solution based on either the chromium or the  $\beta$ -titanium lattice. The  $\beta$ -titanium solution undergoes a eutectoid transformation at low temperatures to form  $\text{Cr}_3\text{Ti}_2$  and  $\alpha$ -titanium.

The mechanism of the contamination of chromium-titanium alloys by oxygen and nitrogen is discussed. It appears that alloys of compositions in the region of the body-centred cubic solid solution are protected against severe hardening due to gas contamination by the precipitation of particles of the hexagonal phase based on  $\alpha$ -titanium, in which the gases are very soluble.

Alloys based on the  $\beta$ -titanium solid solution are likely to have useful mechanical properties.

## I.—INTRODUCTION.

ALTHOUGH both chromium and titanium have in recent years aroused a good deal of interest as possible engineering materials, no complete investigation of the binary system of the two metals has hitherto been published. Vogel and Wenderott<sup>1</sup> studied a section of the system, and concluded that a eutectic between a compound,  $\text{Cr}_2\text{Ti}_3$ , and the solid solution based on the chromium lattice occurred at 1400° C., the eutectic composition being given as 43% titanium. McPherson and Fontana<sup>2</sup> in America have recently studied the properties of some titanium-chromium alloys containing up to 17% chromium.

In the present survey the aim has been the elucidation of the general nature of the system rather than an exact fixing of the phase boundaries of the constitutional diagram; hence the simplest of techniques has been used in all cases. The highly reactive nature of titanium at elevated temperatures complicates the study of the alloys, and prohibits the use of many conventional techniques.

## II.—PREPARATION OF THE ALLOYS.

The chromium used in this work was prepared electrolytically and was found to contain oxygen of the order of 0.05% and less than 0.001%

\* Manuscript received 23 September 1950.

† Formerly Research Officer, Aeronautical Research Laboratory, Melbourne.

nitrogen. The titanium was prepared by the reduction of titanium tetrachloride with magnesium. A typical analysis of the impurities in this material gives the following figures: O 0.35, C 0.40, N 0.14, Si 0.07, Mg 0.25, Fe 0.17, Mn 0.02, Co 0.02 at.-%.

The alloys were melted on a water-cooled copper hearth in a Kroll-type argon arc furnace. Any oxygen or nitrogen remaining in the argon atmosphere after flushing out several times was removed by melting a piece of chromium or titanium on one side of the hearth immediately before melting the alloy. In order to ensure uniform distribution of the two metals, the melted button was turned over and remelted several times. Coring effects were subsequently removed by a homogenizing treatment of 14 days at 1000° C. *in vacuo*, after which the alloys appeared to be uniform when examined under the microscope.

### III.—EXPERIMENTAL TECHNIQUES.

Since alloys containing even relatively small amounts of titanium react in the liquid state with all available refractory materials, it is not possible to determine liquidus, solidus, or eutectic lines in the equilibrium diagram by the normal methods of thermal analysis. All examinations have necessarily to be carried out on quenched materials.

At temperatures of 1000° C. or lower, annealing was carried out in continuously evacuated clear silica tubes, of about 1 cm. dia., heated in small resistance furnaces. In order to quench the specimens, the heating furnace was rapidly removed, and the silica tube immersed in cold water. Although that is not a very rapid method of quenching, it appears to have been rapid enough for these alloys at the temperatures under consideration.

For the higher-temperature work on the chromium-rich alloys, the simple type of vacuum quenching furnace shown in Fig. 1 (a) was used. The heater consisted of two electrically heated molybdenum strips, 0.008 in. thick, 4 in. long, and  $\frac{3}{8}$ – $\frac{1}{2}$  in. wide, arranged between two water-cooled copper electrodes in the form of a bow. The specimen, usually about 0.2 c.c. in volume, was supported in the hot zone between the two strips by a platinum/platinum-rhodium thermocouple which was wrapped completely round it. The electrodes were mounted in the base-plate by means of the vacuum seals shown in Fig. 1 (b). The apparatus was covered by a water-cooled brass bell sealed on to the base-plate by means of a rubber gasket. A metal tube, connected to a water reservoir through a vacuum tap, passed through the top of the bell and terminated immediately above the specimen. At the completion of a heat-treatment, the specimen was very rapidly quenched

by flooding with water from the reservoir. The whole apparatus could be dismantled quickly, and, as it contained no refractory materials, the removal of the water caused no difficulty. The bell was connected to an oil-diffusion pump through a vacuum tap which served to isolate the pumps on quenching.

The highest temperature attained in this apparatus was  $1730^{\circ}\text{C}$ .

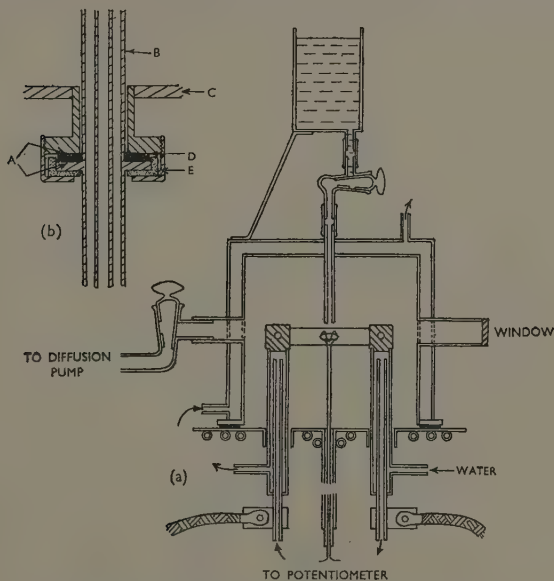


FIG. 1(a).—Vacuum Quenching Furnace.

(b).—Detail of Vacuum-Tight Electrode Mounting.

KEY.

- A Ground surfaces.
- B Electrode.
- C Base plate.
- D Rubber gasket.
- E Bakelite washer.

There seems to be no reason, however, why higher temperatures should not be possible if a tungsten/molybdenum thermocouple is substituted for the platinum/platinum-rhodium couple, and the wax seal at the thermocouple exit moved further from the hot zone. The bow-type of heater is the simplest arrangement, but greater heating efficiency has been obtained with more complicated arrangements which provide an almost totally enclosed space for the specimen. Currents of the order of 300–400 amp. are required.



In the region of 1100°–1200° C. it was found that the temperature recorded by the thermocouple varied by little more than 3° or 4° C. over periods of some hours. At higher temperatures variations were greater, but the necessary heating periods were so much shorter that it was possible to adjust the temperature manually to within  $\pm 5^\circ$  C. during the experiment. A check on the temperature measurement has been provided by the study of a chromium alloy which contained no titanium and could, therefore, be studied by more conventional methods. By using the apparatus described, the eutectic temperature of the alloy was found to lie between 1500° and 1520° C. Thermal analysis showed it to be 1512° C.

Alloy specimens containing about 50 at.-% titanium showed a tendency to react with the platinum thermocouple at temperatures nearing 1400° C. A vigorous exothermic reaction sometimes occurred, during which the specimen and the thermocouple fused together. The high-titanium alloys were, therefore, heated in a platinum-wound furnace with a pure alumina furnace tube, in a static atmosphere of purified argon. The alloys were packed in titanium powder in an alumina boat. This powder protected them both from gas contamination and from reaction with the alumina. The specimens were quenched by withdrawing the boat rapidly, and dropping it into water.

In the preparation of micro-sections no special polishing techniques were necessary. All the alloys, except those containing more than about 85% titanium, were etched electrolytically in an alkaline 10% solution of potassium ferricyanide. Those of very high titanium content were etched in a solution containing 2% nitric acid and 2% hydrogen fluoride. Micrographic examination was supplemented by X-ray work, in which the alloys were examined by powder methods in a 9-cm. camera. Those alloys containing less than about 60% titanium were powdered by crushing in a percussion mortar. The high-titanium alloys were too ductile for this treatment and had to be filed. In most cases the powdered materials were stress-annealed at 600° C. *in vacuo*. Chromium radiation was suitable for alloys at the chromium end of the system, and copper radiation for the titanium-rich alloys. It was not easy, however, to get good pictures of some of the intermediate alloys.

#### IV.—THE CONSTITUTIONAL DIAGRAM.

The constitutional diagram as determined by this investigation is shown in Fig. 2. At temperatures below 1360° C. an intermetallic compound is formed at about 40 at.-% titanium. On each side of this composition, two wide two-phase regions occur, in which the compound is in equilibrium with the body-centred cubic solid solutions based on

the chromium and  $\beta$ -titanium lattices. Microphotographs of these two-phase regions are shown in Figs. 3 and 4 (Plate XLVIII). At a temperature in the region of  $650^{\circ}$ – $700^{\circ}$  C. the solid solution based on the  $\beta$ -titanium lattice undergoes a eutectoid transformation, and is replaced by a solid solution based on the low-temperature hexagonal form of titanium and the compound.

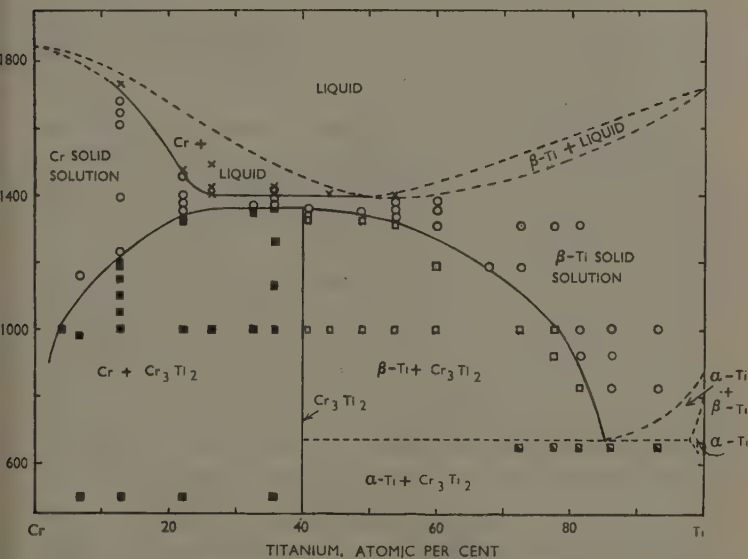


FIG. 2.—The Constitutional Diagram of the Chromium-Titanium System.

In the small region of temperature lying between  $1360^{\circ}$  and  $1400^{\circ}$  C. the elements chromium and titanium appear to be completely soluble in one another.

### 1. The Intermetallic Compound.

The only intermetallic compound formed between chromium and titanium has a composition close to 40 at.-% titanium, and has, therefore, been assigned the formula  $\text{Cr}_3\text{Ti}_2$ . In the preparation of alloys by arc melting, however, it is not possible to control the composition of the alloys within close limits, and an alloy consisting wholly of the compound has not yet been produced. There are several more complicated formulæ which would correspond with a composition of about

40 at.-% titanium, and it is possible that one of them will later prove to be more appropriate to the compound. Until further work is done, however, the simplest formula,  $\text{Cr}_3\text{Ti}_2$ , will be used.

The compound appears to have a very restricted composition range; no appreciable difference in its lattice parameter has been observed in samples from the  $(\text{Cr} + \text{Cr}_3\text{Ti}_2)$  and  $(\beta\text{-Ti} + \text{Cr}_3\text{Ti}_2)$  two-phase regions. It is hard and brittle, as would be expected. An alloy containing 35.7 at.-% titanium, which consists principally of the compound, gave a mean Vickers diamond pyramid hardness value of about 760, although the material tended to break up under the indenter, and the readings were widely scattered.

The crystal structure of the compound is complex, and has not been worked out. The X-ray powder photograph showed a large number of lines, many of which were too faint to be identified positively, but the principal lines on a photograph taken with filtered chromium radiation correspond with the following Bragg angles:  $28.2^\circ$ ,  $30.0^\circ$ ,  $33.8^\circ$ ,  $34.4^\circ$ ,  $35.6^\circ$ ,  $57.5^\circ$ ,  $59.8^\circ$ ,  $64.6^\circ$ , and  $69.8^\circ$ .

The compound is clearly distinguishable in the microstructures of chromium-titanium alloys by the fact that after etching electrolytically in alkaline potassium ferricyanide it appears coloured. The colour assumed may be any of the range of interference colours shown by thin films, and depends on the etching time. The titanium-rich solutions are not affected by the etch, and the chromium-rich solution only on prolonged etching. The coloured film formed on the chromium-rich solution is non-adherent and may be removed by gentle rubbing.

## *2. The Region of Complete Mutual Solubility.*

Although it was evident from the study of the alloys homogenized at  $1000^\circ\text{C}$ . that Vogel and Wenderott's description of the system<sup>1</sup> could not account for the observations at this temperature, it seemed from the appearance of the as-melted specimens, which showed primary dendrites of a solid solution with interdendritic regions of a lamellar material, that a eutectic transformation might occur at a higher temperature. Further examination, however, proved that this could not be the case. It was observed that when an alloy containing 32.7 at.-% titanium, which at  $1355^\circ\text{C}$ . consisted of primary grains of chromium solid solution in a matrix of the compound, was quenched from  $1365^\circ\text{C}$ ., no primary chromium solid solution remained. This is illustrated in Figs. 5 and 6 (Plate XLVIII), which show respectively the structure of the alloy after quenching from  $1355^\circ\text{C}$ . and that of the same alloy quenched from  $1365^\circ\text{C}$ . It will be observed that after quenching from  $1365^\circ\text{C}$ . the alloy consists entirely of a lamellar material. If on heating

to 1365° C. the alloy had passed into the region just below a eutectic horizontal at 1400° C., it would have consisted of the two components of the eutectic, one of which would have been the chromium solid solution. The primary grains of the chromium solid solution would, therefore, be expected to remain. The small rounded light particles in Fig. 6 are thought to be due to gas contamination and will be discussed in Section V.

The author also observed that the X-ray photographs of all the alloys of composition between about 30 and 60 at.-% titanium after quenching from 1360° C. showed only the lines of the intermetallic compound. This provided additional evidence that the lamellar structure seen in the quenched specimens was not associated with the eutectic postulated by Vogel and Wenderott, since the compound  $\text{Cr}_3\text{Ti}_2$  could not be the high-titanium component of a eutectic having a eutectic point at 43% titanium. These lamellar structures which appeared uniformly over the specimens containing from 32 to 47.0 at.-% titanium quenched from temperatures between 1360° and 1390° C. and which differed only in the relative widths of the dark-etching and light-etching lamellæ, led to the belief that the specimens had been quenched from a single-phase region, and that the observed structure was formed only on quenching. It was later found that by carrying out the quenching operations in the vacuum quenching furnace with the greatest possible speed, the breakdown of the single phase could be suppressed except in the grain boundaries (cf. Fig. 7, Plate XLIX). X-ray photographs showed that specimens in which the high-temperature structure was retained had body-centred cubic lattices with parameters between those of pure chromium and  $\beta$ -titanium. The existence of the region of complete mutual solubility was therefore established.

The eutectic-like appearance of the microstructures of some of the as-melted specimens, which probably misled the earlier workers, can be explained quite simply in terms of Fig. 2. When a high-chromium alloy solidifies from the melt, it forms a severely cored solid solution, the first-formed dendrites containing very much less titanium than the material which is last to solidify. If the cooling process is fairly rapid, the solution richest in chromium will be retained at room temperature, and will appear as primary dendrites in the as-melted alloys. The interdendritic titanium-rich material can be retained in the high-temperature form only if the cooling is very rapid indeed, and in normal rapid cooling it will break up to form lamellæ of  $\text{Cr}_3\text{Ti}_2$  which have an appearance similar to that of a eutectic. The process is similar for alloys at the other end of the system, but in this case the primary dendrites are titanium-rich.

The appearance of lines of the compound only, in X-ray photographs of specimens that have lamellar-type transformed structures, is accounted for by the fact that the composition of the body-centred cubic material which remains after the formation of the compound is undoubtedly far from uniform, and any lines given by this material would be expected to be so diffuse as to be indistinguishable from the rather heavy background.

### 3. *The Solidus of the Chromium-Rich Alloys.*

It has been possible to discover something of the nature of the solidus for the chromium-rich alloys by observing the first signs of incipient melting in specimens quenched from successively higher temperatures. The curve thus obtained drops sharply from the melting point of chromium, which has been found in the author's laboratory to be  $1840^{\circ} \pm 10^{\circ}$  C., to about  $1400^{\circ}$  C. at 25 at.-% titanium. At this composition it turns sharply, becoming almost horizontal, and continues thus to 48 at.-% titanium, the highest titanium content studied.

The shape of this curve is similar to that formed by a combination of the usual type of solidus curve and a eutectic or peritectic horizontal at  $1400^{\circ}$  C., and was probably a major cause of the belief in the existence of a eutectic at this temperature.

### 4. *The Liquidus Curve.*

The reactive nature of titanium alloys in the liquid state has prevented the study of the liquidus by thermal analysis. The position of the minimum in the liquidus curve can be obtained, however, from the arc-melted alloys. An alloy of the composition at which the minimum occurs would solidify at a single temperature as does a pure metal, and coring would not occur. Thus just below the freezing point the alloy would consist of a uniform solid solution, which on cooling would break up and precipitate the compound  $\text{Cr}_3\text{Ti}_2$  uniformly over the whole structure. In the microsection of such an alloy, no dendritic material would be visible. In alloys with compositions lying on either side of the minimum, the first material to solidify would be sufficiently rich in either chromium or titanium to be retained on cooling, and it would appear in the microstructure of the as-melted alloy as a dendritic pattern of light-etching material.

Examination of the microstructures of a series of alloys after melting in the arc furnace shows that the minimum must lie between 48.7 and 53.5 at.-% titanium, and it is reasonable to suppose that it is, in fact, 50 at.-%.

## PHOTOMICROGRAPHS OF CHROMIUM-TITANIUM ALLOYS.

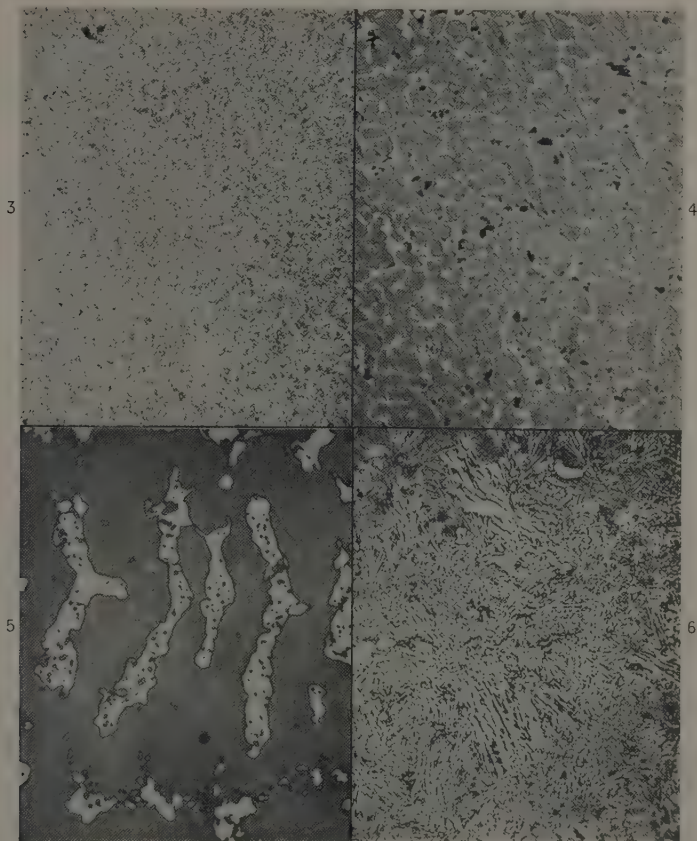


FIG. 3.—22.2 at.-% Ti alloy quenched from 1000° C. Cr solid solution +  $\text{Cr}_3\text{Ti}_2$ .  
 × 100.

FIG. 4.—53.7 at.-% Ti alloy quenched from 1000° C.  $\beta$ -Ti solid solution +  $\text{Cr}_3\text{Ti}_2$ .  
 × 100.

FIG. 5.—32.7 at.-% Ti alloy quenched from 1355° C.  $\text{Cr}_3\text{Ti}_2$  + primary grains of  
 Cr solid solution. × 500.

FIG. 6.—32.7 at.-% Ti alloy quenched from 1365° C. Decomposed single phase.  
 × 500.

All specimens have been electrolytically etched in alkaline 10% potassium  
 ferricyanide solution unless otherwise stated.



## PHOTOMICROGRAPHS OF CHROMIUM-TITANIUM ALLOYS.

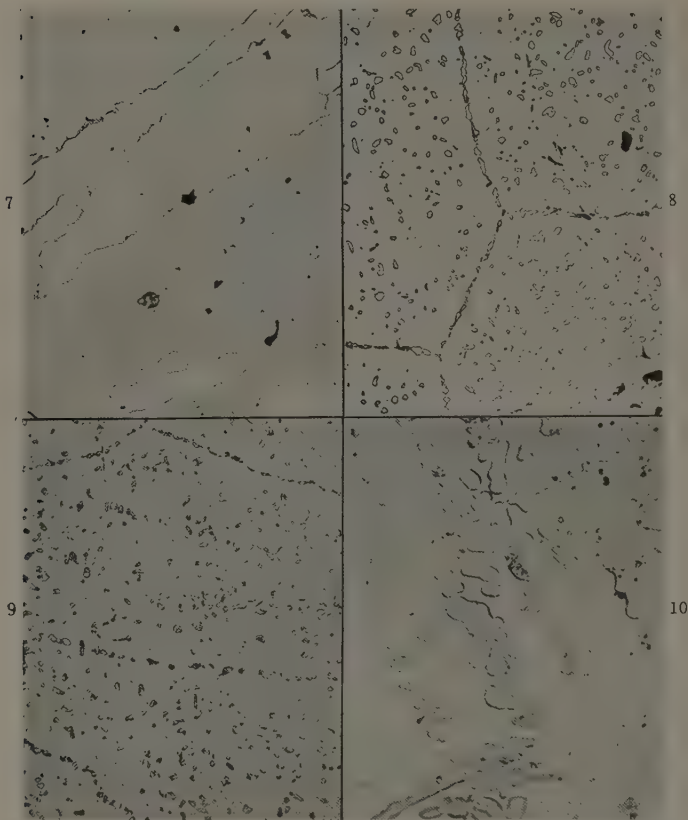


FIG. 7.—32.7 at.-% Ti alloy very rapidly quenched from 1360° C. Single phase, showing beginning of decomposition in grain boundaries.  $\times 100$ .

FIG. 8.—72.5 at.-% Ti alloy quenched from 1000° C.  $\beta$ -Ti solid solution +  $\text{Cr}_3\text{Ti}_2$ .  $\times 100$ .

FIG. 9.—72.5 at.-% Ti alloy quenched from 650° C.  $\alpha$ -Ti solid solution +  $\text{Cr}_3\text{Ti}_2$ .  $\times 100$ .

FIG. 10.—67.6 at.-% Ti alloy badly gas-contaminated, quenched from 1340° C. Unetched.  $\times 500$ .

All specimens have been electrolytically etched in alkaline 10% potassium ferricyanide solution unless otherwise stated.

### 5. The Titanium-Rich Alloys.

Recent work by (A. D.) McQuillan<sup>3</sup> has shown that the impurities present in titanium prepared by magnesium-reduction have a very marked effect on the phase transformations that occur in this metal. The high-titanium part of the system has not, therefore, been studied in detail.

The existence of a eutectoid line lying in the region 650°–700° C. has been established. On passing through this temperature region the  $\beta$ -titanium body-centred cubic solid solution breaks down to form the hexagonal solid solution based on  $\alpha$ -titanium and  $\text{Cr}_3\text{Ti}_2$ . This is illustrated in Figs. 8 and 9 (Plate XLIX). Fig. 8 shows an alloy containing 72.5 at.-% titanium after homogenization at 1000° C. and shows  $\text{Cr}_3\text{Ti}_2$  in a matrix of the  $\beta$ -titanium solid solution. Fig. 9 shows the same alloy after prolonged heating at 650° C. in which the breakdown of the  $\beta$ -titanium and the precipitation of  $\text{Cr}_3\text{Ti}_2$  is clearly seen.

The direction of the phase boundary between the  $\beta$ -titanium solid solution and the ( $\beta$ -Ti +  $\text{Cr}_3\text{Ti}_2$ ) two-phase region indicates that the eutectoid composition is probably about 85 at.-% titanium. The appearance of three-phase regions in these alloys prevents a more precise investigation of the eutectoid temperature and composition using magnesium-reduced titanium. The high-titanium region of the chromium-titanium system is being investigated in greater detail by (A. D.) McQuillan, using van Arkel material.

### V.—GAS CONTAMINATION OF CHROMIUM-TITANIUM ALLOYS.

A few small rounded particles of a very hard white phase frequently appeared in the alloys studied in this work. The author observed that in an alloy lying in the  $\beta$ -titanium solid solution region, which had been accidentally contaminated owing to a vacuum leak, similar particles appeared in much greater quantity and arranged on crystallographic planes, as Fig. 10 (Plate XLIX) shows. They did not appear in the grain boundaries. The two facts (a) that these particles were very similar to those of  $\alpha$ -titanium which have grown out of  $\beta$ -titanium, and (b) that it is a characteristic of the transformation of  $\beta \rightarrow \alpha$  titanium that the process begins on crystal planes in the centres of the grains and not at the grain boundaries, have led to the development of an explanation of the mechanism of gas contamination of chromium-titanium alloys.

It is known that oxygen and nitrogen are very soluble in  $\alpha$ -titanium, but less soluble in  $\beta$ -titanium. This is directly related to the fact that the interstices in the body-centred cubic lattice of  $\beta$ -titanium are too

small to accommodate the gas atoms readily, whereas those in the hexagonal lattice of  $\alpha$ -titanium are large enough to allow extensive take-up of gases. The effect of gas contamination on unalloyed titanium is, therefore, to raise the transformation temperature. The solution of chromium in  $\beta$ -titanium results in a decrease in lattice parameter, and hence a decrease in the size of the already small interstices. It is to be expected that oxygen and nitrogen would, consequently, be even less soluble in the chromium-titanium solid solution than in pure  $\beta$ -titanium, and that the effect of the gases on the transformation temperature of these alloys would be more marked.

The mechanism visualized, therefore, for the process of gas contamination which occurs when these alloys are heated at a temperature in the  $\beta$ -titanium solid solution region, is as follows. The gases first entering the specimen will quickly diffuse through the  $\beta$  lattice, since the diffusion rate is high when the solubility is low, and the gas concentration in the lattice will eventually reach its saturation value for the temperature in question. This means, in effect, that the concentration of gas present at this stage is sufficiently great to raise the transformation temperature to that at which the material is being heated, and the entrance of further gas into the metal results in the precipitation of the  $\alpha$  phase. Since the  $\beta$  phase is already saturated, the gases will not readily diffuse into the alloy, and the precipitation of  $\alpha$  will occur at the surface. A layer of the  $\alpha$  phase, which will thicken as the process of gas contamination proceeds, will thus be built up around the outside of the heated specimen. The diffusion rate of oxygen and nitrogen through  $\alpha$ -titanium is quite slow and though, if heated indefinitely, the whole specimen will eventually transform to  $\alpha$ , the rate of consumption of  $\beta$  by  $\alpha$  does not appear to be great.

Experimental confirmation of this view of the gas-contamination process has been obtained by examining a series of specimens containing about 80 at.-% titanium heated *in vacuo* at temperatures between 650° and 1000° C. for a period of some six weeks. It was expected that after so long an annealing period the specimens would show some increase in hardness owing to unavoidable gas contamination. In fact, the Vickers pyramid hardness values for the specimens were found to have decreased by some 10 points. Examination of the microstructure revealed the presence, round the outer surface of each specimen, of a layer of a hard white material, which broke up at a short distance from the surface to form rounded particles arranged apparently on crystallographic planes. The centres of the specimens were substantially free from the hard phase. It may prove, for practical purposes, that the  $\beta$  phase can be protected from gas contamination by an outer layer

of the  $\alpha$  phase which would be formed automatically when contamination begins. Such a coating would have considerable advantages over other types of surface protection in being completely adherent and very hard.

The presence of the rounded particles which occur throughout the structure in quenched alloys can be accounted for by the same mechanism. The solubility of gases in the  $\beta$  lattice increases with temperature. On quenching from high temperatures, therefore, the  $\beta$  phase suddenly becomes supersaturated, and precipitates out sufficient of the  $\alpha$  phase to accommodate the excess gas. The precipitated  $\alpha$  phase appears as very small particles, which tend to be arranged on crystallographic planes. Fig. 10 (Plate XLIX) illustrates an alloy in which the gas contamination is severe. Under normal experimental conditions, however, the amount of gas present in the  $\beta$  phase at the high temperatures is small, and only occasional scattered particles of the precipitated  $\alpha$  phase, such as those observed in Fig. 6 (Plate XLVIII), appear in the quenched specimen.

Particles similar to those of Fig. 6 have been observed in quenched alloys with compositions varying almost over the whole range of the chromium-titanium system. In high-chromium alloys, the particles are always associated with the titanium-rich phase. Since, at high temperatures, the  $\beta$ -titanium solid solution extends over the whole composition range, it is very probable that the mechanism described operates even at the chromium-rich end of the system.

## VI.—DISCUSSION OF RESULTS.

The existence of a region of complete mutual solubility in the chromium-titanium system is rather surprising in view of the fact that the difference in the atomic diameters of the two elements is close to the 15% limit laid down by Hume-Rothery for the appreciable solubility of one element in the other. The temperature at which complete solubility occurs, however, is very high, and assimilation of foreign atoms by the lattice must be greatly facilitated by the thermal motion of the atoms. This would explain the breakdown of the solid solution and the formation of the compound which occurs on quenching.

No evidence for Vogel and Wenderott's compound  $\text{Cr}_2\text{Ti}_3$  has been found. The alloy with the composition corresponding to this compound showed, in the as-melted condition, primary dendrites of a solid solution and interdendritic material of a lamellar structure, and after homogenizing at  $1000^\circ\text{C}$ . it consisted of about equal proportions of two phases subsequently identified as  $\text{Cr}_3\text{Ti}_2$  and the  $\beta$ -titanium solid solution.

From the practical point of view, the system offers interesting possibilities. Alloys based on the  $\beta$ -titanium solid solution are strong and tough, and appear to operate a self-gettering mechanism which prevents severe hardening of the body-centred cubic matrix by gas contamination. Their Vickers diamond pyramid hardness values lie between 350 and 370. They can withstand a certain amount of cold work, can be hot worked fairly easily, and, although difficult to saw, they can be machined. Since such alloys contain only 10–30% chromium, they have most of the advantages of titanium's low density, without the disadvantages of its hexagonal structure. The rapid change with temperature in the solubility of chromium in  $\beta$ -titanium makes it possible to produce an alloy containing a precipitate of the hard compound finely dispersed in the ductile matrix. Such an alloy should have desirable mechanical properties.

#### VII.—CONCLUSION.

This work has established the type of binary system formed by the metals chromium and titanium, and provides a basis for the consideration of chromium-titanium alloys that can be used as engineering materials. From the scientific point of view it is to be hoped that, when the positions of the phase boundaries are fixed more exactly, the chromium-titanium system will help to throw light on the nature of the binding forces in transition metals.

#### ACKNOWLEDGEMENTS.

This work has been carried out as part of the research programme of the Aeronautical Research Laboratory, Australian Department of Supply, Melbourne.

The chromium used was prepared by Mr. H. T. Greenaway of that laboratory, to whom the author's thanks are due.

#### REFERENCES.

1. R. Vogel and B. Wenderott, *Arch. Eisenhüttenwesen*, 1940, **14**, 279.
2. D. J. McPherson and M. G. Fontana, *Metal Progress*, 1949, **55**, 366.
3. A. D. McQuillan, *J. Inst. Metals*, 1950–51, **78**, 249.

# AN X-RAY STUDY OF THE PHASES IN THE 1313 COPPER-TITANIUM SYSTEM.\*

By NILS KARLSSON.†

## SYNOPSIS.

The copper-titanium system has been investigated by X-ray methods and from powder photographs the general outline of the phase diagram has been drawn. Four intermediate phases with the following approximate titanium contents have been found:  $\beta$  and  $\beta'$ , 21-25 at.-%;  $\gamma$ , 50-53 at.-%;  $\delta$ , 45-50 at.-%; and  $\epsilon$ , 71-75 at.-%. The structure of each phase has been determined.

The  $\beta$  phase has an orthorhombic structure with the ideal composition  $\text{Cu}_3\text{Ti}$ . The structure corresponds to an ordered distribution of the copper and titanium atoms in a slightly deformed hexagonal close-packed lattice. At elevated temperatures the corresponding disordered distribution appears ( $\beta'$  phase). Both the  $\gamma$  and  $\delta$  phases have the ideal formula  $\text{CuTi}$  and have tetragonal symmetry. The structure of the  $\gamma$  phase is of the B11 type and that of the  $\delta$  phase the L10 ( $\text{CuAu}$ ) type. The  $\epsilon$  phase, with the ideal composition  $\text{CuTi}_3$ , also has tetragonal symmetry. The structure may be considered to be of a deformed L12 ( $\text{CuAu}_3$ ) type.

The copper phase dissolves about 6.5 at.-% titanium. No solubility of copper in  $\alpha$ -titanium could be detected. The phase reported by Laves and Wallbaum as having the composition  $\text{CuTi}_2$  has been shown to be  $\text{Cu}_3\text{Ti}_3\text{O}$ , with a structure analogous to that of the carbide  $\text{Fe}_3\text{W}_3\text{C}$ , found in high-speed steel.

## I.—PREVIOUS WORK.

THERE are only a few references to the binary copper-titanium system in the literature, and no complete structure determinations have been published. In 1931 Kroll<sup>1</sup> and Hensel and Larsen<sup>2</sup> experimentally determined the liquidus and solidus curves and published tentative constitutional diagrams up to about 25 wt.-% titanium. Hensel and Larsen reported that X-ray investigations did not give any information about the phase in equilibrium with the copper phase. In two publications on the crystal chemistry of titanium alloys and the alloy chemistry of transition metals, Laves and Wallbaum<sup>3,4</sup> mention that  $\text{Cu}_3\text{Ti}$  has deformed hexagonal close-packing with an ordered structure isomorphous with  $\text{Au}_3\text{Ti}$ ,  $\text{Ni}_3\text{Nb}$ , and  $\text{Ni}_3\text{Ta}$ . They also state that no compound  $\text{CuTi}$  exists, although they found some evidence of a phase near 50 at.-%. They also report that the intermediate phase richest in titanium is  $\text{CuTi}_2$ , isomorphous with  $\text{MnTi}_2$ ,  $\text{FeTi}_2$ ,  $\text{CoTi}_2$ , and  $\text{NiTi}_2$ , which are all face-centred cubic, with 96 atoms per unit cell. No further details are given of the intermediate phases in the system. In 1950 Craighead,

\* Manuscript received 28 December 1950.

† Institute of Chemistry, University of Uppsala, Sweden.



Simmons, and Eastwood <sup>5</sup> published a constitutional diagram between the  $\alpha \rightleftharpoons \beta$  transition point of titanium, and a copper content of about 5 wt.-%.

## II.—EXPERIMENTAL METHODS.

The alloys were prepared from electrolytic copper (Schering-Kahlbaum, *pro analysi*) and titanium hydride (Metal Hydride Corp., Grade R) which was degassed *in vacuo* at a final temperature just below the melting point of pure titanium. The finely powdered metals were carefully mixed, and moulded into tablets. Specimens with a weight of 0.5–1.0 g. were melted in zirconia crucibles in a high-frequency vacuum induction furnace <sup>6</sup> under a pressure of  $10^{-4}$ – $10^{-3}$  mm. mercury. No reaction was noticed between the crucible and melt. Samples were heat-treated by sealing in evacuated silica tubes maintained at various temperatures up to 1200° C. and quenched in cold water. These treatments were not always possible at temperatures above 800° C., however, as reactions between the specimen and the silica tube often occurred. Sometimes fine cracks were found in the walls of the tubes.

The phase analysis and structure determinations were made from powder photographs taken with Cu  $K_\alpha$  radiation on a Guinier-type camera using a bent quartz monochromator. For measurements of the high-angle reflections and for intensity determinations, additional photographs were taken with Phragmén-type focusing cameras. The intensities of the reflections were visually estimated, starting from 4 : 2 : 1 as the relative values of the intensities of Cu  $K_{\alpha_1}$ ,  $K_{\alpha_2}$ , and  $K_\beta$  lines. Relative values of  $p|F|^2$  were calculated by means of the expression, given by Hägg and Regnström : <sup>7</sup>

$$I = c \cdot \frac{\lambda^3}{\mu} \cdot \frac{1 + \cos^2 2\theta}{\sin^2 \theta \cdot \cos \theta} \cdot \frac{1}{\sin(2\theta - \alpha) + \sin \alpha} \cdot A_a \cdot A_p \cdot A_f \cdot p|F|^2,$$

in which the absorption factors of the cameras and the film have been taken into consideration. For a given wave-length, camera, and preparation, all factors preceding  $p$  will be functions of  $\theta$  only. Observed and calculated values of  $p|F|^2$  are given in Tables I–VIII.

Single crystals could not be obtained of any of the intermediate phases.

## III.—THE COMPOSITIONS OF THE PHASES.

The results obtained from the powder-photograph analysis showed the existence of four intermediate phases in the system :  $\beta$ ,  $\gamma$ ,  $\delta$ , and  $\epsilon$ . There is a disordered ( $\beta'$ ) as well as an ordered ( $\beta$ ) structure.

As stated above, difficulties were encountered with the heat-treatments at temperatures above 800° C., especially when the titanium content exceeded 25 at.-%. The main cause of the difficulties was a

reaction between titanium and silica, which gave rise to phases containing silicon and oxygen. As a result phases were found belonging to the copper-silicon (the  $\beta$  and  $\gamma$  phases according to Arrhenius and Westgren<sup>9</sup>), titanium-oxygen, and copper-titanium-oxygen systems. One phase belonging to the last-named system was face-centred cubic with a lattice constant varying from 11.24 to 11.44 Å. It was found to have the ideal composition  $\text{Cu}_3\text{Ti}_3\text{O}$  and to be isomorphous with the carbide  $\text{Fe}_3\text{W}_3\text{C}$ , that occurs in high-speed steel.<sup>8</sup>  $\text{Cu}_3\text{Ti}_3\text{O}$  can dissolve titanium by substitution and the titanium-rich solubility limit probably

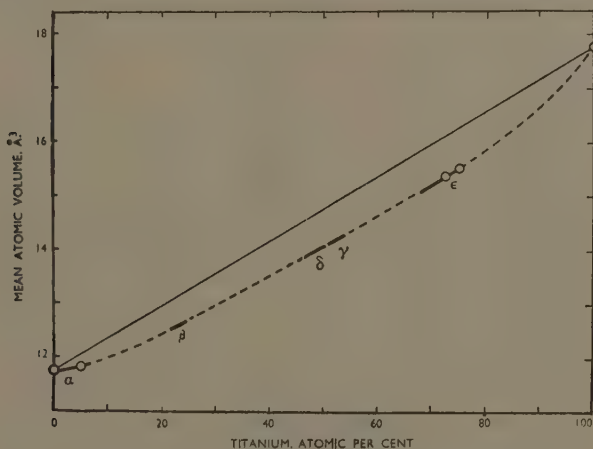


FIG. 1.—Variation of Mean Atomic Volume with Atomic Composition.

lies close to  $\text{Cu}_2\text{Ti}_4\text{O}$ . Evidently, the phase reported by Laves and Wallbaum<sup>3,4</sup> as face-centred cubic with the composition  $\text{CuTi}_2$  and 96 atoms per unit cell, is in fact this oxide phase. During studies on Me-Ti-O systems (Me being a transition element), other oxide phases analogous to  $\text{Cu}_3\text{Ti}_3\text{O}$  have been found to form. The phases  $\text{MnTi}_2$ ,  $\text{FeTi}_2$ ,  $\text{CoTi}_2$ , and  $\text{NiTi}_2$  reported by Laves and Wallbaum are probably identical with these oxide phases. A detailed report of this work will be published later.

As prolonged heat-treatments above 800° C. were rendered difficult by this reaction and equilibrium was often attained very slowly at temperatures below 800° C., there was great uncertainty in the determination of the homogeneity ranges of the copper-titanium phases. From the photographs only one phase appeared to be nearly pure,

the  $\epsilon$  phase. (It should be emphasized, however, that even in this case very weak lines from phases not belonging to the copper-titanium system were visible.) Thus only three fairly reliable points, besides the two for the pure components have been recorded in Fig. 1, in which composition has been plotted against the mean atomic volume. One point has been plotted for the  $\alpha$  phase with dissolved titanium and two for the  $\epsilon$  phase. The straight line drawn between pure copper and pure  $\alpha$ -titanium in accordance with Vegard's law shows that the observed volumes are obviously smaller than the volumes calculated

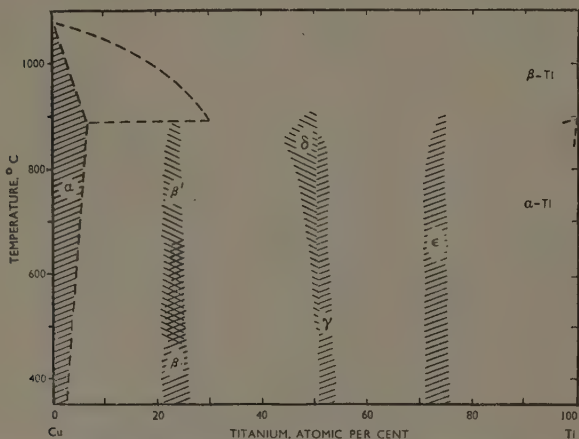


FIG. 2.—General Outline of the Phase Diagram of the Copper-Titanium System. Broken lines indicate the results of other workers (see text).

according to this law. A broken line has been drawn through the five points. The values of the smallest and the largest observed mean atomic volumes of the  $\beta$ ,  $\gamma$ , and  $\delta$  phases have been assumed to lie on this curve, from which the approximate values of the boundaries of the phases have been obtained. This may introduce some errors, but the appearance of the diffraction patterns in the powder photographs showed relatively good agreement with the results obtained by this method. Under the existing circumstances, there was no other way to determine the compositions of the phases. The "ideal compositions", which correspond to the different structures, were also found to lie within the homogeneity ranges determined in this way. From the values obtained from Fig. 1, and the results of the phase analysis by

powder photographs of the specimens that had been heat-treated at different temperatures and quenched, a general outline of the phase diagram has been drawn (Fig. 2). The results of Kroll's,<sup>1</sup> and Hensel and Larsen's<sup>2</sup> investigations of the copper-rich alloys are shown by the broken curves in the diagram, and the results obtained by Craighead, Simmons, and Eastwood<sup>5</sup> on the titanium-rich alloys at temperatures close to the  $\alpha \rightleftharpoons \beta$  transition point of titanium, are similarly shown.

#### IV.—THE STRUCTURE OF THE PHASES.

##### 1. The $\alpha$ Phase.

For pure copper the axial length  $a = 3.609 \text{ \AA}$ . ( $V = 47.01 \text{ \AA}^3$ )\* was determined. The greatest axial length measured for the  $\alpha$  phase was  $a = 3.620 \text{ \AA}$ . ( $V = 47.44 \text{ \AA}^3$ ). If Vegard's law is assumed to apply over the whole composition range from pure copper to pure  $\alpha$ -titanium, this value should correspond to a maximum solubility of 2.0 at.-% titanium. The solubility value is contradicted, however, by the fact that an alloy containing 5.0 at.-% titanium, quenched from  $800^\circ \text{C}$ ., showed the axial length  $a = 3.616 \text{ \AA}$ . ( $V = 27.28 \text{ \AA}^3$ ). This implies a relative contraction  $\Delta V/V = 1.9\%$ . If the same relative contraction is assumed to prevail up to the solubility limit,  $a = 3.620 \text{ \AA}$ . corresponds to a maximum solubility of 6.5 at.-% titanium in the  $\alpha$  phase. Hensel and Larsen<sup>2</sup> indicated a solubility of 5–6.5 at.-% at the eutectic temperature ( $878^\circ \text{C}$ .), but they obtained  $a = 3.61 \text{ \AA}$ . for pure copper and  $a = 3.66 \text{ \AA}$ . for the saturated  $\alpha$  phase. The latter value is remarkably high and suggests a volume increase of 0.6%.

##### 2. The $\beta'$ Phase.

Reflections from this phase appeared faintly in photographs taken with a specimen that contained 8 at.-% titanium. Maximum intensity of the reflections was obtained with a titanium content of about 25 at.-%. Complete equilibrium between this phase and the  $\alpha$  phase could not be obtained. Even samples which had been heat-treated at  $400^\circ$ ,  $600^\circ$ ,  $700^\circ$ , and  $800^\circ \text{C}$ ., for several weeks showed clearly visible copper reflections in the photographs.

The unit cell is orthorhombic with the smallest and largest axial lengths  $a = 2.572$ ,  $b = 4.503$ ,  $c = 4.313 \text{ \AA}$ . ( $V = 49.95 \text{ \AA}^3$ ) and  $a = 2.585$ ,  $b = 4.527$ ,  $c = 4.351 \text{ \AA}$ . ( $V = 50.92 \text{ \AA}^3$ ), respectively. With four atoms in the unit cell these values, according to Fig. 1, give the boundaries at 21 and 25 at.-% titanium for the  $\beta'$ -phase field. The density calculated for an alloy containing 25 at.-% titanium is 7.91, in good agreement with the observed value of 7.75.

\* All values are given in true Ångström units.  $1 \text{ \AA} = 10^{-8} \text{ cm.} = 1/1.00202 \text{ kX. units.}$

The cell evidently corresponds to a slightly deformed close-packed hexagonal lattice. As a comparison it may be mentioned that the orthohexagonal cell with the same volume as the above actual cell at the composition 25 at.-% titanium, should have the axial lengths  $a = 2.62$ ,  $b = 4.53$ , and  $c = 4.27$  Å. The  $a$ -axis has thus been shortened a little, while the  $c$ -axis has been lengthened. The  $\beta'$  phase appears to be isomorphous with the  $\epsilon'$  phases in the silver-tin<sup>10</sup> and silver-antimony<sup>11, 12</sup> systems in which the ideal compositions are  $\text{Ag}_3\text{Sn}$  and  $\text{Ag}_3\text{Sb}$ . Between the silver phase and the  $\epsilon'$  phase in these two systems there appears a hexagonal close-packed phase,  $\epsilon$ , which at a lower silver content is deformed into the orthorhombic  $\epsilon'$  phase. No similar transition seems to exist in the copper-titanium system.

The  $hkl$  reflections were observed only for  $h + k = 2n$ ,  $0kl$  for  $k = 2n$ ,  $h0l$  for  $h = 2n$  and  $l = 2n$ , and  $hk0$  for  $h + k = 2n$ . Thus the probable space-groups are  $D_{2h}^{17}-Cmcm$ ,  $C_{2v}^{12}-Cmc$ , and  $C_{2n}^{16}-Ama$ .\* The only possible positions for the four metal atoms are:

(a) In  $C_{2v}^{12}-Cmc$ , the four-fold position 4 (a):  $0, y, z$ ;  $0, \bar{y}, \frac{1}{2} + z$ ;  $\frac{1}{2}, \frac{1}{2} + y, z$ ;  $\frac{1}{2}, \frac{1}{2} - y, \frac{1}{2} + z$ .

(b) In  $D_{2h}^{17}-Cmcm$ , the four-fold position 4 (c):  $0y\frac{1}{4}$ ;  $0\bar{y}\frac{3}{4}$ ;  $\frac{1}{2}, \frac{1}{2} + y, \frac{1}{4}$ ;  $\frac{1}{2}, \frac{1}{2} - y, \frac{3}{4}$ .

From space considerations  $C_{2v}^{12}-Cmc$  should have  $z = \frac{1}{4}$ , and this value proves to give the best agreement between observed and calculated  $p|F|^2$  values for the  $h0l$  reflections. It implies an increase of the symmetry in the space-group  $D_{2h}^{17}-Cmcm$ . The limits for the

TABLE I.—*The Limits for the Parameter of the  $\beta'$  Phase.*

<i>hkl</i>	Intensity, $p F ^2$						
	Observed	Calculated					
		$y = 0.330$	$y = 0.335$	$y = 0.340$	$y = 0.345$	$y = 0.350$	$y = 0.355$
020	10	19	15	12	9	6	4
110	35	28	31	35	38	42	45
130	25	22	22	21	21	20	18
200	10	11	11	11	11	11	11

parameter  $y$  are given in Table I. The best agreement is obtained for  $y = 0.345$ . In Table II the  $p|F|^2$  values, calculated for this parameter, are compared with the observed values.

\* Notations are according to the "Internationale Tabellen zur Bestimmung von Kristallstrukturen," Berlin. 1935.

TABLE II.—*Observed and Calculated Values of Reflection Angle and Intensity for  $\beta$  and  $\beta'$  Phases.*

<i>hkl</i>		Radiation Cu <i>K</i>	Reflection Angle, $\sin^2 \theta$		Intensity, $p F ^2$	
$\beta'$ Phase Orientation <i>Cmcm</i>	$\beta$ Phase Orientation <i>Pmmn</i>		Observed	Calculated	Observed	Calculated
...	001	<i>a</i>	0.0289	0.0287	1	0.6
...	101	<i>a</i>	0.0512	0.0513	2	1.5
...	110	<i>a</i>	0.0541	0.0538	2	2.0
...	011	<i>a</i>	0.0606	0.0604	1	1.2
...	111	<i>a</i>	0.0823	0.0827	1	0.7
...	200	<i>a</i>	...	0.0890	0	0.2
020	002	<i>a</i>	0.1157	0.1156	10	9.2
110	201	<i>a</i>	0.1178	0.1179	35	38
002	020	<i>a</i>	0.1259	0.1260	55	58
...	102	<i>a</i>	...	0.1380	0	0.5
021	012	<i>a</i>	0.1472	0.1471	80	80
111	211	<i>a</i>	0.1494	0.1494	130	128
...	021	<i>a</i>	...	0.1549	0	0.2
...	112	<i>a</i>	...	0.1694	0	0.1
...	121	<i>a</i>	...	0.1772	0	0.6
...	202	<i>a</i>	...	0.2046	0	0.0
...	220	<i>a</i>	...	0.2150	0	0.2
...	301	<i>a</i>	...	0.2292	0	0.2
...	310	<i>a</i>	...	0.2318	0	0.3
...	212	<i>a</i>	0.2355	0.2361	1	0.4
022	022	<i>a</i>	0.2416	0.2416	6	5.6
112	221	<i>a</i>	0.2433	0.2437	25	24
...	003	<i>a</i>	...	0.2601	0	0.0
...	311	<i>a</i>	...	0.2605	0	0.0
...	122	<i>a</i>	0.2645	0.2639	1	0.4
...	103	<i>a</i>	...	0.2824	0	0.0
...	013	<i>a</i>	...	0.2916	0	0.0
...	130	<i>a</i>	...	0.3058	0	0.0
130	203	<i>a</i>	0.3494	0.3491	25	21
200	400	<i>a</i>	0.3558	0.3560	10	11
131	213	<i>a</i>	0.3813	0.3806	1	1.6
023	032	<i>a</i>	0.3991	0.3991	15	15
113	231	<i>a</i>	0.4009	0.4014	25	24
040	004	<i>a</i>	0.4624	0.4624	6	3.6
220	402	<i>a</i>	0.4716	0.4716	1	2.0
132	223	<i>a</i>	0.4749	0.4751	25	26
202	420	<i>a</i>	0.4822	0.4820	10	13
041	014	<i>a</i>	0.4943	0.4939	6	6.0
221	412	<i>a</i>	0.5031	0.5031	22	22
004	040	<i>a</i>	0.5037	0.5040	35	6
042	024	<i>a</i> <sub>1</sub>	...	0.5874	0	5.2
222	422	<i>a</i> <sub>1</sub>	...	0.5966	0	2.8
024	042	<i>a</i> <sub>1</sub>	...	0.6186	0	1.6
114	241	<i>a</i> <sub>1</sub>	0.6215	0.6210	6	6.4
133	233	<i>a</i> <sub>1</sub>	...	0.6316	0	1.2
043	034	<i>a</i> <sub>1</sub>	...	0.7446	0	5.2
223	432	<i>a</i> <sub>1</sub>	0.7538	0.7539	15	20
150	205	<i>a</i> <sub>1</sub>	...	0.8101	0	0.4
240	404	<i>a</i> <sub>1</sub>	0.8172	0.8170	4	6.4
310	601	<i>a</i> <sub>1</sub>	0.8286	0.8286	0	4.0
151	215	<i>a</i> <sub>1</sub>	0.8417	0.8416	25	26
241	414	<i>a</i> <sub>1</sub>	0.8479	0.8485	6	12
134	243	<i>a</i> <sub>1</sub>	0.8525	0.8518	25	26
204	440	<i>a</i> <sub>1</sub>	0.8581	0.8586	10	14
025	052	<i>a</i> <sub>1</sub>	0.9021	0.9017	10	14
115	251	<i>a</i> <sub>1</sub>	0.9041	0.9040	25	24

$\beta'$  phase: parameter  $y = 0.345$ .

$\beta$  phase: parameters  $x$ ,  $z_a$ ,  $z_b$ , and  $z_c = 0.250, 0.655, 0.345$ , and  $0.155$ .



The four atoms are distributed at random, and at the composition 25 at.-% titanium, each atom is in contact with twelve others at the distances 2.585 Å. (2 atoms), 2.590 Å. (2 atoms), 2.607 Å. (4 atoms), and 2.673 Å. (4 atoms). In the undeformed orthohexagonal cell mentioned above all distances should be 2.62 Å.

### 3. The $\beta$ Phase.

At lower temperatures the disordered structure ( $\beta'$ ) transforms into an ordered one ( $\beta$ ). Thus very weak superlattice reflections appeared in a photograph obtained from a sample which had been cooled from 600° to 100° C. in 16 weeks at a constant rate of cooling. Owing to the very slow rate of diffusion and the small difference in scattering powers between copper and titanium atoms, the  $\beta \rightleftharpoons \beta'$  transition interval could not be determined with any accuracy.

The positions of the reflections showed that the  $a$ -axis of the disordered structure is doubled when ordering occurs, but that the other axes remain the same.

With the exception of  $h0l$  reflections with  $h - l = 2n - 1$ , all the  $hkl$  reflections appeared. Thus the probable space-groups are  $C_{2v}^2 - Pmn$  and  $D_{3d}^{15} - Pm\bar{m}n$ . If no regard is paid to the difference between the copper and titanium atoms, they occupy the same positions as in the disordered cell. The only possible space-group is then  $D_{3d}^{15} - Pm\bar{m}n$  with the following positions:

$$2 (a): 00z; \frac{1}{2}\frac{1}{2}\bar{z}.$$

$$2 (b): 0\frac{1}{2}z; \frac{1}{2}0\bar{z}.$$

$$4 (f): x0z; \bar{x}0z; \frac{1}{2} + x, \frac{1}{2}, \bar{z}; \frac{1}{2} - x, \frac{1}{2}, \bar{z}.*$$

The two titanium atoms may be arbitrarily placed in either 2 (a) or 2 (b). The two-fold position 2 (a) has been chosen and the six copper atoms are then placed in 2 (b) - 4 (f). Since the  $a$ -axis has been doubled the  $a$ -axis parameter becomes  $x = \frac{1}{4}$ ; further: (the parameter  $y$  of the  $\beta'$  phase in  $D_{3d}^{15} - Cmc$  = 0.345,  $z_2 - z_1 = 1$ , and  $z_2 - z_1 = \frac{1}{2}$ . The resulting values of the parameters thus are:  $x = 0.250$ ,  $z_2 = 0.655$ ,  $z_1 = 0.345$ , and  $z_1' = 0.155$ . The  $\sin^2 F^2$  values calculated by means of these parameters are given in Table II, and the interatomic distances are listed in Table III.

The structure of the isomorphous phase  $\text{Ni}_3\text{Ta}$ ,<sup>2,4,13</sup> for which the superlattice reflections are considerably stronger than in the ordered  $\text{Cu}_3\text{Ti}$  phase, was first determined. The following axial lengths were obtained for an alloy with 25 at.-% tantalum:  $a = 5.114$ ,  $b = 4.250$ .

\* The arrangement in "Internationale Tabellen" is maintained. The  $b$ - and  $c$ -axes in the  $\beta'$  phase are therefore interchanged in the  $\beta$  phase.

and  $c = 4.542 \text{ \AA}$ . ( $V = 98.72 \text{ \AA}^3$ ). In this case the  $z_b$  value was also 0.345. Powder photographs taken with specimens quenched from  $600^\circ$ ,  $900^\circ$ , and  $1200^\circ \text{ C}$ . did not show any disordered structure corresponding to the  $\beta'$  phase in the system CuTi.<sup>14</sup>

TABLE III.—*Interatomic Distances in the  $\beta$  Phase (25 at.-% Titanium).*

Atom	Surrounding Atoms	Interatomic Distance, $\text{\AA}$ .
Ti in 2 (a)	2 Cu in 2 (b)	2.585
	2 Cu in 2 (b)	2.590
	4 Cu in 4 (f)	2.607
	4 Cu in 4 (f)	2.673
Cu in 2 (b)	2 Ti in 2 (a)	2.585
	2 Ti in 2 (a)	2.590
	4 Cu in 4 (f)	2.607
	4 Cu in 4 (f)	2.673
Cu in 4 (f)	2 Ti in 2 (a)	2.607
	2 Ti in 2 (a)	2.673
	2 Cu in 2 (b)	2.607
	2 Cu in 2 (b)	2.673
	2 Cu in 4 (f)	2.585
	2 Cu in 4 (f)	2.590

#### 4. The $\gamma$ Phase.

Sets of reflections from two phases ( $\gamma$ ,  $\delta$ ) appeared in the photographs of alloys with compositions approximately 50% copper, 50% titanium. These could not be entirely isolated from each other. It proved impossible to attain equilibrium in spite of a great variety of heat-treatments. The two phases seemed to exist up to a temperature of about  $900^\circ \text{ C}$ .

The photographs indicated a tetragonal cell for the  $\gamma$  phase. The smallest dimensions observed were  $a = 3.108$ ,  $c = 5.887 \text{ \AA}$ .,  $c/a = 1.894$  ( $V = 56.87 \text{ \AA}^3$ ), and the largest dimensions  $a = 3.118$ ,  $c = 5.921 \text{ \AA}$ .,  $c/a = 1.899$  ( $V = 57.58 \text{ \AA}^3$ ). According to the broken curves in Fig. 1 these volumes correspond to the compositions 50 and 53 at.-% titanium respectively. With four atoms in the unit cell the calculated density is 6.57 (50 at.-% titanium). The observed value was 6.46.

The  $hk0$  reflections, for which  $h + k = 2n + 1$ , are absent, as is characteristic of the space-groups  $C_{4h}^3 - P4/n$  and  $D_{4h}^7 - P4/nmm$ . The two- and four-fold positions are the same in the two groups, and for this reason the latter, with the higher symmetry, has been chosen. From space considerations the only possibility is to place the atoms in two-fold positions 2 (c):  $0\frac{1}{2}z$ ;  $\frac{1}{2}0z$ . In this way a structure of the B11 type is obtained.<sup>15</sup>

TABLE IV.—Observed and Calculated Values of Reflection Angle and Intensity for  $\gamma$  Phase.

$hkl$	Radiation Cu K	Reflection Angle, $\sin^2 \theta$		Intensity, $p F ^2$	
		Observed	Calculated	Observed	Calculated
001	$\alpha$	0.0171	0.0172	13	20
002	$\alpha$	...	0.0686	0	0.7
101	$\alpha$	...	0.0787	0	0.0
110	$\alpha$	0.1234	0.1230	75	67
102	$\alpha$	0.1305	0.1302	125	113
111	$\alpha$	0.1408	0.1402	5	5.3
003	$\alpha$	...	0.1544	0	1.1
112	$\alpha$	...	0.1916	0	0.2
103	$\alpha$	0.2156	0.2159	8	9.5
200	$\alpha$	0.2460	0.2460	30	21
201	$\alpha$	...	0.2632	0	3.0
004	$\alpha$	0.2746	0.2744	13	12
113	$\alpha$	...	0.2774	0	1.5
202	$\alpha$	...	0.3146	0	0.1
211	$\alpha$	...	0.3247	0	0.0
104	$\alpha$	...	0.3359	0	0.2
212	$\alpha$	0.3760	0.3761	50	35
114	$\alpha$	0.3968	0.3974	13	13
203	$\alpha$	...	0.4004	0	0.9
005	$\alpha$	...	0.4288	0	1.3
213	$\alpha$	...	0.4619	0	5.3
105	$\alpha$	...	0.4903	0	2.5
220	$\alpha$	0.4914	0.4920	8	7.0
221	$\alpha$	...	0.5092	0	0.7
204	$\alpha$	0.5210	0.5204	8	8.8
115	$\alpha_1$	...	0.5508	0	4.4
222	$\alpha_1$	...	0.5597	0	0.0
301	$\alpha_1$	...	0.5697	0	0.0
214	$\alpha_1$	...	0.5809	0	0.2
310	$\alpha_1$	0.6143	0.6140	8	12
006	$\alpha_1$	...	0.6163	0	0.1
302	$\alpha_1$	0.6210	0.6211	8	10
311	$\alpha_1$	...	0.6311	0	1.2
223	$\alpha_1$	...	0.6453	0	0.3
205	$\alpha_1$	...	0.6736	0	3.5
106	$\alpha_1$	...	0.7777	0	3.6
312	$\alpha_1$	...	0.6825	0	0.0
303	$\alpha_1$	...	0.7067	0	1.8
215	$\alpha_1$	...	0.7350	0	3.2
116	$\alpha_1$	...	0.7391	0	0.2
224	$\alpha_1$	...	0.7651	0	5.9
313	$\alpha_1$	...	0.7681	0	0.8
321	$\alpha_1$	...	0.8153	0	0.0
304	$\alpha_1$	...	0.8265	0	0.1
007	$\alpha_1$	...	0.8389	0	0.8
206	$\alpha_1$	...	0.8619	0	0.2
322	$\alpha_1$	0.8674	0.8667	13*	19
314	$\alpha_1$	0.8870	0.8879	13	15
107	$\alpha_1$	...	0.9003	0	6.0
225	$\alpha_1$	...	0.9192	0	5.2
216	$\alpha_1$	0.9236	0.9233	13	10

This appears to be the first example which can be classified with any certainty as a *B11*-type structure, as all the compounds originally thought to belong to this group, e.g.  $\text{PbO}$ , have since been shown to have the *B10*-type structure.

If the atoms were distributed at random they should be disposed symmetrically in the two positions with  $z = \frac{1}{8}$  and  $\frac{7}{8}$ , which, however, would imply a unit cell with the *c*-axis halved. Consideration of space, in the actual structure, shows that two copper atoms have to be placed in one of the two-fold positions with  $z_{\text{Cu}} < \frac{1}{8}$  and two titanium atoms in the other with  $z_{\text{Ti}} > \frac{1}{2} + \frac{1}{8}$ . The best intensity agreement and the best distribution in space were obtained for the values  $z_{\text{Cu}} = 0.10$  and  $z_{\text{Ti}} = 0.65$ . Calculated and observed  $p|F|^2$  values are recorded in Table IV, and the values of interatomic distances are found in Table V.

TABLE V.—*Interatomic Distances in the  $\gamma$  Phase (50 at.-% Titanium).*

Atom	Surrounding Atoms	Interatomic Distance, Å.
Cu in 2 ( <i>a</i> )	4 Cu	2.494
	4 Ti	2.645
	1 Ti	2.650
Ti in 2 ( <i>a</i> )	4 Ti	2.820
	4 Cu	2.645
	1 Cu	2.650

### 5. The $\delta$ Phase.

Powder reflections from this phase were obtained mainly from alloys with a composition of about 50 at.-% titanium, that had been quenched from about  $800^\circ\text{C}$ . The photographs indicated that the structure of the  $\delta$  phase is of the *L10* type,<sup>16</sup> i.e. isomorphous with the ordered structure of  $\text{AuCu}$ , although the axial ratio  $c/a$  is much lower than for  $\text{AuCu}$  ( $c/a = 0.935$ ).

The dimensions of the tetragonal cell of the  $\delta$  phase varied from  $a = 4.436$ ,  $c = 2.815$  Å.,  $c/a = 0.635$  ( $V = 55.39$  Å.<sup>3</sup>) to  $a = 4.440$ ,  $c = 2.856$  Å.,  $c/a = 0.643$  ( $V = 56.30$  Å.<sup>3</sup>). From Fig. 1 these values correspond to approximately 45 and 50 at.-% titanium. The limits of the homogeneity range of the phase are, therefore, probably situated near these composition values. When the titanium content is increased, the *c*-axis becomes longer, while the *a*-axis remains practically constant. With four atoms in the unit cell the calculated density for the 50 : 50 alloy is 6.664, as compared with the observed density of 6.47.

The *L10* type belongs to the space-group  $D_{4h}^{19}$ — $C4/mmm$ , and the two copper and the two titanium atoms will occupy the positions: 2 Cu in

1 (a) : 000 and 1 (c) :  $\frac{1}{2}\frac{1}{2}0$ , and 2 Ti in 2 (c) :  $0\frac{1}{2}\frac{1}{2}1$ ,  $\frac{1}{2}0\frac{1}{2}1$ . The  $p|F|^2$  values calculated for this structure are compared with the observed values in Table VI. The similarity in scattering power of the copper

TABLE VI. *Observed and Calculated Values of Reflection Angle and Intensity for  $\delta$  Phase.*

$hkl$	Radiation Cu K	Reflection Angle, $\sin^2 \theta$		Intensity, $p F ^2$	
		Observed	Calculated	Observed	Calculated
110	$\alpha$	0.0604	0.0603	1	0.5
001	$\alpha$	0.0727	0.0729	1	1.4
200	$\alpha$	0.1200	0.1205	25	24
111	$\alpha$	0.1328	0.1331	40	38
201	$\alpha$	...	0.1934	0	0.6
220	$\alpha$	0.2415	0.2410	8	6.7
002	$\alpha$	0.2917	0.2914	2	2.6
311	$\alpha$	0.3740	0.3740	14	12
202	$\alpha$	0.4119	0.4119	3	5.8
400	$\alpha$	0.4821	0.4821	2	2.3
222	$\alpha_1$	0.5310	0.5315	5	4.8
420	$\alpha_1$	0.6011	0.6016	3	4.0
331	$\alpha_1$	0.6138	0.6142	3	3.9
113	$\alpha_1$	...	0.7147	0	2.9
402	$\alpha_1$	...	0.7722	0	2.8
511	$\alpha_1$	0.8558	0.8548	5	6.9
422	$\alpha_1$	0.8917	0.8925	5	7.2
313	$\alpha_1$	0.9556	0.9556	14	12
400	$\alpha_1$	...	0.9626	0	3.5

and titanium atoms causes the intensities of the powder reflections to correspond approximately to those of a face-centred lattice.

In the  $\delta$  phase each atom is surrounded by eight atoms of the other kind at the contact distance 2.641 Å., while two groups with two and four atoms of the same kind have their positions at the distances 2.856 and 3.140 Å., respectively.

Both the  $\gamma$  and  $\delta$  phases are homogeneous near the composition CuTi. It has already been stated that the  $\gamma$  phase is homogeneous with an excess of titanium (up to about 3 at.-%), and that the  $\delta$  phase has a homogeneity range at a higher temperature and with an excess of copper (up to about 5 at.-%). The relationship between the two phases is evident from the fact that the former changes into the latter if  $z_{\text{Cu}}$  changes from 0.10 to  $\frac{1}{4}$  = 0.125 and  $z_{\text{Ti}}$  changes from 0.65 to  $\frac{3}{8}$  = 0.625, and Cu in  $0\frac{1}{2}\frac{1}{2}1$  and Ti in  $\frac{1}{2}0\frac{1}{2}1$  change places. Furthermore there appears to be a 3% contraction of the  $c$ -axis and a 1% expansion of the  $a$ -axis.

Quenching experiments were made in order to determine whether there was a temperature above which the lattice of the  $\delta$  phase became disordered. Samples were heated at 600°, 700°, 800°, and 850° C., for

several hours and then quenched, but the relative intensities as well as the positions of the diffraction lines obtained from these samples remained unchanged. The  $\delta$  phase reflections were no longer visible in photographs of samples heated at 950°, 1000°, and 1100° C. and water quenched. This disappearance of the  $\delta$  phase could, however, be caused by the reaction of titanium with the silica tube, which was noticeable at these high temperatures.

#### 6. The $\epsilon$ Phase.

Reflections from a pure phase—the  $\epsilon$  phase—appeared in photographs of alloy samples containing 72.5 and 75.0 at.-% titanium which had been heat-treated at temperatures below 900° C. The composition

TABLE VII.—Observed and Calculated Values of Reflection Angle and Intensity for  $\epsilon$  Phase.

$hkl$	Radiation Cu K	Reflection Angle, $\sin^2 \theta$		Intensity, $p F ^2$	
		Observed	Calculated	Observed	Calculated
100	$\alpha$	0.0344	0.0344	1	1.0
001	$\alpha$	...	0.0466	0	0.3
110	$\alpha$	0.0683	0.0687	0.5	0.4
101	$\alpha$	0.0800	0.0804	0.5	0.6
111	$\alpha$	0.1148	0.1147	50	52
200	$\alpha$	0.1377	0.1374	16	19
210	$\alpha$	...	0.1718	0	0.2
201	$\alpha$	...	0.1834	0	0.2
002	$\alpha$	0.1838	0.1840	5	6.2
211	$\alpha$	0.2178	0.2178	0.5	0.3
102	$\alpha$	...	0.2184	0	0.1
112	$\alpha$	...	0.2527	0	0.1
220	$\alpha$	0.2754	0.2748	5	5.6
202	$\alpha$	0.3216	0.3214	9	8.2
311	$\alpha$	0.3892	0.3895	16	13
222	$\alpha$	0.4589	0.4588	5	4.9
113	$\alpha$	0.4833	0.4827	5	4.8
400	$\alpha_1$	...	0.5486	0	2.5
331	$\alpha_1$	...	0.6631	0	3.5
420	$\alpha_1$	...	0.6858	0	3.2
402	$\alpha_1$	...	0.7323	0	3.1
004	$\alpha_1$	...	0.7347	0	0.8
313	$\alpha_1$	0.7564	0.7562	5	6.0
422	$\alpha_1$	0.8688	0.8695	5	7.2
204	$\alpha_1$	...	0.8719	0	3.6
511	$\alpha_1$	0.9373	0.9374	9	11

of this phase evidently corresponds closely to the formula  $\text{CuTi}_3$  and, incidentally, the structure has been found to be nearly isomorphous with the structure of  $\text{AuCu}_3$  ( $L1_2$  type). The lattice of  $\text{AuCu}_3$  is cubic, but the lattice of the  $\epsilon$  phase is tetragonal. The smallest and largest



dimensions are:  $a = 4.127$ ,  $c = 3.587$  Å.,  $c/a = 0.869$  ( $V = 61.09$  Å.<sup>3</sup>) and  $a = 4.158$ ,  $c = 3.594$  Å.,  $c/a = 0.864$  ( $V = 62.14$  Å.<sup>3</sup>), respectively. These volumes correspond to the phase boundaries at 70 and 75 at.-% titanium. With four atoms in the unit cell the density calculated at the composition  $\text{CuTi}_3$  is 5.57, the observed density being 5.41.

The space-group of the  $\epsilon$  phase is  $D_{4h}^{19}$ — $P4/mmm$  with 1 Cu in 1 ( $a$ ): 000 and 3 Ti in 1 ( $c$ ):  $\frac{1}{2}\frac{1}{2}0$  and 2 ( $e$ ):  $0\frac{1}{2}\frac{1}{2}$ ,  $\frac{1}{2}0\frac{1}{2}$ . The observed and calculated  $p|F|^2$  values for this structure are compared in Table VII and values of interatomic distances are found in Table VIII. It is seen that reflections with any one of the sums  $h + k$ ,  $k + l$ , or  $h + l$  when

TABLE VIII.—*Interatomic Distances in the  $\epsilon$  Phase (75 at.-% Titanium).*

Atom	Surrounding Atoms	Interatomic Distance, Å.
Cu in 1 ( $a$ )	8 Ti in 2 ( $e$ )	2.748
Ti in 1 ( $c$ )	8 Ti in 2 ( $c$ )	2.748
Ti in 2 ( $e$ )	4 Cu in 1 ( $a$ )	2.748
	4 Ti in 1 ( $c$ )	2.748

numerically odd are very weak. This is due to the fact that the scattering power of the copper and titanium atoms have nearly the same values, leading to intensities which practically correspond to a face-centred lattice.\*

It may be well to point out that the structure of the  $\epsilon$  phase can be regarded as a transitional state between the 12 co-ordination in a cubic face-centred cell and the 8 co-ordination in a cubic body-centred cell. With these arrangements ( $F4/mmm$ )  $c/a$  is equal to 1 and  $1/\sqrt{2} = 0.71$ , respectively, while in the  $\epsilon$  phase  $c/a = 0.86$ .

Powder photographs from samples which had been treated at 400°, 600°, 800°, and 850° C. for several hours and then quenched did not suggest any disordered structure. The relative intensities and the positions of the lines remained unchanged.

### 7. Titanium-Rich Alloys.

In powder photographs from specimens with compositions between 75 and 100 at.-% titanium, no reflections indicating any new intermediate phase were visible. Alloy samples with 80, 85, 90, and 95 at.-% titanium which had been quenched from temperatures below

\* A phase isomorphous with the  $\epsilon$  phase has been found in the copper-zirconium system at the composition  $\text{CuZr}_3$ . The dimensions are:  $a = 4.541$ ,  $c = 3.719$  Å.,  $c/a = 0.819$  ( $V = 76.69$  Å.<sup>3</sup>).<sup>14</sup>

900° C. gave diffraction patterns belonging to the  $\epsilon$  phase and to  $\alpha$ -titanium. The  $\epsilon$ -phase lines were very faint with a titanium content of 95 at.-%. Heat-treatment of the samples in silica tubes resulted in reactions with the tubes. Samples, which were quenched from 900°, 1000°, and 1100° C., and which still contained unconsumed titanium phase, did not show any lines of the  $\beta$ -titanium modification.

For pure titanium ( $\alpha$ -Ti) the axial lengths were found to be  $a = 2.953$ ,  $c = 4.709$  Å.,  $c/a = 1.595$  ( $V = 35.56$  Å.<sup>3</sup>). If the  $\alpha$ -titanium lattice is assumed to dissolve copper atoms in a solution of the substitution type, the cell volume may be expected to decrease. No such decrease was, however, noticed.

#### ACKNOWLEDGEMENTS.

The author wishes to express his sincere gratitude to Professor G. Hägg for his encouraging interest in the investigation. The work has been supported by a grant from the Swedish Natural Science Research Council, which is gratefully acknowledged.

#### REFERENCES.

1. W. Kroll, *Z. Metallkunde*, 1931, **23**, 33.
2. F. R. Hensel and E. I. Larsen, *Trans. Amer. Inst. Min. Met. Eng.*, 1932, **99**, 55.
3. F. Laves and H. J. Wallbaum, *Naturwiss.*, 1939, **27**, 674.
4. H. J. Wallbaum, *Naturwiss.*, 1943, **31**, 91.
5. E. M. Cruikhead, O. W. Simmons, and L. W. Eastwood, *Trans. Amer. Inst. Min. Met. Eng.*, 1950, **188**, 491.
6. R. Kiessling, *Jernkontorets Ann.*, 1948, **132**, 237.
7. G. Hägg and G. Rognström, *Arkiv Kemi, Min. Geol.*, 1944, [A], **18**, (5).
8. A. Westgren, *Jernkontorets Ann.*, 1933, **117**, 1.
9. S. Arrhenius and A. Westgren, *Z. physikal. Chem.*, 1931, [B], **14**, 66.
10. O. Nial, A. Almin, and A. Westgren, *Z. physikal. Chem.*, 1931, [B], **14**, 83.
11. A. Westgren, G. Hägg, and S. Eriksson, *Z. physikal. Chem.*, 1929, [B], **4**, 461.
12. S. J. Broderick and W. F. Ehret, *J. Phys. Chem.*, 1931, **35**, 2627.
13. E. Therkelsen, *Metals and Alloys*, 1933, **4**, 105.
14. N. Karlsson, unpublished work.
15. "Strukturbericht 1913-28", Vol. I, p. 94. Leipzig: 1931.
16. *Ibid.*, p. 484.



MAY LECTURE, 1951.

SCIENCE IN THE SERVICE OF THE  
COMMUNITY.

1314

FORTY-FIRST MAY LECTURE TO THE INSTITUTE OF  
METALS, DELIVERED 23 MAY 1951.By The Right Hon. Sir JOHN ANDERSON, P.C., G.C.B., G.C.S.I.,  
G.C.I.E., F.R.S.

## SYNOPSIS.

The remarkable developments of the first half of the present century in the practical application of scientific discoveries to the fields of industry, metallurgy, medicine, biology, agriculture, &c., are briefly reviewed. The potentialities, both for construction and destruction, of the discovery of atomic fission are touched upon, and an urgent plea advanced for a wider dissemination of scientific knowledge as a means of directing these new forces towards ends that will benefit mankind.



## I.—INTRODUCTION.

ONLY in comparatively recent times has science become a significant factor in the life of any nation. Our country has, through the centuries, produced many men of genius who have devoted their lives to the study and elucidation of natural phenomena, and many brilliant discoveries have been made, some of which have had important economic consequences, but these have been sporadic. The creation of a coherent framework of scientific knowledge is a relatively new development.

From the earliest times men have speculated on the true explanation of observed facts, building up what must, I think, be regarded as philosophy rather than science. Some of the theories formulated, after gaining wide acceptance for long periods, have collapsed under more searching investigation. For example, the attribution of the phenomena connected with heat to the influence of an imponderable medium known as *caloric*, supposed to be able to penetrate all forms of matter but also capable of independent existence, survived, like the corpuscular theory of light, until well into the nineteenth century. Those theories were then swept away before a flood of experimental evidence, only, in the latter case, to be eventually re-established in a modified form.

By the end of the last century, however, a long period of blind groping after scientific truth appeared to have come to an end. Atomic

theory and the doctrines of the conservation of matter and the conservation of energy had gained universal acceptance and seemed to provide a solid basis on which to build a satisfactory structure of physical science. As late as the last decade of the century, a man of science of the highest eminence felt able to publish his opinion that all the fundamental discoveries in the field of natural science had already been made, and that for the future progress would be confined to refinements in detail.

Seldom in the history of human affairs can any judgement have been so speedily or so dramatically overthrown. The discovery by Becquerel in 1896 of the wholly unexpected phenomena of radioactivity started a line of investigations in which J. J. Thomson and Rutherford played a leading part, but which quickly involved chemists and physicists all over the world, and resulted within an incredibly short space of time in incontrovertible proof that the atom, so far from being an ultimate indivisible unit, is a complex of smaller particles and that matter and energy are convertible the one into the other.

There followed a veritable renaissance in which every branch of natural science, biological as well as physical, became involved. The course of my own life—and I hope I may be forgiven this personal allusion—was not unaffected, because I was privileged to go to Germany in 1903 to engage in postgraduate work in physical chemistry. Curiously enough, in view of subsequent events, the subject of my research was the radioactivity of uranium, and from that time my interest in atomic theory has been unflagging. But I did not then and then decide to follow a scientific career. This was, I suppose, due to a time factor. It was not until some years later that science—or at any rate academic science—became in this country a rewarding pursuit in any material sense. Let me quote the opening paragraphs of the introductory article in the series of “Surveys on the Progress of Science” published recently by *The Times*:

“The outstanding feature of our civilization in the present century is the intensity of the pursuit and development of scientific research, whether consideration is directed to material results or intellectual endeavour.

“When those who are now senior professors were youngsters, the study of science was a relatively unconsidered part of the activities of our Universities. Practically the only prospect for a student who had let his devotion to a subject lead him to attempt original work was to become a University lecturer at a salary of £100 a year or so, which would be his lot for many years. There was practically no organized industrial research except perhaps in chemistry.”

At the age of twenty-three, I could not afford to be altruistic, and

having previously toyed with the idea of entering the Civil Service, I decided I had better try my luck in the First Division Examination, as it was called, before age ruled me out. The result of the examination determined for good or ill the subsequent course of my life. Ten years later I might have followed a different path.

Since the beginning of the century, developments in every field of scientific investigation have been spectacular, and their influence on our economic life profound. It is with those developments and that influence that I wish to deal.

## II.—A HALF-CENTURY'S PROGRESS.

In 1900, our traditional industries—engineering, metallurgy, heavy chemicals, cotton, woollen and linen textiles, tanning, brewing and distilling, to name only a few—were powerful and efficient. Of the newer industries based on science, now so prominent in the national economy, there was only a modest beginning. It is not generally realized that at the outset of the 1914–18 war, we came near disaster because of our almost complete dependence upon Germany for fine chemicals of all kinds, including synthetic drugs needed in large quantity both for the fighting forces and for the civilian population. Means had to be improvised for securing essential supplies of salvarsan, salicylates, antipyretics, such as aspirin, phenacetin, and antipyrine, local anæsthetics, such as novocaine and beta-eucaine, and a number of other materials, including dulcitol, derived from sugar of milk and essential for bacteriological work.

It is not possible to describe here the measures that were taken. Suffice it to say that but for the vigorous collaboration of University laboratories, under the guidance of the Royal Society and the Medical Research Council, the problem could not have been solved.

There were similar grave shortages of optical glass and dyestuffs, and the discovery of these grave weaknesses in our industrial economy, led quickly to far-reaching developments, so that to-day, in the resources available for the production of fine chemicals of all kinds, including dyestuffs, Britain occupies a leading position.

In the comparatively short period that has elapsed since the first synthetic resin, known as Bakelite, was produced by a Belgian chemist from the condensation of formaldehyde and phenol, the production of plastics has become an industry of the first importance, providing materials now regarded as essential for a great variety of purposes.

In this field, polythene, produced from ethylene, and perspex have been Britain's outstanding contributions. Polythene is the most efficient insulating material known, without which radar, at any rate in its ultimate development, would probably have been impossible.



Allied to plastics chemically, there are the synthetic fibres rayon, nylon, and more recently new fibres called terylene and ardil, of æsthetic value and increasing economic importance in view of the mounting prices of natural fibres.

Finally, there is synthetic rubber in its various forms, some superior for certain purposes to the natural product.

To turn to the sphere of medicine, most doctors would admit that before the dawn of the present century, their art was largely empirical. I say this with some confidence, because as a boy I used to be much interested in reading an admirable publication called "Chambers's Encyclopædia"—only an early edition, it is true—and one sentence has always stuck in my mind. It is this: "Measles belongs nosologically to the miasmatic order of zymotic diseases." The conceptions embodied in that resounding phrase would, I feel sure, be repudiated by every medical man to-day.

Be that as it may, the development of the science of bacteriology, which received a great fillip from the work of Sir Almroth Wright and others in the first European war, coupled with the use of drugs selected for their specific action on pathogenic organisms, has caused a veritable revolution.

I have already referred to salvarsan. Its effectiveness in eliminating the organism responsible for syphilis was established by the German chemist Ehrlich after the trial of a very long series of products, as is evidenced by the number 606 given to it originally. This may perhaps be regarded as the beginning of chemotherapy. Now we have the sulphadiazine drugs, starting with prontosil (sulphanilamide), effective against streptococcal infections but soon discarded in favour of less toxic variants whose names are now almost household words.

There are the mould antibiotics in a remarkable line—penicillin, streptomycin, chloromycetin, and aureomycin, which so far as at present known is the only specific against virus pneumonia. And who knows how many more there may be to come?

For the treatment of malaria there are atabrine and paludrine, far more effective in practice than quinine; and there is antrycide, which is perhaps the long-sought cure and preventive of the disease known as nagana, due to trypanosomes, and of other forms of trypanosomiasis.

The drawback to all these very potent curative agencies is that they are liable to give rise to a resistant strain of the organism which is the target of attack and which in this resistant form continues to flourish until the last condition of the patient is worse than the first. The only way to ensure against this is to administer at the outset sufficiently massive doses to make certain that every organism coming into contact with the drug is killed outright. Low toxicity is of the first import-

ance, or the drug may upset some physiological balance in the subject treated, as happens, I imagine, in certain cases with penicillin. Then again it may work havoc on some benign organism which had been keeping the mischievous one in check. Something of this kind has been experienced in connection with the newer insecticides, such as D.D.T. and Gammexane. It is not much good, for instance, to get rid of green-fly or codlin moth if the result is a plague of red spider.

Study of the action of substances produced in the growing tips of plants, and miscalled hormones on a false analogy with endocrine secretions, has led to the production of a range of weed-killers which act selectively on broad-leaved plants. These have been supplemented by products of an entirely different chemical nature which leave broad-leaved plants untouched but attack grasses and similar botanical species. Methods of promoting root formation and controlling the ripening of fruit have resulted from the same studies. Great practical value attaches, of course, to these developments in agriculture and horticulture.

Concurrently, there has been a progressive elucidation of the properties of materials and of the processes that go on in living tissues. This has been rendered possible by new techniques springing directly from the fundamental discoveries of the last decade of the nineteenth century.

As a student, I was taught that there must be an absolute limit to the degree of magnification attainable by the most perfect microscope, a limit imposed by the size of the molecules of glass and the shortest wave-length of visible light. That seemed wholly reasonable. Now, however, by the use of the electron microscope, employing a beam of electrons instead of ordinary light, and by means of X-ray analysis and of X-ray and electron diffraction, it is possible to measure distances of an order of magnitude of a single molecule and also to determine the arrangement of molecules in a crystal, and even the disposition of atoms in a molecule. The results obtained are of the greatest practical value in metallurgy, and I need not remind members of the Institute of Metals that there are now available new metals with very valuable properties, such as titanium and zirconium, which are coming into use as rapidly as their present high price will allow. Assumptions regarding the properties of various alloys can now be confirmed or disproved, and proportions and working temperatures can be determined with mathematical precision instead of by rule of thumb.

These developments have also been of great value in biology. The conditions under which living cells subdivide and viruses propagate themselves are brought for the first time under direct observation. Studies in this field have been greatly assisted by the availability of radioactive forms of the common elements, by means of which trans-

formations undergone by these elements in living tissues can be traced in detail. The manner in which enzymes, vitamins, and trace elements function is no longer a sealed book.

Are we, then, approaching a solution of the great mystery of life itself? I personally doubt it, but it is beyond question that a flood of light has been thrown on regions that not long ago were thought to be for ever veiled.

The element carbon possesses the unique property of combining with itself to form chains, either straight or having side-chains and rings, with or without cross-linking, in endless variety, some of the larger molecules of, for example, proteins, containing a vast number running into thousands of atoms. The chemistry of such high polymers is now well understood.

Silicon is another element occurring abundantly in nature which has a somewhat similar property, but in this case the combination takes place with intervening atoms of oxygen. The resulting products—known as silicones—have lately come into economic prominence because of their physical characteristics, notably their resistance to temperatures that would destroy any substance containing carbon. Their cost is at present the main deterrent to their wider use, but that will no doubt be overcome.

While I was still a student at Edinburgh fifty-two years ago, the first experiments in radio-telegraphy were under way. I well recall the sensation created when iron filings in the detector—it was then called a “coherer”—arranged themselves in straight lines on the impact of an electromagnetic wave emitted at the other end of the room and thus allowed an electric current to pass. There one had all the essentials of a radio-signalling apparatus. In the interval—a comparatively short interval—between then and now developments have occurred, powerfully stimulated, no doubt, by two world wars, which to the pioneers must have seemed to belong to the region of fantasy. Let us remember, however, that it was a belief in the economic potentialities of electromagnetic waves that determined the character of Rutherford's first work at the Cavendish Laboratory. To the youth of to-day wireless and even television are something to be taken for granted.

Then there is the problem of atomic energy, springing from the discovery, made as recently as 1939, of the fission of the uranium nucleus with accompanying release of energy, followed by conclusive evidence that the conditions conformed to the requirements of a chain reaction. That discovery opened up possibilities of military use and also of economic development. There is, I think, little doubt that but for the war, investigations would have proceeded along the line which they had already taken when war broke out. That is to say, they would have

been concerned with possible industrial applications. If so, it is certain that even less progress would have been made than can be recorded to-day, when we have to recognize that the economic and industrial exploitation of nuclear or sub-atomic energy still lies many years ahead.

There is one intriguing possibility which I should just like to mention. The splitting of the nucleus of a heavy element is not the only process attended by release of atomic energy. A very large amount of energy is also released when the nuclei of some of the light elements are brought together. For example, four nuclei of hydrogen, or it might be two of deuterium, can theoretically be brought together to form one of helium.

Scientists seem to be fairly well agreed that this sort of reaction is responsible for the emission of heat from the sun and the stars. But the reaction is not so simple as I have indicated. It is believed that the first thing that happens under conditions of very high temperature and pressure is that carbon in one of its isotopic forms is created. This splits up to form helium: one atom of carbon, atomic weight 12; three atoms of helium, atomic weight 4. There is, as I have suggested, the possibility that a way may yet be found to develop the production of energy by bringing the nuclei of the lighter atoms together. It has been done in the laboratory, and I believe work is proceeding on this aspect of the problem of nuclear energy. It is not impossible that important economic results may be derived from that line of approach sooner than from the older method of splitting the heavy atoms.

### III.—THE CULTURAL VALUE OF SCIENCE.

I have said enough to show how tremendous a change has come about within the last half century in the part which science plays in our daily lives. In all parts of the world, new industries are being founded and carried on upon the basis of scientific discovery. In this country alone the amount of money devoted by industrial concerns to scientific research and development cannot be less than fifty million pounds a year, and in that connection the establishment of the industrial research associations under the Department of Scientific and Industrial Research has been a peculiarly British development of very great importance.

The output of science graduates from our Universities has increased year by year since the end of the war, and will soon be at a level twice that of 1939. In the matter of technological education—which is no less important than training in pure science—clear lines of development are still lacking, despite more than one high-level investigation of the

problems involved. In my opinion, no one solution of universal validity could be accepted. I should like to see some of our Universities, particularly in recognized centres of some predominant industry, developing a technological faculty or faculties, but I should like also to see one or more specialized Universities established on the lines of the famous Massachusetts Institute of Technology. At the same time, I think that some of our existing technical colleges should be encouraged to raise their academic standard.

In this scientific age upon which we have entered I wish it could be universally recognized that scientific studies no less than the humanities have a cultural value and that applied science is not inferior academically to pure science. I should like to see a much wider dispersal of general scientific knowledge throughout the community, more particularly among public officials, teachers, and business managers.

I make this plea because I am profoundly conscious of the fact that the material progress resulting from the developments of scientific knowledge which I have attempted briefly to outline has gone far ahead of man's capacity to turn it to good account. And I am quite certain that scientists alone cannot save the world from the consequences of this disparity.

The development of transport and communications—thanks to the internal-combustion engine and to radio—has brought the peoples of the earth together physically, but not for more fruitful collaboration. Medical science can now combat plagues that used to decimate the populations of vast areas, but we have made little progress with the task of ensuring adequate sustenance for the steadily mounting populations.

We have found a method of releasing energy from atomic nuclei, but the only practical application so far devised is directed to destruction. I am not, of course, overlooking the immensely valuable results obtainable in medicine and industry by the use of the radio-active products of nuclear reactions. That is a romance in itself. Even a seemingly innocent diversion, such as television, appears to me to have social and economic implications of a serious nature. If I am not mistaken, we shall soon be hearing complaints of children neglecting their homework and men and women avoiding social and domestic obligations and of increasing loss of productive efficiency because of the lure of television programmes.

I end, therefore, on a note of warning. Obviously we cannot call a halt to scientific progress, but at any rate let as high a proportion as possible of the people of the world be trained to think about these matters and the prospect of ultimate salvation will be vastly improved.



## GRAIN-BOUNDARY ENERGIES IN SILVER.\* 1315

By A. P. GREENOUGH,† B.A., STUDENT MEMBER, and RONALD KING,‡  
B.Sc., MEMBER.

## SYNOPSIS.

The variation of grain-boundary energy with the angle between the crystals meeting at the boundary has been investigated for silver by examination of boundary grooves formed during thermal etching. The results are found to be in fair agreement with theoretical prediction based on the treatment of the boundary as a region of transition represented by an assembly of dislocations.

## I.—INTRODUCTION.

DURING recent years, increasing attention has been paid to the nature and properties of crystal boundaries in metals. The older "amorphous cement" theory has given way to the theoretically more attractive picture of the boundary as a region of transition from one crystal orientation to the other, the atoms taking up mean positions dictated by the lattice forces; but when the work described in this paper was started, there existed no positive experimental evidence to distinguish between these two theories. An essential difficulty lay in the determination of a specific boundary property that might be expected to be different for the two cases. Such a property was, however, suggested by the work of Chalmers, King, and Shuttleworth,<sup>1</sup> who, while studying the thermal etching of silver, suggested that the angle at the bottom of the grooves which formed at the grain boundaries when polished silver specimens were heated, was a measure of the excess free energy associated with the boundary. It would be expected that the specific free energy of a region of transition between two crystals would be dependent upon the angle between them, whereas the specific free energy of a truly amorphous phase should be independent of this angle. Qualitative observations on thermally etched specimens<sup>2</sup> did, in fact, suggest that the groove angle depended upon the orientations of the grains, as well as on the orientation of the boundary itself. It was therefore decided to investigate quantitatively the variation in the thermally etched boundary groove with the difference in orientation between the crystals on each side of the boundary.

\* Manuscript received 6 October 1950.

† Scientific Officer, Royal Aircraft Establishment, Farnborough, Hants.

‡ Assistant Director, Davy Faraday Laboratory, The Royal Institution of Great Britain, London; formerly Royal Aircraft Establishment, Farnborough.



While the present work was in progress, there appeared a number of significant papers in this field. Grain-boundary groove angles in thermally etched copper have been measured by Bailey and Watkins,<sup>3</sup> though the variation with relative orientation of the grains was not examined. The variation of boundary energy with orientation of the grains was studied, using a somewhat different method, by Dunn and Lionetti<sup>4</sup> for silicon ferrite, and by Aust and Chalmers<sup>5</sup> for tin. Theoretical calculations of boundary energies, treating the boundary as an assembly of dislocations, have been published by Read and Shockley<sup>6</sup> and by van der Merwe.<sup>7</sup> The results of the investigations on silver now described were found to be in qualitative agreement with the findings of these authors.

## II.—EXPERIMENTAL PROCEDURE.

### 1. *Material.*

Silver was selected as a suitable material for investigation, since considerable experience of its thermal-etching behaviour had already been gained. Its thermal expansion is isotropic, so that no complications occur at the boundary owing to differential expansion of the grains on heating and cooling,<sup>8</sup> and it is readily obtained in a state of high purity. However, it must be noted that, even in silver of the high purity employed, segregation of impurity atoms to the grain boundary could cause a relatively high concentration there, with possibly an appreciable effect upon the specific free energy.

Three batches of silver were used in the preparation of the specimens. Batches *A* and *B* were supplied as spectrographically pure by Messrs. Johnson, Matthey and Co., Ltd., who provided the following information. Batch *A* contained traces only of iron, calcium, magnesium, manganese, sodium, cadmium, and lithium, and batch *B* traces only of iron, calcium, magnesium, silicon, and copper, with a faint trace of sodium. In both the purity was estimated as better than 99.999%. Batch *C* was silver obtained originally for thermocouple calibration. The source of supply was unknown, but spectrographic examination showed its purity to be of the same order as that of *A* and *B*. No increase of impurity content was detected by spectrographic examination of specimens after they had been thermally etched.

### 2. *Preparation of Specimens.*

For the systematic investigation of the variation of groove angle with the relative orientation of the crystals meeting at the boundary, bicrystal specimens, in which the two crystals could be grown at any

required orientations, were an obvious choice. They were prepared by the method used by Chalmers<sup>9</sup> for the production of bicrystal specimens of tin, in which the molten metal is allowed to solidify progressively from two single-crystal "seeds" set at the desired orientations.

Single crystals were first prepared by the standard moving-furnace method in long graphite boats. The boats were contained in a silica tube in which an atmosphere of commercial hydrogen was maintained. The temperature outside the tube was held at 1150° C. and the furnace moved at a rate of 10 in./hr. The crystals produced were about 8 in. long and of roughly V-shaped cross-section, as shown in Fig. 1. Such a single crystal was sawn in half and the two halves set in the seed-crystal

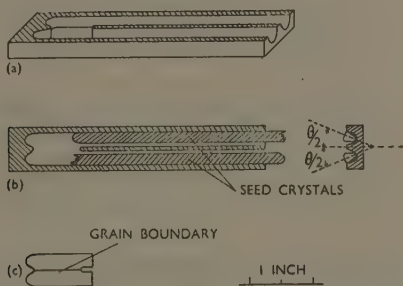


Fig. 1.—Illustrating Preparation of Bicrystal Specimens. (a) Mould; (b) setting of seed crystals in the mould; (c) specimen.

channels of the bicrystal mould (Fig. 1 (a)), the pieces being rotated about their axes through an angle of  $\theta/2$  in opposite senses. The bicrystal end of the mould was charged with silver and the mould was placed in the moving furnace, so that the added silver melted and joined on to the two single crystals. The furnace was then moved away so that the charge solidified progressively from the two seed crystals. The end portion thus grew as a bicrystal, whose component crystals had the orientations of the two seeds. The setting of the seeds complied with the condition established by Chalmers<sup>10</sup> for the production of a straight grain boundary along the axis of the mould and in most cases such a boundary resulted. When a satisfactory specimen had been prepared in this way, the seed-crystal legs were sawn off and used to produce a second specimen in which the angle  $\theta$  between the crystals was different. In this way, from each single crystal a series of bicrystal specimens with progressively increasing values of  $\theta$  was prepared.

### 3. Thermal Etching.

The bicrystal specimens were first held in a vacuum for an hour at 900° C. to remove most of the hydrogen in solution. One surface of each specimen was then ground flat, using emery papers from *F* down to 0000 grade. The specimen was electrolytically polished using the solution described by Shuttleworth, King, and Chalmers<sup>11</sup> (AgCN 35, KCN 30, K<sub>2</sub>CO<sub>3</sub> 38 g./l.). The polishing process was prolonged beyond the time necessary to obtain a polished surface in order to remove the cold-worked layer produced by grinding. The round cast surface of the specimen also became polished at the same time. Several specimens thus prepared were placed in a tube of fused silica, the tube evacuated, and an atmosphere of oxygen-free nitrogen established in it before it was placed in a furnace at 900° C. After heating for 19 hr., the tube was removed and allowed to cool in air, the atmosphere inside being maintained until the specimens had cooled to room temperature.

Nitrogen was chosen as the thermal-etching atmosphere because it is not soluble in silver,<sup>12</sup> and the surface of the latter remains smooth except for the boundary groove.<sup>1</sup> Oxygen-free nitrogen was used, containing less than 10 vol./million of oxygen, less than 50 vol./million of hydrogen, and less than 0.02 g./m.<sup>3</sup> of water vapour at 120 atm. pressure. Even so, it was found that some batches of gas manufactured to this specification still contained sufficient oxygen to cause the surface of the silver to become lightly striated. To obtain reproducible conditions for thermal etching, the gas was further purified by passing it over copper turnings at 900° C., magnesium turnings at 400° C., and finally a second lot of copper turnings at 900° C. The magnesium was necessary to remove the residual oxygen sufficiently fast when the gas was first let into the evacuated specimen tube, and the final passage over copper turnings prevented the development on the silver surface of characteristic striations thought to be caused by sulphur from the magnesium being carried over to the specimen. After being used for about 100 hr., hydrogen was passed over the copper to reduce any oxide formed, and at the same time, the magnesium turnings, which were slowly attacked by the nitrogen, were replaced by fresh turnings.

It was found that heating at 900° C. beyond 19 hr. had little effect on the size of the grooves, and made no apparent difference to the magnitude of the groove angle. Some trouble was experienced initially with boundary migration during thermal etching, but this was minimized by the introduction of lobes at the end of the specimen, which helped to anchor the boundary in its original position.

#### 4. Measurement of the Groove Angle.

After preliminary investigations upon polycrystalline specimens similar to those used by Chalmers, King, and Shuttleworth,<sup>1</sup> the following methods were adopted for the examination of boundary-groove contours.

A layer of silver was electroplated on to the thermally etched surface, and the specimen was sectioned normal to this surface, polished, and etched with a 1 : 1 mixture of 0.4% chromic acid and 0.4% sulphuric acid. From each specimen two values of the groove angle were obtained, one on the flat prepared surface and the other on the rounded cast surface. As the grooves were found to be very shallow and the angle about  $160^\circ$ , taper sections at an angle of approximately  $30^\circ$  to the surface were also prepared. The groove angle  $\gamma$  was measured by a projection microscope or on photographs.

A direct optical method, referred to as the reflected-light method, was also employed to measure the groove angle. This is essentially a goniometric method using a metallurgical microscope. The principle is indicated in Fig. 2.

The vertically illuminating system of the microscope is adjusted to give a thin pencil of light which is focused to produce an image of the field iris on the surface of the specimen. If the specimen is rotated as indicated, the surface as viewed in the microscope remains bright until it is tilted to an angle  $\phi$  such that all the specularly reflected light falls outside the microscope objective. The angle between two inclined portions of the surface may thus be determined by rotating the specimen until this condition is reached, for each of the inclined portions in turn.

An instrument was constructed to fit on the stage of a metallurgical microscope, to enable a thermally etched specimen to be rotated about an axis lying in its surface. Rotational and translational adjustments were provided, so that any line in the specimen could be brought into coincidence with the axis of rotation, and the normal microscope traverse enabled any portion of that line to be brought to the centre of the field of view. The rotation about the horizontal axis in the specimen surface was measured by the movement of a pointer over a protractor.

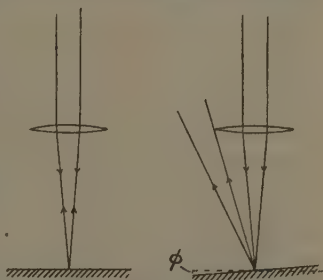


FIG. 2.—Illustrating Principle of Reflected-Light Method for Examination of Boundary-Groove Contours.

Specimens were set up with the boundary groove along the axis of rotation, and were rotated until the condition of Fig. 2 held first for the flat surface and then for the surface at the root of the groove. This gave the angle between the two. Rotation in the opposite sense gave the angle between the flat surface and the surface at the root of the groove on the other side. This method, besides giving the total groove angle, revealed any asymmetry present in the groove. It also had the advantage that the specimen required no special preparation, and a given groove would be investigated along its whole length.

### 5. *Measurement of the Angle Between the Grains.*

After the groove angles had been measured on the sections, the specimens were very deeply etched in 15% nitric acid to reveal clearly the grain boundary.

For the specimens in series 1 (Table I), back-reflection Laue photographs were taken of each of the crystals, the orientations were found by the method described by Greninger,<sup>13</sup> and the angle of rotation necessary to bring one lattice into coincidence with the other determined. For series 2 and 3 a third photograph was taken with the X-ray beam incident on the boundary. The diffraction spots for both crystals appeared on this photograph. The separate photographs of the individual crystals served to identify the two sets of spots, and the angle between the crystals was obtained directly from the third photograph. This method had the advantage that errors due to slight differences in the setting of the specimen for the two separate photographs were avoided. The fact that the diffracted spots for both crystals appeared on the same film made it possible to determine small angles with a much higher accuracy than would otherwise have been the case.

## III.—RESULTS.

Photomicrographs of typical grooves are shown in Figs. 3-5 (Plates L and LI). The shape of the groove is seen to be as suggested by Chalmers, King, and Shuttleworth,<sup>1</sup> though the depth ( $\sim 10^{-4}$  cm.) is smaller than they estimated.

Three complete series of bicrystals were examined. The orientations of the three single crystals from which the seeds were taken are shown in Fig. 6. Fig. 7 indicates the manner in which the pair of seeds of a given series were rotated from their original orientations to give the required angle  $\theta$  between the two crystals of the bicrystal specimen. This angle was varied over as wide a range as was found practicable for each series. The results of the measurement of boundary-groove angles are given in Table I.

#### IV.—DISCUSSION OF RESULTS.

### 1. Accuracy of Measurements.

The methods of measurement of the groove angle were subject to a number of possible errors. From the observations made it is estimated that the angle as measured on both normal and tapered sections could

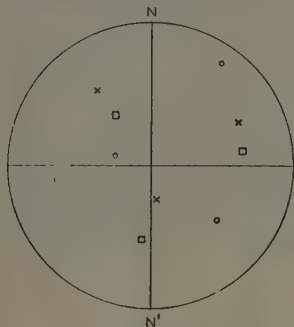


FIG. 6.—Stereographic Projection of {100} Poles of the Three Single-Crystal Seeds.

The long geometrical axes of the seeds are normal to the plane of projection.  $NN'$  is the plane in which the grain boundaries of the bicrystals were produced.

○ Series 1; □ Series 2; × Series 3.

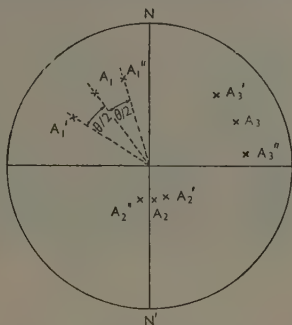


FIG. 7.—Illustrating Rotation of Seeds to Produce a Bicrystal (No. 312, Series 3).

Plane of stereographic projection as in Fig. 6,  $NN'$  being the plane of the grain boundary.

$A = \{100\}$  poles before rotation of the seeds.

$A', A'' = \{100\}$  poles after rotation of the seeds.

$\theta$  = orientation difference.

be subject to an error of at most  $4^\circ$ . The reflected-light method showed a high degree of reproducibility, but it was difficult to assess the absolute accuracy, as this depended on the criterion set by the observer for the disappearance of specularly reflected light in the microscope. Table I, however, shows that there was no serious systematic difference between results obtained by this method and those from the sections.

It is estimated that the values of  $\theta$  quoted for large angles (greater than  $20^\circ$ ) are accurate to within  $\pm 2^\circ$ . It was found that small values of  $\theta$  could be determined more accurately, e.g. when  $\theta$  was  $1^\circ$  the error did not exceed  $\frac{1}{2}^\circ$ .

Though great care was taken over the setting of the seed crystals in the mould, it was found that in a number of cases the orientations of the crystals were not such that they could be brought into coincidence by a rotation about the specimen axis. While in no case did the angle between the specimen axis and the axis about which the rotation had



effectively occurred exceed a few degrees, it is not possible to dismiss this as unimportant. A unique functional relationship between  $\theta$  and  $\gamma$  may only be expected where  $\theta$  measures a rotation about the same axis for all the specimens in the series. It is possible that rotation

TABLE I.—*Measured Grain-Boundary Groove Angles.*

Specimen No.	Groove Angle $\gamma$ , degrees					Orientation Difference $\theta$ , degrees
	Normal Section		Taper Section Flat Side	Reflected-Light Method : Flat Side	Average	
	Flat Side	Cast Side				
Series 1.						
15	174	173	...	173½	173½	5
18	160	162	...	158	160	25
111	164	162	...	160	162	42
19	160	...	...	158	159	46
113	160	161	162	164½	162	75
114	163	162	...	159	161½	96
17	169	168	...	163	166½	129
115	162	...	...	160	161	156
110	...	159	...	159	159	174
Series 2.						
20	174½	174	170	174½	173½	1½
22	172	...	170½	173	172	4
21	166	...	165	169	166½	9
24	168	...	...	170	169	10½
27	161	...	157	...	159	18
23	162	162	159½	160	161	22
25	161	161	160½	167½	162½	22½
26	162	...	164	...	163	72
Series 3.						
31	175	...	175½	175	175	½
32	170	172½	170½	173	171½	1
34	171	...	171	171½	171	1½
35	171½	...	169	174	171½	3
311	163	...	163½	162½	163	13½
39	160	...	155	163½	159½	28½
310	160	161	160	164	161½	34
312	162½	162	163½	168½	164	41
313	159	159	159½	163	160	61

about an axis inclined to this by only a few degrees might cause an appreciable change in the energy of the boundary. However, the main importance attaches to the results for small values of  $\theta$ . For these angles the rotation was reasonably accurately around the specimen axis. Successive use of the seeds changed their shape, and these changes of shape were the main cause of the inaccurate setting of the rotation axis. Thus, since the specimens with the larger values of  $\theta$  were prepared last, these were the ones most subject to this inaccuracy.

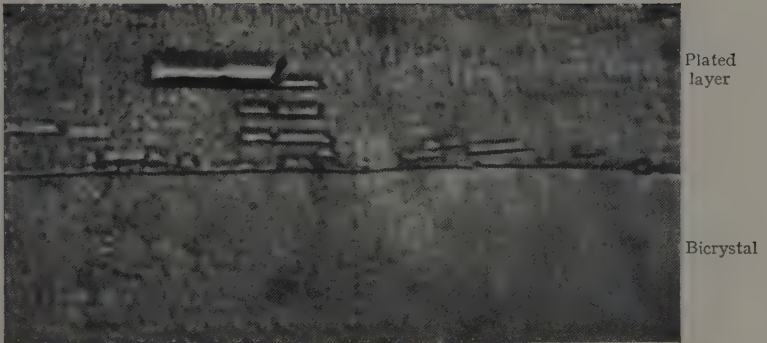


FIG. 3.—Normal Section of Groove in Cast Side of Specimen No. 32.  $\times 2400$ .

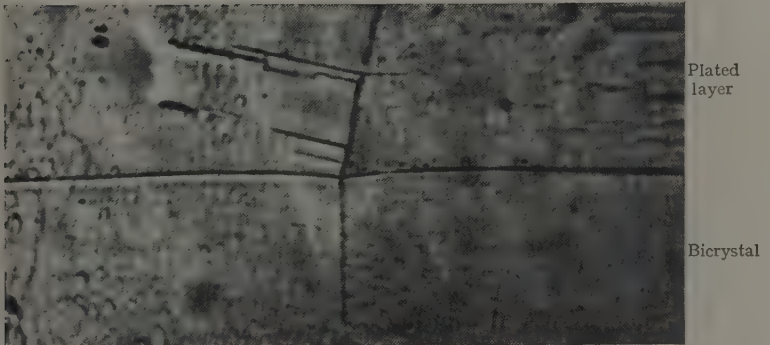


FIG. 4.—Normal Section of Groove in Flat Side of Specimen No. 311.  $\times 2400$ .



FIG. 5.—Taper Section of Groove in Flat Side of Specimen No. 310. Plane of section  $26^{\circ}$  to flat surface.  $\times 2400$ .

## 2. Boundary Energy.

It is clear from Table I that the angle at the bottom of the groove formed by thermal etching varies with the angle  $\theta$  between the two crystals. Following Chalmers, King, and Shuttleworth,<sup>1</sup> the variation of groove angle may be interpreted in terms of the variation of specific free energy of the boundary in the following manner. If the equilibrium configuration at the intersection of the groove with the external surface is as shown in Fig. 8, and  $E_A$ ,  $E_B$ , and  $E_{AB}$  are, respectively, the specific free energies of the surface of crystal A, the surface of crystal B, and the boundary, then :

$$E_{AB}/\sin \gamma = E_A/\sin \alpha = E_B/\sin \beta$$

If it is assumed that the free energy  $E_S$  of the external surface is independent of the crystallographic orientation of that surface, then :

$$E_{AB} = 2E_S \cos \frac{1}{2}\gamma$$

The assumption that the free energy of an external surface is independent of its crystallographic indices is not strictly justified; for example, Fricke<sup>14</sup> calculated that at 25° C. the free energy of a (100) silver surface was 1920 ergs/cm.<sup>2</sup> and that of a (111) surface 1650 ergs/cm.<sup>2</sup>. It is clear, however, that in general the equilibrium conditions specified above could not be met by the intersection of surfaces of simple crystallographic indices, and it is reasonable to suppose that the free energies of the surfaces actually produced at the bottom of the groove would vary but little from specimen to specimen. The fact that the boundary grooves as seen on normal sections showed no asymmetry about the plane of the boundary supports this assumption.

This method of examination of boundary energy has the advantage that it enables a rough estimate to be made of the absolute value of the energy. While no experimental results exist for the free energy of silver surfaces, a very rough estimate may be made on the following considerations. Fricke's<sup>14</sup> theoretical calculations of the free energies of the (100) surfaces for copper and silver at 25° C. yield a ratio of 1.50 : 1 for their respective values. Huang and Wyllie<sup>15</sup> calculated the values of the surface free energy at the melting points of copper and silver. Using the temperature coefficient determined by Udin, Shaler, and Wulff<sup>16</sup> to reduce their calculated value for copper to 960° C., gives for the ratio of the surface free energies at this temperature 1.64 : 1. These two ratios are sufficiently near to justify taking their mean value, 1.57 : 1, which, combined with the figure of 1450 ergs/cm.<sup>2</sup>

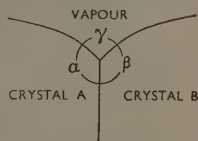


FIG. 8.—Illustrating Method of Interpreting Variation of Groove Angle in Terms of Variation of Specific Free Energy of the Boundary.

obtained by Udin, Shaler, and Wulff for copper at 900° C., gives a value of about 900 ergs/cm.<sup>2</sup> for the free energy of silver at that temperature.

On this assumption, the average value of the free energy for boundaries where  $\theta$  is large is about 300 ergs/cm.<sup>2</sup> at 900° C. This estimate implies that the free energy of the surface is not appreciably affected by the presence of nitrogen. There is no evidence that this is true, and the estimate is made only very tentatively.

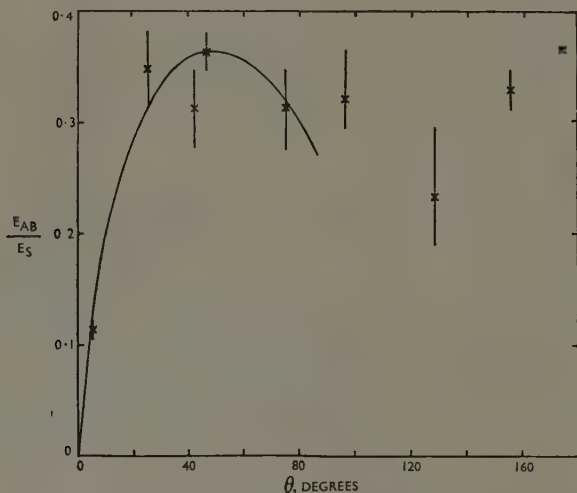


FIG. 9.—The Variation of Boundary Energy with Angle Between the Crystals.  
Series 1.—The full curve represents the relation :

$$E_{AB}/E_S = \theta (0.36 - \log_{10} \theta)$$

### 3. Comparison with the Results of Other Workers.

Bailey and Watkins<sup>3</sup> thermally etched polycrystalline specimens of copper in various atmospheres at two different temperatures. They then prepared metallographic sections normal to the etched surface and, assuming that the groove angle was constant for any given conditions of thermal etching, found a value for this angle by measuring a selection of the smallest groove angles seen in the section. The values of the angle so obtained were: by etching in argon at 900° C. for 2 hr., 160°; in hydrogen at 800° C. for 14 hr., 158°; and in hydrogen at 900° C. for 2 hr., 160°. The results obtained for silver where  $\theta$  is large agree very closely with these figures.

Dunn and Lionetti <sup>4</sup> investigated the variation of boundary energy with relative orientation in silicon ferrite by examination of the equilibrium angles at the junction of three grain boundaries in specially prepared specimens, and Aust and Chalmers <sup>5</sup> similarly studied the relationship in tin. The results now obtained are in good qualitative agreement with theirs, though the energy increases to its maximum value rather more slowly than was found in the case of tin. The results, however, are not strictly comparable, as they refer to metals of dissimilar crystal structure and different degrees of purity.

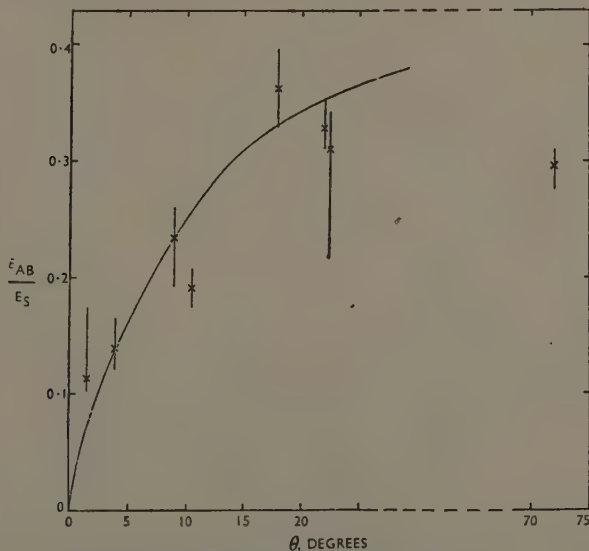


FIG. 10.—The Variation of Boundary Energy with Angle Between the Crystals.  
Series 2.—The full curve represents the relation :

$$E_{AB}/E_S = \theta (0.36 - 1.4 \log_{10} \theta)$$

Considering the boundary as an assemblage of dislocations, Read and Shockley <sup>6</sup> have derived the expression

$$E = E_0 \theta (A - \log_e \theta)$$

where  $E$  is the boundary energy, and  $E_0$  and  $A$  are constants. In Figs. 9, 10, and 11, curves of this type have been very roughly fitted to the present authors' experimental results. The results do not follow the curves closely, but the general nature of the variation of the boundary energy is quite well expressed by the curves up to values of  $\theta$  of



the order of  $50^\circ$ , although the expression was derived for small values of  $\theta$ .

Read and Shockley point out that a detailed consideration of the boundary leads to the conclusion that superimposed upon the curve  $E = E_0\theta(A - \log_e \theta)$  there should be a series of humps separated by cusps, the major cusps lying upon the curve itself. The results of the investigation now described are too inaccurate and widely separated to establish whether these humps are experimentally observable. Their

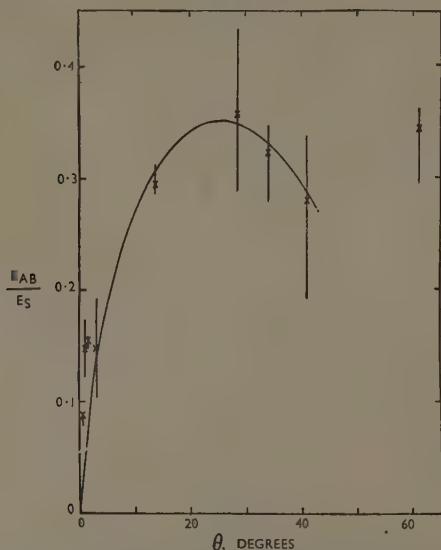


FIG. 11.—The Variation of Boundary Energy with Angle Between the Crystals. Series 3.—The full curve represents the relation :

$$E_{AB}/E_S = \theta (0.12 - 1.9 \log_{10} \theta)$$

existence might, however, to some extent account for the scatter of the experimental results from a smooth curve.

In view of this possibility, no great significance is attached to the exact values of  $E_0$  and  $A$  used in fitting the curves shown in Figs. 9–11. The values obtained are: for  $E_0$  (assuming the surface energy to be 900 ergs/cm.<sup>2</sup>) 380, 540, and 720 ergs/cm.<sup>2</sup> for series 1, 2, and 3, respectively, and for  $A$  0.83, 0.6, 0.15. It is interesting to note, however, that an approximate estimate of  $E_0$ , using the formula due to Read and Shockley, gives for silver a value of about 750 ergs/cm.<sup>2</sup>, while the values of  $A$  are of the order estimated by those authors.

## V.—CONCLUSION.

The experiments, although of no high degree of accuracy, indicate conclusively that boundary energy varies with the angle between the crystal grains. The agreement with theoretical prediction is better than might have been expected, and lends strong support to the consideration of the grain boundary as a region of transition which can be represented as an assembly of dislocations.

The results have justified the interpretation originally given to the formation of the boundary groove by Chalmers, King, and Shuttleworth.

## ACKNOWLEDGEMENTS.

The authors wish to express their thanks to Mr. B. I. Tait for valuable assistance in the preparation of the X-ray photographs from which the orientations of the crystals were determined. Acknowledgement is made to the Chief Scientist, Ministry of Supply, and to the Controller, H.M. Stationery Office, for permission to publish this paper.

## REFERENCES.

1. B. Chalmers, R. King, and R. Shuttleworth, *Proc. Roy. Soc.*, 1948, [A], **193**, 465.
2. P. J. E. Forsyth, R. King, G. J. Metcalfe, and B. Chalmers, *Nature*, 1946, **158**, 875.
3. G. L. J. Bailey and H. C. Watkins, *Proc. Phys. Soc.*, 1950, [B], **63**, 350.
4. C. G. Dunn and F. Lionetti, *Trans. Amer. Inst. Min. Met. Eng.*, 1949, **185**, 125.
5. K. T. Aust and B. Chalmers, *Proc. Roy. Soc.*, 1950, [A], **201**, 210.
6. W. T. Read and W. Shockley, *Phys. Rev.*, 1950, [ii], **78**, 275.
7. J. H. van der Merwe, *Proc. Phys. Soc.*, 1950, [A], **63**, 616.
8. W. Boas and R. W. K. Honeycombe, *Proc. Roy. Soc.*, 1946, [A], **186**, 57.
9. B. Chalmers, *Proc. Roy. Soc.*, 1937, [A], **162**, 120.
10. B. Chalmers, *Proc. Roy. Soc.*, 1949, [A], **196**, 64.
11. R. Shuttleworth, R. King, and B. Chalmers, *Metal Treatment*, 1947, **14**, 161.
12. E. W. R. Steacie and F. M. G. Johnson, *Proc. Roy. Soc.*, 1926, [A], **112**, 542.
13. A. B. Greninger, *Trans. Amer. Inst. Min. Met. Eng.*, 1935, **117**, 61.
14. R. Fricke, *Z. physikal. Chem.*, 1942, [B], **52**, 284.
15. K. Huang and G. Wyllie, *Proc. Phys. Soc.*, 1949, [A], **62**, 180.
16. H. Udin, A. J. Shaler, and J. Wulff, *Trans. Amer. Inst. Min. Met. Eng.*, 1949, **185**, 186.



# THE STUDY OF RECRYSTALLIZATION IN ZINC BY DIRECT OBSERVATION.\*

1316

By G. BRINSON† and A. J. W. MOORE,† B.Sc., Ph.D., MEMBER.

## SYNOPSIS.

Specimens of deformed zinc have been observed under a polarizing microscope while being heated. The changes in the crystal structure during recrystallization were continuously observed and photographed. The authors show that the growth of new crystals is very erratic, and although grain and twin boundaries, inclusions, and local inhomogeneities sometimes markedly affect growth, at other times they have no influence on it. This erratic behaviour implies that a small crystal will not grow uniformly when it is of about the same size as the matrix crystals. The relevance of this to the conclusions reached by previous workers is discussed. The method of observation can be applied to any non-cubic metal that will undergo structural alterations at a temperature at which it can be observed by means of a microscope.

## I.—INTRODUCTION.

ON annealing a deformed metal, recrystallization takes place by what is usually considered to be a process of nucleation and growth. At the same time those properties of the material which are changed by cold work are restored to their original value. Attempts to understand this process have proceeded generally along three directions :

(1) Rates of recrystallization have been widely studied by measuring the rate of change of properties of the deformed materials on annealing. Although these results have yielded little direct information on the mechanism of recrystallization, they are important technically.

(2) Metallographic and X-ray studies have been carried out to determine the effect of such factors as the mode of deformation, the purity of the metal, and the temperature and duration of annealing on the size and orientation of the resultant grains. The results of the experiments suggest that nuclei of undeformed metal form during annealing, and these grow to form new crystals. The rate of nucleation appears to be dependent on the degree of deformation and the temperature, and the rate of growth on the purity and the temperature.

(3) Measurements of actual nucleation, and rates of growth have been carried out by several workers, and quantitative treatments of the problem have been made.

In order to show the relationship of a growing grain to its neigh-

\* Manuscript received 9 October 1950.

† Division of Tribophysics, Commonwealth Scientific and Industrial Research Organization, University of Melbourne, Australia.

hours, it is necessary to observe it at predetermined intervals. This has been done for aluminium by Carpenter and Elam<sup>1</sup> and Karnop and Sachs<sup>2</sup> by interrupting the annealing of the metal for etching and microscopic observation. The repeated heating and cooling of the specimen can, however, introduce stresses which will have an unpredictable effect on the growth of the crystal (Crussard and Aubertin<sup>3</sup>), and it is also probable that the etching so influences the surface that the further development of the crystals is irregular (Stanley and Mehl<sup>4</sup>). These objections have been partly overcome by a statistical type of experiment as used by Stanley and Mehl<sup>4</sup> and Anderson and Mehl.<sup>5</sup> These authors annealed a large number of specimens of very fine-grained material for various periods at a series of temperatures, and from the number and the size distribution of the new grains in each specimen they deduced an average rate of nucleation and growth. These average results, however, apply to a large new grain forming from a fine-grained material, and do not reveal extreme differences of growth from grain to grain, or even within one grain.

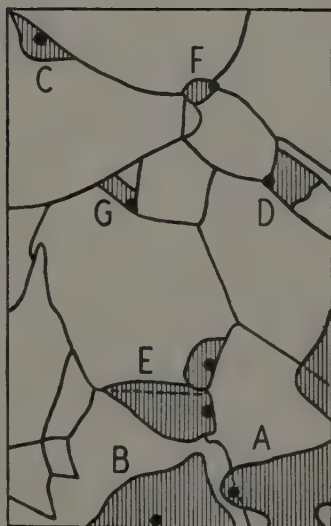
The method described in the present paper allows continuous observation of new grains in deformed zinc without the above complicating factors. It is based on an effect which has been known for many years and described fully by Wright,<sup>6</sup> namely, that the grain structure of a non-cubic metal is revealed when it is observed in a polarizing microscope. A polished surface viewed under crossed nicols shows the true structure at any instant, whereas a normally etched surface requires further preparation to show any changes occurring after the initial etch. Photographic records of the growth of new crystals have revealed marked anisotropy of growth, and the effects of grain boundaries, twins, and inclusions have been observed. The technique was used in 1932 for a film on the "Recrystallization and Grain Growth" of tin and zinc.\* Although the film shows many of the features described in this paper, no detailed study was made nor were the implications discussed.

## II.—EXPERIMENTAL.

The specimens were heated *in situ* on the stage of a standard Vickers projection microscope, and were examined under polarized light, using mercury-arc illumination. A camera body for 35-mm. film, incorporating automatic film transport after each exposure, was attached to the eyepiece tube of the microscope by a Leica microscope adaptor. With this arrangement it was possible to observe the specimen con-

\* Film entitled "Recrystallization and Grain Growth", by E. O. Bernhardt and H. Hanemann, made at the Institut für Metallkunde, Technische Hochschule, Berlin, 1932.

FIG. 2.—Outline of Crystals Shown in  
Plates LIII–LV. Shaded areas indi-  
cate changes taking place during the  
experiments.







FIGS. 3-6.—GENERAL VIEW OF FIELD AT DIFFERENT TIMES DURING RECRYSTALLIZATION OF ZINC.  $\times 110$ .

FIG. 3.—Original Structure.  
FIG. 5.—8½ min.

FIG. 4.—5½ min.  
FIG. 6.—11 min.



FIGS. 7-10.—GENERAL VIEW OF FIELD AT DIFFERENT TIMES DURING RECRYSTALLIZATION OF ZINC.  $\times 110$ .

FIG. 7.— $15\frac{1}{2}$  min.  
FIG. 9.— $20\frac{1}{2}$  min.

FIG. 8.— $17\frac{1}{2}$  min.  
FIG. 10.— $22\frac{1}{2}$  min.



FIGS. 11-14.—GENERAL VIEW OF FIELD AT DIFFERENT TIMES DURING RECRYSTALLIZATION OF ZINC.  $\times 110$ .

FIG. 11.—23½ min.

FIG. 13.—30 min

FIG. 12.—26 min.

FIG. 14.—Repolished.

(a)

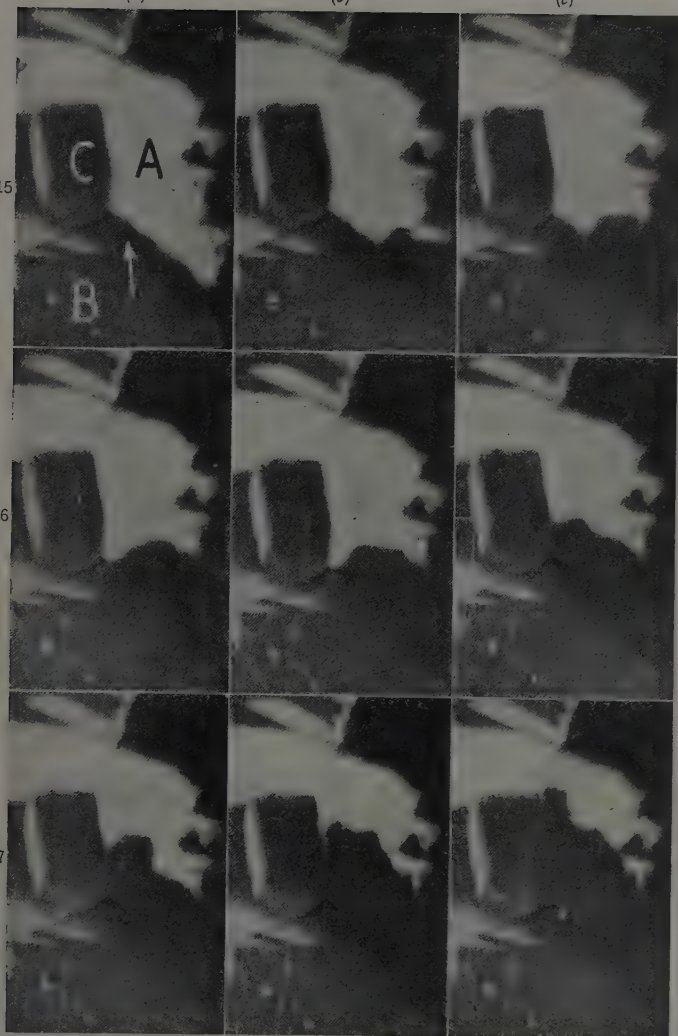
(b)

(c)

15

16

17



FIGS. 15-17.—ERRATIC ABSORPTION OF ONE GRAIN BY ANOTHER DURING RECRYSTALLIZATION.  $\times 220$ .

FIG. 15 (a).—195 sec.

FIG. 15 (b).—295 sec.

FIG. 15 (c).—360 sec.

FIG. 16 (a).—405 sec.

FIG. 16 (b).—425 sec.

FIG. 16 (c).—445 sec.

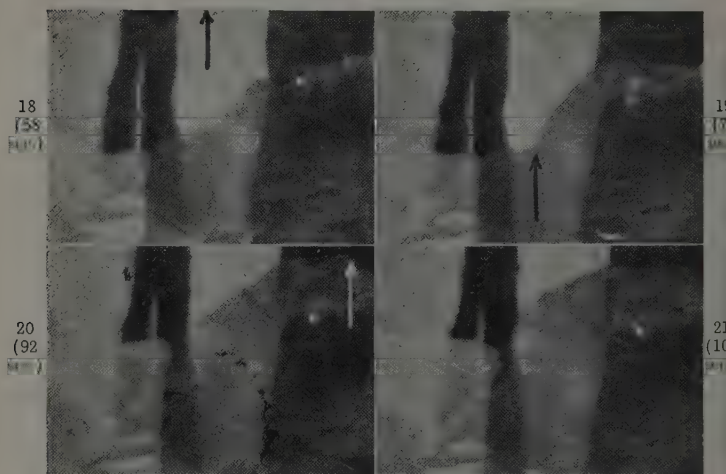
FIG. 17 (a).—465 sec.

FIG. 17 (b).—525 sec.

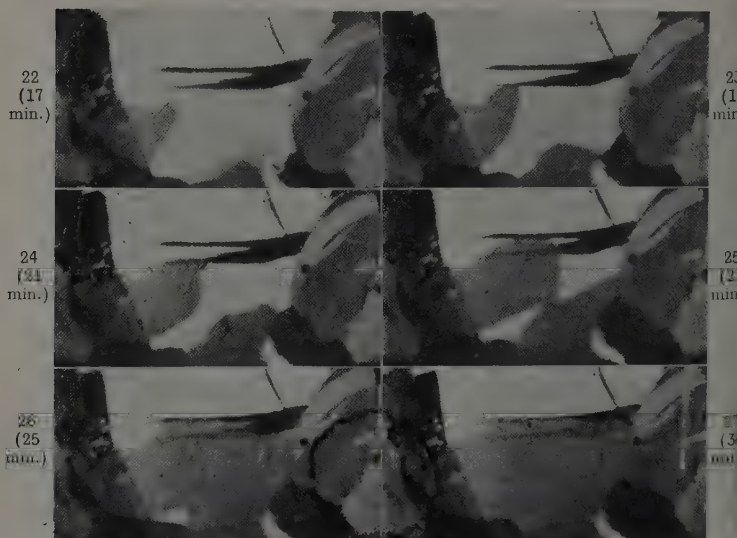
FIG. 17 (c).—585 sec.



THE EFFECT OF TWINS ON GRAIN GROWTH.  $\times 220$ .

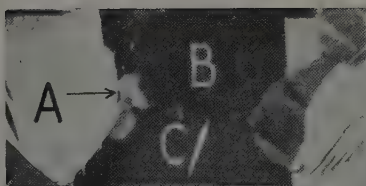


FIGS. 18-21.—Twin boundaries have no great effect on growth of a new grain.

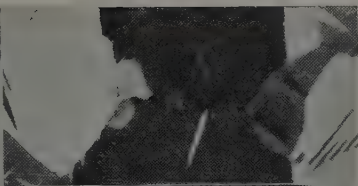


FIGS. 22-27.—Twin boundaries can inhibit growth in some directions.

8  
1  
2  
(n.)



29  
(9  
min.)



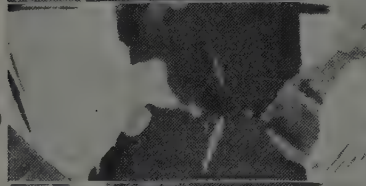
0  
1  
2  
(n.)



31  
(10  
min.)



2  
0  
1  
(n.)



33  
(11  
min.)



4  
1  
2  
(n.)



35  
(14  
min.)



6  
6  
2  
(n.)



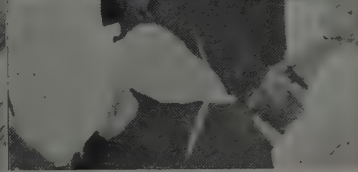
37  
(18  
min.)



8  
0  
1  
(n.)

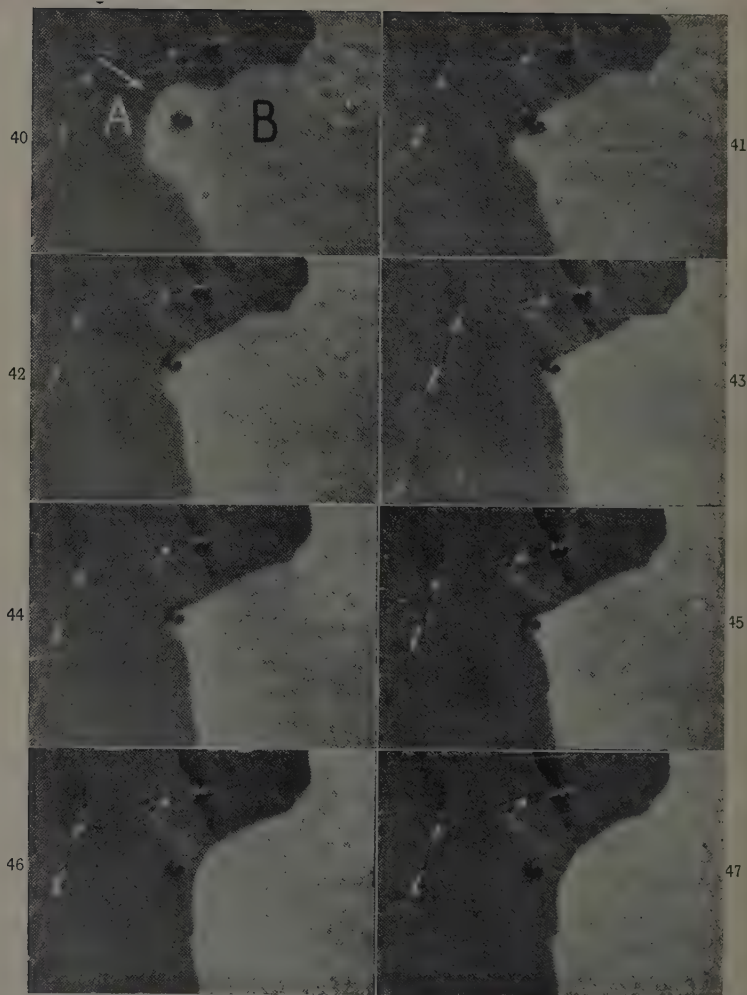


39  
(30  
min.)



FIGS. 28-39.—GROWTH ALONG A GRAIN BOUNDARY WITH VARIABLE GROWTH IN THE ADJACENT GRAINS.  $\times 140$ .





FIGS. 40-47.—THE EFFECT OF A SURFACE INHOMOGENEITY ON GRAIN GROWTH.  $\times 220$ .

FIG. 40.—16 sec.

FIG. 41.—35 sec.

FIG. 42.—64 sec.

FIG. 43.—91 sec.

FIG. 44.—118 sec.

FIG. 45.—127 sec.

FIG. 46.—133 sec.

FIG. 47.—148 sec.

tinually through the eyepiece of the Leica attachment while it was being heated and, when recrystallization commenced, to take a rapid succession of exposures. The intensity of illumination was low, and exposures of about 1 sec. were required when using Ilford HP3 film. By the use of photographic intensifiers, and by a different optical arrangement, it has been possible to reduce the exposure time considerably, but in the present experiments this was not found necessary, as the maximum rate of boundary movement was clearly recorded with exposures at 5-sec. intervals.

The specimen was about 14 mm. in dia. and 2.3 mm. in thickness. It was mounted in a small brass ring that fitted closely into a circular recess in an electrically heated brass block, insulated from the microscope stage by a canvas Bakelite sheet. The temperature was measured by a thermocouple inserted in a hole in the block.

Heat radiation to the objective was reduced by means of a cover glass between the specimen and the lens. The cover glass was partly aluminized to increase the thermal reflectivity, and this only reduced the intensity of illumination by about 20%. The furnace arrangement is shown in Fig. 1.

For most of the experiments the 16-mm. objective was suitable, but it was found that, even with the shorter working distance of the 8-mm. objective, the heating of the lens was not excessive, and although provision was made for cooling the lenses with an air jet, this was not found to be necessary. After preparation, the specimen, mounted in the brass ring, was placed on the microscope stage and a suitable field selected and photographed. The brass block, already adjusted to the required temperature, was then placed over the ring. Owing to the close fit between the ring and the recess, the zinc rapidly reached the temperature recorded by the thermocouple in the block. This was confirmed by preliminary experiments with a thermocouple attached to the specimen. When the experiment was completed, the specimen was removed from the microscope stage and repolished electrolytically. By means of small locating points in the brass ring, the identical field could be located and photographed; this gave an independent check of the structure shown by polarized light. All the essential features of the final photograph were found again on repolishing, apart from minor changes owing to the fact that a different plane was observed after polishing.

The choice of the optimum grain-size in the zinc\* and the best

\* Electrolytic zinc was used, containing Pb 0.0062, Cd 0.0016, Fe 0.0004, Cu 0.0009%. The specimens were cut from cast and swaged rod, and were rendered homogeneous by a 24-hr. anneal at 375° C.

conditions of deformation and temperature required considerable exploratory work. The grain-size was chosen so that it was small enough to give sufficient sites of potential nucleation in any field, and yet large enough to enable the movement of the boundary of any one grain to be easily followed. The optimum grain-size was about 30 grains/mm.<sup>2</sup>. This was obtained by two successive compressions of

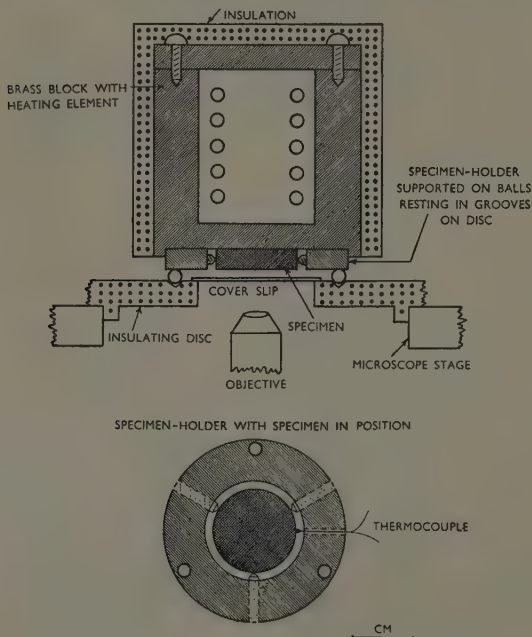


FIG. 1.—General Scheme of Furnace Assembly.

20% reduction in thickness of the homogenized specimens, with an anneal for 1 hr. at 150° C. after each reduction. For the recrystallization experiments, the specimens were deformed 12–15% by compression. With greater deformation, twinning and surface rumpling made the structure too complex for easy interpretation, while with lower deformation the required annealing temperature was unnecessarily high. Most experiments were carried out at about 110° C. In some cases a small increase in temperature occurred during the experiment. Higher temperatures are undesirable, since the movement of grain

boundaries becomes very rapid, and sharp photographs cannot be obtained with the relatively long exposure time used.

Owing to the friction of the platens, deformation by compression was greatest near the middle of the specimen. The specimen was therefore etched in dilute hydrochloric acid on one side only until the thickness was reduced by half. Thus the layers which were originally central could be observed, and, as these layers were the most heavily deformed, they were the most probable sites for nucleation. After careful grinding on wet 600-grade polishing papers, the surface was prepared for examination by electropolishing in orthophosphoric acid (Jacquet<sup>7</sup>). Polishing was continued until all traces of the disturbed layer due to grinding had disappeared.

### III.—RESULTS.

Some typical results are shown in Figs. 3-14 (Plates LIII-LV) which were selected from a series of 46 photographs taken at  $\frac{1}{2}$ -min. intervals during one experiment. It can be seen from Fig. 14 (Plate LV) (which is a photomicrograph of the repolished specimen) that the method shows all changes which have occurred. Since the old grain boundaries sometimes remain clearly visible after the new crystal has grown through them, it may be thought that the growing crystal is only a surface film (possibly a crystal of oxide) growing laterally from some nucleus on the surface. However, the real existence of these shadow crystals is shown in Fig. 14.

To illustrate the changes, Fig. 2 (Plate LII) shows the general outline of the crystals in the field. The shaded portions indicate the new crystals which have developed in the course of the experiment, and the broken lines the old boundaries which are now obscured. The black dot associated with each new crystal marks the point where it was first definitely observed. The photographs show the behaviour of seven nuclei in the first 30 min. of annealing at 110° C. Four of these new crystals (*A*, *B*, *C*, and *D*, Fig. 2) could be seen after  $5\frac{1}{2}$  min. of annealing. Nucleus *E* appeared after  $8\frac{1}{2}$  min., and *F* and *G* after  $15\frac{1}{2}$  and  $17\frac{1}{2}$  min., respectively. Thus there are a number of new crystals which began to grow at different times. However, when the final photographs of the series are examined it can be seen that the age of the crystal bears no relationship to its final size, e.g. nucleus *E* has grown into a crystal much larger than *C* or *D*, although it began to grow later. In all experiments, it has been found that practically all the changes can be traced to the growth of a new undeformed grain. Thus, the phenomena described are principally concerned with recrystallization, and not movement of the boundaries between deformed grains.

As it is not possible to reproduce all the experimental results in detail, the remaining photographs are selected from various experiments to show some of the essential features of recrystallization.

### *1. Growth of New Crystals.*

The growth of new crystals was found to be a very irregular process and very much influenced by such factors as grain boundaries, inclusions, and twinning. However, even when observable discontinuities were absent, erratic growth still occurred. This is shown by Figs. 15-17 (Plate LVI). A light-coloured grain *A* is being absorbed by a dark-coloured grain *B* in the direction shown by the arrow. The boundary, which is initially straight, has parts which grow more rapidly than the remainder, and it therefore develops an irregular contour. The direction of growth is parallel to the boundary between *A* and another dark crystal *C*, and it will be noticed that the presence of the *AC* boundary contributes to the irregular contour. This is discussed below in greater detail in connection with Plate LVII. However, the effects mentioned earlier occur at points distant from this boundary. This erratic growth process has also been observed visually at higher temperatures, which cause an increase in the rate of growth of the new crystal. Under these circumstances, the boundary appears to move in a series of instantaneous jumps.

### *2. Effect of Twin Boundaries.*

Examples can be found showing two opposite effects of twin boundaries on crystal growth. On the one hand, although the growth of a new grain across twinned regions of a crystal shows irregularities, these appear to bear little or no relationship to the twins, but are similar to the erratic growth described in the last section. On the other hand, the movement of a grain boundary can be completely inhibited by a twin. The first effect is shown by Figs. 18-21 (Plate LVII). The new grain is growing in a direction parallel to the long axes of the twins indicated by the arrow in Fig. 18. The growing crystal shows irregularities which often occur in the parts of the old crystal or the twins which are farthest from the twin boundaries (see the points marked with an arrow in Figs. 19 and 20). Thus it appears that twinning does not cause any irregularities in growth additional to those discussed in the previous section.

The second type of behaviour is illustrated by Figs. 22-27 (Plate LVII) which are enlargements of a detail in Plates LIII-LV. A new grain is growing in a direction perpendicular to the long axes of two parallel twins. Within a few minutes it reaches and absorbs the first

twin (Figs. 22-24). On reaching the second twin, the new grain absorbs it also, but growth does not extend further into the untwinned part of the grain, although before reaching the twin the new grain passed through an untwinned region without hindrance. Fig. 27, taken at the end of the experiment, shows the final crystal boundary to be identical with the original twin boundary.

### 3. *Effect of Grain Boundaries.*

The behaviour of a growing grain when it meets a crystal boundary is variable, as in the case of twin boundaries. The growth may be accelerated or retarded, and the magnitude of the effect varies considerably. The authors found, however, that these effects do not always take place exactly at the boundary. The effects are illustrated by Figs. 28-39 (Plate LVIII), which are photographs of another detail selected from the field of Plates LIII-LV. They show a light-coloured crystal *A* (Fig. 28) growing into two dark crystals, *B* and *C*, in a general direction parallel to the *BC* boundary. The growth is always more advanced along the *BC* boundary, but the absorption of *B* and *C* does not occur symmetrically about the boundary. Figs. 28-36 show that *A* has penetrated only a short distance into *C*. Later, growth occurs only in crystal *B* (Figs. 36-39). On the other hand, in Plate LVI there is an example of retardation of growth by the boundary. The growth of crystal *B*, which is in a direction parallel to the *AC* boundary, is retarded at the boundary for some minutes (Figs. 15-16 (*b*)), but the next photograph (Fig. 16 (*c*)), shows a sudden rapid advance along the boundary. Thus Plate LVIII illustrates the case of a crystal growing faster along the boundary of two other crystals, than within either of them and Plate LVI illustrates a boundary retarding growth under apparently similar conditions.

### 4. *Effect of Inclusions and Surface Imperfections.*

Although this has not been systematically studied in the present investigation, the authors noticed that in certain specimens an inclusion or surface imperfection can affect the shape of the growing boundary (Figs. 40-47, Plate LIX). A dark grain *A* is growing into a lighter grain *B*, and part of the boundary (indicated by an arrow in Fig. 40) is approaching what appears to be an inclusion or a pit in the surface. After 35 sec., the boundary has reached this imperfection and begins to grow round it. The growing grain does not absorb it, however, until after 127 sec., when it is rapidly engulfed and growth proceeds. Yet numerous other similar imperfections in other parts of the field did not appear to have any effect on the movement of the boundary.



## IV.—DISCUSSION.

The results show that the growth of a nucleus during recrystallization of deformed zinc is very irregular. Growth varies with the direction, and from point to point in a crystal, and can apparently stop altogether for relatively long periods. In particular, it can be markedly affected by grain and twin boundaries, and by other discontinuities.

Crussard and Aubertin<sup>3</sup> have made a very thorough study of the recrystallization of zinc, and attempted to determine the relationship between grain-size and annealing temperature. They obtained very variable results, which they attributed to the irregular character of the growth process and its marked dependence on localized differences in deformation. The results recorded in the present paper give definite confirmation of their observations.

In a few cases the authors were able to measure the linear dimensions of a growing grain in different directions at various times, and thus to estimate the rate of growth in a number of directions. The results suggested that, although the total growth in different directions varied widely, the actual rates of growth were not subject to such wide variations. However, there were periods of varying duration, when there was little or no growth. It appears, therefore, that for some cases at least, differences in the final dimensions of the grain in various directions are caused by arrests in the uniform growth, rather than by marked differences in the growth rate in various directions.

It may be thought that irregular growth could be caused by the presence of impurities, but this cannot always be a major factor. The zinc specimens were worked and annealed many times before being used in the experiment, and as a result of this treatment, any insoluble impurities would not, in general, coincide with the final grain boundaries, and the soluble ones would be evenly dispersed throughout the metal. The pause in the growth rate occurring in regions near grain boundaries is therefore difficult to explain in terms of impurities. Further, it is even more difficult to associate mechanical twin boundaries with impurity concentrations although these also can be regions of erratic growth.

It is generally agreed that the driving force for the growth of a new crystal in a deformed one, must be primarily due to the deformation energy in the old grain. If this varies throughout the grain, then an erratic growth behaviour can be expected. In recent years there has been a good deal of evidence for the presence of localized inhomogeneities of deformation in metals (Boas<sup>8</sup>). Experiments on aluminium have shown how the distortion can vary between grains as a

result of orientation differences, and within grains as a result of grain-boundary interaction. Zinc, which is non-cubic, would be expected to show these effects even more strongly, and would also be subject to additional distortions, owing to anisotropic thermal expansion (Boas and Honeycombe<sup>9</sup>). The present experiments give additional evidence for the presence of localized distortion.

Finally, the results described suggest the need for a re-examination of the assumptions involved in the statistical method of approach to the recrystallization problem, and can be used to explain certain difficulties. This work emphasizes the care that must be taken in extending the results of statistical investigations to cases where the growing crystal is comparable in size to the deformed grains. Anderson and Mehl<sup>5</sup> measured a rate of nucleation in deformed fine-grained aluminium by counting the number of new grains which appeared after definite intervals. They found an increase of the apparent rate of nucleation with time. At the magnification used, a new grain must be very much larger than the grains of the matrix before it can be observed. In deducing that the true rate of nucleation also increases with time, these authors make the implicit assumption that a nucleus grows at a constant rate to the size necessary for observation. However, at the stage when a new grain is of about the same size as the old grains, and before it can be recognized as such, it must be expected to grow at a most erratic rate.

With these new facts, it is possible to explain the increase of the apparent nucleation rate with time by making the more probable assumption that the true nucleation rate is either independent of, or even decreases slowly with, time. All the true nuclei present at any instant are subject to marked irregularities of growth, both in the crystal in which they first occur and at the grain boundaries of this crystal and its neighbours. However, on the average, a definite fraction of these will be favourably situated for immediate and relatively rapid growth into neighbouring grains. Once the new grain has absorbed one or more of its neighbours, the probability of its growing still larger is increased, since it will come into contact with more neighbours, a statistically constant fraction of which will be favourably situated for further immediate growths.

Hence it may be expected that the period before the growth of a nucleus begins will be extremely variable, and that the growth will be erratic before the regular growth observed by Anderson and Mehl<sup>5</sup> takes place. As long as the number of unobserved true nuclei is increasing with time, the number that grow to an observable size in successive units of time is increasing. Thus the apparent rate of nucleation is increasing.

Cahn<sup>10</sup> has explained the increase in nucleation rate with time, by assuming that the time necessary for a distorted region of a crystal to become an "active" nucleus increases with the local curvature of the crystal planes. Since deformation is inhomogeneous, the curvatures are distributed about a mean, and therefore initially the rate of production of "active" nuclei (called "true" nuclei in previous paragraphs) would increase. Cahn's theory thus applies to the incubation period. The growth beyond this stage is irregular, and this in itself is sufficient to explain the increase in apparent nucleation rate with time. It is possible to make many different assumptions about the rate at which true nuclei become observable, and as long as they lead to the condition that the total number of unobserved nuclei is continually increasing, they all explain the increase in the apparent nucleation rate.

Burgers<sup>11</sup> assumed that Anderson and Mehl measured true nucleation rates, and has explained the increase by suggesting that a growing crystal is able to stimulate new nuclei. In view of the remarks above, it appears that the production of stimulated nuclei is not the major effect in all cases. It is possible, however, that a growing crystal will alter the stress pattern around a nearby small crystal, thereby enabling it to grow more rapidly.

In this paper some direct observations of the growth of new crystals have been described, and their implications with respect to the problem of nucleation have been discussed. The technique can be used for a further detailed investigation of the subsequent growth of these crystals. It is clear, however, that the method also has wider applications, since it enables grain-boundary movements and phase changes to be observed.

#### ACKNOWLEDGEMENTS.

The authors would like to thank Dr. W. Boas for suggesting the problem, and for his continued helpful advice. Thanks are also due to Professor Hartung for laboratory facilities in the Chemistry Department, University of Melbourne.

#### REFERENCES.

1. H. C. H. Carpenter and C. F. Elam, *J. Inst. Metals*, 1921, **25**, 259.
2. R. Karnop and G. Sachs, *Z. Physik*, 1930, **60**, 464.
3. C. Crussard and F. Aubertin, *Métaux et Corrosion*, 1946, **21**, (248), 45; (249), 66.
4. J. K. Stanley and R. F. Mehl, *Trans. Amer. Inst. Min. Met. Eng.*, 1942, **150**, 260.
5. W. A. Anderson and R. F. Mehl, *ibid.*, 1945, **161**, 140.
6. F. E. Wright, *Proc. Amer. Phil. Soc.*, 1919, **53**, 401.
7. P. A. Jacquet, *Métaux, Corrosion, Usure*, 1944, **19**, 71.
8. W. Boas, *Helv. Phys. Acta*, 1950, **23**, 159.
9. W. Boas and R. W. K. Honeycombe, *Proc. Roy. Soc.*, 1946, [A], **186**, 57.
10. R. W. Cahn, *Proc. Phys. Soc.*, 1950, [A], **63**, 323.
11. W. G. Burgers, *Proc. K. Ned. Akad. Wetensch.*, 1947, **50**, 858.

## INTERNAL FRICTION AND GRAIN-BOUNDARY VISCOSITY OF TIN.\*

1317

By L. ROTHERHAM,† M.Sc., MEMBER, A. D. N. SMITH,‡ B.A., and  
G. B. GREENOUGH,§ Ph.D.

## SYNOPSIS.

The internal friction of high-purity tin has been studied over the temperature range 15°–150° C. by measurements made on bars vibrating transversely at audio frequencies in the "free-free" mode. Both polycrystalline specimens and bars consisting of a very few crystals have been examined. A peak in the curve of internal friction plotted against temperature, ascribed to viscous relaxation at the grain boundaries, is found to exist for the former type, but not for the latter. The activation energy associated with the relaxation has been measured, and is consistent with that for steady-state creep of single crystals, but differs greatly from the value for self-diffusion in tin. This is contrary to a theory put forward by Kê that all three values should be the same (*Phys. Rev.*, 1948, [ii], 73, 267).

The variation of Young's modulus with temperature has been observed over the same range for both types of specimen. The results are similar to those obtained by Kê for aluminium (*ibid.*, 1947, [ii], 71, 533), although the magnitude of the effect observed is smaller.

## I.—INTRODUCTION.

DURING recent years internal-friction measurements at very small stresses have been used to shed light on several metallurgical and physical problems. In particular, Kê<sup>1,2</sup> has studied the properties of the grain boundaries in metals, by noting the variation of internal friction in aluminium with temperature, using a torsional pendulum vibrating at about 1 c./s. His results show that in polycrystals, the internal friction ( $Q^{-1}$ ) is low at room temperature, but increases rapidly to a maximum as the temperature is raised, falling to low values again as the temperature rises still further. In single crystals, on the other hand,  $Q^{-1}$  increases very slowly, but steadily, with temperature. Kê deduced that the peak in the polycrystal curve is due to slip of one grain over another at the boundary, under the influence of the applied shear stress, until the relative movement is blocked by the interlocking action of neighbouring grains. This slip gives rise to internal friction,  $Q^{-1} \sim (\text{distance slipped}) \times (\text{shear stress across the boundary})$ . The maximum shear stress that can be applied to the boundary is limited

\* Manuscript received 19 October 1950.

† Division of Atomic Energy (Production), Risley, Warrington, Lancs; formerly Head, Metallurgical Department, Royal Aircraft Establishment, Farnborough.

‡ Metallurgical Department, Royal Aircraft Establishment, Farnborough.

§ Lecturer in Metallurgy, University of Sheffield; formerly Metallurgical Department, Royal Aircraft Establishment, Farnborough.

by the amplitude of vibration of the specimen, while the maximum relative movement that can take place between the grains meeting at the boundary is limited by the interlocking action of the surrounding grains.

Kê explains his results by assuming the grain boundary to be a viscous layer, whose coefficient of viscosity decreases with increasing temperature. At low temperatures the coefficient is so high that the shear stress is insufficient to cause appreciable slip during the period of one vibration. At high temperatures the coefficient is so low that the distance slipped reaches its limiting value while the applied shear stress is still very small, whereupon the stress is no longer applied across the boundary but is transferred to the interlocking units. At both extremes of temperature  $Q^{-1}$  is therefore small, while at some intermediate value  $Q^{-1}$  is high.

Kê found that an activation energy ( $H$ ) is associated with this viscous slip along the boundary, which has approximately the same value as those recorded for steady-state creep of single crystals of aluminium,  $\alpha$ -iron, and  $\alpha$ -brass. It is also the same as the activation energy for self-diffusion in the two pure metals, while in the case of brass it approximates to the energy for diffusion of zinc in copper. On this basis Kê put forward the suggestion<sup>3</sup> that the processes of grain-boundary slip, steady-state creep in single crystals, and diffusion occur by the same kind of mechanism. Thus, he argued that the three activation energies should be the same for all metals.

By assuming that the grain-boundary width was of the order of one atomic distance, Kê estimated the coefficient of viscosity of the grain boundary of aluminium at the temperature at which the maximum internal friction occurred. Then, by using the value obtained for the activation energy, he estimated this coefficient at the melting point, and obtained a value which was in remarkably close agreement with the experimentally determined value for molten aluminium.

Puttick and King<sup>4</sup> have recently reported some experiments using bicrystals of tin with macroscopically straight boundaries. They subjected each specimen to pure shearing forces at relatively high temperatures and observed the initial rate of slip ( $\dot{\epsilon}$ ), which varied with the shear stress ( $\sigma$ ) and the absolute temperature ( $T$ ) according to the equation :

$$\dot{\epsilon} = C \cdot \sigma \cdot \exp \left( \frac{-H}{RT} \right) \quad . \quad . \quad . \quad . \quad (1)$$

where  $R$  is the gas constant,  $H$  is an activation energy, and  $C$  is a constant. This equation shows, as in Kê's experiments, that the initial slip along the grain boundary is viscous, and from it the coefficient of viscosity at any temperature may be found. The value at the melting



point was  $4 \times 10^4$  poises, compared with the experimentally determined value for liquid tin at the same temperature of about 0.02 poise. Thus, it is clear that the grain-boundary slip investigated by Puttick and King is not the same as that studied by Kê. The obvious difference is that in the bicrystal experiments the slip was on a macroscopic scale, the smallest measured displacement between crystals being about  $10^{-4}$  cm., while in Kê's work the slip was on a sub-microscopic scale, the maximum displacement being about  $3 \times 10^{-7}$  cm. Therefore it seems probable that, in spite of the bicrystal boundary being macroscopically straight, sufficient microscopic irregularities existed to cause interlocking between the two crystals. If this were so, then it would seem likely that slip proceeded by creep in the interlocking knobs, in which case the heat of activation ( $H$  in equation (1)) would be the same as that for steady-state creep in single crystals. Puttick and King found  $H$  to be  $19,000 \pm 2000$  cal./mole, which does agree quite well with the value for steady-state creep in a single crystal of tin, stated by Seitz<sup>5</sup> to be 17,300 cal./mole.

It was decided to perform some internal-friction experiments on tin to determine the activation energy associated with the Kê type of grain-boundary slip, and to compare it with these other values. At that time no information was available on the activation energy for self-diffusion in tin, but while the work was in progress Boas and Fensham<sup>6</sup> obtained values of 5900 cal./mole along the  $a$ -axis and 10,500 cal./mole along the  $c$ -axis. This showed that the energies for creep and diffusion differed widely, and therefore that Kê's theory that they should both be identical with the energy for grain-boundary slip could not be true in the case of tin. It was of interest, however, to determine whether this latter energy was identical with that for creep or for self-diffusion, or with neither.

Kê's viscosity equation and the application of internal-friction measurements to the determination of activation energy and Young's modulus are discussed in the Appendix (p. 452).

## II.—EXPERIMENTAL DETAILS.

### 1. *Scope of Investigation.*

The objects of the experiments were, firstly, to determine the activation energy associated with grain-boundary slip for high-purity tin; secondly, to obtain a value for the coefficient of viscosity of the grain boundary at the melting point; and thirdly, to examine the effect of grain-boundary slip on Young's modulus. For this purpose it was essential that the peak in the curves of internal friction plotted against



temperature, due to viscous slip at the boundaries, should occur at a temperature somewhere above  $50^{\circ}\text{C.}$ , since the most useful part of the curve for the determination of activation energy is the rising portion immediately below the peak. Moreover, the allotropic transformation from white to grey tin takes place at  $18^{\circ}\text{C.}$ , and all measurements had to be made above that temperature to avoid possible complications from internal friction associated with the transformation. From Kê's work on aluminium <sup>1</sup> it appeared probable that if the experiments were carried out at the frequencies which he used (1–3 c./s.) then the peak would occur at about room temperature. As explained in the Appendix, an increase in frequency shifts the curve to higher temperatures, and it was therefore decided to make the experiments at audio frequencies. In order to do this, specimens in the form of flat bars were excited into resonant vibration in the "free-free" mode, the internal friction being determined in terms of the logarithmic decrement (log. dec.) of the free decay of vibration that occurred when the exciting unit was switched off. The relation between the logarithmic decrement, internal friction ( $Q^{-1}$ ), and specific damping capacity ( $\Delta E/E$ ) is :

$$\text{log. dec.} = \pi \times Q^{-1} = \frac{\Delta E}{2E}$$

## 2. *Apparatus Used.*

The specimen was suspended horizontally inside an electric furnace by two fine threads. A small piece of low-hysteresis-loss transformer lamination (Permalloy) was firmly fixed to one end of the bar by cold-setting Araldite, and placed immediately below the pole piece of a small electromagnet, consisting of a long, soft iron bar,  $\frac{1}{2}$  in. in dia., on which were wound two coils. The first of these was connected to an accumulator to provide a constant polarizing field, while the second was connected via a power amplifier to a variable-frequency oscillator calibrated with high accuracy. When this latter coil was energized, an alternating force was applied to the Permalloy strip, which in turn caused vibrations in the bar. The amplitude of vibration remained small until the frequency of the oscillator approached either the natural frequency of the bar or one of its harmonics, when it increased to a value depending on the power input and the damping of the specimen.

Vibrations in the bar were transmitted by one of the suspension threads to the needle of a gramophone crystal pick-up, which converted the mechanical energy into a small electrical voltage, whose amplitude was assumed to be proportional to the amplitude of vibration of the bar. After amplification this voltage was displayed on a cathode-ray oscilloscope, thus providing a visual means of tuning the oscillator to resonance.

A special electronic instrument, described in detail elsewhere,<sup>7</sup> was designed to enable measurements of the logarithmic decrement to be made quickly and directly. The principle of operation is to cause two electrical pulses to be emitted during the decay of vibration, the first when the amplitude falls to some value, say,  $A_0$  (which may be varied over a wide range) and the second when it falls to  $A_0/2$ . The time,  $T$ , between these pulses is measured by means of a "Chronotron" instrument, and the logarithmic decrement then found from the equation:

$$\log. \text{dec.} = \frac{\log_e 2}{fT}$$

where  $f$  is the frequency of vibration read directly off the decade dials of the oscillator.

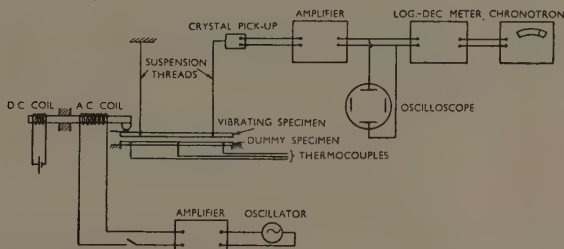


FIG. 1.—Arrangement of Apparatus. Furnace and anti-vibration mounting not shown.

The windings of the furnace were so arranged that two slots were provided through which the suspension threads passed to the pick-up, &c., outside the furnace. The temperature was measured on a dummy specimen, placed close to the vibrating specimen, by means of three iron/Constantan thermocouples which were used to check the temperature gradient along the bar. This gradient increased with temperature, the maximum observed being  $\frac{2}{3}^{\circ}\text{C./in.}$  at  $200^{\circ}\text{C.}$

The arrangement of the apparatus is shown in Fig. 1.

### 3. Preparation of Specimens.

"Chempur" tin, of 99.99% purity, was used in these experiments. The maker's analysis is as follows:

Cu, %	Bi, %	Fe, %	Sb, %	As, %	S, %	Pb, %
0.0006	0.0008	0.0004	0.0032	0.0005	0.0004	0.0021

Ni trace; Co, Zn, Ag, not detected.

Total impurity content . . . . .	0.0080%
Tin (by difference) . . . . .	99.9920%

Two types of specimen were used, one polycrystalline and the other consisting of only a very few crystals. The first kind was usually

obtained by cold rolling a small ingot down to 90% reduction in area, the final dimensions being approx.  $0.06 \times 0.6 \times 4$  in., although one specimen was rolled down only to 80% reduction in area and measured  $0.125 \times 1.15 \times 5.9$  in. (specimen A). These bars were then annealed in air at temperatures ranging from  $125^\circ$  to  $140^\circ$  C. until they had completely recrystallized. The "single-crystal" specimen was grown by the moving-furnace method described by Chalmers,<sup>8</sup> and was somewhat thicker and longer than the polycrystal specimens, measuring about  $0.25 \times 0.5 \times 6.5$  in. In fact, it consisted of several crystals, most of which extended along the greater part of the bar.

#### 4. Measurements Made.

The logarithmic decrement was measured by the method described over a range of temperature, and was plotted either against temperature (as in Fig. 2) or against the reciprocal of the absolute temperature,

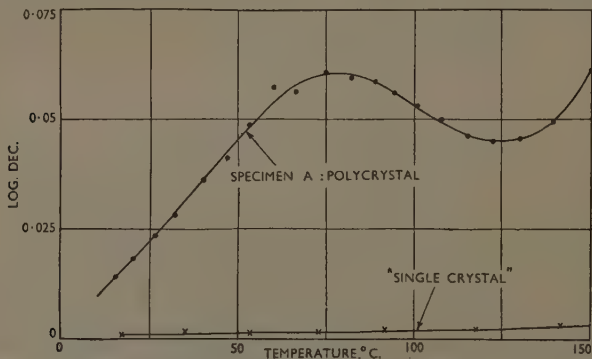


FIG. 2.—Variation of Logarithmic Decrement with Temperature for "Single Crystal" and Polycrystal (Specimen A).

$1/T$  (as in Fig. 3). It was demonstrated by measuring the logarithmic decrement for various initial amplitudes of vibration that the value determined was substantially independent of the strain amplitude. No measurements were made for temperatures greatly in excess of that at which the internal-friction peak occurred, as it was necessary to keep the specimen always below the temperature of preliminary recrystallization. It had proved impossible to anneal the specimens at any higher temperature before carrying out the experiments, because the resultant grain-size was then too large to give an appreciable peak.

As explained in the Appendix, the activation energy may be deter-

mined by obtaining two curves of log. dec. against  $1/T$  for the same specimen at different frequencies, and measuring the shift in  $1/T$  necessary to superpose them. A simple way of obtaining readings at two frequencies with the apparatus described is to excite the bar first into its fundamental resonance and then, at the same temperature, into its first harmonic. For the specimens used, the corresponding frequencies were approx. 300 and 800 c./s. The disadvantage in doing so is that in order to equalize the energy losses through the suspensions (which depend on the distance from the nodes at which they are attached),

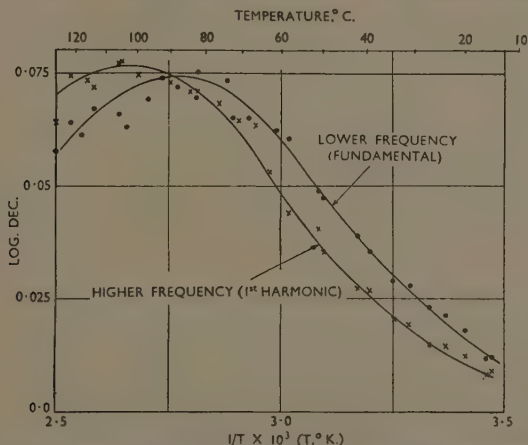


FIG. 3.—Variation of Logarithmic Decrement with the Reciprocal of the Absolute Temperature (Specimen C).

these must be situated midway between the nodes of the fundamental and first harmonic. This means that the energy loss is greater in both cases than it would be for either if the suspensions were close to the corresponding nodes, and hence the measured value of the logarithmic decrement will be greater than it should be. However, the energy loss involved is very small compared with that dissipated at the grain boundaries (it corresponds to a logarithmic decrement of the order of 0.002) and is approximately equal in both cases. The main advantage of the method is that it ensures that no metallurgical factors alter between taking the two sets of readings, and this was thought to outweigh the disadvantage. It was therefore used for specimens B, C, and D.

Theoretically it is possible to determine Young's modulus ( $E$ ) from measurement of the natural frequency of vibration ( $f$ ), provided that

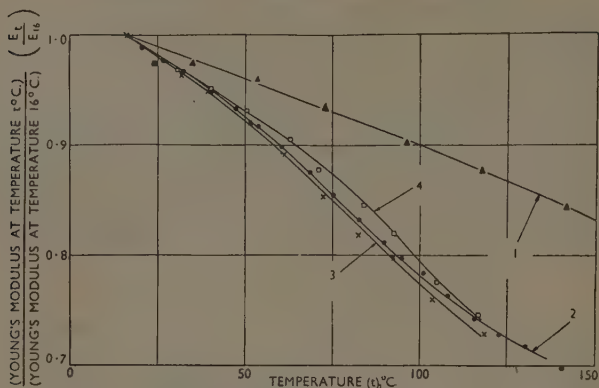


FIG. 4.—Variation of Young's Modulus with Temperature for "Single Crystal" and Polycrystals (Specimens A and C).

KEY. 1. "Single crystal"; unrelaxed modulus. 3. Specimen C; lower frequency.  
2. Specimen A. 4. " " higher frequency.

the dimensions and the density of the specimen are known, but the specimens used were not of sufficiently uniform cross-section to make such a determination accurate enough to be useful. However, the temperature dependence of Young's modulus for any one specimen could be determined quite accurately without knowing the dimensions, since  $E \sim f^2$ . Fig. 4 shows the variation of  $E_t/E_{16}$  with  $t$ , where  $t$  is the temperature in  $^{\circ}\text{C.}$ , for two polycrystalline specimens and for the single

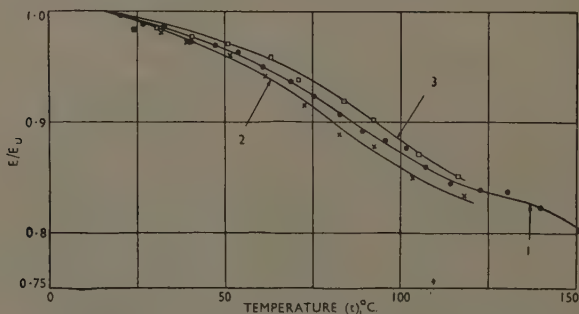


FIG. 5.—Variation of Ratio  $\frac{\text{Young's Modulus for Polycrystal } (E)}{\text{Young's Modulus for Single Crystal } (E_U)}$  with Temperature (Specimens A and C).

KEY. 1. Specimen A. 2. Specimen C; lower frequency. 3. Specimen C; higher frequency.

crystal. Fig. 5 presents a similar curve obtained by dividing  $E_t/E_{16}$  for the polycrystals by the corresponding expression for the single crystal, as discussed in the Appendix.

The magnitude of the longitudinal strain at the moment when measurement of the logarithmic decrement began was determined for one specimen only, at room temperature, by fixing a resistance strain-gauge to the centre of the upper face of the bar. This gave a rough calibration of the strain in terms of the signal amplitude on the oscilloscope, and thus the maximum longitudinal strain, which was of the order of  $5 \times 10^{-6}$ , could be found for each specimen.

The considerable scatter of the points about their respective curves is attributed to a large extent to spurious mechanical vibration of the system as a whole, detected by the very sensitive pick-up. Many efforts were made to eliminate this background "noise" by the use of an anti-vibration mounting and of an electrical filter circuit which allowed a signal of the frequency of the resonant vibration to pass, while substantially reducing low-frequency signals. These two factors helped to reduce the noise to an acceptable level, but it was found impossible to eliminate it entirely.

### III.—RESULTS AND DISCUSSION.

#### 1. *Internal Friction of Polycrystalline Specimens Compared with the "Single Crystal".*

Convincing proof that the effects observed are due to grain-boundary viscosity is obtained by comparing the internal-friction curve for one of the polycrystalline specimens with that for the "single crystal" (see Fig. 2). The latter remains low over the whole temperature range, from which it is concluded that the peak in the other curve is due to the specimen being polycrystalline. The only two types of internal friction peculiar to polycrystals are those attributable to: (a) inter-crystalline thermal currents, and (b) grain-boundary slip.

Zener<sup>9</sup> has developed the theory of internal friction in connection with (a) and has shown that it depends solely on grain-size and frequency, and not on temperature. The frequency change here is much too small to cause a peak in the curve, and in any case it is anticipated that the internal friction from thermal currents would be at least an order of magnitude less than that observed here. Hence the only possible explanation of the peak is that it is due to viscous slip at the grain boundaries.

#### 2. *Activation Energy.*

As pointed out in Section 2 of the Appendix, the two logarithmic decrement curves obtained at the two different frequencies should be



completely superposable by a translation of  $\Delta(1/T)$ . It is clear from Fig. 3, which is typical of the curves obtained for the three specimens, that this is not precisely true. The discrepancy is due to the experimental error in measuring the logarithmic decrement, and the variation of  $\Delta(1/T)$  at different parts of the curves is within the limits of this error. The best value of  $\Delta(1/T)$  is obtained from the parts of the curves where the logarithmic decrement is changing most rapidly with temperature, i.e. at the low-temperature side of the peak, and this value was used in all cases. The difference in the temperatures at which the two peaks occur is not accurate enough to be useful.

Table I gives the values of  $\Delta(1/T)$ , the ratio of the frequencies of vibration during the rising portion of the curve, and the corresponding values of the activation energy,  $H$ , for specimens B, C, and D. It also shows the values of  $1/T$  at each peak and the grain-size of the specimen, including specimen A, internal-friction measurements for which were made at only one frequency.

TABLE I.—*Activation Energy by Two-Frequency Method.*

Specimen	Average Grain Dia., cm.	$T^{-1}$ at Peak, $^{\circ}\text{K.}^{-1} \times 10^3$		Shift in $T^{-1}$ to Superpose the Two Curves, $\Delta(T^{-1}) \times 10^4$	Frequency Ratio	Activation Energy ( $H$ ), cal./mole
		Fundamental	1st Harmonic			
A	0.02	2.85	...	...	...	...
B	0.046	2.83	2.72	1.16	2.72	17,300
C	0.07	2.77	2.67	0.96	2.70	20,700
D	0.027	3.00	2.91	1.03	2.72	19,400

The three values of  $H$  are consistent within the limits of experimental error, the mean value being  $H = 19,000 \pm 2500$  cal./mole. This value for the activation energy associated with grain-boundary slip, on a sub-microscopic scale, in tin is consistent both with that obtained by Puttick and King <sup>4</sup> (19,000 cal./mole) for macroscopic slip of a bicrystal along its boundary, and with the value for steady-state creep of a single crystal quoted by Seitz <sup>5</sup> (17,300 cal./mole). It differs from the activation energy for self-diffusion in tin, found by Boas and Fensham,<sup>6</sup> as already stated, to be 5900 cal./mole along the  $a$ -axis and 10,500 cal./mole along the  $c$ -axis. From results on aluminium,  $\alpha$ -brass, and  $\alpha$ -iron, Kê<sup>3</sup> proposed that the three values should be the same for all metals. The present work shows that tin is an exception to this theory, since only two of the values are approximately equal.

### 3 Coefficient of Viscosity.

The apparent coefficient of viscosity  $\eta$  of the "boundary layer" may be estimated by means of equation (2) in the Appendix. The values of

the various factors involved are those appropriate to the temperature of the internal-friction peak.

The time of relaxation of the shear stress,  $\tau$ , across the boundary, was determined from the frequency of vibration  $f$ , using a relation derived by Zener<sup>10</sup>:

$$\tau = \frac{1}{8f}$$

The value of  $G_U$  was estimated from the shear modulus quoted for tin, allowing for the fact that it falls with increasing temperature in the same manner as does Young's modulus (see Fig. 4). A value of  $2.08 \times 10^{11} \times (1 - 0.0012t)$  dynes/cm.<sup>2</sup> was used, where  $t$  is the temperature in °C. The grain-size of the specimen was determined from

TABLE II.—*Coefficients of Viscosity at the Grain-Boundary Peak Temperatures and at the Melting Point.*

Specimen	Mode of Vibration	Temperature at Peak, °C.	Relaxation Time $\tau$ at Peak, sec. $\times 10^4$	Coefficient of Viscosity, poise		
				At Temperature of the Peak	At the Melting Point (232° C.)	
					Modified Equation	Kê's Equation
A	Fundamental	79	3.84	110	0.028	0.022
B	"	81	4.15	50	0.016	0.013
B	1st Harmonic	95	1.55	20	0.016	0.013
C	Fundamental	89	4.25	35	0.018	0.015
C	1st Harmonic	102	1.58	12	0.018	0.015
D	Fundamental	60	4.21	90	0.005	0.004
D	1st Harmonic	71	1.56	35	0.005	0.004

metallographic examination. For the thickness of the grain-boundary layer,  $d$ , Kê uses a value corresponding to a layer one atom thick. This seems to be very small, but the same width was taken in the present work, i.e.  $d = 3 \times 10^{-8}$  cm. If the grain-boundary layer is assumed to be  $n$  atoms thick, then the calculated coefficient of viscosity would be  $n$  times the values quoted.

The value of the coefficient of viscosity at the melting point was calculated, using equation (4) (see Appendix) and taking the value of  $H$  to be 19,000 cal./mole.

Table II shows the temperature and the value of  $\tau$  at the peak and the calculated values of the coefficient of viscosity, both at the peak and at the melting point, for each specimen at the two frequencies. The values obtained by using Kê's equation for the temperature variation of  $\tau$  (equation (3)) are also shown for comparison.

The mean results for the coefficient of viscosity at the melting point are:

From modified equation: 0.01<sub>5</sub> poise.

From Kê's equation: 0.01 poise.

Experimental value for liquid tin: 0.02 poise.

The agreement between the observed and either of the calculated values is remarkably good, considering that the range over which the extrapolation takes place is so large and the assumptions made in obtaining the equation so approximate.

It is of interest to examine the effect of a change in the value used for the activation energy on the coefficient of viscosity determined at the melting point (it will, of course, make no difference to the coefficient at the temperature of the peak). It may be shown that if  $H$  varies by 10%, then  $\eta$  varies by a factor of 2, approximately.

#### 4. Young's Modulus.

As discussed in the Appendix, Kê's theory of grain-boundary slip states that, when all grain-boundary relaxation has taken place (i.e. at temperatures well above that of the peak in the internal-friction curve), the ratio of the polycrystal modulus to the single-crystal modulus ( $E/E_U$ ) should fall to a fixed value,  $K$ . According to Zener's calculation (equation (10)) this value for tin should be 0.64.

Fig. 4 shows the temperature dependence of Young's modulus ( $E_t/E_{16}$ ) for the two polycrystal specimens for which logarithmic decrement curves are shown, and also for the "single crystal". Fig. 5 shows the value of  $E_t/E_{16}$  for each specimen divided by the corresponding value for the single crystal, and thus the resultant curve gives a measure of the variation in the modulus due to viscous relaxation alone. The fact that the ratio of the two values is unity at 16° C. is purely arbitrary, since no absolute values of  $E$  were determined.

According to theory the curves of  $E/E_U$  shown in Fig. 5 should start as straight lines parallel to the temperature axis, then, at the temperature at which the internal friction begins to rise, they should curve downwards, the slope increasing with temperature until the peak internal friction occurs; finally, the slope should decrease until the internal friction falls to zero, when the modulus approaches its fully relaxed value  $E_R$  and the graph again becomes a straight line parallel to the temperature axis. With tin, however, there is a "background" internal friction superimposed on the grain-boundary peak, which increases with temperature and becomes appreciable soon after the peak is passed (Fig. 2). The cause of this background is not known, but it is only appreciable in polycrystals. Its effect is that the internal friction

never approaches zero at high temperatures, with the result that the modulus curve is not likely to flatten off to a horizontal straight line, since whatever causes the background internal friction will probably produce an associated decrease in the modulus.

The curves in Fig. 5 show trends which agree with the foregoing predictions with the following important exception. At temperatures well above the peak (say, at  $150^{\circ}\text{C.}$ ),  $E/E_U$  is approximately equal to 0.8 (this allows for the fact that the slope of the curve is not zero when  $E/E_U = 1$ , which shows that some relaxation had already taken place in the polycrystal at  $16^{\circ}\text{C.}$ ) instead of Zener's theoretical value of 0.64, Poisson's ratio being 0.33.<sup>11</sup> This difference cannot be due to the background internal friction, since the effect of this would be to reduce  $E/E_U$  rather than to raise it. It seems possible that this result may not be peculiar to tin, since some information about the temperature dependence of the shear modulus of magnesium is available<sup>1</sup> which shows a similar effect. Unfortunately only the polycrystal modulus is included, but a reasonable guess can be made as to the slope of the unrelaxed modulus curve. This indicates that at high temperatures  $G/G_U$  lies between 0.73 and 0.84, compared with the value calculated from Zener's formula of 0.61, taking Poisson's ratio to be 0.33.<sup>12</sup> It is not possible to draw any definite conclusions as to the reason for the discrepancy, but it could be due to an error in Zener's formula, which is based on some very approximate assumptions, or to the fact that for some reason complete relaxation had not taken place.

#### V.—CONCLUSIONS.

The value of the internal friction of tin due to viscous grain-boundary slip obtained from a specimen vibrating at audio frequencies is in qualitative agreement with results obtained by Kê for other metals using torsional vibrations at low frequencies. The activation energy associated with the slip process is found to be  $19,000 \pm 2500$  cal./mole, which is in agreement with Puttick and King's value of  $19,000 \pm 2000$  cal./mole for macroscopic slip along the boundary of a bicrystal of tin. It is also consistent with the value of 17,300 cal./mole for steady-state creep of a single crystal, but differs considerably from both the activation energies for self-diffusion in tin, 5900 cal./mole along the  $a$ -axis and 10,500 cal./mole along the  $c$ -axis. Tin therefore forms an exception to Kê's theory that the activation energies for the three processes are the same.

The coefficient of viscosity of the grain boundary at the melting point, estimated from internal-friction measurements, is consistent with the experimentally determined value for liquid tin.

## ACKNOWLEDGEMENTS.

Acknowledgement is made to the Chief Scientist, Ministry of Supply, and to the Controller, H.M. Stationery Office, for permission to publish this paper. The authors are greatly indebted to their former colleagues, Messrs. Puttick and King, for permission to quote from their unpublished work.

## APPENDIX.

## THEORY OF VISCOUS GRAIN-BOUNDARY SLIP.

1. *Viscosity Equation.*

Kê<sup>1</sup> has derived an equation relating the coefficient of viscosity to the other variables measured. He finds that :

$$\eta = \frac{G_U \cdot d\tau}{(G.S.)} \quad . \quad . \quad . \quad . \quad . \quad (2)$$

where  $\eta$  = coefficient of viscosity of the grain boundary,

$G_U$  = "unrelaxed" shear modulus,

$d$  = width of the grain boundary,

$(G.S.)$  = grain-size,

$\tau$  = time of relaxation of the shear stress along the boundary.

He also states that :

$$\tau = \tau_0 \exp \left( \frac{H}{RT} \right) \quad . \quad . \quad . \quad . \quad . \quad (3)$$

where

$H$  = an activation energy

$R$  = the gas constant

$T$  = the absolute temperature.

$\tau_0$  = a constant

However, Andrade<sup>13</sup> has shown that, for liquids, the coefficient of viscosity varies with temperature approximately as :

$$\eta = A \exp \left( \frac{H}{RT} \right) \quad . \quad . \quad . \quad . \quad . \quad (4)$$

and it is proposed that the grain-boundary viscosity follows the same law. Thus the equation relating  $\tau$  with temperature is a little more complex than Kê's equation.

From equations (2) and (4) :

$$\tau = \frac{A \cdot (G.S.)}{G_U \cdot d} \cdot \exp \left( \frac{H}{RT} \right) \quad . \quad . \quad . \quad . \quad . \quad (5)$$

This contains one more temperature-dependent term,  $G_U$ , than does equation (3). This difference is not large for the range of temperatures used in the experimental work, since  $G_U$  changes only slowly with temperature, but it becomes more important when coefficients of viscosity are calculated at the melting point.

## 2. Determination of Activation Energy.

The activation energy,  $H$ , may be found by comparing the results of two experiments on the same specimen at different frequencies, as will be seen from the following discussion.

If the relaxation time,  $\tau$ , has a single value at some given temperature, then, as Zener<sup>14</sup> has shown, the variation of the internal friction,  $Q^{-1}$ , with the frequency of vibration,  $\omega$ , is:

$$Q^{-1} = \Delta E \frac{\omega\tau}{1 + (\omega\tau)^2} \quad . \quad . \quad . \quad . \quad . \quad (6)$$

where  $\Delta E$  is a constant known as the strength of the relaxation.

In fact, experiments show that there is not a single relaxation time associated with grain-boundary slip, probably owing to the variation in size of different grains, and to possible inequalities in the effective boundary thickness due to differences in orientation between adjacent grains. Moreover, if the material is anisotropic, the shear modulus will depend upon the orientation. Let us suppose then that there are  $n$  relaxation times varying from  $\tau_1$  to  $\tau_n$ , and that the strength of the relaxation associated with  $\tau_r$  is  $\delta E_r$ .

$$\text{Then} \quad Q^{-1} = \sum_{r=1}^n \frac{\omega\tau_r}{1 + (\omega\tau_r)^2} \delta E_r \quad . \quad . \quad . \quad . \quad . \quad (7)$$

$$\text{From (5)} \quad \tau_r = \frac{f(r)}{G_{U_r}} \cdot \exp \left( \frac{H}{RT} \right)$$

where  $f(r)$  is a temperature-independent term.

Now if we alter the frequency from  $\omega_1$ , at temperature  $T_1$ , to  $\omega_2$  at temperature  $T_2$ , the value of  $Q^{-1}$  in each case will be exactly the same, provided that:

$$\omega_1 \exp \left( \frac{H}{RT_1} \right) = \omega_2 \exp \left( \frac{H}{RT_2} \right) \quad . \quad . \quad . \quad . \quad . \quad (8)$$

since every term in the summation (7) will then be the same in both cases, ignoring the temperatures change in  $G$ . From (8):

$$H = R \left( \frac{1}{T_1} - \frac{1}{T_2} \right) \log_e \frac{\omega_2}{\omega_1} \quad . \quad . \quad . \quad . \quad . \quad (9)$$

Thus, if two experiments are performed on the same specimen at different frequencies and  $Q^{-1}$  is plotted against  $1/T$ , two curves should be obtained which are superposable by a sideways shift of the lower-frequency one towards a lower value of  $1/T$ , i.e. towards a higher temperature. The magnitude of this shift,  $\Delta(1/T)$ , may then be used to determine the activation energy by means of equation (9).



## 3. Effect on Young's Modulus.

There is a close relation between the internal friction and the moduli of elasticity, which is very marked in the case of grain-boundary slip. As the temperature rises the amount of slip increases, and hence the modulus falls, since the strain at a given stress increases. The modulus continues to fall with rising temperature, even when the peak in the internal-friction curve is passed, since the amount of slip is still increasing, until finally the interlocking of the grains prohibits further slip, whereupon the modulus approaches a limiting value. This is generally known as the "relaxed modulus",  $M_R$ , as opposed to the "unrelaxed modulus",  $M_U$ , which occurs in single crystals at all temperatures and in polycrystals at low temperatures. It should be remembered that  $M_U$  is not constant, but falls slowly and approximately linearly with temperature. Therefore to examine the effect on the polycrystalline modulus,  $M$ , attributable to grain-boundary slip, it is convenient to plot  $M/M_U$  against temperature. Kê<sup>1</sup> has shown that for aluminium the shear modulus ratio ( $G/G_U$ ) initially has the value unity, but begins to fall as the internal friction starts to rise, and continues to do so until the internal friction is small again, when it approaches a limiting value of 0.67. This is in remarkably close agreement with a theoretical value of 0.64 calculated by Zener,<sup>15</sup> assuming that the grains are uniform spheres with no shearing stresses between them. Zener's formula for the Young's modulus ratio when relaxation is complete is

$$E_R/E_U = \frac{7 + 5\sigma}{2(7 + \sigma - 5\sigma^2)} \cdot \cdot \cdot \cdot \cdot \quad (10)$$

where  $\sigma$  is Poisson's ratio.

## REFERENCES.

1. T.-S. Kê, *Phys. Rev.*, 1947, [ii], 71, 533.
2. T.-S. Kê, *ibid.*, 1947, [ii], 72, 41.
3. T.-S. Kê, *ibid.*, 1948, [ii], 73, 267.
4. K. E. Puttick and R. King, to be published shortly.
5. F. Seitz, "The Physics of Metals", p. 138. 1943: New York (McGraw-Hill).
6. W. Boas and P. J. Fensham, *Nature*, 1949, 164, 1127; 1950, 165, 178.
7. A. D. N. Smith, *J. Sci. Instruments*, 1951, 28, 106.
8. B. Chalmers, *Proc. Roy. Soc.*, 1937, [A], 162, 120.
9. C. Zener, *Phys. Rev.*, 1938, [ii], 53, 90.
10. C. Zener, "Elasticity and Anelasticity of Metals", p. 54. 1948: Chicago (University of Chicago Press).
11. C. L. Mantell, "Tin", p. 20. 1929: New York (Chemical Catalog Co., Inc.).
12. A. Beck, "Technology of Magnesium and Its Alloys", p. 101. 1940: London (F. A. Hughes & Co., Ltd.).
13. E. N. da C. Andrade, *Phil. Mag.*, 1934, [vii], 17, 698.
14. C. Zener, "Elasticity and Anelasticity of Metals", p. 46.
15. C. Zener, *Phys. Rev.*, 1941, [ii], 60, 906.

# ROLLER LEVELLING OF MAGNESIUM ALLOY SHEET.\*

1318

By E. A. CALNAN,† B.Sc., and A. E. L. TATE,† A.I.M.

(Communication from the National Physical Laboratory.)

## SYNOPSIS.

It has been widely suggested that the loss of proof stress in magnesium alloy sheet after roller levelling is due to the untwinning of material twinned by bending in the roller-levelling process. In the present work X-ray diffraction evidence of additional twinned material in roller-levelled sheet has been found. It has been deduced that the loss in proof stress will be avoided by levelling either under tension in the levelling direction or by compression normal to the sheet and that the loss will be reduced by roller levelling in the  $[10\bar{1}0]$  direction when this has a specific direction in the sheet. From an investigation of the influence of previous heat-treatments and deformation, it has been found that previous cold working reduces the loss in proof stress on roller levelling.

## I.—INTRODUCTION.

It is well known that when magnesium alloy sheet is roller levelled it suffers a loss in proof stress in the direction of the passage of the sheet through the levelling apparatus, and it has been widely suggested <sup>1,2</sup> that this is due to the untwinning of material twinned by bending in the roller-levelling process. Beck <sup>1</sup> also states that a further effect of twinning during the straightening operation is that the sheet is thickened and, in the rolling direction, shortened, the degree depending upon the amount of levelling. Ansel and Betterton in later work <sup>3</sup> report similar effects and in certain circumstances advocate the use of cold-rolled sheets for roller levelling.

The work described in the present paper covers an investigation begun in 1946 into the influence of previous conditions of heat-treatment and cold working on the tensile properties of roller-levelled sheet, together with some X-ray observations and a discussion of the associated twinning phenomena.

## II.—MATERIAL AND TESTING.

The material employed was magnesium alloy sheet, containing 7% by weight of aluminium, produced by hot rolling cast ingots from 1.4 to 0.35 in. with alternate passes at right angles to each other, and then

\* Manuscript received 13 October 1950.

† Metallurgy Division, National Physical Laboratory, Teddington.

rolling in one direction to a thickness of 0.1 in. Sheets about  $30 \times 10$  in. were prepared in the following conditions :

- (a) Hot rolled.
- (b) " " and annealed at  $350^{\circ}\text{C}$ .
- (c) " " " " " + 5% reduction by cold rolling.
- (d) " " " " " + 10% " " "
- (e) " " and solution-treated at  $395^{\circ}\text{C}$ . for 10 min.
- (f) " " and solution-treated at  $395^{\circ}\text{C}$ . for 10 min. + 5% reduction by cold rolling.
- (g) Hot rolled and solution-treated at  $395^{\circ}\text{C}$ . for 10 min. + 10% reduction by cold rolling.

The two heat-treatments were chosen in order to compare the conditions after heating at  $395^{\circ}\text{C}$ ., when all the aluminium is in solid solution and a comparatively coarse grain-size is produced, and after annealing for  $\frac{1}{2}$  hr. at  $350^{\circ}\text{C}$ ., when the solid solution may not be quite complete and the grain-size is somewhat finer. The cold rolling to produce 5 and 10% reductions was in the same direction as the final hot rolling.

The roller levelling was carried out at the works of Messrs. James Booth and Co., Ltd., Birmingham. In the roller-levelling process the sheet is passed through a machine consisting essentially of a lower horizontal series of fixed rolls and an upper, also horizontal, series of offset rolls, the rolls being about 2 in. in dia. The distance between the two sets of rolls can be controlled by adjusting the top set, which can also be tilted to give a variation in distance between the sets of rolls in the direction of operation. Sheets passed through the rolls, therefore, are given a series of reverse bends of diminishing intensity. The surfaces of the sheet, during passage through the rolls, undergo alternate compression and tension.

The sheets were all reasonably flat before levelling, but this does not appreciably diminish the amount of work given during roller levelling. One sheet in each of the conditions listed above was passed through parallel to the final rolling direction (i.e. the longitudinal direction) and a second sheet at  $90^{\circ}$  to this direction. Tensile tests were made in duplicate on test lengths cut in both the longitudinal and transverse directions before and after levelling.

The specimens for the first X-ray-diffraction examination were small cylindrical spigots cut parallel to the rolling direction in the sheet and etched down to remove additional cold-working effects. Transmission patterns showing the main low-angle diffraction rings were obtained corresponding to all the sheet conditions both before and after levelling. Subsequently, in order to investigate the presence of twinned material near the surface, samples of the sheets before and after levelling were examined by means of glancing-angle patterns. In this case the beam

of Cu  $K\alpha$  radiation was inclined at about  $15^\circ$  to the surface of a small piece of the sheet and since the effective depth of penetration of the X-rays is approximately 0.01 mm. the diffraction pattern does unquestionably relate to the surface layer.

In addition, some tensile tests were made on specimens which had been bent and straightened in a Glaysheer Bend-Test Machine<sup>4</sup> in which a strip of the sheet is bent through  $90^\circ$  around a former of particular diameter. With a sheet thickness of 0.08 in. formers were chosen to give  $T$  values of 12, 10, and 7,  $T$  being the ratio of former radius to sheet thickness. Since the deformation could be more accurately controlled in this method than in the roller-levelling process it was expected to lead to more exactly comparable results. Material in the hot-rolled, annealed, and annealed and cold-rolled conditions was used.

### III.—RESULTS OF MECHANICAL TESTS.

The mean values of 0.1% proof stress and elongation of the sheet before and after roller levelling are summarized in Table I. Percentage losses on levelling amounting to less than 5% of the proof stress and 10% of the elongation values, were not considered significant and have not been listed.

It will be seen that the loss in proof stress in the longitudinal direction after levelling parallel to this direction is most marked in the annealed and solution-treated materials, 31 and 23%, respectively, and is much less, around 8%, in the hot-rolled material and that subjected to 10% cold reduction. No significant change is observed in the transverse proof stress after this levelling.

With roller levelling in the transverse direction there is some loss, about 10%, in the transverse proof stress of the annealed, solution-treated, and hot-rolled materials, but no change in the longitudinal direction.

The elongation values obtained can hardly be correlated with the condition and directions in the sheet, but it appears that there may be a loss of up to 50% in elongation, rather more marked in the longitudinal direction. There is no significant difference in the effects produced by the two heat-treatments.

The controlled-bend tests (Table II) show that the marked loss of proof stress is virtually unaltered by increasing the severity of the bend from  $T = 12$  to  $T = 7$ , that is to say the maximum effect is reached with a bend of  $T = 12$ . A loss of 50% in proof stress is sustained by sheet in the annealed condition and 25% by sheet that had been cold rolled to give reductions of 5 or 10%. The loss in the hot-rolled con-

TABLE I.—*Effect of Roller Levelling on Tensile Properties.*

Mean values of duplicate tests.

Sheet No.	Condition	Direction of Final Tensile Test Relative to Rolling Direction of Sheet	Roller Levelled at 0° to Rolling Direction				Roller Levelled at 90° to Rolling Direction				Roller Levelled at 0° to Rolling Direction		Roller Levelled at 90° to Rolling Direction	
			0.1% Proof Stress, tons/in. <sup>2</sup>				Elongation, % on 2 in.							
			Before Level-ling	After Level-ling	Loss, %	Before Level-ling	After Level-ling	Loss, %	Before Level-ling	After Level-ling	Before Level-ling	After Level-ling	Before Level-ling	After Level-ling
2546T	Hot rolled.	Long. Trans.	13.8 14.6	12.7 14.7	8 ...	13.8 14.6	14.1 13.1	... 10	17 16	15 15	... ...	15 15	17 16	16 15
2546B	Hot rolled and annealed at 350° C.	Long. Trans.	11.1 11.5	7.6 11.7	31 ...	11.1 11.5	11.1 10.0	... 13	20 16	14 14	30 12	18 14	20 16	18 14
2547T	Hot rolled and annealed at 350° C. + 5% cold reduction.	Long. Trans.	14.0 13.0	12.5 13.5	10 ...	14.0 13.0	14.6 13.5	... ...	13.5 18	10 12	25 33	10 12.5	13.5 8	10 12.5
2547B	Hot rolled and annealed at 350° C. + 10% cold reduction.	Long. Trans.	15.5 15.5	14.4 14.8	7 ...	15.5 15.5	15.2 15.2	... ...	3.5 11.5	4 13	... ...	3.5 15	3.5 11.5	4.5 15
2548T	Hot rolled and solution-treated at 395° C.	Long. Trans.	10.4 11.3	8.0 11.5	23 ...	10.4 11.3	10.6 10.0	... 11.5	18.5 15	19 15	... ...	17 17.5	15.5 15	... ...
2549T	Hot rolled and solution-treated at 395° C. + 5% cold reduction.	Long. Trans.	13.8 13.9	12.2 14.1	11.5 ...	13.8 13.9	13.5 13.3	... ...	10 12.5	8.5 12	15 ...	8 12.5	10 12.5	20 ...
2549B	Hot rolled and solution-treated at 395° C. + 10% cold reduction.	Long. Trans.	15.2 14.8	14.0 15.2	8 ...	15.2 14.8	15.2 14.0	... ...	10 13	5 12	50 ...	9 12.5	10 13.5	10 ...

\* More than 5%.

† More than 10%.

TABLE II.—*Tensile Properties of Magnesium-7% Aluminium Alloy Sheet After Controlled-Bending Tests.*

Thickness of strip 0.08 in.

Specimen No.	Condition	Extent of Bending		Tensile Properties		
		Roller Dia., in.	Ratio of Former Radius to Sheet Thickness <i>T</i>	0.1% Proof Stress	U.T.S.	Elongation, % on 2 in.
				tons/in. <sup>2</sup>		
1	Hot rolled	Unbent		13.4 13.3	20.7 20.7	13.5 14.5
2		2	12	8.8 8.8	21.2 21.0	6.6 8.0
3		1.7	10	8.0 8.5	20.7 20.5	5.5 6.0
4		1.2	7	Broke on bending		
5	Annealed at 350° C.	Unbent		13.2 12.7	20.6 20.6	11.5 10.0
6		2	12	6.7 6.5	19.4 19.4	11.5
7		1.7	10	6.6 6.6	19.2 19.2	11.5 12.0
8		1.2	7	6.3 6.6	18.9 19.0	9.0 10.0
9	Annealed at 350° C. + 5% cold-rolling reduction	Unbent		13.4 13.4	20.4 19.0	10.0 10.0
10		2	12	10.0 10.5	19.1 19.4	4.5
11		1.7	10	10.0 9.9	19.0 19.1	5.0 4.5
12		1.2	7	10.6 10.1	19.3 19.0	7 1.5
13	Annealed at 350° C. + 10% cold-rolling reduction	Unbent		15.1 15.0	21.0 21.0	5.0 3.0
14		2	12	11.3 11.3	21.6 20.7	2.0 2.0
15		1.7	10	11.2 11.2	21.1 20.1	0.0 0.0
16		1.2	7	Broke on bending		



dition is intermediate at approximately 35%. Considering the elongation values, no loss is observed after bending in the annealed condition, but the loss is approximately 50% in the hot-rolled material and somewhat greater in the material previously cold rolled.

Although it is clear from the tensile-test results that the bend tests produce more severe deformation than the roller-levelling process used in this investigation, the relative merits of the previous treatments appear to be the same. Thus, in order of increasing percentage loss of proof stress after roller levelling the materials may be listed: (1) cold rolled, (2) hot rolled, (3) annealed; and in order of increasing percentage loss of elongation (1) annealed, (2) hot rolled, (3) cold rolled.

Metallographic examinations of the specimens were made before and after levelling, but these failed to show any difference, and it may only be inferred with Barrett and Haller<sup>2</sup> that for the estimation of twinning in magnesium sheet this technique is inferior to the X-ray method.

#### IV.—X-RAY OBSERVATIONS.

Although rolled sheet is known to contain varying amounts of twinned material, it has generally been assumed that roller levelling produces additional twinning which under subsequent tension untwins easily and in so doing reduces the proof stress. X-ray evidence of the presence of additional twinned material in roller-levelled sheet was found by Siebel.<sup>5</sup> It would appear that the sheet he examined had suffered more than usually severe deformation in the process, for Barrett and Haller<sup>2</sup> observed no difference in the diffraction patterns before and after roller levelling. They stated, however, that since it was possible that the amount of twinned material did not exceed 1% of the total volume, it might for this reason, not be detected in the transmission X-ray patterns used by them for texture study.

The first X-ray examination of the present authors, using a transmission technique similar to that of Barrett and Haller but carried out before their paper was available, agrees with them in finding no difference before and after levelling. It was expected, however, that the twinning due to compressive stresses caused by bending in the levelling process would be more in evidence near the surface of the sheet, and accordingly glancing-angle patterns were taken. These showed clearly an increase, after levelling, of the intensity of the  $(10\bar{1}0)$  reflection relative to the other adjacent reflections (Fig. 1, Plate LX). Since the magnesium rolling texture may be simply described as that of the hexagonal basal planes (0001) lying in the rolling plane, it will be seen from Fig. 2 that the known twinning habit, about the  $(10\bar{1}2)$  plane, will

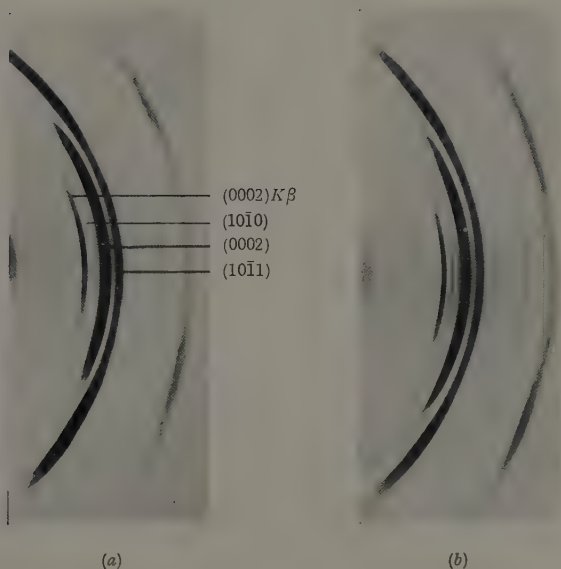


FIG. 1.—Glancing-Angle Patterns from Sheet No. 2549T (a) Before and (b) After Roller Levelling, showing Increase in Intensity of  $(10\bar{1}0)$  Reflection.



bring  $(10\bar{1}0)$  planes to within  $4^\circ$  of the original orientation of the basal planes. Thus in the glancing-angle patterns which record the relative

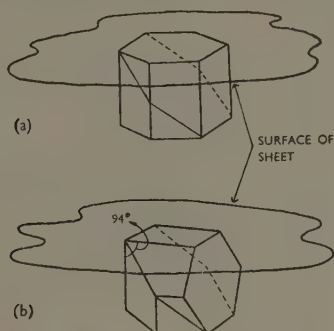


FIG. 2.—(a) Original Orientation. (b) Original and Twinned Orientations.

intensity of those planes lying approximately in the surface of the sheet, this type of twinning will lead to an increased number of  $(10\bar{1}0)$  planes in the surface and a correspondingly augmented X-ray reflection.

TABLE III.—*Tensile Properties and Amount of Twinned Material in the Surface of Roller-Levelled Magnesium Alloy Sheet.*

Sheet No.	Condition	0.1% Proof Stress in Rolling Direction, tons/in. <sup>2</sup>			Proportion of Twinned Material in the Surface, %		
		Before Leveling	After Leveling	Loss, %	Before Leveling	After Leveling	Increase
2546B	Annealed at $350^\circ\text{C}$ .	11.1	7.6	31	4	7	3
2547T	Annealed at $350^\circ\text{C}$ . + 5% cold reduction.	14.0	12.5	10	3	6	3
2547B	Annealed at $350^\circ\text{C}$ . + 10% cold reduction.	15.5	14.4	7	6.5	2.5	-4
2548T	Solution-treated at $395^\circ\text{C}$ .	10.4	8.0	23	5	9	4
2549T	Solution-treated at $395^\circ\text{C}$ . + 5% cold reduction.	13.8	12.2	11.5	1.5	4	2.5
2549B	Solution-treated at $395^\circ\text{C}$ . + 10% cold reduction.	15.2	14.0	8	3	6	3

From the relative intensities of the  $(10\bar{1}0)$  and  $(0002)$  reflections as measured on a Geiger-Müller X-ray spectrometer the proportion of twinned material in the surface layers irradiated was deduced (Table III). From the observed values there is no direct quantitative relationship between the increase of twinned material and the loss of proof

stress. This is to be expected, however, on the grounds that the amount of twinned material is, as discussed in Section V, most directly related to the geometry of the system during bending and is likely to be approximately the same in all these specimens. On the other hand, the loss in proof stress is dependent not only on the amount of twinned material but also on any localized stresses that may obstruct the untwining.

### V.—DISCUSSION.

The levelling process consists essentially in bending the sheet to and fro. Consequently, in an initially flat sheet there should be no more twinned material after levelling than before, and, similarly, levelling a large number of times should produce no more effect than levelling once. There seems little doubt from Siebel's results<sup>5</sup> that

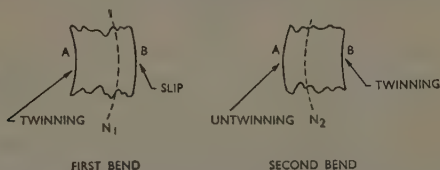


FIG. 3.—Twinning and Untwining Mechanism in Successive Bending.

this is not so, and an explanation of the manner in which the twinned material increases with successive bending may be proposed as below.

In the first bending the stress required for extension by slip on the convex side *B* (Fig. 3) is considerably greater than the stress for twinning on the concave side *A*, and the neutral axis of bending  $N_1$  will be nearer side *B*. In the second bending the stress for extension at *A* will be that for untwining. As a result of some "locking in" of the twins by the accommodating slip around them, this stress will be slightly greater than that for twinning at *B*, and  $N_2$  will be slightly displaced from the centre towards side *A*. Thus for the same angle of bending the extension of *A* will be less than the contraction in the first bend and therefore the re-twinning required will be less than the twinning present and the balance will be retained. For the third bending the axis will shift slightly towards *B* owing to the hardening, and some twinning will be retained at *B*. With this mechanism, and assuming the twinned material at any point to be proportional to the distance from the neutral axis, the proportion in the sheet as a whole may be expected to constitute between one-half and one-quarter of that in the surface layers, 2-4%. Thus the results quoted above

correspond to twinned material comprising approximately 1% of the total volume.

Although the reduced proof stress may be explained simply by the untwinning of this material under applied tension while testing, there is an additional factor which appears to have some influence. The material examined in the present investigation showed that besides the usual texture of basal planes lying approximately in the surface of the sheet, there was a tendency for the  $[11\bar{2}0]$  directions to lie parallel to the longitudinal (final rolling) direction, as has been found by Caglioti and Sachs<sup>6</sup> and by Bakarian.<sup>7</sup> With this orientation, and roller levelling parallel to the longitudinal direction, the twinned material takes up the orientation shown in Fig. 4 (b) and the resolved shear stress on the basal planes for applied tension in either the longi-

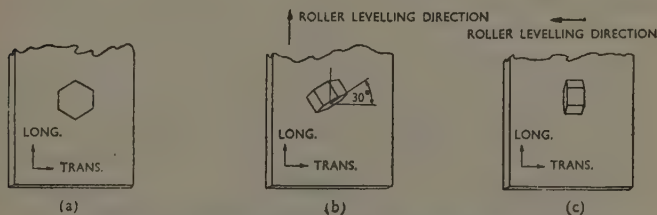


FIG. 4.—Effect on Orientation of Twinned Material of Roller Levelling Parallel (b) and Transverse (c) to Longitudinal Direction.

tudinal or transverse direction will be greater in the twinned material than in the original material. With levelling parallel to the transverse direction, the twinned orientation will be as shown in Fig. 4 (c); where clearly the shear stress is virtually unaltered. This should make the loss in the proof stress in the transverse direction after levelling in the transverse direction slightly less than the loss in the longitudinal direction after levelling in the longitudinal direction. The effect was observed in the tensile results and may be explained on this basis.

Fig. 2 of Barrett and Haller's paper<sup>2</sup> showing the twinned orientations after successive compressions in the longitudinal and transverse directions appears to exhibit the two special orientations illustrated in Fig. 4 of the present paper, i.e. basal planes at  $\pm 30^\circ$  and  $90^\circ$  to the transverse direction.

Summarizing the results, the X-ray method has revealed the presence of additional twinned material in roller-levelled sheet, and it has been shown that previous cold working reduces the loss in proof stress associated with levelling. From purely crystallographic considerations



it may be deduced that the loss in proof stress due to untwinning will be avoided either by levelling under tension in the levelling direction, or by compression normal to the sheet, and that the loss will be reduced by roller levelling in the  $[10\bar{1}0]$  direction when this has a specific direction in the sheet.

#### ACKNOWLEDGEMENTS.

The authors wish to thank Mr. C. Smith of Messrs. James Booth and Co., Ltd., for his early and encouraging interest in the work and to acknowledge the assistance of the Engineering Division of the Laboratory who carried out the tensile testing.

This work forms part of the research programme of the National Physical Laboratory, and the paper is published by permission of the Director of the Laboratory.

#### REFERENCES.

1. A. Beck, "The Technology of Magnesium and Its Alloys". 1940: London (F. A. Hughes & Co., Ltd.).
2. C. S. Barrett and C. T. Haller, Jr., *Trans. Amer. Inst. Min. Met. Eng.*, 1946, **171**, 246 (including subsequent discussion).
3. G. Ansel and J. O. Betterton, Jr., *Non-Ferrous Rolling Practice (Amer. Inst. Min. Met. Eng., Inst. Metals Div. Symposium Series, Vol. 2)*, 1948, 153.
4. G. H. Glaysher, *J. Inst. Metals*, 1942, **68**, 383.
5. G. Siebel, cited by G. Boehme. *Dissertation Tech. Hochschule, Hannover*, 1934; see also A. Beck, "The Technology of Magnesium and Its Alloys," p. 35.
6. V. Caglioti and G. Sachs, *Metallwirtschaft*, 1932, **11**, 1.
7. P. W. Bakarian, *Trans. Amer. Inst. Min. Met. Eng.*, 1942, **147**, 267.

# DISCUSSION ON THE PAPER BY DR. D. TABOR: "THE HARDNESS AND STRENGTH OF METALS."

(*J. Inst. Metals*, this vol., p. 1.)

DR. E. VOCE,\* M.Sc., F.I.M. (Member): While Dr. Tabor's conception of the relationship between hardness and stress is basically sound, and is indeed already fairly well known, it embodies points of detail which are open to criticism, and contains certain assumptions of doubtful validity. It is the purpose of the present contribution to outline a more objective approach, based on experimental data given in the paper. The remarks are confined primarily to the pyramid (or conical) indenter for which the strain is, theoretically at least, independent of the size of the impression. They could, however, be applied with some modification to the more complicated case of the ball hardness test.

Dr. Tabor makes considerable use of the stress/strain equation  $Y = b\epsilon^z$ , quoting Nádai as his authority, and defining  $\epsilon$  as the fractional increase in length, or orthodox strain. He evidently consulted the 1931 edition of Nádai's book, for in the new edition (1950) Nádai, like many other workers, has abandoned this relationship in favour of  $Y = b\eta^z$ , where  $\eta$  is the logarithmic strain, such that  $e^\eta = 1 + \epsilon$ . Nádai, however, is careful to make no more than the most guarded claim for the validity of this equation, saying only that "the natural stress/strain curve for ductile metals may sometimes be approximated in its first steep portion by assuming that the true stress is a power function of the natural (i.e. logarithmic) strains". Moreover, the equation is incomplete in that it takes no account of the original yield stress of the material; apparently a constant,  $Y_0$ , should be added. These observations have a considerable bearing on much of Dr. Tabor's argument. It would seem, for instance, that his equation (13) (p. 10) should be written  $T = (b\eta^z + Y_0) e^{-\eta}$ , making subsequent development much more difficult.

Examination of the data given in Table VI (p. 15) of Dr. Tabor's paper shows that the power function holds neither for the steel nor for the copper, whether orthodox or logarithmic strains be used; plots on double logarithmic paper give shallow curves, not straight lines. On the other hand, all the curves both for stress and hardness, can be represented with great exactitude by the equation proposed in 1948,† namely:

$$S = S_\infty - (S_\infty - S_0) e^{-\eta/\eta_c} \quad . \quad . \quad . \quad . \quad . \quad (1)$$

where  $S$  and  $\eta$  are, respectively, the current true (yield) stress and logarithmic strain; while  $S_0$ ,  $S_\infty$ , and  $\eta_c$  are constants,  $S_0$  being the *threshold stress* for the initiation of plastic deformation,  $S_\infty$  the *asymptotic stress* attained after severe deformation, and  $\eta_c$  (previously called  $k$ ) the *characteristic strain*, i.e. the logarithmic strain required to raise the current stress to the asymptotic stress in the absence of any subsequent change in the plastic modulus,  $dS/d\eta$ . For hardness the comparable equation is:

$$H = H_\infty - (H_\infty - \bar{H}_0) e^{-\bar{\eta}/\eta_c} \quad . \quad . \quad . \quad . \quad . \quad (2)$$

\* Senior Metallurgist, Copper Development Association, Radlett, Herts.

† E. Voce, *J. Inst. Metals*, 1948, 74, 537.

The symbols  $\bar{H}_0$  and  $\bar{\eta}$  are used for the threshold hardness and current strain for reasons that will emerge later.

The constants for the four curves represented by the information in Dr. Tabor's Table VI have been determined by Palm's differential method,\* with the help of a transparent protractor pivoting about a pin and a table of natural tangents. The results are given in Table A, and the precision with which the calculated curves fit the experimental data is revealed by Fig. A. While stresses and hardness numbers greater than the asymptotic values are known to be obtainable for both steel and copper, this aspect of the matter is not relevant to the data at present under discussion.

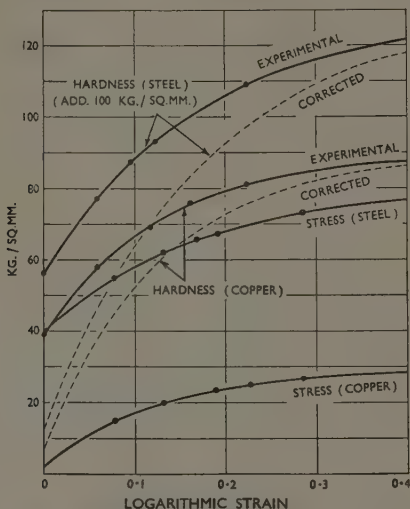


FIG. A.—Curves Calculated from Data in Table VI of Tabor's Paper.

It will be observed that for each material the characteristic strain is the same for the stress and hardness functions. This is a consequence of the linear relationship between yield stress and pyramid hardness demanded by plastic theory, and leads to the following considerations:

Combining equations (1) and (2), it is apparent that, for equal strains:

$$\frac{H_{\infty} - H}{H_{\infty} - \bar{H}_0} = \frac{S_{\infty} - S}{S_{\infty} - S_0} \quad \dots \quad (3)$$

whence

$$H = \left( \frac{\bar{H}_0 S_{\infty} - H_{\infty} S_0}{S_{\infty} - S_0} \right) + \frac{H_{\infty} - \bar{H}_0}{S_{\infty} - S_0} S \quad \dots \quad (4)$$

This is the equation of a straight line (see Fig. B), for which the bracketed constant represents the intercept on the hardness axis, while  $(H_{\infty} - \bar{H}_0)/(S_{\infty} - S_0)$  is the slope. For the steel and copper tested by Dr. Tabor, the intercepts and slopes are those given in Table B.

\* J. H. Palm, *Metallen*, 1950, 5, 13.

TABLE A.—Constants for the Equation  $S = S_{\infty} - (S_{\infty} - S_0) e^{\eta/\eta_c}$  from Data Given in Tabor's Table VI.

Experiment	Threshold Stress or Hardness, kg./mm. <sup>2</sup> $S_0$	Asymptotic Stress or Hardness, kg./mm. <sup>2</sup> $S_{\infty}$	Characteristic Strain in Logarithmic Strain Units $\eta_c$
Mild Steel :			
Stress . . . .	40	81	0.172
Hardness . . . .	156 (E) 113 (C)	229	0.172
Annealed Copper :			
Stress . . . .	2.5	29.5	0.126
Hardness . . . .	39 (E) 7.6 (C)	89.6	0.126

E = experimental.

C = corrected.

A material which has zero yield stress should clearly have no hardness; it follows that the observed intercepts on the hardness axis at zero stress are attributable to the work-hardening caused by the indentation itself. Therefore

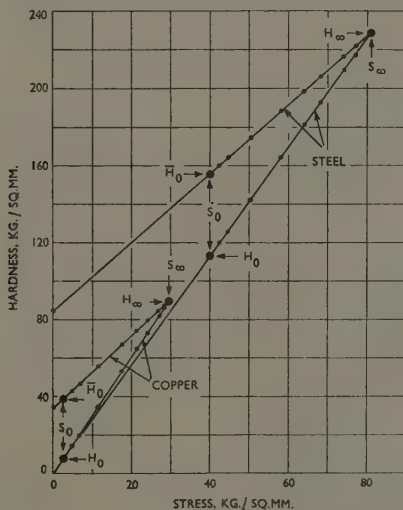


FIG. B.—Relationship Between Hardness and True Stress.

from equation (2) the strain,  $\eta_h$ , which is associated with deformation adjacent to the indentation, and which raises the hardness from zero to the intercept value, is given by :

$$\left( \frac{\bar{H}_0 S_{\infty} - H_{\infty} S_0}{S_{\infty} - S_0} \right) = H_{\infty} - (H_{\infty} - 0) e^{-\eta_h/\eta_c}$$

whence :

$$\epsilon\eta_h/\eta_c = \frac{H_\infty}{S_\infty} \cdot \frac{S_\infty - S_0}{H_\infty - H_0} \quad . \quad . \quad . \quad . \quad . \quad (5a)$$

or :

$$\eta_h = \eta_c \ln \left( \frac{H_\infty}{S_\infty} \cdot \frac{S_\infty - S_0}{H_\infty - H_0} \right) \quad . \quad . \quad . \quad . \quad . \quad (5b)$$

From the constants given in Table A, the values of  $\eta_h$  for the steel and copper are found to be those included in Table B. The value for steel is in good agreement with the equivalent 8% extension mentioned by Dr. Tabor, though that for copper is appreciably smaller. It may be remarked that 8% extension, corresponding to a deformation ratio of 1.08, is equivalent to cosec 68°.

TABLE B.—*Secondary Constants for the Correlation of Hardness with Stress, Based on Data Given in Tabor's Table VI.*

Stresses and hardness numbers in kg./mm.<sup>2</sup>.

Equation No.	Description	Mild Steel	Annealed Copper
4	Direct plot of uncorrected hardness against stress : Intercept on hardness axis Slope of line	84.8 1.78	34.3 1.87
5	Strain associated with hardness test : Logarithmic strain units Deformation ratio Percentage extension Percentage reduction	0.080 1.083 8.3 7.7	0.061 1.063 6.3 5.9
7	Threshold hardness after correcting for strain imposed by the test	113	7.6
9	Ratio of corrected hardness to yield stress (slope)	2.83	3.04
10	Ratio of pressure on indenter to yield stress (slope)	3.06	3.25
11	True stress at maximum load : From hardness data From yield-stress data	69.0 69.1	26.2 26.2
12	Strain at maximum load : Logarithmic strain units Deformation ratio Percentage extension Percentage reduction	0.197 1.218 21.8 17.9	0.283 1.327 32.7 24.7
13	Ordinary tensile strength	56.6	19.7

which represents the ratio of the slant surface of the standard Vickers pyramid to the area of its base. That is to say, the deformation ratio associated with the pyramid-hardness test is approximately equal to the ratio of the total surface area supporting the load on the indenter to the corresponding area before test. The equivalent logarithmic strain is 0.076.

Having thus ascertained the strain associated with the hardness test, the next step is to apply to the hardness numbers a correction for the degree of work-hardening that this strain imposes on the metal. Dr. Tabor proposes to effect the necessary correction by adding 8% to the abscissæ of the true stress/orthodox (percentage) strain curve. Orthodox or percentage strains cannot legitimately be combined by direct addition in this way. For instance, if a bar of initial length  $L_0$  is extended to a length  $L_1$  and then further extended to  $L_2$ , the total (orthodox) strain is clearly  $(L_2 - L_0)/L_0$ , but direct addition of the two individual strains  $(L_1 - L_0)/L_0$  and  $(L_2 - L_1)/L_1$  gives quite a different result. It is even more dangerous to use direct addition if either of the strains happens to be a fractional (percentage) decrease in sectional area or thickness. Strains, unless very small, can be combined only by multiplication of the appropriate deformation ratios, or more simply by the addition of logarithmic strains, thus:

$$(L_1/L_0) \times (L_2/L_1) = (L_2/L_0)$$

or:

$$\ln (L_1/L_0) + \ln (L_2/L_1) = \ln (L_2/L_0)$$

While Dr. Tabor has attempted correlation by selecting appropriate readings from the yield-stress curve, it would seem more logical to apply a correlation to the hardness curve, in which the discrepancy actually arises. Clearly, the experimental hardness number of a material cold-worked to a logarithmic strain  $\bar{\eta}$  should be plotted not against  $\bar{\eta}$  alone, but against  $\bar{\eta} + \eta_h$ . That is to say, the experimental curve should be moved bodily to the right through a distance  $\eta_h$  on the logarithmic strain axis, as shown by the broken lines in Fig. A. The curve so generated then represents the real relationship between each experimental hardness number and the total strain  $\eta = \bar{\eta} + \eta_h$  with which it is associated. Lateral translation of the curve in this manner alters neither its shape, as controlled by  $\eta_c$ , nor its upper asymptote. It does, however, decrease the threshold hardness by exposing, as it were, more of the curve from concealment behind the vertical axis. The equation of the corrected curve is therefore:

$$H = H_\infty - (H_\infty - H_0) e^{-\eta/\eta_c} \quad (6)$$

where  $\eta$  is the total strain, namely  $\bar{\eta} + \eta_h$ , while  $H_0$  is the real threshold hardness in the absence of work-hardening due to the indentation. Here  $\eta$  is identical with  $\eta$  of the stress/strain equation (1), and  $H_0$  is strictly comparable with  $S_0$ . Though the true threshold hardness  $H_0$ , being essentially an extrapolated value, cannot be determined experimentally, it can readily be calculated from the experimental threshold hardness  $\bar{H}_0$  and its associated strain  $\eta_h$ . Thus, from equation (6):

$$\bar{H}_0 = H_\infty - (H_\infty - H_0) e^{-\eta_h/\eta_c}$$

whence:

$$\bar{H}_0 = H_\infty - (H_\infty - H_0) e^{\eta_h/\eta_c} \quad (7a)$$

or:

$$e^{\eta_h/\eta_c} = \frac{H_\infty - H_0}{H_\infty - \bar{H}_0} \quad (7b)$$

On equating this value of  $e^{\eta_h/\eta_c}$  with that given by equation (5a) and simplifying, it is found that:

$$H_0/S_0 = H_\infty/S_\infty \quad (8)$$

This indicates that the ratio of the real, or corrected, hardness to the true stress is the same at the beginning and end of the curves where the total



strains are zero and infinite respectively. Further, by using  $H_0$  instead of  $\bar{H}_0$  in equation (4) and remembering the provisions of equation (8), it is found that the bracketed intercept constant disappears and that the relationship reduces to the simple proportionality:

$$H = S(H_\infty/S_\infty) \quad . \quad . \quad . \quad . \quad . \quad . \quad (9)$$

Thus the geometrical effect of the correction is to pivot the straight line connecting hardness with stress about the point represented by the asymptotic values, until it passes through the origin. The slope is increased from  $(H_\infty - \bar{H}_0)/(S_\infty - S_0)$  to  $H_\infty/S_\infty$  in the process. Numerical values for the corrected slopes in respect of the steel and copper tested by Dr. Tabor are included in Table B.

Theory suggests that it is the pressure under the indenter that is proportional to the yield stress. For the pyramid indenter this is merely a refinement, because the pressure  $P$  is related to the hardness number by  $P = H \operatorname{cosec} \theta$ , where  $\theta$  is the half dihedral angle of the pyramid. Thus for the standard Vickers indenter for which  $\theta = 68^\circ$  equation (9) becomes:

$$P = 1.079 \frac{H_\infty}{S_\infty} S \quad . \quad . \quad . \quad . \quad . \quad . \quad (10)$$

As shown in Table B, the values of the factor  $1.079 H_\infty/S_\infty$  are slightly more than 3 for both steel and copper, though they are not quite identical. They are thus in reasonable accord with plastic theory and with Dr. Tabor's own observations.

It remains to indicate how the tensile properties of a ductile material can be ascertained from the strain-hardening curve. For reasons described earlier\* the true stress at the maximum load or necking point,  $S_m$ , is given by:

$$S_m = S_\infty/(1 + \eta_c) \quad . \quad . \quad . \quad . \quad . \quad . \quad (11)$$

Using this value in equation (1) the corresponding logarithmic strain is found to be  $\eta_m$ , where:

$$\eta_m = \eta_c \ln \left\{ \left( 1 + \frac{1}{\eta_c} \right) \left( 1 - \frac{S_0}{S_\infty} \right) \right\} \quad . \quad . \quad . \quad . \quad (12)$$

Similar relationships hold for the corrected hardness curves, and it is important to note that, because from equation (8)  $H_0/H_\infty = S_0/S_\infty$ , the "necking" strain  $\eta_m$  is the same for corrected hardness as it is for stress. The ordinary tensile strength  $T_m$  is consequently:

$$\begin{aligned} T_m &= S_m e^{-\eta_m} \\ &= \frac{S_\infty}{1 + \eta_c} \left\{ \left( 1 + \frac{1}{\eta_c} \right) \left( 1 - \frac{S_0}{S_\infty} \right) \right\}^{-\eta_c} \quad . \quad . \quad . \quad (13) \end{aligned}$$

If hardness numbers are used instead of stresses, it is necessary to divide by the conversion factor of equation (9), namely  $H_\infty/S_\infty$ , which from the experimental work recorded in this paper can be taken as approximately 2.9, so that:

$$T_m = \frac{1}{2.9} \cdot \frac{H_\infty}{1 + \eta_c} \left\{ \left( 1 + \frac{1}{\eta_c} \right) \left( 1 - \frac{H_0}{H_\infty} \right) \right\}^{-\eta_c} \quad . \quad . \quad (14)$$

The corrected, not the experimental value of  $H_0$  must, of course, be used in this equation.

Values for the true stress and strain at the maximum load point (necking

\* E. Voce, *loc. cit.*

point) and for the ordinary tensile strength of the mild steel and annealed copper tested by Dr. Tabor are included in Table B. It may be remarked that both the tensile strength and hardness of the annealed copper were abnormally low, suggesting that the material might have been superficially "gassed" by annealing in a reducing atmosphere.

It is not, however, essential to determine the constants of the strain-hardening equation in order to derive the tensile properties from hardness tests. The following simple geometrical construction, based on well-established principles outlined in an appendix to the previously mentioned paper,\* can be applied with moderate precision.

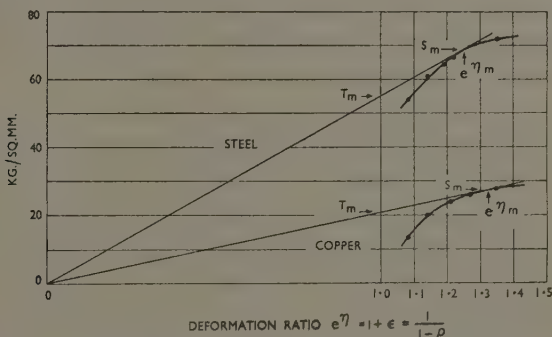


FIG. C.—Geometrical Construction for Determining Tensile Strength.

(1) Tabulate the experimental hardness numbers against the deformation ratios representing the degree of cold work to which the material has been subjected. The deformation ratio is defined as :

$$e^{\eta} = 1 + \epsilon = 1/(1 - \rho) \quad . \quad . \quad . \quad (15)$$

where  $\epsilon$  is a fractional (percentage) *increase* in length under tension or of sectional area under compression, while  $\rho$  is a fractional (percentage) *decrease* in length (thickness) under compression or of sectional area under tension. The distinction between increments and decrements is of the utmost importance. For instance, a reduction in thickness of 60% in strip rolling is equivalent to an increase in length of 150%, and the corresponding deformation ratio is 2.50, not 1.60 as it would be for a 60% increase in length.

(2) Multiply each deformation ratio by, say, 1.08 to correct for the strain imposed by the hardness test itself. It is *not* legitimate to add 8% to the percentage strain.

(3) Divide each experimental hardness number by, say, 2.9 to convert it into stress in kg./mm.<sup>2</sup>, or by  $2.9 \times 1.57 = 4.6$ , if it is desired to obtain tons/in.<sup>2</sup>.

(4) Plot the curve of stress against corrected deformation ratio obtained as described in (2) and (3) above.

(5) Draw the tangent to the curve from the origin as shown in Fig. C. The tangential point then defines the true stress and deformation ratio corresponding to the maximum load or necking point, while the intercept

\* E. Voce, *loc. cit.*

made by the tangent on the ordinate at unit deformation ratio, i.e. the slope of the tangent, represents the ordinary tensile strength.

The tensile strengths obtained by this method are 55.0 kg./mm.<sup>2</sup> for steel and 20.7 kg./mm.<sup>2</sup> for copper, in comparison with 56.6 and 19.7 kg./mm.<sup>2</sup>, respectively, by the more accurate calculation previously described. The discrepancies are attributable to the use of assumed factors (2.9 and 1.08) in translating the hardness numbers into stresses and in correcting the deformation ratios, and not to the geometrical construction, which is capable of quite high precision. This is demonstrated by the fact that the same construction applied directly to the yield-stress data of Dr. Tabor's Table VI gives tensile strengths of 56.4 and 19.9 kg./mm.<sup>2</sup> for steel and copper, respectively, in good agreement with the calculated values. The analysis of a wider range of experimental data covering more materials would doubtless establish the conversion and correction factors with more exactitude, but the suggested figures are probably sufficient for most practical purposes.

The AUTHOR (*in reply*): Dr. Voce has raised a number of matters of interest, and I should like to deal with the minor points first. It is quite true, as Dr. Voce states, that logarithmic strain is the most satisfactory convention for expressing strain. However, for small strains the difference between linear and logarithmic strain is relatively small. Thus, linear strain of 8%, which is, of course, a linear strain of 0.08, is equivalent to a logarithmic strain of 0.076. Even with larger strains the discrepancy is not large. Thus, for a linear strain of 0.20 (or 20%) the logarithmic strain is 0.182; the difference is less than 10%. Again, over a limited strain range the empirical relation representing the stress/strain curve is not greatly changed by a change in the strain convention. For example, a partially annealed aluminium specimen gave a stress/strain curve in tension and compression which was very closely represented by the relation:

$$Y = 12 (\epsilon^*)^{0.28}$$

where  $Y$  is the true yield stress in kg./mm.<sup>2</sup> and  $\epsilon^*$  the logarithmic strain.† The same points could be plotted on linear strain ordinates (linear strain for extension experiments, areal strain for compression experiments) and these points were equally well represented by the relation:

$$Y = 11 (\epsilon)^{0.26}$$

where  $\epsilon$  is the linear (or areal) strain.

Dr. Voce is, of course, quite correct in saying that linear strains cannot be added: only logarithmic strains can be so treated. But for strains of only 8% the difference, as pointed out above, is trivial. A more serious issue, which he overlooks, is that the amount of strain to be added for the indentation process itself is probably *not* constant anyhow. The type of strain pattern produced around the indentation will depend on the rate of strain-hardening of any displaced element. This will not be the same for an annealed metal as it is for a highly worked metal. Indeed, it would seem that the effective strain to be added for the indentation process is less for an annealed than for a worked specimen.

Dr. Voce points out that the 8% strain due to the indentation process, corresponding to a deformation ratio of 1.08, is the same as the ratio of the slant area of the pyramid to its basal area. It would seem that this is largely fortuitous and has no fundamental physical significance. Certainly with

† D. Tabor, "The Hardness of Metals", p. 25. 1951: Oxford (Clarendon Press).

spherical indenters the effective strain is not proportional to the ratio of the curved to the projected area. This would give an effective strain proportional to  $(d/D)^2$ , whereas experiments show that it is much more nearly proportional to  $(d/D)$ . Indeed, using the empirical value of  $20(d/D)\%$  for the indentational strain and applying this to the sphere which fits the Vickers pyramid tangentially ( $d/D = 0.35$ ), we obtain an empirical value for the indentational strain produced by the pyramid of  $20 \times 0.35 = 7\%$ , which is close to the proposed value of  $8\%$ .

One of Dr. Voce's most pertinent criticisms is that I have used a simple power law of the type  $Y = be^z$  to express the stress/strain relation. This is quite clearly a gross oversimplification, and an exponential relation of the type he quotes is very much better. However, for strains of the order of  $25\%$  linear strain, a power law is not a bad approximation except near the origin, and it is significant that the simple theory proposed works quite well over this range of strains. It is only at larger strains that the approximation becomes poor, and in the original paper this was clearly attributed to the fact that the stress/strain curve deviates further and further from the simple power law as the strains extend beyond  $25\%$ . Although Dr. Voce's criticism is perfectly valid, it should be noted that an exponential relation involves three arbitrary parameters; the power law only two.

The main purpose of the original paper was to provide a simple theory of hardness that would explain most of the established empirical relations which have emerged in the hardness literature over the last forty years. Dr. Voce concedes that the fundamental relation proposed between hardness and yield stress is basically sound, but suggests that it is indeed already well known. I wish that were so. The latest technical book on hardness by Lysaght,\* although containing much new empirical data, represents no advance in terms of physical fundamentals on O'Neill's pioneering survey published in 1934. The crucial theoretical study of Prandtl† and of Hencky‡ seems to have been almost completely overlooked in subsequent hardness literature. Although it has long been recognized, in a loose way, that hardness is a measure of some mechanical property of the metal, it was these papers which first showed that the mean pressure resisting local indentation, i.e. the indentation hardness, is directly related to the yield stress  $Y$  and is indeed approximately equal to  $2.8Y$ . When Dr. Voce jumps from his equation (1) to equation (2), he is making a far-reaching physical assumption that the hardness is directly proportional to the yield stress. Any other relation between  $H$  and  $Y$  (or, in his terminology between  $H$  and  $S$ ), would not lead to equation (2). Thus, although he does not explicitly state it, his basic assumption is the one which my paper specifically examined and showed to be valid, namely the Prandtl-Hencky theory of indentation. He also assumes that the additional effective strain produced by a pyramidal indenter is constant. This is another physical assumption which I suggested as being approximately true. Using these assumptions and applying them in very close detail to the deformation characteristics of copper and mild steel, he shows that there is extremely good agreement between the observed stress/strain characteristics and those deduced from the hardness measurements. Indeed, Dr. Voce's detailed treatment is to be welcomed as confirming that the fundamental assumptions described in my original paper are surprisingly well substantiated.

The model given in my paper was admittedly a crude one; it was not

\* V. E. Lysaght, "Indentation Hardness Testing". 1949: New York (Reinhold Publishing Corporation).

† L. Prandtl, *Nachr. Ges. Wiss. Göttingen, Math. physikal. Klasse*, 1920, 74.

‡ H. Hencky, *Z. angew. Math. Mech.*, 1923, 3, 241.

intended to be more. When the crude theory is inadequate, it is essentially because the indentational strain is not truly additive, and because the assumption of a power law for the stress/strain curve is valid only over a limited range.\* These points are made in the original paper, and it is evident that Dr. Voce and I are here in complete agreement. However, although Dr. Voce's treatment is more satisfying in detail, I feel that it obscures the basic simplicity of the relation between hardness and yield stress. To emphasize this relationship, and to derive from it a simple physical explanation of hardness, was the primary purpose of my paper.

DR. E. VOCE (*in further discussion*): In the light of Dr. Tabor's remarks I should like to emphasize that in no sense did I "jump" from equation (1) to equation (2). I thought I had made it clear that both were, in the present case, based objectively and independently on Dr. Tabor's own experimental data.

However, Palm† has already noted the application of the function in question to hardness tests, and has pointed out that the approximate equality of the characteristic strain ( $\eta_c$ ) under stress and hardness leads to a linear relationship between these quantities. I had this work in mind when I said that the relationship between stress and hardness was already fairly well known, as well as van Iterson's theoretical analysis of the subject‡ and my own earlier experimental observations on copper.§ All indicate that the relationship between true (yield) stress and hardness is basically linear.

DR. TABOR (*in further reply*): I am glad to have Dr. Voce's clarification about the linear relationship between indentation hardness and yield stress. Although this was established theoretically in 1920 and has since been recognized by those interested in the physics of metals and the theory of plasticity, it has had practically no impact on hardness literature for 25 years. Indeed, the first specific attempt to correlate this concept with Brinell and Vickers hardness measurements was made, as far as I know, in 1946|| and this was later published in a fuller and more mature form in 1948.¶ The more recent work which recognizes the importance of this relationship is to be welcomed. But until it is firmly entrenched in standard text-books on hardness, it seems to me essential that this fundamental relation should be stressed in any attempt to investigate the physical significance of hardness measurements. Thus Dr. Voce's own contribution—with most of which I entirely agree—does not make clear for the reader interested in the meaning of hardness what are his fundamental postulates. And it seems to me, at this stage, that this is of greater importance than the detailed treatment which Dr. Voce has given. In this sense I wrote that whilst Dr. Voce's detailed analysis is to be warmly welcomed as substantiating the basic assumptions with such accuracy, it tends to obscure rather than to emphasize the simplicity of the fundamental relationship between hardness and yield stress.

\* D. Tabor, *loc. cit.*, pp. 76, 83.

† J. H. Palm, *Trans. Amer. Inst. Min. Met. Eng.*, 1949, 185, 904.

‡ F. K. Th. van Iterson, "Plasticity in Engineering," Chapter XV. London: 1947 (Blackie and Sons).

§ E. Voce, *Metal Treatment*, 1948, 15, 66.

|| D. Tabor, 6th. *Internat. Congr. Appl. Mechanics, Paris*, 1946.

¶ D. Tabor, *Proc. Roy. Soc.*, 1948, [A], 192, 247.



# DISCUSSION ON THE PAPER BY MR. R. W. RUDDLE AND MR. R. A. SKINNER: "HEAT EXTRACTION AT CORNERS AND CURVED SURFACES IN SAND MOULDS."

(*J. Inst. Metals*, this vol., p. 35.)

DR. E. W. FELL\* (Member): My contribution deals with the calculation, by exact methods, of the temperature at different kinds of corner. It may be noted that the corners, referred to below, are of common occurrence in sand moulds.

The mathematical solution of the heat conduction in a wedge of any angle  $\dagger$  enables the temperature to be determined for the particular case of the neighbourhood of a sharp right-angled corner, whether the mould corner be of the kind described in the paper as "external" or as "re-entrant". The mathematical solution may be applied as follows to the conditions associated with Figs. 2, 6, and 7 (pp. 39, 42, 44) of the paper. Taking polar co-ordinates  $r$  and  $\theta$ , we consider the infinite wedge  $r > 0$ ,  $0 < \theta < \theta_0$ , of zero initial temperature, where both faces of the wedge,  $\theta = 0$  and  $\theta = \theta_0$ , are kept at temperature  $V$ , constant, for  $t > 0$ . If  $v$  is the temperature at any point  $(r, \theta)$  of the wedge at time  $t$ , the following equation suggests itself as satisfying the conditions:

$$v = V \left[ 1 - \frac{4}{\theta_0} \sum_{n=0}^{\infty} \sin \frac{(2n+1)\pi\theta}{\theta_0} \int_0^{\infty} e^{-\beta u^2} \frac{J_s(u) du}{u} \right] \quad . \quad . \quad (1)$$

where  $s$  appears to take the values  $(2n+1)\pi/\theta_0$  for  $n = 0, 1, 2, \dots$ ,  $\beta = \kappa t/r^2$ , and  $u$  is a variable. The thermal diffusivity of the substances of which the wedge is composed is denoted by  $\kappa$ . For the corner of a mould described as external, the angle of the wedge ( $\theta_0$ ) would be  $270^\circ$ . For the re-entrant corner of a mould, the angle of the wedge ( $\theta_0$ ) is  $90^\circ$ .

A much simpler method, $\ddagger$  however, of determining the temperature for the  $90^\circ$  re-entrant corner is as follows. Using Cartesian co-ordinates  $x$  and  $y$ , the following equation suggests itself as satisfying the conditions:

$$v = V \left[ 1 - \operatorname{erf} \frac{x}{2\sqrt{\kappa t}} \operatorname{erf} \frac{y}{2\sqrt{\kappa t}} \right] \quad . \quad . \quad . \quad (2)$$

Here, for example, according to Fig. 7 of the paper,  $V = 548^\circ \text{C.}$ , constant, and  $v$  is the required temperature at any point  $(x, y)$  of the corner at time  $t$ .

As regards an external corner where part of the mould surface has the shape of a circular cylinder and the remainder of the surface is a flat end, Professor J. C. Jaeger, in a private communication, informs me that he does not think there is any prospect of a useful exact mathematical solution to the problem of determining the temperature at the corner. The most hopeful line of attack would be numerical. Professor Jaeger offers the suggestion that for small values of the time the temperature distribution near the corners

\* Lecturer in Metallurgy, Technical College, Bradford.

$\dagger$  J. C. Jaeger, *Phil. Mag.*, 1942, [vii], 33, 527.

$\ddagger$  H. S. Carslaw and J. C. Jaeger, "Conduction of Heat in Solids," p. 150. London: 1947 (Oxford University Press).



will not be very different from that in the external corner between two perpendicular planes. He has discussed this and given some figures.\* Possibly these could be used to give an idea of the behaviour at a corner.

Exact solutions are, however, available for a re-entrant corner when the surface of the mould is as described in the previous paragraph. I have calculated the temperature distribution in the neighbourhood of the corner of a solid aluminium cylinder, though for different conditions.† Although the results obtained are considered to be of good accuracy, the use of a small computing machine would have saved much labour and given higher accuracy. Carslaw and Jaeger's book also deals with the re-entrant corner associated with this form of mould surface.

The AUTHORS (*in reply*): We agree with Dr. Fell that equation (1), due to Jaeger, which gives the temperature distribution in a wedge of any angle, could be used to calculate the temperature distribution in the mould around sharp external and re-entrant corners of castings. We did not employ this equation because it is not easy to calculate from it either the flux of heat across the interface per unit surface area (by differentiation after transformation to rectangular co-ordinates), or the total heat extracted in a given time (by subsequent integration of the heat flux with respect to time).

Equation (2) quoted by Dr. Fell is that used to derive the expression given on p. 44 of our paper, for the difference between the heat removed by a plane mould wall and by the mould surrounding a right-angled re-entrant corner of a casting.

We note from Dr. Fell's remarks on the flow of heat in a mould part of whose surface is a right cylinder, that Professor Jaeger suggests that in the case of an internal corner (of a casting) of this kind the temperature distribution in the mould should be closely similar, at small times, to that in the external corner formed by two mutually perpendicular planes. However, since the times involved in foundry work are often quite large, it is clear that caution must be exercised in making assumptions of this nature. From the practical point of view, we feel that the kind of approximations made in our paper offer the most satisfactory method of dealing with the problem.

\* J. C. Jaeger, *loc. cit.*, p. 531 (Tables I and II).

† E. W. Fell, *J. Inst. Metals*, 1947, 73, 252 (Fig. 5).

DISCUSSION ON THE PAPER BY MR. N. B. RUTHERFORD: "THE EFFECT OF MOULD MATERIAL AND ALLOYING ELEMENTS ON METAL/MOULD REACTION IN COPPER-BASE ALLOYS."

(*J. Inst. Metals*, this vol., p. 189.)

DR.-ING. H. LEPP,\* F.I.M. (Member): This interesting paper reminded me of investigations which I carried out many years ago and communicated to the International Foundry Congress held at Prague in 1933, as an official exchange paper from the Nederlandsche Vereeniging van Gieterij Technici.† From the references it appears that Mr. Rutherford and his collaborators have overlooked this paper, which I think should be useful to those readers interested in metal/mould reactions.

The AUTHOR (in reply): I should like to thank Dr. Lepp for calling my attention to his early paper on the effect of the moisture content and other variables of sand moulds on the castings produced. I have read this with interest, and it is evident that the effects with which it is concerned are of the type which arise from bad sand control or poor moulding practice, and usually cause the return of castings to the melting pot before they leave the foundry. The surface reaction dealt with in my own paper occurs even with properly prepared sand and good moulding practice, and is on a finer scale. To emphasize the difference, it may be mentioned that, in Dr. Lepp's paper, it is shown that, in general, trouble is not encountered with high-permeability dry-sand moulds, whereas the evidence in my own and earlier papers‡§|| shows that small-scale reaction is actually worse in a dry mould than in a green mould containing sufficient moisture to exert a slight chilling effect. Even thorough baking at temperatures up to 900° C. does not prevent its occurring.‡ The character of the reaction is most clearly evident from the results quoted by Baker and his colleagues.‡ As Dr. Lepp writes, the effects examined by him occur with all metals and alloys. The phenomenon referred to in my paper does not; thus, bronzes and gun-metals substantially free from phosphorus give no trouble from this cause. Furthermore, the presence of zinc, as in gun-metals, causes an increase in sensitivity, the reaction taking place at lower phosphorus contents than in the tin bronzes. This is a change in the opposite sense to that noted for the effects with which Dr. Lepp's paper is concerned.

\* Consulting Metallurgist, Paris.

† H. Lepp, *Mezinárodní Sjezd Slovárenský Praha*, 1933, 95.

‡ W. A. Baker, F. C. Child, and W. H. Glaisher, *J. Inst. Metals*, 1944, 70, 373.

§ L. W. Eastwood and J. G. Kura, *Foundry*, 1947, 75, (10), 86.

|| B. W. Peck, *B.N.F.M.R.A. Research Rep.*, No. R.R.A. 806, 1918.

## DISCUSSION ON THE PAPER BY MR. G. L. BAILEY: "COPPER-NICKEL-IRON ALLOYS RESISTANT TO SEA-WATER CORROSION."

(*J. Inst. Metals*, this vol., p. 243.)

MR. JOHN R. FREEMAN,\* Jr., S.B. (Member) and MR. A. W. TRACY † : This paper is of very great value to many of us who are interested in the effect of iron on the corrosion-resistance of the cupro-nickels, particularly with reference to their use as condenser tubes. It is apparently an excellent review of the extensive work done in England, much of which was carried out under restrictions of secrecy, so that a comparison of results obtained in the United States has not so far been possible. We could, however, wish for more service data than are given.

Much of our work at the American Brass Co. agrees quite fully with the data given in the paper, but we should like to discuss some points on which there is apparent lack of agreement. All our work has led to the development of an alloy, for condenser-tube service, with a nominal composition of copper 90, nickel 10, iron 0.75%. Simulated service tests made in an experimental condenser at Kure Beach, N. C., with clean sea-water flowing at 11.7 ft./sec., showed cupro-nickel of this composition to be superior to the standard Admiralty brass, aluminium brass, and aluminium bronze (5% aluminium), and almost equivalent to a 70% copper, 30% nickel alloy, with 0.4% iron.‡

An installation of over 100,000 lb. of the 10% alloy of the nominal composition given has now been in service in a large tide-water condenser near Fall River, Mass., on Narragansett Bay, for over 4 years and the tubes are giving excellent service, better than that of the standard alloys mentioned above. The cooling water at this station is partially diluted with fresh water and carries a moderate pollution from domestic sewage and some industrial wastes. Similar results are found in other trial installations. In one, a direct comparison is being made with the standard 70 : 30 cupro-nickel (0.4% iron) and after 3½ years' service, the 10% nickel alloy is showing less corrosion, under conditions of a highly polluted harbour water.

In his conclusions, Mr. Bailey states on p. 274 : "(3) Alloys of low nickel content (5-10%) are greatly inferior to the 70 : 30 alloy if the iron content is below 1%". We have no service experience on alloys with less than 10% nickel, but extensive service experience has shown that the 10% alloy made with a nominal 0.75% iron has given excellent results. Our studies have shown that there is no further significant advantage to be gained by increasing the iron content beyond 1% ; in fact, laboratory tests indicate that corrosion-resistance of the 10% alloy may decrease unless the alloy is quenched from the rather high temperature of 850° C. to retain excess iron in solution. A study of the equilibrium diagram at the 10% and 5% nickel range has been completed recently, and it is hoped to publish the data in the immediate future. Incidentally, this work has demonstrated very interesting precipitation-hardening characteristics of the alloys of higher iron contents.

\* Technical Manager, The American Brass Co., Waterbury, Conn., U.S.A.

† Assistant Metallurgist, The American Brass Co., Waterbury, Conn., U.S.A.

‡ J. R. Freeman, Jr., and A. W. Tracy, *Corrosion*, 1949, 5, 245.

The manufacturing problems involved in considering any heat-treatment procedure should not be overlooked. It is not a happy thought, to say the least, to consider quenching condenser tubes 20 ft. in length from 850° C., in order to retain iron in solution, and produce tubes to meet the very exacting requirements for this type of material. The lower cost of the alloy due to the smaller nickel content would be rapidly absorbed in special manufacturing operations. For these reasons, we find ourselves quite in agreement with the author in his conclusion (8) (p. 274): "The corrosion-resistance of the alloys as normally manufactured in tube form is in normal circumstances not sufficiently below the optimum to justify the troublesome steps necessary to ensure the best possible results".

The 10% alloy with nominal 0.75% iron content has been produced in increasing quantity as a standard item in the mills of the American Brass Co. by standard extrusion and drawing practices for condenser and heat-exchanger tubes. It can be hot rolled readily—in fact with less difficulty than the 70 : 30 alloy—for production of large condenser plates or for strip. It is anticipated that with the present shortage of nickel, the alloy will be adopted for many uses as an equivalent substitute for the 70 : 30 alloy.

MR. A. PRINCE,\* B.Met. (Student Member): Although dealing primarily with the corrosion aspect, the paper includes quite a mine of information on other characteristics of these copper-base alloys and, in view of their importance, it may not be out of place to mention some results recently obtained on their nitriding-resistance. Work at Billingham on the nitriding characteristics of various materials, both ferrous and non-ferrous, has shown that a copper-5% nickel-1% iron alloy has very good resistance to the action of anhydrous ammonia at the usual nitriding temperatures. Very little nitriding was obtained after 500 hr. at 550° C. Surface layers consisted of small amounts of oxides of copper with  $\text{Fe}_3\text{N}$ . Nitrides of copper † and nickel ‡ are unstable at this temperature. Weight increases after 500 hours' nitriding amounted to 0.001 g.

A copper-5% nickel alloy containing no deliberate iron addition has, as would be expected, an even better resistance to nitriding. After 500 hr. at 550° C. no appreciable increase in weight could be detected. Tests extending over longer periods are now in hand.

I am pleased to see that Mr. Bailey includes a few details on the weldability of the copper-5% nickel-1% iron alloy. In the course of our work, we have had occasion to examine the welding characteristics of this particular alloy in the form of annealed  $\frac{1}{4}$ -in. plate. Little work has been done on this subject, and all of it has been confined to the argon-arc method of welding, using strips sheared from the plate as welding wire. A reasonably sound weld, in the mechanical sense, can be obtained by argon-arc welding, in spite of the fact that the welds are invariably exceedingly porous. Results of duplicate tests on butt welds are very similar to those reported by Mr. Bailey and his associates and are tabulated below :

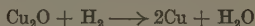
	Test 1	Test 2
Tensile specimens :		
U.T.S., tons/in. <sup>2</sup> .	13.6	13.1
Elongation . . . . .	12% on 2 in.	11% on 1 in.
Bend specimens . . . . .	2 bent through 180°	2 bent through 180°; 1 cracked at 30°

\* Imperial Chemical Industries, Ltd., Billingham Division, Billingham, Co. Durham.

† R. Juza and H. Hahn, *Z. anorg. Chem.*, 1939, **241**, 172.

‡ R. Juza and W. Sachsze, *ibid.*, 1943, **251**, 201.

I wonder if Mr. Bailey would like to comment on the possible causes for this porosity. In one of the tensile specimens blow-holes were observed to extend over one-third of the cross-section and yet the ultimate tensile strength was as high as 13.1 tons/in.<sup>2</sup>. Care was taken to exclude moisture pick-up from welding wire and from adsorbed films on the plates, and I feel that an explanation must not depend on such factors. Ideally, the molten weld pool should be effectively protected by the argon gas flowing over it. If this is not so, it is possible to visualize the rapid absorption of gases by semi-molten regions adjacent to the protected weld pool. With regard to the absorption of gases by such an alloy, it is worth noting that\* the solubility of hydrogen in copper is doubled by the addition of 20 at.-% nickel. The dissolved gases, presumably oxygen and hydrogen, from the water vapour in the atmosphere would then no doubt react in the familiar manner to liberate steam, which is possibly the cause of the blow-holes observed :



DR. I. G. SLATER,† M.Sc., C.I.Mech.E., F.I.M. (Member) : With regard to the engineering aspects of the problem of corrosion in piping, a dominant feature is that many of the troubles are caused by undue water turbulence. Additionally, designs are such that there is much shaping and bending to form of the piping. These two features are, in a measure, inter-related and reflect on past practices in piping layout in which functional requirements have been subordinated to other considerations. Obviously designers have treated metallurgists with much less consideration than was their due. The practical answer is a compromise between the two, and it may be profitable to examine the present position from this point of view.

As Mr. Bailey has indicated, we have in the 70 : 30 cupro-nickel with suitable iron and manganese contents, and in aluminium brass, two materials notably resistant to impingement attack and other forms of marine corrosion. It is valid to ask whether these materials might not have been adopted for the ships' piping and trunking and in this way the corrosion troubles evident with copper avoided. In the early war days, the larger-size piping and sheeting in these alloys was not readily available, but the prospects and potentialities of this must be kept in view in the future. The ability to form and bend tubing in these alloys obviously presents problems, but again the craft of coppersmithing is ever being extended, thanks to newer welding techniques and the further availability of machines for manipulating tubing and sheet. To take full economic advantage of these newer processes it is most desirable that piping layouts and designs should be simplified as far as possible. It is admitted that this is a rather more difficult problem in ships than in shore applications, because of the need to economize in space, which consequently means greater complexity.

A further stimulus to turn away from the older materials, such as copper, used in ships' piping is the need to economize in non-ferrous metals generally. Very substantial tonnages are used for these purposes. The allowance for corrosion deterioration and the low strength properties of copper have meant that the designer has had to employ substantial thicknesses for his piping. Possibly these scantlings might well be halved by using the more corrosion-resistant materials, which incidentally have much better strength properties than copper.

\* C. J. Smithells, "Gases and Metals." 1937 : London (Chapman and Hall).  
A. Sieverts, *Z. Metallkunde*, 1929, 21, 37.

† Director of Research and Development, T.I. Aluminium, Ltd., Birmingham ; formerly Royal Naval Scientific Service.



The value of laboratory tests in indicating service behaviour is a matter of considerable moment in discussion of the present paper. In this connection I should like to quote again some very definite views outlined in an earlier paper by Kenworthy, May, and myself.\* Thus, whilst it is relatively simple to eliminate less satisfactory materials by laboratory and other tests, the firm choice of a really reliable material for more severe use in piping systems is much more difficult. Specific factors which may cause deterioration are elusive and may be of intermittent occurrence, depending on the precise sequence of operating conditions. A final verdict can thus only be approached on statistical lines and trials appropriately extended to an adequate number of systems, to ensure an acceptable probability that some of them will involve potentially damaging conditions.

The AUTHOR (*in reply*): I am particularly glad to have the observations of Mr. Freeman and Mr. Tracy and to learn of parallel investigations in the U.S.A. on these interesting materials. It is not surprising that in the early stages of development of an essentially new series of alloys, initial experience in the two countries does not seem to be identical. The conditions of use are inevitably different, and only when a much larger body of experience has been built up on both sides of the Atlantic can we expect to make a close comparison with advantage. Service experience of the 10% alloys in this country is meagre, but I hope and believe the promising results quoted will encourage more extensive practical trials here. I agree with all that is said about the practical difficulties of quenching tubes from temperatures above 850° C., but laboratory tests at the B.N.F.M.R.A. show that if the iron content of the 10% nickel alloys is of the order of 1.5–2%, the differences in corrosion-resistance resulting from low-temperature annealing are not important. We have no direct experience of the lower-iron alloy favoured by the writers, but should certainly expect even 0.75% iron to effect a large improvement in the resistance of the 90% copper, 10% nickel alloy. I look forward to hearing more in due course of American experience with this and similar compositions.

Regarding the observations of Mr. Prince on the welding of these alloys, I should like to enquire the phosphorus content of his materials. It is usual to add about 0.03% of this element to facilitate castability and improve soundness, and I suggest that a phosphorus addition of this order is not only desirable but necessary in material to be welded, and should suffice to suppress the steam reaction to which Mr. Prince refers. I do not suggest, however, that we are fully satisfied with our knowledge of the welding and other copper-smithing characteristics of these materials.

Dr. Slater's remarks are pertinent. These alloys are offered to the marine engineer as a help in the solution of his problems of corrosion by moving sea-water. It is clear, however, that they only help and do not eliminate the necessity for designing sea-water-carrying systems in such a way as to eliminate that excessive turbulence which is likely to cause corrosion of almost any material. Only by a combination of good design with the use of the most resistant materials can success in service be attained.

\* I. G. Slater, L. Kenworthy, and R. May, *J. Inst. Metals*, 1950, **77**, 309.



# DISCUSSION ON THE PAPER BY DR. MAURICE COOK, MR. R. CHADWICK, AND MR. N. B. MUIR: "OBSERVATIONS ON SOME WROUGHT ALUMINIUM-ZINC-MAGNESIUM ALLOYS."

(*J. Inst. Metals*, this vol., p. 293.)

DR. R. T. PARKER,\* B.Sc., A.R.S.M., F.R.I.C., F.I.M. (Member): I should like to ask the authors to admit the importance of copper as a major alloying constituent in the alloys, by describing them as aluminium-zinc-magnesium-copper alloys. I would not quarrel with any of the ranges used for the investigation of added elements, except perhaps in the cases of silicon and chromium. This disagreement may proceed from some knowledge of what appear to be the optimum levels of these elements in practice, but more information would have been obtained from silicon contents of 0.1, 0.2, and 0.3%, and chromium at zero, 0.15, and 0.25%. With the higher chromium contents in particular, difficulty is likely to arise because of the formation of intermetallics of some size, which might invalidate some of the observations made on corrosion-resistance, for example.

While on the subject of corrosion-resistance, I must query the use of the accelerated testing medium. Have the authors any correlation to offer of their tests with long-time marine exposure? So many tests using accelerated media give a distorted view of the resistance of the metal, that I feel that data such as are given in Fig. 22 (p. 305) and 23 (p. 307) are not of any significant difference.

I question the information given on p. 318 under "Effect of Cold Work and Secondary Heat-Treatment". Since it is stated that cracking occurred in the rolling of the alloy beyond 40% reduction, is the effect shown in Fig. 17 (Plate XLVI) actually corrosion, or the first traces of breakdown in rolling? It would be interesting to learn whether the method of rolling used for these alloys was such as might be expected to overwork the outer surface of sheet. The results of Table IV (p. 319) and the exfoliation of Fig. 18 (Plate XLVI) suggest that the final ageing of 2 hr. at 125° C. is nothing more than a final partial anneal.

Probably the most important point upon which I disagree with the authors is in their belief that the amount of eutectic has some bearing upon the casting properties of these alloys. They have also tied this eutectic quantity in with the rolling and extrusion characteristics, and in this respect they may be correct. In the casting of this type of alloy, however, I believe that the cracking which takes place is essentially "cold cracking", and as such can only be related to stresses formed in casting and to the presence of a brittle structure. Cracking in casting can be correlated with the composition as regards some of the major elements, for example zinc plus magnesium, and some of the minor elements, such as silicon. Unless the authors can relate the presence of their eutectics with the brittle structure necessary for cold cracking, I cannot support their view.

\* Director of Research, Aluminium Laboratories, Ltd., Banbury, Oxon.

MR. H. W. L. PHILLIPS,\* M.A., F.I.M. (Member): The view expressed in the paper that the freezing behaviour of the complex alloys of the D.T.D.687 type is based on that of the ternary alloys of aluminium, zinc, and magnesium is mainly correct, but one point should be emphasized. The authors imply that freezing is completed with the solidification of the aluminium-*T* eutectic complex: this, of course, is only strictly true along the Al-*T* quasi-binary line; in other words, when the magnesium content is about 0.4 of the zinc content. If the magnesium: zinc ratio is less than this, freezing will proceed along the Al-*T* binary valley; it may pass through the peritectic invariants  $T \rightarrow \text{MgZn}_2$  at 475° C.,  $\text{MgZn}_2 \rightarrow \text{MgZn}_5$  at 374° C., and may not terminate until the Al-MgZn<sub>5</sub>-Zn ternary eutectic is reached at about 350° C. If, on the other hand, the magnesium: zinc ratio much exceeds 0.4, freezing will proceed along the other branch of the Al-*T* valley, and may not be completed until the Al-Mg<sub>2</sub>Al<sub>3</sub>-*T* ternary eutectic is reached at 447° C. In either case, therefore, freezing may continue over a long temperature range.

From our work at the Research Laboratories of The British Aluminium Co., Ltd., we confirm that the addition of chromium tends to lead to the formation of stringers of CrAl<sub>3</sub>, often large in size, and our results suggest that the primary CrAl<sub>3</sub> field may be entered at chromium contents of the order of 0.3-0.5%. In this connection it is worth remembering that increases in the amount of manganese and of iron cause this field to be entered at lower percentages of chromium. In these alloys, silicon tends to enter into combination with magnesium to form Mg<sub>2</sub>Si, and this constituent can be detected when the silicon content is well below 0.1%. We also find that, with high manganese contents, the manganese occurs almost wholly as MnAl<sub>6</sub>, and that the formation of this constituent is favoured by an increase in the iron content. With low manganese contents, there is some formation of the  $\alpha$  script constituent, but we cannot yet say at what manganese content the line of demarcation falls. It must lie below 0.4% manganese because at that content and with normal silicon, the manganese-bearing constituent is predominantly MnAl<sub>6</sub>.

DR. I. G. SLATER,† M.Sc., C.I.Mech.E., F.I.M. (Member): Some danger exists in interpreting the accelerated laboratory corrosion tests reported on a practical basis. Failures of aluminium alloys in service due to stress-corrosion are in my experience extremely rare. To produce stress-corrosion effects in the laboratory is a very different matter, and the relationship between such tests and service behaviour is indeed obscure. It is opportune to suggest that we get "back to nature" in planning future testing procedures.

Regarding the evaluation of the alloys by simple tensile tests, it must be realized that aircraft components fabricated from these high-strength alloys are subjected to complex stress systems, which demand more of the metal than may be exhibited by the simple tensile properties. Thus, directional properties, sensitivity to notches and other stress raisers, liability to catatrophic rupture (as in brittle-fracture phenomena), fatigue, shock, &c. are of vital concern to the aircraft designer. A further factor is the strength properties of the alloy "in the piece", as distinct from properties determined on carefully machined test samples. Extrusions, in particular, are of concern in the latter connection. I have noted with interest an extrusion speed of upwards of 22 ft./min. for one of the alloys. This is certainly outstanding and merits further comment as to the nature of the extrusion.

\* Metallurgist, Research Laboratories of The British Aluminium Co., Ltd., Gerrards Cross, Bucks.

† Director of Research and Development, T.I. Aluminium, Ltd., Birmingham.

The AUTHORS (*in reply*): While we are gratified to note the interest that this paper has aroused in the more practical aspects of the utilization of high-strength alloys based on the aluminium-zinc-magnesium system, many of the comments are more concerned with the long-range testing of the alloys and with properties required for special applications, and are not altogether relevant. Such further stages in the development of the alloys are obviously important, but lie outside the scope of the present paper.

Too much has been assumed both by Dr. Parker and by Dr. Slater about the significance attaching to the results of the corrosion tests. There was no question of relating the results of such tests to service behaviour in this investigation. Indeed, it should be apparent from the very nature of the work that a well-established corrosion test was used solely with the object of comparing the relative resistance to corrosion of the various alloys studied. In the authors' experience the salt-peroxide accelerated test is one of the best and most reproducible of those in current use, and it would therefore be most unwise to assume, as Dr. Parker does, that evidence of the kind shown in Figs. 22 and 23 is without significance.

Naturally, more information would have been obtained by studying more alloys, but there has to be a limit to the number of compositions investigated and those chosen were regarded as adequate, as the results themselves confirm, for a general survey of the kind made. The inclusion of the extra alloys mentioned by Dr. Parker would lead only to additional intermediate points being obtained for the curves plotted in Figs. 23 and 24 and would not materially affect any of our conclusions.

In connection with composition, as Mr. Phillips has pointed out, his own observations indicate that the primary  $\text{CrAl}_7$  field may be entered when the chromium content reaches about 0.3-0.5%, although this range may be affected in the downward direction by the presence of manganese and iron. In so far as they are comparable, Mr. Phillips's observations confirm our finding that, with compositions investigated, stringer formations of chromium-rich segregates appear when the chromium content exceeds about 0.25%.

Concerning the point raised by Dr. Parker on the effect of cold work and secondary heat-treatment, the short answer is that the example of cracking to which he refers is due to corrosion and not to breakdown in rolling. There was no evidence that a reduction of 30% induced excessive working at the surface, for no cracking occurred on samples that were rolled without being subsequently exposed to corrosion tests. Whether the treatment by heating for 2 hr. at 125° C. is to be regarded as a final partial anneal or not is merely a matter of words, but it is quite clear both from the figures given in Table IV and from the microstructure that such a treatment does improve the ductility as well as the resistance to corrosion.

We find it difficult to understand Dr. Parker's view that the presence or quantity of eutectic has no influence on casting characteristics, since it is one of the basic concepts of metal technology, that the relative amounts of different phases and their freezing temperature or range constitute some of the essential and particular factors which influence what is, in general, termed the casting characteristics of an alloy. That the incidence of so-called "cold cracking", when it does occur in continuously cast aluminium alloys, is related to internal stresses, is generally agreed. It is, however, going much too far to suggest, as Dr. Parker does, that the quantity of eutectic cannot, as a result of the freezing conditions involved, ultimately affect the distribution and intensity of the stresses in casting. By reducing the eutectic constituent to a minimum, it is possible to operate under conditions which lead to minimum stress effects and least risk of "cold cracking". Thus, the stresses are intensified by the slow rate of casting necessary to avoid hot tearing in an alloy of long freezing range, but, as the eutectic content is reduced, the casting speed can be in-

creased and internal stresses thereby diminished. On the other hand, if casting conditions are such as to give rise to high internal stresses in the ingot, "cold cracking" is likely to occur irrespective of composition within wide limits.

Apart from the increased difficulty in hot rolling and extrusion, a long freezing range necessarily gives rise to segregation in casting, so that the optimum mechanical properties of the alloy cannot be realized in the wrought product. Homogeneity and consistency of properties, especially in heat-treatable alloys, depend to such an extent upon the uniformity and freedom from defects in the castings, that any factors which improve ingot quality in these respects must be regarded as beneficial.

On the more detailed aspects of the solidification of the alloys, we agree with Mr. Phillips's remarks. The formation of  $MgZn_5$  by a peritectic reaction is known to be sluggish, and the most careful examination has failed to reveal this compound in any of the alloys investigated. It follows, therefore, that the ternary eutectic at  $350^{\circ}C.$  is not involved, nor was it, in fact, observed. The number of alloys in which the magnesium : zinc ratio exceeded 0.4 was quite small, and even where an arrest of considerable magnitude occurred at  $475^{\circ}C.$ , the ternary eutectic at  $447^{\circ}C.$  was not detected.

# DISCUSSION ON THE PAPER BY MR. L. ROTHERHAM, MR. A. D. N. SMITH, AND DR. G. B. GREENOUGH: "INTERNAL FRICTION AND GRAIN-BOUNDARY VISCOSITY OF TIN."

(*J. Inst. Metals*, this vol., p. 439.)

DR. J. SAWKILL,\* B.Sc. (Student Member): The authors find, at temperatures well above the grain-boundary peak, a value of 0.8 for  $E/E_u$ , compared with Zener's theoretical value of 0.64. They state that this discrepancy could be due to an error in Zener's formula, or to the fact that for some reason complete relaxation had not taken place. However, Zener's formula does agree remarkably well with the observations of Kê, so that the alternative explanation deserves serious consideration.

If there is some factor inhibiting relaxation at the boundaries, the internal friction ( $\log.\text{dec.}/\text{temperature}$ ) curves will be affected. The magnitude of the grain-boundary peak will be reduced; while any activation energy deduced from the effect of frequency on the curve, will not be the activation energy for true grain-boundary slip. The value of  $H = 19,000 \pm 2500$  cal./mole may then be the activation energy associated with grain-boundary slip with this inhibiting factor present at the boundaries.

It may be significant that with aluminium Kê found the value of the internal friction ( $Q^{-1}$ ) at the grain-boundary peak to be 0.09 when the maximum amount of stress relaxation was in agreement with Zener's theoretical value; whereas here, where the amount of stress relaxation is less than Zener's value, the value  $Q^{-1}$  at the peak is only 0.019.

Kê showed that impurities at the boundaries can block grain-boundary slip. However, the purities of the aluminium and the tin giving the above values are almost the same. Is it possible that it is the nature and not the quantity of impurity at the boundary that is the important factor in blocking slip?

The AUTHORS (*in reply*): We agree that the apparently incomplete relaxation of Young's modulus and the relatively small grain-boundary peak are probably related. Both effects could be due to impurities at the grain boundaries, and, if this were the case, Dr. Sawkill's suggestion that the nature, rather than the amount, of the impurity is the critical factor is probably correct. Clearly, elements which concentrate at the boundaries will be far more effective in blocking slip than those that are uniformly distributed.

The effect of grain-boundary impurities will depend on their arrangement. If they are in the form of small particles which lock the two grains together at various points in the boundary, then the amount of the relaxation will be reduced, but the value of the activation energy for the grain-boundary slip deduced from the experimental observations should be identical with that for the pure metal. On the other hand, a film of impurity in the form of a solid solution at the grain boundaries should not influence the amount of the relaxation, but it will affect the activation energy for the process.

Without a careful examination of the effects of minute quantities of impurity on the results, it is impossible to say whether either effect is present.

\* Post-Graduate School of Physical Metallurgy, Sheffield University.

JOINT DISCUSSION ON THE PAPERS BY DR. H. K. HARDY: "THE EFFECT OF SMALL QUANTITIES OF Cd, In, Sn, Sb, Tl, Pb, OR Bi ON THE AGEING CHARACTERISTICS OF CAST AND HEAT-TREATED ALUMINIUM-4% COPPER-0.15% TITANIUM ALLOY," AND "THE TENSILE PROPERTIES OF HEAT-TREATED ALUMINIUM-COPPER AND ALUMINIUM-COPPER-CADMIUM ALLOYS OF COMMERCIAL PURITY."

(*J. Inst. Metals*, 1950-51, **78**, 169, 657.)

DR. H. K. HARDY\*: I wish to describe briefly some of the results obtained by subsequent work. Probably the most important point is that we have been able to produce aluminium-copper-cadmium alloys on a technical scale as extrusions, forgings, and sheet. The alloy has a most remarkable workability for a strong aluminium alloy and can be hot rolled with almost complete absence of edge-cracking. The tensile properties of the sheet and forgings are given in Table A, from which it will be seen that the results have confirmed the promise suggested.

TABLE A.—*Tensile Properties of Al-4½% Cu-0.6% Mn-0.1% Cd Alloys. Heat-treated in air at 530° C., C.W.Q. and Aged 6 hr. at 185° C.*

Material	0.1% Proof Stress, tons/in. <sup>2</sup>	U.T.S., tons/in. <sup>2</sup>	Elongation, %
Sheet (T) . . .	23½	29	9½
Forging (L) . . .	24	30	14

T = transverse. L = longitudinal.

There are two points to be made concerning the papers themselves. First, the reduction in natural-ageing capacity of the super-purity cast aluminium-copper alloys by additions of cadmium, indium, or tin does not occur to anything like the same extent in wrought alloys or in materials of commercial purity. Of course, the rate of natural ageing is still very much below that of Duralumin-type alloys, so that the aluminium-copper-cadmium can be stored between solution heat-treatment and forming. Secondly, the fully heat-treated cadmium-containing alloy has a good resistance to unstressed and stressed corrosion in NaCl solution. Figs. A and B (Plate LXI) show, respectively, intercrystalline corrosion in an aluminium-copper alloy and intracrystalline corrosion in an aluminium-copper-cadmium alloy.

The effect of certain trace elements on reactions in alloys is very in-

\* Remarks made in introducing his paper at the Autumn Meeting of the Institute held in Venice, September 1951.



teresting. It is known that very small quantities of arsenic, copper, zinc, or cadmium\*† can influence the ageing of lead-tin and lead-tin-antimony alloys. Boron shows up the sub-eutectoid reaction in steel,‡ and 0.05% magnesium does the same for zinc-aluminium alloys.§

MR. R. CHADWICK,|| M.A., F.I.M. (Member): In the first paper the author has made a systematic study of the effect of several elements on the ageing characteristics of an aluminium-copper alloy, which has led to important and well-established conclusions of both theoretical and practical value. The second paper includes a number of observations on several short series of cast and wrought alloys based on aluminium-4% copper with cadmium and other additions, which do not appear to constitute either a systematic study or to be concerned with any one particular theoretical aspect of alloying. While some interesting facts emerge, many of the data are slight and conclusions are often based on differences in properties so small as to be of doubtful significance. In Tables I, II, and III (pp. 659-661), for example, the very considerable effect on mechanical properties of a small addition of cadmium is amply confirmed by the weight of evidence, but other conclusions concerned with the effects of iron and manganese additions would seem to be less reliable, especially since no information is provided on the reproducibility of results which, on material in the form of cast or cast and forged bars, would normally be low even with the most careful experimental techniques. In other instances, factors which might significantly influence the results are ignored. For instance, in Table IV (p. 662), which is concerned with the properties of wrought aluminium-copper-magnesium alloys with varying cadmium, iron, and manganese contents, the quite considerable differences in magnesium content within the series are likely to have a greater effect on properties than deliberate variations in iron and manganese.

The only corrosion results included (Table VII, p. 664), are perhaps the least satisfactory feature of the paper. The basis material, a wrought aluminium-4.5% copper alloy is, especially in the artificially aged condition, notably susceptible to corrosion of an intercrystalline type and has little value as an industrial material for this reason. It is indeed surprising that after exposure to salt spray for 3 months the loss in strength experienced should be so slight. The author does not state, however, under what atmospheric conditions the tests were conducted. The corrosion behaviour of the six alloys is compared by reference to loss-in-strength values ranging from 1.2 to 4.3 tons/in.<sup>2</sup>, tests being carried out only in duplicate. Even in a wrought material made by methods providing a much higher degree of uniformity than exists in forged bars, I should hesitate to make deductions from such a series of values, and the only justification for the author's conclusions is the micrographic evidence of the improvement in corrosion-resistance associated with the presence of cadmium.

It would be interesting to know whether Dr. Hardy has any information on the wrought aluminium-copper-magnesium-cadmium alloy known as Aeral, to which reference was made in a list of proprietary alloys published in 1936.¶

\* W. Hofmann, A. Schrader, and H. Hanemann, *Z. Metallkunde*, 1937, **29**, 39.  
M. Bluth and H. Hanemann, *ibid.*, 1937, **29**, 48.

W. Hofmann and H. Hanemann, *ibid.*, 1938, **30**, 416.

† H. C. J. de Decker, *Rec. Trav. Chim.*, 1946, **65**, 300.

‡ M. C. Udy, *Metal Progress*, 1947, **52**, 257.

§ E. Gebhardt, *Z. Metallkunde*, 1941, **33**, 328.

|| Assistant Research Manager, Imperial Chemical Industries, Ltd., Metals Division, Birmingham.

¶ A. v. Zeerleder, "The Technology of Aluminium and Its Light Alloys." 1936: Amsterdam (Nordeman Publishing Company); London (Crosby Lockwood and Son, Ltd.).



FIG. A.—Inter crystalline Corrosion in Wrought Al-4.5% Cu-Fe-Mn Alloy (F461 of Table VII, p. 664 of paper).

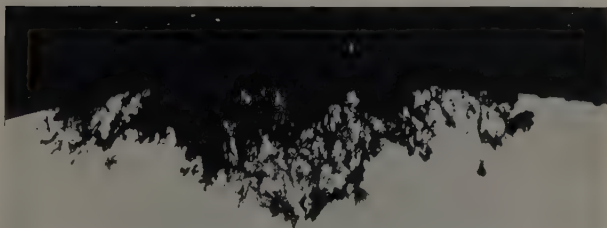


FIG. B.—Intracrystalline Corrosion in Wrought Al-4.5% Cu-Fe-Mn Alloy Containing 0.08% Cd (F462 of Table VII).

Both sprayed once daily for 3 months with NaCl solution.  $\times 50$ .  
(Hardy.)



A specimen of this alloy in the form of 1-in.-dia. wrought bar, which I examined some years ago, contained about 1.2% cadmium, and its properties in the fully heat-treated condition were not significantly different from those of a standard type of aluminium-copper-magnesium alloy in the form of extruded and drawn rod with comparable heat-treatment, although there was a measurable improvement in corrosion-resistance and greatly improved machinability. The microstructure showed small particles of cadmium dispersed in stringer formation, but no information was available on the method of working into rod. In view of the failure of the author to hot work material with more than 0.25% cadmium, it would be interesting to have his comments on the probable method of manufacture of this material.

PROFESSOR DR.-ING. A. VON ZEERLEDER\* (Honorary Corresponding Member to the Council for Switzerland), DR. F. ROHNER\* (Member), and MR. H. HUG\*: Dr. Hardy, in discussing the mechanism of the action of cadmium, indium, and tin in aluminium-copper alloys, rejects the possibility that they exercise a hardening effect of their own by causing the formation of a new phase. We agree with him that these elements act rather by influencing the precipitation process of the copper. They could, according to Dr. Hardy, either affect the rate of diffusion of the copper or its rate of nucleation. He discusses the second case, but thinks it hazardous to speculate about the first. From the point of view of precipitation and pre-precipitation theories of age-hardening no simple and satisfactory explanation of the effects of these elements attributable to an influence on the rate of diffusion can be deduced. However, if age-hardening is regarded from another aspect, a very easy and straightforward solution seems possible.

In very general terms our picture of age-hardening is as follows. The hardening effects are due to some kind of disorder in the parent lattice, which is a by-product of the rejection and precipitation of copper atoms from the supersaturated solid solution. Whether the disorder takes the form of internal strains, dislocations, or vacant lattice sites, is unimportant. Now let us assume that cadmium, indium, and tin impede diffusion in the aluminium-copper system. The result will be that natural ageing is retarded, because the diffusion of copper atoms is reduced. In artificial ageing we may visualize that disorder of the matrix is caused by the rejection of copper atoms in much the same way, but at a considerably greater rate. However, the disorder is no more stable at these higher temperatures, because self-diffusion in the aluminium matrix sets in at about 35° C.† and is very marked at, say, 150° C. The rate of artificial ageing is therefore determined by the difference between the rate at which disorder is created (dependent on the diffusion of copper) and that at which order is restored (dependent on the self-diffusion of aluminium). We know that self-diffusion is more temperature-dependent than the diffusion of foreign atoms in the same matrix. By assuming that the diffusion of copper in aluminium, as well as the self-diffusion of aluminium, is hindered by cadmium, indium, or tin, but that the self-diffusion is the more strongly affected, the acceleration of artificial ageing could be understood.

Dr. Hardy's explanation of the neutralizing effect of magnesium seems convincing and is applicable both to his hypothesis involving nucleation, and to our own involving diffusion.

We are much interested in Dr. Hardy's second paper, since we made similar investigations in 1926.‡ With an addition of 0.05% cadmium, binary

\* Research Laboratories, S.A. pour l'Industrie de l'Aluminium Chippis, Neuhausen-am-Rheinfall, Switzerland.

† G. F. Hüttig, *Arch. Metallkunde*, 1948, 2, 95.

‡ Swiss Patents Nos. 124,793 and 133,722.

aluminium-copper casting alloys showed a slight decrease in tensile properties after solution-treatment at 530° C. and age-hardening at room temperature. Artificially aged alloys, on the other hand, gave a considerable increase, particularly in tensile strength. While the effect of a corresponding addition of tin is apparent after ageing at 140° C., the hardening affect of cadmium occurs only after ageing at somewhat higher temperature (see Table A).

TABLE A.—*Effect of Cadmium Additions on Tensile Properties of Cast Al-Cu Alloys.*

(a) Cu 4.5, Fe 0.22, Si 0.1, Ti 0.15% (Hardy, Table I).

Cadmium Addition, %	Aged 14 days at room temperature			Aged 16 hr. at 165° C.		
	0.1% Proof Stress, kg./mm. <sup>2</sup>	Max. Stress, kg./mm. <sup>2</sup>	Elongation, %	0.1% Proof Stress, kg./mm. <sup>2</sup>	Max Stress, kg./mm. <sup>2</sup>	Elongation, %
Nil	11.9	27.8	17	23.4	34.5	6
0.05	11.8	26.1	14	30.8	36.7	3

(b) Cu 4, Fe 0.2% (v. Zeerleder *et al.*).

Cadmium Addition, %	Ageing Treatment	0.2% Proof Stress, kg./mm. <sup>2</sup>	Max Stress, kg./mm. <sup>2</sup>	Elongation, % 11.3√(area)	Brinell Hardness, kg./mm. <sup>2</sup>
Nil	Room temp.	12.5	27.5	12	64
0.05		11.0	25.5	12.5	62
Nil	16 hr. at 140° C.	13.9	24.9	5	79
0.05		14.8	25.5	5.5	81
Nil	16 hr. at 160° C.	10.6	22.6	6.5	63
0.05		31.5	34.2	1	111

Aluminium-copper casting alloys containing magnesium (Alufont II; magnesium 0.2%) do not exhibit an enhanced hardening effect after addition of 0.05% cadmium, even when aged at 160° C. The behaviour of wrought alloys is similar. Ageing at room temperature after addition of cadmium did not increase the tensile properties; artificial ageing did so only at temperatures above 140° C. (see Table B).

As regards corrosion-resistance, we obtained much the same results as Dr. Hardy. In alloys containing cadmium we even found a slight improvement in the tendency to intercrystalline attack.

Later investigations on binary aluminium-copper alloys (iron 0.2, silicon 0.1%) revealed an acceleration of artificial ageing with increasing cadmium content. While no improvement in the tensile properties of sheet containing 0.05% cadmium was found after artificial ageing for 48 hr. at 140° C., an addition of 0.2% resulted in a remarkable increase in strength after 6 hr. (see Table B (c)). Higher additions up to 1% produced no further improvement.

Addition of cadmium to aluminium-magnesium-silicon alloys caused an improvement of 3 kg./mm.<sup>2</sup> in both yield strength and U.T.S., without detrimental effect on the corrosion-resistance.

Owing to working difficulties and insufficient demand for the improved mechanical properties obtained, our alloys have not found much application in practice. It will be interesting to see whether the new attempt to introduce

TABLE B.—Effect of Cadmium Additions on Tensile Properties of Wrought Al-Cu Alloys.

(a) Cu 4.5, Fe 0.24, Si 0.1% (Hardy, Table II).

Cadmium Addition, %	Aged 14 days at room temperature			Aged 16 hr. at 165° C.		
	0.1% Proof Stress, kg./mm. <sup>2</sup>	Max. Stress, kg./mm. <sup>2</sup>	Elongation, %	0.1% Proof Stress, kg./mm. <sup>2</sup>	Max. Stress, kg./mm. <sup>2</sup>	Elongation, %
Nil	9.4	26.9	35	14.8	30.4	22.5
0.08	9.1	26.1	32.5	34.0	42.0	15

(b) Cu 4, Fe 0.2% (v. Zeerleder *et al.*).

Cadmium Addition, %	Ageing Treatment	0.2% Proof Stress, kg./mm. <sup>2</sup>	Max Stress, kg./mm. <sup>2</sup>	Elongation, % 11.3√(area)	Brinell Hardness, kg./mm. <sup>2</sup>
0	Room temp.	10.5	27.5	21.5	66
0.05		9.5	27.0	22.5	64
0	48 hr. at 100° C.	18.8	35.0	22	90
0.05		17.0	33.5	22.5	86
0	48 hr. at 140° C.	18.5	36.5	20.5	99
0.05		18	36	21	96
0	48 hr. at 160° C.	23	35	14.5	101
0.05		31.8	40.5	9.5	120

(c) Cu 4, Fe 0.2, Si 0.1% (v. Zeerleder *et al.*).

Cadmium Addition, %	Ageing Treatment at 140° C.	0.2% Proof Stress, kg./mm. <sup>2</sup>	Max. Stress, kg./mm. <sup>2</sup>	Elongation, % 11.3√(area)	Brinell Hardness, kg./mm. <sup>2</sup>
Nil	48 hr.	18.5	36.5	20.5	99
0.05	48 hr.	18	36	21	96
0.22	6 hr.	33.8	40.7	9	122
0.22	24 hr.	36.7	42.6	97	124

such alloys will be more successful. Working equipment has, of course, been greatly improved in the meantime, and there is much scope for higher-quality materials.

The AUTHOR (*in reply*): I am rather at a loss to understand Mr. Chadwick's remarks on the tensile properties of the aluminium-copper-cadmium alloys containing iron and manganese. Although only single figures have been quoted, it is stated that these are average results. In practice a number of bars were tested, and consistent values were always obtained. Similar remarks apply to Table IV, in which only very small variations of magnesium occurred within each series of alloys. The corrosion specimens were kept in a spray cabinet in the laboratory, and the results in Table VII are the averages



on three uncorroded and three corroded specimens. The small change in strength is probably to be associated with the diameter of the test-piece (0.423 in.), but Mr. Chadwick's comment that only the metallographic evidence confirms an improved corrosion-resistance of the cadmium-bearing materials is unacceptable. The cadmium-free and manganese-free alloys gave strength losses two to three times as great as the corresponding alloys with cadmium. The changes in ductility show exactly the same effects. I have no information on Aeral, but do not anticipate improved tensile properties in view of the magnesium content.

It is interesting to have Professor von Zeerleder's comments on the mechanism by which cadmium, indium, or tin atoms exert their marked effect on aluminium-copper alloys. However, I do not find his picture of the ageing process at all simple, as it seems to be independent of any nucleation process, while the metallographic evidence (Figs. 15-18, Plate XXX) shows that additions of cadmium greatly increase the number of particles of precipitate.

I was aware of the Swiss Patents to which Professor von Zeerleder refers. These indicate that aluminium-3% copper alloys with 0.5% tin, 0.5% cadmium, or 0.25% tin and 0.25% cadmium, respond to solution heat-treatment and artificial ageing. One Brinell hardness value, in the range 100-130, is given for each of the three alloys aged at 130° C. It is pleasing to know that other work of Professor von Zeerleder's confirms the results in my own papers.

I am unable to understand Professor von Zeerleder's reference to working difficulties. We have found that aluminium-copper-cadmium alloys possess outstanding hot-working properties and the cadmium content can safely be raised above the 0.1% limit referred to in the second paper. For example, an alloy containing 4.5% copper, 0.15% cadmium was hot rolled from 5 in. thick to 0.25-in. slab without the slightest signs of edge cracking.

# DISCUSSION ON THE PAPER BY MR. R. W. RUDDLE AND MR. A. L. MINCHER: "THE INFLUENCE OF ALLOY CONSTITUTION ON THE MODE OF SOLIDIFICATION OF SAND CASTINGS."

(*J. Inst. Metals*, 1950-51, 78, 229.)

DR. R. T. PARKER,\* B.Sc., A.R.S.M., F.R.I.C., F.I.M. (Member): A particular point upon which I should like to comment concerns the method of solidification of eutectics, a matter which the authors have to admit still remains obscure. The difficulty they have had to contend with is the apparent progress of solidification without the presence of a thermal gradient, and I cannot feel satisfied with their earlier explanation that gravity and convection can account for the loss of heat. The experiment described in the present paper to check this hypothesis does not help to clear up the matter. Can we be assured that the temperature gradients, in horizontally and vertically cast blocks, and in the different alloys, were still of too small a size adequately to explain normal heat loss?

Another point worth confirming is that the alloys can really be regarded as eutectic in composition. The "few per cent." of primaries mentioned at the bottom of p. 244 may well be enough to form a network modifying, among other properties, the pour-out characteristics. I feel that the solidification of eutectics, which appear always to be capable of a form of "modification" by alteration of cooling rate, can be expected to vary in behaviour between that of a pure metal and an alloy with a freezing range, depending upon composition and cooling rate together.

The suggestion of movement of metal, either solid or liquid, is also mentioned in the description of the work on the solid-solution alloys. On p. 241 the formation of interdendritic fissures in magnesium and in aluminium alloys is suggested as being a result of metal movement, but without an illustration it is difficult to visualize whether these fissures occur at the block axis, and transverse to the cylinder wall, or further out and parallel to it. In either case it seems there are alternative explanations of their formation: either that the cracks are due to hot tears or bridging with consequent lack of feeding, or that they are due to cold cracking. I should like to hear the authors' reasons for ruling out these possibilities, which I imagine they must have considered.

Another point of great interest is the extension of the authors' findings to higher freezing rates. Assuming that alloys of certain freezing ranges will behave as skin-forming alloys under higher speeds of chilling, it should be possible to reverse the process and use the change-point from skin-formation to pasty freezing as a measure of change of temperature gradient. This would imply a recognizable alteration in structure accompanying the two different mechanisms of freezing. Does any evidence yet collected by the authors help in this connection?

DR. I. G. SLATER,† M.Sc., C.I.Mech.E., F.I.M. (Member): The work could profitably be extended to more rapid rates of solidification. Experimental

\* Director of Research, Aluminium Laboratories, Ltd., Banbury, Oxon.

† Director of Research and Development, T.I. Aluminium, Ltd., Birmingham.

difficulties might be substantial and complexities arise, but the prospects of obtaining valuable information are bright. With these higher solidification rates, as in the production of slabs and billets for subsequent fabrication, the actual solidification mechanism has a significant effect on the properties of the resulting material. Thus, higher rates may not always have a beneficial effect on the product, as instanced by the fact that aluminium sheet rolled from die-cast slabs has superior deep-drawing and directional properties to that produced from continuously cast slab. Factors relating to inverse-segregation effects and to the significance of dissolved gases in the melt might also be further elucidated by the techniques evolved.

The AUTHORS (*in reply*): We agree with Dr. Parker that our explanation for the loss of heat in the absence of a temperature gradient during the solidification of eutectics cannot be regarded as fully satisfactory; and that the matter remains obscure. Dr. Parker suggests that, with increased accuracy of measurement, it might be found that small temperature gradients exist in the casting which could account for the flow of heat. In the experiments described in our paper, the temperatures were measured to better than  $\pm 0.5^{\circ}\text{C.}$ ; since there were thermocouples at the surface of the casting, at the centre, 5 in. away, and at intermediate points, it follows that we should have detected any gradients in excess of  $0.1^{\circ}\text{C./in.}$  As pointed out in an earlier paper,\* gradients of a lesser order than this are much too small to account for the flow of heat into the mould. Particular attention was devoted to this point in the earlier work,\* and the original finding that there is a considerable period during the solidification of eutectiferous aluminium-copper alloys during which the casting is at substantially the same temperature throughout, was confirmed by more sensitive measurements made with differential thermocouples. There seems little doubt therefore that, even if a very small temperature gradient does exist during the period of apparent constant temperature, it cannot be large enough to account for the flux of heat into the mould.

As Dr. Parker points out, the alloys used were, in most cases, not exactly of eutectic composition and we agree that such small discrepancies, combined with variations in cooling rate, might greatly affect the mode of solidification. It is evident that a long and detailed study will be necessary to clear up the matter completely.

Dr. Parker asks about the disposition of the fissures observed in the magnesium and aluminium-magnesium alloys. These were in general neither parallel nor perpendicular to the cylindrical walls of the casting, but were arranged with their length along the isotherms present during solidification (the shapes of these isotherms were similar to those previously observed in aluminium-4% copper alloy cylinders and depicted in Figs. 6 and 7 of the paper cited\*). Some of the fissures were cruciform in shape, the shorter arms being at right angles to the isotherms. We assumed that these fissures were interdendritic and were caused by incomplete mass feeding, because they had regular wavy outlines which strongly suggested that they had resulted from pulling apart of the dendrites. The fact that the fissures always lay along the isotherms supported this view, by indicating that the stresses responsible for the fissuring were always directed from the heat centre of the casting towards the colder regions. This type of fissuring, of course, really amounts to hot tearing, in which the stresses are produced in the pasty mass of solidifying dendrites by the opposition which the semi-rigid mass offers to the forces which normally promote mass feeding (i.e. gravity, atmospheric pressure, &c.). As we visualize it, compacting of the semi-solid and semi-rigid

\* R. W. Ruddle, *J. Inst. Metals*, 1950, 77, 1.

mass, to take up the shrinkage during freezing, probably proceeds discontinuously, small regions suddenly compacting in succession. As the mass is steadily becoming more rigid as solidification advances, it is unlikely that some of the last regions to compact will be able to do so completely, and fissures will develop in these regions. Gas rejected from solution during solidification might aid the production of these fissures.

Both Dr. Parker and Dr. Slater consider that work of the kind we have been doing could usefully be extended to more rapid rates of solidification, and we entirely agree with this view. The effect of freezing rate on the properties of the casting is complex and, as Dr. Slater indicates, higher rates may not always be beneficial. For example, work carried out some years ago by Baker\* showed that 1-in.-dia. magnesium alloy sand-cast bars have higher strength when allowed to solidify slowly than when solidification is speeded up by uniformly chilling the mould.

Dr. Parker enquires whether the two different freezing mechanisms give rise to different structures. We would not like to be too definite on this point, but we have always observed predominantly columnar structures in castings which have solidified by skin formation and equi-axial structures in castings which have frozen in a pasty manner. Certain alloys (e.g. high-tensile brass) generally show columnar structures when chill cast and equi-axial structures when sand cast, suggesting that altering the rate of freezing causes a change in the mode of solidification.

\* W. A. Baker, *J. Inst. Metals*, 1945, 71, 165.

# JOINT DISCUSSION ON THE PAPERS BY MR. R. F. TYLECOTE : " THE ADHERENCE OF OXIDE SCALES ON COPPER " AND " THE OXIDATION OF COPPER AT 350°-900° C. IN AIR."

(*J. Inst. Metals*, 1950-51, **78**, 301, 327.)

DR. F. D. RICHARDSON \* : The large differences between the properties of scales formed on pure copper and those formed on copper containing arsenic or phosphorus, are most interesting, particularly when it is remembered that only 0.44% arsenic and 0.034% phosphorus are involved. The parallel between the powers of adherence of the scales to the basis metal, and the ductility of the scales alone, seems to be important, though the precise relationship between the two is by no means clear. The poor adherence and ductility of scales formed from the phosphorus-containing copper, is attributed to the formation of a copper phosphate glass, spread out between the oxide grains. It appears certain that such a phase exists, but premature to assume that this is the cause of brittleness until more is known about its properties. A glassy phase might quite possibly confer plasticity rather than brittleness, by acting as a plastic bond between the grains.

The author has said little regarding the manner in which his work adds to the general picture of scale formation so far developed. There are, however, some interesting points to be deduced from his results.

The current view of the oxidation of copper, and indeed of a number of other metals, is as follows. Copper ions move out from the metal, through the copper oxide, to the surface, where there is a deficit of copper in the lattice (i.e. of  $\text{Cu}^+$  ions) due to the presence of  $\text{Cu}^{++}$  ions. As the copper atoms reach the surface, they combine with oxygen atoms from the gas, and so build up more copper oxide on the surface of the growing scale. Actually, most published researches can be explained in terms of movement of oxygen atoms back, but this movement has generally been discounted on account of the much greater size of the oxygen atoms, and the greater activation energy consequently required for their movement in the lattice. If, however, oxidation is effected only by the movement of copper ions outwards, the complete oxidation of a wire should lead to the formation of a central cavity, provided oxidation is uniform. The porosity shown in Figs. 5-8 (Plates XXXVI and XXXVII of the first paper) is so widely distributed that it can be taken as proof of the movement of oxygen atoms during oxidation, the oxygen atoms sliding backwards in a random manner. This fits in with recent work on the movement of  $^{18}\text{O}$  in  $\text{CoO}$  and  $\text{NiO}$ , which changes from slow to fast around 700° C.†

Another interesting point is the manner in which single crystals generally grow upwards from the metal through the scale. This is well illustrated in Figs. 6 (Plate XXXVI) and 10 (Plate XXXVIII) of the first paper, where etched cross-sections are shown. We have noted exactly similar behaviour

\* Head of Nuffield Research Group in Extraction Metallurgy, Royal School of Mines, London.

† J. A. Allen and I. Lander, *Nature*, 1949, **164**, 142.

with the oxidation of iron, though we have not obtained etched cross-sections. The oxidation of polycrystalline iron specimens has always led to the formation of an oxide with a surface crystal pattern following that of the iron beneath it.

In our experiments with iron strips and wires, we have found that in the neighbourhood of scratches, and in places where the basis metal has been disorganized (e.g. at the edges where strips have been cut), long spikey crystals of oxide grow rapidly outwards from the metal. These consist sometimes of single spikes, and sometimes of tree-like clusters, ranging up to 0.0001 in. long. We have so far been unable to explain this phenomenon satisfactorily. We should like to know whether Mr. Tylecote has ever observed such growths with his copper scale, and if so, whether they failed to appear in electropolished specimens.

DR. H. K. HARDY,\* M.Sc., A.R.S.M., A.I.M. (Member): Unfortunately I have not seen the spikey crystals described, but wonder whether they are in any way related to the dislocations in the underlying metal. Frank's theory of crystal growth requires the presence of screw dislocations giving rise to a small ledge at which atoms can easily be attached to the solid. The lattice structure of the solid frequently controls the orientation of the surface film, and it is reasonable to suppose that screw dislocations in the solid may sometimes be carried on by screw dislocations in the lattice of the oxide film. Since the axis of the screw dislocation may provide a relatively easy diffusion path, the oxide film might thicken preferentially in such a region. Each spike would then represent the position at which a screw dislocation in the solid had been successfully continued into the surface film. I hope that experimental work will be able to confirm or deny this hypothesis.

MR. K. SACHS,† M.Sc., A.I.M. (Junior Member): A paper as full of new facts as that on the adherence of oxide scales on copper must naturally raise a number of questions. Two of these concern the practical applications of the work. The author states on p. 304 that some of the inner scale layer is retained even when "complete" exfoliation is recorded in Table III. Is the flaking off of the "outer scale layer" sufficient to overcome most of the difficulties sometimes caused by adherent oxide scales in subsequent fabrication? The characteristic behaviour of scales formed on phosphorus-containing copper is attributed to the presence of a phase that is liquid above about 500° C. Does this lead to accelerated oxidation and, particularly, to severe roughening of the surface of the metal below the scale?

The presence of the liquid phase in scales on phosphorus-containing copper raises another question of theoretical interest. In a footnote to p. 313 it is pointed out that scale formed on pure copper extended 16% when broken quickly (15 sec.) at 700° C. and 25% when the load was applied gradually (7 min.), and it was concluded that elongation was predominantly plastic rather than viscous. The presence of a liquid, particularly a glassy, phase, even in very small quantities, may well confer viscous properties on the scale, and information on the behaviour of the corresponding phosphorus-containing "oxide wire" under conditions of gradual loading at 700° C. would be of interest. This idea is supported by the contrast between the tensile tests on completely oxidized wires in Fig. 22 (p. 314), where the elongation at 800° C. of scale formed on the phosphorus-containing copper NTF is lower than that on the "pure" copper NTB even at 400° C., and the torsion test, Tables V

\* Head of Physical Metallurgy Section, Fulmer Research Institute, Stoke Poges, Bucks.

† Research Metallurgist, The Mond Nickel Co., Ltd., Birmingham.



and VI (p. 310), where the scale NTF tested at 800° C. is much more ductile than that formed on "pure" copper tested at 400° C.

The microstructures of the "oxide wires" tend to show an inner core whose structure differs a little from the rest. It is most sharply delineated, at least on one side, in the wire from "pure" copper, Fig. 6 (Plate XXXVI), and is characterized by a constituent of intermediate tone in the wire from copper containing 0.03% phosphorus (Fig. 7, Plate XXXVII). Is the author able to account for these cores in any way?

Mr. Tylecote finds that scale formed on pure copper at 900° C. and cooled to temperatures below 600° C. is much more ductile than scale formed at these low temperatures (Tables V and VI). Is this because less cupric oxide is formed at 900° C., in which case it would follow that cupric oxide embrittles the scale? Or can it be attributed to the heavier scale deposit formed at 900° C., in which case it would follow that in thin layers the ductility of the bulk oxide is overshadowed by poor adhesion at the scale/metal interface?

Reference is made on p. 312 to the importance of the scale/metal interface in connection with the effect of prolonged oxidation at 900° C. on the ductility in the torsion test of scale formed on arsenical copper. Here the thick deposit cracks more easily than the thin one. The same effect can be deduced from the exfoliation experiments. Arsenical copper oxidized more rapidly than the other samples used (p. 312). At higher temperatures, when this would lead to appreciably thicker scale, the tendency to exfoliation is as strong as in other samples; at lower temperatures, however, the scale flakes off less readily than with the other types of copper (p. 319). The bulk properties (p. 314) and the microstructure (p. 317) of scale formed on arsenical copper resemble those of scales formed on phosphorus-containing copper, while the relatively high ductility of this type of scale exhibited in exfoliation and torsion tests falls off as the scale thickens. Could the anomalous behaviour of these scales on arsenical copper be due to the brittleness of the bulk oxide being overshadowed by tighter adherence at the scale/metal interface? Is there any direct evidence to suggest that the scale on arsenical copper is more intimately bonded with the metallic core than that on pure copper? It is known that in some alloy steels the adherence of the scale is enhanced by the mutual penetration of oxide and metal at the interface.

Mr. Tylecote's mechanical tests on completely oxidized wires are of particular interest, and one would like to compare his results with the bulk properties of pure oxides.

The AUTHOR (*in reply*): It is true that neither of the papers has added much to our knowledge of the mechanism of scale formation. That was not the main object of the work reported, but it will be the subject of a further paper.

With regard to the long spikey crystals of oxide, mentioned by Dr. Richardson, I have recently observed on electropolished specimens, oxidized under certain conditions, a general superimposed growth of "hairs" of oxide. These appear to consist of CuO, and are not restricted to the edges but are more widespread.

In reply to Mr. Sachs, where exfoliation takes place, it is clear that in the majority of cases the greater portion of the scale formed comes off. But it seems that in some cases of oxidation in the lower range of temperature a thin film of Cu<sub>2</sub>O is left behind. It is also possible for a film to form during cooling after exfoliation, since this process often starts at temperatures as high as 500° C. Films present owing to either of these causes would be thin and not likely to cause much trouble in subsequent working processes.

There is no doubt that the presence of 0.4% arsenic leads to accelerated oxidation at 900° C. But 0.04% phosphorus has very little effect, if any, on

the oxidation rate. Roughening of the surface of the copper below the scale seems to occur in all high-temperature oxidation of copper.

With reference to Fig. 6 (Plate XXXVI) of the paper on adherence, the area on the right-hand side is merely a large cavity. However, in the centre of Fig. 7 (Plate XXXVII) there is a large amount of the phosphorus-rich constituent. This can be explained on the basis of the formation of this phase on the copper/cuprous oxide interface. During the consumption of the metal during oxidation, this interface moves inwards, and at the end of oxidation one would expect to find it in the centre of the specimen.

I should not like to be dogmatic about the reasons for the difference in behaviour of scales formed at high temperatures and at low temperatures. Either of Mr. Sachs's suggestions may be correct. I should not expect the adherence of the arsenical scale to be very different from that of the phosphorus-containing scale, and certainly not greater than that of pure copper. I agree that adherence would be enhanced by mutual penetration of oxide and metal. Present work appears to show that the scale is more adherent on rough surfaces than on electropolished ones.

## DISCUSSION ON THE PAPER BY MR. H. G. BARON AND PROFESSOR F. C. THOMPSON : " FRICTION IN WIRE DRAWING."

(*J. Inst. Metals*, 1950-51, **78**, 415.)

PROFESSOR H. FORD,\* Ph.D., D.Sc. (Member) : It is, I think, true to say that until recently investigations into plastic deformation in the various industrial metal-working processes have run along distinctly separate lines. It is now clear that a comparative study at an earlier stage would have speeded up the general progress being made, certainly as far as cold-working processes are concerned.

If we consider first the points of similarity in wire drawing, cold rolling, and deep drawing, it is apparent that we are concerned with two fundamental quantities in attempting an analysis of the forces involved and the nature of the deformation occurring : (i) the stress/strain curve connecting the current yield stress with the corresponding amount of strain reckoned from the initial condition of the material being deformed ; and (ii) the coefficient of friction between the deforming metal and the die or roll. Using the theory of plasticity to derive an equation for the stress distribution in the process, no other quantities are involved, and if these two quantities were accurately known, an immediate test of the adequacy or otherwise of the underlying theory could be obtained. Unfortunately, no direct way of measuring the coefficient of friction is at present available.

In the past, methods of measuring the overall forces, such as drawing force, die load, roll force, or roll torque were not sufficiently accurate nor sufficiently carefully controlled to yield consistent data ; empirical correcting factors had to be applied which masked the essential simplicity of the problem.

For example, if the yield-stress curve can be considered fixed, by some such technique as described by Mr. Baron and Professor Thompson, then only one factor—the coefficient of friction—remains as the adjustable factor when comparing theory with experiment. That is in fact the procedure followed by the authors. Quite recently, MacLellan, after a careful assessment of all the published data on drawing force, &c., found that the coefficient of friction determined in this way required to vary from 0.09 to 0.4 as between the various experimental results, a variation so great as to make any conclusions worthless.

Until a few years ago, a similar spread of values was quoted in cold rolling, but in both rolling and deep drawing, the latest studies have narrowed the range to 0.04-0.1 for the whole range of lubricants and surface finish. The wire-drawing process, giving such vastly different values, has been the black sheep of the family and caused doubt to be cast on the much lower values found in the other processes and it is to be questioned whether a coefficient of friction exists at all, in the normally understood sense, when surfaces are pressed together under high load. The authors, by careful experiment and examination of existing theories of wire drawing, have been able to show that the coefficient, determined as the empirical adjusting factor, assuming the drawing force and yield-stress curve to be known, now comes into

\* Professor of Applied Mechanics, Imperial College of Science and Technology, London.

line with other investigations. This paper therefore must be looked upon as a real milestone on the road to progress in the fundamental knowledge of metal-working, because it lends support to the view that we are, in fact, chasing a real coefficient of friction and not just deriving an empirical constant.

Summing up the authors' findings, it would seem that the results given yield an average coefficient of friction of 0.053, when using a good lubricant, a value agreeing very well with the range 0.05-0.06 found for good lubricants in cold rolling and deep drawing.

The scatter of the results is, however, rather greater than found in other processes, and I should like to know whether the authors have reversed the calculation procedure: that is, have they taken  $\mu$  at the mean value, and recalculated the drawing force over all the data, e.g. for soap *B*, on this value, and then compared the answer with the experimental results? One would expect the differences to be not more than  $\pm 5\%$  for most of the tests, with  $\pm 10\%$  as an absolute limit. The importance of this point is that to predict drawing force, given a yield-stress curve and  $\mu$ , is the practical requirement in wire drawing.

The authors describe in detail their method of determining the yield-stress curve of their material. This is the method which I devised about 1946 for cold rolling.\* The cold-rolling process does not have the advantage of an axi-symmetric distribution of stress and therefore the redundant-work term is not negligible. In rolling, small contact angles cannot be associated with large deformations.

In this connection I should like to ask whether the authors have considered the redundant-work term proposed by Körber and Eichinger, who used the equations for equivalent stress and strain to derive the additional term:

$$A_2(k_1 + k_2) \frac{2}{3\sqrt{3}} \theta.$$

My experience would suggest that the authors are correct in considering redundant work as negligible where  $\theta$  is small, but it would be interesting to know whether, where  $\theta$  is not small and using the values of  $Y_m$  and  $\mu$  they have already determined, this correction term provides satisfactory agreement. On p. 431, in equation (2), the authors give a relationship for determining  $Y_m$ , the true mean yield stress, and say that this method "although somewhat obvious does not appear to have been used before". They may intend this to refer only to wire drawing: it has certainly been used before in cold rolling.

It is felt that much more must be known about the nature of friction between highly loaded surfaces in metal-working processes before it can be established that hydrodynamic conditions exist.

DR. G. D. S. MACLELLAN †: With their careful measurements Mr. Baron and Professor Thompson have established further interesting phenomena concerning the behaviour of wire during the drawing process, and clarified many doubtful points. Their conclusions show how much more is known about the factors influencing the wire-drawing process than a few years ago, and it is now becoming possible to make recommendations for improving the techniques of industrial wire-drawing practice upon a truly scientific basis.

In the paper, however, there are a number of detailed points which merit further consideration and discussion, and it is simplest to take them in the order in which they occur.

(1) The effect of parallel extensions on the total frictional drag has been

\* H. Ford, *Proc. Inst. Mech. Eng.*, 1948, 159, 115.

† Engineering Laboratory, Cambridge University.

considered theoretically in my own work.\* The following relation was obtained for the additional drawing stress  $W_p$  required to overcome friction in the "parallel":

$$W_p = (Y_2 - W_0)(1 - e^{-4\mu l})$$

where  $W_0$  is the observed drawing stress "without parallel";  $Y_2$  is the yield stress at exit from the deformation zone;  $\mu$  is the coefficient of friction in the "parallel", assumed constant; and  $l$  is the length of the "parallel" expressed as a fraction of the final diameter of the wire.

The other assumptions involved in the derivation of this relation are similar to those of Baron and Thompson (p. 429), namely, that the wire remains in contact with the die, i.e. it does not "neck down", and that the maximum shear stress in the parallel extension is constant and equal to  $Y_2$ . If this relation is used to calculate the additional drag that would be caused by a parallel extension of length  $l = 1.5$  (approximately the average figure for the dies used) and a coefficient of friction  $\mu = 0.060$  (a typical value for soap *B*), the results shown in the fourth column of Table A are obtained from the authors' Table I (p. 435).

TABLE A.—*Calculations of the Additional Drag Due to Parallel Extension, and of  $\mu$ .*

$r$	$W_0$	$Y_1$	$W_p$	$W_0 + W_p$	$\mu$	
					MacLellan	Davis & Dokos
0.135	4.3	20	4.7	9.0	0.086 †	...
0.27	9.6	30	6.2	15.8	0.068	0.056
0.37	16.5	36	5.9	22.4	0.063	0.054
0.48	25.1	41	4.8	29.9	0.063	0.060

† Neglecting the "redundant work" discussed by the authors.

The values of  $(W_0 + W_p)$ , if plotted on Fig. 9 (p. 427), are high compared with the observed values for  $W_0$  with "parallel", and  $W_p$  is nearly double the observed effect. I found considerably better agreement in many cases (*loc. cit.*), but the estimate is sensitive to variations in  $l$  and  $\mu$ , for the dies both with and without "parallel".

(2) The authors' values of  $\mu$  calculated from Davis and Dokos's equation, which they consider the most reliable, are subject to some error because the variation of  $Y$  with  $\epsilon (= \log_e \frac{A_1}{A_2})$  is not linear but, for the brass used, almost exactly parabolic. In fact,  $Y = Y_0 \cdot \epsilon^{\frac{1}{2}}$ , where  $Y_0 = 52$  tons/in.<sup>2</sup>, fits the envelope curve of Fig. 4 (p. 422) within about 2% for values of  $\epsilon$  between 0.1 and 0.8. The relation obtained by generalization of Sachs's theory, to allow for variation of  $Y$  in this parabolic manner, can only be expressed in the form of a series, but for practical values of  $\epsilon$ ,  $\mu$ , and  $\alpha$  only the first three or four terms need be considered.

The general solution is:

$$W_0 = Y_0(1 + \lambda)\epsilon^{3/2} \left[ \frac{2}{1.3} - \frac{2^2}{1.3.5}(\lambda\epsilon) + \frac{2^3}{1.3.5.7}(\lambda\epsilon)^2 - \dots \right]$$

where  $\lambda = \mu \cot \alpha$ . In the absence of friction this reduces to  $W_T = \frac{2}{3} \cdot Y_0 \cdot \epsilon^{3/2}$ , as it should, by direct integration; this equation corresponds to the curve for

\* G. D. S. MacLellan, *Ph.D. Dissert., Camb. Univ., 1948.*

$W_T$  shown in Fig. 9, with negligible error over the whole range. Values of  $\mu$  calculated from the relation, using the first three terms and, where necessary, a slight correction for the fourth term of the series, are given in Table A for comparison with those obtained by the authors from Davis and Dokos's equation, and with similar results shown in Table IV of the paper (p. 445), obtained from back-pull experiments.

Calculations for other results show discrepancies of the same order as compared with the authors' results using Davis and Dokos's equation.

(3) The authors make some use of data obtained from a paper by Hill and Tupper.\* It is necessary to accept the latter's semi-empirical correction for converting from two-dimensional results to three-dimensional with considerable reserve. Fig. A shows a sketch of the deformation zone and deformation pattern of an initially square grid in strip drawing, following Hill and Tupper. They argue that the stress distribution for the wire and for the two-dimensional model will correspond if the ratio of wire areas before and

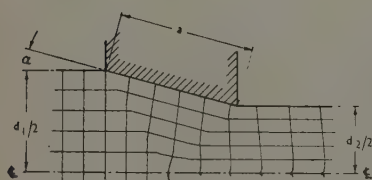


FIG. A.—Theoretical Deformation Pattern Derived by Hill and Tupper for Strip Drawing.

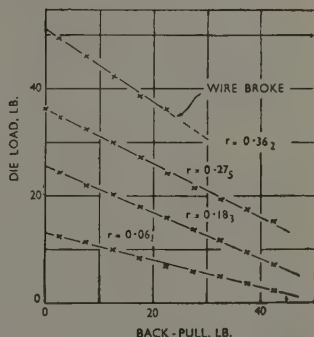


FIG. B.—Curves for Copper Wire Drawn at 1 ft./min. through a Diamond Die.

after drawing ( $A_1/A_2$ ) is the same as the ratio of the strip thickness ( $d_1/d_2$ ). One must therefore assume that the same correspondence will hold for the deformation patterns, since the boundaries of the plastic zone are involved in the determination of the stresses. However, for the reduction of 34.1%, with  $\alpha = 15^\circ$ , for which the diagram is drawn,  $a/d = 0.654$  for the model and  $a/d_1 = 0.36$  for the wire,  $a$  being the length of the contact area in the die. The deformation patterns are therefore far from similar, and the analogy must break down.

(4) The authors present convincing evidence for a small but appreciable variation of  $\mu$  with mean interfacial pressure, part of the evidence being consistent deviations of the back-pull curves from linearity. In support of my claim † that such deviations have in the past been due to inadequate experimental control, Fig. B is reproduced above ‡. This shows curves for a series of copper wires of different sizes drawn at 1 ft./min. through a diamond die for which  $\alpha = 11.5^\circ$  and  $D_2 = 0.0405$  in., the lubricant being castor oil. There are slight departures from linearity, but scarcely sufficient to justify any con-

\* R. Hill and S. J. Tupper, *J. Iron Steel Inst.*, 1948, **159**, 353.

† G. D. S. MacLellan, *J. Iron Steel Inst.*, 1948, **158**, 347.

‡ G. D. S. MacLellan, *Ph.D. Dissert., Camb. Univ.*, 1948.



clusions as to a consistent decrease of  $\mu$  with decreasing interfacial pressure. These results are typical of very many others using liquid lubricants, and it is hoped to publish a fuller account shortly.

(5) Lastly, the authors claim that they used "conical dies without parallel extension" in many of their investigations. It would be of interest if they could give an estimate of the approximate radius of curvature at the throat of such dies. From the normal method of preparation it seems improbable that the die channel could be strictly conical to the throat, and then diverge with precise geometrical conformity to the design, and I have found that in some dies which are nominally conical the relation between drawing force and reduction of area is best explained by the presence of an effective "parallel", having values of  $l$  between 0.1 and 0.25. Such an effect would help to explain the discrepancy noted in (1) above.

The AUTHORS (*in reply*): We have not recalculated the drawing forces from the values of  $\mu$ , but this is a matter to which attention might well be given, and we are grateful to Professor Ford for the suggestion. We had overlooked the fact that he had previously used the same method as ourselves for determining the yield stress of the material, and apologize for the omission of a reference to this. We have not employed the redundant-work term proposed by Körber and Eichinger. It would be interesting to see what sort of result this relationship will give.

Dr. MacLellan's dissertation was not available to us, but the impression gained is that his technique leads to higher values of the coefficient of friction than that obtained from, for instance, the Davis and Dokos equation. We can hardly agree that we have provided evidence for "a small but appreciable variation of  $\mu$  with mean interfacial pressure". The values given in Table V (p. 447), based on direct work, show that the interfacial pressure increases the coefficient of friction, and does so appreciably.

We agree with Dr. MacLellan that wire-drawing dies without parallel extension do not, in actual fact, consist of two conical portions meeting sharply, and that it is not strictly true to speak of the die being without parallel extension. Perhaps what ought to have been stated was that these dies were made carefully and without intentional parallel extension.

## FURTHER DISCUSSION ON THE PAPER BY PROFESSOR A. H. COTTRELL AND DR. V. AYTEKIN: "THE FLOW OF ZINC UNDER CONSTANT STRESS."

(*J. Inst. Metals*, 1950, 77, 389, 597.)

Dr. A. LATIN,\* M.Eng. (Member): I feel that Professor Cottrell's kind reply to the points I raised in the discussion on his paper with Dr. Aytekin calls for some further comment.

I should like to take up first the view Professor Cottrell expresses that statements such as "to say hardening is balanced by recovery is simply to state that neither occurs", could be "dangerous"; the actual statement I made was worded somewhat cautiously, but if pressed on the point, I would state that it is almost a logical truism and certainly less dangerous than the use of analogy. As regards the example Professor Cottrell gives, I cannot myself see any very close analogy between the forces acting on a body falling through the atmosphere and the hardening and recovery processes. The presence of forces, even of zero resultant, acting on real bodies, can be demonstrated, for example, by the stress/strain system they produce. There may be perhaps a closer analogy with acceleration, but again it would seem to me almost if not quite a logical truism to say that when constant velocity is reached, neither acceleration nor deceleration occur.

All this does not mean that the device of using the hardening/recovery type of theory may not give the correct result, and, if it can be proved without doubt that it does so, it is justified. However, some suspicion of artificiality could be avoided, or the theory completely vindicated by confirmation, if a further attempt at a more direct treatment could be undertaken. The fact that the hardening/recovery theory "requires only that the activation energy for recovery should be a smoothly decreasing function of the internal stress" does not smooth out the difficulty that it is necessary to account fully for such a function. As regards the direction on which one might wish to develop the diffusion view of (quasi-viscous) creep, I would point out that a treatment of the matter has been given by McCance in his Hatfield Memorial lecture.† He does not deal with the stress relationship; the sort of treatment involved there, I would suggest, would be somewhat on the lines given by Orowan.‡ The latter's calculations were for a fully disordered structure; they would need to be replaced by calculations based on the conceived type of diffusion motion through a crystal lattice structure.

\* British Insulated Callender's Cables, Ltd., London.

† Sir A. McCance, *J. Iron Steel Inst.*, 1949, 163, 241.

‡ E. Orowan, *J. West Scotland Iron Steel Inst.*, 1946-47, 54, 45.

## OBITUARY.

## PROFESSOR THOMAS TURNER.

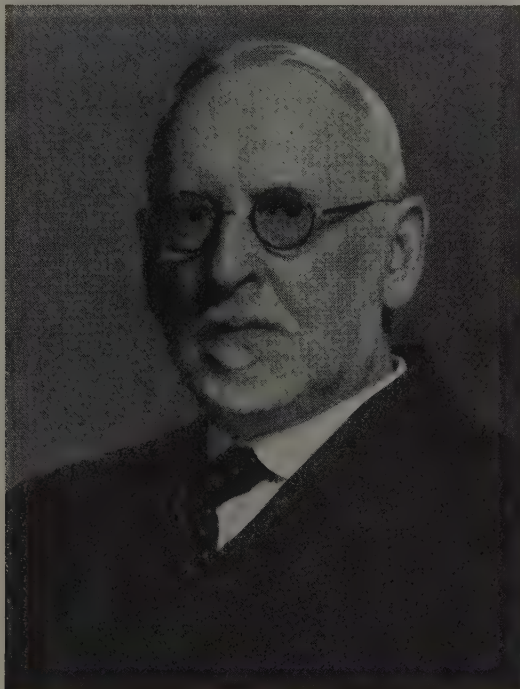
The death of Professor Thomas Turner on January 31st, 1951, marked the close of a long and distinguished career devoted unceasingly to the advancement of metallurgy over a very wide field. Born in Birmingham in 1861, he had reached his 90th year, and until quite recent years he had been seen as a welcome and honoured figure at metallurgical gatherings. His presence gave evidence of his sustained interest in metallurgical science, in which, during his long life, he had witnessed such remarkable progress. To this progress he had himself made many valuable contributions, both by his own researches and by the training of others to realize, as he had found, how very much worth while the pursuit of metallurgy may be.

It is difficult to realize that one who was so recently with us and whose friendship one had valued for so many years, had entered the Royal School of Mines as a student of 17 so long ago as 1878, the year in which Thomas and Gilchrist gave to the world the results of their epoch-making efforts in regard to basic steel. Dr. John Percy still occupied the Chair of Metallurgy at the time of the triumph of his two former students, but his retirement took place in the following year, so that Turner completed the course as one of Roberts-Austen's first students. It was, however, directly due to Percy's personal instigation and encouragement that Turner responded to an appeal made by him to young metallurgists in his Presidential Address to the Iron and Steel Institute in 1885. Turner was then occupying a position at Mason's College, Birmingham, as Demonstrator in Chemistry, and had already contributed several papers to the chemical journals as a result of his skill in metallurgical analysis, the real basis, if one may say so, of all metallurgical training. Percy's appeal had been for someone to co-ordinate and interpret the results of chemical analysis, and Turner's response was a remarkable paper of some 28 pages which he presented to the Iron and Steel Institute in the following year (1886) on "The Constituents of Cast Iron". This paper received the warm commendation of Percy and of others who were present, among them Sir Lowthian Bell, Sir Frederick Abel, Professor Huntington, and Professor Bauerman. Thus, it was in the realms of ferrous metallurgy that he achieved success and recognition in the 80's of the last century. His paper is remembered chiefly for the clear exposition he gave of the relations of iron to silicon in cast iron, though it was by no means confined to this aspect of the metallurgy of cast iron.

After a period of ten years or so at Mason's College as Lecturer in Metallurgy, his services were sought, in 1894, by the Staffordshire County Council to organize and direct technical instruction in that area. It was while here that his work "The Metallurgy of Iron" was published. This received world-wide recognition, and has been a standard text-book on the subject ever since.

With the establishment of a University at Birmingham in 1902, Turner became the first to occupy the Chair of Metallurgy. To him fell the responsibility of planning and equipping the Metallurgical Department in the new University Buildings which were being erected at Edgbaston. This task he carried out so successfully that Birmingham was furnished with laboratories as fine as any in the kingdom. Those engaged in the non-ferrous industries of the district gave generous support to the Department and, as its head, Pro-

fessor Turner increased his already close association with these industrialists. With them, he saw the need for setting up some appropriate body for ensuring a closer contact between the members of these industries. It was in Birmingham that the decision was reached to form a Society for this purpose, and the Institute of Metals came into being in 1908 with temporary quarters in the University itself, with Shaw Scott as the first Secretary and Turner undertaking the duties of Honorary Treasurer. It was not long before suitable headquarters were found in London, and with the late Sir William White as



its first President, the Institute was successfully launched on its career. Meanwhile, from 1902 onwards, Turner had been steadily building up a school of metallurgy at Birmingham, with Dr. O. F. Hudson, from the outset and for some time, as his only Lecturer. Later on he was joined by the late Dr. G. D. Bengough, who was succeeded by Dr. Donald M. Levy when Bengough went to Liverpool. Hudson remained with Turner until 1916. The sincere regard in which he was held and a generous appreciation of his services have been expressed to the writer on many occasions by Professor Turner.

One could compile a long list of those of Turner's students who have since gained distinction as metallurgists, but mention may perhaps be made of two who subsequently achieved distinction on an even wider horizon. It was always

a source of justifiable pride to Turner that he had numbered among his students Stanley Baldwin and Neville Chamberlain, two future Prime Ministers.

So, when the time came for his retirement from the University in 1926, with the title of Professor Emeritus, he could look back on the 24 years of his occupancy of the Chair of Metallurgy with satisfaction and with the full assurance that the foundation upon which the Department had been built would sustain even greater things in the future, and it must have been a great reward to him to have lived to witness the subsequent and remarkable developments that have taken place. Turner, who had seen the parallel growth of the science and practice of Ferrous and of Non-Ferrous Metallurgy, lived to see the inevitable tendency to recognize their virtual indivisibility.

For many years after his retirement, and indeed up to the time of his death, Professor Turner acted as Consultant to Fry's Metal Foundries, Ltd., London.

Many honours and distinctions came to him in the course of his long life, among them the De la Beche Medal of the Royal School of Mines, as long ago as 1883, the Bessemer Gold Medal of the Iron and Steel Institute in 1925, and also Gold Medals awarded by the Institute of British Foundrymen and by the American Foundrymen's Association. He was president of the Institute of Metals from 1924 to 1926, and was elected a Fellow in 1929. In 1939 the wheel had made a full turn when the Governing Body of the Imperial College of Science and Technology (of which the School of Mines, to which he had gone 60 years before, forms an integral part), elected him an Honorary Fellow.

Quite apart from his profession as a metallurgist, Professor Turner always appeared to have mastered the art of living, as in fact he had. There was a composure in his demeanour and a spiritual detachment from the more mundane aspects of his profession which were traceable, perhaps, to the happy relationships that he and his family enjoyed. He married in 1887 Miss Christian Smith, who survived him for only a short time, and they had two sons and two daughters. One of the sons, Mr. T. Henry Turner, is of course, well known in the metallurgical world, and the elder daughter is the wife of Mr. G. Shaw Scott, Secretary of the Institute from 1908 to 1944.

S. W. SMITH.

## NAME INDEX.

- Ahmad, Shafiq. Elected member, xvii.  
 Allard, Marc. Elected member, xix.  
 Améen, Einar Louis. Elected member, xx.  
 Anderson, (Sir) John. May Lecture, 1951: "Science in the Service of the Community", 407.  
 Andresen, Erling. Elected member, xx.  
 Arden, Lawrence L. Elected member, xxii.  
 Atkins, John William. Elected student member, xiv.  
 Auld, John Hugh. Elected junior member, xxi.  
 Bailey, G. L. Paper: "Copper-Nickel-Iron Alloys Resistant to Sea-Water Corrosion", 243; reply to discussion, 481.  
 Baron, H. G., and F. C. Thompson. Reply to discussion on "Friction in Wire Drawing", 504.  
 Beishon, Ronald John. Elected student member, xiv.  
 Binder, William Oakley. Elected member, xxii.  
 Blyth, Howard Neville. Elected member, xix.  
 Bolliger, Max. Elected member, xvii.  
 Braine, William Alan. Elected student member, xx.  
 Brinson, G., and A. J. W. Moore. Paper: "The Study of Recrystallization in Zinc by Direct Observation", 429.  
 Broadbent, Brian Lynn. Elected member, xx.  
 Broennimann, Markus. Elected member, xiv.  
 Brook, G. B. *See* Perryman, E. C. W.  
 Brown, Derek James. Elected junior member, xxii.  
 Buckman, Peter. Elected member, xviii.  
 Bullen, Francis Peter. Elected student member, xix.  
 Bunton, John Darrah. Elected member, xix.  
 Burke, Thomas Joseph. Elected member, xviii.  
 Burrill, William James. Elected student member, xiv.  
 Bushell, Thomas Wyvern. Elected member, xv.  
 Cahn, R. W. Paper: "Slip and Polygonization in Aluminium", 129.  
 Caldicott, Peter David. Elected student member, xix.  
 Calnan, E. A., and A. E. L. Tate. Paper: "Roller Levelling of Magnesium Alloy Sheet", 455.  
 Chadwick, R. Discussion on "The Effect of Small Quantities of Cd, In, Sn, Sb, Tl, Pb, or Bi on the Ageing Characteristics of Cast and Heat-Treated Aluminium-4% Copper-0.15% Titanium Alloy", and "The Tensile Properties of Heat-Treated Aluminium-Copper and Aluminium-Copper-Cadmium Alloys of Commercial Purity", 488; *see also* Cook, Maurice.  
 Chandler, Henry. Elected member, xx.  
 Chen, Neng-Kuan. Elected member, xix.  
 Cina, Bernard. Elected student member, xxiii.  
 Claxton, Cyril Charles. Elected member, xix.  
 Clayton, William Wikeley Ward. Elected member, xxi.  
 Cole, Alan Giffard. Elected member, xv.  
 Coleman, Geoffrey. Elected member, xiii.  
 Collier, Claude William. Elected member, xviii.  
 Colmant, Raymond. Elected member, xxii.  
 Cook, Maurice, R. Chadwick, and N. B. Muir. Paper: "Observations on Some Wrought Aluminium-Zinc-Magnesium Alloys", 293; reply to discussion, 484.  
 Cookson, Roland Antony. Elected member, xiv.  
 Corfield, Reginald Holbeche. Elected member, xxi.  
 Coudel, Jean. Elected member, xv.  
 Crooks, Laurence Edward. Elected member, xxii.  
 Daccò, Aldo. Elected member, xviii.  
 Davies, David Howell. Elected student member, xiv.  
 Davies, Ivor Bowen. Elected member, xxi.  
 Dawihl, Walther. Elected member, xxii.  
 Dawkins, Alfred Ernest. Elected member, xv.  
 Defreyn, Joseph Emile Ghislain. Elected member, xviii.



- De Merre, Marcel. Elected member, xiii.
- Devereux, Robert Wayne. Elected junior member, xxii.
- Devereux, Wallace Deane. Elected member, xxii.
- Dewhirst, Eric Victor. Elected member, xxi.
- Donovan, Maurice. Elected student member, xix.
- Duncan, John Alexander. Elected student member, xiv.
- Dunlop, Samuel Hamilton. Elected member, xiii.
- Dupont, Max. Elected member, xiv.
- Duran Rigol, Enrique. Elected member, xxi.
- Eglinton, Samuel Sydney Edward. Elected member, xv.
- Eichen, Erwin. Elected student member, xiv.
- El Liethy, Kadry Foad. Elected member, xviii.
- Ellis, Dennis Thomas. Elected member, xix.
- Elstub, St. John. Elected member, xxii.
- Elton, Miles. Elected member, xviii.
- English, Alan. Elected member, xix.
- Evans, Ronald Ernest. Elected student member, xxi.
- Fattah, Mohamed Ahmed Abdel. Elected member, xix.
- Fell, E. W. Discussion on "Heat Extractions at Corners and Curved Surfaces in Sand Moulds", 475.
- Ferrall, Lorin L. Elected member, xxii.
- Fiedler, Howard C. Elected student member, xv.
- Fitzgerald, Timothy. Elected member, xv.
- Fletcher, Frank. Elected member, xxii.
- Ford, H. Discussion on "Friction in Wire Drawing", 500.
- Fox, Kenneth William. Elected member, xviii.
- Freeman, John R., Jr. Discussion on "Copper-Nickel-Iron Alloys Resistant to Sea-Water Corrosion", 478.
- Frejaques, Jean Leon Maurice. Elected member, xviii.
- Freynik, Henry Stanley. Elected member, xv.
- Fricker, Dennis John. Elected student member, xv.
- Frost, Michael Andrew. Elected student member, xv.
- Frye, John H., Jr. Elected member, xviii.
- Gifkins, Robert Cecil. Paper: "The Variation with Strain-Rate of the Mechanism of Deformation of a Lead-Thallium Alloy", 233; elected member, xxi.
- Gillespie, William George. Elected member, xiii.
- Goicoechea, Manuel. Elected member, xxii.
- Graham, Robert. Elected member, xxii.
- Greenough, A. P., and Ronald King. Paper: "Grain-Boundary Energies in Silver", 415.
- Greenough, G. B. See Rotherham, L.
- Hagel, William P. Elected junior member, xxii.
- Hall, Edward George. Elected student member, xv.
- Hamer, Robert Dennis. Elected member, xiii.
- Hancock, Peter Francis. Elected member, xxi.
- Hannaford, Robert Heath. Elected student member, xv.
- Hardwick, Henry Cecil. Elected student member, xix.
- Hardy, H. K. Paper: "The Ageing Characteristics of Binary Aluminium-Copper Alloys", 321; discussion on "The Effect of Small Quantities of Cd, In, Sn, Sb, Tl, Pb, or Bi on the Ageing Characteristics of Cast and Heat-Treated Aluminium-4% Copper-0.15% Titanium Alloy" and "The Tensile Properties of Heat-Treated Aluminium-Copper and Aluminium-Copper-Cadmium Alloys of Commercial Purity", 487, 491; discussion on "The Adherence of Oxide Scales on Copper" and "The Oxidation of Copper at 350°-900° C. in Air", 497.
- Hardy, John. Elected member, xiv.
- Harris, Arthur Clement. Elected member, xix.
- Harris, Ian Robert. Elected junior member, xxii.
- Haut, Frederick Joseph Georg. Elected member, xix.
- Hayward, Eric. Elected member, xiii.
- Head, A. K. See Wood, W. A.
- Heaton, Roger Noel. Elected member, xiii.
- Henschker, Erhard Rudolf. Elected member, xiv.
- Hines, John Grahame. Elected student member, xxi.
- Hogan, Leonard McNamara. Elected member, xxi.
- Holder, Sydney George, Jr. Elected student member, xxiii.

- Houghton, Frank. Elected member, xxii.
- Howell, Leonard Philip. Elected member, xv.
- Hu, Hsun. Elected student member, xix.
- Hull, Derek. Elected student member, xix.
- Hyam, Elmer Donald. Elected student member, xv.
- Isgar, John Ernest. Elected student member, xiv.
- Ismail, Yousef. Elected member, xviii.
- Jolivet, Henri. Elected member, xxii.
- Jonah, David Alonzo. Elected member, xiv.
- Jones, (Sir) Lewis. Elected member, xix.
- Karlsson, Nils. Paper: "An X-Ray Study of the Phases in the Copper-Titanium System", 391.
- Kendrick, George André. Elected member, xviii.
- King, Ronald. *See* Greenough, A. P.
- Kirkpatrick, Leonard Henry. Elected member, xiv.
- Kirkup, William Brookes. Elected member, xxi.
- Klement, John F. Elected member, xiii.
- Latin, A. Discussion on "The Flow of Zinc Under Constant Stress", 505.
- Lawley, Bernard. Elected member, xiii.
- Lawley, Gerald. Elected member, xiii.
- Lawrie, John Arthur Noel. Elected junior member, xix.
- Lepp, H. Discussion on "The Effect of Mould Material and Alloying Elements on Metal/Mould Reaction in Copper-Base Alloys", 477.
- Leroy, André Georges Paul. Elected member, xxi.
- Lewis, George Leonard. Elected member, xix.
- Littlewood, Frederick Richard Edward. Elected member, xix.
- Liu, Tien Shih. Elected student member, xxiii.
- Lloyd, Eric Gilbert. Elected member, xviii.
- Lodder, Jacob. Elected member, xv.
- Lombardi, Paolo. Elected member, xix.
- McConnell, John Lawson. Elected member, xiii.
- McKinlay, Dudley Frederick Alexander. Elected junior member, xxi.
- MacLean, Timothy Lachlan. Elected student member, xv.
- MacLellan, G. D. S. Discussion on "Friction in Wire Drawing", 501.
- McLennan, John Andrew. Elected student member, xx.
- McQuillan, A. D. Papers: "The Application of Hydrogen Equilibrium-Pressure Measurements to the Investigation of Titanium Alloy Systems", 73; "The Titanium-Hydrogen System for Magnesium-Reduced Titanium", 371.
- McQuillan, (Mrs.) M. K. Paper: "A Provisional Constitutional Diagram of the Chromium-Titanium System", 379.
- MacWatters, Gerald. Elected member, xiii.
- Madine, James Aloysius. Elected member, xviii.
- Malcor, Henri. Elected member, xxi.
- Martinez, Giorgio. Elected member, xxii.
- Matuschka, Bernhard. Elected member, xxi.
- Metzl, John. Elected member, xviii.
- Mincher, A. L. *See* Ruddle, R. W.
- Mirza, Mohammad Razi. Elected student member, xx.
- Mitchell, Neville Meruyan. Elected junior member, xx.
- Moghe, Dinker. Elected member, xv.
- Moore, A. J. W. *See* Brinson, G.
- Morcos, Shoukry. Elected member, xviii.
- Muir, Neil Baird. Elected member, xxi; *see also* Cook, Maurice.
- Murphy, A. J. Presidential Address, 117.
- Myers, Rupert Horace. Elected member, xviii.
- Naylor, Graham Lewis. Elected student member, xx.
- Nicolau, Jean Pierre. Elected member, xviii.
- Nourse, Louis M. Elected member, xxii.
- O'Connor, Kenneth James. Elected member, xix.
- Orlando, Guiseppe. Elected member, xx.
- Owe, Aage Willand. Elected member, xxii.
- Parker, R. T. Discussion on "Observations on Some Wrought Aluminium-Zinc-Magnesium Alloys", 482; discussion on "The Influence of Alloy Constitution on the Mode of Solidification of Sand Castings", 493.
- Peplow, Douglas Boraston. Elected member, xx.

- Perryman, E. C. W., and G. B. Brook. Paper: "Mechanism of Precipitation in Aluminium-Magnesium Alloys", 19.
- Petersen, Edward Jacob. Elected member, xviii.
- Phillips, H. W. L. Discussion on "Observations on Some Wrought Aluminium-Zinc-Magnesium Alloys", 483.
- Pitts, Gordon Roy. Elected junior member, xxi.
- Plackett, John Ronald. Elected student member, xx.
- Plantema, Frederik J. Elected member, xxi.
- Poole, Howard John. Elected member, xviii.
- Porro, Giovanni. Elected member, xviii.
- Prasad, Rajendra. Elected member, xx.
- Pratt, J. N., and G. V. Raynor. Paper: "The Intermetallic Compounds in the Alloys of Aluminium and Silicon with Chromium, Manganese, Iron, Cobalt, and Nickel", 211.
- Price, Bartlett Root. Elected member, xxii.
- Prichard, Evan Wynne. Elected member, xiii.
- Prince, A. Discussion on "Copper-Nickel-Iron Alloys Resistant to Sea-Water Corrosion", 479.
- Pryor, Horace. Elected member, xx.
- Rachinger, W. A. See Wood, W. A.
- Raynor, G. V. See Pratt, J. N.
- Reynolds, Thomas. Elected member, xiv.
- Richardson, F. D. Discussion on "The Adherence of Oxide Scales on Copper" and "The Oxidation of Copper at 350°-900° C. in Air", 496.
- Ridge, Charles William. Elected member, xxi.
- Roberts, William James. Elected member, xviii.
- Robinson, Eric Arthur. Elected member, xx.
- Rolls, Roger. Elected student member, xx.
- Rotherham, L., A. D. N. Smith, and G. B. Greenough. Paper: "Internal Friction and Grain-Boundary Viscosity of Tin", 439; reply to discussion, 486.
- Rowley, Edward. Elected member, xviii.
- Ruddle, R. W., and A. L. Mincher. Reply to discussion on "The Influence of Alloy Constitution on the Mode of Solidification of Sand Castings", 494.
- and R. A. Skinner. Paper: "Heat Extraction at Corners and Curved Surfaces in Sand Moulds", 35; reply to discussion, 476.
- Rushworth, David. Elected member, xx.
- Rutherford, N. B. Paper: "The Effect of Mould Material and Alloying Elements on Metal/Mould Reaction in Copper-Base Alloys", 189; reply to discussion, 477.
- Sachs, K. Discussion on "The Adherence of Oxide Scales on Copper" and "The Oxidation of Copper at 350°-900° C. in Air", 497.
- Salah el-Din Nessim, Ahmed. Elected member, xx.
- Sandberg, Alexander Christer Edward. Elected member, xx.
- Sandström, Karl Eric Viktor. Elected member, xxii.
- Sargeant, Colin Wilfred. Elected member, xx.
- Sawkill, J. Discussion on "Internal Friction and Grain-Boundary Viscosity of Tin", 486.
- Schenkel, John Robert Harry. Elected member, xiv.
- Scheuer, E., S. J. Williams, and J. Wood. Paper: "The Effect of Copper, Silicon, and Magnesium on the Mechanical Properties of Aluminium Alloys of the D.T.D. 424 Type", 57.
- Scortecchi, Massimo. Elected member, xx.
- Shami, Wahid-Uz-Zaman. Elected student member, xv.
- Sherwood, Charles Noel. Elected member, xxii.
- Siebel, Gustav. Elected member, xviii.
- Skinner, R. A. See Ruddle, R. W.
- Slater, I. G. Discussion on "Copper-Nickel-Iron Alloys Resistant to Sea-Water Corrosion", 480; discussion on "Observations on Some Wrought Aluminium-Zinc-Magnesium Alloys", 483; discussion on "The Influence of Alloy Constitution on the Mode of Solidification of Sand Castings", 493.
- Smith, A. D. N. See Rotherham, L.
- Snedden, George Thomas. Elected member, xx.
- Sparks, Edward John. Elected member, xx.
- Staples, Ronald Thomas. Elected member, xxi.
- Sudbury, Michael Peter. Elected student member, xix.
- Suiter, John William. Elected student member, xix.
- Sully, William John. Elected member, xiv.

- Tabor, D.** Paper: "The Hardness and Strength of Metals", 1; reply to discussion, 472, 474.
- Tagliaferri, Leone.** Elected member, xxii.
- Talini, Renzo.** Elected member, xx.
- Tate, A. E. L.** See Calnan, E. A.
- Taylor, Ian.** Elected student member, xxi.
- Tenland, Waldemar.** Elected member, xxii.
- Theobald, John Richard.** Elected member, xiv.
- Thomas, Wilbert Roy.** Elected student member, xxiii.
- Thompson, F. C.** See Baron, H. G.
- Thompson, Ronald Alexander.** Elected junior member, xiv.
- Thorley, Raymond Thomas.** Elected student member, xix.
- Toor, Amanullah Khan.** Elected student member, xv.
- Turner, Thomas.** Obituary notice, 506.
- Tylecote, R. F.** Reply to discussion on "The Adherence of Oxide Scales on Copper" and "The Oxidation of Copper at 350°-900° C. in Air", 498.
- Vanick, James Sebold.** Elected member, xxii.
- Vargas, Fernando Gonzalez.** Elected member, xxi.
- Vaughan, Thomas Bernard.** Elected junior member, xxi.
- Voce, E.** Discussion on "The Hardness and Strength of Metals", 465, 474.
- Waldron, M. B.** Paper: "The Stability of the  $\text{Co}_2\text{Al}_9$ -Type Structure in the Aluminium-Rich Alloys of the Aluminium-Iron-Cobalt-Nickel System", 103.
- Walton, Ronald Newton.** Elected member, xviii.
- Ward, Samuel Henry Dewick.** Elected member, xviii.
- Watson, Nigel.** Elected member, xiv.
- White, Charles M.** Elected member, xxii.
- Whitehead, Trevor Joseph.** Elected student member, xiv.
- Williams, Dean Nesbit.** Elected student member, xix.
- Williams, S. J.** See Scheuer, E.
- Williams, Thomas Howard.** Elected student member, xv.
- Willners, Sven Harry.** Elected member, xxii.
- Wilms, G. R.** See Wood, W. A.
- Windle, John Michael.** Elected student member, xiv.
- Wood, David Baker.** Elected member, xviii.
- Wood, Harold Carrington.** Elected member, xx.
- Wood, J.** See Scheuer, E.
- Wood, W. A., and A. K. Head.** Paper: "Some New Observations on the Mechanism of Fatigue in Metals", 89.
- **G. R. Wilms, and W. A. Rachinger.** Paper: "Three Basic Stages in the Mechanism of Deformation of Metals at Different Temperatures and Strain-Rates", 159.
- Worner, H. W.** Paper: "The Constitution of Titanium-Rich Alloys of Iron and Titanium", 173.
- Yates, Harry.** Elected member, xx.
- v. Zeerleder, A.** Discussion on "The Effect of Small Quantities of Cd, In, Sn, Sb, Tl, Pb, or Bi on the Ageing Characteristics of Cast and Heat-Treated Aluminium-4% Copper-0.15% Titanium Alloy" and "The Tensile Properties of Heat-Treated Aluminium-Copper and Aluminium-Copper-Cadmium Alloys of Commercial Purity", 489.

PRINTED IN GREAT BRITAIN BY  
RICHARD CLAY AND COMPANY, LTD.  
BUNGAY, SUFFOLK.







